National Research
Council Canada

Conseil national
de recherches Canada

NRC · CNRC

Canadian Journal of Fisheries and Aquatic Sciences

Journal canadien des sciences halieutiques et aquatiques

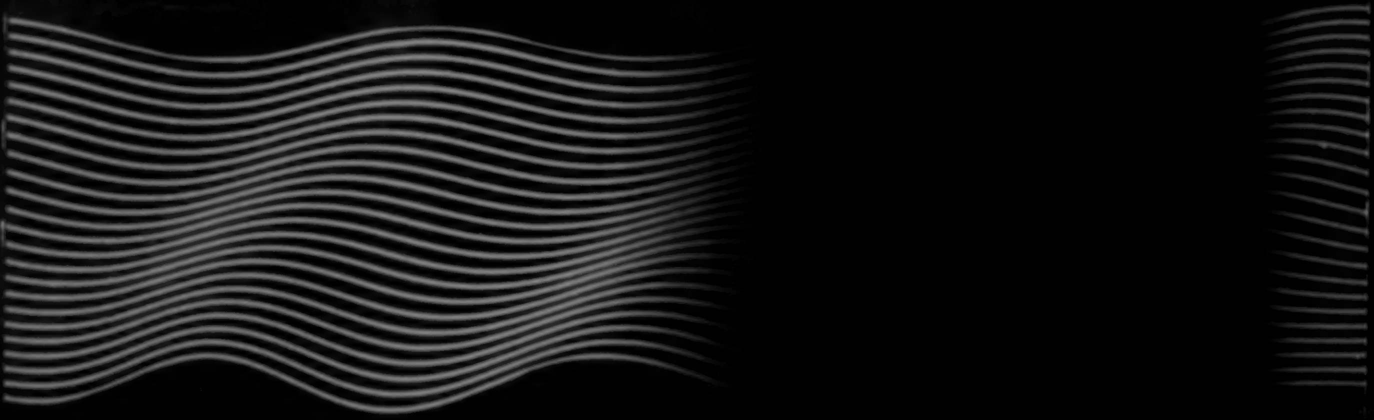

http://cjfas.nrc.ca

http://jcsha.cnrc.ca

ISSN 0706-652X / CJFSDX 63(10) 2149–2389 (2006)

The *Canadian Journal of Fisheries and Aquatic Sciences*, previously published as *Contributions to Canadian Biology* 1901–1925, *Contributions to Canadian Biology and Fisheries* 1926–1934, *Journal of the Biological Board of Canada* 1934–1937, and *Journal of the Fisheries Research Board of Canada* 1938–1979, is issued monthly to form annual volumes of 12 numbers plus supplements.

Editorial policy. The Journal publishes original research articles, perspectives (syntheses, critiques, re-evaluations), discussions (comment and reply), and rapid communications. Manuscripts may concern cells, organisms, populations, communities, ecosystems, or processes that affect aquatic systems. They may cover a range of disciplines including biology and ecology of marine and freshwater organisms, limnology, oceanography, physiology, toxicology, genetics, economics, disease, and management. Preference will be given to manuscripts that emphasize understanding of observed phenomena and interpretation of experimental results. The Journal encourages papers that lead from clearly stated purpose or rationale and from testable hypotheses, concepts, or questions to identifiable conclusions or syntheses. Such papers may amplify, modify, question, or redirect accumulated knowledge embodied in contemporary perceptions of a particular state of aquatic sciences. The Journal discourages papers that are essentially descriptive, except in emerging disciplines; have only site-specific or local applications (a certain year, place, taxon, chemical compound, etc.); only confirm previously established principles; or apply standard techniques without breaking new methodological ground.

Manuscripts for publication should be submitted to the Editorial Office via NRC Research Press' online submission and peer review system (**OSPR**EY) at http://pubs.nrc-cnrc.gc.ca/cjfas/osprey. Alternatively, manuscripts may be submitted to the Senior Editor, *Canadian Journal of Fisheries and Aquatic Sciences*, Department of Integrative Biology, Building #006, Room 118, University of Guelph, Guelph, ON N1G 2W1, Canada (519-824-4120 ext. 52646; fax: 519-767-9798; e-mail: cjfas@uoguelph.ca).

Submissions in either English or French are acceptable. The information must be original, that is, not copyrighted, published, or submitted elsewhere except in abstract form or unless by written consent of the Editor.

Correspondence concerning accepted manuscripts and corrected proofs should be sent to NRC Research Press, National Research Council of Canada, Ottawa, ON K1A 0R6, Canada (fax: 613-952-7656; e-mail: pubs@nrc-cnrc.gc.ca).

Instructions to Authors are published once a year in the first issue of each volume. Copies are available from NRC Research Press or at http://cjfas.nrc.ca. The **Publication Policy** of NRC Research Press is available at http://pubs.nrc-cnrc.gc.ca.

Microfilm. Issues from 1934 through the current volume can be purchased on 16- or 35-mm microfilm. Photocopies of individual articles or issues can be purchased from University Microfilms International, 330 North Zeeb Road, Ann Arbor, MI 48106, USA.

The *Canadian Journal of Fisheries and Aquatic Sciences*, ISSN 0706-652X, is published monthly, 12 times per year, by NRC Research Press, c/o USACAN Media Dist. Srv. Corp. at 26 Power Dam Way, Suite S1-S3, Plattsburgh, NY 12901. Periodicals postage paid at Plattsburgh, NY, and at additional mailing offices. POSTMASTER: Send address changes to *Canadian Journal of Fisheries and Aquatic Sciences*, c/o NRC, P.O. Box 2888, Plattsburgh, NY 12901.

Publié sans interruption depuis 1901, le *Journal canadien des sciences halieutiques et aquatiques* a paru sous plusieurs titres : *Contributions to Canadian Biology* 1901–1925, *Contributions to Canadian Biology and Fisheries* 1926–1934, *Journal of the Biological Board of Canada* 1934–1937, et *Journal of the Fisheries Research Board of Canada* 1938–1979. Le Journal paraît tous les mois, formant ainsi un volume de 12 numéros, et offre en plus jusqu'à deux suppléments par année.

Politique éditoriale. On publie, dans le Journal, des articles rendant compte de recherche originale, des perspectives (synthèses, critiques et réévaluations), des discussions (commentaires et réponses) et des communications rapides. Les documents peuvent porter sur les cellules, organismes, populations, communautés, écosystèmes ou processus qui affectent les systèmes aquatiques. Ils peuvent relever de divers domaines y compris la biologie et l'écologie des organismes marins et d'eau douce, la limnologie, l'océanographie, la physiologie, la toxicologie, la génétique, l'économie, la pathologie et la gestion. On accorde la préséance aux articles qui contribuent à la compréhension de phénomènes observés et à l'interprétation de résultats expérimentaux. On invite les auteurs à soumettre des articles ayant des objectifs précis ou relevant d'hypothèses, de concepts ou de questions vérifiables et se terminant par de solides conclusions ou d'utiles synthèses. Ces articles enrichissent, changent, mettent en question ou réorientent les connaissances acquises sur divers aspects des sciences aquatiques. On décourage toutefois la soumission d'articles simplement descriptifs (à moins qu'il ne s'agisse de nouvelles disciplines), d'application très limitée (applicables à une seule année, une seule région ou un seul taxon, portant sur un unique composé chimique, etc.); d'articles qui ne font que reprendre les principes énoncés dans des articles précédents; et d'articles rendant compte de l'application de normes sans gain de méthodologie.

Les auteurs sont invités à soumettre leur **manuscrit** au Bureau de la rédaction par le truchement du Système de soumission et d'examen en direct des articles (**OSPR**EY) des Presses scientifique du CNRC à http://pubs.nrc-cnrc.gc.ca/jcsha/osprey. Sinon, ils peuvent transmettre leur manuscrit par la poste à la directrice scientifique principale, *Journal canadien des sciences halieutiques et aquatiques*, Département de biologie intégrative, édifice 006, bureau 118, University of Guelph, Guelph, ON N1G 2W1, Canada (519-824-4120 poste 52646; télécopieur : 519-767-9798; courriel : cjfas@uoguelph.ca).

Les contributions peuvent être en anglais ou en français. Elles doivent être originales, c.-à.-d. qu'elles ne doivent pas avoir fait l'objet d'un copyright, avoir été publiées ou soumises ailleurs, sauf sous forme abrégée ou avec le consentement du rédacteur. Le CNRC ne se tient en aucune façon responsable des opinions exprimées par un collaborateur ou des déclarations qui pourrait faire ce dernier.

La correspondance ayant trait aux manuscrits acceptés et les **épreuves corrigés** doivent être envoyées aux Presses scientifiques du CNRC, Conseil national de recherches du Canada, Ottawa, ON K1A 0R6, Canada (télécopieur : 613-952-7656; courriel : pubs@nrc-cnrc.gc.ca).

Les Recommandations aux auteurs sont publiées une fois par année dans le premier numéro de chaque volume. Des copies sont disponibles auprès du Bureau de la rédaction aux Presses scientifiques du CNRC ou au http://jcsha.cnrc.ca. **La Politique de publication** est disponible auprès des Presses scientifiques du CNRC ou au http://pubs.nrc-cnrc.gc.ca.

Microfilms. On peut acheter sur microfilms de 16 ou 35 mm tous les numéros depuis 1934. Des photocopies d'articles ou de numéros individuels sont aussi en vente auprès de University Microfilms International, 330 North Zeeb Road, Ann Arbor, MI 48106, É.-U.

This Journal is indexed or abstracted in / Cette revue est signalée ou résumée dans
ABSEARCH; Applied Science and Technology Index and Abstracts; Aquatic Sciences and Fisheries Abstracts; Biological Abstracts; Biological and Agricultural Abstracts; CAB Abstracts; Chemical Abstracts; Current Contents; Elsevier BIOBASE; Environmental Abstracts; ETDE Energy Database; General Science Index and Abstracts; GEOBASE; GeoRef; Life Sciences Collection; Meteorological and Geoastrophysical Abstracts; Oceanic Abstracts; PASCAL Database; Science Citation Index.

Volume 63, Number 10, October 2006

Canadian Journal of Fisheries and Aquatic Sciences

Published by the National Research Council of Canada

Volume 63, numéro 10, octobre 2006

Journal canadien des sciences halieutiques et aquatiques

Publié par le Conseil national de recherches du Canada

Senior Editor / Directrice scientifique principale Moira M. Ferguson

Editors / Directeurs

Jeffrey A. Hutchings, *Dalhousie University, Halifax*
Pierre Pepin, *Northwest Atlantic Fisheries Centre, DFO/MPO, St. John's, Newfoundland*
W. Gary Sprules, *University of Toronto at Mississauga*
Assistant to the Editors / Adjointe aux directeurs scientifiques **Holly Foster**

Associate Editors / Directeurs scientifiques associés

D. Boisclair, *Université de Montréal*
U. Borgmann, *Environment Canada, Burlington*
M.J. Bradford, *DFO/MPO and Simon Fraser University*
S.E. Campana, *DFO/MPO, Dartmouth*
R. Carignan, *Université de Montréal*
K.T. Frank, *DFO/MPO, Dartmouth*
J.W.A. Grant, *Concordia University*
M.M. Hansen, *Danish Institute for Fisheries Research, Silkeborg, Denmark*
R. Hilborn, *University of Washington*
D.F. Houlihan, *University of Aberdeen*
F.A. Huntingford, *University of Glasgow*
J.M. Jech, *NFSC/NOAA, Woods Hole, Mass.*
B. Jonsson, *Norwegian Institute for Nature Research, Oslo, Norway*
K.A. Kidd, *University of New Brunswick*
D.L. MacLatchy, *University of New Brunswick, Saint John*
P. Magnan, *Université du Québec à Trois Rivières*
C.T. Marshall, *University of Aberdeen*
R.B. Millar, *University of Auckland, New Zealand*
W.P. Patterson, *University of Saskatchewan*
Y.T. Prairie, *Université du Québec à Montréal*
T.J. Quinn II, *University of Alaska–Fairbanks, Juneau, Alaska*
T.P. Quinn, *University of Washington*
C.W. Ramcharan, *Laurentian University*
J.S. Richardson, *The University of British Columbia*
B. Sainte-Marie, *DFO/MPO, Mont-Joli*
R.E.H. Smith, *University of Waterloo*
S.J. Smith, *DFO/MPO, Dartmouth*
E.B. Taylor, *The University of British Columbia*
W.F. Vincent, *Université Laval*
R.D. Vinebrooke, *University of Alberta*
C.J. Walters, *The University of British Columbia*
B. de Young, *Memorial University of Newfoundland*

NRC Research Press / Presses scientifiques du CNRC

Editor-in-Chief / Directeur scientifique en chef **Bruce P. Dancik**
Assistant Editor-in-Chief / Adjoint au directeur scientifique en chef **Iain E.P. Taylor**

Journals Program / Programme des revues

Fax / Télécopieur : 613-952-7656; e-mail / courriel : pubs@nrc-cnrc.gc.ca; URL / URL : pubs.nrc-cnrc.gc.ca
Director / Directeur **Cameron D. Macdonald**
Business Manager / Gestionnaire des affaires **Jason Charron**
Manager, Journals Program / Gestionnaire, Programme des revues **Carolyn Brown**
Managing Editor / Rédactrice administrative **Cecily M. Pearson** (613-993-9099)
Publication Officers / Agents de publication **Jennifer McColl, Thad Costigan**
Advertising and reprints / Annonces publicitaires et tirés à part **Roxanne Landriault** (613-990-2254)
Subscriptions / Abonnements **Eileen Evans-Nantais** (613-990-7873)

The National Research Council of Canada accepts no responsibility for statements or opinions expressed by a contributor. Acceptance of an advertisement, announcement, or other material does not imply endorsement by either the Journal's Senior Editor or the National Research Council.

© National Research Council of Canada 2006. All rights reserved.

No part of this publication may be reproduced, stored, or transmitted in any form or by any means, without the written permission of the publisher, except as stated below.

The National Research Council of Canada grants **permission*** to individuals to make single copies of articles for personal use. Any person may reproduce short excerpts from articles in the journal for any purpose that respects the moral rights of authors, provided that the source is fully acknowledged. As a courtesy, the consent of authors of such material should be obtained directly from the author.

Authorization to reproduce items for other than personal use, as stated above, is granted by the National Research Council of Canada provided that the copyright fee of $7.00 per copy is paid directly to Access Copyright, The Canadian Copyright Licensing Agency, One Yonge Street, Suite 800, Toronto, ON M5E 1E5, Canada.

*The above permission does not extend to other kinds of copying, such as copying for general distribution, for advertising, or promotional purposes, for creating new collective works, or for resale. For such copying, arrangements must be made with the publisher, National Research Council of Canada, Ottawa, ON K1A 0R6, Canada.

Subscription information

The *Canadian Journal of Fisheries and Aquatic Sciences* (ISSN 0706-652X) is published monthly by the National Research Council of Canada. The 2007 annual subscription rates (second class postage) for Canada are $1051CAN institutional and $325CAN personal, for US & foreign $1051US institutional and $325US personal. For air mail add $150US to foreign rate. Canadian customers please include 6% GST (business no. 12149 1807 RT 0275). Subscriptions are entered for the calendar year. Remittances should be made payable to the Receiver General for Canada, credit NRC. Price for regular single issues: institutional, $110.00; personal, $35.00. Supplements will be priced separately. Special rates apply to members of Canadian scientific and engineering societies if they subscribe through their respective societies.

There are no refunds on cancelled subscriptions once delivery has begun. Claims for missing issues should be made within four months (N. America) or six months (outside N. America) following the date of publication. The publisher expects to supply missing issues only when losses have occurred in transit and when the reserve stock will permit. For change of address and subscription enquiries: Subscription Office, NRC Research Press, National Research Council of Canada, Ottawa, ON K1A 0R6, Canada; tel.: 613-993-9084; fax: 613-952-7656; e-mail: pubs@nrc-cnrc.gc.ca.

Microform backfiles are available from UMI, P.O. Box 1346, Ann Arbor, MI 48106-1346, USA, and Micromedia Ltd., 20 Victoria St., Toronto, ON M5C 2N8, Canada.

All issues of the *Canadian Journal of Fisheries and Aquatic Sciences* since 1996 are available on the Web. Pricing information can be found at http://pubs.nrc-cnrc.gc.ca.

Le Conseil national de recherches du Canada ne se tient en aucune façon responsable des opinions exprimées par un collaborateur ou des déclarations que pourrait faire ce dernier. La publication d'annonces publicitaires, d'avis et autres n'implique pas l'endossement de leur contenu par la directrice principale de la Revue ou le CNRC.

© Conseil national de recherches du Canada 2006. Tous droits réservés.

Il est interdit de reproduire, de sauvegarder ou de transmettre quelque partie de la présente publication dans quelque format ou de quelque façon sans le consentement écrit de l'éditeur, à l'exception des conditions suivantes.

Le Conseil national de recherches du Canada accorde aux particuliers le droit de faire des copies individuelles pour leur usage personnel. Toute personne peut reproduire de courts extraits des articles de la Revue pour autant que les droits moraux de l'auteur soient respectés et que la mention de provenance soit clairement indiquée. Il est de convenance de demander le consentement de l'auteur avant de faire mention de son travail.

On obtiendra l'autorisation de reproduire des articles à d'autres fins que l'usage personnel (tel qu'on l'a décrit ci-dessus) auprès du Conseil national de recherches du Canada pour autant que des redevances de droits d'auteurs de 7,00 $/copie soient versées au Access Copyright, The Canadian Copyright Licensing Agency, 1, rue Yonge, bureau 800, Toronto, ON M5E 1E5, Canada.

*La permission ci-dessus ne s'applique pas à la reproduction à grande échelle, telle que la reproduction aux fins de distribution générale, publicitaire ou promotionnelle, de compilation de nouveaux ouvrages collectifs ou de revente. Dans de tels cas, il faudra ratifier une entente particulière avec l'éditeur, le Conseil national de recherches du Canada, Ottawa, ON K1A 0R6, Canada.

Renseignements sur l'abonnement

Journal canadien des sciences halieutiques et aquatiques (ISSN 0706-652X) est une publication mensuelle du Conseil national de recherches du Canada. Le prix de l'abonnement annuel en 2007 au Canada (courrier de deuxième classe) est de 1051 $CAN pour les organismes et de 325 $CAN pour les particuliers. À l'étranger (y compris les É.-U.), le prix de l'abonnement est de 1051 $US pour les organismes et de 325 $US pour les particuliers. L'expédition par avion exige des frais de 150 $US en sus du prix d'abonnement à l'étranger. Les clients du Canada doivent ajouter la TPS de 6 % (numéro d'entreprise 12149 1807 RT 0275). Les abonnements sont pour l'année civile. Tout paiement doit être adressé au Receveur général du Canada, crédit du CNRC. Le prix par numéro est de 110 $ pour les organismes et de 35 $ pour les particuliers. Le prix des hors-série varie. Les membres des sociétés canadiennes de sciences et de génie bénéficient de taux préférentiels en s'abonnant via leurs sociétés respectives.

Aucun remboursement ne sera accordé ni aucune annulation acceptée une fois que les livraisons auront commencé. Les réclamations de numéros manquants devront être soumises dans les quatre mois (Amérique du Nord) ou dans les six mois (à l'extérieur de l'Amérique du Nord) suivant la date de publication. L'éditeur ne fournira de numéros manquants que si le document a été perdu pendant l'expédition et que si le stock le permet. Adressez tout changement d'adresse ou toute question quant à l'abonnement au : Bureau des abonnements, Presses scientifiques du CNRC, Conseil national de recherches Canada, Ottawa, ON K1A 0R6, Canada; téléphone : 613-993-9084; télécopieur : 613-952-7656; courriel : pubs@nrc-cnrc.gc.ca.

On peut obtenir les fichiers rétrospectifs sur **microforme** auprès de UMI, P.O. Box 1346, Ann Arbor, MI 48106-1346, É.-U., et auprès de Micromedia Ltée, 20, rue Victoria, Toronto, ON M5C 2N8, Canada.

À partir de 1996, tous les numéros de *Journal canadien des sciences halieutiques et aquatiques* sont accessibles sur le Web. On trouvera des renseignements sur les tarifs à http://pubs.nrc-cnrc.gc.ca.

RAPID COMMUNICATION / COMMUNICATION RAPIDE

The cost of overfishing and management strategies for new fisheries on slow-growing fish: orange roughy (*Hoplostethus atlanticus*) in New Zealand

Ray Hilborn, John Annala, and Daniel S. Holland

Abstract: The history of orange roughy (*Hoplostethus atlanticus*) stocks, primarily in New Zealand and Australia, is commonly used as an example of the inability to manage fisheries resources. We review the history and status of the New Zealand orange roughy fishery and show that the total loss of potential biological yield from overfishing is no more than 8.3% (1260 tonnes (t)·year^{-1}) of the potential yield. The losses from underfishing are estimated to be 810 t·year^{-1}. We consider the biological and economic consequences of alternative management approaches to the New Zealand orange roughy fishery. We suggest that given the uncertainty in stock abundance and productivity and market and processing capacity limits, the management of New Zealand orange roughy stocks has been close to economically optimal and has produced near maximum sustainable yield from the resource.

Résumé : On utilise souvent l'histoire des stocks de l'hoplostèthe orange (*Hoplostethus atlanticus*), particulièrement de Nouvelle-Zélande et d'Australie, comme exemple pour montrer que les ressources halieutiques sont impossibles à gérer. Nous passons en revue l'histoire et le statut de la pêche commerciale de l'hoplostèthe orange en Nouvelle-Zélande et démontrons que la perte totale de rendement biologique potentiel dû à la surpêche ne dépasse pas 8,3 % (1260 tonnes (t)·an^{-1}) du rendement potentiel. Les pertes dues à la sous-exploitation sont estimées à 810 t·an^{-1}. Nous examinons les effets biologiques et économiques des diverses approches de rechange pour la gestion de la pêche de l'hoplostèthe de Nouvelle-Zélande. Nous croyons qu'étant donné l'incertitude de l'abondance et de la productivité des stocks et des limites de capacité du marché et de l'industrie de la transformation, la gestion des stocks de l'hoplostèthe orange en Nouvelle-Zélande s'est maintenue à un niveau proche de l'optimum économique et qu'elle a produit à peu près le rendement potentiel à long terme de cette ressource.

[Traduit par la Rédaction]

Introduction

Overfishing has attracted enormous public attention in recent years, and orange roughy (*Hoplostethus atlanticus*) in New Zealand is often used as an example of one of the most egregious cases of poor fisheries management (Roberts 2002). The New Zealand (NZ) orange roughy fishery developed very rapidly in the late 1970s and early 1980s as new stocks were found and fisheries were developed. The early total allowable catches (TACs) were based on limited research biomass surveys and early productivity assumptions but have been shown to be overly optimistic. As more extensive research data and analyses indicated that orange roughy stocks were less abundant and less productive than initially assumed, the TACs were reduced over several years to sustainable levels (Clark et al. 2000).

The four largest fisheries (Northeast Chatham Rise (NECR), South Chatham Rise (SCR), Mid East Coast North Island (MEC), and Challenger Plateau (7A)) have produced more than 90% of the total NZ orange roughy catch (Table 1). In the case of the NECR, SCR, and MEC fisheries, beginning in 1989 TACs were reduced to sustainable levels in a stepped fashion over a 5- to 6-year period to ameliorate impacts on the fishing industry. In the 7A fishery, the TAC was doubled from 6000 to 12 000 tonnes (t) as part of an experimental adaptive management program. Once updated es-

Received 2 June 2006. Accepted 31 July 2006. Published on the NRC Research Press Web site at http://cjfas.nrc.ca on 18 August 2006.
J19346

R. Hilborn.[1] School of Aquatic and Fishery Sciences, Box 355020, University of Washington, Seattle, WA 98195-5020, USA.
J. Annala and D.S. Holland. Gulf of Maine Research Institute, 350 Commercial Street, Portland, ME 04101, USA.

[1] Corresponding author (e-mail: rayh@u.washington.edu).

Can. J. Fish. Aquat. Sci. 63: 2149–2153 (2006) doi:10.1139/F06-115

Table 1. Stock status of the major New Zealand orange roughy (*Hoplostethus atlanticus*) stocks, the estimated maximum sustainable yield (MSY), and the amount of loss due to overfishing and underfishing.

Stock	Unfished biomass (1000 t)	Current biomass (1000 t)	Current level as fraction of unfished	Percent loss in potential yield	MSY (1000 t)	Annual loss from overfishing (1000 t)	Annual loss from underfishing (1000 t)
NWCR	67	23	0.347	–0.02	1.3	0.00	0.03
NECR	373	166	0.445	–0.10	7.2	0.00	0.72
SCR	104	37	0.356	–0.03	2.0	0.00	0.06
Puysegur	17	1.1	0.065	0.37	0.3	0.12	0.00
East Cape	21	5.1	0.243	0.00	0.4	0.00	0.00
MEC	101	26	0.253	0.00	2.0	0.00	0.00
7A	91	2.5	0.027	0.65	1.8	1.14	0.00
7B	14.5	5	0.345	–0.03	0.3	0.00	0.01
Total	789	266	0.337		15.2	1.3	0.81

Note: Negative loss in potential yield indicates stock is underfished. NWCR, Northwest Chatham Rise; NECR, Northeast Chatham Rise; SCR, Southern Chatham Rise; MEC, Mid East Coast North Island; 7A, Challenger Plateau (west of North Island); 7B, Cook Canyon (west of South Island). All values are from 2005 stock assessments found in Sullivan et al. (2005). t, tonnes.

timates of biomass and productivity became available, the sustainable yield was re-estimated and the TAC was reduced to 2500 t in one year and then closed completely several years later when the catch rate continued to decline.

During the development of the fishery, orange roughy yields were much higher than the sustainable level as the virgin biomass was fished down to the level where long-term yield is maximized (Fig. 1*a*). The concept of a period of nonsustainable yields during a fishing-down phase is well understood among fisheries scientists (Hilborn and Walters 1992), but the general public, and particularly environmental groups, repeatedly interpreted the TAC declines in the early 1990s as an indication that the management strategy had failed and that overfishing had led to a TAC reduction. Since the early 1990s, total removals have been at about the same level as the overall maximum sustained yield (MSY) using current biological assumptions.

The objectives of fisheries management are diverse and include the production of food, economic wealth, employment, and preservation of ecosystems. Most national legislations specify that the primary objective is MSY and often contain only marginal wording relating to social, economic, and environmental impacts (Hilborn 2006). For this reason we will concentrate on analyzing the loss of biological yield relative to MSY resulting from overfishing in the NZ orange roughy fishery.

Secondly, we will explore the history of the NZ orange roughy fishery and compare a range of alternative development strategies to determine what the economically optimal strategy would have been, given perfect hindsight about the size and productivity of the orange roughy stock.

Materials and methods

The status of NZ orange roughy stocks is summarized in an annual report of the stock assessment plenary meeting (Sullivan et al. 2005). Where the plenary report contained multiple scenarios, we used the value of current stock size and unfished stock size for each orange roughy stock averaged across the various scenarios presented.

To calculate the loss of yield resulting from overfishing, we used the standard fisheries age-structured model that forms the core of all NZ stock assessments (Bull et al. 2005) and calculated the yield that would be obtained at the current stock size and divide this by the maximum possible yield. In all cases we used the biological parameters assumed for Chatham Rise orange roughy. Although there are some slight variations in these parameters from stock to stock, they constitute a trivial difference.

We calculated the MSY for each stock from the production relationship and compared that with the yield at the current stock size using the method of Lawson and Hilborn (1985). These represented both ideal and equilibrium conditions. The resulting MSY was generally greater than the MSY assumed by NZ working groups, which are based on maximizing yield under a risk tolerance (Sullivan et al. 2005) rather than under equilibrium assumptions. We calculated potential yield by assuming that the stock could be maintained at the biomass supporting MSY, with no natural variability or management error. Assuming our estimates of the current stock size and unfished stock size were correct, we overestimated the loss in yield because the denominator was a theoretical MSY, not one that would result under an MSY policy.

A simple economic model was used to evaluate alternative management histories. Revenues from fishing were calculated as

$$(1) \qquad R_t = C_t P$$

where R_t is fishing revenue at year t, C_t is catch at year t, and P is fish price.

We assumed that the catch in tonnes per tow was proportional to stock abundance, so

$$(2) \qquad \mathrm{CPUE}_t = qB_t$$

where B_t is stock abundance at year t.

Assuming vessels could make five tows per day, the effort (in vessel days) required to achieve any annual catch was calculated as

$$(3) \qquad E_t = \frac{C_t}{5\mathrm{CPUE}_t}$$

Fig. 1. (*a*) The annual catch of orange roughy (*Hoplostethus atlanticus*) in New Zealand (vertical bars) and the estimated maximum sustainable yield summed over all stocks (solid line). (*b*) The relationship between stock size and potential yield for New Zealand orange roughy, with each stock plotted on the curve at its current size. NWCR, Northwest Chatham Rise; NECR, Northeast Chatham Rise; SCR, Southern Chatham Rise; MEC, Mid East Coast North Island; 7A, Challenger Plateau (west of North Island); 7B, Cook Canyon (west of South Island). (*c*) Trends in stock biomass and stock size using a fixed escapement policy with exploitation rate capped at 10% of the stock biomass.

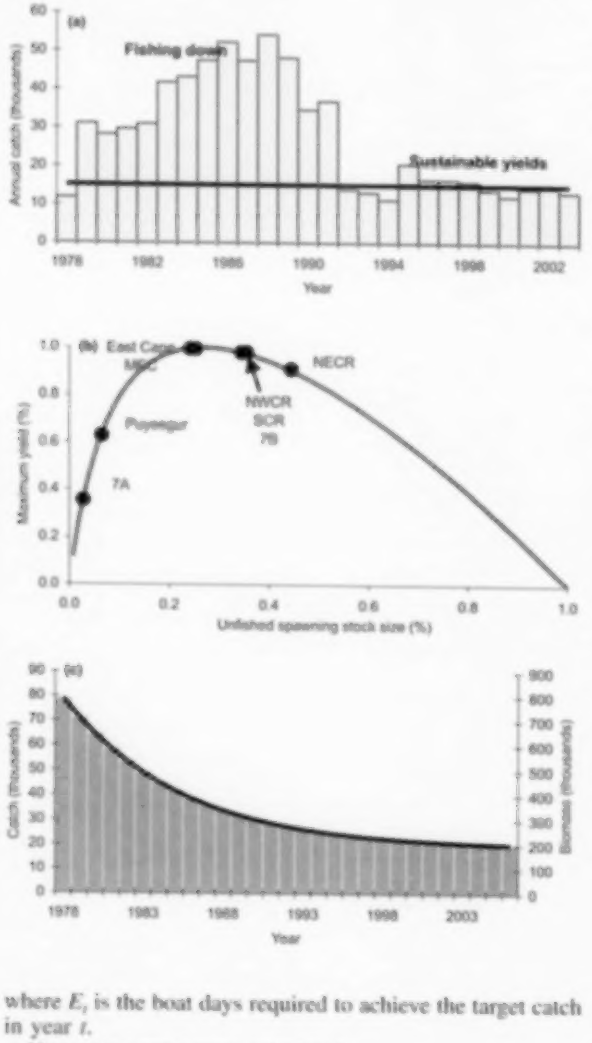

where E_t is the boat days required to achieve the target catch in year t.

Harvesting costs were calculated as

$$(4)\qquad H_t = E_t V \text{ and } \pi_t = R_t - H_t$$

where H_t is harvesting costs at year t, V is the price of operating a vessel for one day, and π_t is profits at year t.

The net present value (NPV) of the profit stream, simulated from 1978 to 2078, is

$$(5)\qquad \mathrm{NPV} = \sum_{t=1}^{t=100} \frac{\pi_t}{(1+r)^t}$$

where r is the discount rate and $t = 1$ in 1978.

We used the following economic parameters to qualitatively address the potential biases caused by the assumptions that harvest volume had no impact on price and that there were no fixed investment costs: a price per tonne of NZ$ 4500, which represented an average of port price and export price, a discount rate of 8%, a vessel cost per day of NZ$ 30 000, and vessel efficiency set at 50 t/day in the unfished state. These costs and revenues are in 2006 dollars and are based on nonpublished industry sources.

We explored a range of alternative harvest strategies including: (*i*) a fixed escapement policy, (*ii*) a fixed escapement policy constrained by a 10% maximum harvest rate, and (*iii*) a two-staged harvest rate in which there is one harvest rate during the fishing-down period and another harvest rate during the period of sustainable management. We maximized the NPV in 1978 for each policy simulated over a 100-year period by searching over the parameters that controlled the harvest strategy.

Results

The production relationship for orange roughy, based on the assumptions used in NZ stock assessments, showed that the sustainable yield was maximized at about 30% of unfished spawning stock biomass, but the yield was very close to the MSY value over the range of 20%–40% of virgin biomass (Fig. 1*b*). This is a typical result for most fisheries population models, and nothing in the life history of orange roughy makes this species unusual in this respect. The key assumption is the steepness value used in NZ assessments of 0.75. Lower values of steepness would result in more lost yield and higher values would result in less lost yield; 0.75 has been chosen for NZ orange roughy as an average of a range of fish stocks as none of the data sets for orange roughy provides information on this parameter.

The key inputs and outputs for each NZ orange roughy stock are shown (Table 1). The majority of the orange roughy stock are near the stock sizes that produce MSY. The 7A stock is the most depleted and shows the most loss relative to the MSY, losing 65% of the potential yield at the current low stock size, estimated to be 1140 t·year^{-1}, from a total loss across all stocks of 1260 t·year^{-1}. There is also a loss from underfishing (primarily for the NECR stock) of 810 t·year^{-1}. The 1260 t·year^{-1} loss from overfishing from a total 15 190 t of potential yield constitutes a loss of 8.3% per year.

We explored three alternative harvest strategies. As expected from economic theory, a fixed escapement policy maximized the net present value of the resource at NZ$ 2.6 billion. This policy involved fishing the stock down to 23% of its virgin biomass in the first year and then setting a subsequent annual catch at about 14 000 t. The fixed escapement policy with the exploitation rate capped at 10% was similar to the highest exploitation rate ever observed. This resulted in a more gradual development of the fishery and reduced the NPV to NZ$ 1.8 billion. In this scenario, the stock was held at 24% of its virgin biomass. We show the trend in catch and biomass (Fig. 1*c*), where there is a gradual decline in catch as the stock declines under the 10% harvest rate, then the catch and biomass approach equilibrium values.

Another strategy would have been to fish at a high harvest rate during a fishing-down phase and then apply a lower, long-term harvest rate. The optimal policy under this strategy would be to fish-down rapidly, with an annual harvest rate of 27%, and then cut the harvest rate back to 7% during the period of sustainable management. This policy produced a NPV of NZ$ 2.1 billion. In comparison, the actual catch history for the stock resulted in a NPV of NZ$1.2 billion, the lower value primarily due to the slower increase in yields in the early years of the fishery.

We explored the sensitivity of the results to the choice of discount rate. Although the absolute value of the NPV is much higher with lower discount rates, the basic results are the same, with rapid development and fishing-down to low but sustainable levels always the optimal path. The primary impact of discount rates is that the long-term population size is higher at lower discount rates; for instance, at a 2% discount rate, the long-term population size is about 25% higher than at an 8% discount rate.

Discussion

Given that the popular conception around the world is that orange roughy stocks in NZ have collapsed, our estimated 8.3% loss in yield will come as a surprise to most readers. Only two of the stocks, Puysegur and 7A, have been reduced to such low levels that yield is appreciably reduced, and both of those fisheries have been closed.

The bioeconomic analysis showed that without accounting for marketing, processing, and capacity constraints, the NPV of the resource would have been maximized by a rapid fishing-down period followed by long-term sustainable management at a similar level as presently exists. Such a policy would have been unrealistic because of market, harvest, and processing constraints. Price would also likely be affected by the high level of catches in a single year.

The third management scenario, high initial harvest rates followed by lower sustained fishing, was similar to what happened in NZ, although the actual fishing-down of the orange roughy stocks was much slower. The harvest rate required during the fishing-down period in this scenario would also have been constrained by markets and harvesting capacity. Obvious limitations to the model used are the assumptions that there is no impact of harvest volume on price and that there are no fixed or investment costs. In addition, our calculations of lost yield were dependent on the assumptions of the stock assessment. If there is less compensation in the spawner recruit curve and the B_{MSY} (biomass that produces maximum sustainable yield) occurs at a higher level than assumed, we have underestimated lost yield, whereas if there is more compensation than assumed, we will have overestimated lost yield.

Many fisheries agencies now use B_{MSY} as a lower limit and strive to keep the stocks above this level. This is in part due to the historical performance of many fisheries that have kept the stocks, on average, below this level and in part because some of the objectives of fisheries management are enhanced by larger stock sizes.

Some members of the public have the desire to maintain pristine marine ecosystems. However, it is an unfortunate fact of harvesting natural populations that one cannot produce harvest from pristine ecosystems, and the more one attempts to maximize yield, the lower the stock size will be. It is not widely understood outside the fisheries science community that depleting a stock to 20%–40% of its original state is required to achieve the management objective of MSY, not an indication of management failure. Development trajectories such as found in NZ orange roughy have led to orange roughy stocks in NZ and Australia being proposed under World Conservation Union (IUCN) criteria as threatened or endangered.

There are now widespread controversies over the status of fish stocks that revolve around those who see low abundance as a symptom of fisheries failure and those who see low abundance as a consequence of maximization of yield. Jackson et al. (2001) refer to Gulf of Maine cod (*Gadus morhua*) as "ecologically extinct" yet the average surplus production for that stock in the 1980s and 1990s was as high or higher than any period in the 20th century (authors' calculations based on NOAA catch data and stock assessments http://www.nefsc.noaa.gov/nefsc/publications/crd/crd0118/). Although Myers and Worm (2003) argued that large pelagic fish stocks throughout the world were depleted to less than 10% of their original abundance by 1980, the catches of this group of species have continued to rise for the last 25 years (authors' calculations from the Food and Agricultural Organization of the United Nations catch statistics (http://www.fao.org/fi/default.asp)) and are much higher than they were during the period when they were supposedly being depleted. Authors who focus on stock size rarely examine the productivity of the stocks and tend to describe stocks at low abundance as "depleted" or "crashed", even if they are producing near optimal yields. Indeed, if Myers and Worm's estimates of abundance trends are correct, then the large pelagics, as a group, exhibited negative surplus production until they reached low abundance.

There is a widely perceived risk of "stock collapse" when stocks are harvested down to low abundance. Analyses by Myers et al. (1995) and Liermann and Hilborn (1997) suggested that fish stocks rarely show depensatory dynamics that would lead to heavily overfished stocks not recovering or showing dramatic declines in rates of increase at low densities. Hutchings (2000) has argued that many stocks do not recover from overfishing when fishing pressure is reduced, but in most cases that he examined, the fishing pressure was reduced but still remained considerable. At present, there is no accepted measure of the "risk" associated with overfishing. In NZ, both orange roughy fisheries that are thought to be well below the level that produced MSY are completely closed to fishing.

Orange roughy do pose considerable challenges to management, particularly because abundance is difficult to index using either acoustic or trawl survey methodologies. However, the widespread use of NZ orange roughy as an example of failed fisheries management seems misguided, and although mistakes have been made and lessons learned, the overall outcome has produced sustainable biological and economic benefits that appear to be nearly as high as could be expected.

Acknowledgements

We thank Paul Starr, Trevor Branch, Doug Butterworth, Pamela Nelle, and an anonymous reviewer for extensive comments on an earlier draft of this manuscript.

References

Bull, B., Francis, R.I.C.C., Dunn, A., McKenzie, A., Gilbert, D.J., and Smith, M.H. 2005. CASAL (C++ algorithmic stock assessment laboratory): CASAL user manual v2.07–2005/08/21. National Institute for Water and Atmosphere (NIWA) No. 127.

Clark, M.R., Anderson, O.F., Francis, R., and Tracey, D.M. 2000. The effects of commercial exploitation on orange roughy (*Hoplostethus atlanticus*) from the continental slope of the Chatham Rise, New Zealand, from 1979 to 1997. Fish Res. (Amst.), **45**: 217–238.

Hilborn, R. 2006. Defining success in fisheries and conflicts in objectives. Marine Policy. doi:10.1016/j.marpol.2006.05.014. *Available at* www.elsevier.com/locate/marpol.

Hilborn, R., and Walters, C.J. 1992. Quantitative fisheries stock assessment: choice, dynamics and uncertainty. Chapman and Hall, New York.

Hutchings, J.A. 2000. Collapse and recovery of marine fishes. Nature (London), **406**: 882–885.

Jackson, J.B.C., Kirby, M.X., Berger, W.H., Bjorndal, K.A., Botsford, L.W., Bourque, B.J., Bradbury, R.H., Cooke, R., Erlandson, J., Estes, J.A., Hughes, T.P., Kidwell, S., Lange, C.B., Lenihan, H.S., Pandolfi, J.M., Peterson, C.H., Steneck, R.S., Tegner, M.J., and Warner, R.R. 2001. Historical overfishing and the recent collapse of coastal ecosystems. Science (Washington, D.C.), **293**: 629–638.

Lawson, T.A., and Hilborn, R. 1985. Equilibrium yields and yield isopleths from a general age-structured model of harvested populations. Can. J. Fish. Aquat. Sci. **42**: 1766–1771.

Liermann, M., and Hilborn, R. 1997. Depensation in fish stocks: a hierarchic Bayesian meta-analysis. Can. J. Fish. Aquat. Sci. **54**: 1976–1984.

Myers, R.A., and Worm, B. 2003. Rapid worldwide depletion of predatory fish communities. Nature (London), **423**: 280–283.

Myers, R.A., Barrowman, N.J., Hutchings, J.A., and Rosenberg, A.A. 1995. Population dynamics of exploited fish stocks at low population levels. Science (Washington, D.C.), **269**: 1106–1108.

Roberts, C.M. 2002. Deep impact: the rising toll of fishing in the deep sea. Trends Ecol. Evol. **17**: 242–245.

Sullivan, K.J., Mace, P.M., Smith, N.W.M., Griffiths, M.H., Todd, P.R., Livingston, M.E., Harley, S.J., Key, J.M., and Connell, A.M. 2005. Report from the fishery assessment plenary, May 2005: stock assessments and yield estimates. New Zealand Ministry of Fisheries, ASB Bank House, 101–103 The Terrace, P.O. Box 1020, Wellington, New Zealand.

Interannual variation in large-scale movement of Atlantic bluefin tuna (*Thunnus thynnus*) determined from pop-up satellite archival tags

John R. Sibert, Molly E. Lutcavage, Anders Nielsen, Richard W. Brill, and Steven G. Wilson

Abstract: Data from pop-up satellite archival tags (PSATs) deployed on Atlantic bluefin tuna (*Thunnus thynnus*) in 1999, 2000, and 2002 were analyzed synthetically using variants of a state–space statistical model to estimate tag shedding positions, in situ position estimation errors, and movement parameters. Geographic position estimates were computed from PSAT data for 30% to 50% of the days at liberty for each tag. Such relatively low position reporting rates may present biased impressions of movement for brief times at liberty. The respective longitude and latitude errors were estimated by the state–space Kalman filter model to be approximately 0.4° and 1.0° for the 1999 deployments, 0.4° and 2.1° for the 2000 deployments, and 0.9° and 2.1° for the 2002 deployments. Estimated movement parameters were used in stochastic simulation models to predict the distribution of tagged fish after times at liberty that exceed observed reporting dates. The distributions predicted by parameters estimated from the 2002 deployments were more restricted than those estimated from the 1999 deployments. Atlantic bluefin dispersal patterns appear to be age- or size-dependent and linked to shifts in oceanographic conditions. Future fisheries management measures should address interannual differences in stock distribution identified by electronic tags.

Résumé : Nous avons analysé de manière synthétique des données enregistrées par des étiquettes satellites auto-détachables à archivage (PSATs) fixées sur des thons rouges (*Thunnus thynnus*) en 1999, 2000 et 2002 à l'aide de variantes du modèle statistique état–espace afin d'estimer les positions de libération des étiquettes, les erreurs des estimations de position in situ et les paramètres du déplacement. Nous avons calculé les estimations des positions géographiques à partir des données de PSAT pour 30 % à 50 % des jours de liberté pour chaque étiquette. De tels taux faibles de signalisation des positions peuvent donner des impressions erronées des déplacements pour les courtes périodes en liberté. Nous avons estimé à l'aide du modèle état–espace de filtre de Kalman les erreurs de longitude et de latitude qui sont respectivement d'environ 0,4° et 1,0° pour les déploiements de 1999, de 0,4° et 2,1° pour ceux de 2000 et de 0,9° et 2,1° pour ceux de 2002. Les paramètres estimés du déplacement ont servi dans des modèles de simulation stochastique à prédire la répartition des poissons marqués après des périodes de liberté qui surpassent les dates de signalisation observées. Les répartitions prédites par les paramètres estimés à partir des déploiements de 2002 sont plus restreintes que celles faites à partir des déploiements de 1999. Les patrons de dispersion des thons rouges de l'Atlantique semblent être dépendants de l'âge ou de la taille et reliés à des changements dans les conditions océaniques. Les mesures futures de gestion des pêches devraient tenir compte des différences interannuelles de répartition des stocks signalées par les étiquettes électroniques.

[Traduit par la Rédaction]

Introduction

Transatlantic movements of Atlantic bluefin tuna (*Thunnus thynnus*) have been well-documented by classical mark and recapture techniques since the 1950s (NRC 1994). Catch records from high-seas longline fishing (Wilson 1965; Shingu et al. 1975) also indicate that bluefin tuna use mid-Atlantic habitat (Lutcavage et al. 1999). Recent tagging studies using electronic tags have confirmed transatlantic movements and use of mid-Atlantic habitats (Block et al. 2001, 2005; Wilson et al. 2005). Atlantic bluefin tuna have been managed as separate stocks since the 1980s, with an arbitrary boundary at 45° W longitude. This policy is based on assumptions of low mixing rates (1%–4% annually), sepa-

Received 10 January 2006. Accepted 22 May 2006. Published on the NRC Research Press Web site at http://cjfas.nrc.ca on 15 September 2006.
J19098

J.R. Sibert[1] and A. Nielsen. Joint Institute of Marine and Atmospheric Research, University of Hawai'i at Manoa, Honolulu, HI 96822, USA.
M.E. Lutcavage. Department of Zoology, University of New Hampshire, Durham, NH 03824, USA.
R.W. Brill. Virginia Institute of Marine Science, Gloucester Point, VA 23062, USA.
S.G. Wilson. Hubbs-SeaWorld Research Institute, 2595 Ingraham Street, San Diego, CA 92109, USA.

[1] Corresponding author (e-mail: sibert@hawaii.edu).

Can. J. Fish. Aquat. Sci. **63**: 2154–2166 (2006) doi:10.1139/F06-114

rate spawning areas, and spawning site fidelity (Sissenwine et al. 1998). A recent electronic tagging study (Block et al. 2005) concluded that bluefin tuna forage throughout the Atlantic but exhibit spawning site fidelity to either the Mediterranean or the Gulf of Mexico. However, results from other tagging studies are not entirely consistent with these conclusions (Lutcavage et al. 1999; Wilson et al. 2005), and information on the reproductive status of bluefin tuna outside of the known spawning areas is extremely limited and does not rule out other spawning areas (Richards 1976; Mather et al. 1995).

Modern electronic tagging devices offer biologists a wealth of information on movement and distribution of fishes (Arnold and Dewar 2001). Pop-up satellite archival tags (PSATs) are externally attached to fish and record time, light intensity, hydrostatic pressure, and temperature. After a preset date, the tags detach themselves from the fish, rise to the sea surface, and transmit the stored information to a central location via satellite. Daily geographic position estimates are computed from the record of light intensity. The record of water pressure and temperature provides insights into the depth associations and habitat preferences of the fish and may assist in detecting tag shedding. The utility of these devices depends on retention of the device on the fish during the time at liberty and successful transmission of data. Tag shedding is a widespread problem in all tagging studies, but is seldom discussed in the realm of electronic tagging (Holland and Braun 2003). The current generation of PSATs detect and report premature releases, but earlier models lacked this capability and also did not record pressure. Thus, detection of tag shedding in early model PSATs is difficult because ambient temperature was the only additional variable recorded by the tags. Such data, when interpreted against sea surface temperature records, do not necessariy reflect whether the tag had remained on the fish (Lutcavage et al. 1999).

Parametric representation of horizontal movement (Sibert and Fournier 2001; Sibert et al. 2003) offers the possibility of using data from electronic tags to objectively detect such changes in behavior. Statistical tests can be applied to the differences in the numerical values of parameters estimated from the horizontal movements recorded by the tags under different movement hypotheses. Such changes in movement may indicate tag shedding or actual changes in behavior, such as would be required for a fish residing in the western Atlantic to begin a transatlantic migration. In addition, the estimated movement parameters can be used to extrapolate movements of tagged fish over periods of time that exceed the duration of the attachment.

We augment the PSAT data used by Wilson et al. (2005) with earlier data from PSATs deployed on larger fish (Lutcavage et al. 2000, 2001) to explore possible interannual differences in movements of Atlantic bluefin tuna in the western Atlantic Ocean. Variants of the state–space model estimated by the extended Kalman filter (Sibert and Fournier 2001; Sibert et al. 2003) are used (*i*) to estimate in situ position estimation errors and movement parameters, (*ii*) to detect apparent changes in movement, and (*iii*) to evaluate alternative hypotheses about movement. The estimated movement parameters are applied in simple simulations, using a biased random walk model, to predict the distribution of tagged fish after times at liberty extending beyond the reporting dates. In the process of conducting this analysis, we became aware of certain practical problems with the interpretation of PSAT data. We will briefly discuss these problems and their implications for the use of PSATs for the study of large-scale fish movement.

Materials and methods

Data from PSATs deployed in 1999, 2000, and 2002 were reanalyzed. Details of deployment and attachment methods are described briefly here and in more detail elsewhere (Lutcavage et al. 1999, 2001). All deployments used PTT-100 tags from Microwave Telemetry Inc. (MWT) (Columbia, Maryland, USA). During the period from 1999 through 2002, the tag manufacturer made several improvements to both the hardware and software in the tags. Tag attachment methods were improved and deployment strategies were modified. In addition, availability of fish suitable for tagging differed because tagging was conducted from commercial fishing boats using harpoon, rod and reel, and purse seine capture methods.

In 1999 and 2000, the tags were attached to dorsal musculature of the fish using a medical-grade nylon dart and 1.68 mm monofilament fishing line. Tags were deployed on the commercial fishery size class known as "giant bluefin" (size >140 kg in weight or 205 cm curved fork length, CFL) captured by rod and reel in September and October in the southern Gulf of Maine in the northwest Atlantic Ocean and were programmed to release and transmit after 1, 2, 3, or 4 quarters of a year at liberty. These tags did not have pressure sensors or fail-safe mechanisms (see below). Consequently, there is some uncertainty that all data transmitted by the tag were recorded while the tag was actually attached to the fish.

In 2002, the tags were equipped with depth sensors and attached to the dorsal musculature of the fish with flat metal darts constructed of both stainless steel and titanium (Wildlife Computers Inc., Redmond, Washington, USA). The 2002 MWT tag software incorporated a fail-safe mechanism that initiated release and data transmission if the tag approached its depth limit (~1200 m) or remained at a constant depth for 4 days (i.e., if the fish was dead on the bottom or the tag had prematurely detached and was floating at the surface). Most tags were deployed after capture via purse seiner in the southern Gulf of Maine (one was deployed off North Carolina). Groups of up to 20 fish from the same school were captured and released (Wilson et al. 2005). Most in the 2002 deployments were in the commercial category "large medium" (105 kg < weight < 140 kg; 185 cm < CFL < 205 cm) fish. Tags were all programmed to detach from the fish and initiate data transmission on 1 June 2003. In addition to the usual light and temperature sensors, these tags were also equipped with pressure sensors. Details of all tag deployments are given in Table 1.

Times of sunrise and sunset are used to estimate geographic position for each day of transmitted data using the MWT proprietary algorithm. Geographic positions are not estimated for every day at liberty because either no data are received for that day or the light record is not informative of geographic position. We define "reporting rate" for position, temperature, and depth as the proportion of days at liberty with position estimates, temperature records, and

Table 1. Summary of release and reporting information for all tags.

					Position		Depth		Temperature	
Tag No.	Release date	Report date	Weight at release (kg)	Days at liberty	Days	%	Days	%	Days	%
1999–2000 deployment										
2966	24 Sept. 1999	30 June 2000	260.5	281	192	68.3	—	—	—	—
X5312	24 Sept. 1999	30 June 2000	135.9	281	178	63.4	—	—	—	—
3631	25 Sept. 1999	14 Apr. 2000	362.4	203	68	33.5	—	—	—	—
3652	27 Sept. 1999	14 Apr. 2000	226.5	201	133	66.2	—	—	—	—
2975	2 Oct. 1999	14 Sept. 2000		349	169	48.4	—	—	—	—
2974	3 Oct. 1999	14 Sept. 2000	317.1	348	79	22.7	—	—	—	—
X5325	8 Oct. 1999	25 Dec. 1999	158.6	79	62	78.5	—	—	—	—
2979	8 Oct. 1999	25 Dec. 1999	181.2	79	51	64.6	—	—	—	—
3656	8 Oct. 1999	14 Apr. 2000	226.5	190	150	79.0	—	—	—	—
5328	8 Oct. 1999	14 Apr. 2000	181.2	190	123	64.7	—	—	—	—
2982	8 Oct. 1999	31 Aug. 2000	203.9	329	161	48.9	—	—	—	—
3704	8 Oct. 1999	31 Aug. 2000	158.6	329	153	46.5	—	—	—	—
3648	14 Sept. 2000	1 Sept. 2001	181.0	353	129	36.5	—	—	—	—
3665	14 Sept. 2000	1 Sept. 2001	249.2	353	74	21.0	—	—	—	—
3667	14 Sept. 2000	1 Sept. 2001	215.2	353	93	26.4	—	—	—	—
2002 deployment										
4659	17 July 2002	27 July 2002	181.4	11	6	54.6	6	54.6	6	54.6
5026	17 July 2002	29 July 2002	181.4	13	11	84.6	13	100.0	13	100.0
A188	17 July 2002	4 Aug. 2002	136.1	19	9	47.4	10	52.6	10	52.6
5028	17 July 2002	16 Sept. 2002	158.7	62	18	29.0	60	96.8	61	98.4
A191	17 July 2002	18 Sept. 2002	204.1	64	8	12.5	31	48.4	32	50.0
A202	17 July 2002	18 Sept. 2002	204.1	64	20	31.3	33	51.6	33	51.6
A189	17 July 2002	22 Jan. 2003	136.1	190	2	1.1	13	6.8	18	9.5
5027	17 July 2002	20 Feb. 2003	136.1	219	39	17.8	114	52.1	101	46.1
5024	17 July 2002	17 Mar. 2003	113.4	244	68	27.9	120	49.2	113	46.3
5025	17 July 2002	18 Mar. 2003	136.1	245	78	31.8	118	48.2	112	45.7
5280	1 Aug. 2002	15 Sept. 2002	136.1	46	18	39.1	46	100.0	46	100.0
A208	1 Aug. 2002	5 Oct. 2002	136.1	66	4	6.1	2	3.0	7	10.6
A199	1 Aug. 2002	19 Oct. 2002	113.4	80	20	25.0	36	45.0	35	43.8
A205	1 Aug. 2002	29 Oct. 2002	113.4	90	17	18.9	42	46.7	43	47.8
5283	1 Aug. 2002	6 Nov. 2002	90.7	98	32	32.7	92	93.9	93	94.9
5269	1 Aug. 2002	27 Nov. 2002	136.1	119	37	31.1	98	82.4	103	86.6
5267	1 Aug. 2002	9 Dec. 2002	136.1	131	45	34.4	109	83.2	115	87.8
5279	1 Aug. 2002	13 Dec. 2002	181.4	135	19	14.1	95	70.4	90	66.7
A206	1 Aug. 2002	14 Dec. 2002	181.4	136	19	14.0	2	1.5	4	2.9
A190	1 Aug. 2002	29 Dec. 2002	181.4	151	26	17.2	59	39.1	60	39.7
5281	1 Aug. 2002	2 Jan. 2003	90.7	155	30	19.4	130	83.9	129	83.2
5282	1 Aug. 2002	22 Jan. 2003	204.1	175	56	32.0	131	74.9	128	73.1
5272	1 Aug. 2002	25 Jan. 2003	136.1	178	54	30.3	121	68.0	123	69.1
A195	1 Aug. 2002	30 Jan. 2003	136.1	183	37	20.2	17	9.3	17	9.3
5274	1 Aug. 2002	7 Feb. 2003	181.4	191	44	23.0	109	57.1	108	56.5
5271	1 Aug. 2002	20 Feb. 2003	136.1	204	66	32.4	135	66.2	114	55.9
5276	1 Aug. 2002	7 Mar. 2003	158.7	219	51	23.3	107	48.9	116	53.0
5273	1 Aug. 2002	7 Apr. 2003	181.4	250	84	33.6	70	28.0	90	36.0
5270	1 Aug. 2002	7 May 2003	136.1	280	78	27.9	89	31.8	92	32.9
5275	1 Aug. 2002	1 June 2003	181.4	305	107	35.1	133	43.6	125	41.0
5278	1 Aug. 2002	1 June 2003	158.7	305	69	22.6	130	42.6	152	49.8
5362	9 Aug. 2002	18 Aug. 2002	158.7	10	10	100.0	10	100.0	10	100.0
5305	9 Aug. 2002	18 Aug. 2002	136.1	10	10	100.0	10	100.0	10	100.0
5302	9 Aug. 2002	21 Aug. 2002	90.7	13	12	92.3	12	92.3	12	92.3
5019	9 Aug. 2002	31 Aug. 2002	136.1	23	19	82.6	23	100.0	23	100.0
5021	9 Aug. 2002	19 Sept. 2002	136.1	42	13	31.0	42	100.0	42	100.0
5020	9 Aug. 2002	24 Sept. 2002	158.7	47	24	51.1	47	100.0	47	100.0

Table 1 (*concluded*).

Tag No.	Release date	Report date	Weight at release (kg)	Days at liberty	Position		Depth		Temperature	
					Days	%	Days	%	Days	%
5314	9 Aug. 2002	26 Oct. 2002	158.7	79	17	21.5	74	93.7	76	96.2
5320	9 Aug. 2002	4 Nov. 2002	136.1	88	30	34.1	83	94.3	84	95.5
5374	9 Aug. 2002	11 Dec. 2002	136.1	125	35	28.0	110	88.0	110	88.0
5023	9 Aug. 2002	15 Dec. 2002	158.7	129	52	40.3	108	83.7	102	79.1
5310	9 Aug. 2002	19 Dec. 2002	147.4	133	38	28.6	81	60.9	81	60.9
5376	9 Aug. 2002	16 Feb. 2003	136.1	192	45	23.4	126	65.6	125	65.1
5301	9 Aug. 2002	22 Feb. 2003	136.1	198	43	21.7	98	49.5	104	52.5
5268	9 Aug. 2002	7 Mar. 2003	90.7	211	40	19.0	116	55.0	108	51.2
5367	9 Aug. 2002	1 June 2003	113.4	297	39	13.1	181	60.9	173	58.3
5303	17 Aug. 2002	1 Mar. 2003	113.4	197	34	17.3	56	28.4	55	27.9
X5325	6 Sept. 2002	25 Sept. 2002	204.1	20	3	15.0	20	100.0	20	100.0
X5312	30 Sept. 2002	6 Oct. 2002	226.8	7	2	28.6	7	100.0	7	100.0
5365	30 Sept. 2002	6 Oct. 2002	249.4	7	5	71.4	7	100.0	7	100.0
5377	30 Sept. 2002	8 Oct. 2002	181.4	9	3	33.3	9	100.0	9	100.0
5313	30 Sept. 2002	12 Oct. 2002	294.8	13	2	15.4	13	100.0	13	100.0
5307	30 Sept. 2002	16 Oct. 2002	272.1	17	5	29.4	17	100.0	17	100.0
5352	30 Sept. 2002	24 Oct. 2002	204.1	25	3	12.0	25	100.0	25	100.0
5299	30 Sept. 2002	1 Nov. 2002	204.1	33	9	27.3	33	100.0	33	100.0
5369	30 Sept. 2002	1 Feb. 2003	226.8	125	17	13.6	74	59.2	73	58.4
5265	10 Oct. 2002	16 Oct. 2002	181.4	7	3	42.9	7	100.0	7	100.0
5328	10 Oct. 2002	9 Nov. 2002	272.1	31	17	54.8	31	100.0	31	100.0
5326	14 Jan. 2003	11 May 2003	124.7	118	65	55.1	99	83.9	98	83.1
Median (1999 releases)			203.9	242	142	64.0	—	—	—	—
Median (2000 releases)			215.2	353	93	26.4	—	—	—	—
Median (2002 releases)			147.4	118	20	28.6	59	70.4	60	69.1

Note: Days at liberty is the number of days between the dates of release and reporting. The columns of Position, Depth, and Temperature report the number of days and the percentage of days at liberty with position, depth, and temperature estimates, respectively. No data were available for Depth and Temperature for releases in 1999 and 2000.

depth records, respectively. MWT PSATs broadcast estimate time of sunrise and sunset and temperature records covering 1 day in a single transmission to the tag manufacturer via the Argos satellite network. For tags with pressure sensors, the pressure records for the day are broadcast in a second transmission (P.W. Howey, Microwave Telemetry Inc., Columbia, Maryland, USA, personal communication). Since there is a only a small number of transmission windows available on any given day, tags which broadcast pressure records report only 50% as many sunrise and sunset records during a day as tags that do not broadcast pressure records. As a result, the position reporting rate for pressure-recording tags will be lower than that of tags that only transmit sunrise and sunset records.

The sequence of geographic positions estimated by the MWT geolocation tracks were analyzed using several variants of a state–space model estimated by the extended Kalman filter. Strictly speaking, the Kalman filter is a likelihood method that is applied to estimate the parameters of a state–space model. The term Kalman filter is often used to refer to the combined state–space and likelihood models. For simplicity, we will refer to the state–space model estimated by the extended Kalman filter as the Kalman filter or KF. The KF and the several variants used in this paper are described in the supplementary material[2] and Nielsen (2004). The model parameterizes movement as a biased random walk partitioning movement into directed movement (i.e., the eastward (u) and northward (v) bias of the random walk) and dispersive movement (i.e., random variation in movement, D). The KF also estimates the in situ geolocation errors as the longitude (σ_x) and average latitude (σ_{y_0}) standard deviations. The equinox singularity model (Sibert et al. 2003) was used to estimate latitude geolocation errors. This parameterization enables estimation of latitude during the several days surrounding the equinox, when latitude as a function of day length is indeterminate. Two additional parameters are estimated: the maximum equinox error adjustment (a_0) and the number of days that the maximum equinox error is shifted towards the boreal summer solstice (b_0) (Hill and Braun 2001).

The first two model variants pertain to whether movement is assumed to be homogeneous during the entire time at liberty. The "change-point" model (Nielsen 2004) treats the track as a sequence of two distinct behaviors: an early and a

---

[2] Supplementary data for this article are available on the journal Web site (http://cjfas.nrc.ca) or may be purchased from the Depository of Unpublished Data, Document Delivery, CISTI, National Research Council Canada, Building M-55, 1200 Montreal Road, Ottawa, ON K1A 0R6, Canada. DUD 5074. For more information on obtaining material refer to http://cisti-icist.nrc-cnrc.gc.ca/irm/unpub_e.shtml.

Fig. 1. Temporal distribution of position estimates for the combined 1999 and 2000 (*a*, *b*) and the 2002 (*c*, *d*) deployments. Frequency of position estimates by 10-day period during the first 200 days liberty are shown in panels *a* and *c*. Frequency of position estimates by 10-day period in relation to the equinoxes are shown in panels *b* and *d*. Negative days indicate days prior to the equinox; positive days indicate days after the equinox. For longer periods at liberty, the histograms include observations relative to both equinoxes.

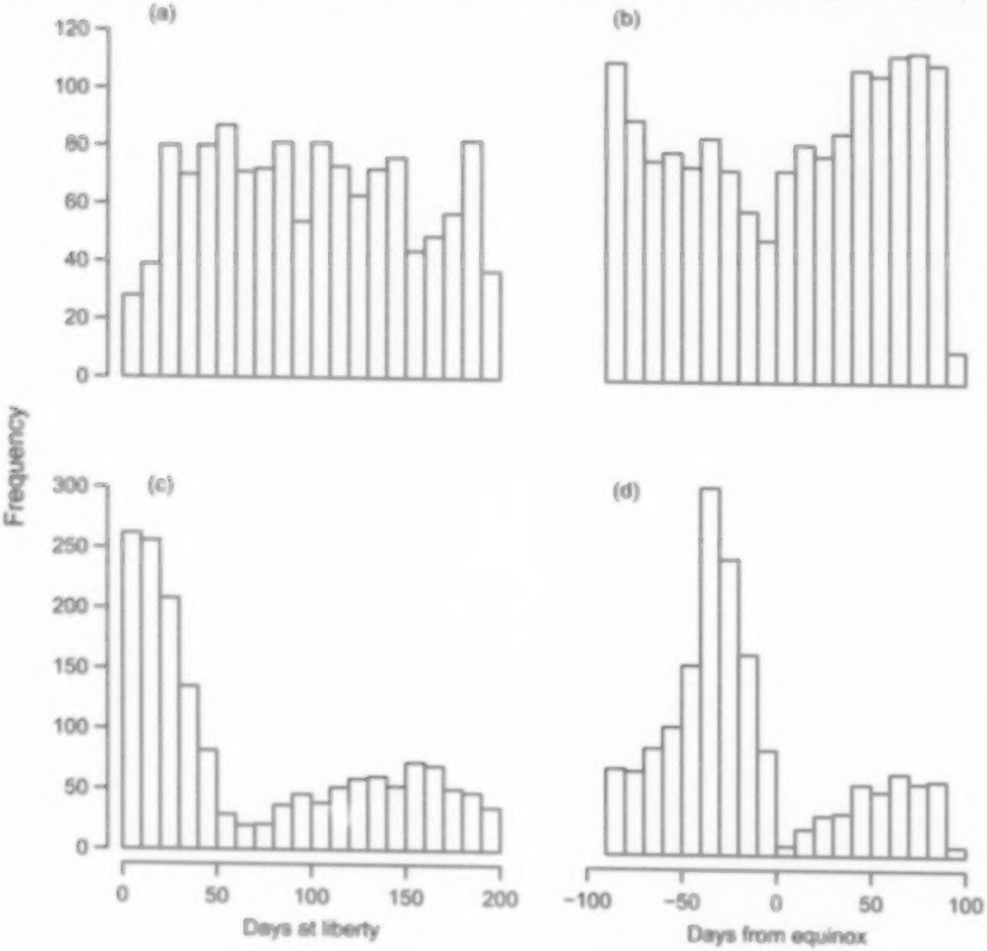

later period. The change point (i.e., the exact time when the behavior switches (τ)) is estimated by maximum likelihood. The change-point track is represented by 11 parameters: three movement parameters for each segment (u_1, v_1, D_1; and u_2, v_2, D_2), the change point (τ), and four error parameters (σ_x, σ_{y_e}, a_0, and b_0). The multisegment KF variant accommodates variation in behavior by estimating different values of the movement parameters in different arbitrary geographic areas. The third KF variant pertains to whether the tracks are treated as unique events or as samples from a population. A single track model assumes that each track is unique and has distinct parameters for each track. The multitrack KF model assumes that tracks are samples from a population and represents all tracks by a single (small) set of parameters.

The state–space model represents movement as a biased random walk, the Lagrangian analog of the advection diffusion model applied to tagged tuna by Sibert et al. (1999). The biased random walk model is also the basis of the model used by Humston et al. (2000) to simulate attraction of bluefin tuna to temperature fronts. The model parameters estimated by the KF can be applied in either an advection–diffusion model or in a biased random walk. We apply a biased random walk to simulate movements of individual tagged fish to project their movements beyond the tag shedding dates. The simulated release position was near 68°W by 41°N, near the actual release positions off Cape Cod in the northwest Atlantic. The movement parameters were those estimated from the 1999 and 2002 deployments by the two-region, multitrack model. The movements of populations of 100 tagged fish were simulated for 360 days, and their positions were reported after 30, 90, and 360 days at liberty.

All variants of the KF were implemented in AD Model Builder (Otter Research Ltd. 1994–1999). Model parameters were estimated by numerical minimization of the extended KF likelihood function either by a quasi-Newton function minimizer or by Markov chain Monte Carlo (MCMC) optimization (Geyer 1996; Gelman et al. 2004).

Results

Details of the deployment and reporting are presented in Table 1. The earliest reporting tags (X5325 and 2979; 25 December 1999) were the first PSAT reports from deployments on a marine vertebrate. Fish tagged in 1999 and 2000 (>200 kg) were substantially larger than those tagged in 2002 (<150 kg) because almost all fish in 2002 were tagged and released from a commercial purse seiner that primarily captured large medium fish during the 2002 season. The median number of days at liberty for the 1999, 2000, and 2002 deployments were 242, 352, and 118 days, respectively, reflecting differences in programmed reporting date. The number of days with position estimates were 142, 93, and 20, respectively. Approximately 64% of the days at liberty for 1999 tags had position estimates compared with 26% to 29% for the 2000 and 2002 tags. The temperature and depth reporting rates for the 2002 tags were both approximately 70%, about twice the position reporting rate.

The distribution of position estimates over the days at liberty was not uniform (Fig. 1). The rate of recovery of position estimates was lowest around the time of the equinoxes for both tag groups. All of the 1999 and 2000 tags were released within 2 weeks of 21 September, the height of the New England bluefin fishing season and the approximate date of the boreal autumnal equinox. The position recovery rate was low for these tags during the first month at liberty and relatively constant thereafter. Most of the 2002 releases were in July and August, well before the equinox, and the position recovery rate was high during the first month at liberty. The tags deployed in September and October 2002 were at liberty for relatively short periods and had low rates of position reporting.

Substantial gaps occur in the time series of position estimates. The time interval between successive geolocation estimates (Δt) ranges from 1 to 120 days, the maximum gap recorded in the 2002 deployments. The 1999 and 2002 deployments are similar, with 50% of the observations separated by gaps of 1 and 2 days (Fig. 2). The observations from the 2000 deployment are more dispersed, with 50% of the observations separated by gaps of 1–4 days and a large number of gaps of more than 4 days.

The change-point variant of the KF requires 11 parameters; therefore, only tracks with 20 or more data points were analyzed (Table 2). The median estimated longitude geolocation errors, σ_x, ranges from 0.35° for the 2000 deployments to 0.93° for the 2002 deployments. The median estimated latitude geolocation error, σ_{y_0}, ranges from 1.03° for the 1999 deployments to 2.11° for the 2002 deployments. The parameters of the equinox singularity latitude error correction are not well-determined by the data, especially for the 2002 tags. The timing parameter, b_0, is in some cases on its upper bound of 50 days. Consequently, extremely large values of σ_{y_0} are estimated for some of the 2002 tags.

The two-segment change-point model provides a significantly better description of the data at the 95% confidence level than the one-segment model for nearly all tracks, as determined by likelihood ratio tests (Table 3). Estimates of the directed movement parameters, u and v, are near zero for both segments of most tracks. Estimates of nondirected movement parameters, D, are highly variable. All of the reporting positions and most of estimated change-point positions for the 1999 and 2000 deployments occurred in the North Atlantic Subtropical Gyre (NAST) biogeochemical province (Longhurst 1998). The reporting positions and estimated change-point provisions for the 2002 deployments occurred closer in shore, usually within Northwest Atlantic Shelves (NWCS) province (Fig. 3). The distribution of the estimated change points for the 1999 deployment is very similar to the time to shedding recorded by the tags for the 2002 deployment (Fig. 4). The median days at liberty to the estimated 1999 change point is 122 compared with the 118 days for the median days to shedding for the 2002 deployments.

Fig. 2. Frequency distribution of time intervals between geolocation estimates (Δt) for the 1999, 2000, and 2002 deployments. The boxes indicate the interquartile range (i.e., the area encompassing the central 50% of the time intervals). The horizontal line within the box indicates the median. The range bars extend outside the boxes to the most extreme data point, which is no more than 1.5 times the interquartile range. The circles are individual outliers. The ordinate has been truncated at 10 days.

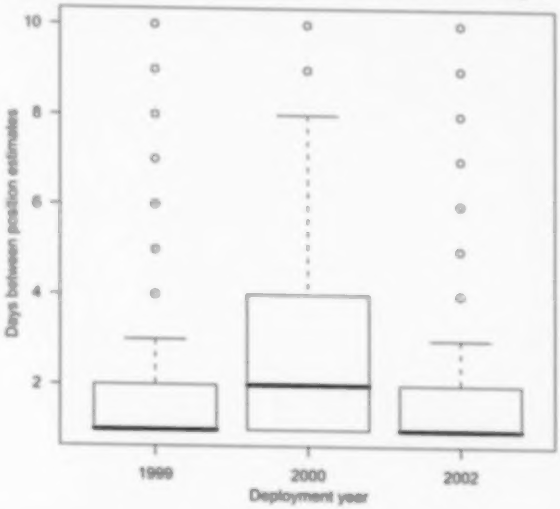

The data from the three deployments were analyzed by the multitrack Kalman with two regions separated by the approximate boundary between the NWCS and Gulf Steam (GFST) provinces. Tracks from the 1999 and 2000 deployments were truncated on the day closest to the estimated change point and the positions of the change points assumed to be "known" reporting positions (i.e., fixed endpoints) in the KF analysis (Table 4).

The geolocation errors estimated by the combined multitrack model were slightly higher than medians of the estimates from the single-track models (Table 2). Estimated values of the dispersive movement parameter (D) for the multitrack models were higher than the median estimates from single-track models, and the absolute values of directed movement parameters (u, v) were also higher than for the single-track models.

Table 2. Summary of parameter estimates for all tags using the change-point variant of the Kalman filter model.

Tag	u_1	v_1	D_1	u_2	v_2	D_2	σ_x	σ_{y_0}	a_0	b_0
2966*	7.79	1.00	535.6	0.78	–3.60	175.5	0.38	0.91	0.0427	20.26
X5312*	—	—	363.3	—	—	4.3	0.44	1.46	0.0055	11.69
3631*	19.75	–1.79	1997.6	6.22	5.93	317.7	0.37	1.11	0.0651	17.07
3652*	—	—	1061.4	—	—	163.2	0.45	1.07	0.0154	14.69
2974*	7.16	–0.62	680.4	3.71	0.48	89.0	0.54	0.89	0.0198	14.58
2975*	6.91	–3.41	542.9	0.32	1.81	115.5	0.44	0.92	0.0314	24.95
X5325*	—	—	1755.1	—	—	584.2	0.45	0.68	0.0202	37.39
2979*	—	—	1837.2	—	—	330.4	0.00	1.12	0.1534	–50.00
3656*	4.01	–1.69	870.4	5.05	–7.73	137.1	0.22	1.35	0.0563	13.85
5328*	23.11	–2.78	1656.9	3.33	–1.59	266.9	0.29	1.13	0.0369	13.02
2982*	3.84	–4.51	3117.8	5.29	0.08	288.6	0.50	0.84	0.0131	12.20
3704*	—	—	665.5	—	—	130.0	0.36	1.00	0.0277	16.25
3648*	—	—	540.9	—	—	155.4	0.29	1.37	0.0000	–0.04
3665*	—	—	457.4	—	—	158.5	0.35	2.62	0.0003	–1.07
3667*	—	—	2777.1	—	—	138.0	0.49	2.09	0.0001	–0.76
5374*	—	—	1983.4	—	—	301.9	0.00	1.56	0.9614	0.90
5303*	—	—	67.1	—	—	5208.7	1.40	1.65	0.0000	–1.02
5326*	—	—	11.3	—	—	2216.1	0.90	2.49	0.2163	–3.85
5376	—	—	1174.5	—	—	212.1	0.40	2.23	0.5548	23.29
A195*	—	—	2.1	—	—	254.2	0.69	1.11	0.1060	–10.68
5023*	—	—	2786.3	—	—	132.0	0.22	1.31	0.2151	–37.32
5024*	—	—	8.7	—	—	780.3	1.07	1.72	0.4363	20.27
A199	—	—	641.7	—	—	123.0	0.92	2.43	0.1304	50.00
5025*	—	—	151.1	—	—	6.6	0.95	2.10	0.3086	43.40
A202*	—	—	946.5	—	—	9.0	0.00	0.26	0.0047	–8.59
5367	—	—	516.9	—	—	1397.1	0.98	2.86	1.5738	50.00
5027*	—	—	81.8	—	—	1274.5	1.03	2.42	1.7289	–42.86
5301*	—	—	297.9	—	—	4.6	0.84	2.39	0.5868	15.86
5267*	—	—	513.1	—	—	3.5	0.53	2.51	1.5494	50.00
5268*	—	—	3.0	—	—	983.6	0.85	1.56	0.3146	2.52
5269*	—	—	1233.3	—	—	106.6	0.53	1.22	0.0000	28.84
5270	—	—	323.3	—	—	94.4	0.93	3.36	2.2457	50.00
5271*	—	—	4263.1	—	—	318.3	1.42	2.70	0.5467	8.43
5272*	—	—	204.4	—	—	2231.7	0.89	0.71	0.0663	–29.81
5273*	—	—	159.3	—	—	1032.1	1.12	2.05	0.2941	22.71
5274	—	—	599.3	—	—	227.1	0.78	0.91	0.1472	–5.79
5275*	—	—	291.0	—	—	1788.0	1.23	2.26	0.2801	28.50
5276*	—	—	50.5	—	—	2329.1	1.01	15.00	32.1238	–50.00
5281	—	—	47.6	—	—	418.4	1.11	2.13	0.5864	50.00
5282	—	—	24.0	—	—	316.5	1.40	12.52	23.7936	49.99
5283*	—	—	26.6	—	—	1579.1	0.48	1.35	0.0711	8.09
5310*	—	—	5.1	—	—	366.7	1.41	1.08	0.2505	–25.32
5320*	—	—	1658.3	—	—	122.8	1.09	2.58	0.9150	50.00
Median 1999	3.92	–0.31	965.9	0.55	0.00	169.4	0.41	1.03	0.0296	14.64
Median 2000	0.00	0.00	540.9	0.00	0.00	155.4	0.35	2.09	0.0001	–0.76
Median 2002	0.00	0.00	247.7	0.00	0.00	317.4	0.93	2.11	0.0312	12.14

Note: An asterisk (*) after a tag number indicates that division of the track into two segments is statistically significant ($P < 0.05$). A dash (—) indicates parameters were not significantly different from zero. (Estimates of the change points are listed in Table 3.)

Larger data sets were constructed by combining tracks from the three deployments. The significance of the difference between the 1999 and 2002 tracks was evaluated by a likelihood ratio test comparing the combined data with the aggregated results for the 1999 and 2002 tracks. The fit to the combined data produced a log likelihood of –8946.57 with 10 parameters, and the aggregate model had a higher likelihood of –8501.06 (2825.38 + 5675.68) with 20 parameters (Table 4). The resulting χ^2 statistic was 891.02 with 10 degrees of freedom, significant at $P < 0.001$. The aggregate model consisting of two 10-parameter models was significantly more consistent with the combined 1999–2002 data than a single 10-parameter model. That is, the movements recorded by the 1999 and 2002 deployments were significantly different.

This result is not surprising, since the parameters estimated from these two data sets differ in almost all respects. The geolocation errors are higher for the 2002 deployments than for the 1999 deployments. The estimates of both dispersive and directed movement parameters are higher for the 1999 deployment. The directions of movement, particularly in the offshore area, also differ. The movement of tags from the 1999 deployment show a strong easterly orientation (H_2 = 92°) compared with a northwest orientation for the 2002 deployment (H_2 = 319°).

The positions of 100 simulated tagged fish after different periods at liberty (Fig. 5) using the movement parameters estimated from the 1999 and 2002 deployments are shown in Table 4. These two sets of movement parameters produce very different tag distributions over time. The distribution predicted from the 1999 estimated movement pattern covers most of the North Atlantic Ocean, with nearly all tags crossing the 45°W stock separation line in less than 12 months. In contrast, the distribution predicted from the estimated 2002 movement pattern is largely confined to the western North Atlantic, with no tags crossing 45°W longitude.

Discussion

Estimation of latitude from light data is nearly impossible during the time period surrounding the equinox because day length is nearly the same at all latitudes. The equinox latitude error model in the KF compensates for this problem by amplifying the error in latitude estimation during equinox periods. The reporting rate of geolocation estimates from PSATs is lowest around the equinoxes and generally less than 50%. When field operations require release of tagged fish at times of year when PSAT data yield few position estimates, the resulting data will be a biased sample of the movement pattern. For example, tags released within 2 weeks of the equinox will not sample the behavior of the animal during its first months at liberty. The 2002 release strategy effectively improved reporting during the first part of the track by releasing more tags earlier in the year during periods not affected by the equinox. Use of multisegment movement models can alleviate this problem by estimating separate parameters for the first and and last part of the track. The multitrack model may further improve coverage of geographically variable behavior by distributing observations more evenly among regions.

The inherent limits of light-based algorithms at the equinox do not entirely account for low position reporting rates in the 2000 and 2002 data. Transmission to Argos satellites is constrained to approximately 10 transmission windows per day (P.W. Howey, Microwave Telemetry Inc., Columbia, Maryland, USA, personal communication). The 1999 tags were transmitting only light and temperature data and were able to transmit a complete daily record in one transmission. The 2000 and 2002 tags were also transmitting depth data and therefore required two transmissions for a complete daily record. These difference could explain the roughly twofold change in position reporting rate. There are multiday gaps in all tracks at times of year other than around the equinox. The loss of 1 day of transmission from the 1999 tags could cause a 10-day gap in the track, and loss of 1 day of transmission from the 2000 and 2002 tags would cause a roughly 5-day gap. Whether these gaps are due to weather or to localized interference with transmission from the tag to the

Table 3. Summary of Kalman filter change-point estimates of all tags.

Tag	τ	Date	*P*	Longitude (°E)	Latitude (°N)
2966	153	24 Feb. 2000	0.0010	318.43	42.42
X5312	252	2 June 2000	0.0001	300.55	33.71
3631	49	13 Nov. 1999	<0.0001	311.93	39.86
3652	136	10 Feb. 2000	<0.0001	315.91	36.89
2974	153	4 Mar. 2000	0.0001	315.35	40.75
2975	203	22 Apr. 2000	<0.0001	320.82	30.29
X5325	33	10 Nov. 1999	0.0315	285.13	34.31
2979	71	18 Dec. 1999	0.0124	302.25	39.76
3656	137	22 Feb. 2000	<0.0001	302.49	33.58
5328	42	19 Nov. 1999	<0.0001	308.80	38.35
2982	86	2 Jan. 2000	<0.0001	294.63	36.05
3704	206	1 May 2000	<0.0001	308.09	33.21
3648	209	11 Apr. 2001	0.0002	307.36	33.63
3665	204	6 Apr. 2001	0.0164	311.57	33.44
3667	90	13 Dec. 2000	<0.0001	311.31	39.70
5374	19	27 Aug. 2002	0.0006	290.29	40.60
5303	132	27 Dec. 2002	<0.0001	289.02	43.15
5326	84	8 Apr. 2003	0.0002	285.37	34.39
5376	20	28 Aug. 2002	0.0801	293.53	37.78
A195	40	10 Sept. 2002	0.0184	290.78	41.97
5023	50	27 Sept. 2002	<0.0001	290.08	37.61
5024	30	16 Aug. 2002	0.0007	290.95	41.99
A199	11	12 Aug. 2002	0.2444	290.17	40.77
5025	156	20 Dec. 2002	0.0092	285.65	36.60
A202	41	27 Aug. 2002	<0.0001	290.18	40.29
5367	19	27 Aug. 2002	0.1706	293.92	43.67
5027	138	2 Dec. 2002	0.0012	288.08	40.13
5301	162	17 Jan. 2003	0.0189	297.77	43.31
5267	112	21 Nov. 2002	0.0074	283.01	34.29
5268	32	9 Sept. 2002	0.0001	290.82	41.86
5269	39	9 Sept. 2002	0.0264	290.46	36.82
5270	107	16 Nov. 2002	0.1162	284.83	37.17
5271	14	15 Aug. 2002	0.0052	290.40	39.74
5272	169	17 Jan. 2003	0.0055	297.27	39.89
5273	206	23 Feb. 2003	0.0396	283.34	33.86
5274	106	15 Nov. 2002	0.1722	294.69	45.31
5275	199	16 Feb. 2003	0.0082	283.20	39.59
5276	162	10 Jan. 2003	<0.0001	290.86	39.66
5281	115	24 Nov. 2002	0.0797	291.80	40.94
5282	125	4 Dec. 2002	0.1632	292.09	42.43
5283	29	30 Aug. 2002	0.0062	288.20	41.37
5310	13	21 Aug. 2002	0.0475	291.03	41.90
5320	9	17 Aug. 2002	0.0119	290.05	38.40

Note: τ is the estimated day at liberty estimated for the change point; Date is the estimated date of the change; *P* is the significance level of the improvement in fit of the two-segment model over the one-segment model; and Longitude and Latitude are the estimated position of the change.

Fig. 3. Reporting and estimated change-point locations for pop-up satellite archival tags (PSATs) released in 1999 and 2000 (*a*) and in 2002 (*b*). Reporting points are given by triangles (△). Change points for $P \leq 0.05$ are plotted with open squares (□); change points for $P > 0.05$ are plotted with open circles (○). The inverted triangles (▽) indicate release position. The heavy black line indicates the boundary between the regions used in the two-segment multitrack analyses. The gray lines indicate the boundaries of the Longhurst (1998) biogeographic provinces in the Northwest Atlantic. NWCS, Northwest Atlantic Shelves; NADR, North Atlantic Drift; GFST, Gulf Steam; NAST, North Atlantic Subtropical Gyre.

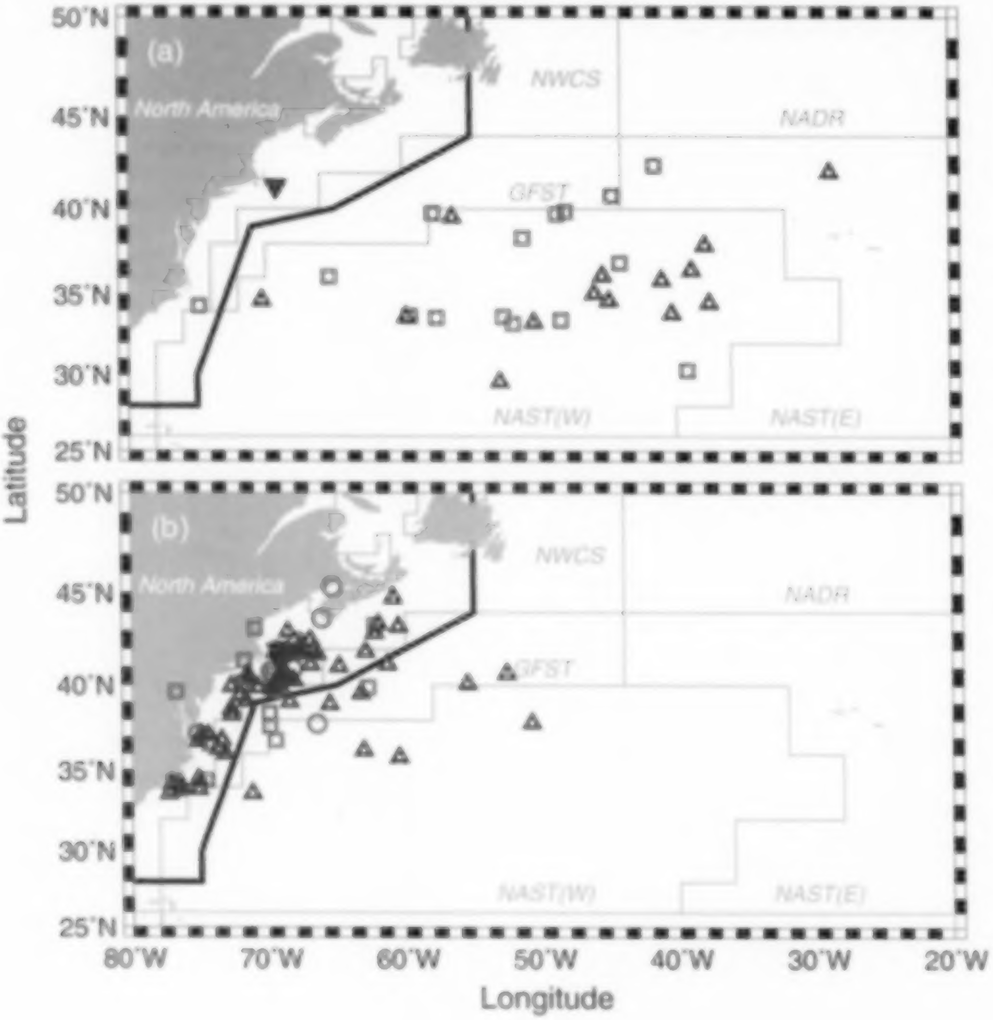

satellite is unknown. However, examination of available weather and wave height records during the deployments cannot simply account for the observed transmission gaps.

Wilson et al. (2005) found no evidence of movement east of 45°W longitude based on the positions reported for the 2002 deployment through 1 June 2003. Simulations based on the same data are consistent with this conclusion. The most important difference between the two deployments is between the estimated movement direction in the offshore region. The estimated heading for the 2002 deployments is 319°, a heading that would return a fish to coastal waters if it had moved into the offshore area. In contrast, the estimated heading in the offshore area for the 1999 deployment is 92°, a heading that would start a fish on a transatlantic migration.

Changes in oceanographic conditions such as thermocline depth and sea surface temperature fronts occurred over the tagging periods (M.E. Lutcavage, unpublished data), and shifts in availability of surface schools were reflected in declines in catch per unit of effort (CPUE) for harpoon and purse seine fisheries. PSAT data also recorded shifts in modal depth preferences for bluefin tuna, with fish in 2002 remaining somewhat deeper than fish tagged in 1999–2001 (Wilson et al. 2005).

The result of the two-segment multitrack analysis of the 1999–2001 data is consistent with the hypothesis that bluefin

Table 4. Results of multitrack Kalman filter analyses for the 1999, 2000, and 2002 deployments.

(*a*) The negative log-likelihood value, number of parameters, and estimates of geolocation errors.

Year	Tracks	$-\log L$	n	σ_x	σ_y	σ_{y_0}	a_0	b_0
1999	12	2825.38	10	0.38	1.20	1.26	0.00585	14.07
2000	3	787.836	10	0.43	2.48	2.51	0.00047	−0.60
2002	28	5675.68	10	1.07	2.36	2.59	0.54144	20.25
1999+2002	40	8946.57	10	0.85	1.51	1.73	0.04658	14.25
Aggregate	40	8501.06	20					

(*b*) Estimates of movement parameters for the inshore and offshore regions.

		Inshore						Offshore					
Year	Tracks	T_1	u_1	v_1	D_1	S_1	H_1	T_2	u_2	v_2	D_2	S_2	H_2
1999	12	149	2.86	−14.00	1221.3	14.29	168.4	588	7.29	−0.28	812.6	7.30	92.2
2000	3	47	5.61	3.00	1984.3	6.36	61.9	119	3.70	−1.46	317.8	3.98	111.5
2002	28	1139	1.04	−1.33	334.8	1.69	142.1	228	−1.20	1.39	685.8	1.83	319.2
1999+2002	40	1280	1.21	−2.11	486.0	2.43	150.2	913	3.15	0.11	632.5	3.16	88.0

Note: Tracks refers to the number of tracks included in the model. Aggregate is the aggregated model consisting of the sum of the 1999 and 2002 models.

Fig. 4. Days at liberty prior to tag shedding. Data for 1999–2000 illustrates days prior to the estimated change point for the 1999 and 2000 deployments; data for 2002 illustrates days prior to reporting date for 2002 deployments. The boxes indicate the interquartile range (i.e., the area encompassing the central 50% of the time intervals). The horizontal line within the box indicates the median. The range bars extend outside the boxes to the most extreme data point, which is no more than 1.5 times the interquartile range.

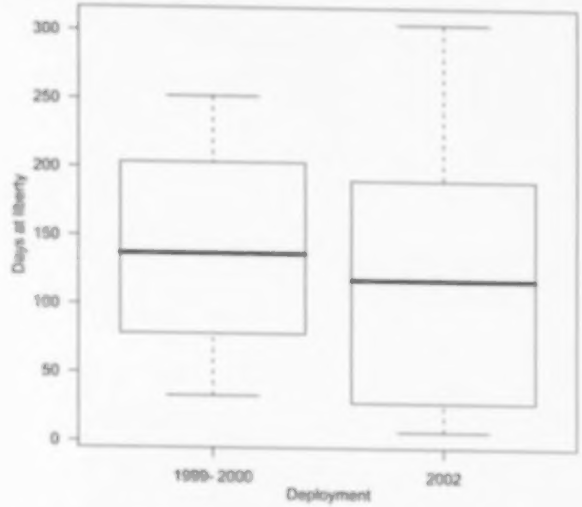

tuna change their behavior when they move away from the coast and the NWCS province to begin a transatlantic migration. After leaving the shelf, bluefin feeding dependencies shift from demersal fishes (i.e., Atlantic herring (*Clupea herrengus*), Atlantic mackerel (*Scomber scombrus*), and American sand lance (*Ammodytes americanus*)) to squid, octopods, and mesopelagic fishes (Matthews et al. 1977). Longline catches (Wilson 1965; Shingu et al. 1975) and also PSAT data show that depth associations shift, especially near the Gulf Stream boundary (Wilson et al. 2005).

Differences in apparent behavior recorded by the tags deployed in different years suggest significant interannual variability in the movement and distribution of Atlantic bluefin tuna. Mather (1980) showed that transatlantic migration of large and small bluefin tuna varied strongly from year to year and hypothesized that it might be linked to oceanographic conditions. The fish tagged in 1999 and 2000 were larger than those tagged in 2002, and there were environmental differences between the two periods as well. In 1996, the North Atlantic Oscillation (NAO) index exhibited the largest single-year drop in the 20th century, attaining a negative value not seen since the 1960s, and hydrographic conditions in the mid-Atlantic Bight did not return to their pre-1996 state until the end of 1999 (Smith et al. 2001; Greene and Pershing 2003). These changes had a profound impact on water temperatures (Slonosky and Yiou 2002) and zooplankton communities (Smith et al. 2001) and almost certainly altered the forage base for bluefin tuna. For example, the chlorophyll content in the NWCS during the summer months of 1999 was 25% lower than during the summer months of 2002 (Fig. 6). The 1999 deployment occurred during a pe-

Fig. 5. Simulated positions of 100 tagged fish after 30 days (•), 90 days (△), and 1 year (○) at liberty. Distribution was computed using *u*, *v*, and *D* estimated from the 1999 (*a*) and 2002 (*b*) deployments. The broken line at 45°W longitude is the line used to separate bluefin tuna (*Thunnus thynnus*) stock management units. The inverted triangle (▽) indicates release position.

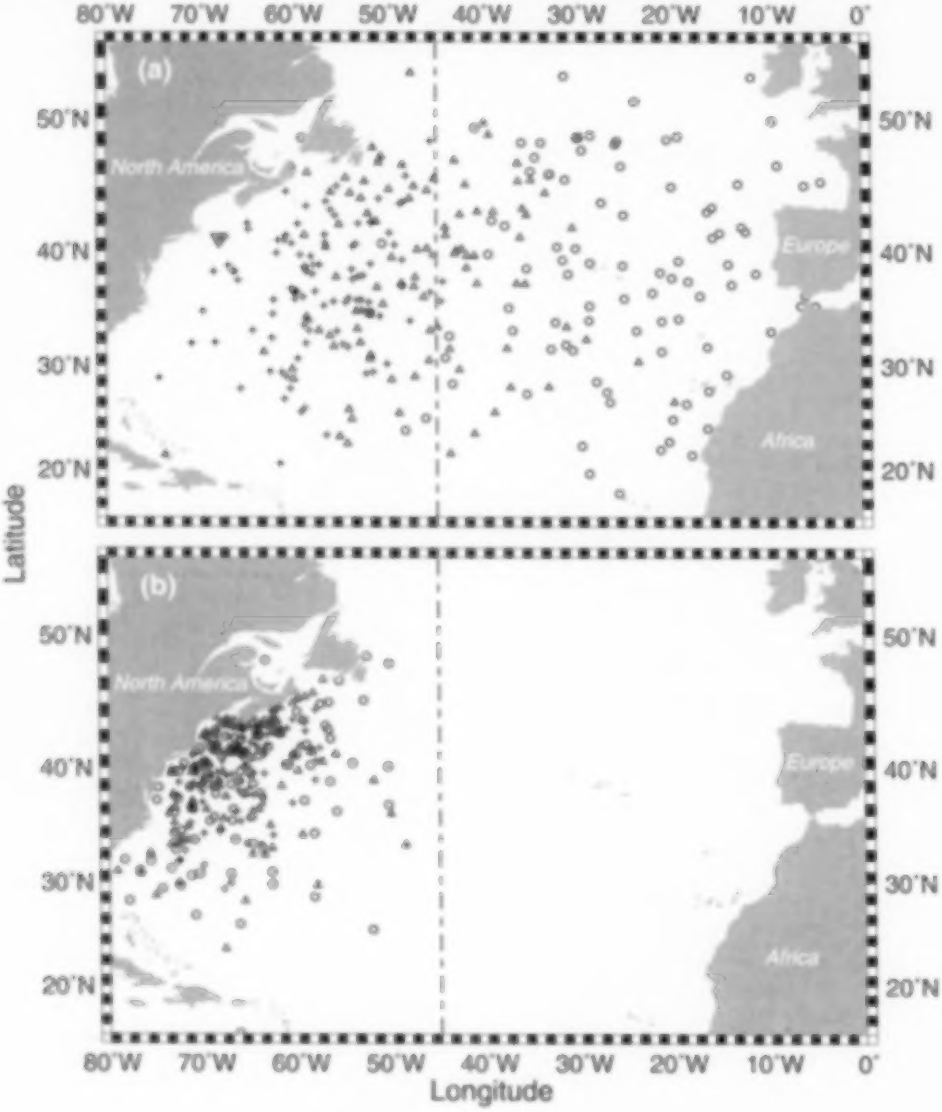

riod of rapid transition from a negative to a positive phase of the NAO just prior to the end of the recovery period from this major oceanographic change (Fig. 7). Changes in thermal structure and chlorophyll content are not equivalent to changes in tuna forage. Some lapse of time is required for a forage base for top predators to develop from primary productivity (Vinogradov 1981; Jaquet and Whitehead 1996; Gascuel et al. 2005). Lehodey et al. (1998) modeled the forage base for Pacific skipjack tuna (*Katsuwonus pelamis*) using a time lag of 90 days between primary production and forage production. Low productivity from May through July could translate into low forage abundance in September, when the fish tagged in 1999 exited the NWCS province. Our results are consistent with Mather's hypothesis that transatlantic migration is size-dependent and related to environmental conditions in the western Atlantic.

Tag shedding is an chronic problem in the use of pop-up tags (Holland and Braun 2003). The tags used in 2002 were equipped to detect shedding, but that technology was not available in the first generation PSATs used for the 1999 and 2000 deployments. We address the tag shedding problem in data from these tags by attempting to estimate the shedding date and position using the change-point variant of the KF model. The change-point model was able to detect substan-

Fig. 6. Average monthly chlorophyll content of the water in the Northwest Atlantic Shelves province from SeaWiFS data. The horizontal lines indicate the average chlorophyll content in the province for the months of May, June, July, and August. Inverted triangles indicate deployment dates.

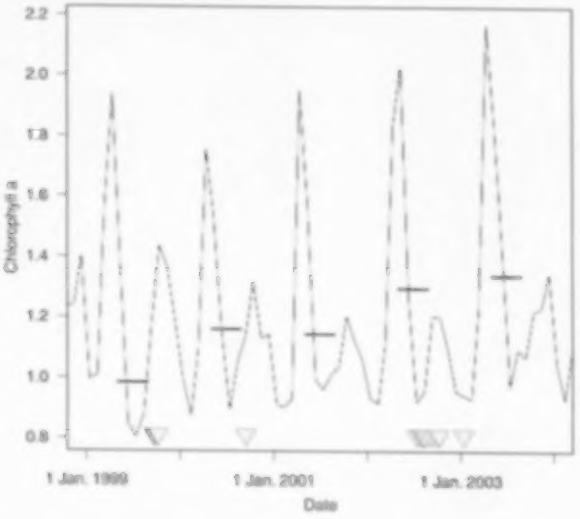

Fig. 7. Twelve-month leading moving average of the North Atlantic Oscillation for 1999 through 2003. Inverted triangles indicate deployment dates. Data are from the National Oceanic and Atmospheric Administration (NOAA) Climate Prediction Center website (http://www.cpc.ncep.noaa.gov/data/teledoc/nao.shtml).

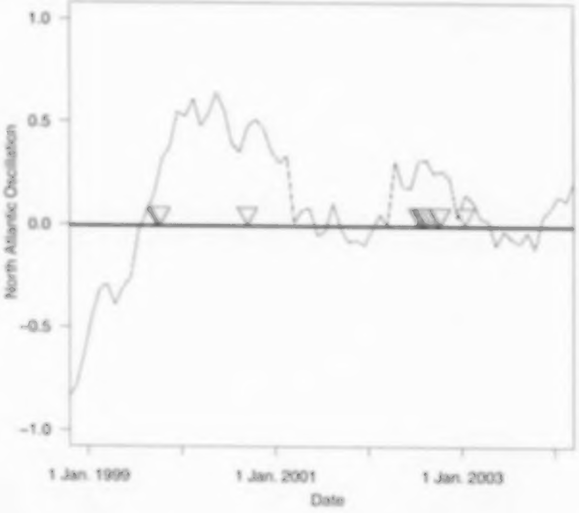

tial differences in apparent movement in two-segment tracks, and the estimated times to shedding are comparable with those recorded by the tags used in the 2002 deployment. Thus we accept the conclusion that the results of the combined 1999 multitrack analysis represent the movement of the bluefin population during the last quarter of 1999. The results of treating the tracks from the two deployment periods as samples of a larger population of tracks using the multitrack model strongly indicate interannual differences in movement.

The joint influence of environment and age on the distribution of bluefin tuna is well known. Mather (1980) indicated that transatlantic mixing could be attributed to both environmental variability and size, and Tiews (1963) attributed eastward movement to the availability of food. Since the fish taggged in 2002 were considerably smaller than those taged in 1999–2000, the results presented here cannot discrimate between envrionment and age. Indeed, it is probably unrealistic to search for a single cause. Regardless of the causes of the interannual variability, the differences have profound fishery management implications, because in some years, most of the population may cross the current stock separation line at 45°W longitude. Other spatially fixed management frameworks, such as those recently proposed by International Commission for the Conservation of Atlantic Tunas (ICCAT 2002), will also be impacted by interannual variability, as noted by Powers and Porch (2004). The possibility of environmental controls mediating the distribution of the stock should be seriously considered by fishery managers when geographically assigning catch quotas or in defining alternative fishery management strategies.

Acknowledgements

The work described in this paper was partly sponsored by the University of Hawai'i Pelagic Fisheries Research Program under cooperative agreement No. NA17RJ1230 from the National Oceanic and Atmospheric Administration, a grant from the National Marine Fisheries Service (grant No. NA15FM2840) to Molly Lutcavage, and the Scaling from Individual to Population (SLIP) research school under the Danish Network for Fisheries and Aquaculture Research (www.fishnet.dk) financed by the Danish Ministry for Food, Agriculture and Fisheries and the Danish Agricultural and Veterinary Research Council. We thank Pierre Kleiber and Alain Fonteneau for assistance with mapping the Longhurst provinces, Paul Howey of Microwave Telemetry Inc. for taking the time to clearly explain the fine points of transmitting tag data via the Argos system, and Russell Moffitt for aggregating the chlorophyll data into the Longhurst provinces. We also thank the SeaWiFS Project (Code 970.2) and the Goddard Earth Sciences Data and Information Services Center – Distributed Active Archive Center (Code 902) at the Goddard Space Flight Center, Greenbelt, Maryland, for the production and distribution of these data, respectively, activities which are sponsored by NASA's Earth Science Enterprise.

References

Arnold, G., and Dewar, H. 2001. Electronic tags in marine fisheries research: a 30-year perspective. *In* Electronic tagging and tracking in marine fisheries reviews: methods and technologies in fish biology and fisheries. *Edited by* J.R. Sibert and J.L. Nielsen. Kluwer Academic Press, Dordrecht. pp. 7–64.

Block, B.A., Dewar, H., Blackwell, S.B., Williams, T.D., Prince, E.E., Farwell, C.J., Boustany, A., Teo, S.L., Seitz, A., Walli, A., and Fudge, D. 2001. Migratory movements, depth preferences, and thermal biology of Atlantic bluefin tuna. Science (Washington, D.C.), **293**: 1310–1314.

Block, B.A., Teo, S.L., Walli, A., Boustany, A., Stokesbury, M., Farwell, C.J., Weng, K., Dewar, H., and Williams, T. 2005. Electronic tagging and population structure of Atlantic bluefin tuna. Nature (London), **334**: 1121–1127.

Gascuel, D., Bozec, Y., Chassot, E., Colomb, A., and Laurans, M. 2005. The trophic spectrum: theory and application as an ecosystem indicator. ICES J. Mar. Sci. **62**: 443–452.

Gelman, A., Carlin, J.B., Stern, H.S., and Rubin, D.B. 2004. Bayesian data analysis. Chapman and Hall Inc., New York.

Geyer, C.J. 1996. Estimation and optimization of functions. *In* Markov chain Monte Carlo in practice. *Edited by* W.R. Gilks, S. Richardson, and D.J. Spiegelhalter. Chapman and Hall Inc., New York, London. pp. 241–258.

Greene, C.H., and Pershing, A.J. 2003. The flip-side of the North Atlantic Oscillation and modal shifts in slope-water circulation patterns. Limnol. Oceanogr. **48**: 319–322.

Hill, R.D., and Braun, M.J. 2001. Geolocation by light-level. The next step: latitude. *In* Electronic tagging and tracking in marine fisheries reviews: methods and technologies in fish biology and fisheries. *Edited by* J. Sibert and J. Nielsen. Kluwer Academic Press, Dordrecht. pp. 443–456.

Holland, K.N., and Braun, M.J. 2003. Proceedings of "Tying One On" — A Workshop on Tag Attachment Techniques for Large Marine Animals, 4–5 December 2002, Honolulu [online]. School of Ocean and Earth Science and Technology (SOEST) Publ. No. 03-02. Joint Institute for Marine & Atmospheric Research Contribution (JIMAR) 03-349. Available from http://www.soest.hawaii.edu/PFRP/soest_jimar_rpts/holland_braun.pdf [accessed 30 August 2006].

Humston, R., Ault, J., Lutcavage, M., and Olson, D. 2000. Schooling and migration of large pelagic fishes relative to environmental cues. Fish. Oceanogr. **9**: 136–146.

ICCAT (International Commission for the Conservation of Atlantic Tunas). 2002. ICCAT Workshop on Bluefin Mixing. ICCAT Coll. Vol. Sci. Pap. **54**: 261–352.

Jaquet, N., and Whitehead, H. 1996. Scale-dependent correlation of sperm whale distribution with environmental features and productivity in the South Pacific. Mar. Ecol. Prog. Ser. **135**: 1–9.

Lehodey, P., Andre, J., Bertignac, M., Hampton, J., Stoens, A., Menkes, C., Memery, L., and Grima, N. 1998. Predicting skipjack tuna forage distributions in the equatorial Pacific using a coupled dynamical biogeochemical model. Fish. Oceanogr. **7**: 317–325.

Longhurst, A.R. 1998. Ecological geography of the sea. Academic Press, London, UK.

Lutcavage, M., Brill, R., Skomal, G., Chase, B., and Howey, P. 1999. Results of pop-up satellite tagging of spawning size class fish in the Gulf of Maine: do North Atlantic bluefin tuna spawn in the mid-Atlantic? Can. J. Fish. Aquat. Sci. **56**: 173–177.

Lutcavage, M., Brill, R., Porter, J., Skomal, G., Chase, B., and Howey, P. 2000. Presliminary results from the joint US–Canada pop-up satellite tagging of giant bluefin tuna in the Gulf of Maine and Canadian Atlantic region, 1998–99. Int. Comm. Conserv. Atlantic Tunas Coll. Vol. Sci. **LI**: 847–854.

Lutcavage, M., Brill, R., Porter, J., Howey, P., Murray, E., Mendillo, A., Chaprales, W., Genovese, M., and Rollins, T. 2001. Summary of pop-up satellite tagging of giant bluefin tuna in the joint US–Canadian program, Gulf of Maine and Canadian Atlantic. Int. Comm. Conserv. Atlantic Tunas Coll. Vol. Sci. **52**: 759–770.

Mather, F.J. 1980. A preliminary note on migratory tendencies and distributional pattens of Atlantic bluefin tuna based on recently acquired and cumulative tagging results. ICCAT Coll. Vol. Sci. Pap. **IX**: 478–491 (SCRS/79/76).

Mather, F.J., Mason, J.M., and Jones, A.C. 1995. Historical document: life history and fisheries of Atlantic bluefin tuna. NOAA Tech. Mem. NMFS-SEFSC-370.

Matthews, F.D., Damaker, D.M., Knapp, L.W., and Collette, B.B. 1977. Food of western North Atlantic tunas (*Thunnus*) and lancet fishes (*Alepisaurus*). NOAA Tech. Rep. NMFS SSRF-706.

National Research Council (NRC). 1994. An assessment of Atlantic bluefin tuna. National Academy Press, Washington.

Nielsen, A. 2004. Estimating fish movement. Ph.D. thesis, The Royal Veterinary and Agricultural University, Denmark. ISBN: 87-7611-065-6.

Otter Research, Ltd. 1994–1999. AD Model Builder documentation [online]. Otter Research Ltd., Sidney, British Columbia. Available from http://otter-rsch.com/admodel.htm [accessed 29 August 2006; updated September 2004].

Powers, J.E., and Porch, C.E. 2004. Approaches to developing management procedures which incorporate mixing. Col. Vol. Sci. Pap. ICCAT, **56**: 1144–1152.

Richards, W.J. 1976. Spawning of bluefin tuna (*Thunnus thynnus*) in the Atlantic Ocean and adjacent seas. ICCAT Coll. Vol. Sci. Pap. Madrid, **5**: 267–278.

Shingu, C., Hisada, K., Kume, S., and Honma, M. 1975. Biological information on Atlantic blueifn tuna caught by longline fishery and some views on the management of the resources. ICCAT Coll. Vol. Sci. Pap. **4**: 145–160.

Sibert, J.R., and Fournier, D.A. 2001. Possible models for combining tracking data with conventional tagging data. *In* Electronic tagging and tracking in marine fisheries reviews: methods and technologies in fish biology and fisheries. *Edited by* J. Sibert and J. Nielsen. Kluwer Academic Press, Dordrecht. pp. 443–456.

Sibert, J.R., Hampton, J., Fournier, D.A., and Bills, P.J. 1999. An advection–diffusion–reaction model for the estimation of fish movement parameters from tagging data, with application to skipjack tuna (*Katsuwonus pelamis*). Can. J. Fish. Aquat. Sci. **56**: 925–938.

Sibert, J., Musyl, M., and Brill, R.W. 2003. Horizontal movements of bigeye tuna (*Thunnus obesus*) near Hawaii determined by Kalman filter analysis of archival tagging data. Fish. Oceanogr. **12**: 141–152.

Sissenwine, M.P., Mace, P.M., Powers, J.E., and Scott, G.P. 1998. A commentary on western Atlantic bluefin tuna assessments. Trans. Am. Fish. Soc. **127**: 838–855.

Slonosky, V., and Yiou, P. 2002. Does the NAO index represent zonal flow? The influence of the NAO on North Atlantic surface temperature. Climate Dynamics, **19**: 17–30.

Smith, P.C., Houghton, R.W., Fairbanks, R.G., and Mountain, D.G. 2001. Interannual variability of boundary fluxes and water mass properties in the Gulf of Maine and on Georges Bank: 1993–1997. Deep-Sea Res. II, **48**: 37–70.

Tiews, K. 1963. Synopsis of bioloigcal data on bluefine tuna *Thunnus thynnus* (Linneaus) 1758 (Atlantic and Mediterranean). Food and Agricultural Organization (FAO), Rome. FAO Fisheries Biology Synopsis, **58**: 422–481.

Vinogradov, M.E. 1981. Ecosystems of equatorial upwellings. *In* Analysis of marine ecosystems. *Edited by* A.R. Longhust. Academic Press, New York. pp. 69–93.

Wilson, P.C. 1965. Review of the development of Atlantic coast tuna fisheries. Comm. Fish. Rev. **27**: 1–10.

Wilson, S.G., Lutcavage, M.E., Brill, R.W., Genovese, M.P., Cooper, A.B., and Everly, A.W. 2005. Movements of bluefin tuna (*Thunnus thynnus*) in the northwestern Atlantic Ocean recorded by pop-up satellite archival tags. Mar. Biol. **146**: 409–423.

Effect of lipid extraction on the interpretation of fish community trophic relationships determined by stable carbon and nitrogen isotopes

Brent A. Murry, John M. Farrell, Mark A. Teece, and Peter M. Smyntek

Abstract: Stable isotopes of carbon (C) and nitrogen (N) are commonly used to evaluate trophic relationships and food web structure; however, the decision to extract lipids or not may influence the interpretation of results. Lipid extraction is not a universal practice, thus pooling or comparing results across studies may not always be appropriate. Additionally, common lipid extraction techniques remove not only lipids, but also N-containing compounds that may alter the $\delta^{15}N$ value of a sample. We examined differences in the interpretation of fish community trophic structure derived from $\delta^{13}C$ and $\delta^{15}N$ stable isotope data based on lipid-extracted and nonextracted samples from nine freshwater fish species. Lipid extraction significantly increased $\delta^{13}C$ and $\delta^{15}N$, causing a positive shift in overall food web placement. The magnitude of isotopic change did not, however, differ among species, such that the overall interpretation of the fish community structure was not altered. The consistent increase in both C and N isotopes did, however, significantly alter the placement of the food web in coordinate space relative to nonextracted webs. Cross-study comparisons need to consider these procedural inconsistencies when drawing conclusions from multiple studies.

Résumé : Les isotopes stables de carbone (C) et d'azote (N) servent couramment à évaluer les relations trophiques et la structure des réseaux alimentaires; cependant, la décision d'extraire ou non les lipides peut influencer l'interprétation des résultats. Comme l'extraction des lipides n'est pas une procédure universelle, il peut ne pas être approprié de mettre en commun ou de comparer les résultats provenant d'études différentes. De plus, les techniques courantes d'extraction des lipides retirent non seulement les lipides, mais aussi des composés N, ce qui peut modifier la valeur de $\delta^{15}N$ d'un échantillon. Nous avons examiné les différences des interprétations de la structure trophique d'une communauté de poissons obtenues à partir de données de $\delta^{13}C$ et de $\delta^{15}N$ d'isotopes stables d'échantillons avec et sans extraction de lipides chez neuf espèces de poissons d'eau douce. L'extraction des lipides augmente significativement les valeurs de $\delta^{13}C$ et de $\delta^{15}N$, ce qui cause un glissement positif du positionnement dans le réseau alimentaire global. L'importance du changement isotopique ne varie pas, cependant, en fonction des espèces, si bien que l'interprétation globale de la communauté de poissons n'est pas modifiée. L'accroissement uniforme à la fois des isotopes de C et de N change la position du réseau alimentaire dans l'espace des coordonnées par comparaison aux réseaux basés sur des échantillons sans extraction. Les comparaisons de plusieurs travaux doivent donc tenir compte de ces divergences dues à la procédure avant de tirer des conclusions d'études multiples.

[Traduit par la Rédaction]

Introduction

The naturally occurring stable isotopes of carbon (^{13}C) and nitrogen (^{15}N) are commonly used in population and community ecology to elucidate trophic relationships, such as food web structure (Fry et al. 1999), trophic position (Vander Zanden and Rasmussen 1999; Post 2002), time-integrated diets (Beaudoin et al. 1999), ontogenetic diet shifts (Vander Zanden et al. 1998), and benthic–pelagic coupling (Vadeboncoeur et al. 2002), and also to determine the relative contribution of energy derived from different primary sources (France 1995; Post 2002; Vander Zanden and Vadeboncoeur 2002). The utility of stable isotopes in addressing these issues rests upon the measured or assumed isotopic fractionation (change in value) from diet to consumer that occurs during assimilation (Peterson and Fry 1987). The stable carbon isotope ratio ($\delta^{13}C$) is generally used as an indicator of energy sources, while the stable nitrogen isotope ratio ($\delta^{15}N$) indicates trophic position (Vander Zanden et al. 1997; Kelly 2000; Post 2002). There is rela-

Received 31 October 2005. Accepted 20 June 2006. Published on the NRC Research Press Web site at http://cjfas.nrc.ca on 13 September 2006.
J18971

B.A. Murry[1] and J.M. Farrell. Faculty of Environmental and Forest Biology, 242 Illick Hall, State University of New York, College of Environmental Science and Forestry (SUNY-ESF), 1 Forestry Drive, Syracuse, NY 13210, USA.
M.A. Teece and P.M. Smyntek. Faculty of Chemistry, 415 Jahn Laboratory, SUNY-ESF, 1 Forestry Drive, Syracuse, NY 13210, USA.

[1] Corresponding author (e-mail: bamurry@syr.edu).

doi:10.1139/F06-116

tively little fractionation of C from diet to consumer (generally <1‰; see reviews by France and Peters 1997; Vander Zanden and Rasmussen 1999; Post 2002). Additionally, owing to differences in photosynthetic pathways among different primary producers (e.g., C_3 and C_4 plants), energy derived from different sources (i.e., littoral algae and phytoplankton) often exhibit disparate δ^{13}C values, making C an excellent indicator of energy sources (Park and Epstein 1961; Kelly 2000). The relative contribution of energy from each of these potential sources is generally determined through the use of mixing models (Post 2002). The δ^{15}N value of a consumer is generally more enriched than its diet (mean fractionation of +3.4‰) making it more suitable to infer trophic position (Vander Zanden and Rasmussen 2001; Post 2002).

Food web studies using stable isotopes depend on consistent measurement of isotopic signatures at the individual, population, and species levels. The consistency and accuracy of these measurements may, however, be called into question because of the lack of standardized protocols and poor understanding of the effects of different sample preparation techniques (Gannes et al. 1997). Inconsistent procedures include the use of whole organisms versus individual tissues (Sotiropoulos et al. 2004), sample acidification (Bunn et al. 1995), sample preservation techniques (Kaehler and Pakhomov 2001; Arrington and Winemiller 2002; Sarakinos et al. 2002), and sample lipid extraction (Sotiropoulos et al. 2004). These methodological inconsistencies inhibit our ability to appropriately pool data across studies and may adversely affect data interpretation within studies.

The exclusive use of a particular tissue, for instance white muscle tissue in fish, and lipid extraction are standard protocols intended to minimize violations of assumptions and reduce data variance (Pinnegar and Polunin 1999). However, lipid extraction is a technique that is used by some researchers (e.g., Kling et al. 1992; Beaudoin et al. 1999; Post 2002) but not others (e.g., Fry et al. 1999; Vander Zanden and Rasmussen 1999; Johnson et al. 2002). Because of fractionation during their biosynthesis, lipids are depleted (about 6‰–7‰) in ^{13}C relative to protein (DeNiro and Epstein 1977; Focken and Becker 1998). The variation in lipid content among species, populations, sexes, and temporally within individuals affects the consistency and magnitude of the δ^{13}C values within otherwise homogenous samples (Focken and Becker 1998), such as white muscle tissue, potentially altering individual data points (Gu et al. 1996; Sotiropoulos et al. 2004) and the interpretation of observed relationships within a food web (Rau et al. 1992).

Because commonly used solvents (i.e., chloroform–methanol or dichloromethane–methanol, Bligh and Dyer 1959) are not lipid-specific, some nitrogenous compounds are also removed during lipid extraction (Radin 1981). Sotiropoulos et al. (2004) presented data on three ecologically similar fish species (brook stickleback (*Culaea inconstans*), fathead minnow (*Pimephales promelas*), and dace (*Phoxinus* sp.)) in which both the δ^{13}C and the δ^{15}N values were slightly enriched in extracted samples versus nonextracted control samples. The magnitude of change in the isotope values due to lipid extraction, although small (<1‰), was greater than the analytical error for both the C and N isotopes. Though the magnitude of change in individual samples was regarded as ecologically insignificant, the authors suggested that derived food web relationships might be affected.

The goal of this paper is to expand upon these studies by examining differences in the fish community structure and relative trophic position of nine different species using paired food webs derived from extracted and nonextracted samples. Because of the variation in lipid content among species and individuals, we hypothesize that lipid extraction may differentially alter individual sample signatures, more for high lipid content species and less for low lipid content species, such that food webs derived from extracted and nonextracted samples may differ in the observed placement of individual species within the food web.

We present data testing the hypotheses that lipid extraction (*i*) causes a differential shift in both the δ^{13}C and the δ^{15}N values among different species and (*ii*) shifts resulting from lipid extraction may alter the interpretation of food web structure (species grouping and spacing) when compared with food webs reconstructed using non-lipid-extracted samples.

Materials and methods

All fish were collected throughout the 2002 summer growing season from United States waters of the Thousand Islands region of the upper St. Lawrence River. This region of the St. Lawrence River is directly downstream of Lake Ontario and contains a wide variety of habitat types and a very diverse fish community (Edwards et al. 2002). Fish were collected in nearshore littoral nursery bays between Cape Vincent and Alexandria Bay, New York, USA, primarily by seining but also some gillnetting. Fish were held live in coolers and returned to the State University of New York, College of Environmental Science and Forestry's (SUNY-ESF) Thousand Islands Biological Station (TIBS) for processing.

We measured the total length of each fish (Table 1) and then filleted a small section of skinless white muscle tissue from the dorsal caudal peduncle region. All samples were immediately frozen on dry ice and stored frozen until they were freeze-dried and divided into two aliquots. Lipids were exhaustively extracted from one aliquot using dichloromethane–methanol (1:1). Solvent was evaporated under inert nitrogen gas (N_2). The second aliquot was not extracted. All samples were then weighed (350–650 μg) into tin cups and stable C and N compositions were measured using a Costech elemental analyzer coupled to a Thermo Finnigan Delta XP-Plus isotope ratio mass spectrometer at the Environmental Science Stable Isotope Laboratory (EaSSIL), SUNY-ESF. Stable isotope ratios are expressed in the delta (δ) notation as parts per thousand (‰) difference from a known standard:

$$\delta^{13}\mathrm{C} \text{ or } \delta^{15}\mathrm{N} = [(R_{\mathrm{sample}} - R_{\mathrm{standard}})/R_{\mathrm{standard}}] \times 1000$$

where *R* is the ratio of ^{13}C/^{12}C or ^{15}N/^{14}N. Results are reported relative to the international standards: Vienna Pee Dee Belemnite for C and atmospheric nitrogen for N. Approximately 10% of the samples were analyzed in triplicate to assess analytical error, which was ~0.1‰ for both δ^{15}N and δ^{13}C. For each species, we report the average value of all

Table 1. Species, name abbreviation, and mean total length (mm) of fish used in this study.

Common name	Scientific name	Abbreviation	*n*	Total length (range)
Bullhead	*Ameiurus* sp.	BH	9	113.4 (55–285)
Blackchin shiner	*Notropis heterodon*	BLCH	5	54.2 (52–57)
Bluntnose minnow	*Pimephales notatus*	BLNO	5	55.2 (54–60)
Banded killifish	*Fundulus diaphanus*	K	8	77.5 (68–94)
Pumkinseed	*Lepomis gibbosus*	PUMP	6	81.0 (29–156)
Rock bass	*Ambloplites rupestris*	RB	11	67.2 (29–122)
Yellow perch	*Perca flavescens*	YP	11	117.7 (77–158)
Muskellunge (YOY)[a]	*Esox masquinongy*	M	4	116.5 (96–151)
Northern pike	*Esox lucius*	NP	8	470.0 (111–665)

[a] Muskellunge (YOY) indicates that these were all young-of-the-year fish.

individuals within each group plus or minus one standard error (SE).

We examined the effect of lipid extraction on each species using paired *t* tests. Next we examined the relative distance between paired extracted and nonextracted points measured horizontally along the C (*x*) axis ($\Delta^{13}C_{\text{extracted-nonextracted}}$), vertically along the N (*y*) axis ($\Delta^{15}N_{\text{extracted-nonextracted}}$), and diagonally ($\Delta\text{Diag}_{\text{extracted-nonextracted}}$; Fig. 1). Each of these measures was compared across species testing the null hypothesis that the shift in coordinate space due to the lipid extraction procedure was the same for all species. Relative distances between paired points of each species were compared using multivariate analysis of variance (MANOVA). Significantly different ($p < 0.05$) distances between paired points are indicative of differences in extracted and nonextracted food web structures, whereas nonsignificant differences in distances between paired points suggests homogenous shifting of points and no difference in food web structure resulting from the two procedures.

We also examined the variance associated with extracted and nonextracted data sets using Levene's homogeneity of variance test (Levene 1960). We tested the overall data (pooling across all species), as well as the variance associated with each individual species. SAS was used for all statistical analyses (SAS Institute Inc., Cary, North Carolina). Most data were normally distributed; however, in the few instances where data did not meet the assumption of normality, parametric and nonparametric measures of significant differences (i.e., paired *t* test and sign-rank test) were identical. In all cases, parametric results are reported.

Results

Effect of lipid extraction on individual samples

The $\delta^{13}C$ and $\delta^{15}N$ values of lipid-extracted samples were significantly and consistently enriched in the heavier isotope relative to the nonextracted samples in every pair-wise case ($p < 0.05$; Figs. 2*a*, 2*b*). The mean $\Delta^{13}C_{\text{extracted-nonextracted}}$ was +1.07‰ (±0.069‰ SE, $n = 67$), whereas the mean $\Delta^{15}N_{\text{extracted-nonextracted}}$ was +1.59‰ (±0.071‰ SE, $n = 67$), which constitutes a mean increase of nearly half a trophic position (assuming 1 trophic position = +3.4‰).

Effect of lipid extraction on food web structure

Lipid extraction did cause minor changes in the order of species arranged from low to high mean $\delta^{13}C$ and $\delta^{15}N$ (Figs. 2*a*, 2*b*). However, because of the very close proximity of the species involved, the relative error about each mean, and the homogenous shift of each species location due to extraction, the changes in sequence were not ecologically or statistically significant. The relative distance along the C (*x*) axis, the N (*y*) axis, and the respective diagonal distances between paired samples did not differ among species (MANOVA, $\lambda = 0.70$, $F_{[24,163]} = 0.90$, $p = 0.60$).

Fig. 1. Measurements of isotopic shift due to the lipid extraction procedure. $\Delta^{13}C$ measures the horizontal distance, $\Delta^{15}N$ measures the vertical distance, and ΔDiag measures the straight-line distance between the paired nonextracted and extracted points in coordinate space.

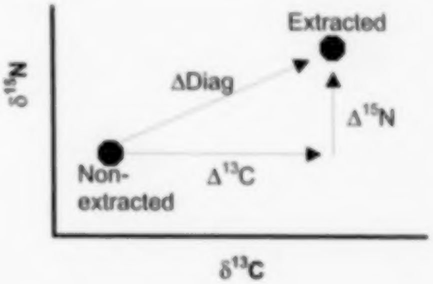

Effect of lipid extraction on food web position

The location of food webs, developed from nonextracted and extracted samples, in $\delta^{13}C$ and $\delta^{15}N$ (*x*,*y*) coordinate space (Fig. 3) were compared with a MANOVA consisting of two response variables ($\delta^{13}C$ and $\delta^{15}N$), two independent variables (method (extracted or not) and species), as well as the interaction of the two independent variables. The interaction was not significant ($\lambda = 0.98$, $F_{[16,230]} = 0.15$, $p = 1.00$), but both main effects were significant (method: $\lambda = 0.39$, $F_{[2,115]} = 89.57$, $p < 0.05$; species: $\lambda = 0.25$, $F_{[16,230]} = 14.65$, $p < 0.05$). Subsequent ANOVAs of each response variable resulted in no interaction among main effects in both cases ($\delta^{13}C$: $F_{[8,17]} = 0.04$, $p = 1.00$; $\delta^{15}N$: $F_{[8,17]} = 0.26$, $p = 0.98$). Similarly in both cases, as expected, species were a significant main effect, but were utilized only to isolate variation due to the method. Both the $\delta^{13}C$ and $\delta^{15}N$ across all species were significantly shifted (right and up, respectively) because of the extraction method ($\delta^{13}C$: $F_{[1,17]} = 12.99$, $p < 0.05$; $\delta^{15}N$: $F_{[1,17]} = 174.70$, $p < 0.05$).

Fig. 2. Mean (±standard error) nonextracted (solid squares) and extracted (open squares) values for (*a*) δ^{13}C and (*b*) δ^{15}N. The species, labeled along the *x* axis in each panel, are ordered from low to high according to each respective *y*-axis value. Abbreviated fish names are as follows: BLCH, blackchin shiner (*Notropis heterodon*); BH, bullhead (*Ameiurus* sp.); BLNO, bluntnose minnow (*Pimephales notatus*); YP, yellow perch (*Perca flavescens*); PUMP, pumpkinseed (*Lepomis gibbosus*); K, banded killifish (*Fundulus diaphanus*); RB, rock bass (*Ambloplites rupestris*; M, young-of-the-year (YOY) muskellunge (*Esox masquinongy*); NP, northern pike (*Esox lucius*).

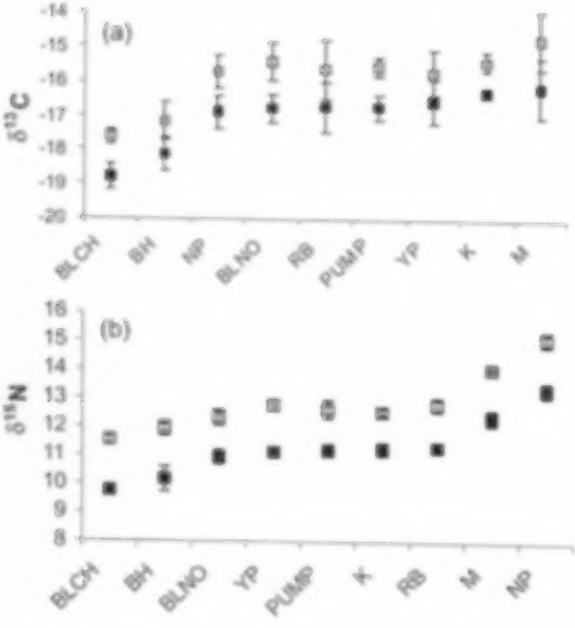

Fig. 3. Food web structure evaluated using δ^{13}C and δ^{15}N values (±standard error). The solid circles are nonextracted samples; the open circles are lipid-extracted samples.

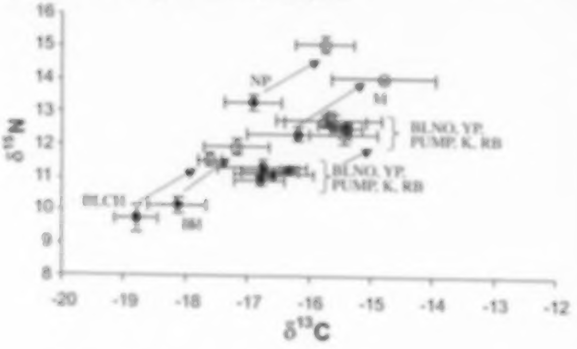

Table 2. Levene's test for homogeneity of variance.

Response variable	Species	df	F	P
δ^{13}C	Pooled	1, 132	0.20	0.66
δ^{15}N	Pooled	1, 132	0.00	0.96
δ^{13}C	Blackchin shiner	1, 8	2.27	0.17
	Bluntnose minnow	1, 8	2.25	0.17
	Bullhead	1, 16	0.13	0.73
	Killifish	1, 14	3.57	0.08
	Muskellunge	1, 6	0.01	0.93
	Northern pike	1, 14	0.01	0.91
	Pumpkinseed	1, 10	0.54	0.48
	Rock bass	1, 20	0.14	0.71
	Yellow perch	1, 20	0.00	0.97
δ^{15}N	Blackchin shiner	1, 8	1.23	0.30
	Bluntnose minnow	1, 8	3.33	0.11
	Bullhead	1, 16	0.00	0.98
	Killifish	1, 14	0.07	0.79
	Muskellunge	1, 6	2.90	0.14
	Northern pike	1, 14	0.17	0.69
	Pumpkinseed	1, 10	3.78	0.08
	Rock bass	1, 20	0.17	0.69
	Yellow perch	1, 20	0.32	0.58

Note: Extraction did not influence the observed sample variance.

Effect of lipid extraction on sample variance

Lipid extraction did not influence the collective (all species pooled) sample variance nor the variance associated with individual species (Table 2).

Discussion

Lipid extraction is intended to remove isotopically depleted lipids to obtain an unbiased C isotope value and reduce intersample variability (DeNiro and Epstein 1977; Focken and Becker 1998; Pinnegar and Polunin 1999). A similar study conducted by Sotiropoulos et al. (2004) using sticklebacks and two minnow species found that lipid extraction from muscle tissue produced a very slight (<1‰), ecologically nonsignificant shift in both δ^{13}C and δ^{15}N values. We found, however, a significant and larger increase in the extracted samples of both the δ^{13}C values (all species average = +1.07‰ ± 0.07‰ SE) and the δ^{15}N values (all species average = +1.59‰ ± 0.07‰ SE) relative to the paired, nonextracted samples for all nine fish species we studied. However, similar to the findings of Sotiropoulos et al. (2004), the variance of δ^{13}C and δ^{15}N was not influenced by lipid extraction. Although lipid extraction did not alter the relative position of species, and thus did not distort the interpretation of food web relationships, it did significantly shift the location of the entire web relative to the same nonextracted food web. Future literature reviews and meta-analyses attempting to draw conclusions from multiple isotope studies need to be cognizant of this shift, which is due to differing sample preparation protocols rather than an ecological cause. Standardization procedures, using mixing models (Vander Zanden et al. 1997; Post 2002), should be used cautiously, as lower trophic groups that are used as isotopic bases often contain a greater proportion of lipids compared with fish (Bilkovic and Lehman 1997), thereby altering actual differences in δ values.

Overall, although we observed a significant shift in position, lipid extraction did not have an influence on our interpretation of trophic relationships within the studied fish community. Our sampling was conducted midway through the summer growing season, thus we would not expect high lipid levels relative to the late fall and pre-spawn seasons (Bradford 1993; Miranda 1993; Malavesi et al. 2004). Samples collected during these times may produce different results. Gu et al. (1996), for instance, compared extracted and nonextracted samples of gizzard shad (*Dorosoma cepedianum*) muscle tissue. They found no differences between sample preparation procedures for any fish less than 125 mm and males greater then 125 mm, but extracted samples of female fish greater than 125 mm were 2.1‰ enriched in ^{13}C relative to nonextracted samples, which is over twice as much change due to extraction as observed in this study, demonstrating that reproductive status, sex, and seasonality can influence data interpretation.

The enrichment of the C isotope value after lipid extraction is not unexpected because lipids are known to be depleted in ^{13}C owing to fractionation processes during lipid biosynthesis (DeNiro and Epstein 1977). However, the enrichment in the N isotope value resulting from lipid extraction is curious. Sotiropoulos et al. (2004) suggest that the loss of N through lipid extraction is the result of cellular proteins being leached out in association with the polar lipids of the cell membrane. That explanation in and of itself does not, however, explain why in all cases, the resultant $\delta^{15}N$ value of the muscle tissue increases. The N leaving the sample must be heavily depleted in ^{15}N relative to the remaining tissue for the $\delta^{15}N$ value to increase. It has been demonstrated that specific amino acids differ in isotopic composition (McClelland and Montoya 2002; Schmidt et al. 2004), such that perhaps the amino acid – protein groups extracted in association with the polar lipids (Pinnegar and Polunin 1999), under this hypothesis, are isotopically lighter than the primary muscle proteins.

An alternative explanation for the consistent enrichment of the $\delta^{15}N$ values due to lipid extraction may be the removal of nitrogenous wastes resulting from cellular respiration of proteins (Bearhop et al. 2000). Protein metabolism in fish produces ammonia (NH_3) and ammonium (NH_4^+), which is carried by the blood and released via gill exchange, with approximately 10% being converted to urea and excreted through the kidneys (Moyle and Cech 2004). Secondary consumers preferentially retain the heavier isotopes (Peterson and Fry 1987), and thus the ammonia–ammonium produced as a byproduct of protein metabolism is expected to be isotopically light. Both ammonium and ammonia are soluble in lipids and organic solvents and may be removed with lipid extraction.

The source of the ^{15}N-depleted nitrogen that is removed through lipid extraction is an important issue. We may not want to remove structural proteins, whereas we may want to remove nitrogenous waste from the sample, as it may introduce unnecessary bias. Should further research determine that structural proteins are the cause of the change in the N signature, we share the recommendation of Sotiropoulos et al. (2004) to use two sample aliquots, one extracted for C and the other nonextracted for N. Alternatively, Radin (1981) suggested the use of a hexane–isopropanol solvent to avoid removing N, but in preliminary studies this technique was found to remove N from fish tissue at a similar magnitude as the dichloromethane–methanol method (B.A. Murry, unpublished data). If, however, the N removed by extraction is determined to be nitrogenous waste (Bearhop et al. 2000), we recommend removal through solvent-based extraction.

In conclusion, this is the only known direct examination of the influence of lipid extraction on the interpretation of fish community structure. We found that lipid extraction did produce a significant, differential change of both $\delta^{13}C$ and $\delta^{15}N$ values among species, but these differences did not alter our interpretation of food web structure within the studied fish community. Therefore, in the majority of situations lipid extraction may not be necessary. There may, however, be certain extenuating situations, such as studies during the reproductive season or studies including species known to have higher than typical lipid content, where lipids may pose a legitimate concern and should be removed. In these cases, researchers should bear in mind that lipid extraction significantly shifted the entire food web positively in both the $\delta^{13}C$ and $\delta^{15}N$ directions. This point is especially relevant if cross-study meta-analyses are to be conducted.

Acknowledgements

The authors acknowledge the assistance of Adam Storch in reviewing an early draft and making comments that greatly improved the manuscript. Funding was provided by a Federal Aid in Sportfish Restoration Grant No. FA-5-R. This research is a contribution of the State University of New York, College of Environmental Science and Forestry's Thousand Islands Biological Station (TIBS).

References

Arrington, D.A., and Winemiller, K.O. 2002. Preservation effects on stable isotope analysis of fish muscle. Trans. Am. Fish. Soc. **131**: 337–342.

Bearhop, S., Teece, M.A., Waldron, S., and Furness, R.W. 2000. Influence of lipid and uric acid on $\delta^{13}C$ and $\delta^{15}N$ values of avian blood: implications for trophic studies. Auk, **117**: 504–507.

Beaudoin, C.P., Tonn, W.M., Prepas, E.E., and Wassenaar, L.I. 1999. Individual specialization and trophic adaptability of northern pike (*Esox lucius*): an isotope and dietary analysis. Oecologia, **120**: 386–396.

Bilkovic, D.M., and Lehman, J.T. 1997. Lipid concentration and size variation of *Bythotrephes* (Cladocera: Cergopagidae) from Lakes Erie, Huron, and Michigan. J. Gt. Lakes Res. **23**: 149–159.

Bligh, E.G., and Dyer, W.J. 1959. A rapid method of total lipid extraction and purification. Can. J. Biochem. Physiol. **37**: 911–917.

Bradford, R.G. 1993. Role of spawning condition in the determination of the reproductive traits of spring- and autumn-spawning Atlantic herring from the southern Gulf of St. Lawrence. Can. J. Zool. **71**: 309–317.

Bunn, S.E., Loneragan, N.R., and Kempster, M.A. 1995. Effects of acid washing on stable isotope ratios of C and N in penaeid shrimp and seagrass: implications for food-web studies using multiple stable isotopes. Limnol. Oceanogr. **40**: 622–625.

DeNiro, M.J., and Epstein, S. 1977. A mechanism of carbon isotope fractionation associated with lipid synthesis. Science (Washington, D.C.), **197**: 261–263.

Edwards, P.A., Stewart, T.J., and Mathers, A. 2002. St. Lawrence River fish community. *In* Lake Ontario fish communities and fisheries 2001. Annual report of the Lake Ontario Management Unit. Lake Ontario Committee Great Lakes Fishery Commission, Picton, Ont., Canada.

Focken, U., and Becker, K. 1998. Metabolic fractionation of stable carbon isotopes: implications of different proximate compositions for studies of aquatic food webs using δ^{13}C data. Oecologia, **115**: 337–343.

France, R.L. 1995. Differentiation between littoral and pelagic food webs in lakes using stable carbon isotopes. Limnol. Oceanogr. **40**: 1310–1313.

France, R.L., and Peters, R.H. 1997. Ecosystem differences in the trophic enrichment of ^{13}C in aquatic food webs. Can. J. Fish. Aquat. Sci. **54**: 1255–1258.

Fry, B., Mumford, P.L., Tam, F., Fox, D.D., Warren, G.L., Havens, K.E., and Steinman, A.D. 1999. Trophic position and individual feeding histories of fish from Lake Okeechobee, Florida. Can. J. Fish. Aquat. Sci. **56**: 590–600.

Gannes, L.Z., O'Brien, D.M., and Martinex del Rio, C. 1997. Stable isotopes in animal ecology: assumptions, caveats, and a call for more laboratory experiments. Ecology, **78**: 1271–1276.

Gu, B., Schelske, C.L., and Hoyer, M.V. 1996. Stable isotopes of carbon and nitrogen as indicators of diet and trophic structure of the fish community in a shallow hypereutrophic lake. J. Fish Biol. **49**: 1233–1243.

Johnson, B.M., Martinez, P.J., and Stockwell, J.D. 2002. Tracking trophic interactions in coldwater reservoirs using naturally occurring stable isotopes. Trans. Am. Fish. Soc. **131**: 1–13.

Kaehler, S., and Pakhomov, E.A. 2001. Effects of storage and preservation on the δ^{13}C and δ^{15}N signatures of selected marine organisms. Mar. Ecol. Prog. Ser. **219**: 299–304.

Kelly, J.F. 2000. Stable isotopes of carbon and nitrogen in the study of avain and mammalian trophic ecology. Can. J. Zool. **78**: 1–27.

Kling, G.W., Fry, B., and O'Brian, W.J. 1992. Stable isotopes and planktonic trophic structure in arctic lakes. Ecology, **73**: 561–566.

Levene, H. 1960. Robust test for equality of variance. *In* Contributions to probability and statistics: essays in honor of Harold Hotelling. *Edited by* I. Olkin. Stanford University Press, Stanford, Calif. pp. 278–292.

Malavesi, S., Fiorin, R., Franco, A., and Torricelli, P. 2004. Somatic energy storage and reproductive investment in the grass goby *Zosterisessor ophiocephalus*. J. Mar. Biol. Assoc. U.K. **84**: 455–459.

McClelland, J.W., and Montoya, J.P. 2002. Trophic relationships and the nitrogen isotopic composition of amino acids in plankton. Ecology, **83**: 2173–2180.

Miranda, L.E. 1993. Length-dependent winter survival and lipid composition of age-0 largemouth bass in Bay Springs Reservior, Mississippi. Trans. Am. Fish. Soc. **123**: 80–87.

Moyle, P.B., and Cech, J.J., Jr. 2004. Fishes: an introduction to ichthyology. 5th ed. Prentice Hall, Upper Saddle River, N.J.

Park, R., and Epstein, S. 1961. Metabolic fractionation of C13 and C12 in plants. Plant Physiol. **36**: 133–138.

Peterson, B.J., and Fry, B. 1987. Stable isotopes in ecosystem studies. Annu. Rev. Ecol. Syst. **18**: 293–320.

Pinnegar, J.K., and Polunin, N.V.C. 1999. Differential fractionation of δ^{13}C and δ^{15}N among fish tissues: implications for the study of trophic interactions. Funct. Ecol. **13**: 225–231.

Post, D.M. 2002. Using stable isotopes to estimate trophic position: models, methods, and assumptions. Ecology, **83**: 703–718.

Radin, N.S. 1981. Extraction of tissue lipids with a solvent of low toxicity. Methods Enzymol. **72**: 5–7.

Rau, G.H., Ainley, D.G., Bengtson, J.L., Torres, J.J., and Hopkins, T.L. 1992. 15N/14N and 13C/12C in Weddell sea birds, seals, and fish: implications for diet and trophic structure. Mar. Ecol. Prog. Ser. **84**: 1–8.

Sarakinos, H.C., Johnson, M.L., and Vander Zanden, M.J. 2002. A synthesis of tissue-preservation effects on carbon and nitrogen stable isotope signatures. Can. J. Zool. **80**: 381–387.

Schmidt, K., McClelland, J.W., Mente, E., Montoya, J.P., Atkinson, A., and Voss, M. 2004. Trophic-level interpretation based on δ^{15}N values: implications of tissue-specific fractionation and amino acid composition. Mar. Ecol. Prog. Ser. **266**: 43–58.

Sotiropoulos, M.A., Tonn, W.M., and Wassenaar, L.I. 2004. Effects of lipid extraction on stable carbon and nitrogen isotope analyses of fish tissues: potential consequences for food web studies. Ecol. Freshw. Fish, **13**: 155–160.

Vadeboncoeur, Y., Vander Zanden, M.J., and Lodge, D.M. 2002. Putting the lake back together: reintegrating benthic pathways into lake food web models. Bioscience, **52**: 44–54.

Vander Zanden, M.J., and Rasmussen, J.B. 1999. Primary consumer δ^{13}C and δ^{15}N and the trophic position of aquatic consumers. Ecology, **80**: 1395–1404.

Vander Zanden, M.J., and Rasmussen, J.B. 2001. Variation in δ^{15}N and δ^{13}C trophic fractionation: implications for aquatic food web studies. Limnol. Oceanogr. **46**: 2061–2066.

Vander Zanden, M.J., and Vadeboncoeur, Y. 2002. Fishes as integrators of benthic and pelagic food webs in lakes. Ecology, **83**: 2152–2161.

Vander Zanden, M.J., Cabana, G., and Rasmussen, J.B. 1997. Comparing trophic position of freshwater fish calculated using stable nitrogen isotope ratios (δ^{15}N) and literature dietary data. Can. J. Fish Aquat. Sci. **54**: 1142–1158.

Vander Zanden, M.J., Hulshof, M., Ridgway, M.S., and Rasmussen, J.B. 1998. Application of stable isotope techniques to trophic studies of age-0 smallmouth bass. Trans. Am. Fish. Soc. **127**: 729–739.

Growth and survival of age-0 walleye (*Sander vitreus*): interactions among walleye size, prey availability, predation, and abiotic factors

R. John H. Hoxmeier, David H. Wahl, Ronald C. Brooks, and Roy C. Heidinger

Abstract: We examined the importance of prey availability, predation, and abiotic factors in determining growth and survival of age-0 walleye (*Sander vitreus*) across 15 Illinois reservoirs during 7 years. Multiple life stages were examined by stocking walleye at three different size groups: larval (6 mm total length (TL)), small (46 mm TL), and large (100 mm TL). Factors affecting growth and survival of walleye varied depending on walleye size. Growth of small and large walleye increased with benthic invertebrate density. Temperature had a positive effect on larval and small walleye growth but a negative effect on large walleye growth. Prey availability was an important factor for walleye survival across all size groups, whereas temperature affected only larval and large walleye. Juvenile centrarchid density had a negative effect on larval walleye survival, presumably caused by predation. Our best predictive models explained substantial variation in survival for larval (97%), small (57%), and large (83%) walleye. We also explained a high proportion of variation in growth of large (98%), small (55%), and larval (52%) walleye. Our study demonstrates the importance of examining multiple life stages to predict growth and survival and leads to a better understanding of walleye recruitment and recommendations for stocking strategies.

Résumé : Nous avons examiné l'importance de la disponibilité des proies, de la prédation et des facteurs abiotiques dans la détermination de la croissance et de la survie chez les dorés (*Sander vitreus*) d'âge 0 dans 15 réservoirs de l'Illinois pendant 7 ans. Nous avons étudié plusieurs stades de vie en empoissonnant avec des dorés de trois classes de taille différentes, des larves (6 mm de longueur totale (TL)), des petits (46 mm TL) et des grands (100 mm TL) dorés. Les facteurs qui affectent la croissance et la survie du doré varient en fonction de la taille des poissons. La croissance des petits et grands dorés augmente en fonction de la densité des invertébrés benthiques. La température a un effet positif sur la croissance des larves et des petits dorés, mais un effet négatif sur la croissance des grands dorés. La disponibilité des proies est un facteur important pour la survie des dorés de toutes tailles, alors que la température n'affecte que les larves et les grands dorés. La densité des jeunes centrarchidés a un effet négatif sur la survie des larves de dorés, probablement à cause de la prédation. Nos meilleurs modèles prédictifs expliquent une partie substantielle de la variation de la survie chez les larves (97 %), les petits (57 %) et les grands (83 %) dorés. Nous pouvons aussi expliquer une forte proportion de la variation de la croissance chez les grands (98 %) et les petits (55 %) dorés et chez les larves (52 %). Notre étude démontre l'importance d'examiner plusieurs stades de vie pour prédire la croissance et la survie; elle apporte une meilleure compréhension du recrutement chez le doré et elle propose des recommandations sur les stratégies d'empoissonnement.

[Traduit par la Rédaction]

Introduction

Growth and survival of young fish can be dependent on predation, prey availability, and abiotic factors. These factors can play an important role in both natural recruitment and stocking success and are often dependent on fish size. For example, abiotic factors often have the greatest effect on growth and survival during initial life stages (Houde 1987; Claramunt and Wahl 2000). Similarly, smaller fish are more susceptible to predation and starvation than larger fish (Rice et al. 1987; Miller et al. 1988). Resident predators can be an important source of mortality for a number of stocked fish species (Wahl and Stein 1989; Hoxmeier and Wahl 2002; Henderson and Letcher 2003). These variables can affect

Received 11 October 2005. Accepted 23 May 2006. Published on the NRC Research Press Web site at http://cjfas.nrc.ca on 13 September 2006.
J18929

R.J.H. Hoxmeier[1,2] **and D.H. Wahl.** Kaskaskia Biological Station, Illinois Natural History Survey, RR 1, Box 157, Sullivan, IL 61951, USA.
R.C. Brooks and R.C. Heidinger. Fisheries and Illinois Aquaculture Center, Southern Illinois University, Carbondale, IL 62901, USA.

[1] Corresponding author (e-mail: john.hoxmeier@dnr.state.mn.us).

[2] Present address: Minnesota Department of Natural Resources, 1801 South Oak Street, Lake City, MN 55041, USA.

doi:10.1139/F06-087

Table 1. Surface area, latitude, and number of stockings for three size classes[a] of walleye (*Sander vitreus*) stocked into 15 Illinois lakes from 1991–1997.

Lake	Area (ha)	Latitude (N)	Number of stockings		
			Larval	Small	Large
Bloomington	250	39°69′98″		5	
Dutchman	53	37°30′00″	3	1	
East Fork	379	38°45′43″	5	2	
Fox Chain	2663	42°28′26″	3	2	
George	68	41°25′58″		4	
Kinkaid	1114	37°46′25″		4	2
Leaquana	16	42°25′08″	5	5	7
Pierce	66	42°20′43″		7	
Randolph	26	37°58′25″	5	5	5
Ridge	6	39°27′08″	4	2	3
Sam Dale	78	39°00′52″		5	
Sara	237	39°20′01″	1	4	
Shelbyville	4455	39°25′07″	6	5	3
Springfield	1715	39°42′43″	5		1
Sterling	53	42°28′26″	4	4	5
Total			41	55	26

[a] Size classes: larval (6 mm total length (TL)); small (46.0 ± 0.9 mm TL (mean ± 1 standard error)); large (99.7 ± 2.0 mm TL).

growth and survival at multiple life stages, suggesting that recruitment may not be set at a single stage (Parkos and Wahl 2002).

Assessments of which variables are important in determining recruitment during early life stages of walleye (*Sander vitreus*) are needed for this important sportfish. A number of studies have assessed the importance of individual factors, but few have either examined them in combination to determine their relative effects or assessed their importance across size. Variability in water temperature and spring water levels can affect age-0 walleye survival (Serns 1982; Quist et al. 2003). Younger stocked walleye are more susceptible to change in water temperature than larger individuals (Santucci and Wahl 1993; Clapp et al. 1997). Predation can also be a limiting factor in walleye survival, especially in lakes with dominant centrarchid populations. For example, white crappie (*Pomoxis annularis*) abundance has been negatively related to walleye recruitment (Quist et al. 2003). In addition, largemouth bass (*Micropterus salmoides*) consumed up to 17% of a stocked walleye population (Santucci and Wahl 1993). Predation rates on walleye are also related to size, with smaller walleye being more susceptible to predation than larger walleye (Santucci and Wahl 1993). Prey resources important to walleye change during their first year of life through ontogenetic diet shifts. Walleye begin feeding on zooplankton after endogenous feeding at about 8 mm total length (TL) and then switch to macroinvertebrates (35–50 mm TL) and eventually to fish (60–80 mm TL) (Priegel 1969; Mathias and Li 1982; Galarowicz and Wahl 2005). The availability of these resources during the appropriate life stage can influence both growth and survival. An increase in zooplankton density and species composition has been shown to affect both growth and survival of larval walleye (Mayer and Wahl 1997; Hoxmeier et al. 2004), whereas larger walleye have been shown to rely on larger prey items such as benthic invertebrates and fish (Priegel 1969; Mathias and Li 1982; Kolar et al. 2003).

Stocking walleye to create or supplement existing populations is a common practice in North America. Often times, a single size is stocked throughout a region because of its availability or because a particular size has generally been shown to have high survival. Survival varies by lake and year (Brooks et al. 2002), but specific underlying mechanisms are not well understood. Matching the size of stocked walleye to the appropriate lake characteristics could further increase survival. Prey availability, predators, and abiotic factors could all affect growth and survival of stocked walleye.

The interaction between walleye size and factors influencing their growth and survival is likely complex. Most studies have examined these relationships in laboratory settings rather than in natural environments. Previous field studies have generally focused on the importance of a single factor on recruitment or stocking success. The objectives of our study were to determine factors influencing the growth and survival of walleye during the first year of life. Specifically, we examined the effects of prey (zooplankton, benthic invertebrates, and fish), predation, and abiotic factors (temperature and transparency) on three sizes of walleye stocked into Illinois reservoirs. Our hypothesis was that the relative importance of these factors would change with walleye size. Based on our results, we also present guidelines to help increase success of walleye stocking programs.

Materials and methods

Study area

We sampled 15 lakes across Illinois ranging in size from 6 to 4500 ha (Table 1), with depths from 8 to 24 m. Lakes also varied in latitude, productivity, prey resources, and predator abundances. Largemouth bass were the most abundant predator and were present in all study lakes. Sunfish (*Lepomis* spp.), white bass (*Morone chrysops*), yellow bass (*Morone mississippiensis*), crappie (*Pomoxis* spp.), and channel catfish (*Ictalurus punctatus*) were abundant in most lakes. Gizzard shad (*Dorosoma cepedianum*), sunfish, and brook silversides (*Labidesthes sicculus*) were the primary prey species. Naturally reproducing walleye were not present at the time of stocking in any of our study lakes and no unmarked fish were recovered. Aquatic vegetation consisted primarily of pondweed (*Potomogeton* spp.), coontail (*Certatophyllum demersum*), water milfoil (*Myriophyllum* spp.), and niad (*Najas* spp.).

Walleye were stocked as larval (6 mm TL), small (46.0 ± 0.9 mm TL, mean ± 1 standard error (SE)), or large (99.7 ± 2.0 mm TL) sizes during 1991 through 1997. We monitored the success of 41 larval, 55 small, and 26 large walleye stockings in the 15 study lakes (Table 1). All three size classes were stocked in five lakes, whereas six lakes were stocked with two size classes, and four lakes were stocked with small walleye only. Walleye were typically stocked in April as larvae, June for the small size class, and August for the large size class. Walleye were obtained from Jake Wolf Memorial Fish Hatchery and LaSalle Fish Hatchery, Illinois. Before stocking, all size classes of walleye were given a distinct mark for future identification. Larval and small walleye were marked by immersing them in 500 $mg \cdot L^{-1}$ oxytetracycline (OTC) for 6 h before stocking (Brooks et al. 1994). Larval walleye had OTC marks located close to the otolith nucleus, whereas small walleye had OTC marks further out from the otolith center. Large walleye were marked by removing either the right or left pelvic fin, depending on the year stocked. Stocking rates for larval walleye ranged from 1000 to $7000 \cdot ha^{-1}$ but were most often stocked at around $3000 \cdot ha^{-1}$. Target numbers for stocking were $90 \cdot ha^{-1}$ for small and $65 \cdot ha^{-1}$ for large size classes, but varied with availability in some instances. Larvae were transported to the lake in oxygenated bags in styrofoam coolers, whereas the larger size classes were transported in oxygenated hauling tanks. To reduce mortality from stocking stress (Clapp et al. 1997), walleye larvae were tempered by floating the hatchery bags in the lake until water temperatures in the bag and lake were within 1 °C. Larger size classes were acclimated by transferring lake water into the hauling tanks until water temperatures were equalized. We measured 50 individuals (TL, mm) for each walleye stocking event.

To examine success of stocked walleye, we conducted night shoreline electrofishing twice monthly in each lake during fall (September–December). All walleye were measured, weighed, and examined for clips. A subsample of unclipped walleye was frozen for later examination of OTC marks. Within 2 weeks of being removed from individual walleye, otoliths were examined for marks in the laboratory, using a compound microscope equipped with a 100-watt ultraviolet light source, 450–490 nm excitation filter, 515 nm barrier filter, and a 510 nm dichroic mirror. Population estimates were completed with the Schnable multiple census method. Because population estimates were not possible on a number of lakes because of an insufficient number of recaptures, survival of stocked walleye was subsequently based on catch-per-unit-effort (CPUE) from electrofishing. CPUE was highly correlated to number of fish per hectare ($N \cdot h^{-1}$) based on population estimates (log-transformed, r = 0.79, n = 27, $P < 0.0001$). Stomach contents of potential predators on stocked walleye were examined by gastric flushing (Foster 1977). Predator diets were examined for three consecutive days following each stocking and weekly thereafter until walleye were no longer found. Growth of walleye was calculated as the difference in TL between time of stocking and collection in fall.

Data for abiotic and biotic variables that may influence age-0 walleye survival were collected at the time of stocking and at biweekly intervals thereafter through October. Zooplankton were collected at six sites on each sampling date in each lake with a 0.5 m diameter zooplankton net with 64 μm mesh. Samples were taken from the thermocline to the surface during stratification or the entire water column when the lake was not thermally stratified. Zooplankton samples were preserved in a 4% Lugol's solution and returned to the laboratory for processing. Zooplankton samples were adjusted to a volume of 100 mL and were subsampled by 1 mL aliquots until 200 organisms from the major groups were counted or until 10% of the sample was counted (Welker et al. 1994). Copepods were identified as either cyclopoids or calanoids, and cladacerans were identified to genus. Individuals (N = 30) from each taxonomic group were measured (nearest 0.01 mm) with the aid of a digitizing pad. Copepod nauplii and rotifers were not included in density estimates because they are rarely consumed by age-0 walleye (Houde 1967; Mathias and Li 1982; Hoxmeier et al. 2004). Benthic invertebrates were collected at four sites in each lake with a Ponar bottom sampler. Samples were passed through a 600 μm sieve and preserved in a Rose bengal – ethanol solution. Samples were returned to the laboratory where they were counted and identified to order.

To estimate forage fish densities, we sampled both larval and juvenile prey fish in each lake. Larval fish were collected by towing a 0.5 m diameter ichthyoplankton net with 500 μm mesh behind the boat for 5 min at six offshore sites in each lake. Volume of water filtered was estimated from a flowmeter mounted in the opening of the net. Larval fish were preserved in ethanol and identified to genus. Seine hauls were taken with a 9.2 m bag seine (3.2 mm mesh) along the shoreline at four sites to estimate juvenile fish densities. Fish collected in the seine were identified to species, counted, and measured (nearest 1.0 mm). We used the number of fish between 20 and 50 mm TL per seine haul as a relative measure of prey fish abundance based on preferred prey sizes reported for walleye in the literature (Parsons 1971; Einfalt and Wahl 1997).

Abiotic variables examined included dissolved oxygen, turbidity, and water temperature. Dissolved oxygen and water temperature readings were taken every 2 weeks at 1 m depth intervals with a YSI oxygen meter (YSI Inc., Yellow Springs, Ohio) at the deepest area in the lake. Water transparency was measured with a secchi disk at the same location. Because we did not have daily water temperature data for all lakes, air temperature data from the Illinois State Water Survey were analyzed as a metric of lake temperature conditions. Cooling degree-days (CDDs) were obtained for each lake from the nearest weather station and were highly correlated with mean summer water temperatures from a subset of the study lakes ($r = 0.86$, $n = 22$, $P < 0.0001$). Warmer summer air temperatures are indicated by higher number of cooling degree-days.

Correlational analysis was used to examine individual relationships between environmental variables and walleye survival and growth. Multiple regression was used to examine the contribution of select variables to walleye growth and survival. Variables were added to the model in a hierarchical approach based on their presumed causal priority and results from individual correlations (Cohen and Cohen 1983). Independent variables were only added to the model if they were significant at $\alpha = 0.1$. To avoid temporal pseudoreplication, growth rates and CPUE of walleye, along with summer means of biotic and abiotic variables, were averaged across years for each lake when conducting regression analysis. Because some individual lakes were not stocked all of the 7 years, sample sizes for mean environmental variables differed. Data were tested with the UNIVARIATE procedure in SAS (SAS Institute Inc. 2001) and were log-transformed as needed to normalize the distributions before analyses. Because of the high variability associated with field data, we used $\alpha = 0.1$ to denote significance. Lake Leaquana was removed from regression analysis for larval sizes as the lake was atypical of the rest of the study lakes because of extremely high nutrient loads and hypoxic conditions at the time of stocking.

Results

Survival

Survival of young-of-year (YOY) walleye varied across lakes and size classes. Small fingerlings had higher survival than both larval and large size classes across most lakes; however, in some lakes, larval or large sizes had the highest survival (Brooks et al. 2002). Although stocking densities sometimes varied, we did not see an effect on survival for any size class (larval, $r = -0.03$, $n = 40$, $P = 0.86$; small, $r = -0.16$, $n = 53$, $P = 0.27$; large, $r = -0.02$, $n = 22$, $P = 0.96$). Prey availability, predators, and latitude were important variables determining the survival of walleye; however, the importance of these variables varied by fish size. Benthic invertebrates and juvenile fish density were the most important prey influencing walleye survival. Higher benthic invertebrate densities resulted in increased survival for both larval ($P = 0.01$) and large ($P = 0.03$; Fig. 1) walleye. However, the small walleye size class was not affected by benthic invertebrate density ($P = 0.15$). Bluegill (*Lepomis macrochirus*), gizzard shad, and brook silversides were the most common forage fish species found in both larval and seine samples. Mean summer larval fish abundance ranged from 0.01 to 16.4 m^{-3} across lakes but was not correlated with survival of larval ($r = -0.21$, $n = 9$, $P = 0.60$), small ($r = 0.37$, $n = 14$, $P = 0.20$), or large ($r = 0.11$, $n = 7$, $P = 0.81$) sizes of walleye. However, abundance of forage fish based on shoreline seining was important for small ($P = 0.01$; Fig. 2) but not larval ($r = -0.57$, $n = 9$, $P = 0.11$) or large ($r = -0.27$, $n = 7$, $P = 0.55$) walleye.

Fig. 1. Survival of (*a*) larval, (*b*) small, and (*c*) large fingerling stocked walleye (*Sander vitreus*) related to benthic invertebrate densities ($N \cdot m^{-2}$). Catch-per-unit-effort (CPUE) is the mean number of walleye collected per hour of night electrofishing the following fall after stocking. Each data point represents a mean value of CPUE and invertebrate density across years for each lake.

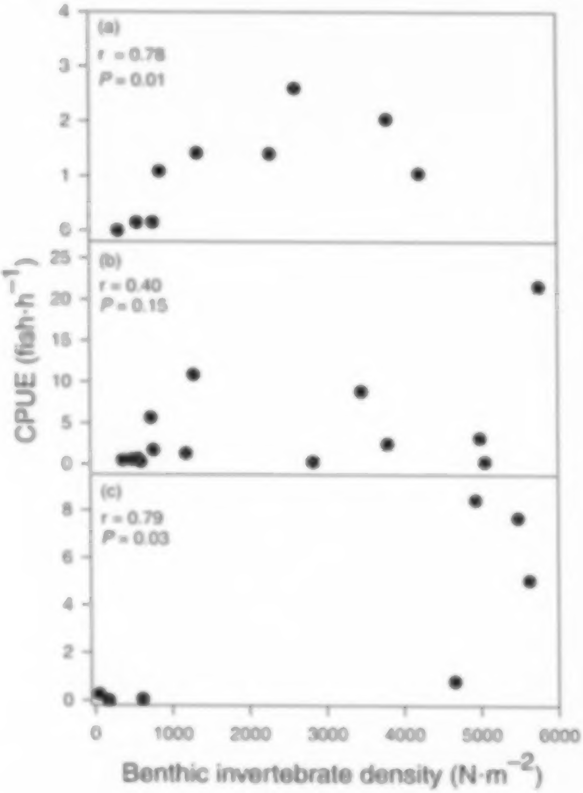

Mean zooplankton densities during summer ranged from 12 to 420 L^{-1} (excluding copepod nauplii and rotifers) across lakes. Despite the wide range in zooplankton density, we did not detect any affect on survival of larval ($r = 0.17$, $n = 9$, $P = 0.65$), small ($r = -0.17$, $n = 14$, $P = 0.55$), or large ($r = 0.53$, $n = 7$, $P = 0.22$) size classes. Because zooplankton density at the time of stocking could be particularly important for larval walleye, we also examined these relationships. Zooplankton densities at the time of larval walleye stocking also ranged widely from 3 to 396·L^{-1}. However, similar to results for summer densities, there were no significant effects of zooplankton on survival of larval fish ($r = 0.16$, $n = 9$, $P = 0.68$).

Predation had more of an effect on survival of larval walleye than on the survival of larger size classes. Although we did not directly assess predation on larval walleye at the time of stocking, survival of larval walleye was negatively correlated with juvenile centrarchid density ($P = 0.01$; Fig. 3). We were able to directly measure the amount of predation on fingerling walleye because of their larger size. However, the number of predators with walleye in their diet

Fig. 2. Survival of small walleye (*Sander vitreus*) related to the number (N) of forage fish (20–50 mm) per metre of shoreline. Catch-per-unit-effort (CPUE) is the mean number of walleye collected per hour of night electrofishing the fall following stocking. Each data point represents a mean value of CPUE and forage fish density across years for each lake.

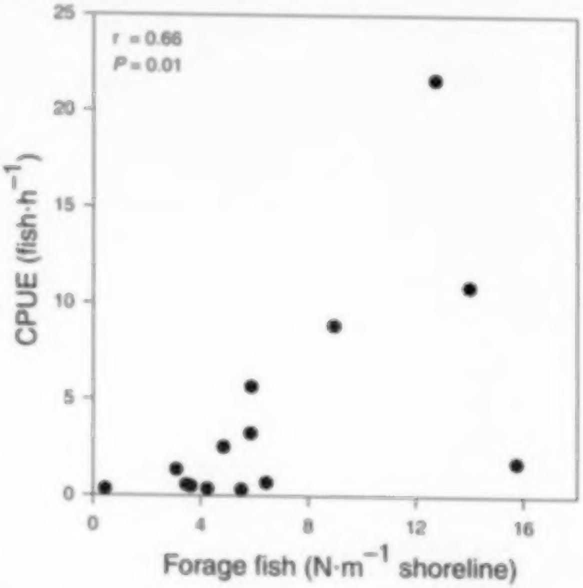

Table 2. Numbers of predator fish containing age-0 walleye (*Sander vitreus*) collected by electrofishing after stocking.

Predator species	Stomachs examined (N)	Diets with walleye N	Diets with walleye %
Bluegill	184	2	1.1
Largemouth bass	12 226	200	1.6
Muskellunge	384	9	2.3
Smallmouth bass	248	2	0.8
Walleye	10 026	43	0.4
Crappie spp.	240	6	2.6
White bass	216	3	1.4
Total	23 524	265	1.1

Note: Predator diets were examined for three consecutive days following each stocking and weekly thereafter until walleye were no longer found. Data are combined across 15 lakes in Illinois from 1991 to 1997. N, number.

Fig. 3. Survival of larval walleye (*Sander vitreus*) related to juvenile centrarchid densities ($N \cdot m^{-1}$ shoreline). Catch-per-unit-effort (CPUE) is the mean number of walleye collected per hour of night electrofishing the fall following stocking. Each data point represents a mean value of CPUE and centrarchid density across years for each lake.

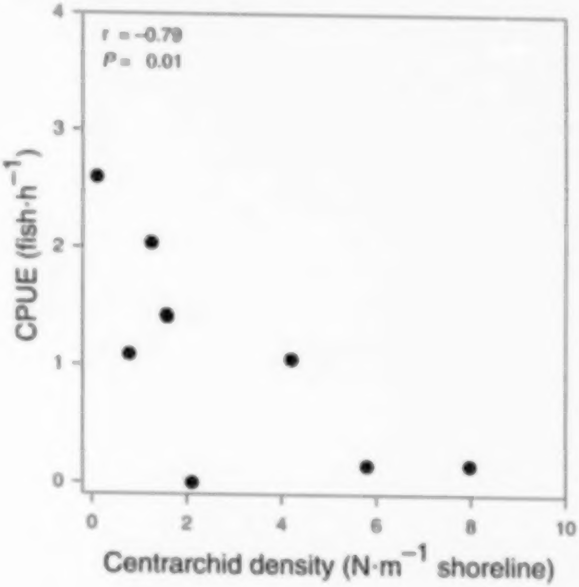

was low for both small and large walleye size classes (1.1%; Table 2). The most abundant predators on small and large walleye in our study lakes were largemouth bass. Similar to results from stomach analyses, adult (>200 mm TL) largemouth bass abundance was not significantly correlated with survival for either small (r = 0.14, n = 14, P = 0.64) or large (r = –0.49, n = 7, P = 0.27) size classes.

Larval and large walleye had higher survival in lakes located in cooler latitudes as measured by CDDs (larval, P < 0.01; large, P = 0.04; Fig. 4). CDDs ranged from 456 to 1705 and were directly related to the latitude at which the lake was located. In contrast, small walleye survival was not related to CDDs (P = 0.53).

We developed predictive models using multiple regression to further explore relationships with walleye survival. The combination of CDDs, benthic invertebrate densities, and juvenile centrarchid density accounted for 97% of the variability in larval walleye survival (multiple regression, P < 0.01; Table 3). A high proportion of the variability in survival for small walleye (57%) was accounted for by prey fish density and benthic invertebrate densities (P < 0.01; Table 3). The best model for large walleye survival included benthic invertebrate density and CDDs (R^2 = 0.83, P = 0.03; Table 3).

Growth

Factors important in determining growth were different than those for survival across all size classes of walleye. CDDs had a positive effect on larval walleye growth (P = 0.04) but a negative effect on large walleye growth (P = 0.08; Fig. 5). Larval walleye at more northern latitudes were around 180 mm TL when collected in the fall, whereas those collected in southern latitudes were over 220 mm TL. Large walleye grew over 50 mm from the time they were stocked until they were collected at northern latitudes but only grew 36 mm in the same time period at more southern latitudes.

Zooplankton density did not affect growth of larval (r = –0.10, n = 8, P = 0.81), small (r = 0.01, n = 14, P = 0.96), or large (r = 0.25, n = 5, P = 0.68) walleye. However, growth of both small and large walleye increased with benthic invertebrate density. Large walleye were influenced by total ben-

Table 3. Multiple regression analysis of factors affecting survival (fall catch-per-unit-effort) of three size classes of stocked walleye (*Sander vitreus*) in Illinois lakes from 1991 to 1997.

Size	Variable	Coefficient	Partial R^2	Model R^2	F value	P value
Larval	Log(cooling degree-days)	−1.49	0.73	0.73	5.66	0.06
	Log(benthic invertebrate density)	1.13	0.13	0.86	23.23	<0.01
	Log(centrarchid density)	−1.35	0.11	0.97	16.90	<0.01
	Overall model	2.73*		0.97	50.52	<0.01
Small	Forage fish density	0.06	0.44	0.44	10.56	<0.01
	Benthic invertebrate density	0.00008	0.13	0.57	3.42	0.09
	Overall model	−0.05*		0.57	7.37	<0.01
Large	Benthic invertebrate density	0.0007	0.63	0.63	5.06	0.09
	Log(cooling degree-days)	−13.93	0.20	0.83	4.56	0.10
	Overall model	42.8*		0.83	9.51	0.03

*Intercept value for multiple regression model.

Fig. 4. Survival of (*a*) larval, (*b*) small, and (*c*) large fingerling walleye (*Sander vitreus*) related to cooling degree-days (CDDs) in Illinois during 1991–1997. Catch-per-unit-effort (CPUE) is the mean number of walleye collected per hour of night electrofishing the fall following stocking. Each data point represents a mean value of CPUE and CDDs across years for each lake.

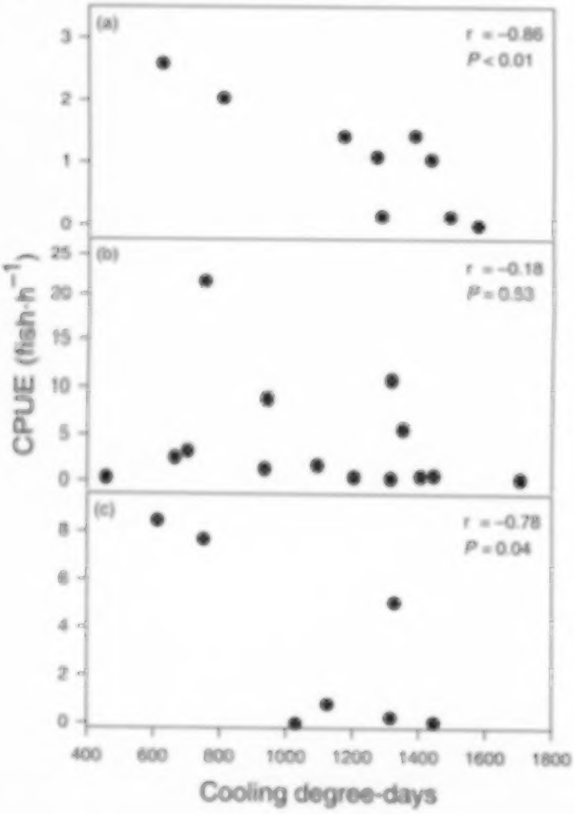

Fig. 5. Growth of (*a*) larval, (*b*) small, and (*c*) large fingerling walleye (*Sander vitreus*) related to cooling degree-days (CDDs). Growth is presented as the difference in total length (TL) between time stocked and time collected in fall. Each data point represents a mean value of growth and CDDs across years for each lake.

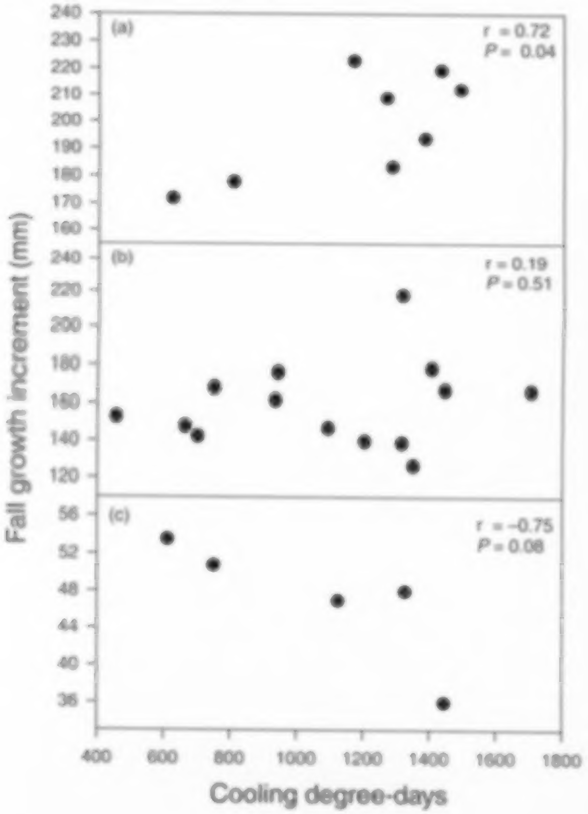

thic invertebrate density (P = 0.03; Fig. 6), whereas small walleye growth was related to chironomid density (P = 0.03; Fig. 6). Despite the fact that forage fish were important for survival, there were no relationships with growth of larval (r = 0.42, n = 8, P = 0.29), small (r = −0.18, n = 14, P = 0.55), or large (r = −0.08, n = 5, P = 0.89) walleye.

Total benthic invertebrate density and CDDs explained 98% of the variability in large fingerling walleye growth (multiple regression, P = 0.02; Table 4). Growth of small fingerlings was best explained by chironomid density and CDDs (R^2 = 0.55, P = 0.01; Table 4). Most of the variability in growth of larval walleye was accounted for by CDDs

Table 4. Multiple regression analysis of factors affecting first-year growth of three size classes of stocked walleye (*Sander vitreus*) in Illinois lakes from 1991 to 1997.

Size class	Variable	Coefficient	Partial R^2	Model R^2	F value	P value
Larval	Log(cooling degree-days)	79.76		0.52	6.4	0.04
	Overall model	–35.38*		0.52	6.4	0.04
Small	Chironomid density	0.02	0.34	0.34	12.67	<0.01
	Log(cooling degree-days)	71.39	0.22	0.55	5.29	0.04
	Overall model	–73.81*		0.55	6.80	0.01
Large	Benthic invertebrate density	0.002	0.82	0.82	43.30	0.02
	Log(cooling degree-days)	–19.43	0.16	0.98	21.24	0.04
	Overall model	96.18*		0.98	65.11	0.02

*Intercept value for multiple regression model.

Fig. 6. Growth of (*a*) large and (*b*) small walleye (*Sander vitreus*) related to invertebrate densities ($N\cdot m^{-2}$). Growth is presented as the difference in total length (TL) between time stocked and time collected in fall. Each data point represents a mean value of growth and invertebrate densities across years for each lake.

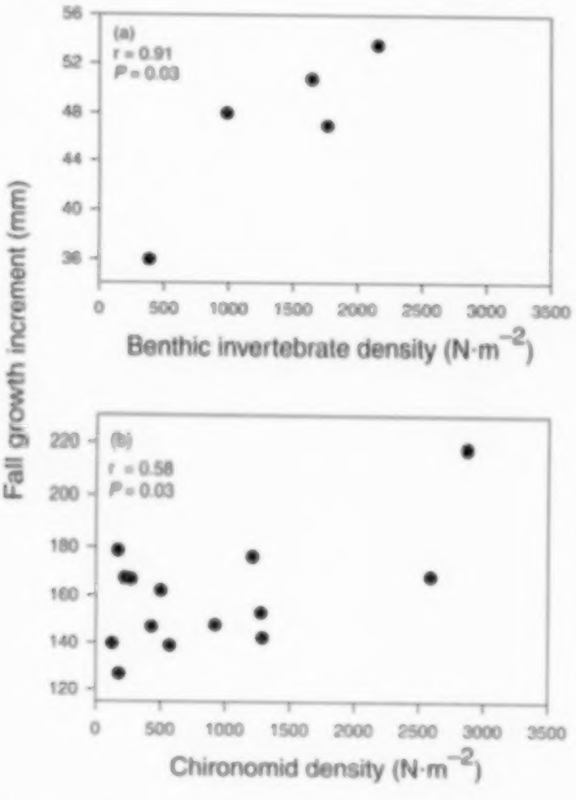

($r^2 = 0.52$, $P = 0.04$; Table 4) and was not improved by the addition of other variables.

Discussion

Factors affecting the growth and survival of fish change during the first year of life and are often dependent on fish size (Mathias and Li 1982; Ludsin and DeVries 1997). Interactions between environmental variables and fish size have led to a broader (i.e., multiple life stage) approach to understanding fish recruitment. For example, largemouth bass recruitment depends on hatch date, the timing of piscivory, and overwinter survival, all of which are interdependent (Olson 1996; Ludsin and DeVries 1997; Parkos and Wahl 2002). Our study demonstrates that growth and survival of walleye are also size-dependent and that important mechanisms vary with size. Prey abundance was important in determining growth and survival of all sizes of walleye, but importance of specific taxa varied with size. Predation only affected larval walleye survival, whereas temperature affected growth and survival of both larval and large walleye.

Despite zooplankton being an important food resource for age-0 walleye (Houde 1967; Priegel 1969; Hoxmeier et al. 2004), zooplankton abundance was not correlated with either growth or survival of any size group of walleye in our study. In controlled manipulative experiments, zooplankton density has been shown to be important for growth and survival of larval walleye during the first 3 weeks of life (Li and Mathias 1982; Mayer and Wahl 1997; Hoxmeier et al. 2004). Despite attempts to collect larval walleye several weeks after stocking, we were unable to effectively sample walleye until the first fall. If zooplankton abundance did affect early growth and survival of larval walleye, we may not have been able to detect it given the long duration between stocking and subsequent estimates of survival. These results suggest that although zooplankton abundance could be important in determining early growth and survival, other factors during later life stages can mask its effect on overall first-year success.

Growth and survival for all size classes of walleye increased with benthic invertebrate density (with the exception of larval growth), indicating the importance of these prey items for age-0 walleye. Previous studies have shown that 35–50 mm TL walleye depend on macroinvertebrates as prey, particularly chironomids (Priegel 1969; Mathias and Li 1982; Fox 1989). Although fish can be an important diet item for age-0 walleye (Parsons 1971; Hartman and Margraf 1992; Kolar et al. 2003), we did not observe any influence of forage fish on walleye growth for any size class of walleye. In addition, forage fish abundance did not effect survival of either larval or large walleye. Similar to our results, Fielder (1992) did not find a relationship between juvenile fish abundance and walleye survival in Lake Oahe. Several possible explanations exist for why we did not find an effect of forage fish on walleye growth or survival. First, our study lakes had abundant centrarchid prey, which can result in slower growth of age-0 walleye than other taxa (Santucci and Wahl 1993). Second, juvenile centrarchids may have been acting as direct competitors with age-0 walleye for prey resources. Lastly, not all forage fish may have been vulnerable to predation by stocked walleye because of differing habitat preferences or gape limitations. In contrast to other size classes, survival of small fingerling walleye was positively affected by forage fish density. Positive relationships have also been observed between small fingerling saugeye (*Sander vitreus* × *S. canadensis*) (34–39 mm TL) survival and larval fish abundance (Stahl and Stein 1994; Stahl et al. 1996). For larval and large sizes, our results suggest that invertebrate prey can be beneficial to growth and survival of age-0 walleye, especially in lakes with abundant centrarchids. That small fingerlings relied more on fish prey than invertebrates suggests that the importance of prey type is dependent on walleye size.

Diet selection for age-0 walleye depends on both body size and prey availability (Priegel 1969; Mathias and Li 1982; Hoxmeier et al. 2004). Differences in prey importance in our study for various sizes of walleye may relate to the timing of walleye introduction. Larval walleye were stocked before their diet shift to benthic invertebrates, thus they were able to take full advantage of these prey, as indicated by the strong relationship we observed with growth and survival. Because walleye typically feed on invertebrates and fish for a longer time period than zooplankton during the first year of life, the importance of zooplankton may have been reduced. In contrast, small and large walleye were stocked at a size when they should have been feeding primarily on fish. Walleye typically switch to a predominantly fish diet once they reach 60–80 mm TL (Priegel 1969; Galarowicz and Wahl 2005). Although our large walleye were beyond those sizes, their survival was not related to prey fish abundance. Large walleye at the time of stocking were smaller than sizes achieved by earlier stocked larval and small size classes (see Brooks et al. 2002). Gape limitation may have prevented the large size class from taking advantage of age-0 forage fish. The lack of appropriately sized fish prey may have forced large walleye to feed on invertebrates (Kolar et al. 2003). Potential relationships between large sizes of walleye and prey fish abundance also could have been obscured by the short time period between stocking and recapture (2 months). However, abundance the following spring also did not show any relationship with prey fish. Conversely, small walleye were stocked at a time when they were able to feed on most available juvenile prey fish, resulting in strong relationship for both growth and survival.

Predation can be an important source of mortality for age-0 fish (Forney 1976; Kim and DeVries 2001) and can reduce the survival of stocked fish (Santucci and Wahl 1993; Wahl et al. 1995). Predation rates on young walleye can vary with walleye size (Santucci and Wahl 1993), abundance, species composition, and size distribution of the predator population (Wahl et al. 1995) and presence of alternate prey (Forney 1976). The negative relationship between small centrarchids and walleye fry survival in our study suggests that predation was an important source of mortality for these sizes. Predation on larval fish is difficult to assess directly in the field because of fast digestion of fish larvae. However, several studies have demonstrated high mortality for recently stocked larval fish of other species based on stomach contents of predators (Johnson and Dropkin 1992; Henderson and Letcher 2003), supporting our conclusions. Additionally, experimental studies have shown that centrarchids can reduce larval fish abundance through predation (Kim and DeVries 2001; Quist et al. 2003). In contrast with larval fish, we did not observe an effect of predation on larger size classes. Our study lakes had abundant centrarchid predator populations when compared with other studies in which predation has been found to be important (Santucci and Wahl 1993). However, fish communities in this previous work contained only centrarchid prey, and the presence of gizzard shad as alternate prey in our study systems may have reduced predation rates on fingerling walleye. Similarly, predation did not effect saugeye survival in Ohio reservoirs that had high shad densities (Stahl et al. 1996).

Latitude influenced both growth and survival of walleye. Cooler water temperatures in northern lakes when walleye were introduced probably increased initial survival because of lower stocking stress (Santucci and Wahl 1993; Clapp et al. 1997). Large sizes also survived and grew better in northern latitudes, where water temperatures were closer to those reported for optimal growth (22 °C; Huh et al. 1976), than in southern lakes. Increased growth of larval and small walleye in southern latitudes may have resulted from warmer spring water temperatures. Warmer water temperatures in early summer have been shown to increase growth of age-0 walleye (Forney 1966; Serns 1982). In addition to obvious climatic differences across latitudes, benthic invertebrate densities also covaried, with higher densities in northern latitude lakes. Future studies will be required to separate the relative importance of invertebrate densities and water temperatures across broad geographic areas.

Prediction has recently been revisited as an important goal in fisheries management (Pace 2001). However, predicting the success of stocking or recruitment of naturally reproducing walleye has been difficult given the changing requirements with size during the first year of life. Despite the dynamic nature of these relationships, our best predictive models explained a high proportion of both survival (57%–97%) and growth (52%–98%) across sizes. Previous studies in single lakes also explained a high proportion of natural recruitment. Spawner abundance, gizzard shad abundance the previous fall, and spring warming rate explained 92% of the variation in walleye recruitment in Lake Erie (Madenjian et al. 1996), and in Escanaba Lake, Wisconsin, 89% was explained by spawner abundance, May water temperatures, and yellow perch abundance (Hansen et al. 1998). However, when multiple lakes have been used in predictive models, often times much less variation in recruitment is explained. For example, in a number of Kansas reservoirs, only 31% of the variation in walleye recruitment was explained by spring water temperatures, white crappie abundance, and spring storage ratio (Quist et al. 2003). We believe that our high predictive values are a result of including important variables that influence a number of life stages of walleye. In addition, in contrast to previous models, because walleye in our study were not naturally produced, spawning stock could not affect recruitment. Our results suggest that prey abundance, predators, and abiotic factors can all affect recruitment independent of parental stock size. The models we developed can be combined with estimates of larval or juvenile densities to effectively forecast walleye recruitment to the fishery.

Our models can also be useful in matching the size of walleye and the appropriate lake characteristics to optimize stocking success. Walleye stocking is an important management tool used throughout North America, although success of this practice often varies. Stocking larger sizes generally increases survival (Paragamian and Kingery 1992; Santucci and Wahl 1993); however, recent studies have shown that this is not always the best strategy (Koppelman et al. 1992; Olson et al. 2000; Brooks et al. 2002). Our results suggest that size of walleye to be stocked should be based on lake characteristics. Because walleye fry are less expensive to produce than fingerlings, these practices may be effective in northern latitude lakes with low centrarchid densities. In northern lakes in which centrarchid predation is high, large sizes of walleye should be considered for stocking. In lakes with high abundance of small cyprinids and other prey fish, small sizes of walleye fingerlings can be effective regardless of latitude.

Acknowledgements

We thank staff of the Kaskaskia, Sam Parr, and Ridge Lake Biological Stations, Illinois Natural History Survey, and the Fisheries Research Laboratory at Southern Illinois University for their help in the field and laboratory, especially R. Anderson, J. Boase, M. Desjardins, L. Einfalt, K. Eisenbarth, T. Galarowicz, M. Garthaus, K. Goodwin, D. Harrison, P. Hayes, M. Herbert, M. Hooe, J. Jonas, C. Kolar, R. Mauk, C. Mayer, B. Nerbonne, D. Pavlik, D. Partridge, J. Ross, K. Schnake, B. Simms, E. Stark, J. Waddell, and R. Wagner. D. Clapp was instrumental in initial design and implementation of the study. J. Parkos and the Aquatic Ecology Discussion Group of the Kaskaskia Biological Station provided helpful reviews of this manuscript. D. Austen, K. Cottrell, J. Mick, M. Conlin, and L. Dunham coordinated activities with the Illinois Department of Natural Resources (IDNR). Walleye were provided by S. Krueger of Jake Wolf Memorial Fish Hatchery, IDNR, and E. Hansen of LaSalle Fish Hatchery, IDNR. This project was funded in part by the IDNR through Federal Aid in Sport Fish Restoration, Project F-118-R.

References

Brooks, R.C., Heidinger, R.C., and Kohler, C.C. 1994. Mass-marking otoliths of larval and juvenile walleyes by immersion in oxytetracycline, calcein, or calcein blue. N. Am. J. Fish. Manag. **14**: 143–150.

Brooks, R.C., Heidinger, R.C., Hoxmeier, R.J.H., and Wahl, D.H. 2002. Relative survival of three sizes of walleyes stocked into Illinois lakes. N. Am. J. Fish. Manag. **22**: 995–1006.

Clapp, D.F., Bhagwat, Y., and Wahl, D.H. 1997. The effect of thermal stress on walleye fry and fingerling mortality. N. Am. J. Fish. Manag. **17**: 429–437.

Claramunt, R.M., and Wahl, D.H. 2000. The effects of abiotic and biotic factors in determining larval fish growth rates: a comparison across species and reservoirs. Trans. Am. Fish. Soc. **129**: 835–851.

Cohen, J., and Cohen, P. 1983. Applied multiple regression/correlation analysis for the behavioral sciences. 2nd ed. Lawrence Erlbaum Associates, Hillsdale, New Jersey.

Einfalt, L.M., and Wahl, D.H. 1997. Prey selection by juvenile walleye as influenced by prey morphology and behavior. Can. J. Fish. Aquat. Sci. **54**: 2618–2626.

Fielder, D.G. 1992. Evaluation of stocking walleye fry and fingerlings and factors affecting their success in lower Lake Oahe, South Dakota. N. Am. J. Fish. Manag. **12**: 336–345.

Forney, J.L. 1966. Factors affecting first-year growth of walleyes in Oneida Lake, New York. N.Y. Fish Game J. **13**: 146–167.

Forney, J.L. 1976. Year-class formation in the walleye (*Stizostedion vitreum vitreum*) population of Oneida Lake, New York, 1966–73. J. Fish. Res. Board Can. **33**: 783–792.

Foster, J.R. 1977. Pulsed gastric lavage: an efficient method of removing the stomach contents of live fish. Prog. Fish-Cult. **39**: 166–169.

Fox, M. 1989. Effect of prey density and prey size on growth and survival of juvenile walleye (*Stizostedian vitreum vitreum*). Can. J. Fish. Aquat. Sci. **46**: 1323–1328.

Galarowicz, T.L., and Wahl, D.H. 2005. Foraging by a young-of-year piscivore: the role of predator size, prey type, and density. Can. J. Fish. Aquat. Sci. **62**: 2330–2342.

Hansen, M.J., Bozek, M.A., Newby, J.R., Newman, S.P., and Staggs, M.D. 1998. Factors affecting recruitment of walleyes in Escanaba Lake, Wisconsin, 1958–1996. N. Am. J. Fish. Manag. **18**: 764–774.

Hartman, K.J., and Margraf, F.J. 1992. Effects of prey and predator abundances on prey consumption and growth of walleyes in western Lake Erie. Trans. Am. Fish. Soc. **121**: 245–260.

Henderson, J.N., and Letcher, B.H. 2003. Predation on stocked Atlantic salmon (*Salmo salar*) fry. Can. J. Fish. Aquat. Sci. **60**: 32–42.

Houde, E.D. 1967. Food of pelagic young of the walleye, *Stizostedion vitreum vitreum*, in Oneida Lake, New York. Trans. Am. Fish. Soc. **96**: 17–24.

Houde, E.D. 1987. Fish early life dynamics and recruitment variability. *In* 10th Annual Larval Fish Conference. *Edited by* R.D. Hoyt. Am. Fish. Soc. Symp. **2**: 17–29.

Hoxmeier, R.J.H., and Wahl, D.H. 2002. Evaluation of supplemental stocking of largemouth bass across reservoirs: effects of predation, prey availability, and natural recruitment. *In* Black bass: ecology, conservation, and management. *Edited by* D.P. Philipp and M.S. Ridgeway. Am. Fish. Soc. Symp. **31**: 639–647.

Hoxmeier, R.J.H., Wahl, D.H., Hooe, M.L., and Pierce, C.L. 2004. Growth and survival of larval walleyes in response to prey availability. Trans. Am. Fish. Soc. **133**: 45–54.

Huh, H.T., Calbert, H.E., and Stuiber, D.A. 1976. Effects of temperature and light on growth of yellow perch and walleye using formulated feed. Trans. Am. Fish. Soc. **105**: 254–258.

Johnson, J.H., and Dropkin, D.S. 1992. Predation on recently released larval American shad in the Susquehanna River basin. N. Am. J. Fish. Manag. **12**: 504–508.

Kim, G.W., and DeVries, D.R. 2001. Adult fish predation on freshwater limnetic fish larvae: a mesocosm experiment. Trans. Am. Fish. Soc. **130**: 189–203.

Kolar, C.S., Wahl, D.H., and Hooe, M.L. 2003. Piscivory in juvenile walleyes: relative importance of prey species, timing of spawning of prey fish, and density on growth and survival. Trans. Am. Fish. Soc. **132**: 679–690.

Koppelman, J.B., Sullivan, K.P., and Jeffries, P.J., Jr. 1992. Survival of three sizes of genetically marked walleyes stocked into two Missouri impoundments. N. Am. J. Fish. Manag. **12**: 291–298.

Li, S., and Mathias, J.A. 1982. Causes of high mortality among cultured larval walleyes. Trans. Am. Fish. Soc. **111**: 710–721.

Ludsin, S.A., and DeVries, D.R. 1997. First-year recruitment of largemouth bass: the interdependency of early life stages. Ecol. Appl. **7**: 1024–1038.

Madenjian, C.P., Tyson, J.T., Knight, R.L., Kershner, M.W., and Hansen, M.J. 1996. First-year growth, recruitment, and maturity of walleyes in western Lake Erie. Trans. Am. Fish. Soc. **125**: 821–830.

Mathias, J.A., and Li, S. 1982. Feeding habits of walleye larvae and juveniles: comparative laboratory and field studies. Trans. Am. Fish. Soc. **111**: 722–735.

Mayer, C.M., and Wahl, D.H. 1997. The relationship between prey selectivity and growth and survival in a larval fish. Can. J. Fish. Aquat. Sci. **54**: 1504–1512.

Miller, T.J., Crowder, L.B., Rice, J.A., and Marschall, E.A. 1988. Larval size and recruitment mechanisms in fishes: toward a conceptual framework. Can. J. Fish. Aquat. Sci. **45**: 1657–1670.

Olson, M.H. 1996. Ontogenetic niche shifts in largemouth bass: variability and consequence for first year growth. Ecology, **77**: 179–190.

Olson, M.H., Brooking, T.E., Green, D.M., VanDeValk, A.J., and Rudstam, L.G. 2000. Survival and growth of intensively reared large walleye fingerlings and extensively reared small fingerlings stocked concurrently in small lakes. N. Am. J. Fish. Manag. **20**: 337–348.

Pace, M.L. 2001. Prediction and the aquatic sciences. Can. J. Fish. Aquat. Sci. **58**: 63–72.

Paragamian, V.L., and Kingery, R. 1992. A comparison of walleye fry and fingerling stockings in three rivers in Iowa. N. Am. J. Fish. Manag. **12**: 313–320.

Parkos, J.J., III, and Wahl, D.H. 2002. Towards an understanding of recruitment mechanisms in largemouth bass. *In* Black bass: ecology, conservation, and management. *Edited by* D.P. Philipp and M.S. Ridgeway. Am. Fish. Soc. Symp. **31**: 25–45.

Parsons, J.W. 1971. Selective food preferences of walleyes of the 1959 year class in Lake Erie. Trans. Am. Fish. Soc. **100**: 474–485.

Priegel, G.R. 1969. Food and growth of young walleyes in Lake Winnebago, Wisconsin. Trans. Am. Fish. Soc. **98**: 121–124.

Quist, M.C., Guy, C.S., and Stephen, J.L. 2003. Recruitment dynamics of walleyes (*Stizostedion vitreum*) in Kansas reservoirs: generalities with natural systems and effects of a centrarchid predator. Can. J. Fish. Aquat. Sci. **60**: 830–839.

Rice, J.A., Crowder, L.B., and Binkowski, F.P. 1987. Evaluating potential mortality for larval bloater (*Coregonus hoyi*): starvation and vulnerability to predation. Can. J. Fish. Aquat. Sci. **44**: 467–472.

Santucci, V.J., Jr., and Wahl, D.H. 1993. Factors influencing survival and growth of stocked walleye (*Stizostedion vitreum*) in a centrarchid-dominated impoundment. Can. J. Fish. Aquat. Sci. **50**: 1548–1558.

SAS Institute Inc. 2001. SAS/STAT user's guide. Release 8.02 ed. SAS Institute Inc., Cary, N.C.

Serns, S.L. 1982. Influence of various factors on density and growth of age-0 walleyes in Escanaba Lake, Wisconsin, 1958–1980. Trans. Am. Fish. Soc. **111**: 299–306.

Stahl, T.P., and Stein, R.A. 1994. Influence of larval gizzard shad (*Dorosoma cepedianum*) density on piscivory and growth of young-of-year saugeye (*Stizostedion vitreum* × *S. canadense*). Can. J. Fish. Aquat. Sci. **51**: 1993–2002.

Stahl, T.P., Thiede, G.P., Stein, R.A., Lewis, E.M., Austin, M.R., and Culver, D.A. 1996. Factors affecting survival of age-0 saugeye *Stizostedion vitreum* × *S. canadense* stocked in Ohio reservoirs. N. Am. J. Fish. Manag. **16**: 378–387.

Wahl, D.H., and Stein, R.A. 1989. Comparative vulnerability of three esocids to largemouth bass (*Micropterus salmoides*) predation. Can. J. Fish. Aquat. Sci. **46**: 2095–2103.

Wahl, D.H., Stein, R.A., and DeVries, D.R. 1995. An ecological framework for evaluating the success and effects of stocked fishes. *In* Uses and effects of cultured fishes in aquatic ecosystems. *Edited by* H.L. Schramm, Jr., and R.G. Piper. Am. Fish. Soc. Symp. **15**: 176–189.

Welker, M.T., Pierce, C.L., and Wahl, D.H. 1994. Growth and survival of larval fishes: roles of competition and zooplankton abundance. Trans. Am. Fish. Soc. **123**: 703–717.

Ultraviolet vision and foraging in juvenile bluegill (*Lepomis macrochirus*)

Dina M. Leech and Sönke Johnsen

Abstract: Ultraviolet (UV) photoreceptors have been reported in a wide variety of freshwater and marine organisms, suggesting that UV vision is prominent in aquatic ecosystems. However, its adaptive significance remains speculative. The present study tested whether the foraging of juvenile bluegill (*Lepomis macrochirus*) is enhanced in the presence of UV radiation (UVR). Laboratory feeding trials were conducted in a laminar flow tank in which *L. macrochirus* juveniles between 2.3 and 3.5 cm standard length were fed the cladoceran *Daphnia magna*. Sighting and striking distances, as well as capture success, were measured in the presence and absence of UVR. Mean sighting and striking distances and capture success did not differ significantly between the two light treatments. There were also no significant differences in the frequency distributions of sighting and striking distance. These results suggest that UV vision may not be used to enhance foraging in *L. macrochirus* on *Daphnia* within the size class tested.

Résumé : Les photorécepteurs d’ultraviolet (UV) sont connus chez une grande variété d’organismes d’eau douce et d’organismes marins, ce qui laisse croire que la vision UV est importante dans les écosystèmes aquatiques. Cependant, on ne peut que spéculer sur leur signification adaptative. Notre étude vérifie si la recherche de nourriture chez de jeunes crapets arlequins (*Lepomis macrochirus*) est améliorée en présence de radiation ultraviolette (UVR). Nous avons fait des essais alimentaires en laboratoire dans un aquarium à flux laminaire dans lequel des jeunes *L. macrochirus* de 2,3–3,5 cm de longueur standard ont été nourris de cladocères *Daphnia magna*. Nous avons mesuré les distance de repérage et d’attaque, de même que le succès de capture, en présence et en l’absence de UVR. Il n’y a pas de différence significative dans les distances moyennes de repérage et d’attaque, ni dans les taux moyens de capture, dans les deux régimes lumineux. Il n’y a pas non plus de différences significatives dans les distributions de fréquence des distances de repérage et d’attaque. Ces résultats indiquent que la vision UV ne sert sans doute pas à améliorer la recherche de nourriture chez les *L. macrochirus* sur les *Daphnia* de la classe de taille examinée.

[Traduit par la Rédaction]

Introduction

Ultraviolet (UV) vision is widespread throughout the animal kingdom, including terrestrial and aquatic organisms (Goldsmith and Bernard 1985; Jacobs 1992; Tovee 1995). Among aquatic organisms, most UV photoreceptors have been described in fish species, although UV photosensitivity has also been reported in annelids, cnidarians, and crustaceans (reviewed by Leech and Johnsen 2003). UV sensitivity, in coordination with other photoreceptor channels, allows the visual systems of organisms that contain them to make certain discriminations, such as the electric field vector, or e-vector, distribution of polarized skylight (Hawryshyn 1992; Parkyn and Hawryshyn 1993) and color (Jacobs 1992; Coughlin and Hawryshyn 1994). Recognition and communication between conspecifics and mates at UV wavelengths is suggested in certain species of coral reef fish (Shashar 1994; Losey et al. 1999; Siebeck 2004) and is demonstrated in the guppy, *Poecilia reticulata* (Smith et al. 2002), and the Panuco swordtail, *Xiphophorus nigrensis* (Cummings et al. 2003).

UV vision is also thought to enhance prey contrast (Loew et al. 1993; Browman et al. 1994; Shashar 1994). Relatively transparent planktonic prey, both freshwater and marine, absorb light at UV wavelengths (Loew and McFarland 1990; Johnsen and Widder 2001). Because of this, these zooplankters may appear darker against a bright UV-rich background. In addition, planktonic prey also scatter or reflect UV and thus may appear lighter or darker depending on the direction of illumination (Loew and McFarland 1990). Laboratory experiments have demonstrated that larval fish and salmonid alevins within the genera *Lepomis*, *Perca*, and *Oncorhynchus* catch more prey (Loew et al. 1993) and have longer pursuit distances (Browman et al. 1994) in the presence of UV radiation (UVR). Furthermore, some species can feed under UV-A radiation alone (Loew et al. 1993). Predation rates of African cichlids feeding on *Artemia* spp. were greater for species with UV sensitivity compared with those without (Jordan et al. 2004). However, recent experiments with rainbow trout, *Oncorhynchus mykiss*, suggest that UV vision does not enhance foraging under natural levels of solar radiation (Rocco et al. 2002). Similar results also were found for the guppy feeding on *Daphnia pulex* under artificial illumination (White et al. 2005). Interestingly, although guppy for-

Received 9 December 2005. Accepted 18 May 2006.
Published on the NRC Research Press Web site at
http://cjfas.nrc.ca on 16 September 2006.
J19041

D.M. Leech[1,2] and S. Johnsen. Biology Department, Duke University, Durham, NC 27708, USA.

[1] Corresponding author (e-mail: dmleech@email.unc.edu).
[2] Present address: Department of Environmental Sciences and Engineering, University of North Carolina, Chapel Hill, NC 27599, USA.

Can. J. Fish. Aquat. Sci. 63: 2183–2190 (2006) doi:10.1139/F06-107

aging efficiency was not enhanced by UV, a significant UV effect on mate choice has been demonstrated in previous experiments (Smith et al. 2002).

The objective of the present study was to determine if prey detection in juvenile bluegill (*Lepomis macrochirus*) improves in the presence of UVR. We chose bluegill feeding on *Daphnia* as our model system as both are widely distributed in fresh waters across North America and have been the focus of numerous feeding studies in the past. For example, Vineyard and O'Brien (1976) reported a reduction in the reaction distance of bluegill feeding on daphnia as visible illumination decreased and turbidity increased. Luecke and O'Brien (1981) noted that bluegill (5–9 cm in length) are better able to feed when presented daphniid prey in the forward hemisphere, and sighting distances are often greater than striking distances at both low and high light intensities.

Here laboratory feeding trials were conducted in a laminar flow tank in which sighting and striking distances of bluegill feeding on *Daphnia* prey were measured in the presence and absence of UVR. Placing the fish in laminar flow allows for better control of fish location and orientation and offers a promising technique for testing similar types of behavioral questions. UV and visible spectral reflectance of *Lepomis* and *Daphnia* were also measured.

Materials and methods

Study organism

Bluegill juveniles were collected from a shallow pond in Gainesville, Florida (29.7°N, 82.3°W), on 21 January 2003 (M. Allen, Department of Fisheries and Aquatic Sciences, University of Florida, Gainesville, FL 32611, USA) and were housed in a 50-gallon tank in the laboratory at Duke University, Durham, North Carolina, USA. Fish were kept at 22–23 °C under room illumination and fed fish pellets. All fish were cared for in accordance with established humane protocols (Duke University IACUC Protocol Number A-153-02-05).

Lepomis UV sensitivity test

UV photoreceptors have been detected in pumpkinseed, *Lepomis gibbosus* (Loew et al. 1993), and unusually large beta band absorption has been observed in the red photoreceptor of juvenile bluegill (E. Loew, Program in Physiology, Cornell University, Ithaca, NY 14853, USA, unpublished data). Together, these suggested that bluegill may also have UV sensitivity, via either a UV photopigment or beta band absorption of the red pigment, as is the case for some bats (e.g., *Glossophaga soricina*, Winter et al. 2003). UV sensitivity associated with a beta band would not allow for a chromatic mechanism in the UV, but nevertheless allows for sensitivity to UVR. Preliminary experiments tested for UV sensitivity in the following manner. Ten juvenile bluegill similar in size to those used in the experimental study were adapted to a dim incandescent light and then exposed to flashes of UVR using a UV lamp (UVL-21, UVP, Upland, California, USA) fitted with a Hoya U-330 visible-blocking filter (Edmund Optics, Barrington, New Jersey, USA). The wavelength of peak emission was 366 nm, with a full-width half-maximum of 12 nm (measured using the USB2000 spectroradiometer fitted with a cosine collector; CC3, Ocean Optics Inc., Dunedin, Florida, USA). The integrated irradiance at 5 cm from the lamp was 1.5×10^{15} photons·cm^{-2}·s^{-1}, which is approximately equal to the irradiance in this waveband at noon. No radiation at visible wavelengths could be measured. The low level of fluorescence induced by the UV source was insignificant compared with the adapting illumination and could not be detected. In response to these flashes of UVR, the fish initially exhibited a jerking response and would sometimes swim towards the lamp. These responses do not confirm that the bluegill possess UV-A photoreceptors but do demonstrate UV sensitivity.

Reflectance measurements

Diffuse reflectance of fish and *Daphnia* were measured using the USB2000 spectroradiometer fitted with a reflectance probe (R400-7, Ocean Optics). The sensor was placed at a 45° angle and calibrated using a white standard (WS-1, Ocean Optics). Fish and *Daphnia* were patted dry, placed on a white background, and measured. UV and visible reflectance was averaged over three to five measurements. For the bluegill, measurements were taken at different locations on the body from the head to the tail, including the abdomen, caudal peduncle, and the caudal fin.

Experimental apparatus and lamp setup

Experiments were conducted in a laminar flow tank designed and built by S. Vogel, Duke University (Fig. 1). The tank consists of a rectilinear working section (76 cm × 10 cm × 12.5 cm), connected at both ends with 7 cm diameter polyvinyl chloride (PVC) tubing. A propeller connected to a variable-speed motor (Master Motor 20000 Series, Minarik Corp., Glendale, California, USA) is housed at one end of the working section. Laminar flow is maintained using honeycombs of hollow tubes (diameter = 5 mm) placed upstream and downstream of the working section. The flow tank was kept in a darkened room and filled with 48 µm filtered, clear water taken from the 50-gallon housing tank. A 1 cm^2 grid was placed along the back wall of the working section of the tank to measure sighting and striking distances of the fish, and a video camera was placed on the opposite side of the rectilinear working section from the grid to record experiments.

One 1.2 m Vita-Lite (Duro-Test Corporation, Philadelphia, Pennsylvania, USA) was mounted 20 cm directly above the surface of the water. The same UV lamp used in the preliminary studies, but without the visible-blocking filter, was placed directly above the surface of the working section 23 cm downstream from a white Nytex mesh screen. The lamp was angled such that the UVR reflected off the screen upstream of the fish, increasing UV radiance in the horizontal direction. UV irradiance in the flow tank was controlled by placing either UV-transparent (OP-4, Cyro Industries, New Jersey, USA) or UV-opaque (UF3, Polycast Inc., Stamford, Connecticut, USA) acrylic over the working section. The flow tank itself was constructed out of UV-opaque acrylic so that UVR could only enter the tank from above. Preliminary experiments showed that under the full output of the Vita-Lite, the presence or absence of UVR had no effect on the sighting or striking distance of the fish. Therefore, metal window screening was used to reduce the lamp output and replicate twilight conditions. Juvenile bluegills are thought to feed

Fig. 1. Schematic of the experimental laminar flow tank and lamp setup.

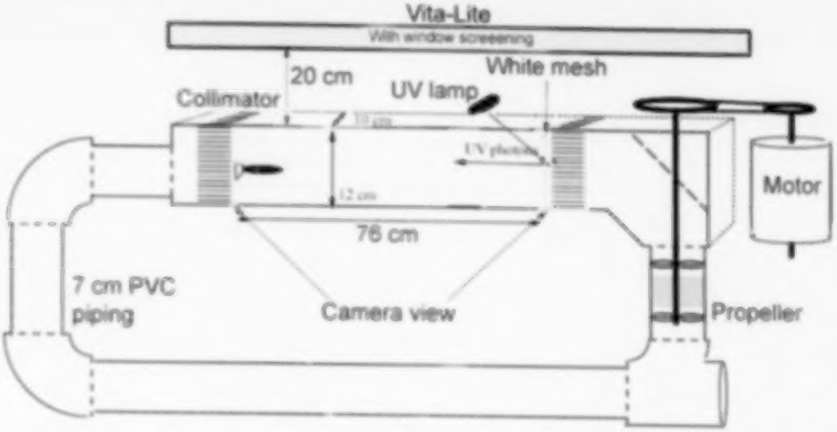

more actively at crepuscular periods (Keast and Welsh 1968), and the ratio of UV to visible light is also greater during these times of day (Novales-Flamarique and Hawryshyn 1997; Leech and Johnsen 2003). Downwelling quantal irradiance between 350 and 700 nm was kept constant between UV+ and UV– treatments by moving the tank 5.5 cm closer to the overhead lamp, as well as reducing the amount of window screening in the UV– treatment (Fig. 2).

Light measurements

The total number of photons in the fish's field of view was measured using a portable spectroradiometer (USB2000, Ocean Optics Inc., Dunedin, Florida, USA), calibrated using a NIST-traceable UV-visible calibration source (DH-2000-CAL, Ocean Optics). A 1 mm diameter fiber optic cable with an angle of acceptance of 24.8° was fitted to the spectroradiometer. The cable was placed at the position of the fish and directed towards the white Nytex mesh screen. The total number of photons within the field of view was measured from 300 to 700 nm under both UV+ and UV– lighting conditions (Fig. 2). The integrated quanta between the UV+ and UV– treatments were within 9.5% of each other (5.12×10^{11} and 4.65×10^{11} photons·cm^{-2}·s^{-1}, respectively). The light levels approximated those at civil twilight, which is defined as the period when the sun is between 0° and 6° below the horizon.

Experimental design

Fish were starved for 24 h before the start of the experiments. A fish (2.5–3.5 cm total length) was then randomly selected from the housing tank and placed into the flow tank. The lamps were turned on and the fish was allowed to acclimate for 2 h. After acclimation, the flow was incrementally increased to 3 cm·s^{-1}, at which point the fish oriented towards the oncoming current. Fish that did not orient were removed from the study. This flow rate represented the minimum speed at which the fish would orient. Additional speeds were not examined as the focus of our study was on sighting and striking distances in the presence and absence of UVR.

Once oriented, the fish was allowed to acclimate to the flow for an additional 10–15 min before the feeding trial began. Ten *D. magna* (1.3–1.5 mm total length) were introduced to the flow tank one at a time from a pipette placed at the upstream end of the flow tank. Each daphniid could only pass by the fish once, after which a successive daphniid was introduced. Daphnia that were not eaten were trapped behind the white mesh at the upstream end of the flow tank.

Fig. 2. Spectra of the ultraviolet plus (UV+) (solid line) and ultraviolet minus (UV–) (shaded line) treatments.

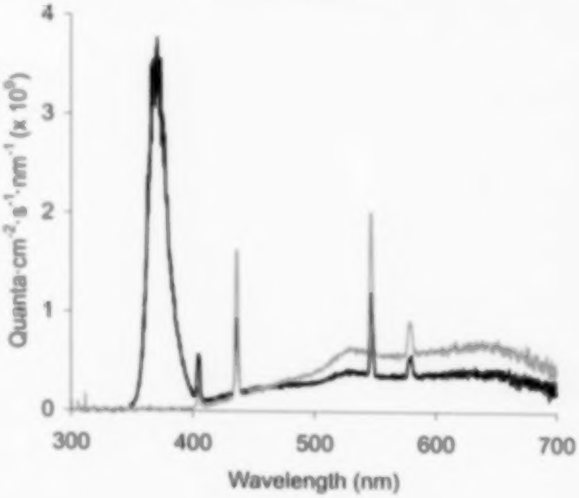

Feeding trials were videotaped and measurements of the sighting distance, striking distance, and capture success were measured later. Sighting distance was defined as the distance between the prey and the snout of the fish at the moment that the fish first cued into the prey (denoted by a d[illegible] positioning of the head towards the prey). Typically [illegible] sighted prey in a forward-looking position (i.e., infl[illegible] by flow), between 6 and 23 cm upstream. Daphnia w[illegible]cated closer to the surface of the water at times and n[illegible] bottom of the tank at other times. Striking distance [illegible]fined as the distance between the snout of the fish and the position of the prey at the moment that the fish lunged after the prey. Daphnia were termed missed if the fish did not see or strike at them or if they were missed during attempted strikes. Eleven fish were tested under UV+ conditions and 13 were tested under UV− conditions.

Statistics

Mean sighting and striking distances, as well as the mean number of missed daphniids, were calculated for each treatment. The mean ratios of sighting to striking distances were also computed. Using SigmaStat (SPSS Inc. 2003), one-way analyses of variance (ANOVA) were performed to test for significant differences between the two light treatments for sighting distance, striking distance, and capture success. A two-group, one-sided power analysis was also performed using SigmaStat to assess the strength of these statistical tests, assuming equal variances and $\alpha = 0.05$. A one-sided test was performed because it was predicted that sighting and striking distances would be greater in the presence of UV.

In addition, the data were analyzed as frequency distributions. The Kolmogorov–Smirnov (K–S) two-sample test was used to detect significant differences between the frequency distributions of the mean sighting and striking distance for each fish in the presence and absence of UVR (after Browman et al. 1994).

Results

Reflectance

Although overall diffuse reflectance was low (less than 6%), both the bluegills and the Daphnia had increased reflectance at UV wavelengths compared with visible wavelengths (Fig. 3). In bluegill, peak UV reflectance occurred at 335 nm, with similar peak reflectance values across the length of the body, except for the tail. Integrated reflectance in the UV spectrum (300–400 nm) was approximately 33% of that in the visible (400–700 nm). *Daphnia magna* peak reflectance occurred at 320 nm, with an additional broad peak occurring at 610 nm associated with the red coloration of the Daphnia carapace. Integrated reflectance in the UV spectrum was approximately 20% of that in the visible.

Sighting distance, striking distance, and capture success

There was no significant difference in the mean sighting distance ($F_{[1,23]} = 0.669$, $P = 0.42$) or striking distance ($F_{[1,23]} = 0.748$, $P = 0.40$) of the bluegills between the two light treatments (Fig. 4). The frequency distributions of the sighting and striking distances also did not differ significantly between the two light treatments ($P > 0.05$; Fig. 5). The ratio of sighting to striking distance was greater, although not significant, in the presence of UV ($F_{[1,23]} = 3.03$, $P = 0.10$; Fig. 4). An a posteriori power analysis indicated that with our sample size we had an 80% chance of detecting a statistically significant difference between UV+ and UV− treatments if the magnitude of differences between treatments was at least 26% (i.e., 4.1 cm) in sighting distance and at least 49% (i.e., 3.5 cm) in striking distance.

In addition, the number of missed Daphnia per fish did not differ significantly between the two light treatments ($F_{[1,23]} = 0.052$, $P = 0.82$; Fig. 4). On average, bluegill missed 2.5 ± 0.6 standard error (SE) daphnia per fish in both light treatments. The a posteriori power analysis indicated that we had an 80% chance of detecting a statistically significant difference between UV+ and UV− treatments if the difference was 99% or greater.

Fig. 3. Ultraviolet and visible reflectance measurements for (*a*) the bluegill sunfish (*Lepomis macrochirus*) body (solid line) and tail (shaded line) and (*b*) the cladoceran *Daphnia magna*.

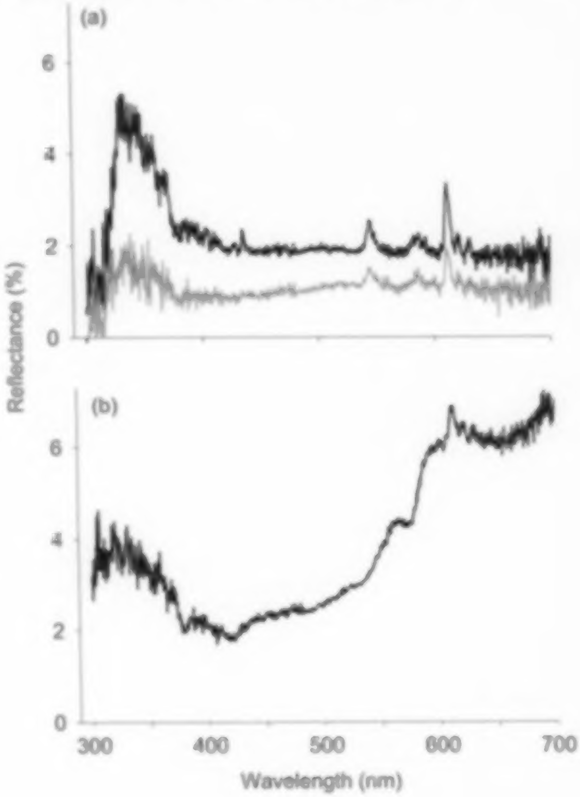

Discussion

In high-UV environments, UV sensitivity has been reported in over one-half of the fish species examined, spanning a wide diversity of freshwater and marine families (reviewed in Leech and Johnsen 2003). However, in low-UV environments, the percentage of fish with UV sensitivity decreases dramatically, suggesting that UV vision has some adaptive function (Douglas et al. 1998; Fuller et al. 2004). Although great strides have been made in identifying UV photoreceptors among fish species, our understanding of the roles of UV vision in fish and other aquatic organisms is limited.

In the present study, average sighting and striking distances, as well as capture success, did not significantly differ in the presence and absence of UVR, suggesting that UVR does not enhance bluegill foraging on *Daphnia* within the size class tested and may be used for other adaptive purposes. Similar results were found in juvenile rainbow trout (Rocco et al. 2002) and guppies (White et al. 2005), i.e., the presence of natural or artificial UV illumination did not enhance the number of prey eaten, prey choice, or sighting distances. However,

Fig. 4. Mean values for (*a*) *Lepomis* sighting and striking distance and (*b*) the ratio between sighting and striking distance and the number of missed *Daphnia* in the presence and absence of ultraviolet (UV) radiation. Solid symbols represent the UV+ treatment, open symbols represent the UV− treatment. Shaded lines denote range; error bars denote standard error.

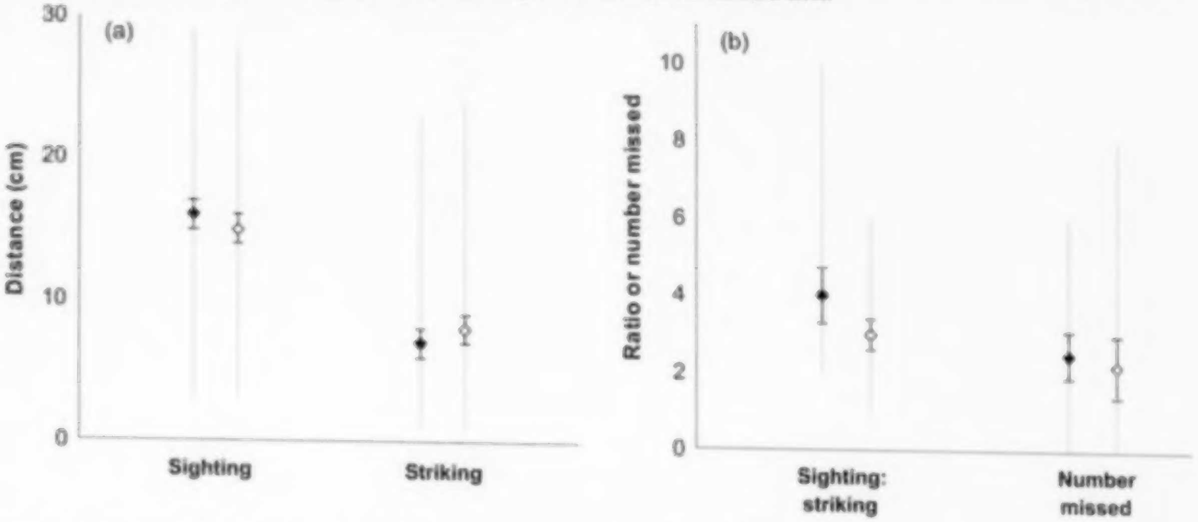

Fig. 5. Frequency distributions of (*a*) sighting distance and (*b*) striking distance for bluegill sunfish (*Lepomis macrochirus*) foraging in the presence (solid bars) and absence (open bars) of ultraviolet radiation.

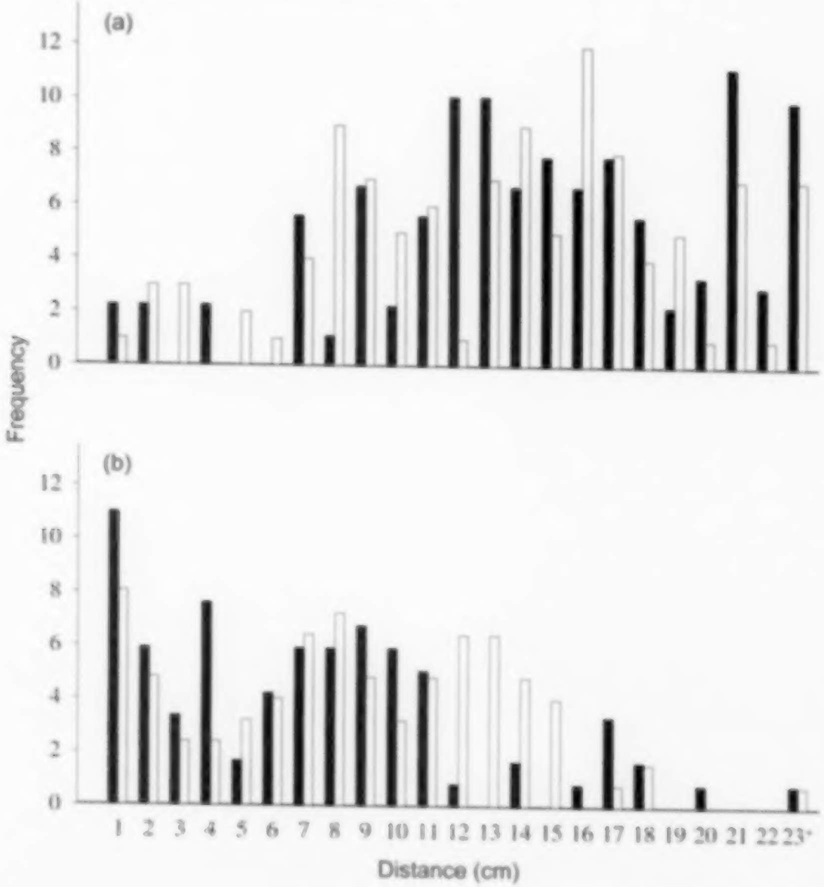

these results are in contrast to those reported by others in which pursuit distances in rainbow trout and number of prey eaten in pumpkinseed increased in the presence of UVR (Loew et al. 1993; Browman et al. 1994). Furthermore, laboratory experiments demonstrated that yellow perch (*Perca flavescens*) feed better under UV-A radiation alone compared with visible light, even when the quantal flux was less than that at longer wavelengths (Loew et al. 1993).

One possible explanation for the lack of enhanced UV foraging is that the addition of UVR did not sufficiently increase daphniid visibility. Although others have demonstrated that Daphnia scatter UVR (reviewed in Leech and Johnsen 2003), measured diffuse reflectance in the present study was low. UV reflectance was 20% less than visible reflectance, although the integrated visible range was three times larger (400–700 nm) than the UV (300–400 nm). In addition, daphniids typically do not absorb UVR because of a lack of UV-absorbing pigments in the cuticle. Copepods, however, are often highly UV absorptive, and thus using copepods instead of daphniids may have yielded a greater positive effect in UV foraging.

In the present study, as well as in others (Rocco et al. 2002; Jordan et al. 2004), it is important to note the size of the fish examined. Different populations of fish lose their UV photoreceptors at different sizes and (or) ages, thus using length and (or) weight as the sole criteria for presence or absence of UV photoreception is equivocal. It is possible that the bluegill used in our study did not possess UV-A photoreceptors even though UV sensitivity was demonstrated in the preliminary experiments. The presence of a UV-A photoreceptor could have yielded a greater UV effect on foraging than UV sensitivity associated with a beta band (e.g., increased chromatic contrast; Loew et al. 1993).

Experimental lighting conditions are also important to note. To maintain the same total quanta in the UV+ and UV– treatments, the tank was moved closer to the Vita-Lite in the UV– treatment, resulting in 33% more quanta in the visible spectrum of the UV– treatment compared with the UV+ treatment. If the fish were relying solely on visible light for foraging, one might expect an increase in sighting distance with increased visible light. However, based on theoretical modeling of visual summation under dim lighting conditions, the effect on contrast threshold is likely to be small (approximately 23% as calculated by the inverse square root of the photon flux; Theobald et al. 2006). In addition, the use of the white mesh created a bright UV-rich background upon which the daphniids were viewed in the horizontal direction, and a darker background may have provided different results. We chose to use the white mesh to more closely replicate natural conditions. In clear surface waters, the number of UV-A photons often approaches 40% of the total photons seen in the horizontal and downward directions (Losey et al. 1999). Finally, increased blue light relative to shorter wavelength UV can override or shut down the UV channel in some species (Hawryshyn 1991).

We recognize that a larger sample size would have increased the power of our study and may have revealed a significant difference in foraging between the two light treatments. We were able to detect significant UV effects on sighting distance with a difference of approximately 25% or greater with 80% power. It is possible that smaller effects on sighting distance may be present that were not detected. To detect a 10% (i.e., 1.55 cm) or greater difference in sighting distance, a sample size of 158 fish would be needed. Because of the high variability in striking distance, only a 49% or greater difference in this parameter could be detected with 80% power, and at least 215 fish would be needed to detect a 10% (i.e., 0.72 cm) or greater difference. This is even truer in the case of missed strikes. These differences in distance may seem small. However, foraging models generally consider foraging efficiency to be proportional to the sighting distance squared (Aksnes and Giske 1993). Predators are assumed to make tubes of observed territory as they travel, and the radius of the tube is equal to the sighting distance. Thus, a 10% increase in sighting distance leads to a 21% increase in foraging. A 20% increase leads to a 44% increase. Nevertheless, bluegill sighting and striking distances in the present study are within the same range reported by others (Vineyard and O'Brien 1976; Luecke and O'Brien 1981).

This is the first time that UV foraging has been tested in flowing waters. Conducting the experiments in the laminar flow tank allowed for better control of the positioning and orientation of the fish versus the appearance of the prey. The length of the working section of the flow tank (76 cm) also allowed us to measure longer sighting and striking distances than previously reported. Bluegills typically inhabit both moving and non-moving waters. However, it is possible that UV foraging in bluegill may be more efficient in lakes than in streams and rivers because of the lack of current influencing the prey's position and reduced variability in background contrast upon which the prey are viewed. Recently, Mussi et al. (2004) conducted experiments in a flow tank of similar design and observed that the feeding reaction of shiner perch (*Cymatogaster aggregata*) occurred at longer distances when fed semitransparent artemia (i.e., natural) compared with artemia injected with black ink. The authors suggest that the semitransparent artemia were visible at greater distances because of their increased scattering or diffuse reflectance, making them appear brighter against a dark background. In the present study, daphniids displayed low diffuse reflectance and possessed dark gut contents. These factors are likely to make them appear darker against a brighter background in both light treatments.

Many species of larval and juvenile fish feed more actively during crepuscular periods (i.e., dawn and dusk) (Keast and Welsh 1968). At these times of day, the ratio of UVR to visible light is greater because the light field is mostly composed of skylight, which contains a higher proportion of scattered shorter-wavelength radiation than direct sunlight (Novales-Flamarique and Hawryshyn 1997; Leech and Johnsen 2003). We simulated this in our experiments, with respect to irradiance only, by decreasing visible light intensity using window screening. However, it is possible that there was still sufficient visible light in both treatments to facilitate foraging, and even dimmer conditions with increased relative UVR may have resulted in a stronger UV response. In addition, the fish used in this study were collected from a productive, shallow pond, receiving less UVR than those living in less productive systems. Typically, organisms inhabiting low-UV environments have little to no expression of UV photoreception (Cronin et al. 2002; Fuller et al. 2004).

Future studies comparing animals collected from populations inhabiting both high- and low-UV environments may therefore be of interest.

If bluegill are not using UV vision in foraging, then it may play an important role in communication and recognition between conspecifics and (or) predators. The advantage of signaling at UV wavelengths is that it cannot be detected by predators or prey without UV vision (Losey et al. 1999; Cummings et al. 2003). In the present study, bluegill were shown to be UV reflective, excluding the tail. Another possibility is that the fish are using UV vision to avoid depths at which levels of solar UVR could be potentially damaging. Increased mutation and mortality rates have been noted in both fish eggs and larvae resulting from increased UV exposure (Williamson et al. 1994; Browman et al. 2000), and adult *Lepomis* construct their nests for rearing young deeper in high-UV lakes compared with low-UV lakes (Gutierrez-Rodriguez and Williamson 1999). These early life history stages are particularly susceptible to UV damage because of their often transparent, dermal tissue. Certain species of fish possess photoprotective compounds and DNA repair mechanisms to help protect or alleviate some of the damage associated with UV exposure, whereas others are able to actively avoid high-UV environments. For example, shade-seeking behavior and UV avoidance were observed in larval coho salmon (*Oncorhynchus kisutch*) in outdoor enclosures that provided fish with a choice of light environment (Kelly and Bothwell 2002). Although *O. kisutch* has not been examined for UV photoreceptors, other species within this genus are known to have UV vision (Browman et al. 1994). Negative phototactic responses of *Lepomis* larvae to UVR, as well as intense visible light, have been observed in the field (D. Leech, personal observation); however, UVR avoidance has not been directly tested in bluegill.

Acknowledgements

We thank Steve Vogel (Duke University) for the use of his laminar flow tank, Mike Allen and Galen Kaufman (University of Florida, Gainesville) for collecting the bluegill, and Ellis Loew (Cornell University) for measuring bluegill spectral sensitivity. This work was supported in part by a Duke University Postdoctoral Fellowship given to DML.

References

Aksnes, D.L., and Giske, J. 1993. A theoretical model of aquatic visual feeding. Ecol. Model. **67**: 233–250.

Browman, H.I., Novales-Flamarique, I., and Hawryshyn, C.W. 1994. Ultraviolet photoreception contributes to prey search behavior in two species of zooplanktivorous fishes. J. Exp. Biol. **186**: 187–198.

Browman, H.I., Rodriguez, C.A., Beland, F., Cullen, J.J., Davis, R.F., Kouwenberg, J.H.M., Kuhn, P.S., McArthur, B., Runge, J.A., St-Pierre, J.F., and Vetter, R.D. 2000. Impact of ultraviolet radiation on marine crustacean zooplankton and ichthyoplankton: a synthesis of results from the estuary and Gulf of St. Lawrence, Canada. Mar. Ecol. Prog. Ser. **199**: 293–311.

Coughlin, D., and Hawryshyn, C.W. 1994. The contribution of ultraviolet and short-wavelength sensitive cone mechanisms to color vision in rainbow trout. Brain Behav. Evol. **43**: 219–232.

Cronin, T.W., Caldwell, R.L., and Erdmann, M.V. 2002. Tuning of photoreceptor function in mantis shrimp species occupying a range of depths. I. Visual pigments. J. Comp. Physiol. A, **188**: 179–186.

Cummings, M.E., Rosenthal, G.G., and Ryan, M.J. 2003. A private ultraviolet channel in visual communication. Proc. R. Soc. Lond. B, **270**: 897–904.

Douglas, R.H., Partridge, J.C., and Marshall, N.J. 1998. The eyes of deep-sea fish. I: Lens pigmentation, tapeta and visual pigments. Prog. Retin. Eye Res. **17**: 597–636.

Fuller, R.C., Carleton, K.L., Fadool, J.M., Spady, T.C., and Travis, J. 2004. Population variation in opsin expression in the bluefin killifish, *Lucania goodie*: a real-time PCR study. J. Comp. Physiol. A, **190**: 147–154.

Goldsmith, T.H., and Bernard, G.D. 1985. Visual pigments in invertebrates. Photochem. Photobiol. **42**: 805–809.

Gutierrez-Rodriguez, C., and Williamson, C.E. 1999. Influence of solar ultraviolet radiation on early life-history stages of the bluegill sunfish, *Lepomis macrochirus*. Environ. Biol. Fishes, **55**: 307–319.

Hawryshyn, C.W. 1991. Light adaptation properties of the ultraviolet sensitive cone mechanism in comparison to the other receptor mechanisms of goldfish. Vis. Neurosci. **6**: 293–301.

Hawryshyn, C.W. 1992. Polarization vision in fish. Am. Sci. **80**: 164–175.

Jacobs, G.H. 1992. Ultraviolet vision in vertebrates. Am. Zool. **32**: 544–554.

Johnsen, S., and Widder, E.A. 2001. Ultraviolet absorption in transparent zooplankton and its implications for depth distribution and visual predation. Mar. Biol. **138**: 717–730.

Jordan, R., Howe, D., Juanes, F., Stauffer, J., Jr., and Loew, E. 2004. Ultraviolet radiation enhances zooplanktivory rate in ultraviolet sensitive cichlids. Afr. J. Ecol. **42**: 228–231.

Keast, A., and Welsh, L. 1968. Daily feeding periodicities, food uptake rates, and dietary changes with hour of day in some lake fishes. J. Fish. Res. Board Can. **25**: 1133–1144.

Kelly, D.J., and Bothwell, M.L. 2002. Avoidance of solar ultraviolet radiation by juvenile coho salmon (*Oncorhynchus kisutch*). Can. J. Fish. Aquat. Sci. **59**: 474–482.

Leech, D.M., and Johnsen, S. 2003. Behavioral responses: UV avoidance and vision. *In* UV effects in aquatic organisms and ecosystems. *Edited by* W. Helbling and H. Zagarese. The Royal Society of Chemistry, Cambridge. pp. 455–481.

Loew, E.R., and McFarland, W.N. 1990. The underwater visual environment. *In* The visual system of fish. *Edited by* R.H. Douglas and M.B.A. Djamgoz. Chapman and Hall Press, London. pp. 1–44.

Loew, E.H., McFarland, W.N., Mills, E.L., and Hunter, D. 1993. A chromatic action spectrum for planktonic predation by juvenile yellow perch, *Perca flavescens*. Can. J. Zool. **71**: 384–386.

Losey, G.S., Cronin, T.W., Goldsmith, T.H., Hyde, D., Marshall, N.J., and McFarland, W.N. 1999. The UV visual world of fishes: a review. J. Fish Biol. **54**: 921–943.

Luecke, C., and O'Brien, W.J. 1981. Prey location volume of a planktivorous fish — a new measure of prey vulnerability. Can. J. Fish. Aquat. Sci. **38**: 1264–1270.

Mussi, M., McFarland, W.N., and Domenici, P. 2004. Visual cues eliciting the feeding reaction of a planktovorous fish swimming in a current. J. Exp. Biol. **208**: 831–842.

Novales-Flamarique, I., and Hawryshyn, C.W. 1997. Is the use of underwater polarized light by fish restricted to crepuscular periods? Vis. Res. **37**: 975–989.

Parkyn, D.C., and Hawryshyn, C.W. 1993. Polarized light sensitivity in the rainbow trout (*Oncorhynchus mykiss*): characterization from multiunit responses in the optic nerve. J. Comp. Physiol. **172**: 493–500.

Rocco, V., Barriga, J.P., Zagarese, H., and Lozada, M. 2002. How much does ultraviolet radiation contribute to the feeding performance of rainbow trout, *Oncorhynchus mykiss*, juveniles under natural illumination? Environ. Biol. Fishes, **63**: 223–228.

Shashar, N. 1994. UV vision by marine animals: mainly questions. *In* Ultraviolet radiation and coral reefs. *Edited by* D. Gulko and P.L. Jokiel. Hawaiian Institute of Marine Biology (HIMB) Tech. Rep. No. 41. University of Hawaii UNIHI-Sea Grant-CR-95-03.

Siebeck, U.E. 2004. Communication in coral reef fish: the role of ultraviolet colour patterns in damselfish territorial behaviour. Anim. Behav. **68**: 273–282.

Smith, E.J., Partridge, J.C., Parsons, K.N., White, E.M., Cuthill, I.C., Bennett, A.T.D., and Church, S.C. 2002. Ultraviolet vision and mate choice in the guppy (*Poecilia reticulata*). Behav. Ecol. **13**: 11–19.

SPSS Inc. 2003. SigmaStat [computer software]. Version 3.0.1. SPSS Inc., Chicago, Illinois.

Theobald, J.C., Greiner, B., Weislo, W.T., and Warrant, E.J. 2006. Visual summation in night-flying sweat bees: a theoretical study. Vis. Res. **46**: 2298–2309.

Tovee, M.J. 1995. Ultra-violet photoreceptors in the animal kingdom: their distribution and function. Trends Ecol. Evol. **10**: 455–459.

Vineyard, G.L., and O'Brien, W.J. 1976. Effects of light and turbidity on reactive distance of bluegill (*Lepomis macrochirus*). J. Fish. Res. Board Can. **32**: 2845–2849.

White, E.M., Church, S.C., Willoughby, L.J., Hudson, S.J., and Partridge, J.C. 2005. Spectral irradiance and foraging efficiency in the guppy, *Poecilia reticulate*. Anim. Behav. **69**: 519–527.

Williamson, C.E., Zagarese, H.E., Schulze, P.C., Hargreaves, B.R., and Seva, J. 1994. The impact of short-term exposure to UV-B radiation on zooplankton communities in north temperate lakes. J. Plankton Res. **16**: 205–218.

Winter, Y., Lopez, J., and von Helversen, O. 2003. Ultraviolet vision in a bat. Nature (London), **425**: 612–614.

Recruitment variability in Baltic Sea sprat (*Sprattus sprattus*) is tightly coupled to temperature and transport patterns affecting the larval and early juvenile stages

H. Baumann, H.-H. Hinrichsen, C. Möllmann, F.W. Köster, A.M. Malzahn, and A. Temming

---

Abstract: Recruitment patterns of Baltic Sea sprat (*Sprattus sprattus*) were correlated to time series of (*i*) month- and depth-specific temperature conditions and (*ii*) larval drift patterns inferred from long-term Lagrangian particle simulations. From the latter, we derived an index that likely reflected the variable degree of annual larval transport from the central, deep spawning basins to the shallow coastal areas of the Baltic Sea. The drift index was significantly ($P <$ 0.001) correlated to sprat recruitment success and explained, together with sprat spawning stock biomass, 82% of the overall variability between 1979 and 2003. Years of strong larval displacement towards southern and eastern Baltic coasts corresponded to relative recruitment failure, while years of retention within the deep basins were associated with relative recruitment success. The strongest correlation between temperature and recruitment occurred during August in surface waters, explaining 73% of the overall variability. Together, the two approaches advocate that new year classes of Baltic sprat are predominantly composed of individuals born late in the season and are determined in strength mainly by processes acting during the late larval and early juvenile stages. However, prior to be included in recruitment predictions, the biological mechanisms underlying these strong correlations may need to be better resolved.

Résumé : Nous avons mis en corrélation les patrons de recrutement du sprat (*Sprattus sprattus*) de la Baltique avec des séries chronologiques (*i*) de conditions de température en fonction du mois et de la profondeur et (*ii*) de patrons de dérive des larves obtenus à partir de simulations de Lagrange à long terme de particules. D'après ces simulations, nous avons élaboré un indice qui représente vraisemblablement le degré variable de transport annuel des larves depuis les bassins de fraye centraux et profonds vers les zones côtières peu profondes de la Baltique. L'indice de dérive est en corrélation significative ($P < 0{,}001$) avec le succès du recrutement du sprat; combiné à la biomasse du stock reproducteur du sprat, il explique 82 % de la variabilité globale entre 1979 et 2003. Les années de fort déplacement des larves vers les côtes du sud et de l'est de la Baltique correspondent à des insuccès relatifs du recrutement, alors que les années de rétention dans les bassins profonds sont associées à un succès relatif du recrutement. La corrélation la plus forte entre la température et le recrutement s'observe en août dans les eaux superficielles, ce qui explique 73 % de la variabilité globale. Ensemble, les deux approches indiquent que les nouvelles classes d'âge annuelles des sprats de la Baltique se composent principalement d'individus nés tard dans la saison et que la force des classes est déterminée par des processus qui agissent à la fin de la vie larvaire et durant les stades juvéniles. Cependant, il faut mieux élucider les mécanismes sous-jacents à ces fortes corrélations avant de les inclure dans les prédictions du recrutement.

[Traduit par la Rédaction]

Received 11 October 2005. Accepted 1 June 2006. Published on the NRC Research Press Web site at http://cjfas.nrc.ca on 15 September 2006.
J18927

H. Baumann[1] and A. Temming. Institute for Marine Ecosystems and Fisheries Science, Olbersweg 24, 22767, Hamburg, Germany.
H.-H. Hinrichsen. Leibniz Institute of Marine Science, Düsternbrooker Weg 20, 24105, Kiel, Germany.
C. Möllmann and F.W. Köster. Danish Institute for Fisheries Research, Charlottenlund Castle, DK-2920, Charlottenlund, Denmark.
A.M. Malzahn. Alfred Wegener Institute for Polar and Marine Research, Biologische Anstalt Helgoland, Ostkaje 1118, 27498 Helgoland, Germany.

[1] Corresponding author (e-mail: hannes.baumann@uni-hamburg.de).

doi:10.1139/F06-112

Introduction

Explaining and predicting recruitment variability are perennial goals in fisheries science (Sissenwine 1984). In sprat, *Sprattus sprattus*, currently the most abundant, commercially exploited fish species in the Baltic Sea, recruitment variability has increased considerably at the beginning of the 1990s (ICES 2005*a*), thereby coinciding with other profound changes in the Baltic ecosystem that affected all trophic levels (Alheit et al. 2005).

Previous studies have found significant but weak correlations between recruitment strength and (*i*) spawning stock biomass (SSB) and (*ii*) temperature conditions experienced during the egg and early larval stages of Baltic Sea sprat (Köster et al. 2003; MacKenzie and Köster 2004). However, Köster et al. (2003) noted that estimates of egg and larval abundance are generally well correlated, whereas larval production poorly predicts recruitment levels. It has been argued, thus, that year-class strength in Baltic Sea sprat may rather be determined by environmental influences during the late larval and early juvenile stages (Voss et al. 2005). Thus, to improve current sprat recruitment models, potential environmental effects may need to be considered throughout all pre-recruit life stages.

Feeding sprat larvae predominantly occur in surface waters (Voss et al. 2003), where variable, wind-driven circulation patterns may transport them either to suitable or unsuitable nursery areas (Sinclair 1988). Previously, we followed this rationale by using a hydrodynamic circulation model in combination with Lagrangian particle tracking to simulate 23 years of larval sprat drift patterns (Baumann et al. 2004). Our retention index, defined as the annual proportion of drifters collected within predefined rectangles in and outside of the Bornholm Basin, a major sprat spawning area (Köster et al. 2001), was significantly related to the number of age-0 sprat recruits in the central Baltic. The relationship suggested that retention within the deep basin would be beneficial for recruitment, while dispersion and transport to southeastern Baltic shores would lead to relative recruitment failure. Shortcomings of the previous approach were that the index (*i*) did not explain the full recruitment time series but only the most recent 12 years, (*ii*) was restricted to sprat from the Bornholm Basin, and (*iii*) relied on the definition of arbitrary rectangles in the model domain (Baumann et al. 2004).

Here we present an improved drift index to explain sprat recruitment variability within the entire Baltic Sea and over the whole, extended time series of 25 years (1979–2003). The index was again based on hydrodynamic modelling in conjunction with Lagrangian particle simulations, but instead of final horizontal drifter positions (previous approach), we now integrated the entire drift period by considering the average water depth across all daily particle positions to be a proxy of larval transport from the deep spawning basins to the coast. The underlying rationale was that years of predominant larval retention or coastal transport should result in anomalously deep or shallow particle distributions, respectively.

In a second line of investigation, we evaluated the relationship between recruitment variability and month- and depth-specific temperature conditions based on 30 years of observations. In contrast with previous studies, our approach did not make any a priori assumptions regarding the time and the water depth (and thus the life stage affected) of such potential temperature–recruitment correlations, thereby encompassing possible effects prior, during, and after the main spawning season of Baltic Sea sprat.

Materials and methods

Hydrodynamic circulation model

A comprehensive description of the hydrodynamic model and the Lagrangian particle-tracking technique has recently been published by Hinrichsen et al. (2005). Briefly, the three-dimensional, baroclinic circulation model of the Baltic Sea (Lehmann 1995; Lehmann and Hinrichsen 2000) is an adaptation of the free surface Bryan–Cox–Semtner model (Killworth et al. 1991), with a model domain that encompasses the entire Baltic Sea, including the Gulf of Bothnia, Gulf of Riga, the Belt Seas, Kattegat, and the Skagerrak, with a realistic bottom topography. The horizontal resolution is 5 km, and 60 vertical levels are specified with a thickness chosen to best represent the different sill depths in the Baltic Sea. The model is forced by atmospheric data provided on a 1° × 1° grid (i.e., geostrophic wind, 2 m air temperature, 2 m relative humidity, surface pressure, cloudiness, and precipitation; Swedish Meteorological and Hydrological Institute, Norrköping) and river runoff taken from a mean runoff database (Bergstrom and Carlsson 1994). The model was run for a time series of 25 years (1979–2003). Three-dimensional velocity fields extracted from the circulation model were used to predict the trajectories of passive Lagrangian drifters using a 4th order Runge–Kutta scheme (Hinrichsen et al. 1997), which allowed particles to be tracked independently from the resolution of the hydrodynamic circulation model. Along each particle's drift path, corresponding bottom depths (i.e., the water depth at the current position of each particle) were initially stored in 6 h intervals, but later averaged to obtain daily estimates.

Particle releases and indices

Initial horizontal drifter positions were based on average sprat egg distributions in the Baltic Sea (Köster 1994; A. Makarchouk, Latvian Fisheries Research Institute, Daugavgrivas St. 8, Riga, LV-1007, Latvia, unpublished data), assumed to be a proxy for the spatial distribution of first-feeding sprat larvae. The vast majority of particles was released inside the 40 m isobath of the four major Baltic spawning grounds: Arkona Basin, Bornholm Basin, Gdansk Deep, and Gotland Basin (Fig. 1*b*). All drifters were seeded and forced to remain within the 5–10 m depth layer, because feeding sprat larvae predominantly occur in surface waters and appear not to exhibit clear vertical migration patterns (Voss et al. 2005). Each year, particle cohorts representing batches of first-feeding, passively drifting sprat larvae were released on 21 April (day 111) and then every 10 days until 10 July (day 191) to cover the entire average spawning season of Baltic Sea sprat (Köster and Möllmann 2000; Karasiova 2002). Each of these nine larval pulses per year consisted of 2671 particles that were seeded in regular spatial intervals of about 5 km (Fig. 1*b*).

Fig. 1. Distributions of 2671 Lagrangian particles (black dots) released on 10 July (day 191) within areas of Baltic Sea sprat (*Sprattus sprattus*) spawning effort and tracked for 50 days in (*a*) 1997 and (*b*) 1998. The bathymetry of the study area is shown in panel *a*; the particle seeding pattern (grey dots) is depicted in panel *b*. Water abbreviations: AB, Arkona Basin; BB, Bornholm Basin; GB, Gotland Basin; GD, Gdansk Deep. Land abbreviations: DK, Denmark; Ger, Germany; Lat, Latvia; Li, Lithuania.

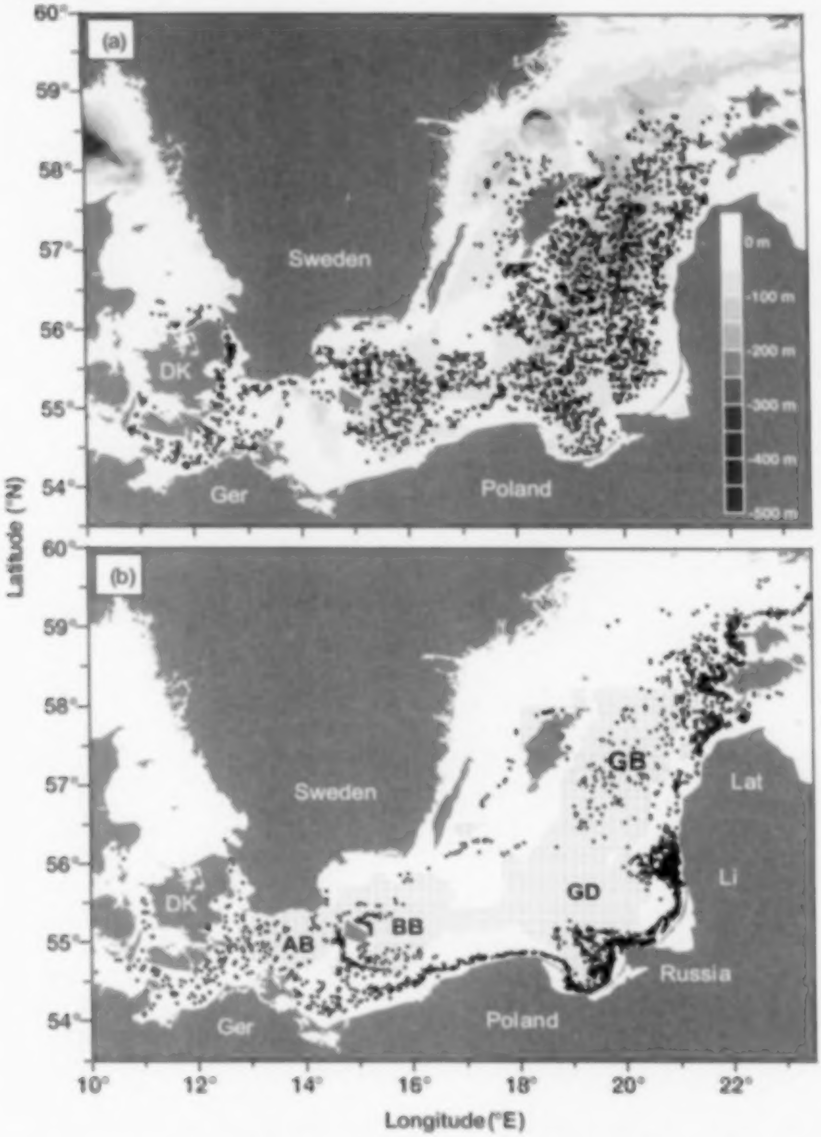

Two different approaches were tested regarding the end of the simulations. First, particles were tracked through the model domain for variable drift periods of 50–130 days, until a common collection date on 28 August (day 240). This arbitrary date was chosen to compromise sufficient drift times for late-released larval batches while avoiding too long drift periods for oldest larvae, because active swimming for the latter becomes likely. In a second approach, drifters were tracked for fixed periods of 50 days, entailing nine different collection dates (9 June to 28 August).

For an integrated view of annual drift patterns, daily bottom depths were averaged by year and release date across all 2671 particles, regardless of their individual positions in model domain. Then, because we were interested in anomalies rather than absolute values, average daily bottom depths (D_{ikl}) were standardized to zero mean and unit deviation across all 25 years modelled (i.e., $S_{ikl} = (D_{ikl} - m_{kl})\mathrm{SD}_{kl}^{-1}$, where S_{ikl} is the standardized bottom depth of the *i*th year, the *k*th release, and the *l*th day; and *m* and SD are the day- and release-specific mean and standard deviation of bottom depth across all 25 years, respectively). Finally, daily standardized bottom depths were averaged over the considered simulation period (i.e., either over 50 days after release (fixed drift periods) or over release-specific variable drift periods (fixed collection date)). Annual, mean, standardized bottom depths are hereafter referred to as bottom depth anomalies (BDAs).

Temperature, recruitment, and larval abundance

Temperatures in the Baltic Sea were compiled from the International Council for the Exploration of the Sea (ICES) Oceanographic Database (http://www.ices.dk/ocean/), containing two main data sets of (*i*) surface temperatures (0–10 m) and (*ii*) depth-specific CTD (conductivity–temperature–depth) and bottle measurements. From the combined data, we selected all available temperatures between 1974 and 2003 within the area of the major Baltic Sea sprat stock abundance (53°–60°N, 13°–23°E, ICES 2005*b*). Data were subsequently aggregated to obtain monthly means per year and 10 m depth stratum down to a water depth of 70 m (i.e., 0 to <10, 10 to <20, …, 60 to <70 m). Temperature means were derived from, on average, 223 observations available per month, depth stratum, and year.

Both temperature and BDA time series were correlated to the abundance of age-0 sprat during the 3rd quarter of each year in the entire Baltic Sea (ICES subdivisions 22–32). The abundance estimates (1974–2003) were taken from the most recent area-aggregated, multispecies virtual population analysis (MSVPA; ICES 2005*b*), which also provided the updated time series of sprat SSB. Data on larval sprat abundance were available from various ichthyoplankton surveys in the Bornholm Basin, Gdansk Deep, and Gotland Basin between 1979 and 1999 (stations deeper than 60 m), as described by Köster et al. (2003).

Baltic Sea Index (BSI)

To obtain a general impression of how atmospheric conditions over the Baltic Sea influence transport and temperature patterns, we applied the BSI (Lehmann et al. 2002), which is defined as the difference of normalized sea level pressure anomalies between Oslo (Norway) and Szczecin (Poland). Positive indices correspond to anomalous sea level pressures associated with westerly winds, whereas negative indices indicate predominantly easterly winds over the Baltic Sea. BSIs were recorded in 3 h intervals, but later averaged over the desired periods of larval drift simulations.

Correlations between time series of BDA, temperature, BSI, and sprat recruitment were studied using Pearson's bivariate, two-sided correlation coefficient (SPSS 13.0.1, SPSS Inc., Chicago, Illinois).

Results

Transport (BDA) and recruitment

For all nine drifter cohorts per year, final particle positions on day 240 (28 August) were indicative of considerable interannual differences in Baltic circulation patterns. Two main scenarios could be distinguished: (*i*) years of predominant particle retention within the central deep basins, likely induced by prevailing weak to variable easterly winds in summer (e.g., 1997; Fig. 1*a*), and (*ii*) years of large-scale particle displacement and dense accumulation along southern, southeastern, and eastern Baltic coastlines, probably as a consequence of prevailing strong to variable westerly winds in summer (e.g., 1998; Fig. 1*b*). Particle displacement towards Swedish coastlines (westward drift) was generally negligible.

Fig. 2. Release-specific bottom depth anomalies (BDAs) derived from long-term Lagrangian particle simulations. Shaded lines correspond to BDAs derived from releases 1–8 (day 111 – day 181), while BDAs based on the last release 9 (day 191) is shown by the dash-dotted line. BDA_9 was best correlated to Baltic Sea sprat (*Sprattus sprattus*) 0-group abundance (solid dark line), which was estimated by area-aggregated multispecies virtual population analysis (MSVPA).

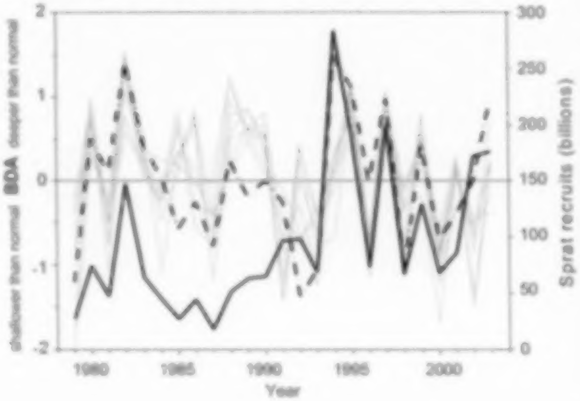

Release-specific BDAs (BDA_{1-9}) reflected these interannual differences well, with positive and negative BDAs indicating years when the majority of sprat larvae likely drifted over deeper-than-normal or shallower-than-normal waters, respectively, (Fig. 2). Indices derived from variable drift periods (fixed collection on 28 August) were all significantly cross-correlated ($P < 0.05$), in contrast with indices based on fixed 50-day drift periods, where significant cross-correlations did not exceed two subsequent release dates (e.g., BDA_3 was correlated to BDA_2 and BDA_{4-5}, but not to BDA_{6-9}). Within a given drift period, the coefficient of variation (CV) of daily average bottom depths ranged between 4% and 32% (temporal transport variability).

Drift indices based on early release dates 1–7 (BDA_{1-7}) were not significantly correlated to sprat age-0 abundance ($P > 0.05$), irrespective of fixed or variable simulation periods. In contrast, highly significant positive correlations occurred between sprat recruitment and BDA_8 (release 30 June, $P = 0.003$, $r^2 = 0.32$) and BDA_9 (release 10 July, $P < 0.001$, $r^2 = 0.50$). For the latter, an exponential function of the form $y = ab^x$ best fitted the data ($r^2 = 0.64$). However, the residuals of the fitted BDA_9–recruitment curve showed a clear decadal pattern; residuals between 1979 and 1990 were all negative, in contrast with all positive residuals between 1991 and 2003 (except 1996). If separate exponential curves were fitted to these two periods, BDA_9 explained 92% of the variability between 1979 and 1990 and 84% between 1991 and 2003 (Fig. 3). The shift in the relationship between BDA_9 and recruitment coincided with the strong increase in Baltic Sea sprat SSB at the end of the 1980s (Fig. 4).

Temperature and recruitment

Out of 84 correlations (12 months × 7 depth strata), temperature was significantly ($P < 0.05$) and positively corre-

Fig. 3. Relationship between bottom depth anomaly 9 (BDA_9) and Baltic Sea age-0 sprat (*Sprattus sprattus*) recruitment (*R*). Exponential curves ($R = a \cdot b^{BDA_9}$) best fitted the periods 1979–1990 ($r^2 = 0.92$, squares) and 1991–2003 ($r^2 = 0.84$, circles).

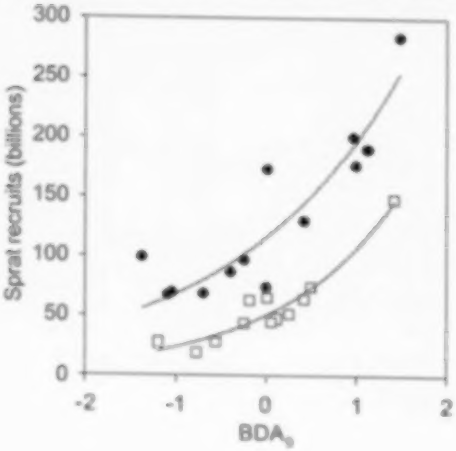

Fig. 4. Time series of Baltic Sea sprat (*Sprattus sprattus*) spawning stock biomass (SSB, solid line) and mean larval abundance (shaded line) in the main Baltic spawning grounds Bornholm Basin, Gdansk Deep, and Gotland Basin between May and July.

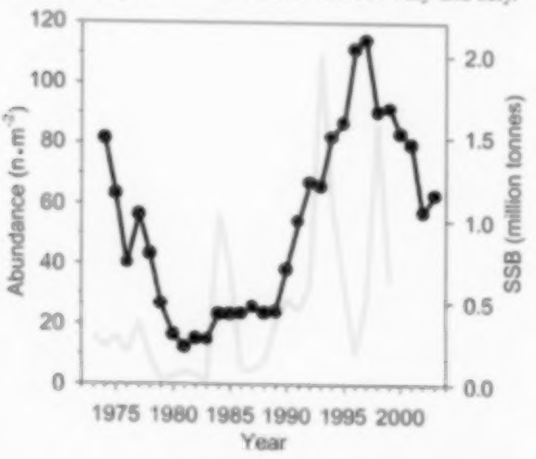

Fig. 5. Summarizing the month- and depth-specific temperature–recruitment correlations of Baltic Sea sprat (*Sprattus sprattus*) based on 30 years of observations (1974–2003). Shading and isolines correspond to r^2 and *P* values, respectively, while crosses refer to the data grid points used to create the contour plot (i.e., Kriging).

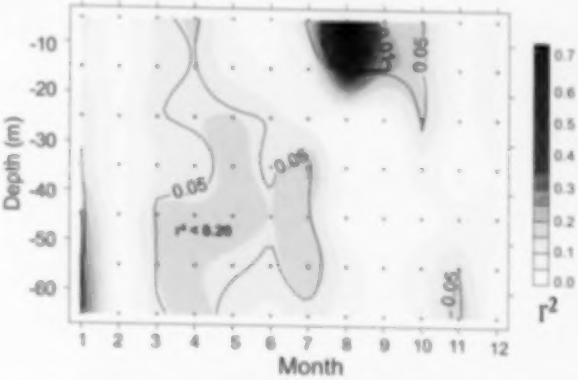

lated to Baltic Sea sprat recruitment success in 31 cases, thereby showing a characteristic month- and depth-specific pattern (Fig. 5). Significant temperature–recruitment correlations were already observed in January and in depths between 40 and 70 m ($r^2_{max} = 0.34$). February temperatures were uncorrelated to recruitment. Between March and July, significant but weak correlations to recruitment developed mostly in midwater depths (20–60 m, $r^2_{max} = 0.21$), with April correlations having the broadest depth range. From July to August, correlations shifted notably to surface waters, with August temperatures in 0–10 m explaining 66% of sprat recruitment variability between 1974 and 2003 (Fig. 5). A quadratic fit to the data, however, explained 73% of the overall recruitment variability. A shift in the relationship between decades, as observed for BDA_9, was not apparent for temperature. Surface temperatures were still significantly correlated to recruitment strength in September and October ($r^2_{max} = 0.22$), whereas in November, a weak but significant correlation reappeared in deeper water layers (50–70 m, $r^2_{max} = 0.20$; Fig. 5).

The BSI averaged between 10 July and 28 August (days 191–240) was found to be significantly and negatively correlated to the corresponding drift index (BDA_9, $P = 0.001$, $r^2 = 0.38$) and surface temperature in August ($P = 0.003$, $r^2 = 0.35$; Fig. 6). The relationships indicated that differences in sea level pressure associated with westerly winds (positive BSIs) induced both coastal particle transport and relatively cold surface temperatures, while negative BSIs and easterly winds were conducive to warm years and particle retention.

Recruitment models

The strong cross-correlation between surface temperature in August and BDA_9 ($P < 0.001$, $r^2 = 0.46$) precluded the inclusion of both variables in a common recruitment model. SSB alone explained 28% of the recruitment variability ($P = 0.007$) and was significantly cross-correlated to August temperature ($P = 0.023$) but not to BDA_9 ($P = 0.75$). We therefore constructed two different models, the first using BDA_9 and SSB and the second using only August surface temperature (*T*) as independent variables to predict the MSVPA estimates of sprat age-0 abundance (Table 1). The used model functions were

$$\text{(1)} \qquad \text{age 0 sprat} = a^{BDA_9} + b \cdot \text{SSB}$$

$$\text{(2)} \qquad \text{age 0 sprat} = a \cdot T^2 + b \cdot T$$

The explained variability in the BDA_9+SSB model was 82% (1979–2003; Fig. 7*a*) and therefore slightly better than the recruitment prediction using August temperature only (1974–2003, $r^2 = 0.73$; Fig. 7*b*). However, both models predicted different years of sprat recruitment success differently and with a differing quality of prediction. While sprat recruitment was considerably underestimated by the

Table 1. Parameter estimates and their 95% confidence limits, significance levels, and r^2 values for the two recruitment models using bottom depth anomalies plus spawning stock biomass (BDA_9+SSB) (abundance (R) = $a^{BDA_9} + b \cdot SSB$) and August surface temperature ($R = a \cdot T^2 + b \cdot T$ + constant) to predict the multispecies virtual population analysis (MSVPA) estimates of age-0 sprat, *Sprattus sprattus*, in the entire Baltic Sea.

Dependent variable	Time series	Independent variable(s)	Parameter	Parameter estimate	95% confidence limits: Lower	95% confidence limits: Upper	P	r^2_{adj}
R'	1979–2003	BDA′, SSB (entire Baltic)	a	4.478	4.177	4.779	<0.001	0.82
			b	5.47×10^{-5}	4.26×10^{-5}	6.69×10^{-5}		
R	1974–2003	August temperature (0–10 m)	Constant	1.33×10^{12}	-9.99×10^{10}	2.77×10^{12}		
			a	5.84×10^{9}	1.26×10^{9}	1.04×10^{10}	<0.001	0.73
			b	-1.74×10^{11}	-3.37×10^{11}	-1.14×10^{10}		

Note: Transformed variables were used to fit the BDA+SSB model (i.e., $BDA' = BDA_9 + 2$ and $R' = R \times 10^{-9}$).

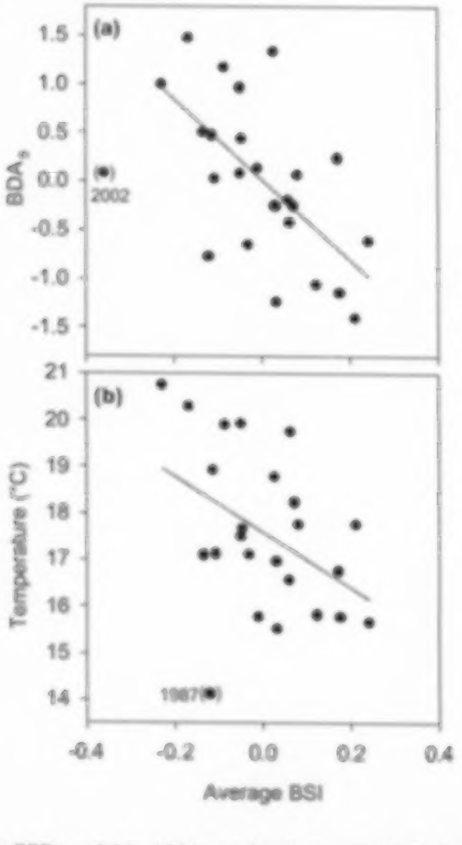

Fig. 6. Relationship between the Baltic Sea Index (BSI) and (*a*) bottom depth anomaly (BDA, 1979–2003, $r^2 = 0.38$) and (*b*) surface temperature in August (1974–2003, $r^2 = 0.35$). Data indicated with parentheses were years that were not included in the regression.

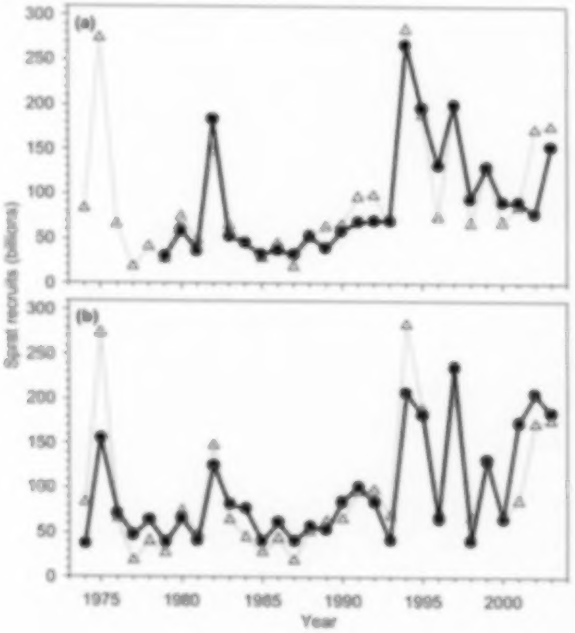

Fig. 7. Time series of observed (triangles, shaded line) and predicted (circles, solid line) Baltic Sea sprat (*Sprattus sprattus*) recruitment. (*a*) BDA+SSB (bottom depth anomaly plus spawning stock biomass) model explaining 82% of the recruitment variability between 1979 and 2003. (*b*) Temperature model (August, 0–10 m) explaining 73% of recruitment variability between 1974 and 2003.

BDA_9+SSB model in 1996 and 2002, the quadratic temperature model yielded much closer estimates. Conversely, temperature-based predictions were considerably poorer than the BDA_9+SSB model in 1994 and particularly in 2001 (Fig. 7).

Interestingly, residuals scaled by observed recruitment numbers were significantly and negatively correlated to the variability around BDA_9 ($P = 0.02$, $r^2 = 0.36$), indicating that years of highly variable transport patterns increasingly led to recruitment overestimation (Fig. 8).

Discussion

BDA as a drift proxy

We found BDAs a meaningful way to condense and quantify the large amounts of information produced by long-term Lagrangian simulations. BDAs reflected well the variable degree of annual particle transport from the central deep

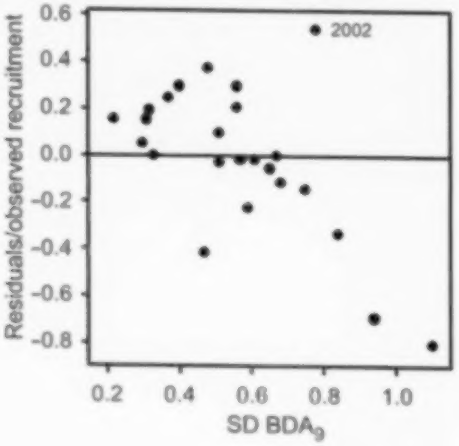

Fig. 8. Relative deviations of recruitment predictions made by the BDA+SSB (bottom depth anomaly plus spawning stock biomass) model as a function of BDA_9 variability (SD BDA_9; i.e., standard deviation of standardized bottom depths between days 191 and 240), showing increased recruitment overestimation for years of high drift variability ($P = 0.02$, $r^2 = 0.36$).

spawning basins of the Baltic Sea to shallower coastal waters. In addition, averaging daily standardized bottom depths along particle trajectories effectively integrated the drift information over the entire simulation period, which was advantageous over our previous approach using only the final horizontal particle positions (Baumann et al. 2004). This did not affect the key results, though, which were similar for both studies and indicated that years of relative particle retention or coastal displacement corresponded to relative sprat recruitment success or failure, respectively. Both studies were also consistent in finding the strongest correlations to recruitment for particles released late in the season.

However, when moving from particles to living organisms, inferences drawn from Lagrangian simulations rely on the assumption that passive drifter trajectories reflect the average transport patterns of the planktonic species or life stage studied. In demersal fish like cod or flatfish, juvenile settlement concludes the susceptibility to ocean circulation and thus sets a natural limit to drift studies (e.g., 65 days; Hinrichsen et al. 2003). Such a limit is not as readily defined in pelagic species like sprat. The onset of active swimming behaviour or schooling may not necessarily preclude Lagrangian drift simulations if late larvae or early juveniles keep moving randomly within a water body that is subject to predictable physical forcing. For example, Allain et al. (2003) successfully used a hydrodynamic model to infer likely origins of approximately 100-day-old and 80 mm long (Cermeno et al. 2003) juvenile European anchovy, *Engraulis encrasicolus*, in the Bay of Biscay. For the Baltic Sea, Hinrichsen et al. (2005) compared average Lagrangian drifter distributions with field data on 0-group sprat abundance, as determined by annual hydroacoustic surveys. They found model and field distributions in generally good accordance, with the highest mean October abundance of sprat juveniles along the southern and eastern Baltic coasts. The authors also reported that the inclusion of simulated larval vertical migration did not produce contradictory results. It may, therefore, be justified to assume that average transport patterns of sprat larvae and early juveniles were generally reflected by the present drift model.

Still, longer simulation periods increase uncertainty, which could have been a contributory but not the only reason for the lack of correlation between early released particles and recruitment strength, because fixed and variable drift periods produced similar results. Furthermore, both approaches did not show a gradual but a very sudden shift from nonsignificant to highly significant BDA–recruitment correlations from early- (April–June) to late-released particles (July), possibly reflecting the seasonally different contribution of larval production to recruitment. In other words, sprat larvae born early in the season may play a negligible role in the recruitment process, while new sprat year classes appear to consist predominantly of individuals born relatively late in the season. The hypothesis is supported by recent findings of Voss et al. (2005), who studied larval sprat survival and condition in relation to food availability in the central Baltic Sea during 2002. The authors presented evidence that the late larval stages critically relied on the abundance of larger copepodites and adult copepods, which were scarce in April–May but significantly more abundant in June–July 2002. In addition, Baumann et al. (2006*a*) inferred distributions of days-of-first-feeding (DFF, a proxy for hatch date) from otolith microstructure analyses in newly recruited 0-group sprat caught in October 2002 in the Baltic Sea. Depending on the Baltic region, DFF distributions of sprat survivors peaked between the end of June and mid-July 2002, which is consistent with the present conclusion.

If recruitment levels are mainly determined by variable survival patterns of individuals born late in the season, what potential mechanisms could cause the observed dependence on circulation variability? Previous studies on other species and different marine systems (reviewed by Sissenwine 1984; Leggett and Deblois 1994) have mostly attributed the coupling between recruitment success and advective processes to food availability (e.g., Borja et al. 1998; Skogen 2005; Zeldis et al. 2005) or feeding success (Crecco and Savoy 1987). For Baltic Sea cod (*Gadus morhua*) larvae, Hinrichsen et al. (2003) showed that retention to but also advection out of the central Bornholm Basin could have beneficial effects to survival, depending on the season and the abundance of the calanoid copepod *Pseudocalanus acuspes*. For Baltic Sea sprat, stock size and 0-group numbers (Kornilovs, et al. 2001; Alheit et al. 2005) appear to be correlated to long-term trends in abundance of the two most important prey species, *Acartia* spp. and *Temora longicornis*, which showed significant, temperature-related increases during the 1990s (Möllmann et al. 2000). However, these observations did not resolve potential differences between Baltic basins and coastal areas. The latter normally support a higher primary and secondary production, which appears contradictory to our findings of poor recruitment levels associated to years of high larval onshore transport.

Apart from influencing transport, variable forcing conditions also affect turbulence, which is potentially important for larval feeding success (MacKenzie et al. 1994). On the population level, however, this mechanism is not unequivocally supported by field studies and appears to be of less im-

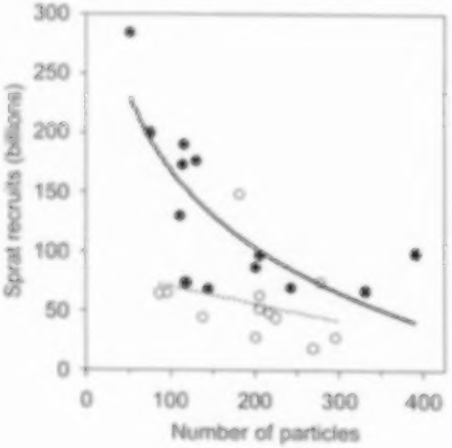

Fig. 9. Relationship between sprat (*Sprattus sprattus*) recruitment success and the number of Lagrangian drifters (out of 2671) that had at least one next neighbour within a 0.5 km radius of their final position. A significant ($r^2 = 0.62$, $P = 0.001$) logarithmic relationship was found only for the period 1991–2003 (solid circles, solid line). The nonsignificant relationship between 1979 and 1990 (open circles) is shown by a broken line. Particles were released on 10 July (release 9) and tracked for 50 days.

portance for older larvae and early juveniles, where turbulence levels probably need to be unnaturally high to hamper feeding success (MacKenzie 2000).

It has also been suggested that density-dependent processes operating during the late larval – early juvenile stages may substantially modify recruitment levels (Cushing 1974; Leggett and Deblois 1994). To test this hypothesis with our drift model, we calculated the distance between each particle and its next neighbour on 28 August (end of simulation). During years of large-scale coastal transport (e.g., 1998), particles were found in much denser aggregations than during retention years (e.g., 1997), with particle density being significantly ($P < 0.05$) and inversely related to recruitment strength (Fig. 9). The fact that such a relationship was only apparent throughout the last decade may be explained by the, on average, higher larval abundance during the 1990s. In addition, Baumann et al. (2006*b*) compared otolith-based growth rates of sprat recruits caught in October 2003 in the western Baltic Sea with those of pre-recruits caught at the end of August in very shallow coastal waters. The authors presented evidence that a sudden growth decline observed exclusively in pre-recruit otoliths likely resulted from severely depleted food resources. It could thus be argued that coastal areas may not always comprise the most suitable nursery grounds for Baltic Sea sprat, particularly if high summer temperatures in shallow waters lead to increased energetic demands and thus food requirements (Houde 1989) of post-larvae and early juveniles.

The strong increase of the sprat spawning stock at the end of the 1980s may have increased the potential impact of transport-related, density-dependent processes. This is supported by the fact that over a similar range of BDA values, the magnitude of recruitment fluctuations almost doubled from the 1980s to the 1990s. It does not imply a greater sensitivity of recruitment to transport, since BDAs during the 1980s were more closely related to recruitment variability than during the 1990s. However, although SSB may have been the most important factor responsible for the shift in the drift–recruitment relationship, it co-occurred with a whole suite of changes in the Baltic ecosystem that affected all trophic levels (Alheit et al. 2005). Particularly, the unknown effects of pronounced shifts in Baltic zooplankton composition and dynamics (Möllmann et al. 2000) could have increased unexplained variability around the drift–recruitment relationship.

Temperature and recruitment

As with transport, studies that show significant temperature–recruitment correlations are numerous across species and marine systems (e.g., Campana 1996; Fowler and Jennings 2003; Zeldis et al. 2005), but often a multitude of interrelated mechanisms, acting on different life stages, are proposed to have caused these relationships. Temperature-enhanced growth rates certainly appear to reduce cumulative predatory losses in early larval populations (Pepin 1991; Heath 1992), as formulated by the "bigger-is-better", the "stage-duration", or "growth-selective predation" hypotheses (Takasuka et al. 2004). In many cases, the temperature effect of enhanced survival through higher growth rates is probably augmented by temperature-dependent zooplankton dynamics (Limburg 1996). For Baltic Sea sprat, significant temperature effects on recruitment strength have so far been attributed to the limited tolerance of sprat eggs and early larvae to low midwater temperatures after severe winters (Nissling 2004).

The present analysis of month- and depth-specific temperature–recruitment relationships has broadened our perception of when and where ambient temperature conditions interact with recruitment variability. Three main cores of such temperature–recruitment relationships were found: the first is in January and at depths below 40 m, which may reflect positive effects on the gonad development of prespawning adults, which are known to overwinter in the deep Baltic basins (Stepputtis et al. 2003). The second core encompassed correlations in midwater depths between March and July and is consistent with the body of published work on temperature-dependent sprat egg and early larval survival (Karasiova and Zezera 2000; Köster et al. 2003). However, the third core has not previously been reported and occurred between July and October in Baltic surface waters, with August relationships having a much higher explanatory power than all temperature correlations earlier in the year. This indicates that temperature-related survival processes during the late summer months, and therefore throughout or after metamorphosis (Baumann et al. 2005, 2006*a*), explain most of the recruitment variability in Baltic Sea sprat. Furthermore, the fact that August and September correlations occurred only in surface waters may reflect the predominant vertical distribution of pre-recruit sprat late in summer.

Although Houde (1992) found survival until metamorphosis to be 45 times lower in marine than in freshwater fish, and consequently suggested that "in marine species larval stage dynamics will have a greater influence on recruitment success", studies concluding just the opposite have become numerous. Bradford (1992) analysed abundance data of fish eggs and larvae compiled from the literature and suggested that "recruitment levels are fixed after the early-larval period", while Leggett and Deblois (1994) more explicitly proposed that "interannual variability in survival during the juvenile life stage is the most important contributor to recruitment variability". Small pelagic clupeoids appear to fit into this concept, as indicated by the present and other recent studies (e.g., by Wilhelm et al. 2005 on Cape anchovy, *E. encrasicolus*, and Takahashi and Watanabe 2005 on Japanese anchovy, *Engraulis japonicus*).

In the case of post-larval Baltic Sea sprat, we need to reconsider the mechanisms responsible for the apparently strong temperature–recruitment relationship. It is noteworthy that all of the established temperature–growth–survival hypotheses for fish larvae imply size- or growth-rate-selective predation to act as the ultimate mortality agent. Following this rationale, years of high surface temperatures in August would increase population growth and thus body size at the end of summer, which then somehow confers a survival advantage with respect to predation. However, the only major predator of Baltic sprat was assumed to be Baltic cod (Köster et al. 2003), before stocks dramatically declined because of a combination of climate-induced recruitment failures and overfishing (Bagge and Thurow 1993). This has caused an estimated fivefold decrease in predation mortalities of 0-group sprat from the mid 1970s to the early 1990s and thereafter (ICES 2005*b*), which did not affect the persistently strong temperature–recruitment relationship. Recent studies on Atlantic cod in the North Sea also suggested that relatively small prey size differences (e.g., due to temperature) have very limited consequences for the total predation mortality (Floeter and Temming 2003). Whether other Baltic piscivores, particularly in shallow coastal areas, can significantly prey on 0-group sprat remains to be demonstrated (e.g., Patokina and Feldman 1998). We argue that the predation by Atlantic cod on post-larval and juvenile sprat cannot be regarded as the major mechanism underlying the observed strong coupling between recruitment and late summer surface temperature.

However, bigger sizes due to accelerated growth in summer may not necessarily grant immediate survival benefits but could also lead to lower mortality throughout the subsequent first winter (e.g., Henderson et al. 1988). Smaller fish have lower energy reserves than bigger conspecifics and could therefore be physiologically less tolerant against low temperatures during overwintering (Sogard 1997). This may be particularly important in a species like sprat, for which the Baltic Sea comprises the northern extreme of its geographical distribution (MacKenzie and Köster 2004). We note that our approach of considering sprat age-0 estimates does not rule out this possibility, because MSVPAs are predominantly driven by catch-at-age data starting at age 1 and are therefore insensitive to potential interannual variations in age-0 overwinter mortality. To assess the magnitude of this potential mechanism, future studies should compare independent abundance time series of sprat recruits prior to and after their first winter.

The strong correlations among long-term data of surface temperature, modelled transport patterns, and sprat recruitment variability advocate that new year classes of Baltic Sea sprat are (*i*) mainly composed of individuals born late in the season and (*ii*) determined in strength by processes acting during the late larval and early juvenile stages. Furthermore, recruitment and atmospheric processes appear to be tightly coupled in the Baltic Sea. The significant relationships between both recruitment proxies and the BSI suggested that temperature and transport have a combined and coherent influence on sprat recruitment. Positive BSIs are characteristic for prevailing westerly winds (Lehmann et al. 2002), which cause eastward and southeastward larval transport and result in lower summer surface temperatures because of increased cloud cover and precipitation (i.e., maritime weather). Conversely, larval retention and high summer surface temperatures appear to be linked through prevailing weak easterly winds (negative BSIs; i.e., continental weather). For these two scenarios, the temperature and the drift model were reliably consistent, suggesting that recruitment levels can be predicted with relatively high confidence. However, a potential decoupling of temperature and transport may happen and will result in inconsistent and therefore less confident predictions (e.g., 2001 and 2002). The drift model may presently be advantageous to the temperature model, given (*i*) that it explicitly includes SSB as a biologically sensible variable, (*ii*) that it is based on a reasonable and testable mechanism (i.e., density-dependent processes in coastal areas), and (*iii*) because of its higher explanatory power.

Correlational studies are useful means to detect long-term trends and general relationships between environmental variables and fish recruitment, which are instrumental for hypothesis generation (e.g., MacKenzie and Köster 2004; Ottersen et al. 2006). Process-oriented field and laboratory studies including all pre-recruit life stages are inevitable for hypothesis testing and exploration of the mechanisms driving such environment–recruitment correlations, which will contribute to improved recruitment models less prone to postpublication failure. The intended revenue of such efforts may be an increased readiness of fisheries managers to include environmentally based projections into regular assessment procedures.

Acknowledgements

Owing to the constructive criticism of the two anonymous reviewers, revising an earlier version of this paper became an enjoyable and creative process. The study was funded by the German Global Ocean Ecosystem Dyanmics (GLOBEC) program (FKZ 03F0320E).

References

Alheit, J., Möllmann, C., Dutz, J., Kornilovs, G., Loewe, P., Mohrholz, V., and Wasmund, N. 2005. Synchronous regime shifts in the Central Baltic and the North Sea in the late 1980s. ICES J. Mar. Sci. **62**: 1205–1215.

Allain, G., Petitgas, P., Grellier, P., and Lazure, P. 2003. The selection process from larval to juvenile stages of anchovy (*Engraulis encrasicolus*) in the Bay of Biscay investigated by Lagrangian simulations and comparative otolith growth. Fish. Oceanogr. **12**: 407–418.

Bagge, O., and Thurow, F. 1993. The Baltic cod stock: fluctuations and possible causes. ICES Mar. Sci. Symp. **198**: 254–268.

Baumann, H., Hinrichsen, H.-H., Köster, F.W., and Temming, A. 2004. A new retention index for the central Baltic Sea: long-term hydrodynamic modelling used to study recruitment variability in central Baltic sprat, *Sprattus sprattus*. ICES CM 2004/L:02.

Baumann, H., Peck, M.A., and Herrmann, J.-P. 2005. Short-term decoupling of otolith and somatic growth induced by food level changes in post-larval Baltic sprat, *Sprattus sprattus*. J. Mar. Freshw. Res. **56**: 539–547.

Baumann, H., Gröhsler, T., Kornilovs, G., Makarchouk, A., Feldman, V., and Temming, A. 2006*a*. Temperature-induced regional and temporal growth differences in Baltic young-of-the-year sprat, *Sprattus sprattus*. Mar. Ecol. Prog. Ser. **317**: 225–236.

Baumann, H., Peck, M.A., Götze, E., and Temming, A. 2006*b*. Starving early juvenile sprat, *Sprattus sprattus* L., in Western Baltic coastal waters: evidence from combined field and laboratory observations in August/September 2003. J. Fish Biol. (In press).

Bergstrom, S., and Carlsson, B. 1994. River runoff to the Baltic Sea: 1950–1990. Ambio, **23**: 280–287.

Borja, A., Uriarte, A., Egaña, J., Motos, L., and Valencia, V. 1998. Relationships between anchovy (*Engraulis encrasicolus*) recruitment and environment in the Bay of Biscay (1967–1996). Fish. Oceanogr. **7**: 375–380.

Bradford, M.J. 1992. Precision of recruitment predictions from early life stages of marine fishes. Fish. Bull. **90**: 439–453.

Campana, S.E. 1996. Year-class strength and growth rate in young Atlantic cod *Gadus morhua*. Mar. Ecol. Prog. Ser. **135**: 21–26.

Cermeno, P., Uriarte, A., de Murguia, A.M., and Morales-Nin, B. 2003. Validation of daily increment formation in otoliths of juvenile and adult European anchovy. J. Fish. Biol. **62**: 679–691.

Crecco, V.A., and Savoy, T.A. 1987. Effects of climatic and density-dependent factors on intra-annual mortality of larval American shad. Am. Fish. Soc. Symp. **2**: 69–81.

Cushing, D.H. 1974. The possible density-dependence of larval mortality and adult mortality in fishes. *In* The Early Life History of Fish. Proceedings of an International Symposium held at the Dunstaffnage Marine Research Laboratory of the Scottish Marine Biological Association at Oban, Scotland. pp. 103–111.

Floeter, J., and Temming, A. 2003. Explaining diet composition of North Sea cod (*Gadus morhua* L.): prey size preference vs. prey availability. Can J. Fish. Aquat. Sci. **60**: 140–150.

Fowler, A.J., and Jennings, P.R. 2003. Dynamics in 0+ recruitment and early life history for snapper (*Pagrus auratus*, Sparidae) in South Australia. Mar. Freshw. Res. **54**: 941–956.

Heath, M.R. 1992. Field investigations of the early life stages of marine fish. Adv. Mar. Biol. **28**: 1–174.

Henderson, P.A., Holmes, R.H.A., and Bamber, R.N. 1988. Size-selective overwintering mortality in the sand smelt, *Atherina boyeri* Risso, and its role in population dynamics. J. Fish. Biol. **33**: 221–233.

Hinrichsen, H.-H., Lehmann, A., St. John, M.A., and Brügge, B. 1997. Modelling the cod larvae drift in the Bornholm Basin in summer 1994. Cont. Shelf Res. **17**: 1765–1784.

Hinrichsen, H.-H., Lehmann, A., Möllmann, C., and Schmidt, J.O. 2003. Dependency of larval fish survival on retention/dispersion in food limited environments: the Baltic Sea as a case study. Fish. Oceanogr. **12**: 425–433.

Hinrichsen, H.-H., Kraus, G., Voss, R., Stepputtis, D., and Baumann, H. 2005. The general distribution pattern and mixing probability of Baltic sprat juvenile populations. J. Mar. Sys. **58**: 52–66.

Houde, E.D. 1989. Comparative growth, mortality, and energetics of marine fish larvae: temperature and implied latitudinal effects. Fish. Bull. **87**: 471–495.

Houde, E.D. 1992. Are marine and freshwater fish larvae different? ICES CM 1992/L:26.

ICES. 2005*a*. Report of the Baltic Fisheries Assessment Working Group. ICES CM 2005/ACFM:19.

ICES. 2005*b*. Report of the Study Group on Multispecies Assessment in the Baltic (SGMAB). ICES CM 2005/H:06.

Karasiova, E.M. 2002. Variability of sprat peak spawning and larvae appearance timing in the southeastern Baltic Sea during the past six decades. Bull. Sea Fish. Inst. Gdynia, **156**: 57–67.

Karasiova, E.M., and Zezera, A.S. 2000. On influence of long-term variability of temperature regime in the Gdansk Deep of the Baltic Sea on the sprat reproduction and the offspring survival. ICES CM 2000/L:06.

Killworth, P.D., Stainforth, D., Webbs, D.J., and Paterson, S.M. 1991. The development of a free-surface Bryan–Cox–Semtner ocean model. J. Phys. Oceanogr. **21**: 1333–1348.

Kornilovs, G., Sidrevics, L., and Dippner, J.W. 2001. Fish and zooplankton interaction in the Central Baltic Sea. ICES J. Mar. Sci. **58**: 579–588.

Köster, F.W. 1994. Der Einfluß von Bruträubern auf die Sterblichkeit früher Jugendstadien des Dorsches (*Gadus morhua*) und der Sprotte (*Sprattus sprattus*) in der zentralen Ostsee. Ber. Inst. Meereskunde Kiel, **261**.

Köster, F.W., and Möllmann, C. 2000. Egg cannibalism in Baltic sprat *Sprattus sprattus*. Mar. Ecol. Prog. Ser. **196**: 269–277.

Köster, F.W., Möllmann, C., Neuenfeldt, S., St. John, M.A., Plikshs, M., and Voss, R. 2001. Developing Baltic cod recruitment models. I. Resolving spatial and temporal dynamics of spawning stock and recruitment for cod, herring, and sprat. Can. J. Fish. Aquat. Sci. **58**: 1516–1533.

Köster, F.K., Hinrichsen, H.-H., Schnack, D., St. John, M.A., MacKenzie, B.R., Tomkiewicz, J., Möllmann, C., Kraus, G., Plikshs, M., Makarchouk, A., and Aro, E. 2003. Recruitment of Baltic cod and sprat stocks: identification of critical life stages and incorporation of environmental variability into stock–recruitment relationships. Sci. Mar. **67**(Suppl.1): 129–154.

Leggett, W.C., and Deblois, E. 1994. Recruitment in marine fishes: is it regulated by starvation and predation in the egg and larval stages? Neth. J. Sea Res. **32**: 119–134

Lehmann, A. 1995. A three-dimensional baroclinic eddy-resolving model of the Baltic Sea. Tellus, **47A**: 1013–1031.

Lehmann, A., and Hinrichsen, H.-H. 2000. On the thermohaline variability of the Baltic Sea. J. Mar. Sys. **25**: 333–357.

Lehmann, A., Krauss, W., and Hinrichsen, H.-H. 2002. Effects of remote and local atmospheric forcing on circulation and upwelling in the Baltic Sea. Tellus, **54A**: 299–316.

Limburg, K.E. 1996. Growth and migration of 0-year American shad (*Alosa sapidissima*) in the Hudson River estuary: otolith microstructural analysis. Can. J. Fish. Aquat. Sci. **53**: 220–238.

MacKenzie, B.R. 2000. Turbulence, larval fish ecology and fisheries recruitment: a review of field studies. Oceanol. Acta, **23**: 357–375.

MacKenzie, B.R., and Köster, F.W. 2004. Fish production and climate: sprat in the Baltic Sea. Ecology, **85**: 784–794.

MacKenzie, B.R., Miller, T.J., Cyr, S., and Leggett, W.C. 1994. Evidence for a dome-shaped relationship between turbulence and larval fish ingestion rates. Limnol. Oceanogr. **79**: 1–16.

Möllmann, C., Kornilovs, G., and Sidrevics, L. 2000. Long-term dynamics of main mesozooplankton species in the central Baltic Sea. J. Plankton Res. **22**: 2015–2038.

Nissling, A. 2004. Effects of temperature on egg and larval survival of cod (*Gadus morhua*) and sprat (*Sprattus sprattus*) in the Baltic Sea — implications for stock development. Hydrobiologia, **514**: 115–123.

Ottersen, G., Hjermann, D.Ø., and Stenseth, N.C. 2006. Changes in spawning stock structure strengthen the link between climate and recruitment in a heavily fished cod (*Gadus morhua*) stock. Fish. Oceanogr. **15**: 230–243.

Patokina, F.A., and Feldman, V.N. 1998. Peculiarities of trophic relations between Baltic herring (*Clupea harengus membras* L.) and sprat in the south eastern Baltic Sea in 1995–1997. ICES CM 1998/CC:7.

Pepin, P. 1991. Effect of temperature and size on development, mortality, and survival rates of the pelagic early life history stages of marine fish. Can. J. Fish. Aquat. Sci. **48**: 503–518.

Sinclair, M. 1988. Marine populations: an essay on population regulation and specification. University of Washington Press, Seattle, Wash.

Sissenwine, M.P. 1984. Why do fish populations vary? *In* Exploitation of marine communities. *Edited by* R. May. Springer-Verlag, Berlin. pp. 59–94.

Skogen, M.D. 2005. Clupeoid larval growth and plankton production in the Benguela upwelling system. Fish. Oceanogr. **14**: 64–70.

Sogard, S.M. 1997. Size-selective mortality in the juvenile stage of teleost fishes: a review. Bull. Mar. Sci. **60**: 1129–1157.

Stepputtis, D., Hinrichsen, H.-H., Goetze, E., and Boetticher, U. 2003. How behaviour of clupeid fishes in the Central Baltic Sea depends on physical factors. ICES CM 2003/P:13.

Takahashi, M., and Watanabe, Y. 2005. Effects of temperature and food availability on growth rate during late larval stage of Japanese anchovy (*Engraulis japonicus*) in the Kuroshio–Oyashio transition region. Fish. Oceanogr. **14**: 223–235.

Takasuka, A., Aoki, I., and Mitani, I. 2004. Three synergistic growth-related mechanisms in the short-term survival of larval Japanese anchovy *Engraulis japonicus* in Sagami Bay. Mar. Ecol. Prog. Ser. **270**: 217–228.

Voss, R., Köster, F.W., and Dickmann, M. 2003. Comparing the feeding habits of co-occurring sprat (*Sprattus sprattus*) and cod (*Gadus morhua*) larvae in the Bornholm Basin, Baltic Sea. Fish. Res. **63**: 97–111.

Voss, R., Clemmesen, C., Baumann, H., and Hinrichsen, H.-H. 2005. Baltic sprat larvae: coupling food availability, larval condition and survival. Mar. Ecol. Prog. Ser. **308**: 243–254.

Wilhelm, M.R., Painting, S.J., Field, J.G., Kerstan, M., and Durholtz, M.D. 2005. Impact of environmental factors on survival of larval and juvenile Cape anchovy *Engraulis encrasicolus* (G.) in the southern Benguela upwelling region, determined from hatchdate distributions: implications for recruitment. Mar. Freshw. Res. **56**: 561–572.

Zeldis, J.R., Oldman, J., Ballara, S.L., and Richards, L.A. 2005. Physical fluxes, pelagic ecosystem structure, and larval fish survival in Hauraki Gulf, New Zealand. Can. J. Fish. Aquat. Sci. **62**: 593–610.

Response of the residential piscivorous fish community to introduction of a new predator type in a mesotrophic lake

Torsten Schulze, Ulrich Baade, Hendrik Dörner, Reiner Eckmann, Susanne S. Haertel-Borer, Franz Hölker, and Thomas Mehner

Abstract: Although the effects of introduced predators on prey populations in aquatic ecosystems have been studied frequently, less is known about the interactions between predators. We performed a whole-lake experiment by stocking a non-native top predator (pikeperch (*Sander lucioperca*)) to two residential piscivores (Eurasian perch (*Perca fluviatilis*) and northern pike (*Esox lucius*)). By analyzing spatial distribution, diet composition, growth, and consumption rates of the piscivores before and after pikeperch introduction, we tested how both density-dependent and trait-mediated responses affected interactions between the three predators. Total piscivore biomass increased 1.5 times and annual consumption by the piscivores increased 1.7 times after stocking, attributable to the stocked pikeperch and increased northern pike abundances. Abundance, distribution, and consumption data indicated that northern pike was hardly affected by pikeperch stocking and even increased its biomass, whereas piscivorous perch shifted its habitat use towards the littoral lake areas in response to competition with pikeperch. Furthermore, all piscivores increasingly fed on small perch. The forced habitat shift of piscivorous perch in combination with increased predation on small perch led to a decreased abundance of large perch, attributable to the compensatory effects of intraguild predation and cannibalism.

Résumé : Alors que les effets des prédateurs introduits sur les populations de proies dans les écosystèmes aquatiques ont souvent été étudiés, les interactions entre les prédateurs eux-mêmes sont moins bien connues. Dans une expérience à l'échelle d'un lac, nous avons ajouté un prédateur supérieur non indigène (« pikeperch » (*Sander lucioperca*)) à un peuplement de poissons ichtyophages résidents (la perche (*Perca fluviatilis*) et le grand brochet (*Esox lucius*)). L'analyse de la répartition spatiale, de la composition du régime alimentaire, de la croissance et des taux de consommation avant et après l'introduction du pikeperch nous a permis de vérifier comment les réactions liées à la densité et celles reliées aux caractéristiques biologiques affectent les interactions entre les trois prédateurs. Après l'empoissonnement, la biomasse totale des poissons piscivores a augmenté de 1,5 fois et la consommation annuelle des piscivores de 1,7 fois; cela s'explique par l'introduction des pikeperch et l'abondance accrue des grands brochets. Les données sur l'abondance, la répartition et la consommation indiquent que le grand brochet est à peine affecté par l'introduction du pikeperch et qu'il augmente même sa biomasse, alors que la perche piscivore modifie son utilisation de l'habitat et choisit de préférence les zones littorales du lac en réaction à la compétition par le pikeperch. De plus, tous les piscivores se nourrissent davantage de petites perches. Le changement forcé d'habitat des perches piscivores combiné à la prédation accrue sur les petites perches a pour effet de diminuer l'abondance des perches de grande taille, ce qui est attribuable aux effets compensatoires de la prédation et du cannibalisme au sein de la guilde.

[Traduit par la Rédaction]

Received 2 June 2005. Accepted 22 April 2006. Published on the NRC Research Press Web site at http://cjfas.nrc.ca on 21 September 2006.
J18721

T. Schulze,[1,2] H. Dörner,[3] F. Hölker, and T. Mehner. Department of Biology and Ecology of Fishes, Leibniz-Institute of Freshwater Ecology and Inland Fisheries, P.O. Box 850 119, 12561 Berlin, Germany.
U. Baade.[4] Department of Biology and Ecology of Fishes, Leibniz-Institute of Freshwater Ecology and Inland Fisheries, P.O. Box 850 119, 12561 Berlin, Germany, and Department of Biology, Limnological Institute, University of Constance, 78457 Constance, Germany.
R. Eckmann and S.S. Haertel-Borer.[5] Department of Biology, Limnological Institute, University of Constance, 78457 Constance, Germany.

[1] Corresponding author (e-mail: torsten.schulze@igb-berlin.de).

[2] Present address: University of Natural Resources and Applied Life Sciences, Department of Water, Atmosphere and Environment, Institute of Hydrobiology and Aquatic Ecosystem Management, Max-Emanuel-Straße 17, A-1180 Vienna, Austria.

[3] Present address: European Commission, Joint Research Centre, IPSC Institute for the Protection and Security of the Citizen, AGRIFISH Unit, TP 266, 21020 Ispra, Italy.

[4] Deceased.

[5] Present address: Swiss Fisheries Advisory Service (FIBER), c/o EAWAG, Seestr. 79, 6047 Kastanienbaum, Switzerland.

Can. J. Fish. Aquat. Sci. **63**: 2202–2212 (2006) doi:10.1139/F06-099

Introduction

Species invasions and introductions may be considered as one of the major threats to global biodiversity and ecosystem stability (Simberloff 1981; Coblentz 1990). Nevertheless, deliberate or intended introductions are widespread in freshwater ecosystems in which stocking of certain fish species is still recommended and a common practice (Lehtonen et al. 1984; Mehner et al. 2004). Within the fisheries perspective, the aims of introducing fish cover several aspects such as filling a "vacant niche", replacing native species with more productive alien species, or controlling water quality (Welcomme 2001). The effects provoked in the stocked ecosystem can be those that were desired, as in the case of biomanipulation (Lathrop et al. 2002), but also devastating effects of introduced piscivorous fish have occurred (Craig 1992).

Whether predator introductions have the desired ecosystem effects depends, among others, on the degree of knowledge available on species interactions. Although direct and indirect effects of predators on their prey populations were often considered (Carpenter and Kitchell 1993; Hansson et al. 1998; Hölker and Mehner 2005), the possible interactions between stocked and residential piscivorous fish species have often been neglected. Coexistence of species faced by competitive interactions is often facilitated by resource segregation along the diet, time, or habitat niche axes (Schoener 1974). Accordingly, niche shifts of the resident competitors in response to introduced competitors might occur. Secondly, because many predators have to grow to large sizes to become piscivorous, size-structured predator–prey interactions between several developmental stages of the piscivores are likely affected (Werner and Gilliam 1984). Intraguild predation and cannibalism are frequent interactions, among others, that may dampen the expected direct density effects on the prey populations (Polis et al. 1989; Arim and Marquet 2004; Claessen et al. 2004). Furthermore, the response of the predators may be additionally influenced by both density-dependent and trait-mediated responses in the prey fish communities (Brabrand and Faafeng 1993; Christensen and Persson 1993; Jacobsen and Perrow 1998).

To elucidate the variety of resulting interactions, we studied the response of two residential predatory species, large Eurasian perch (*Perca fluviatilis*; >20 cm total length (L_T); referred to hereafter as perch) and northern pike (*Esox lucius*), to the experimental introduction of a new predator, pikeperch (*Sander lucioperca*), in a small lake in northern Germany. Northern pike and perch are distributed in Europe, Asia, and North America (northern pike only) and are the top piscivores in many lakes of the northern German lowlands (Maitland and Campbell 1992; Mehner et al. 2005*a*). Northern pike rely on the ambush technique (sit-and-wait predator type), feeding solitarily mainly in the littoral zone, being mostly active during day and twilight (Eklöv 1992; Maitland and Campbell 1992; Craig 1996). In contrast, perch is a less specialized, predominantly day-active fish undergoing several ontogenetic niche shifts and foraging mainly in the pelagic zones (Popova and Sytina 1977; Craig 1987). Into this set of residential predators, we introduced pikeperch, a species that naturally did not occur in northern Germany but has been introduced into many waters to enhance fisheries yield and to suppress unwanted cyprinid species in biomanipulation approaches (Mehner et al. 2004). Pikeperch is a solitary ambush–pursuit predator patrolling the pelagic zones of lakes (Popova and Sytina 1977; Maitland and Campbell 1992). In contrast to perch and northern pike, pikeperch is found highly active during twilight and also at night (Popova and Sytina 1977; Fedorova and Drozzhina 1982).

Empirical data on sympatric populations of northern pike, large perch, and pikeperch are scarce (Svärdson and Molin 1973). According to the single-species studies available, we expected that pikeperch would more strongly interfere with perch than with northern pike because of the stronger habitat overlap among the two percids. Furthermore, we expected that the introduction of pikeperch would lead to both competitive and predator–prey interactions within the piscivorous feeding guild. We considered four not mutually exclusive effects of the ecosystem perturbation. (*i*) The residential northern pike and perch share their prey resources with pikeperch such that growth and consumption rates will decline in the two residential species, but probably at different magnitudes. (*ii*) At least one of the two residential predator species responds to introduction by a habitat shift in comparison with usual habitat preference at allopatry (Werner and Hall 1977). (*iii*) At least one of the two residential predators responds with a shift to other fish prey (Hanson and Leggett 1986) or even includes new prey resources, for example, from benthic origin (Persson 1986). (*iv*) Because of diet switches and altered prey selectivity, predator–prey relationships become the dominant interaction type between the piscivores, and thus intraguild predation and cannibalism will lead to a biomass decline in at least one of the predators. This diet switch might then, in the long term, lead to a return of the overall piscivorous fish abundance to its initial state (Murdoch 1969).

By analyzing spatial distribution, diet composition, growth, and consumption rates of the residential piscivores before and after pikeperch introduction, we tested which of the alternatives contributed strongest to the expected response within the piscivorous fish guild. Furthermore, by studying abundances and distribution of the prey fish populations, we aimed to elucidate whether the response in the residential piscivores was additionally influenced by changes in prey density or behavior.

Material and methods

Study site

Lake Großer Vätersee (12 ha, maximum depth 11.5 m, mean depth 5.2 m) is situated about 70 km northeast of Berlin, Germany (60 m above sea level). The mesotrophic lake has no inflow or outflow, the water level depends on groundwater and the catchment is mostly covered by forest (see Kasprzak et al. (2000) for further details). Most of the lakeshore and the adjacent littoral zones are covered by reed (*Phragmites australis*) and *Chara* sp. There is no commercial fishery at the lake, and angling was forbidden for the duration of the experiment. According to the lake owner, pikeperch has not occurred in the lake during the past 100 years such that the residential piscivores were naive to its experimental introduction. Biological features of the lake ecosystem were studied during a 2-year period both before

(1997 and 1998) and after (2001 and 2002) pikeperch stocking: 782 (183.8 kg) and 301 (101.4 kg) age-2 pikeperch were stocked in spring 2001 and spring 2002, respectively. Pikeperch were measured (mean L_T ± standard deviation (SD): 2001, 30.6 ± 3.5 cm; 2002, 34.3 ± 4.1 cm) and weighed (see below), and all pikeperch were tagged with passive integrated transponders (PIT tags, TROVAN; except for 152 pikeperch marked by fin clips in 2001) before stocking.

Data of the period without pikeperch were taken, in part, from a study by Haertel et al. (2002). During the period after pikeperch stocking, data collection and processing were performed using the same methods as in Haertel et al. (2002) whenever possible. The methods used in either period are described below.

Fishing, food analyses, and abundance estimates

To minimize the impact of fishing on piscivorous fish (i.e., large perch, northern pike, and pikeperch), only nonlethal sampling methods were used, and fish were released into the lake after processing. Fishing was done once or twice per month from April to November in 1997 and 2001 and from March to November in 1998 and 2002. In all years, electric fishing was done with low current (~200V; electrofishing gear with accumulator; Bretschneider Spezialelektronik, Germany) during night and day from a boat with an electrical engine. During night, single fish resting in shallow littoral areas were detected with a spotlight and anaesthetized by a short, low-current pulse. In 2001 and 2002, a set of gill nets with mesh sizes of 25, 32, 40, and 50 mm was also used. Nets were set at day (sunrise to sunset), twilight (sunset to total darkness and total darkness to sunrise), and night (total darkness) and at different depths (littoral zone, 3 m; pelagic zone, 6 m, 8 m (2002 only); surface) for short time intervals (45 to 120 min, depending on water temperature) to minimize mortality. To describe diel activity patterns, standardized fish numbers (catch per unit effort (CPUE) calculated per 100 m^2 net panel and exposure time, individuals·(h·100 $m^2)^{-1}$) were calculated from all nets except the set at the depth of 8 m because of anoxic conditions during summer. The proportion of habitat use by both prey species was calculated from the simultaneously obtained littoral and pelagic CPUE, separately for day and night periods. From these values, an annual average use (percent of total CPUE) of the littoral (or pelagic) zone was calculated only for those sampling intervals in which ≥2 perch or pikeperch were caught. In contrast, catches with only one fish (i.e., 100% in either littoral or pelagic areas) were considered to be not representative of the distributions and thus were omitted. To increase the number of fish available for abundance estimates (see below), a fyke net (length of leader, 65 m; mesh size, 16 mm; height, 4.5 m; mesh size of hoop, 12 mm) set perpendicular to the shore was used in addition to the other nets during all sampling months in 2002. A beach seine (length of each wing, 300 m; mesh size, 26–18 mm; height, 20 m) hauled by a mooring winch was used to remove most of the pikeperch from the lake at the end of the experimental period in November 2002.

All fish were measured and weighed to the nearest 0.5 cm L_T and gram wet mass, respectively. Fishes caught by gill nets, electrofishing, and the beach seine were used for diet analyses. Stomach contents, obtained from anaesthetized fish (tricaine methanesulfonate, MS 222) by flushing them with a compression sprayer, were preserved in 70% alcohol (1997–1998) or deep frozen (–18 °C; 2001–2002) until further processing in the laboratory. Stomach contents were examined under a stereoscopic microscope. Prey fish were determined to species level and, in case of advanced digestion, identified from remaining hard structures. Prey fish were counted, length was measured, and mass was then backcalculated from length–mass relationships or hard part length–mass relationships obtained from Lake Großer Vätersee fish and crayfish samples. Vertebra length in fish and carapax or claw lengths in crayfish were used to calculate total length and biomass. Index of food selectivity of predators was calculated for the main prey species small roach (*Rutilus rutilus*, 6–16 cm) and small perch (6–15 cm) according to Strauss (1979), based on the biomass proportions of these size classes in the calculated yearly consumption rates (see below) and on the lake-wide prey biomass.

On each sampling occasion, all piscivores were checked for tags, and untagged ones were individually tagged with PIT tags injected into the back muscle and released. Population densities were estimated from the mark–recapture data according to Schumacher and Eschmeyer (in Ricker 1975). Population biomass was then derived from the age group (perch) or length class (northern pike) proportions in the samplings and the respective length–mass relationships. For pikeperch, abundance and biomass data were calculated for two groups according to the stocking occasions.

Abundances of prey fish species (small roach and perch) were estimated by multiple mark–recapture experiments in 1998 (Haertel et al. 2002) and 2002. To minimize handling mortality at higher water temperatures, these estimates were restricted to early spring (Haertel et al. 2002). Moreover, a short time frame better approximates the assumption of a closed population in mark–recapture models. Fishes were caught by electrofishing (see above), anaesthetized (MS 222), and measured (L_T, to the nearest 1 mm). All fish were tagged with coded wire tags (NMT, Salisbury, USA), which were injected into the dorsal musculature in 1998 (Haertel et al. 2002) or into the head (snout tissue or cheek muscle) in 2002. Tag presence was checked by a portable sampling detector. At each electrofishing operation, all fish were checked for tags, unmarked fish were tagged, and all fish were subsequently released. Population size was calculated according to model M_t (Otis et al. 1978; White et al. 1982). Population biomass was derived from length–weight relationships obtained from Lake Großer Vätersee fish samples.

Habitat use of prey fish was investigated in the littoral (≤3 m water depth) and the pelagic zones. Both habitats were sampled simultaneously during day and night. Sampling took place monthly from May to September 1997 and from May to October 1998 (Haertel et al. 2002). In 2001 and 2002, sampling took place from May to October. All fishing was done by gillnets of 8–15 mm bar mesh size. In the littoral zone, the nets were set perpendicular to the shoreline at the bottom. In the pelagic zone, floating nets 6 m high were used, fishing almost the entire zone where fish can survive as the lake is thermally stratified from late April to late October, with an anoxic zone beginning at about 7 m deep (Kasprzak et al. 2000). The nets were set for 2 h during day (1000–

Fig. 1. Abundance (open bars) and biomass (shaded bars) ± upper and lower 95% confidence limits of northern pike (*Esox lucius*), perch (*Perca fluviatilis*; >20 cm L_T), and pikeperch (*Sander lucioperca*) in Lake Großer Vätersee in the pikeperch-free (1997–1998) and pikeperch (2001–2002) periods, estimated by multiple mark–recapture census.

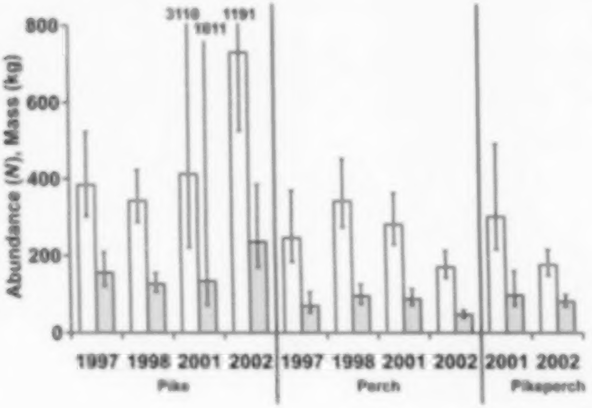

1200) and immediately after nightfall. The fish length was measured and CPUE was calculated per 100 m^2 net panel and 2 h exposure time. CPUE was calculated only for those sampling intervals with ≥2 perch or roach simultaneously caught with littoral and pelagic nets.

Growth and consumption estimates

For calculating daily rations of northern pike, perch, and pikeperch, a computerized bioenergetics model was used (Fish Bioenergetics, Hanson et al. 1997). Species-specific parameters for perch were taken from Kitchell et al. (1977), for northern pike from Bevelhimer et al. (1985), and for pikeperch from Wysujack and Mehner (2002). Percent composition by mass on a monthly basis was used as diet input. In the pikeperch-free period, water temperature was recorded at a water depth of 1 m at 1-h intervals throughout the sampling season (ONSET; Optic StowAway® temperature logger). For each day of the simulation period, the mean water temperature was calculated. In the pikeperch period, temperature was interpolated from biweekly measurements using a mean temperature at depths of 0–5 m (0.5 m intervals). Yearly mass increment of fish was modeled between 1 April and 5 November (218 days), because fish diet could not be sampled during winter months. Water temperature was, however, below 8 °C during the winter, and therefore growth should have been negligible. Mean yearly mass increment per age or length class was used as somatic growth model input, based on age–length keys from scales (northern pike) and opercula (perch; caught in November 2002) or directly determined from individual growth rates of tagged fish (northern pike and pikeperch in 2001–2002, minimum distance between captures >30 days). Individual consumption estimates were expanded to population estimates by taking into account the relative abundances of the several age groups or length classes per species of piscivorous fish. For growth comparisons of perch and northern pike between both periods, the individual growth data were used.

Table 1. Differences in the abundance of northern pike, perch (>20 cm L_T), and pikeperch between the years 1997, 1998, 2001, and 2002, based on Student's *t* test and Bonferroni correction.

Year	Northern pike	Perch	Pikeperch
2002 vs. 2001	0	–	–
2002 vs. 1998	+	–	nd
2002 vs. 1997	+	–	nd
2001 vs. 1998	0	0	nd
2001 vs. 1997	0	0	nd
1998 vs. 1997	0	0	nd

Note: +, increase; –, decrease; 0, no significant difference; nd, no data.

Statistical methods

Data were checked for normality. The level of significance was $p < 0.05$. Predator abundances were tested for differences among years using Student's *t* test on the reciprocal abundances calculated by the Schumacher and Eschmeyer model (in Ricker 1975) and a Bonferroni correction according to Holm (in Rice 1989). All other tests were calculated using SPSS 9.0 (SPSS Inc. 1999).

Results

Abundance, biomass, and growth of predatory fish

During the first month after stocking, 25 pikeperch were found dead in 2001 and 60 in 2002. In both the pikeperch-free (1997 and 1998) and the pikeperch (2001 and 2002) periods, a total of 892 northern pike, 951 perch (> 20 cm), and 245 pikeperch were caught (including recaptures). The number of sampling occasions varied between species and ranged from 10 to 17 each year. Total biomasses of piscivorous fish before pikeperch stocking were 226 kg and 223 kg in 1997 and 1998, respectively (Fig. 1). After pikeperch stocking, piscivorous fish biomass rose to 320 kg and 366 kg in 2001 and 2002, respectively. Pikeperch contributed 31% in 2001 and 22% in 2002 to the total biomass of piscivorous fish. Northern pike biomass was relatively constant between 1997 and 2001 (134–156 kg) but significantly increased in 2002 (236 kg). Partially because of low and heterogeneous recapture rates, the confidence limits of the abundance estimates in northern pike were high in 2001 and 2002 (Fig. 1). Perch biomass never exceeded 96 kg and dropped below 50 kg in 2002. After the first stocking in 2001, pikeperch biomass was estimated at 98 kg, whereas 82 kg were estimated in the second year of stocking. Abundances were significantly higher for northern pike and lower for perch and pikeperch in 2002 than in the previous years (Student's *t* test, Bonferroni correction, $p < 0.05$; Table 1).

Median lengths (minimum–maximum) of northern pike were 36.0 (5.0–101.0) cm in 1997–1998 and 32.0 (12.5–92.0) cm L_T in 2001–2002, whereas median lengths of piscivorous perch were 27.5 (20.5–39.5) cm and 28.0 (20.5–7.0) cm L_T in 1997–1998 and 2001–2002, respectively. Median lengths of pikeperch were 34.0 (28.0–49.0) cm and 38.5 (29.5–55.0) cm L_T in 2001 and 2002, respectively.

Fig. 2. Yearly consumption in terms of biomass of different prey types by populations of northern pike (*Esox lucius*), perch (*Perca fluviatilis*; >20 cm L_T), and pikeperch (*Sander lucioperca*) in the pikeperch-free (1997–1998) and pikeperch (2001–2002) periods in Lake Großer Vätersee, estimated by bioenergetics modeling. Prey are perch (hatched bars), roach (solid bars), other and unidentified fish (stippled bars), *Orconectes limosus* (open bars), and other invertebrates (shaded bars).

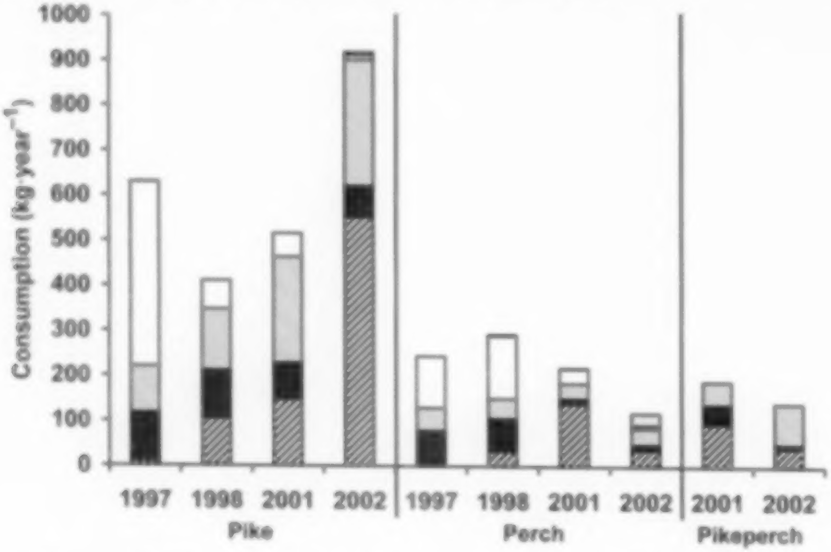

Length-specific growth rates of different size classes of northern pike and perch determined from individual tagging did not differ between the pikeperch and the pikeperch-free period (Mann–Whitney *U*, length class, *p*, *n* (pikeperch-free/pikeperch): northern pike: L_T < 30 cm, p = 0.869, n = 23/4; L_T = 30–45 cm, p = 0.806, n = 48/3; L_T = 35–40 cm, p = 0.214, n = 59/6; L_T > 40 cm, p = 0.870, n = 45/9; perch: L_T = 20–25 cm, p = 0.883, n = 26/21; L_T = 25–30 cm, p = 0.795, n = 56/60; L_T > 30 cm, p = 0.802, n = 42/55).

Diet and consumption

Spiny-cheek crayfish (*Orconectes limosus*) and small roach dominated the diet of northern pike and large perch before pikeperch stocking, whereas small perch was the main food item of all three piscivorous species after stocking with pikeperch (Fig. 2). Although consumption of small perch as prey rose from 20% of total consumption in the pikeperch-free period to 54% in 2002, the proportion of small roach declined from more than 20% in the pikeperch-free period to 15% and 7% in the years 2001 and 2002, respectively. Consumption of *O. limosus* declined from 60% in 1997 (523 kg) to only 1% (18 kg) in 2002. Other fish consumed were cyprinids other than small roach, juvenile northern pike, ruffe (*Gymnocephalus cernuus*), pikeperch, and unidentified fish. Other invertebrates consumed were mainly *Chaoborus* sp. in perch and *Asellus* sp. in northern pike.

Annual consumption of all piscivorous fishes was in the same range in the years 1997, 1998, and 2001 (874, 703, and 923 kg, respectively) and rose to 1178 kg in 2002 (Fig. 2). The relative annual consumption rates of the three species largely reflected their contribution to the biomass of the piscivorous guild. Consumption rates were always highest for northern pike (56%–72% of total consumption in the years 1997, 1998, and 2001, and even 78% in 2002; Fig. 2). In contrast, large perch consumed between 24% and 42% of the piscivorous guild in the years 1997, 1998, and 2001, but contributed only 10% to total consumption in 2002. Pikeperch contributed 21% and 12% to total consumption in the years 2001 and 2002, respectively. Annual mass-specific individual energy consumption increased in northern pike from about 14 300 to 17 000 kJ·kg^{-1}·year^{-1}, but declined in perch from 13 700 to 10 700 kJ·kg^{-1}·year^{-1} over the period from 1997 to 2002 (Table 2). In pikeperch, the lowest relative energy consumption rates were estimated.

According to selectivity indices for prey fish, small perch was continuously preferred over small roach by all piscivorous species, and the discrepancy in preference between both species was even enhanced after the stocking with pikeperch (Fig. 3). The differences between the pikeperch-free and the pikeperch periods were significant for both northern pike and large perch as predators (Student's *t* test, p < 0.05, northern pike feeding on small perch, df = 100; northern pike on small roach, df = 128; large perch on small perch, df = 168; large perch on small roach, df = 116).

Diel patterns in habitat use

Before pikeperch stocking, in an unrepeated sampling operation in June 1997, 89% of large perch (n = 45) was caught by gill nets in the pelagic zone during the day, and no large perch have been caught by any passive fishing gear during the night (Haertel et al. 2002). After pikeperch stocking, more large perch were caught in the littoral zone, and the use of littoral habitats even increased from 2001 to 2002 such that almost 69% of perch were caught in littoral areas during the day in 2002 (Fig. 4). In contrast, pikeperch was caught predominantly in the pelagic zone, although a similarly enhanced use of the littoral zone as in perch was found

Table 2. Energy consumption per biomass estimated by bioenergetics modeling of northern pike (*Esox lucius*), perch (*Perca fluviatilis*; >20 cm L_T), and pikeperch (*Sander lucioperca*) in Lake Großer Vätersee before (1997–1998) and after (2001–2002) stocking with pikeperch.

	Specific consumption (kJ·kg^{-1}year^{-1})		
	Northern pike	Perch	Pikeperch
1997	14 284	13 668	
1998	14 211	11 637	
2001	15 923	10 122	8682
2002	17 020	10 668	7620

Fig. 3. Index of selectivity ± standard deviation (Strauss 1979) for small perch (*Perca fluviatilis*) and small roach (*Rutilus rutilus*) in the diet of northern pike (*Esox lucius*), large perch (>20 cm L_T), and pikeperch (*Sander lucioperca*) in Lake Großer Vätersee in the years 1998 (open bars) and 2002 (shaded bars). Asterisks (*) indicate that selectivities were significantly different between the two years (*t* test, $p < 0.05$).

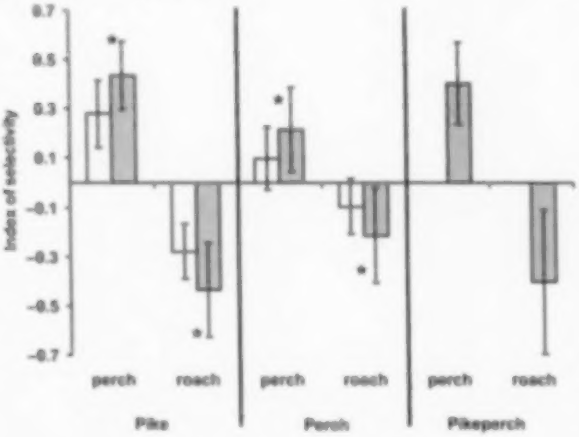

Fig. 4. Percent of gill net catch (catch per unit effort, CPUE; columns: median of all catches with ≥2 individuals) of perch (*Perca fluviatilis*; >20 cm L_T) and pikeperch (*Sander lucioperca*) in the pikeperch period obtained from littoral (open bars) or pelagic (shaded bars) habitats in Lake Großer Vätersee during day, twilight (twil.), and night. Numbers above columns indicate the number of sampling occasions, numbers in parentheses indicate the number of fishes caught for distribution estimates. Please note that no large perch were caught at all during two nightly sampling occasions in 2002.

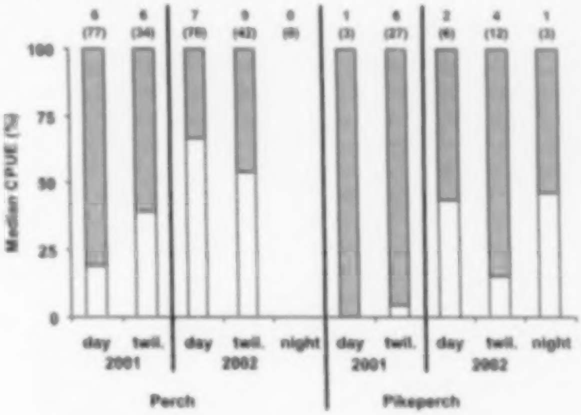

in 2002 (Fig. 4). Further, although perch was caught by gill nets only during day and twilight, pikeperch was also caught during night. Northern pike was only occasionally ($n = 11$) caught by gill nets (never during night). During both the pikeperch-free (Haertel et al. 2002) and pikeperch periods, northern pike were predominantly caught in *Chara* sp. beds (<3 m depth) or in reed stands in the littoral zone.

Abundance and distribution of prey

Biomasses of prey populations (mean ± SD) were 25.8 (±1.2) kg·ha^{-1} for small roach and 7.2 (±1.6) kg·ha^{-1} for small perch in 1998 (Haertel et al. 2002) and 14.7 (±4.1) kg·ha^{-1} for small roach and 10.4 (±1.7) kg·ha^{-1} for small perch in 2002 (Fig. 5). The number of sampling occasions were 19 and 17 in 1998 and 13 and 16 in 2002 for small roach and small perch, respectively. In the pikeperch-free period, small roach exclusively used the littoral zone during daytime, whereas almost all small roach were caught in the pelagic zone during night (Fig. 6). This was different in the pikeperch period when small roach reduced its diel horizontal migration and used the pelagic zone less rigorously during night. No difference in diel habitat use was observed for small perch, which were caught mostly in the littoral zone during day. No conclusion can be drawn from the gill net catches about the habitat use of small perch during night after the pikeperch stocking because only two individuals were caught during two sampling occasions. In contrast, perch of all size classes were observed resting in high numbers in shallow littoral areas before and after the pikeperch stocking during night (Haertel et al. 2002; T. Schulze, personal observations) and were not even caught with active fishing methods in the pelagic zone (purse seine) during night in the pikeperch period (H. Dörner, unpublished data; see Mehner et al. (2005*b*) for details on fishing methods). This indicates a nearly exclusive inactive use of littoral habitats by small perch during night in the pikeperch period, whereas active perch were caught in both habitats during night in the pikeperch-free period.

Discussion

Our study demonstrates that the introduction of a new predator type had strong impacts on the residential fish community in Lake Großer Vätersee on both the prey and predator levels. The lake-wide piscivore biomass increased 1.42–1.64 times as a result of pikeperch stocking and the accompanying increase in northern pike abundance. The biomass of piscivorous fish in the pelagic area almost doubled as a result of pikeperch stocking in comparison with the period before stocking when large perch was the sole pelagic predator. Therefore, a severe density-mediated perturbation could be expected. Beyond the density-mediated effects on the prey fish population (consumption rates of predators), changes in a behavioral trait (reduced diel horizontal migration

Fig. 5. Abundance (open bars) and biomass (shaded bars) ± standard deviation of small roach (*Rutilus rutilus*; 6–16 cm L_T) and small perch (*Perca fluviatilis*; 6–15 cm L_T) in Lake Großer Vätersee in the periods before (1988) and after (2002) pikeperch (*Sander lucioperca*) stocking, as estimated by multiple mark–recapture census.

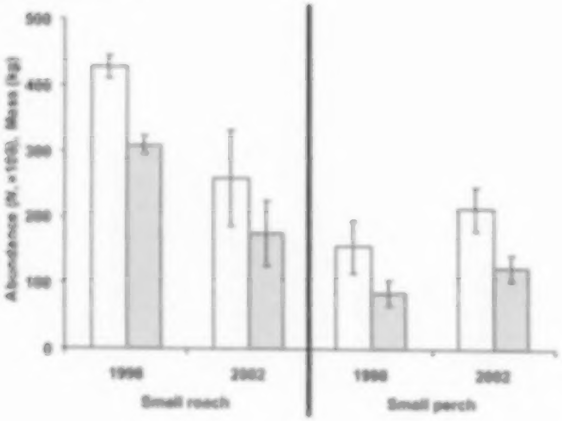

Fig. 6. Percent of gill net catch (catch per unit effort, CPUE; columns: median of all catches with ≥2 individuals) of small roach (*Rutilus rutilus*) and small perch (*Perca fluviatilis*) in the periods before (PP free; 1997–1998) and after (PP; 2001–2002) pikeperch (*Sander lucioperca*) stocking, obtained from littoral (open bars) or pelagic (shaded bars) habitats in Lake Großer Vätersee during day and night. Numbers above columns indicate the numbers of sampling occasions, numbers in parentheses indicate the number of fishes caught for distribution estimates. Please note that only two small perch were caught during two nightly sampling occasions in 2002, which were not considered to be representative of habitat use.

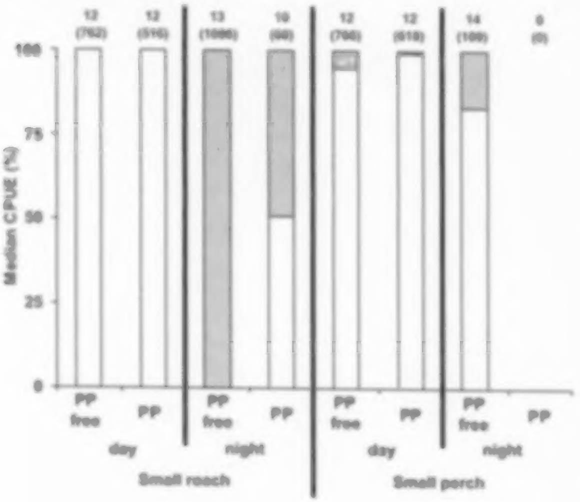

of small roach) were also observed. Furthermore, among the residential predators, the introduced pikeperch induced both density-mediated effects (cannibalism and intraguild predation) and changes in habitat use and prey selectivity. The latter may be a trait-mediated indirect effect of the behavioral changes of the prey species (reduced diel horizontal migration). These complex interactions have, to the best of our knowledge, never been reported in empirical studies to date and underline that the immediate expectation, i.e., introduced predators suppressing unwanted prey fish and improving fisheries yield, will not necessarily be fulfilled because of compensatory mechanisms affecting the piscivorous guild.

Pikeperch stocking affected habitat use and diet composition of piscivorous perch. Because both species are predominantly pelagic hunters, strong interspecific competition for pelagic-living prey fish could be expected (Craig 1987). However, according to literature, the main diel activity phases differ between perch and pikeperch with pikeperch being more active during the twilight and night phases and perch being a day-active species (Craig 1987). In contrast, in Lake Großer Vätersee diel gill net catches of large perch and pikeperch indicated a stronger temporal overlap. Although perch were almost exclusively caught during day and twilight, pikeperch were caught over the full diel cycle, reflecting a simultaneous hunting activity of both species at least during daytime and twilight. Also, the spatial segregation between large perch and pikeperch remained weak, with both species being caught in the littoral and pelagic zones. Accordingly, there was only low niche segregation between perch and pikeperch, and competition was probably strong. However, there was a strong tendency for perch to increasingly respond to the pelagic presence of pikeperch by shifting their daytime habitat towards a stronger use of the littoral area as a higher proportion of perch was caught in nearshore areas in 2002 as compared with 2001, and the differences were even more pronounced in comparison with the situation before pikeperch stocking (Haertel et al. 2002). This may indicate strong interference competition for the pelagic zone, with the larger pikeperch being the stronger competitor. Aggressive pelagic interference was also found to be responsible for reduced vertical space use by Dolly Varden (*Salvelinus malma*) living in sympatry with cutthroat trout (*Oncorhynchus clarkii*) (Hindar et al. 1988). Furthermore, size is an important factor determining competitive displacements in predator communities in which intraguild predation occurs (Fedriani et al. 2000; Suutari et al. 2004), thus underlining the possibility of asymmetric interference competition between the larger pikeperch (55 cm maximum L_T) and the smaller perch (39.5 cm maximum L_T).

A different impact of pikeperch stocking was found on northern pike. Because the feeding habitats differ between northern pike and pikeperch, a strong spatial segregation could be expected. Indeed, in Lake Großer Vätersee, only a few northern pike (five in each year in 2001 and 2002; Schulze 2005) were caught by the pelagic or deep littoral gill nets, indicating a close association of northern pike with reed stands and *Chara* sp. beds. In contrast, no pikeperch were caught in the littoral reed stands where northern pike occurred during the day and night. Because there was no response in habitat preferences or activity patterns of northern pike in response to pikeperch stocking, competition for feeding habitat between both predators was assumed to be very low in Lake Großer Vätersee as a consequence of the stable spatial segregation between northern pike and pikeperch. Comparably, habitat use and hence diet compositions of northern pike and pikeperch differed in an empirical study in Lake Peipsi (Kangur and Kangur 1998) such that the authors concluded that interspecific competition between these predators was probably not strong. However, northern pike and pikeperch may still compete for the same food resources in Lake Großer Vätersee because of the diel and seasonal migrations of small fish between littoral and pelagic sites (this study; see also Jacobsen and Berg 1998; Okun and Mehner 2005).

Northern pike may have even benefited from stocking with pikeperch. In direct comparison between the pikeperch-free and the pikeperch periods, northern pike abundance was significantly higher in 2002 than the years before pikeperch stocking, and biomass almost doubled after the pikeperch introduction. An explanation may be a higher recruitment from larvae into the juvenile size classes, indicated by the declining median length of northern pike in the pikeperch period. Recruitment is correlated with the availability of food and vegetative shelter for the juveniles against cannibalism (Craig 1996; Skov and Koed 2004). Because of altered habitat use and abundances of prey fish, the prey availability in the littoral zone increased after the introduction of pikeperch (please see below for further discussion). Specific consumption rates of northern pike were indeed higher in the pikeperch period, and cannibalism in northern pike was found only in very few cases in Lake Großer Vätersee (Schulze 2005).

According to the improved performance of northern pike after pikeperch stocking, perch was also the inferior competitor to northern pike in the littoral zone. This may be indicated by the decreased specific consumption rates in perch after the pikeperch stocking and is in accordance with other studies in which juvenile northern pike was found to be the more effective forager compared with perch in complex littoral structures (Jacobsen and Perrow 1998). Furthermore, only the northern pike growth rates increased in experiments when northern pike only treatments were contrasted with treatments in which perch and northern pike co-occurred. In contrast, perch could not benefit from competitive release because their growth rates were similar in both treatments (Eklöv and VanKooten 2001). However, the specific growth rates (one of the input parameters of the bioenergetics models) of northern pike and perch were not different between the two periods in the present study. Consequently, in Lake Großer Vätersee, piscivorous perch responded to competition with pikeperch in the pelagic zone by a partial habitat shift and increased cannibalism, but was faced with similarly strong competition and a higher predation rate on perch juveniles by northern pike in the littoral areas. Therefore, both pikeperch and northern pike are supposed to be the specialists for piscivorous feeding in their favored habitats, leading to the more generalist perch being sandwiched between northern pike (littoral zone) and pikeperch (pelagic zone) and becoming the weaker competitor for fish. A similar sandwiching was described for juvenile perch switching between planktivory and benthivory in competition with the benthivorous specialist ruffe and the planktivorous specialist roach such that perch growth rates were always lower than those of the competing species (Bergman and Greenberg 1994). It can be assumed, therefore, that specialists with a highly efficient feeding strategy in one habitat may outcompete a generalist (perch) in relatively stable environments like Lake Großer Vätersee. The generalist is then forced to respond with diet and (or) habitat shifts to avoid severe competition (Larkin 1956).

The interactions between the predators were furthermore directly influenced by changes in prey fish abundance and behavior. Small roach, the dominant prey species in the pikeperch-free period, responded to pikeperch stocking with reduced diel horizontal migrations. In the pikeperch-free period, small roach inhabited the littoral zone during the day, being protected against predation by large perch in the pelagic zone, but moved into the zooplankton-richer pelagic area during the night (Haertel et al. 2002). After pikeperch introduction, however, the occurrence of small roach in littoral habitats also remained high during the night. Such a shift in a behavioral trait was also observed in other lakes in response to pikeperch stocking (Brabrand and Faafeng 1993). Accordingly, the availability of small roach in the pelagic areas declined for both pikeperch and perch, but increased for northern pike in the littoral zone, which may have contributed to the higher recruitment of northern pike. Brabrand and Faafeng (1993) similarly argued that the modification of roach behavior by pikeperch stocking in Lake Gjersjoen (Norway) may have increased the prey availability for littoral predators.

The abundance of the alternative prey species, small perch, slightly increased in the years after pikeperch stocking. Further, small perch inhabited mostly the littoral areas during the day and were exclusively found in littoral habitats during the night in the pikeperch period. This predominant littoral occurrence may have contributed to the habitat shifts of the piscivorous perch and the partial littoral habitat use of pikeperch and has furthermore increased the availability of perch as prey for northern pike. As a consequence, cannibalism and intraguild predation on small perch substantially increased in 2001, which may have led to a reduced recruitment from small to large perch and eventually to a reduced density of large perch in 2002. Further, the predation impact relative to the standing stock of small perch became very high in 2002. Nevertheless, year-class strength of small perch in 2002 was high, indicated by slightly higher abundances of small perch in spite of the high predation pressure. Introduction of pikeperch into Scandinavian waters inhabited by perch resulted in comparable interactions where predation on juvenile perch by pikeperch explained the strong decrease in commercial catches of perch, and also, in naturally sympatric populations, perch catches were inversely correlated with those of pikeperch (Svärdson and Molin 1973).

Overall, feeding of all piscivores on the prey populations was asymmetrical, although both small perch and small roach concentrated in the littoral zone. Consumption on perch increased, whereas that on small roach decreased. Firstly, this simply reflects the differing population developments of small perch and small roach, with perch densities increasing and roach densities declining after pikeperch stocking. Also, in other lakes, diet composition of piscivorous perch, northern pike, and pikeperch were mainly influenced by relative availabilities of prey species (Popova and Sytina 1977; Fedorova and Drozzhina 1982; Dörner et al. 2003). Secondly, selectivity indices for roach feeding did decline and that for perch increased. Small perch are very vulnerable to predators as they have to move continuously while feeding on benthic organisms and therefore face a high risk of encountering predators. In contrast, roach show effective behavioral antipredator traits, such as shoaling and jumping out of the water, that have been found to reduce the number of roach eaten by littoral predators (Christensen and Persson 1993; Eklöv and Persson 1995; Persson and Eklöv 1995). Further, in a habitat structured by artificial vegetation (Christensen and Persson 1993) similar to the reed stands in the littoral zone of Lake Großer Vätersee, small perch was found to be preferred over small roach by predators because of different antipredator traits. Therefore, small roach were probably less vulnerable than small perch to all piscivorous predators in Lake Großer Vätersee after pikeperch had been introduced, and thus passive selectivity (sensu Turesson et al. 2002) for roach feeding declined and that for perch increased under strong predation pressure leading to strong intraguild predation on small perch. Similar findings were made at high piscivorous fish biomass in Bautzen Reservoir, where small benthivorous perch were the preferred prey of piscivorous perch, pikeperch, and eel (Dörner et al. 1999, 2003; Dörner and Benndorf 2003).

The preferential consumption of small perch indicated that besides competitive interactions, predator–prey relationships between the predators also became increasingly important and contributed decisively to the density-mediated effects of the pikeperch introduction. The mutual predation on potential competitors, both within and across the species borders, is widespread in many aquatic and terrestrial species (Arim and Marquet 2004) and has fundamental impacts on food web dynamics and ecosystem stability (Claessen et al. 2004). In pikeperch, strong inter- and intra-cohort cannibalism was found to stabilize year-class strengths and was seen as population density self-regulation (Frankiewicz et al. 1999). Furthermore, adaptive feeding of predators stabilizes food webs (Murdoch 1969) and promotes species coexistence in modeled systems because adaptive foraging changes interaction strength in food webs, which relaxes competition between species (Krivan 2003).

The results presented here give empirical support for the compensatory effects of adaptive feeding strategies in predators, which include cannibalism and intraguild predation. As a consequence, for Lake Großer Vätersee, we expect that the total biomass of piscivorous fish will fall back to that biomass that was estimated before stocking because the piscivorous trophic level in four-level mesotrophic lakes is strongly dependent on the productivity of the system (Persson et al. 1992). Indeed, predation pressure of piscivorous fish on their prey populations was already high before the stocking (Haertel et al. 2002) and the trophic state of the lake has not changed during the experiment. Thus, although predator biomass was substantially enhanced, we suggest that several self-regulating mechanisms will, in the long term, prevent a higher energy transfer to the piscivores in comparison with the situation before stocking.

Nevertheless, populations of the residential predator species responded very differently to stocking with a new predator type in mesotrophic lakes. Our results suggest that introductions and stocking programs with pikeperch or other piscivorous fish species are likely to result in a decrease of guild member abundances because of increased competition and trait-mediated interactions (i.e., changes in behavioral traits leading to alterations in prey selectivity as in the present study). Accordingly, each introduction of a new piscivorous fish species might be a trade-off (in the long term) between gaining a new species for commercial or game fisheries and altering or even decreasing the abundances of the residential piscivorous species, especially when prey resources are already limited.

Acknowledgements

We thank Christian Helms and Alexander Türck for supporting all kinds of labor-intensive fieldwork. We thank all members of the Department of Biology and Ecology of Fishes and the Lake Vätersee working group for their support during the stocking and fishing programs and for valuable discussions. The study was financed by the German Research Foundation (DFG, EC 146/2-1+2, and ME 1686/4-1+2).

References

Arim, M., and Marquet, P.A. 2004. Intraguild predation: a widespread interaction related to species biology. Ecol. Lett. **7**: 557–564.

Bergman, E., and Greenberg, L.A. 1994. Competition between a planktivore, a benthivore, and a species with ontogenic diet shifts. Ecology, **75**: 1233–1245.

Bevelhimer, M.S., Stein, R.A., and Carline, R.F. 1985. Assessing significance of physiological differences among three esocids with a bioenergetics model. Can. J. Fish. Aquat. Sci. **42**: 57–69.

Brabrand, A., and Faafeng, B. 1993. Habitat shift in roach (*Rutilus rutilus*) induced by pikeperch (*Stizostedion lucioperca*) introduction: predation risk versus pelagic behaviour. Oecologia, **95**: 38–46.

Carpenter, S.R., and Kitchell, J.F. 1993. The trophic cascade in lakes. Cambridge University Press, Cambridge, UK.

Christensen, B., and Persson, L. 1993. Species-specific antipredatory behaviors — effects on prey choice in different habitats. Behav. Ecol. Sociobiol. **32**: 1–9.

Claessen, D., De Roos, A.M., and Persson, L. 2004. Population dynamic theory of size-dependent cannibalism. Proc. R. Soc. Lond. Ser. B Biol. Sci. **271**: 333–340.

Coblentz, B.E. 1990. Exotic organisms: a dilemma for conservation biology. Conserv. Biol. **4**: 261–265.

Craig, J.F. 1987. The biology of perch and related fish. Croom Helm Ltd., Kent, UK.

Craig, J.F. 1992. Human-induced changes in the composition of fish communities in African Great Lakes. Rev. Fish Biol. Fish. **2**: 93–124.

Craig, J.F. 1996. Pike: biology and exploitation. Chapman & Hall, London, UK.

Dörner, H., and Benndorf, J. 2003. Piscivory by large eels on young-of-the-year fishes: its potential as a biomanipulation tool. J. Fish Biol. **62**: 491–494. doi:10.1046/j.0022-1112.2003.00035.x.

Dörner, H., Wagner, A., and Benndorf, J. 1999. Predation by piscivorous fish on age-0 fish: spatial and temporal variability in a biomanipulated lake (Bautzen reservoir, Germany). Hydrobiologia, **408–409**: 36–46.

Dörner, H., Berg, S., Jacobsen, L., Hülsmann, S., Brojerg, M., and Wagner, A. 2003. The feeding behaviour of large perch (*Perca* *fluviatilis* (L.)) in relation to food availability: a comparative study. Hydrobiologia, **506–509**: 427–434.

Eklöv, P. 1992. Group foraging versus solitary foraging efficiency in piscivorous predators — the perch, *Perca fluviatilis*, and pike, *Esox lucius*, patterns. Anim. Behav. **44**: 313–326.

Eklöv, P., and Persson, L. 1995. Species-specific antipredator capacities and prey refuges — interactions between piscivorous perch (*Perca fluviatilis*) and juvenile perch and roach (*Rutilus rutilus*). Behav. Ecol. Sociobiol. **37**: 169–178.

Eklöv, P., and VanKooten, T. 2001. Facilitation among piscivorous predators: effects of prey habitat use. Ecology, **82**: 2486–2494.

Fedorova, G.V., and Drozzhina, K.S. 1982. Daily feeding rhythm of pikeperch, *Stizostedion lucioperca*, and perch, *Perca fluviatilis*, from Lake Ladoga. J. Ichthyol. **22**: 52–60.

Fedriani, J.M., Fuller, T.K., Sauvajot, R.M., and York, E.C. 2000. Competition and intraguild predation among three sympatric carnivores. Oecologia, **125**: 258–270.

Frankiewicz, P., Dabrowski, K., Martyniak, A., and Zalewski, M. 1999. Cannibalism as a regulatory force of pikeperch, *Stizostedion lucioperca* (L.), population dynamics in the lowland Sulejow reservoir (Central Poland). Hydrobiologia, **408–409**: 47–55.

Haertel, S.S., Baade, U., and Eckmann, R. 2002. No general percid dominance at mesotrophic lake conditions: insights from the quantification of predator–prey interactions. Limnologica, **32**: 1–13.

Hanson, J.M., and Leggett, W.C. 1986. Effect of competition between two freshwater fishes on prey consumption and abundance. Can. J. Fish. Aquat. Sci. **43**: 1363–1372.

Hanson, P.C., Johnson, T.B., Schindler, D.E., and Kitchell, J.F. 1997. Fish bioenergetics. Version 3.0 for Windows. University of Wisconsin–Madison, Centre for Limnology and University of Wisconsin Sea Grant Institute, Madison, Wisconsin.

Hansson, L.A., Annadotter, H., Bergman, E., Hamrin, S.F., Jeppesen, E., Kairesalo, T., Luokkanen, E., Nilsson, P.A., Sondergaard, M., and Strand, J. 1998. Biomanipulation as an application of food-chain theory: constraints, synthesis, and recommendations for temperate lakes. Ecosystems, **1**: 558–574.

Hindar, K., Jonsson, B., Andrew, J.H., and Northcote, T.G. 1988. Resource utilization of sympatric and experimentally allopatric cutthroat trout and Dolly Varden charr. Oecologia, **74**: 481–491.

Hölker, F., and Mehner, T. 2005. Simulation of trait- and density-mediated indirect effects induced by piscivorous predators. Basic Appl. Ecol. **6**: 289–300.

Jacobsen, L., and Berg, S. 1998. Diel variation in habitat use by planktivores in field enclosure experiments: the effect of submerged macrophytes and predation. J. Fish Biol. **53**: 1207–1219.

Jacobsen, L., and Perrow, M.R. 1998. Predation risk from piscivorous fish influencing the diel use of macrophytes by planktivorous fish in experimental ponds. Ecol. Freshw. Fish, **7**: 78–86.

Kangur, A., and Kangur, P. 1998. Diet composition and size-related changes in the feeding of pikeperch, *Stizostedion lucioperca* (Percidae), and pike, *Esox lucius* (Esocidae), in the Lake Peipsi (Estonia). Ital. J. Zool. **65**: 255–259.

Kasprzak, P., Gervais, F., Adrian, R., Weiler, W., Radke, R.J., Jäger, I., Riest, S., Siedel, U., Schneider, B., Böhme, M., Eckmann, R., and Walz, N. 2000. Trophic characterization, pelagic food web structure and comparison of two mesotrophic lakes in Brandenburg (Germany). Int. Rev. Hydrobiol. **85**: 167–189.

Kitchell, J.F., Stewart, D.J., and Weininger, D. 1977. Applications of a bioenergetics model to perch (*Perca flavescens*) and walleye (*Stizostedion vitreum vitreum*). J. Fish. Res. Board Can. **34**: 1922–1935.

Krivan, V. 2003. Competitive co-existence caused by adaptive predators. Evol. Ecol. Res. **5**: 1163–1182.

Larkin, P.A. 1956. Interspecific competition and population control in freshwater fish. J. Fish. Res. Board Can. **13**: 327–342.

Lathrop, R.C., Johnson, B.M., Johnson, T.B., Vogelsang, M.T., Carpenter, S.R., Hrabik, T.R., Kitchell, J.F., Magnuson, J.J., Rudstam, L.G., and Stewart, R.S. 2002. Stocking piscivores to improve fishing and water clarity: a synthesis of the Lake Mendota biomanipulation project. Freshw. Biol. **47**: 2410–2424.

Lehtonen, H., Miina, T., and Frisk, T. 1984. Natural occurrence of pike-perch (*Stizostedion lucioperca* (L.)) and success of introduction in relation to water quality and lake area in Finland. Aqua Fenn. **14**: 189–196.

Maitland, P.S., and Campbell, R.N. 1992. Freshwater fishes. Harper Collins Publishers, London, UK.

Mehner, T., Arlinghaus, R., Berg, S., Dörner, H., Jacobsen, L., Kasprzak, P., Koschel, R., Schulze, T., Skov, C., Wolter, C., and Wysujack, K. 2004. How to link biomanipulation and sustainable fisheries management: a step-by-step guideline for lakes of the European temperate zone. Fish. Manag. Ecol. **11**: 261–275.

Mehner, T., Diekmann, M., Brämick, U., and Lemcke, R. 2005*a*. Composition of fish communities in German lakes as related to lake morphology, trophic state, shore structure and human-use intensity. Freshw. Biol. **50**: 70–85.

Mehner, T., Ihlau, J., Dörner, H., and Hölker, F. 2005*b*. Can feeding of fish on terrestrial insects subsidize the nutrient pool of lakes? Limnol. Oceanogr. **50**: 2022–2031.

Murdoch, W.W. 1969. Switching in general predators: experiments on predator specificity and the stability of prey populations. Ecol. Monogr. **39**: 335–354.

Okun, N., and Mehner, T. 2005. Distribution and feeding of juvenile fish on invertebrates in littoral reed (*Phragmites*) stands. Ecol. Freshw. Fish, **14**: 139–149.

Otis, D.L., Burnham, K.P., White, D.C., and Anderson, D.R. 1978. Statistical inference from capture data on closed animal populations. Wildl. Monogr. **62**: 1–135.

Persson, L. 1986. Effects of reduced interspecific competition on resource utilization in perch (*Perca fluviatilis*). Ecology, **67**: 355–364.

Persson, L., Diehl, S., Johansson, L., Andersson, G., and Hamrin, S. 1992. Trophic interactions in temperate lake ecosystems: a test of food chain theory. Am. Nat. **140**: 59–84.

Persson, L., and Eklöv, P. 1995. Prey refuges affecting interactions between piscivorous perch and juvenile perch and roach. Ecology, **76**: 70–81.

Polis, G.A., Myers, C.A., and Holt, R.D. 1989. The ecology and evolution of intraguild predation: potential competitors that eat each other. Annu. Rev. Ecol. Syst. **20**: 297–330.

Popova, O.A., and Sytina, L.A. 1977. Food and feeding relations of Eurasian perch (*Perca fluviatilis*) and pikeperch (*Stizostedion lucioperca*) in various waters of the USSR. J. Fish. Res. Board Can. **34**: 1559–1570.

Rice, W.R. 1989. Analyzing tables of statistical tests. Evolution, **43**: 223–225.

Ricker, W.E. 1975. Computation and interpretation of biological statistics of fish populations. Bull. Fish. Res. Board Can. **191**: 1–382.

Schoener, T.W. 1974. Resource partitioning in ecological communities. Science (Washington, D.C.), **185**: 27–39.

Schulze, T. 2005. Changes in structure and function of the fish community in a mesotrophic lake ecosystem after stocking a non-native top predator. PhD. thesis, University of Potsdam, Potsdam, Germany.

Simberloff, D. 1981. Community effects of introduced species. *In* Biotic crises in ecological and evolutionary time. *Edited by* M.H. Nitecki. Academic Press, New York. pp. 53–81.

Skov, C., and Koed, A. 2004. Habitat use of 0+year pike in experimental ponds in relation to cannibalism, zooplankton, water transparency and habitat complexity. J. Fish Biol. **64**: 448–459.

SPSS Inc. 1999. SPSS 9.0. SPSS Inc., Chicago, Illinois.

Strauss, R.E. 1979. Reliability estimates for Ivlev's electivity index, the forage ratio, and a proposed linear index of food selection. Trans. Am. Fish. Soc. **108**: 344–352.

Suutari, E., Rantala, M.J., Salmela, J., and Suhonen, J. 2004. Intraguild predation and interference competition on the endangered dragonfly *Aeshna viridis*. Oecologia, **140**: 135–139.

Svärdson, G., and Molin, G. 1973. The impact of climate on scandinavian population of the sander, *Stizostedion lucioperca* (L.). Inst. Freshw. Res. Drottningholm, **53**: 112–139.

Turesson, H., Persson, A., and Brönmark, C. 2002. Prey size selection in piscivorous pikeperch (*Stizostedion lucioperca*) includes active prey choice. Ecol. Freshw. Fish, **11**: 223–233.

Welcomme, R.L. 2001. Inland fisheries. Ecology and management. Blackwell Science, Oxford, UK.

Werner, E.E., and Gilliam, J.F. 1984. The ontogenetic niche and species interactions in size-structured populations. Annu. Rev. Ecol. Syst. **15**: 393–425.

Werner, E.E., and Hall, D.J. 1977. Habitat partitioning in a freshwater fish community. J. Fish. Res. Board Can. **34**: 360–370.

White, G.C., Anderson, D.R., Burnham, K.P., and Otis, D.L. 1982. Capture–recapture and removal methods for sampling closed populations. Los Alamos National Laboratory, Los Alamos, New Mexico.

Wysujack, K., and Mehner, T. 2002. Comparison of losses of planktivorous fish by predation and seine-fishing in a lake undergoing long-term biomanipulation. Freshw. Biol. **47**: 2425–2434.

Bioaccumulation of newly deposited mercury by fish and invertebrates: an enclosure study using stable mercury isotopes

Michael J. Paterson, Paul J. Blanchfield, Cheryl Podemski, Holger H. Hintelmann, Cynthia C. Gilmour, Reed Harris, Nives Ogrinc, John W.M. Rudd, and Ken A. Sandilands

Abstract: Enriched stable mercury (Hg) isotopes were added to four 10 m diameter enclosures in Lake 239 at the Experimental Lakes Area to increase inorganic Hg loading. Our main objectives were to (*i*) follow low-level additions (spikes) of isotope-enriched Hg through the biogeochemical cycle and into the food web and (*ii*) determine the relative contribution of newly deposited Hg to methyl Hg (MeHg) accumulation by fish and other biota. The experiment ran for two summers (2000, 2001), with different enriched Hg isotopes being added each year. Within 1 month of beginning additions in 2000, spike Hg was detected in water, zooplankton, and benthic invertebrates as MeHg, and in fish as total Hg (THg: the sum of inorganic and organic Hg). In 2001, concentrations in water of inorganic spike Hg added in 2000 were near detection limits, but concentrations of 2000 spike MeHg in water and biota remained unchanged or greater. Despite comparatively large increases in inorganic Hg loading, accumulation of ambient, non-spike MeHg predominated in all organisms, and spike MeHg never comprised more than 15%, even after 1 year. Our results suggest that changes in Hg loading will affect MeHg concentrations in fish and other biota, but that steady state may not be achieved for at least 10–30 years under conditions similar to our enclosures.

Résumé : Nous avons ajouté des isotopes stables enrichis de mercure (Hg) à quatre enclos de 10 m de diamètre au lac 239 dans la Région des lacs expérimentaux afin d'augmenter la charge de Hg inorganique. Nos objectifs principaux étaient (*i*) de suivre des additions de faible niveau (pics) d'Hg enrichi d'isotopes à travers le cycle biogéochimique et dans le réseau alimentaire et (*ii*) de déterminer la contribution relative du Hg nouvellement déposé à l'accumulation de méthyl Hg (MeHg) par les poissons et les autres organismes. L'expérience s'est poursuivie pendant deux étés (2000, 2001) avec différents isotopes enrichis de Hg ajoutés chaque année. En moins de 1 mois après le début des additions en 2000, un pic a pu être détecté sous forme de MeHg dans l'eau, le zooplancton et les invertébrés benthiques et sous forme d'Hg total (THg, la somme du Hg inorganique et organique) chez les poissons. En 2001, les concentrations dans l'eau du pic de Hg inorganique ajouté en 2000 étaient à la limite de la détection, mais les concentrations du pic de MeHg de 2000 dans l'eau et les organismes étaient les mêmes ou avaient augmenté. Malgré des augmentations relativement importantes de la charge de Hg inorganique, l'accumulation du MeHg ambiant non relié au pic prédomine chez tous les organismes et le MeHg du pic ne représente jamais plus de 15 % même après 1 an. Nos résultats indiquent que des changements de la charge de Hg affectent les concentrations de MeHg chez les poissons et les autres organismes, mais que l'équilibre ne sera pas atteint avant 10–30 ans sous des conditions comparables à celles de nos enclos.

[Traduit par la Rédaction]

Introduction

Concentrations of methyl mercury (MeHg) are elevated in fish from many lakes in Canada and the United States. This has resulted in the closure of fisheries and the issuance of consumption advisories in many provinces and states. Even lakes located far from point source inputs of Hg often have high concentrations of MeHg in fish, and there is increasing

Received 10 November 2005. Accepted 22 June 2006. Published on the NRC Research Press Web site at http://cjfas.nrc.ca on 19 September 2006.
J18995

M.J. Paterson,[1] P.J. Blanchfield, C. Podemski, J.W.M. Rudd,[2] and K.A. Sandilands. Fisheries and Oceans Canada, Freshwater Institute, 501 University Crescent, Winnipeg, MB R3T 2N6, Canada.
H.H. Hintelmann and N. Ogrinc.[3] Trent University, Department of Chemistry, 1600 West-Bank Drive, Peterborough, ON K9J 7B, Canada.
C.C. Gilmour. Smithsonian Environmental Research Center, 647 Contees Wharf Road, Edgewater, MD 21037, USA.
R. Harris. Tetra Tech Inc., 180 Forestwood Drive, Oakville, ON L6J 4E6, Canada.

[1] Corresponding author (e-mail: patersonm@dfo-mpo.gc.ca).
[2] Present address: R & K Research Inc., 675 Mt. Belcher Heights, Salt Spring Island, BC V8K 2J3, Canada.
[3] Present address: Jozef Stefan Institute, Department of Environmental Sciences, Jamova 39, 1000 Ljubljana, Slovenia.

Can. J. Fish. Aquat. Sci. 63: 2213–2224 (2006) doi:10.1139/F06-118

recognition of the importance of atmospheric Hg loading (Jackson 1997; Fitzgerald et al. 1998). A large proportion of atmospheric Hg is generated from anthropogenic emissions, particularly from coal-fired power plants (Mason et al. 1994). As a result, reductions of anthropogenic Hg emissions to the atmosphere of 50% or more have been proposed in both Canada and the United States, with the aim of reducing MeHg concentrations in fish (North American Implementation Task Force on Mercury 2000).

Once deposited in a lake, inorganic Hg that predominates in precipitation must be converted to MeHg before transfer to fish. Although it is widely agreed that levels of atmospheric Hg deposition are probably linked to levels of MeHg in fish (e.g., Johansson et al. 1991; Downs et al. 1998), this relationship has been difficult to demonstrate. In part, this is because the amount of stored Hg in soils and sediments of terrestrial and aquatic ecosystems is hundreds to thousands of times greater than annual deposition. As a result, it is not clear whether most of the Hg methylated in any given year was deposited during that year or during many previous years. Large differences in factors affecting Hg methylation and MeHg availability to the food web further obscure the relationship between Hg deposition and Hg accumulation by fish (Wiener et al. 2003).

An understanding of the relative contribution of recently deposited Hg to Hg accumulation by fish and other biota is required to predict whether changes in fish Hg will occur slowly or rapidly following changes in Hg emissions. If MeHg accumulated by fish and other biota is primarily derived from newly deposited Hg, then concentrations in fish should change rapidly following changes in Hg emissions. Alternatively, if much of the Hg in fish is derived from Hg deposited in past years, MeHg concentrations in fish will change more slowly with changes in atmospheric Hg deposition. For example, Hrabik and Watras (2002) observed simultaneous declines in Hg in fish and deposition to Little Rock Lake, a seepage lake in Wisconsin. From this, they inferred that newly deposited Hg predominantly contributed to the Hg accumulated by fish in this lake.

Our study was undertaken using large enclosures in Lake 239 (L239) at the Experimental Lakes Area (ELA) in northwestern Ontario and was completed in advance of a whole-lake Hg isotope addition experiment called METAALICUS (Mercury Experiment To Assess Atmospheric Loading in Canada and the United States). The METAALICUS study is exploring the effect of changes in inorganic Hg deposition rates on Hg accumulation by fish and their associated food web. In both our enclosure study and the whole-lake experiment, recently deposited Hg is being distinguished from old Hg by adding Hg that is enriched with certain stable isotopes. Stable isotopes of Hg have rarely been used in an ecosystem context or to follow patterns of food web transfer (e.g., Hintelmann et al. 2002; Pickhardt et al. 2002, 2005). Our objectives in the enclosure study were to (*i*) assess the use of low-level additions of isotope-enriched Hg to follow Hg through the biogeochemical cycle and into the food web; (*ii*) determine the timing and relative contribution of newly deposited Hg to Hg accumulation by fish and other biota; and (*iii*) compare results from enclosures receiving isotopically enriched Hg in a single annual dose versus multiple doses over the summer.

Table 1. Percent contribution of different stable isotopes to the Hg spikes added to the L239 enclosures in 2000 and 2001.

Isotope	2000	2001
^{196}Hg	<0.02	<0.10
^{198}Hg	0.13	<0.10
^{199}Hg	0.99	0.01
^{200}Hg	96.41	0.30
^{201}Hg	1.46	0.10
^{202}Hg	0.10	99.20
^{204}Hg	0.10	<0.05

Materials and methods

Experimental design

Four large enclosures (10 m diameter × approximately 1.5–2 m deep) open to both lake sediments and the atmosphere were installed in L239 at the ELA (49°39′N, 93°43′W) on 6–7 June 2000. Enclosure walls were made of woven polyethylene supported by a foam collar at the surface and anchored to the bottom with two rings of sandbags placed on a skirt sewn to the enclosure wall. Such enclosures are not completely water tight. Orihel (2005) estimated water losses from identical enclosures installed in nearby Lake 240 (L240) using additions of ^{3}H. She found average water leakage of 6.6% between June and September of 2002.

Our experiment started in June 2000 and continued through to September 2001. A spike enriched with different isotopes of Hg was added each summer. In 2000, enclosures were amended with a spike solution enriched with ^{200}Hg and in 2001 with ^{202}Hg (the exact isotopic composition of each spike is listed in Table 1). Because neither spike solution consisted entirely of a single isotope, we determined the excess concentration of the major spike isotope in each sample and mathematically corrected the final concentration of each spike, taking into account the concentrations of minor isotopes in the spike solutions (Hintelmann and Ogrinc 2003). This allowed us to separate naturally occurring background (or ambient) Hg from the isotopically enriched spike Hg. Below, we refer to the two spikes as the 2000 spike and the 2001 spike.

We increased annual wet Hg loading by adding 30 μg·m^{-2} of spike Hg to each enclosure. Long-term annual wet deposition of Hg at ELA is approximately 4 μg·m^{-2} and was between 7.1 and 7.9 μg·m^{-2} from 1998 to 2001 (St. Louis et al. 2004). Additions were made according to two different regimes. Two enclosures (E1 and E2) each received a single 30 μg·m^{-2} addition on 15 June 2000 (day 1) and 13 July 2001 (day 395). In each summer, additions were made to E3 and E4 every 2 weeks for 5 weeks with lower doses (6 μg·m^{-2}) so that the cumulative additional loading in all enclosures was the same.

The isotope stock solutions were made by dissolving the isotope-enriched Hg (as Hg^0) in dilute HCl. Prior to addition, an aliquot of HgCl$_2$ solution was added to 500 mL of L239 water and allowed to equilibrate for at least 4 h. The spike solution was then added at dusk from a raft in the center of each enclosure and mixed in using a paddle in 2000 and a small electric trolling motor in 2001.

Water and sediment sampling

Samples for the determination of water chemistry and dissolved and particulate Hg were collected from a raft held in the center of each enclosure. Samples were collected at least biweekly in 2000, whereas in 2001 a diminished sampling schedule was used to follow only longer term changes in Hg accumulation. Water samples for Hg analysis were pumped from a depth of 0.75 m and filtered through a pre-ashed quartz fiber filter (Whatman QM-A; 0.7 μm nominal pore size) housed in an in-line Teflon cartridge system. Clean hand – dirty hand protocols were used throughout (Horowitz et al. 1994). Samples were collected and stored in 250 mL acid-cleaned Teflon bottles. For particulate Hg, an additional 500–1000 mL of water was filtered to obtain sufficient mass for analysis.

Sediments were collected monthly in 2000 and twice in 2001 from the enclosure rafts using 4.8 cm diameter polyvinyl chloride (PVC) core tubes mounted on a PVC tube fitted with a clamp to seal the headspace. On each sampling date, three cores were collected from each enclosure from randomly selected locations. Great care was taken to minimize sediment disturbance during sampling. Cores were sectioned and preserved by freezing within hours of collection.

Invertebrate sampling

Zooplankton were collected weekly in 2000 using horizontal sweeps of a 150 μm net attached to a wooden pole. In 2001, zooplankton were sampled only once in September. Samples were prepared for MeHg analysis using methods described in Paterson et al. (1998). Zooplankton consisted predominantly of Cladocera (*Bosmina longirostris*, *Diaphanosoma birgei*, *Daphnia mendota*), cyclopoid copepods (*Mesocyclops edax*, *Tropocyclops extensus*), and calanoid copepods (*Diaptomus minutus*). Benthic invertebrates were collected monthly in 2000 using an Ekman dredge, with care being taken to minimize the amount of sediment released into the water column. Dredge contents were washed through a sieve outside the enclosures. In 2001, macroinvertebrates were collected only in September using a d-frame dipnet. After collection, invertebrates were removed from debris while alive, sorted to the lowest practical taxonomic level, and frozen. Samples were freeze-dried, ground to a powder using acid-washed glass rods, and weighed to the nearest 0.1 μg. They were then transferred to a 5 mL conical bottom Teflon vial for digestion.

Fish stocking and sampling

Immediately after enclosure installation in 2000, baited minnow traps and small-mesh gill nets were used in an attempt to remove all fish from the enclosures. Finescale dace (*Phoxinus neogaeus*) were then purchased from a local baitfish supplier, and 30 were added to each enclosure on 14 June 2000. At initial stocking, 10 finescale dace were kept as a reference sample. The density of fish in each enclosure (0.35 fish·m^{-2}) approximated densities used in other enclosure experiments (Bodaly and Fudge 1999) and in shallow lakes at the ELA (Eddy 2000). In June 2001, as many fish as possible were again removed from the enclosures using minnow traps and gillnets. On 18 July (day 398), we stocked each enclosure with 15 finescale dace collected from ELA Lake 114. To differentiate newly added fish, all stocked finescale dace received a clip on the upper caudal fin.

In 2000, fish were collected monthly using overnight sets of minnow traps and then killed, measured (fork length), weighed, and frozen. In 2001, enclosures were sampled for fish only in September. There was large, unexplained mortality of finescale dace after the first sampling period in E2 and E3 in 2000 and in E1 and E2 in 2001. As a result, data presented for 2000 include only fish collected from E1 and E4, and data for 2001 include only fish from E3 and E4. At least four finescale dace were captured on all dates for which data are presented. In addition to finescale dace, a few small yellow perch (*Perca flavescens*; mostly young of the year and age 1+) were also captured (n = 1–7 from each enclosure on each sampling date). These fish naturally inhabit L239 and presumably were trapped when the enclosure walls were dropped in June 2000.

After collection, stomachs were removed from larger fish and preserved in 95% ethanol. Approximately 0.2 g of muscle tissue was removed from each fish, placed into a clean glass scintillation vial, and frozen prior to analysis for total Hg (THg; the sum of inorganic and organic Hg). THg was measured because generally >90% of the Hg in fish muscle is MeHg (Bloom 1992; Turner and Rudd 1983). We analysed the stomach contents of finescale dace (n = 44) and yellow perch (n = 7) that were captured in enclosures E1 and E4 in 2000. Each stomach was cut open and all items were counted individually and identified to order using a compound microscope. Organisms from the same order were grouped and oven-dried to determine their contribution by weight to fish diet.

Analytical methods

Water chemistry other than Hg was analysed using methods in Stainton et al. (1977). THg in water samples was determined after oxidation of 50 mL samples by adding 0.25 mL of BrCl. The method for digesting particles collected on filters has been modified from Morrison and Watras (1999). Filters were fitted into 30 mL Teflon vials and 10 mL of Milli-Q water were added. Particles were digested by adding 0.1 mL concentrated HCl and 0.1 mL BrCl (0.2 mol·L^{-1}). Fish samples were weighed into 25 mL glass vials and digested by adding 10 mL of a HNO_3–H_2SO_4 (7:3) mixture. Samples were heated to 80 °C until the formation of brown NO_x gases had ceased. All samples were then diluted and analyzed. Prior to digestions, water and particulate samples received 20 μL and fish samples 500 μL of a ^{201}Hg(II) standard solution (2.3 ng·mL^{-1}) to serve as an internal standard. Ionic Hg in the water and particulate digests was reduced using stannous chloride and the generated Hg^0 purged onto gold traps, which were heated to release the Hg. THg in fish was quantified using an on-line flow injection system described in Hintelmann and Ogrinc (2003). Measurements were performed by inductively coupled plasma mass spectrometry (ICP-MS, Micromass Platform). Sediment analysis was performed on thawed, homogenized, wet samples. Digestion methods for THg and distillation methods for MeHg in sediments are described in Gilmour et al.

Table 2. Average water chemistry in the study enclosures in 2000.

Parameter	E1	E2	E3	E4	Lake 239[a]
pH	7.1 (0.1)	7.2 (0.1)	7.2 (0.1)	7.3 (0.1)	7.0 (0.1)
Total phosphorus ($\mu g \cdot L^{-1}$)	7.2 (3.7)	9.2 (3.0)	6.4 (1.9)	8.3 (2.0)	8.1 (5.4)
Chlorophyll *a* ($\mu g \cdot L^{-1}$)	1.6 (1.0)	1.3 (0.8)	1.5 (1.2)	1.2 (0.7)	2.6 (0.7)
Suspended carbon ($\mu g \cdot L^{-1}$)	558 (222)	611 (226)	492 (128)	493 (136)	750 (177)
DOC ($mg \cdot L^{-1}$)	6.9 (0.3)	7.0 (0.4)	6.5 (0.3)	6.4 (0.3)	8.1 (0.9)
Zooplankton biomass (μg dry weight$\cdot L^{-1}$)	84.4 (99.1)	50.6 (73.5)	57.0 (59.4)	55.6 (79.0)	16.1 (7.7)

Note: Numbers in brackets are 1 standard deviation. DOC, dissolved organic carbon.

[a] Parameter values for Lake 239 are for the epilimnion at centre-buoy, except for zooplankton, which is a whole-water-column estimate.

Table 3. Average, time-weighted ambient Hg concentrations in the enclosures in 2000 and 2001 (all enclosures).

	2000	2001
Water		
Unfiltered THg ($ng \cdot L^{-1}$)	1.6 (0.4)	1.1 (0.1)
Unfiltered MeHg ($ng \cdot L^{-1}$)	0.11 (0.02)	0.06 (0.01)
Sediment (0–2 cm)		
THg ($ng \cdot g^{-1}$ dw)	17.6 (4.4)	15.6 (5.8)
MeHg ($ng \cdot g^{-1}$ dw)	0.54 (0.21)	0.57(0.13)
Invertebrates		
Zooplankton MeHg ($ng \cdot g^{-1}$ dw)	108 (26)	58 (20)
Ceratopogonidae MeHg ($ng \cdot g^{-1}$ dw)	81 (32)	—
Chironomidae MeHg ($ng \cdot g^{-1}$ dw)	47 (17)	38 (14)
Ephemeroptera MeHg ($ng \cdot g^{-1}$ dw)	41 (16)	44 (6)
Hydracarina MeHg ($ng \cdot g^{-1}$ dw)	220 (194)	53 (15)
Pisidiidae MeHg ($ng \cdot g^{-1}$ dw)	44 (60)	13 (4)
Fish		
Finescale dace THg (*Phoxinus neogaeus*; $ng \cdot g^{-1}$ ww)	108 (27)	174 (46)
Yellow perch THg (*Perca flavescens*; $ng \cdot g^{-1}$ ww)	76 (25)	109 (54)

Note: Numbers in brackets are 1 standard deviation. Ceratopogonidae were not encountered in the 2001 samples. THg, total Hg (the sum of inorganic and organic Hg); MeHg, methyl Hg; dw, dry weight; ww, wet weight.

(1998). All sediment analyses were undertaken using a Perkin Elmer Elan DRC ICP-MS.

MeHg determinations were slightly modified from procedures described in detail by Horvat et al. (1993), Bloom (1989), and Hintelmann and Ogrinc (2003). Water samples (50 mL) were distilled in a glass distillation apparatus consisting of two 50 mL glass tubes connected via an air-cooled glass distillation bridge (inner diameter 8 mm). Particles collected on filters were distilled in a similar fashion, except that 30 mL Teflon bottles were used instead of the glass distillation system. Filters were placed in the vial and then 10 mL of Milli-Q water and reagents were added. Extraction of MeHg from freeze-dried zooplankton and zoobenthos was accomplished by treating the samples with a 20% (*w/v*) KOH–MeOH solution at 50 °C over 8 h, following Bloom (1992). MeHg in sample distillates and alkaline leaching solutions was measured after aqueous phase ethylation using $NaBEt_4$ (Hintelmann and Ogrinc 2003). Volatile Hg species were purged and trapped onto Tenax, and MeHg was measured after thermodesorption and GC separation using ICP-MS detection. To correct for procedural recoveries, $Me^{201}HgCl$ additions of 20 and 50 pg were made to water and biota samples, respectively, prior to distillation or digestion.

Samples of similar weight of a certified reference material (DORM-2, National Research Council of Canada (NRC), Ottawa, Ontario; NBS-1566 oyster tissue, National Bureau of Standards) were submitted to the same procedures; measured THg and MeHg concentrations in the reference materials were not significantly different from certified values ($p < 0.05$).

Terminology

In the discussion below, we use the following terms to distinguish the various forms of Hg in the enclosures. Methyl Hg (MeHg) refers to monomethyl Hg. Ambient THg or ambient MeHg refers to background THg or MeHg, respectively, not associated with the isotope-enriched Hg spikes. The 2000 spike refers to the Hg spike enriched with ^{200}Hg added in 2000, whereas the 2001 spike refers to the Hg spike enriched with ^{202}Hg added in 2001.

Spike/ambient ratios

We used the ratio of spike and ambient Hg as a measure of the amount by which THg or MeHg concentrations were changed by the addition of isotopically enriched Hg. For example, a spike/ambient ratio of 1.0 indicates that concentra-

Fig. 1. Changes in concentrations of (*a*) 2000 and 2001 spike total mercury (THg, the sum of inorganic and organic Hg) in unfiltered water samples (±1 standard error of the mean (SEM)); (*b*) 2000 and 2001 spike methyl mercury (MeHg) in unfiltered water samples (±1 SEM); (*c*) 2000 and 2001 spike THg in 0–2 cm sediments (±1 SEM); and (*d*) 2000 and 2001 spike MeHg in 0–2 cm sediments (±1 SEM). Standard errors reflect variability among enclosures receiving either a single Hg isotope addition (E1, E2) or multiple additions (E3, E4). Data for 18 July 2001 (day 396) are for water samples filtered through a quartz fiber filter. For MeHg, data points below detection were not included in averages. Symbols are as follows: 2000 spike, single addition (solid circles, solid line); 2000 spike, multiple additions (open circles, dotted line); 2001 spike, single addition (solid triangles, solid line); 2001 spike, multiple additions (open triangles, dotted line).

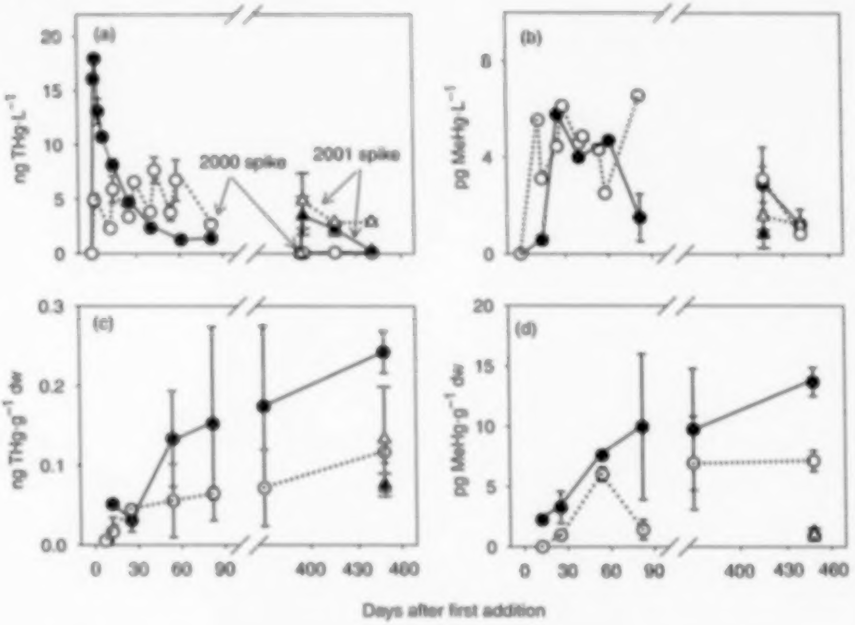

tions of spike and ambient Hg are equal and that the sum of spike and ambient Hg concentrations has increased by two times as compared with ambient Hg alone. The use of spike/ambient ratios facilitates comparisons of relative changes between different forms of Hg (MeHg, THg) and among different media and biotic groups (e.g., water, zooplankton, benthos, and fish). Spike/ambient ratios also help to normalize seasonal variations in overall Hg transfer and accumulation.

At the beginning of each year, finescale dace stocked in enclosures contained ambient Hg accumulated prior to their introduction. In 2000, initial ambient Hg concentrations were 86.8 ± 17.7 ng·g^{-1} wet weight (ww; mean ± 1 standard deviation) and in 2001, 178.8 ± 34.6 ng·g^{-1} ww. Most of this was presumably MeHg (Bloom 1992) that was probably retained for most of the 3-month duration of each summer period of the experiment. For example, the model of Trudel and Rasmussen (1997) indicates that a 3 g fish (similar to the size of finescale dace in the enclosures) depurates MeHg with a half-life of >250 days. Because we were interested in determining changes in the accumulation of spike versus ambient Hg while biota inhabited the enclosures, we calculated spike/ambient ratios for finescale dace using estimates of new ambient Hg accumulated during the experiment. This was done by subtracting the average muscle burden of ambient Hg in finescale dace collected on day 0 from the muscle burden of ambient Hg measured in fish on different sampling days. Muscle burdens of Hg were estimated as

$$(\mu\text{g THg} \cdot \text{g}^{-1}\ \text{ww}) \times (\text{ww of muscle in each fish})$$

The weight of muscle (g) was assumed to be 49% of body weight (J. Van Wallegham, 501 University Crescent, Winnipeg, MB, Canada, R3T 2N6, personal communication, 2005). Spike/ambient ratios were then estimated as muscle burden of spike Hg divided by muscle burden of newly accumulated ambient Hg.

No such correction was necessary for invertebrate spike/ambient ratios because most of their population biomass (and associated MeHg) was accumulated during the experiment. Zooplankton have generation times of days to weeks in midsummer, and most macroinvertebrates at ELA are univoltine and undergo their greatest periods of growth during the summer months. No correction for ambient Hg in yellow perch was possible because no determinations of Hg burden were made at the experiment's initiation. As a result, we only consider spike/ambient ratios for the 2000 spike in yellow perch collected in September 2001. These perch had presumably accumulated most of their ambient Hg in the enclosures, because they had lived in them for more than 1 year.

Results

Water chemistry

Water chemistry was very similar among the enclosures, and most parameters changed minimally over the course of the experiment (Table 2). As is typical for lakes on the Canadian Shield, L239 is oligotrophic, circumneutral, and relatively high in dissolved organic carbon (DOC). Conditions within the enclosures were similar to the epilimnion of L239, except that concentrations of DOC, suspended carbon, and chlorophyll *a* were lower. In part, this reflects greater settling of particles in the more quiescent water column of the enclosures. DOC concentrations were lower because the enclosures were isolated from water exchange with the rest of the lake. This resulted in lower import of DOC in runoff from the watershed and, possibly, greater DOC loss from flocculation, sedimentation, and photobleaching. Water in the enclosures did not strongly stratify or become anoxic.

Ambient Hg concentrations

Concentrations of ambient THg and MeHg were generally low and typical for lakes on the Canadian Shield (Table 3). There were no obvious changes in concentrations of ambient Hg associated with the addition of the Hg spikes in 2000 or 2001. There was also no evidence that disturbance of lake sediments during enclosure installation or benthic sampling strongly affected ambient Hg concentrations in the water column or biota. Concentrations of unfiltered THg and MeHg from L239 were only measured in the enclosures, but were similar to those measured simultaneously in L240, which is immediately downstream of L239 (L240 THg = 1.37 ± 0.26 $ng \cdot L^{-1}$; MeHg = 0.06 ± 0.03 $ng \cdot L^{-1}$). Comparisons of unfiltered THg and MeHg collected within and outside of identical enclosures in a second experiment conducted in L240 in 2002 and 2003 revealed no statistically significant differences between the lake and enclosures (D. Orihel, 501 University Crescent, Winnipeg, MB, Canada, R3T 2N6, personal communication, 2006). Concentrations of unfiltered THg also did not increase in samples collected immediately after benthic sampling as compared with samples collected before sampling (paired *t* test, $p > 0.4$). In 2000, concentrations of ambient MeHg in L239 zooplankton collected within and outside of the enclosures were statistically indistinguishable (average time-weighted concentration in enclosures = 108 ± 26 $ng \cdot g^{-1}$ dry weight (dw); in L239 = 74 ± 23 $ng \cdot g^{-1}$ dw; paired *t* test, $p > 0.2$).

Where data were available, there were few consistent directional changes in concentrations of ambient THg or MeHg during the course of each summer. Exceptions were Ceratopogonidae, which increased in average ambient MeHg concentrations from 75 to 110 $ng \cdot g^{-1}$ dw, and finescale dace, which increased in average THg concentrations from 87 to 122 $ng \cdot g^{-1}$ ww between June and September 2000. Overall, concentrations of ambient THg and MeHg in water and invertebrates were lower in 2001 than in 2000.

Spike Hg and MeHg concentrations

Water and sediments

In enclosures receiving a single Hg addition (E1 and E2), concentrations of the added spikes as THg in water declined rapidly in both 2000 and 2001 (Fig. 1*a*). In enclosures receiving multiple Hg doses (E3 and E4) in 2000, concentrations of the spike increased immediately after each addition and then diminished to create a sawtooth pattern over time. This pattern was not discernable in 2001 because of less intensive sampling. In September 2000 (day 82), concentrations of spike THg in unfiltered water were similar in enclosures receiving single and multiple doses. In 2001, very little of the 2000 spike was still detectable in water (average concentrations <3%). Enclosures receiving multiple additions usually had higher concentrations of 2001 spike THg than enclosures receiving a single addition. The reason for this difference is uncertain.

Fig. 2. Changes in concentrations of the 2000 and 2001 spike methyl mercury (MeHg) in zooplankton (±1 SEM). Standard errors reflect variability among enclosures receiving either a single Hg isotope addition (E1, E2) or multiple additions (E3, E4). Symbols are as follows: 2000 spike, single addition (solid circles, solid line); 2000 spike, multiple additions (open circles, dotted line); 2001 spike, single addition (solid triangles); 2001 spike, multiple additions (open triangles).

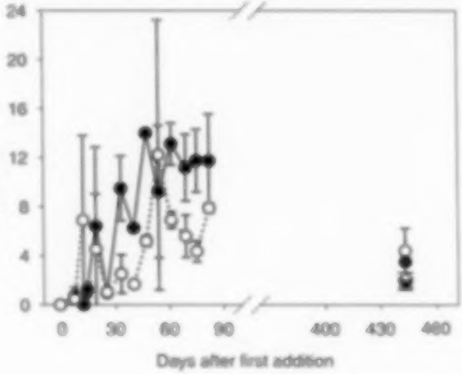

Concentrations of spike MeHg in water were low and often near detection limits. In 2000, spike MeHg was first detected in all enclosures 2–5 weeks after the first addition (Fig. 1*b*). For the 2000 spike, concentrations of MeHg did not diminish in 2001 as did concentrations of THg. There were no obvious differences between enclosures receiving single versus multiple spikes.

In 2000, concentrations of spike THg and MeHg in 0–2 cm sediments increased through time in all enclosures (Figs. 1*c* and 1*d*). Heterogeneity among sediment samples was high, and spike THg and MeHg concentrations were often near detection limits. In 2001, concentrations of 2000 spike THg and MeHg were similar to concentrations measured in September 2000. In September 2001, sediment concentrations of MeHg generated from the 2001 spike were much lower than the September 2000 levels of MeHg produced from the 2000 spike The reason for this difference is uncertain.

In the enclosures, the majority of Hg added as spikes in 2000 and 2001 was lost via evasion to the atmosphere (Amyot et al. 2004; C.C. Gilmour, unpublished data). Mass-balance estimates indicate that by September of each year, an average of 83% ± 3.4% of spike Hg added in 2000 and 85% ± 10.9% of spike Hg added in 2001 was evaded. In September of 2000 and 2001, respectively, an average of 12.2% ± 5.1% and 9.7% ± 9.5% of spike Hg added in the

Fig. 3. Changes in concentrations of the 2000 and 2001 spike methyl mercury (MeHg) in four groups of benthic invertebrates (±1 SEM): (*a*) Chironomidae, (*b*) Pisidiidae (shell removed), (*c*) Hydracarina, and (*d*) Ephemeroptera. Standard errors reflect variability among enclosures receiving either a single Hg isotope addition (E1, E2) or multiple additions (E3, E4). Symbols are as follows: 2000 spike, single addition (solid circles, solid line); 2000 spike, multiple additions (open circles, dotted line); 2001 spike, single addition (solid triangles); 2001 spike, multiple additions (open triangles).

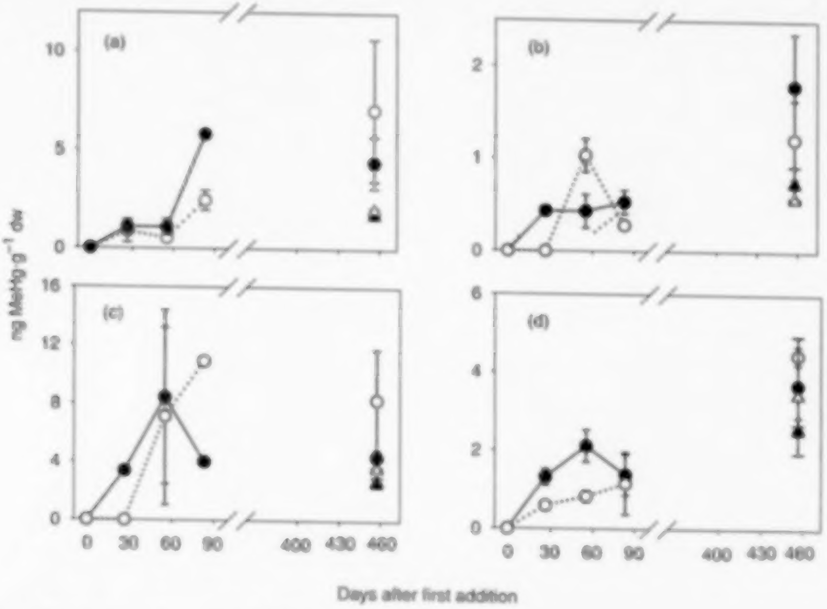

same year remained in the water column, and 4.5% ± 4.5% and 4.5% ± 2.8% was incorporated in enclosure sediments. The remainder (<1%) was accumulated in sediment pore water and in periphyton growing on the enclosure walls. In 2001, <1% of the 2000 spike occurred in the water column and 7.5% ± 3.1% was found in the sediments.

Zooplankton

In 2000, there was considerable variability in concentrations of spike MeHg in zooplankton (Fig. 2). Spike MeHg was first detected within 2–4 weeks of beginning additions, and concentrations increased through the summer. In September 2001 (day 448), the 2000 spike was still readily detectable as MeHg in zooplankton, indicating that the 2000 spike continued to be available to the food web 1 year after its addition to the enclosures.

Benthic invertebrates

In 2000, spike MeHg was detected in all benthic invertebrate groups after 4–8 weeks, and concentrations of spike MeHg generally increased through the summer (Fig. 3). As with the zooplankton, the 2000 spike continued to be available to benthic invertebrates 1 year after addition. In September 2001 (day 462), concentrations of MeHg derived from the 2001 spike were similar to those for the 2000 spike as measured in September 2000 (day 83). The highest concentrations of spike and ambient MeHg were observed in predatory Hydracarina and the lowest concentrations in sphaeriid clams (i.e., Pisidiidae) after shell removal (Fig. 3; Table 3). Chironomids, ceratopogonids, and ephemeropterans (*Hexagenia* spp. and *Caenis* spp.) had intermediate concentrations of spike and ambient MeHg (Table 3).

Fish

Finescale dace showed steady growth in all enclosures in both 2000 and 2001 and approximately doubled in weight by September (2000: initial weight = 2.0 ± 0.3 g, final weight = 3.9 ± 0.5 g; 2001: initial weight = 2.1 ± 0.8 g, final weight = 4.0 ± 1.4 g). The diet of finescale dace was numerically dominated by Cladocera, but the percent contribution by weight was split almost equally between zooplankton and benthic invertebrates (Table 4). Yellow perch had a diet similar to finescale dace, but with an even greater reliance on Cladocera (>60% by weight). Within dates, strong correlations between Hg concentrations and fish weight were not observed.

After only 1 month, newly deposited spike Hg was detected in fish from enclosures that had received both single and multiple spike additions (Fig. 4*a*). Concentrations of the 2000 spike in finescale dace from E1 (single addition) increased rapidly and reached a plateau by July 2000, whereas concentrations of this spike steadily increased through the season in fish from E4 (multiple additions). In September 2001 (day 461), concentrations of the 2001 spike were similar to those observed for the 2000 spike in September 2000 (day 85). In September of 2000, large differences in concentrations of spike Hg in enclosures receiving multiple or single spikes were not evident.

Spike/ambient ratios

Spike/ambient ratios provide an indication of changes in accumulation of spike Hg relative to ambient Hg. We assume that most of the ambient Hg accumulated by biota in the enclosures is derived from past deposition. This is be-

Table 4. The occurrence and percentage by weight of dietary items in stomachs from finescale dace (*Phoxinus neogaeus*) and yellow perch (*Perca flavescens*) captured in E1 and E4 in 2000.

	Finescale dace		Yellow perch	
	Occurrence	% of diet by weight	Occurrence	% of diet by weight
Zooplankton				
Cladocera	3839	47.8	1982	61.9
Copepoda	1	0.4	20	4.1
Benthic invertebrates				
Pisidiidae	9	16.6		
Amphipoda	1	0.2		
Chironomid pupae	12	2.8	57	18.1
Ephemeroptera			1	9.8
Trichoptera	11	6.7	1	3.0
Unidentified Insecta	23	25.1		
Detritus	1	0.4		

Note: Of the 44 finescale dace stomachs examined, six were found to be empty. The stomach contents of seven yellow perch were examined.

cause deposition of ambient Hg to our enclosures was small relative to existing pools in the enclosure sediments and water column and because the enclosures were isolated from ambient Hg inputs from the watershed.

Immediately after additions to single-dose enclosures in both 2000 and 2001, spike/ambient ratios for unfiltered THg in water increased to between 2 and 6 and rapidly diminished thereafter (Fig. 5*a*). In 2000, peak spike/ambient ratios for THg in multiple-dose enclosures varied between approximately 1 and 3 immediately after Hg additions, with lower values at other times. In general, spike/ambient ratios for THg were higher for the 2001 spike because of lower concentrations of ambient THg in that year (Table 3). In 2001, little of the spike Hg added in 2000 remained in the water column, and average spike/ambient ratios were below 0.1 (Table 5). Our detection limit for spike/ambient ratios was ~0.01. Over the course of each summer, average time-weighted spike/ambient ratios for unfiltered spike THg added in that year were between 1.0–3.1, with an overall average of 1.2 (Table 5).

Spike/ambient ratios for MeHg in water were markedly lower than those for THg. Spike/ambient ratios for MeHg in water were always less than 0.3, with overall averages below 0.1 (Fig. 5*b*; Table 5). In 2001, spike/ambient ratios for the 2000 spike did not decrease for MeHg in water as much as they did for THg. This indicates that the 2000 spike continued to be available as MeHg in 2001.

In both 2000 and 2001, spike/ambient ratios for spike THg added in each year and measured in 0–2 cm sediments were far lower than in the overlying water column (overall average = 0.01 ± 0.01; Table 5). This is a result of dilution of spike Hg in the large pool of older ambient Hg in the enclosure sediments. For the 2000 spike, spike/ambient ratios for MeHg in 0–2 cm sediments were similar in magnitude to those for THg. Spike/ambient ratios for sediment MeHg derived from the 2001 spike were lower than those from the 2000 spike. These data suggest that low spike/ambient ratios for MeHg in water reflect the low proportion of spike THg in enclosure sediments.

In 2000, MeHg spike/ambient ratios for zooplankton and benthic invertebrates steadily increased to approximately 0.05 to 0.1 by September (Figs. 5*c*, 5*d*; Table 5). As with MeHg in water, spike/ambient ratios for the 2000 spike in zooplankton and benthic invertebrates did not diminish in 2001. By September 2001, spike MeHg concentrations and spike/ambient ratios for MeHg derived from the 2000 spike increased and were greater for benthic invertebrates than for zooplankton. In part, this may reflect the longer life spans of benthic invertebrates and their longer period of exposure to spike-enriched MeHg. Across all dates and enclosures, average spike/ambient ratios in zooplankton and benthic invertebrates were similar in magnitude to those of MeHg in water for the 2000 and 2001 spikes and in sediments for the 2000 spike (Table 5).

Spike/ambient ratios for finescale dace were also much lower than for dissolved THg (0.04–0.22) (Fig. 4*b*). The highest spike/ambient ratios for finescale dace were observed in fish collected from E1 (single addition) during the first sampling interval in 2000. In subsequent sampling intervals, spike/ambient ratios decreased to average values below 0.1, and in 2000, ratios were similar for fish collected from the multiple and single spike enclosures. In September 2001, spike/ambient ratios for the 2000 spike in finescale dace were similar to those observed 1 year previously and to those observed for zooplankton and benthic invertebrates collected at the same time (Table 5). Once again, this indicates that the 2000 spike continued to be available for uptake by fish 1 year after its addition to the enclosures. Spike/ambient ratios for the 2001 spike in September 2001 were slightly lower than those for the 2000 spike in September 2000, although concentrations of spike Hg in finescale dace were similar.

In September 2001, spike/ambient ratios for the 2000 spike were higher in yellow perch than in finescale dace, possibly because the yellow perch had lived for 15 months in the enclosures, whereas the finescale dace were added in June 2001.

Discussion

The use of Hg stable isotopes to assess the effects of changes in Hg loading rates

This study was initiated in advance of a whole-lake Hg isotope addition experiment to assess the suitability of using environmentally realistic additions of enriched stable isotopes of Hg to determine the effect of changes in Hg deposition rates on accumulation by fish and other biota. Our results demonstrate that this approach is highly effective. Throughout the experiment, we were easily able to follow the added isotopes as they accumulated in the aquatic food web. The use of stable isotopes greatly enhanced our ability to detect the effect of changes in Hg loading rates. If we had added Hg in a nonisotopic form and sought to determine changes in overall Hg accumulation by biota, we would have been unable to detect any change. This was because of the small relative contribution of added spike Hg to bioaccumulation and background variability in concentrations of ambient Hg.

A further advantage of using Hg stable isotopes was the availability of different isotopes that allowed us to separate the contributions of spikes added in different years. Overall, the dynamics of the Hg spikes added in 2000 and 2001 were very similar. Concentrations and spike/ambient ratios of the two Hg spikes in water, sediments, invertebrates, and fish were similar in September of the year in which they were added. Hence, our results were repeatable among years.

Contribution of newly deposited Hg to Hg accumulation by fish and other biota

Overall, increases in Hg loading to our enclosures contributed to greater MeHg accumulation by fish and other aquatic biota. This suggests that changes in Hg deposition should result in changes in Hg accumulation by fish. Within weeks of beginning additions, the enriched Hg isotopes were detectable as MeHg in water, sediments, zooplankton, and benthic invertebrates. This indicates that a portion of the newly deposited Hg was almost immediately methylated and made available to the food web. Overall, however, increases in MeHg in biota were comparatively small (on average 3%–10%) despite relatively large increases in inorganic Hg loading (200% to >400%). This suggests that most of the Hg accumulated by biota was derived from a large store of Hg deposited in past years.

Fig. 4. (*a*) Changes in concentrations (±1 SEM) of the 2000 and 2001 Hg spike in finescale dace (*Phoxinus neogaeus*). (*b*) Changes in spike ambient ratios (±1 SEM) for the 2000 and 2001 spike in finescale dace. No finescale dace were captured from E2 or E3 in 2000 or from E1 or E2 in 2001. Spike/ambient ratios for finescale dace were corrected for initial ambient body burdens as described in the text. Symbols are as follows: 2000 spike, single addition (E1) (solid circles, solid line); 2000 spike, multiple additions (E3; 2001 only) (open circle); 2000 spike, multiple additions (E4) (open squares, dotted line); 2001 spike, multiple additions (E3) (open triangle); 2001 spike, multiple additions (E4) (open inverted triangle). Standard errors for each enclosure reflect variability among individual fish (not individual enclosures as in previous figures). THg, total mercury (the sum of inorganic and organic Hg).

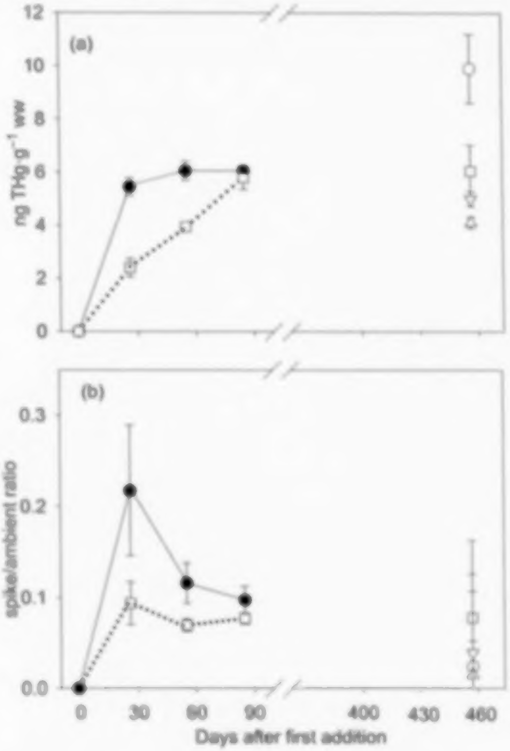

In our study, we increased inorganic Hg loading to the enclosures considerably over average atmospheric loading at the ELA. Over the course of each summer, average spike/ambient ratios for THg in water were 1.2–1.9 in 2000 and 1.2–6.1 in 2001, which further indicates that the sum of ambient and spike THg increased considerably. Despite these large increases of THg in water, changes in MeHg in biota were much smaller (spike/ambient ratios of 0.04–0.1) and similar for all taxa examined. Spike/ambient ratios for biota were also similar to spike/ambient ratios for MeHg in water and 0–2 cm sediments, suggesting that spike MeHg bioaccumulation was roughly proportional to its availability in the environment. Although we added the equivalent of at least one additional year of Hg loading (and probably more) in each of 2000 and 2001, MeHg accumulation by biota increased by only 3%–10% annually. This suggests that it would take at least 10–30 years for this system to achieve steady state with the new Hg additions, if continued indefinitely. This long response time was driven at least in part because of the small proportion of Hg spike in enclosure sediments, the main site of MeHg production in the enclosures.

Our conclusions are further supported by the observation that spike Hg added in 2000 continued to be as available to biota as MeHg in 2001 as in 2000. Despite large decreases in spike THg in water, there was no sign that the availability of spike MeHg to biota had substantially declined 1 year after its introduction to the enclosures. For organisms with

Fig. 5. Changes in spike/ambient ratios (±1 SEM) for (*a*) unfiltered total mercury (THg, the sum of inorganic and organic Hg) in water; (*b*) unfiltered methyl Hg (MeHg) in water; (*c*) MeHg in zooplankton; and (*d*) MeHg in Chironomidae larva. Changes in spike/ambient ratios for other groups of benthic invertebrates were similar to Chironomidae. Standard errors reflect variability among enclosures receiving either a single Hg isotope addition (E1, E2) or multiple additions (E3, E4). Symbols are as follows: 2000 spike, single addition (solid circles, solid line); 2000 spike, multiple additions (open circles, dotted line); 2001 spike, single addition (solid triangles, solid line); 2001 spike, multiple additions (open triangles, dotted line).

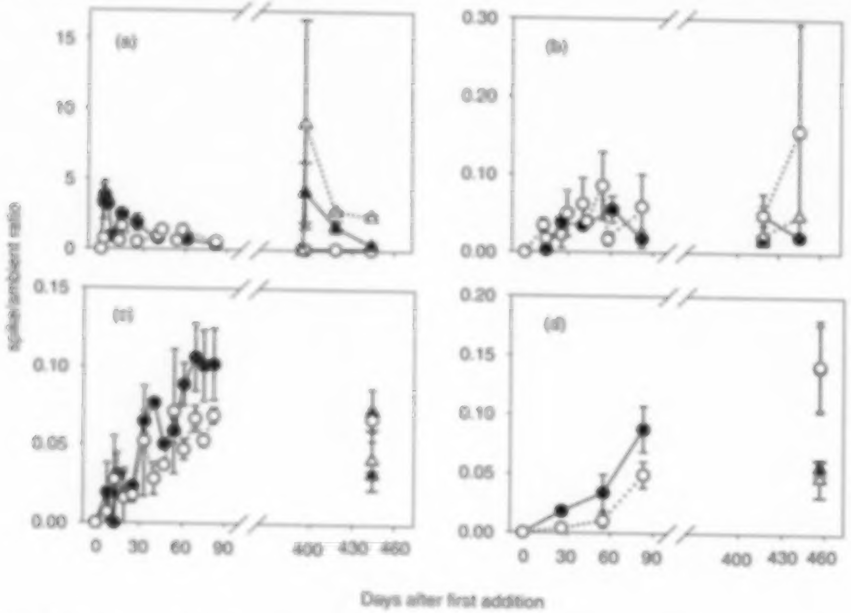

Table 5. Average spike/ambient ratios in the study enclosures in 2000 and 2001.

	Year 2000	Year 2001	
	2000 spike	2000 spike	2001 spike
Water			
Unfiltered THg	1.16 (0.18)	0.08 (0.01)	3.14 (1.06)
Unfiltered MeHg	0.03 (0.01)	0.09 (0.03)	0.03 (0.01)
Sediments (0–2 cm)			
THg	0.01 (0.01)	0.01 (0.01)	0.01 (0.01)
MeHg	0.01 (0.01)	0.02 (0.01)	0.002 (0.001)
Invertebrate MeHg			
Zooplankton	0.08 (0.02)	0.07 (0.01)	0.04 (0.01)
Ceratopogonidae	0.05 (0.01)	—	—
Chironomidae	0.07 (0.02)	0.14 (0.02)	0.05 (0.01)
Ephemeroptera	0.05 (0.01)	0.09 (0.01)	0.07 (0.01)
Hydracarina	0.06 (0.02)	0.12 (0.02)	0.06 (0.01)
Pisidiidae	0.04 (0.01)	0.11 (0.02)	0.05 (0.01)
Fish THg			
Finescale dace (*Phoxinus neogaeus*)	0.09 (0.01)	0.05 (0.02)	0.03 (0.01)
Yellow perch (*Perca flavescens*)	—	0.13 (0.03)	—

Note: Data for Hg concentrations in water are time-weighted June–September averages, whereas all other data are for September samples only. Ceratopogonidae were not encountered in the 2001 samples. Spike/ambient ratios for finescale dace were corrected for initial ambient muscle burdens as discussed in the text. Numbers in brackets are 1 standard error of the mean and reflect variation among enclosures. THg, total Hg (the sum of inorganic and organic Hg); MeHg, methyl Hg.

longer life spans such as benthic invertebrates and yellow perch, spike MeHg concentrations increased from 2000 to 2001. For organisms with short life spans (e.g., zooplankton) or for organisms introduced to the enclosures each year (finescale dace), spike Hg concentrations and spike/ambient ratios were similar in September 2000 and 2001. Given the comparatively short duration of our experiment, extrapolations beyond 1 year are not possible.

Many features of natural lakes differ substantially from our enclosures. As a result, natural lakes may respond differently to changes in Hg deposition. For example, the enclosures were shallow and lacked anoxic water, which may support substantial Hg methylation (Eckley et al. 2005). We also observed considerable photoreduction and evasion of Hg from the enclosures, which decreased the amount of Hg available for methylation (Amyot et al. 2004). It is uncertain whether the evasion rates observed in our enclosures were anomalously high as compared with natural lakes. While these factors may result in faster responses in natural lakes, others may result in a slower response relative to our enclosures. For example, a considerable proportion of Hg in lakes is derived from the surrounding watershed, as opposed to direct deposition to the lake surface, as in our study. There are many potential delays in the transfer of newly deposited Hg from a catchment to the lake itself (e.g., Hintelmann et al. 2002). Average temperatures were higher in our enclosures than in many lakes, which may increase relative rates of methylation. In addition, large, old fish in natural lakes may take many years to depurate MeHg accumulated during previous growth. Notwithstanding these potentially important differences between enclosures and natural lakes, our data may be applicable to shallow systems dominated by littoral sediments. Clearly, further study is required.

Single versus multiple additions

By September of both 2000 and 2001, there were no large differences in spike Hg concentrations in biota from enclosures receiving single or multiple additions. Overall, this suggests that long-term results (>6 months) were not strongly affected by the method of spike addition (multiple versus single spikes). Presumably this is because spike Hg was diluted into a comparatively large pool of ambient Hg and because there were time lags in the conversion of inorganic Hg to MeHg and subsequent accumulation by biota.

In contrast with the September results, Hg concentrations in finescale dace collected during the first 8 weeks of 2000 had higher concentrations of spike Hg in the single dose enclosure (E1) than in the multiple dose enclosure (E4). This result is surprising because there was no indication of higher concentrations of spike MeHg in invertebrates collected from E1 versus E4 at the time. In addition, spike/ambient ratios for finescale dace in the single dose enclosure were much higher than for their food resources: benthic invertebrates and zooplankton. One possible explanation for this result is that Hg in fish was measured as THg, whereas Hg in invertebrates was measured as MeHg. Under natural conditions, >90% of the Hg in fish is MeHg and THg is a sufficient measure of MeHg concentrations (Bloom 1992). In the early stages of our experiment, however, concentrations of inorganic spike Hg were briefly increased to very high levels relative to MeHg because there was insufficient time for methylation of the spike to achieve steady state with the new loading rates. As a result, much of the spike Hg incorporated by finescale dace in the first few weeks may have been inorganic Hg.

Although our use of THg may have biased our short-term results for fish, we believe that by September of each year, these biases were greatly reduced. Within weeks of addition, much of the added inorganic Hg was lost from the enclosures and probably newly accumulated inorganic Hg was largely depurated by fish. The model of Trudel and Rasmussen (1997) indicates that inorganic Hg is depurated by a 3 g fish with a half-life of approximately 10 days. In contrast, MeHg depuration would have a half-life of >250 days in similarly sized fish. With time, an increasingly larger proportion of the spike Hg in the enclosures was also methylated and relative incorporation of spike MeHg by fish presumably became increasingly important. Turner and Rudd (1983) and Hecky et al. (1991) found that >60% and >85%, respectively, of newly accumulated Hg added as radioactive ^{203}Hg occurred as MeHg in fish collected from large enclosures similar to ours after 60 days. By September in our enclosures, spike/ambient ratios for fish and invertebrates were very similar. Concentrations and spike/ambient ratios for the 2000 spike were also similar in September 2000 and 2001, further suggesting that the system was moving toward a new steady state with respect to MeHg–THg dynamics.

In summary, our study clearly demonstrates the utility of using stable isotopes of Hg to examine Hg accumulation in aquatic communities. The enriched isotopes were clearly detectable in biota, and the availability of different isotopes facilitated among-year comparisons. Our data suggest that changes in deposition of inorganic Hg will result in changes in MeHg accumulation by fish and other biota. Although long-term changes in Hg deposition should result in changes in MeHg accumulation by biota in such systems, it may take much more than a decade for steady-state conditions to be achieved. More study is required to determine to what extent these data from enclosures can be extrapolated to natural lakes.

Acknowledgements

This study was funded by the Electric Power Research Institute (EPRI), the Natural Sciences and Engineering Research Council of Canada (NSERC) through the Collaborative Mercury Research Network (COMERN), the US Environmental Protection Agency (EPA STAR program R82-7631)), and Fisheries and Oceans Canada through the Environmental Science Strategic Research Fund (ESSRF) and Toxic Substances Research Initiative (TSRI). We thank all those that assisted with enclosure installation, sample collection, processing, and analysis, including Tyler Bell, Brian Dimock, Michelle Dobrin, Cynthia Evans, Andy Majewski, Anja Naepfal, Hong Thi Nguyen, Diane Orihel, Bryan Page, Georgia Riedel, Alex Salki, Justin Shead, Mike Tate, and Shawn Tratch. We are also very grateful for the advice and support of Carol Kelly, Drew Bodaly, and Jim Hurley. Water chemistry other than Hg was determined by the Freshwater Institute Chemical Laboratory. Drew Bodaly, Ray Hesslein, Diane Orihel, and two anonymous referees provided valuable comments on earlier drafts of this manuscript.

References

Amyot, M., Southworth, G., Lindberg, S.E., Hintelmann, H., Lalonde, J.D., Ogrinc, N., Poulain, A.J., and Sandilands, K.A. 2004. Formation and evasion of dissolved gaseous mercury in large enclosures amended with $^{200}HgCl_2$. Atmos. Environ. **38**: 4279–4289.

Bloom, N.S. 1989. Determination of picogram levels of methylmercury by aqueous phase ethylation, followed by cryogenic gas chromatography with cold vapor atomic fluorescence detection. Can. J. Fish. Aquat. Sci. **46**: 1131–1140.

Bloom, N.S. 1992. On the chemical form of mercury in edible fish and marine invertebrate tissue. Can. J. Fish. Aquat. Sci. **49**: 1010–1017.

Bodaly, R.A., and Fudge, R.J.P. 1999. Uptake of mercury by fish in an experimental boreal reservoir. Arch. Environ. Contam. Toxicol. **37**: 103–109.

Downs, S.G., Macleod, C.L., and Nester, J.N. 1998. Mercury in precipitation and its relations to bioaccumulation in fish: a literature review. Water Air Soil Pollut. **108**: 149–187.

Eckley, C.S., Watras, C.J., Hintelmann, H., Morrison, K., Kent, A.D., and Regnell, O. 2005. Mercury methylation in the hypolimnetic waters of lakes with and without connection to wetlands in northern Wisconsin. Can. J. Fish. Aquat. Sci. **62**: 400–411.

Eddy, J.B. 2000. Estimation of the abundance, biomass and growth of a northwestern Ontario population of finescale dace (*Phoxinus neogaeus*), with comments on the sustainability of local commercial baitfish harvests. Master of Natural Resource Management thesis, University of Manitoba, Winnipeg, Man.

Fitzgerald, W.F., Engstrom, D.R., Mason, R.P., and Nater, E.A. 1998. The case for atmospheric mercury contamination in remote areas. Environ. Sci. Technol. **32**: 1–7.

Gilmour, C.C., Riedel, G.S., Ederington, M.C., Bell, J.T., Benoit, J.M., Gill, G.A., and Stordal, M.C. 1998. Methylmercury concentrations and production rates across a trophic gradient in the northern Everglades. Biogeochemistry, **40**: 327–345.

Hecky, R.E., Ramsey, D.J., Bodaly, R.A., and Strange, N.E. 1991. Increased methylmercury contamination in fish in newly formed freshwater reservoirs. *In* Advances in mercury toxicology. *Edited by* T. Suzuki, N. Imura, and T.W. Clarkson. Plenum Press, New York. pp. 33–52.

Hintelmann, H., and Ogrinc, N. 2003. Determination of stable mercury isotopes by ICP/MS and their application in environmental studies. *In* Biogeochemistry of environmentally important trace elements. *Edited by* Y. Cai and C.O. Braids. American Chemical Society, Washington, D.C. pp. 321–338.

Hintelmann, H.H., Harris, R., Heyes, A., Hurley, J.P., Kelly, C.A., Krabbenhoft, D.P., Lindberg, S., Rudd, J.W.M., Scott, K.J., and St. Louis, V.L. 2002. Reactivity and mobility of new and old mercury deposition in a boreal forest ecosystem during the first year of the METAALICUS study. Environ. Sci. Technol. **36**: 5034–5040.

Horowitz, A.J., Demas, C.R., Fitzgerald, K.K., Miller, T.L., and Rickert, D.A. 1994. U.S. Geological Survey protocol for collection and processing of surface-water samples for the subsequent determination of inorganic constituents in filtered water. US Government Printing Office, Washington, D.C. USGS Open File Rep. 94-539.

Horvat, M., Liang, L., and Bloom, N.S. 1993. Comparison of distillation with other current isolation methods for the determination of methyl mercury compounds in low level environmental samples. Anal. Chim. Acta, **282**: 153–168.

Hrabik, T.R., and Watras, C.J. 2002. Recent declines in mercury concentration in a freshwater fishery: isolating the effects of de-acidification and decreased atmospheric mercury deposition in Little Rock Lake. Sci. Tot. Environ. **297**: 229–237.

Jackson, T.A. 1997. Long-range atmospheric transport of mercury to ecosystems, and the importance of anthropogenic emissions — a critical review and evaluation of the published evidence. Environ. Rev. **5**: 99–120.

Johansson, K., Aastrup, M., Andersson, A., Bringmark, L., and Iverfeldt, A. 1991. Mercury in Swedish forest soils and waters — assessment of critical load. Water Air Soil Pollut. **56**: 267–281.

Mason, R.P., Fitzgerald, W.F., and Morel, F.M. 1994. The biogeochemical cycling of elemental mercury: anthropogenic influences. Geochim. Cosmochim. Acta, **58**: 3191–3198.

Morrison, K.A., and Watras, C.J. 1999. Mercury and methyl mercury in freshwater seston: direct determination at picogram per litre levels by dual filtration. Can. J. Fish. Aquat. Sci. **56**: 760–766.

North American Implementation Task Force on Mercury. 2000. North American regional action plan on mercury: phase II [online]. Available from http://www.cec.org/programs_projects/pollutants_health/smoc/pdfs/Hgnarap.pdf [accessed November 2005].

Orihel, D.M. 2005. The effects of changes in atmospheric mercury deposition on the bioaccumulation of mercury in fish. Master of Natural Resource Management thesis, University of Manitoba, Winnipeg, Man.

Paterson, M.J., Rudd, J.W.M., and St. Louis, V. 1998. Increases in total and methylmercury in zooplankton following flooding of a peatland reservoir. Environ. Sci. Technol. **32**: 3868–3874.

Pickhardt, P.C., Folt, C.L., Chen, C.Y., Klaue, B., and Blum, J.D. 2002. Algal blooms reduce the uptake of toxic methylmercury in freshwater food webs. Proc. Natl. Acad. Sci. U.S.A. **99**: 4419–4423.

Pickhardt, P.C., Folt, C.L., Chen, C.Y., Klaue, B., and Blum, J.D. 2005. Impacts of zooplankton composition and algal enrichment on the accumulation of mercury in an experimental freshwater food web. Sci. Tot. Environ. **339**: 89–101.

Stainton, M.P., Capel, M.J., and Armstrong, F.A.J. 1977. The chemical analysis of fresh water. 2nd ed. Can. Fish. Mar. Serv. Misc. Spec. Publ. No. 25.

St. Louis, V.L., Rudd, J.W.M., Kelly, C.A., Bodaly, R.A., Paterson, M.J., Beaty, K.G., Hesslein, R.H., Heyes, A., and Majewski, A.R. 2004. The rise and fall of mercury methylation in an experimental reservoir. Environ. Sci. Technol. **38**: 1348–1358.

Trudel, M., and Rasmussen, J.B. 1997. Modeling the elimination of mercury by fish. Environ. Sci. Technol. **31**: 1716–1722.

Turner, M.A., and Rudd, J.W.M. 1983. The English–Wabigoon River system. III. Selenium in lake enclosures: its geochemistry, bioaccumulation, and ability to reduce mercury bioaccumulation. Can. J. Fish. Aquat. Sci. **40**: 2228–2240.

Wiener, J.G., Krabbenhoft, D.P., Heinz, G.H., and Scheuhammer, A.M. 2003. Ecotoxicology of mercury. *In* Handbook of ecotoxicology. Lewis Publishers, Boca Raton, Fla. pp. 409–463.

A multifrequency method to classify and evaluate fisheries acoustics data

J. Michael Jech and William L. Michaels

Abstract: Acoustic surveys have been conducted on Georges Bank from 1998 to present to estimate Atlantic herring (*Clupea harengus*) population abundance. Acoustic data were collected with a 12 or 18, 38, and 120 kHz Simrad EK500 scientific echo sounder. A pelagic trawl and underwater video images were used to collect biological information and to verify the species composition of acoustic backscatter. A multifrequency classification method was developed to improve the efficiency and accuracy of classifying species from acoustic echograms. In this method, a volume backscatter (S_v) threshold was applied equivalently to all echograms, and then a composite echogram was created based on which frequencies had S_v greater than or less than the S_v threshold. The results of this method were compared with the standard method of visually scrutinizing regions, and metrics were developed to evaluate the accuracy of classification algorithms relative to current methods, as well as to assess the effects of classification methods on population abundance estimates. In general, this method matched visually scrutinized Atlantic herring regions, but with consistent biases in classifying 38 kHz backscatter. The metrics highlighted spatial and temporal changes in the acoustic landscape, which may be indicative of intra- and inter-annual biological changes.

Résumé : Des inventaires acoustiques sur le banc Georges de 1998 à aujourd'hui cherchent à estimer l'abondance de la population de harengs de l'Atlantique (*Clupea harengus*). Les données acoustiques ont été recueillies à l'aide d'une écho-sonde scientifique Simrad EK500 de 12 ou 18, 38 et 120 kHz. Un chalut pélagique et des images vidéo sous-marines ont servi à amasser des renseignements biologiques et à vérifier la composition spécifique de la rétrodiffusion acoustique. Nous avons mis au point une méthode de classification à fréquences multiples pour améliorer l'efficacité et la précision de la classification des espèces à partir des échogrammes acoustiques. Dans cette méthode, un seuil de volume de rétrodiffusion (S_v) est appliqué de façon équivalente à tous les échogrammes et un échogramme composite est créé à partir des fréquences qui ont des S_v plus grands ou plus faibles que le seuil de S_v. Nous avons comparé les résultats de cette méthode à la méthode standard qui consiste à scruter visuellement les régions et nous avons mis au point des métriques pour évaluer la précision des algorithmes de classification par rapport aux méthodes courantes ainsi que pour déterminer les effets des méthodes de classification sur les estimations d'abondance de la population. En général, notre méthode se compare à celle de l'examen visuel des régions contenant des harengs, mais avec des déformations uniformes dans la classification des rétrodiffusions de 38 kHz. Les métriques mettent en lumière les changements spatiaux et temporels du paysage acoustique, qui peuvent peut-être représenter des changements biologiques intra- et inter-annuels.

[Traduit par la Rédaction]

Introduction

Identification of acoustic backscatter to taxa is one of the grand challenges of fisheries acoustics (MacLennan and Holliday 1996). In this paper, identification is defined as the objective determination of acoustic backscatter to genus or species, whereas classification is defined as the less rigorous product of objectively categorizing acoustic backscatter to some anatomical feature or lower-level taxon. For example, acoustic backscatter may be classified or categorized as fish with a gas-filled swimbladder or as non-gas-bearing zooplankton, but the species comprising either group may only be broadly known. Interpretation of acoustic data currently involves verification of backscatter in conjunction with visual scrutiny of echograms (Reid et al. 1998). Scrutinization is the process of visually interpreting an echogram and selecting and allocating backscatter to a species. Verification of acoustic backscatter primarily involves physical capture with nets and, to a lesser extent, optical imaging. Visual interpretation of echograms is highly dependent on the experience of the person scrutinizing the data, and consequently, biases are difficult to quantify. Objective identification or classification methods are preferable to subjective methods because objective classification can be applied as data are collected; biases due to personal experience are minimized or eliminated; objective methods can be transferred among

Received 18 January 2006. Accepted 6 June 2006. Published on the NRC Research Press Web site at http://cjfas.nrc.ca on 21 September 2006.
J19116

J.M. Jech[1] and W.L. Michaels. Northeast Fisheries Science Center (NOAA/NMFS), 166 Water Street, Woods Hole, MA 02543, USA.

[1]Corresponding author (e-mail: michael.jech@noaa.gov).

Can. J. Fish. Aquat. Sci. **63**: 2225–2235 (2006) doi:10.1139/F06-126

surveys without transferring "experienced" specialists; data analyses are more efficient, timely, less sensitive to subjective interpretation, and potentially more accurate; error and bias are more amenable to quantification; and spatial and temporal distributions and changes in these distributions can be efficiently characterized.

The dependence of backscatter by zooplankton and fish on acoustic frequency and size of the animal has long been recognized (e.g., Anderson 1950; Haslett 1965) and has been used to separate size classes (McNaught 1969; Holliday 1977) or classify or identify organisms (Zakharia and Sessarego 1982). Utilizing this frequency dependence for remotely estimating organism size or identifying species requires a wide acoustic bandwidth. Widening the frequency bandwidth can be achieved with broadband signals and (or) multiple, narrowband echo sounders (multifrequency). Broadband signals transmit and receive continuous energy over a broad (greater than 10% of the center frequency) frequency range. Broadband methods have been used to measure spectral responses from individuals (Kjærgaard et al. 1990; Reeder et al. 2004), compare spectra among different species (Simmonds and Armstrong 1990), and differentiate species using neural networks (Simmonds et al. 1996). These methods have had some success in the laboratory but have had limited application to fisheries surveys (Zakharia et al. 1996). A drawback to broadband technology is that the energy per frequency is lower than with narrowband systems, so that the detection of targets at the ranges required for most fisheries assessments is limited.

Alternatively, multiple narrowband frequencies (multifrequency) can be used to widen the acoustic bandwidth. The two common methods of analyzing multifrequency data are an inverse approach (Holliday 1977) and the difference in mean volume backscattering strength (ΔMVBS) (Madureira et al. 1993) or "dB differencing" (Higgenbottom et al. 2000). These techniques have been used to separate fish with gas-filled swimbladders from fish with no swimbladder (Kirkegaard and Lassen 1990) and swimbladder-bearing fish from zooplankton (Sætersdal et al. 1982; Cochrane et al. 1991; Kang et al. 2002), to generate size-based estimates of zooplankton (Greenlaw and Johnson 1983; Holliday and Pieper 1995; Mitson et al. 1996), to estimate swimbladder sizes (Holliday 1972; Kalish et al. 1986), and to discriminate squid from other targets (Goss et al. 1998). The nearly ubiquitous availability of two or three narrowband echo sounders on fisheries research vessels has driven the use of the ΔMVBS method, and it is becoming a standard technique for separating gas-bearing organisms from those without a gas-bearing organ (e.g., Korneliussen and Ona 2002, 2003) and in ecological studies (Simard and Lavoie 1999; Swartzman et al. 1999).

The ΔMVBS method uses ratios of volume backscatter ($s_v(f)$ ($\mathrm{m}^2 \cdot \mathrm{m}^{-3}$)) or, in the logarithmic domain, the difference between $S_v(f)$ (dB) values, where f denotes the frequency dependence. The general success of this method to discriminate zooplankton and fish is apparent when the frequency-dependent backscatter for gas-bearing organisms versus those organisms without a gas-bearing feature is compared. However, the ΔMVBS method uses the ratio of two frequencies regardless of how many frequencies are available. When three or more frequencies are available, ratios of two frequencies are compared with other ratios of two frequencies. Comparing ratios of ratios is a cumbersome method to analyze data from three or more frequencies. In this paper, a method is presented that incorporates information from multiple frequencies to investigate the potential for classifying Atlantic herring (*Clupea harengus*) in the Northwest Atlantic. This method is evaluated by comparison with visually scrutinized data, and the benefits and limitations of this method for surveys are discussed.

Materials and methods

Data were collected during the Northeast Fisheries Science Center's (NEFSC) annual Atlantic herring acoustical survey. These surveys consisted of systematic parallel or zigzag transects conducted during September and October in the Gulf of Maine and Georges Bank regions (Fig. 1). The primary survey is designed to survey the offshore component of the Atlantic herring population, which migrates to Georges Bank in the fall to spawn.

Acoustic data

Acoustic data were collected from 1995 to 2004 on the NOAA R/V *Delaware II* with a Simrad EK500 scientific echo sounder (Simrad, Horton, Norway). Before 1999, acoustic data were collected as part of pilot projects to investigate the potential for using acoustic methods to estimate abundance and biomass of pelagic species. During 1999–2001, the EK500 operated a hull-mounted, single-beam, 12 kHz transducer (model 12-16) and hull-mounted 38 kHz (ES38-12) and 120 kHz (ES120-7) split-beam transducers. From 2002 to present, the 12 kHz transducer was replaced with an 18 kHz (ES18) split-beam transducer. Beam widths, as measured by the manufacturer at the half-power points, were 16°, 12°, 12°, and 7° for the 12, 18, 38, and 120 kHz transducers, respectively. The 38 and 120 kHz transducers were located on the keel, with the 120 kHz transducer 1.24 m aft of the 38 kHz transducer. The 12 and 18 kHz transducers were located 2.97 m forward and 0.66 m to the port of the 38 kHz transducer. Each frequency was transmitted simultaneously at a rate of 1 ping per 2 s. Pulse durations were 1 ms for the 38 and 120 kHz echo sounders, 3 ms for the 12 kHz echo sounder, and 2 ms for the 18 kHz echo sounder. Although it may be advantageous to maintain consistent pulse durations among all frequencies, the signal to noise ratio for the 12 and 18 kHz systems was unacceptable at shorter pulse durations. The 18, 38, and 120 kHz systems were calibrated before each survey and often were calibrated during and (or) immediately after the survey period using the standard target method (Foote et al. 1987). The 12 kHz system was successfully calibrated in 1999 and 2001. Target strength and volume backscatter calibration gains varied less than 0.5 dB for the 12 and 18 kHz systems, 0.3 dB for the 38 kHz system, and 0.8 dB for the 120 kHz system over the period from 1999 to 2004.

Acoustic signals were processed by the EK500 by applying $20\log R$ time-varying gain, frequency-dependent absorption coefficients, and calibration gains. A –90 dB S_v threshold was set during data collection. These data were vertically inte-

Fig. 1. Systematic parallel acoustic survey conducted on Georges Bank during 18–26 September 2002. Areal backscatter (s_A) values at 38 kHz are based on volume backscatter allocated to Atlantic herring (*Clupea harengus*).

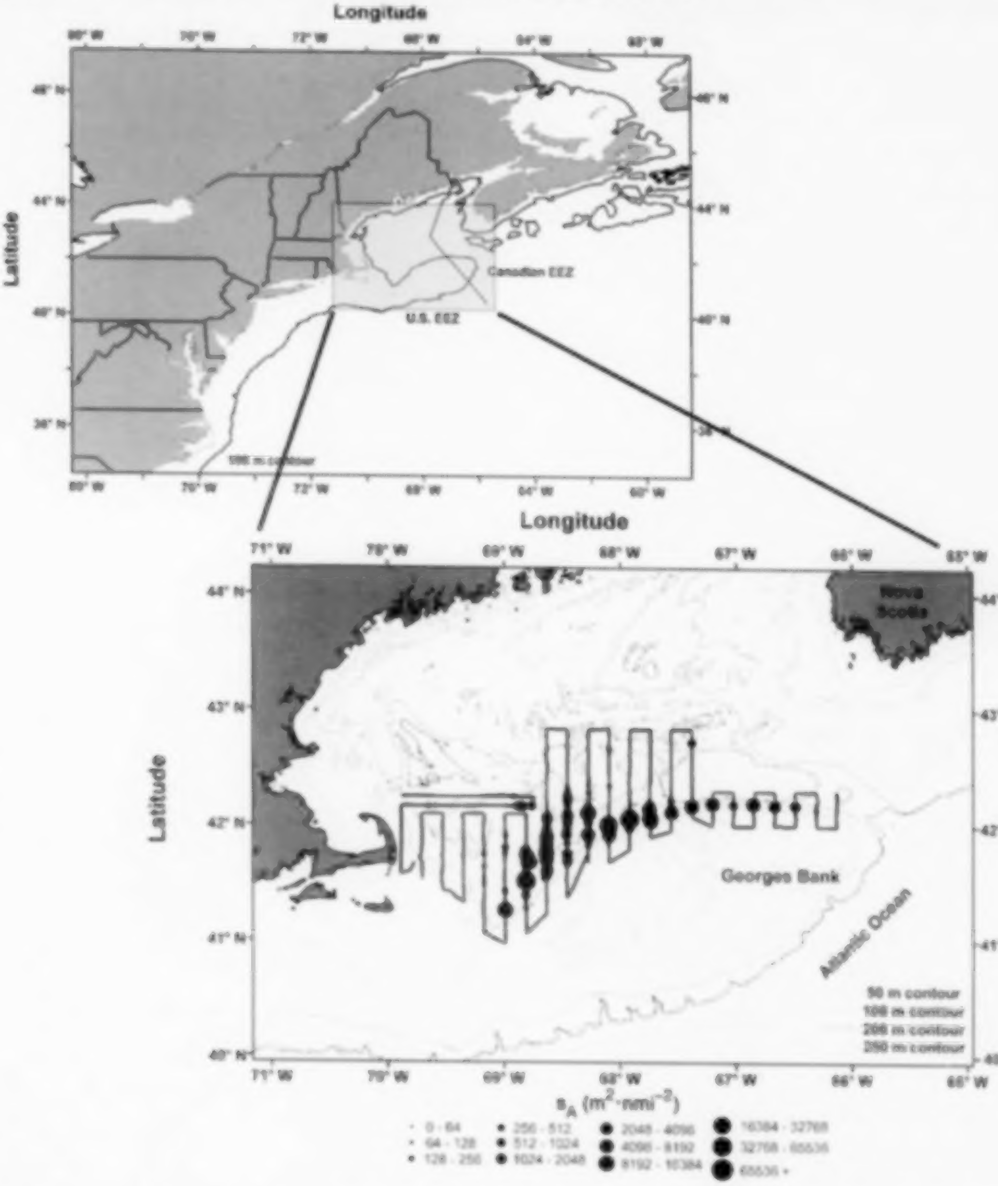
Longitude
80° W
76° W
72° W
68° W
64° W
60° W
48° N
44° N
40° N
36° N
Latitude
Canadian EEZ
U.S. EEZ
100 m contour
Longitude
71° W
70° W
69° W
68° W
67° W
66° W
65° W
44° N
43° N
42° N
41° N
40° N
Latitude
Nova Scotia
Georges Bank
Atlantic Ocean
50 m contour
100 m contour
200 m contour
250 m contour
s_A (m²·nmi⁻²)
0 - 64
64 - 128
128 - 256
256 - 512
512 - 1024
1024 - 2048
2048 - 4096
4096 - 8192
8192 - 16384
16384 - 32768
32768 - 65536
65536 +

grated at 0.5 m intervals (1999 and 2000) or 1 m intervals (2001–2004) for volume backscatter (S_v (dB·m^{-3})). Volume backscatter data collected in 1999 and 2000 were transferred via Ethernet to a UNIX workstation in Simrad's BI500 data format. Volume backscatter data collected from 2001 to 2004 were transferred via Ethernet to a personal computer (PC) and logged with SonarData's Echolog software (SonarData Pty Ltd., Hobart, Tasmania).

Volume backscatter data were postprocessed using SonarData's Echoview software. Data shallower than 10 m were removed from analyses to eliminate the transmit pulse and reduce backscatter by surface bubbles. Data deeper than 0.5 m above the seafloor echo were removed from analyses. The seafloor echo was selected using Echoview's "Maximum Sv with backstep" algorithm, where the backstep was set at 0.5 m. The bottom detection was then visually inspected and corrected if necessary.

Volume backscatter data were horizontally averaged over 0.5 nautical miles (nmi) for measures of areal backscatter (s_A (m^2·nmi^{-2})). This equivalent sampling distance unit (ESDU) was based on analyses of Atlantic herring abundance and biomass estimates using traditional statistics and geostatistical methods and was determined to be optimal for deriving abundance and biomass estimates of Atlantic herring during the annual surveys (William Overholtz, NEFSC, 166 Water Street, Woods Hole, MA 02543, USA, personal communication).

During postprocessing, an S_v threshold of –66 dB was applied equivalently to all echograms and all frequencies. This threshold was determined by analyzing a subset of data collected in 1999. Data were selected from transects where the greatest concentrations of Atlantic herring were observed. Total water-column s_A and s_A apportioned to herring were calculated at 0.5 nmi intervals for S_v thresholds ranging from –91 to –43 dB in 6 dB steps. The mean s_A was calculated at each S_v threshold and then normalized to the maximum mean value (Fig. 2*a*). Mean water-column s_A and herring s_A decreased slightly for S_v thresholds from –91 to –70 dB. For thresholds above –70 dB, mean water-column s_A deviated from the maximum at a greater rate than did the mean herring s_A. The mean water-column s_A was reduced to 91% of the maximum at an S_v threshold of –61 dB, whereas mean herring s_A was only reduced to 97% of the maximum. The final choice of –66 dB as the postprocessing S_v threshold was based on these results and the qualitative ability to visually select Atlantic herring.

Acoustic backscatter attributed to Atlantic herring was visually selected (i.e., "scrutinized") in near-real time during the surveys. Selection of Atlantic herring was accomplished through experience and examination of trawl catches. Two sets of areal backscatter values were exported from Echoview and imported into an Oracle® database: s_A for the entire water column and s_A apportioned to Atlantic herring.

Biological data

A high-speed midwater rope trawl (HSMRT) was used to collect biological samples and verify species composition of acoustic backscatter. This trawl was designed for fishing at relatively high speeds (4–5 knots) with minimal drag. Its symmetrical four-seam box design had 53.1 m footrope, headrope, and breast lines, providing a mouth opening of roughly 300–350 m^2 when fishing. The trawl was rigged with four 54.8 m bridles and 1.8 m^2 US Jet double-foiled suberkrub-type doors with double door weights. Optimal tow configuration was set to a total (forward and aft sections) setback of 2.5 m with 275 kg tom weights for each side. A Simrad FS903 third-wire trawl monitoring system was used to determine net configuration while towing and to estimate the catch amount to collect a representative sample of the organisms comprising acoustic backscatter.

Trawl locations, tow depths, and tow durations were chosen on an ad hoc basis to sample Atlantic herring aggregations, as well as unknown backscatter. Because tow duration was not standardized, trawl catches were not used for abundance estimates. Trawl catch data were recorded, audited, and archived using the Fisheries Scientific Computer System (FSCS). FSCS has been developed within NOAA Fisheries as an electronic on-board data entry system. Catch data are imported to an Oracle® database for data auditing and archiving. The trawl catch was separated by species, and the total weight of each species was recorded. Fork lengths to the nearest centimetre were recorded for a sample of 100–150 fish for all species, except Atlantic herring. A sample of 100–150 Atlantic herring was randomly selected and individual fork lengths to the nearest millimetre and individual weights to the nearest gram were recorded. A subsample of one herring per centimetre interval was selected for measurements of sex, maturity, stomach contents, and otolith extraction for age estimation.

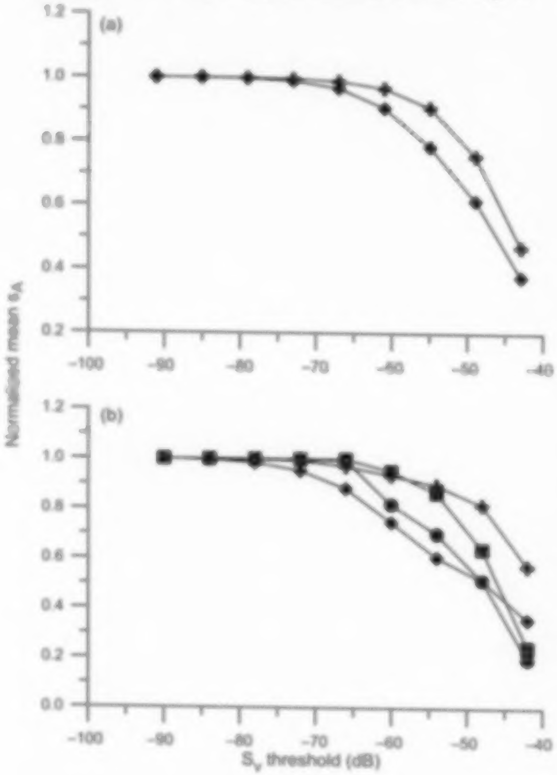

Fig. 2. Mean 38 kHz areal backscatter (s_A) integrated throughout the entire water column (s_A(WC), +), in visually selected herring regions ($s_A(AH_V)$, ◆), in cells where all three frequencies were present throughout the water column ($s_A(WC_{123})$, ●), and in cells where all three frequencies were present within visually selected herring regions ($s_A(AH_{123})$, ■) as a function of 38 kHz volume backscatter (S_v) threshold. Data presented in (*a*) were collected in September 1999 and data presented in (*b*) were collected in September 2003 along the transect shown in Fig. 8.

Other data

Conductivity–temperature–depth (CTD) profiles were obtained at the beginning and end of each transect and before each trawl haul. The on-board data recording and entry system, Scientific Computer System (SCS), was used to record time series of time (GMT), geographic position, and the EK500 vessel log, as well as electronically enter events such as the beginning and end of transects and deployments. This event log was audited and imported to an Oracle® database. The event log, biological data, and acoustic data are all linked within Oracle®.

Table 1. Year, beginning and end dates, number of transects in each survey, and the survey design for Atlantic herring (*Clupea harengus*) acoustic surveys in the Georges Bank region.

Survey year	Begin date	End date	No. of transects	Survey design
1999*a*	25 September	27 September	13	Systematic zigzag
1999*b*	27 September	28 September	13	Systematic zigzag
2000*a*	11 September	16 September	17	Systematic parallel
2000*b*	04 October	06 October	7	Systematic parallel
2000*c*	06 October	08 October	7	Systematic parallel
2001	18 September	23 September	18	Systematic parallel
2002	18 September	26 September	22	Systematic parallel
2003*a*	04 September	10 September	18	Systematic parallel
2003*b*	18 September	24 September	18	Systematic parallel
2003*c*	03 October	10 October	18	Systematic parallel
2004	21 September	27 September	17	Systematic parallel

Classification method

A method is introduced that records whether the S_v in an echogram "cell" (1 m or 0.5 m vertical by 1 ping horizontal) is greater than the S_v threshold and then codes each cell depending on which frequencies are greater than the S_v threshold ("present") or less than the S_v threshold ("absent"). The number of present or absent combinations can be calculated from Pascal's triangle. For three frequencies, there are eight possible outcomes: - - -, 1- -, 12-, 123, 1-3, -2-, -23, and - - 3, where "1" denotes the presence of 12 or 18 kHz S_v, "2" denotes the presence of 38 kHz S_v, "3" denotes the presence of 120 kHz S_v, and "-" denotes the absence of a frequency. A series of virtual echograms was created in Echoview (Higgenbottom et al. 2000) and the final result of the classification was applied to the 38 kHz S_v data.

Through experience with visually scrutinizing echograms and examining trawl catches, backscatter by Atlantic herring appeared to correspond closely with S_v that was present in all three frequencies (code value "123"). Overall, Atlantic herring dominated (>90% by number or weight) pelagic trawl catches within 10–15 nmi of Georges Bank. For the entire survey area on Georges Bank (Fig. 1), Atlantic herring, silver hake (*Merluccius bilinearis*), and Acadian redfish (*Sebastes fasciatus*) typically comprised 95% or greater of the trawl catches. Therefore, those cells where all three frequencies are present were hypothesized to be Atlantic herring.

Thirty-eight kHz s_A values were exported from Echoview and imported to an Oracle® database for analysis. The following data categories were used for analysis: s_A values for the entire water column (s_A(WC)); s_A values for visually selected Atlantic herring regions (s_A(AH$_V$)); s_A values for the entire water column where S_v was present in all three frequencies (s_A(WC$_{123}$)); and s_A values within visually selected Atlantic herring regions where S_v was present in all three frequencies (s_A(AH$_{123}$)). Only s_A values along systematic zigzag (1999) or parallel (2000–2004) transects were selected for analysis and s_A values during deployments, transits, and crossover transects were excluded (Table 1).

Analysis and comparisons

Objective classification methods require evaluation of the accuracy and precision of the method and consideration of how the method affects long-term time series of population estimates. Evaluating the accuracy of classification methods in situ is often very difficult because of the limited ability at sea to accurately verify all acoustic backscatter. For these analyses, the classification method is compared with the de facto standard of visually scrutinizing echograms.

To assess whether the frequency combination where all three frequencies were present corresponded to the visually selected Atlantic herring regions (AH$_V$), the number of visually selected Atlantic herring regions was compared with the number of these regions containing S_v where all three frequencies were present (AH$_{123}$).

To evaluate which frequency combinations, if any, were more prevalent in visually selected Atlantic herring regions (AH$_V$) relative to the water column, the proportion of cells for each frequency combination (FC) within Atlantic herring regions ($p_{\mathrm{AH_V}}$(FC)) was compared with the proportion in the water column (p_{WC}(FC)):

$$(1) \qquad P(\mathrm{FC}) = \frac{p_{\mathrm{AH_V}}(\mathrm{FC})}{p_{\mathrm{WC}}(\mathrm{FC})}$$

where $p_{\mathrm{AH_V}}$(FC) was the number of cells for each frequency combination within visually selected Atlantic herring regions divided by the total number of cells within those regions, and p_{WC}(FC) was the number of cells for each frequency combination in the water column divided by the total number of cells. Water-column cells comprised all cells except those within Atlantic herring regions along the entire survey. Values of P(FC) greater than one indicate a greater proportion of that frequency combination within visually selected regions, values less than one indicate a greater proportion of that frequency combination in the water column, and values of one indicate equivalent proportions.

This classification method is dependent on the S_v threshold used to postprocess the echograms. If the S_v threshold is set such that all cells have volume backscatter greater than the threshold, then the entire water column will be classified homogeneously. Conversely, setting a high S_v threshold will eliminate all volume backscatter. Similar to the S_v-threshold analysis in 1999, data collected along a transect during 21 September 2003 were analyzed to examine the effects of S_v threshold on the classification method; s_A(WC), s_A(AH$_V$),

Fig. 3. Echograms of three frequency (12, 38, and 120 kHz) data (lower three panels) and corresponding composite echogram (top panel) from the classification method. In the composite echogram, volume backscatter cells are color-coded based on the frequency combinations, where "1", "2", or "3" denotes the presence of 12, 38, or 120 kHz S_v values, respectively, and "-" denotes the absence of a frequency. The cyan color represents all three frequencies greater than the S_v threshold, and these cells are hypothesized to represent Atlantic herring (*Clupea harengus*). Note that color in the composite echogram does not represent magnitude. nmi, nautical mile.

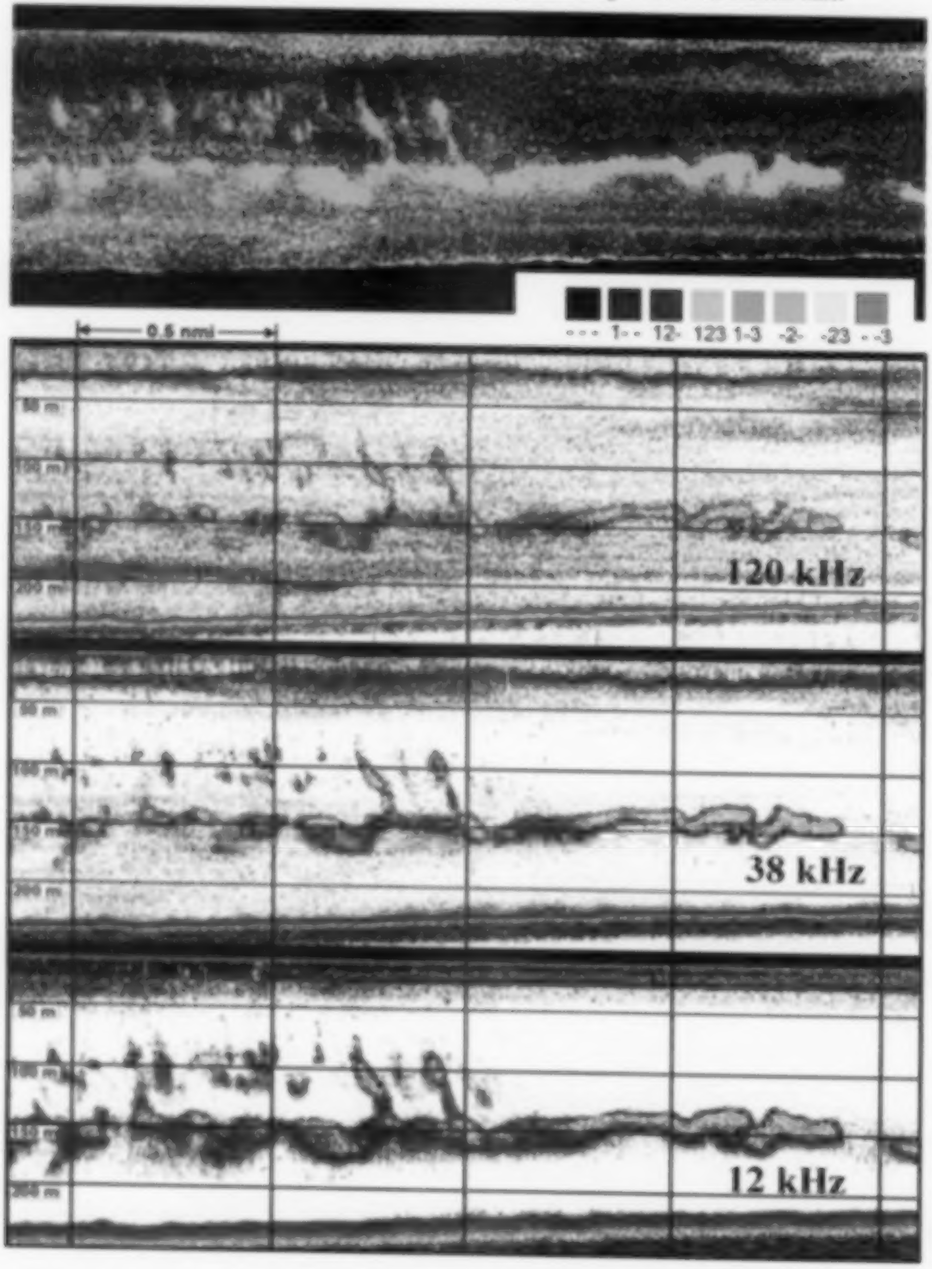

$s_A(WC_{123})$, and $s_A(AH_{123})$ were averaged over 0.5 nmi intervals for S_v thresholds ranging from −90 to −42 dB in 6 dB steps. The mean s_A was calculated at each S_v threshold and then normalized to the maximum mean value.

Areal backscatter values are used for abundance estimates. Three comparisons of s_A values were done. For these comparisons, water-column cells comprised all echogram cells, including those within Atlantic herring regions. The first comparison was the ratio of $s_A(AH_{123})$ to $(s_A(AH_V)$. This ratio provides a metric of the proportion of backscatter objectively classified as Atlantic herring relative to the backscatter visually allocated to herring:

Table 2. Number of regions visually selected and the number of visually selected regions with cells where all three frequencies were present.

Survey	No. of visually selected regions	No. of regions with all three frequencies present
1999*a*	14	14
1999*b*	14	14
2000*a*	25	25
2000*b*	19	19
2000*c*	16	16
2001	29	29
2002	25	25
2003*a*	28	27*
2003*b*	57	57
2003*c*	39	39
2004	30	30

Note: With the exception of one region in survey 2003*a* (indicated by *), all visually selected regions had S_v values that had all three frequencies present. The s_A for the single region in survey 2003*a* was 27 $m^2 \cdot nmi^{-2}$.

$$(2) \qquad R(s_A(AH_{123}){:}s_A(AH_V)) = \frac{\sum s_A(AH_{123})}{\sum s_A(AH_V)}$$

where the summation is over the entire survey. This ratio can be used to quantify a change in abundance indices when using the objective method.

The second comparison was the ratio of $s_A(WC_{123})$ to $s_A(WC)$. This ratio provides a metric of the total water-column backscatter relative to the backscatter objectively classified as Atlantic herring:

$$(3) \qquad R(s_A(WC_{123}){:}s_A(WC)) = \frac{\sum s_A(WC_{123})}{\sum s_A(WC)}$$

where the summation is over the entire survey. This ratio measures the proportion of backscatter within the water column that can be potentially classified as Atlantic herring.

The third comparison provides a metric of $s_A(AH_V)$ relative to $s_A(WC_{123})$:

$$(4) \qquad R(s_A(AH_V){:}s_A(WC_{123})) = \frac{\sum s_A(AH_V)}{\sum s_A(WC_{123})}$$

where the summation is over the entire survey. This ratio measures the proportion of backscatter in the water column that could be objectively classified as Atlantic herring to that backscatter visually allocated.

Results

Mean water-column s_A ($s_A(WC)$) and visually apportioned herring s_A ($s_A(AH_V)$) decreased slightly for S_v thresholds less than –72 dB for data collected in 2003 (Fig. 2*b*). For thresholds above –70 dB, mean $s_A(WC)$ deviated from the maximum at a greater rate than did the mean $s_A(AH_V)$ and at a greater rate than in 1999 (Fig. 2*a*). The mean $s_A(WC)$ was reduced to 75% of the maximum at an S_v threshold of –60 dB, whereas mean $s_A(AH_V)$ was only reduced to 94% of the maximum. For backscatter where all three frequencies were above the S_v threshold, mean $s_A(WC_{123})$ and $s_A(AH_{123})$ were insensitive to S_v threshold at thresholds less than –66 dB. At thresholds greater than –66 dB, similar to results in 1999, the mean $s_A(WC_{123})$ deviated from the maximum at a greater rate than did the mean $s_A(AH_{123})$. At thresholds less than –60 dB, mean $s_A(AH_{123})$ was less sensitive to the S_v threshold than was the mean $s_A(AH_V)$, whereas for thresholds above –60 dB, the opposite trend occurred.

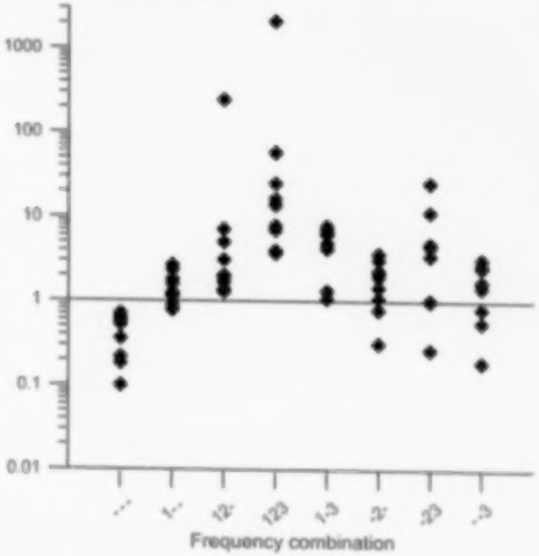

Fig. 4. The proportion of each frequency combination within visually selected Atlantic herring (*Clupea harengus*) regions relative to the proportion of frequency combinations in the water column. Each point represents the cumulative proportion for each survey. Frequency combinations are coded as "1", "2", or "3" where each value denotes the presence of 12 or 18, 38, or 120 kHz S_v, respectively, and "–" denotes the absence of a frequency. Values greater than 1 represent a greater proportion of a frequency combination within regions relative to the water column. Values less than 1 represent a smaller proportion of a frequency combination within regions relative to the water column, and a value of 1 represents equivalent proportions between regions and the water column.

Conventional echograms commonly display S_v in color, where color is used to represent backscattering intensity. For this method $S_v(f)$ frequency combinations are visualized by color coding each frequency combination and displaying the results as an echogram (Fig. 3). The use of color is a powerful tool to display data, to highlight features, and to interpret the data (Swartzman et al. 1999; Kloser et al. 2002; Towler et al. 2003). For these data, cyan represents S_v data where all three frequencies were greater than the S_v threshold. This frequency combination is hypothesized to be representative of Atlantic herring.

To evaluate whether visually selected Atlantic herring regions were objectively categorized as Atlantic herring, the number of visually selected regions were compared with the number of regions that contained S_v where all three frequencies were present. Every visually selected Atlantic herring region, with the exception of one region selected in 2003, contained cells with S_v where all frequencies were greater

Fig. 5. Ratio of 38 kHz areal backscatter based on 38 kHz volume backscatter where all three frequencies were present within visually selected herring regions ($s_A(AH_{123})$) to the 38 kHz areal backscatter based on volume backscatter within visually selected regions ($s_A(AH_V)$) for each survey.

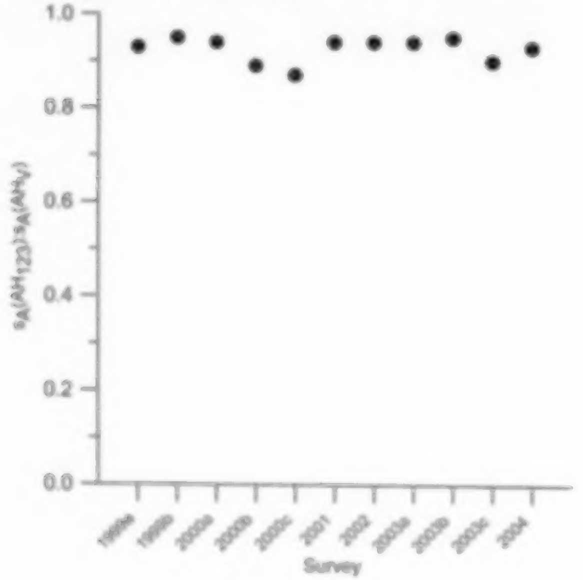

Fig. 6. Ratio of 38 kHz areal backscatter based on volume backscatter where all three frequencies were present throughout the water column ($s_A(WC_{123})$) to 38 kHz areal backscatter throughout the water column ($s_A(WC)$) for each survey.

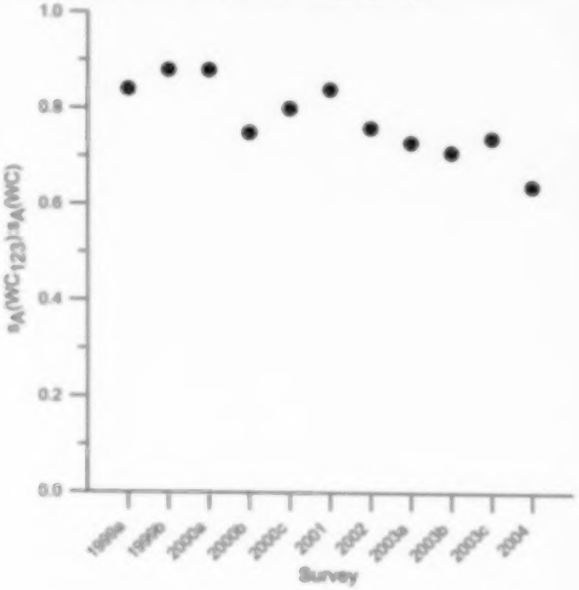

than the S_v threshold (Table 2). The single region in 2003 was a small aggregation, horizontal dimension less than 0.5 nmi, with an s_A of 27 $m^2 \cdot nmi^{-2}$.

In general, the proportion of each frequency combination relative to the other combinations within Atlantic herring regions was greater than the proportion of each corresponding frequency combination in the water column (Fig. 4). For the frequency combination where all frequencies were less than the S_v threshold, the proportion of empty cells was greater in the water column than in scrutinized regions. However, this comparison is biased because scrutinized regions were created to minimize the number of empty cells. Three frequency combinations (12 or 18 and 38 kHz (frequency combination code "12-"), 12 or 18, 38, and 120 kHz ("123"), and 12 or 18 and 120 kHz ("1-3")) had greater proportions within scrutinized Atlantic herring regions for all surveys, whereas the other frequency combinations were not consistently greater or less than the proportion of those combinations in the water column.

Within regions scrutinized for Atlantic herring, 38 kHz s_A derived from S_v cells with all three frequencies greater than the S_v threshold was 5%–13% lower than the 38 kHz s_A from corresponding visually selected regions (Fig. 5). The ratio $s_A(AH_{123})$ to $s_A(AH_V)$ varied between 93% and 95% for surveys conducted in September, whereas the three surveys conducted in October had the lowest ratios (2000*b*, 89%; 2000*c*, 87%; 2003*c*, 90%).

Water-column 38 kHz s_A values derived from S_v cells with all three frequencies greater than the S_v threshold ($s_A(WC_{123})$) were 88% to 64% of the 38 kHz water-column s_A ($s_A(WC)$) (Fig. 6). The ratio of $s_A(WC_{123})$ to $s_A(WC)$ showed a decreasing trend from 1999 to 2004.

The s_A values from scrutinized Atlantic herring regions relative to water-column cells where all three frequencies were greater than the S_v threshold ($s_A(AH_V)$ to $s_A(WC_{123})$) ranged from 100% to 20% (Fig. 7). Ratios of $s_A(AH_V)$ to $s_A(WC_{123})$ were considerably lower during 2000, ranging from 20% to 31% in 2000 versus 75% to 100% during the other years. There appears to be a disjunct in these ratio values between 2001 and 2002, where $s_A(AH_V):s_A(WC_{123})$ values were near 100% during 1999 and 2001 and in the 70%–90% range during 2002–2004.

Discussion

The S_v threshold used in this analysis is that used for estimating Atlantic herring abundance at the Northeast Fisheries Science Center and was chosen as a compromise between the ability to visually scrutinize echograms for Atlantic herring and minimizing the effect of S_v threshold on areal backscatter and the resulting abundance estimates. The classification method was less sensitive to S_v threshold at lower thresholds than was visually scrutinizing the data. This suggests that echogram cells where all three frequencies are above the threshold dominate the total backscatter. Interestingly, at higher thresholds, the classification method was more sensitive to S_v threshold. The overall response (a flat response and then a relatively sharp drop) of the classification method to S_v threshold suggests that an objective classification method could be used to select an optimal S_v threshold.

The acoustic data were neither spatially smoothed (e.g., Korneliussen and Ona 2003) nor corrected for beam-width or pulse-duration effects (e.g., Diner 2001). During these surveys, the herring are queuing to spawn on Georges Bank

Fig. 7. Ratio of 38 kHz areal backscatter based on volume backscatter within visually selected herring regions ($s_A(\mathrm{AH_V})$) to 38 kHz areal backscatter based on volume backscatter where all three frequencies were present throughout the water column ($s_A(\mathrm{WC}_{123})$) for each survey.

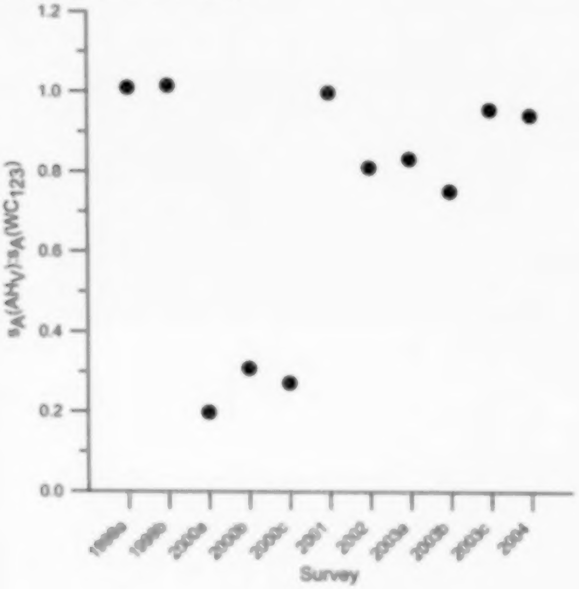

and are observed in fairly large and continuous aggregations. The spatial extent of the aggregations along the transects tends to be on the order of miles, which is much larger than the beam-width dimensions. Corrections described by Diner (2001) were applied to a subset of the data to determine whether these corrections should be applied to the data before applying the classification method. Corrections ranged from 0.1 to 0.4 dB and thus were deemed negligible for these data. During other surveys at other times and locations, Atlantic herring are observed in smaller aggregations and smoothing and other corrections may be required.

Through experience in scrutinizing multifrequency data collected during the Atlantic herring surveys, it was hypothesized that echogram cells that had S_v greater than the threshold for all three frequencies could be classified as Atlantic herring. In support of this hypothesis, essentially every scrutinized region contained cells that met this criterion. In addition, the proportion of cells with all three frequencies greater than the S_v threshold was consistently greater in scrutinized regions than in the water column. However, all frequency combinations occurred in scrutinized regions and the frequency combination of all three frequencies greater than the S_v threshold did occur, sometimes in significant magnitude, outside of scrutinized regions. Examination of trawl catches showed that the backscatter outside of scrutinized regions was not attributable to Atlantic herring, thus demonstrating that this method is not sufficient for identification of Atlantic herring alone. However, it does appear that this method may be used to discriminate between gas-bearing organisms, such as swimbladder-bearing fish, and non-gas-bearing organisms, such as euphausiids or shrimp.

At present, this method must be used in a supervised mode where the classification is applied to the echograms and then the data are scrutinized. This two-step process changes the scrutinize paradigm from asking "what is?" to "what is not?" For our Atlantic herring surveys, the objective method effectively classifies a subset of the total backscatter as potentially herring, and then the scrutinizer selects from only that subset. This allows the scrutinizer to focus on a smaller set of data and may enhance the efficiency of scrutinizing echograms.

When utilizing multiple frequencies, the choice of frequencies is potentially more important than the number of frequencies (Horne and Jech 1999). Our results suggest that incorporating 12 or 18 kHz data is valuable for classifying swimbladder-bearing fish. There were consistently higher proportions of the frequency combinations that included the lower frequency within visually scrutinized regions than in the water column. This result is consistent with acoustic scattering theory where zooplankton are in the Rayleigh scattering region at the lower frequencies and thus are less sensitive to detection by the 12 or 18 kHz echo sounders.

When new classification schemes, whether they are subjective or objective, are applied to acoustic data that are used for long-term abundance indices, the effects of that method must be quantified relative to the index. Evaluating the accuracy in situ of acoustic classification or identification algorithms is difficult because of size-selectivity and catchability biases of physical capture gear, spatial and temporal displacement between acoustic sampling and verification sampling, and other limitations in verification methods. For these analyses, the classification method was compared with the standard method of visually scrutinizing echograms. Although this does not directly address the accuracy of the objective method, it does provide a means to quantify the effects of a new classification scheme on a long-term index. For these Atlantic herring surveys, areal backscatter was consistently 5%–10% lower using the multifrequency algorithm presented here than when the data were scrutinized. The cause of this reduction is not known, but it is most likely due to eliminating S_v from scatterers other than swimbladder-bearing fish. It is interesting to note that at the scale of a survey, the cumulative effect of this scattering is small relative to the scattering by swimbladder-bearing fish. The ultimate issue of whether to adjust estimates from prior surveys (in this case decreasing estimates by 5%–10%) or adjust future estimates (increasing estimates by 5%–10%) remains. This choice will be dictated by the confidence in the classification method and the long-term effects on the population assessments and must be made in cooperation with the fisheries managers.

An advantage to objective classification or identification methods is that real-time interpretation can be used to direct sampling. Although the method presented did not entirely succeed at identifying Atlantic herring, it did provide insights to the acoustic landscape. When viewing composite echograms for these surveys, spatial patterns (i.e., color-coded frequency combinations) emerged that were attributable to Atlantic herring, but other patterns were observed, the origins of which can only be speculated on at this time. These patterns could be used to select times, locations, and types of gear to optimally sample the backscatter, which

Fig. 8. Composite echogram of 18, 38, and 120 kHz data collected along a transect conducted during 21 September 2003 (0950–2010 GMT). The transect is oriented north to south (left to right). In the composite echogram, volume backscatter cells are color-coded based on the frequency combinations, where "1", "2", or "3" denotes the presence of 18, 38, or 120 kHz S_v values, and "–" denotes the absence of a frequency. The grey band at the surface designates the upper 10 m of the water column, which was not used in the analyses. The image is vertically distorted to highlight details of the backscattering patterns. The purple "streaks" throughout the water column are 18 kHz noise, most likely caused by cavitation at the transducer. nmi, nautical miles.

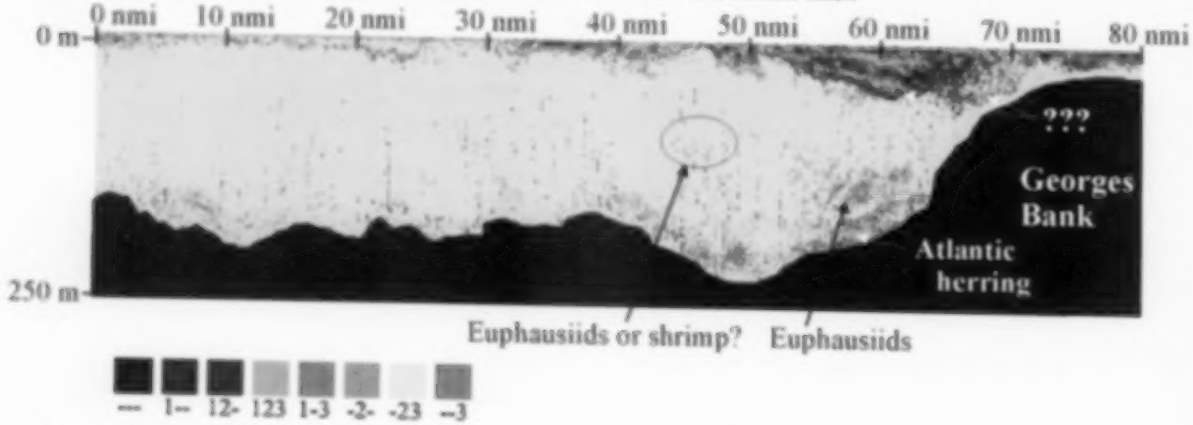

would reduce the uncertainty in acoustic classification and ultimately improve abundance estimates.

Metrics developed to evaluate classification methods may also have utility for monitoring interannual changes in backscatter patterns, which may be indicative of biological or ecosystem changes. A dramatic change in the ratio of 38 kHz backscatter within scrutinized regions to backscatter in the water column was observed in surveys conducted in 2000. During the three surveys conducted in 2000, the level of 38 kHz backscatter was considerably greater in the water column relative to the level of backscatter in scrutinized regions than in the other years. The cause of this change is unknown, but inspection of the echograms during this year showed high backscatter within the top 20 m of the surface, and it is thought that this backscatter may be due to siphonophores or possibly other small gas-bearing fish or organisms. Only a few trawls were directed at this layer and the trawl was not optimized for towing near the surface. However, no Atlantic herring were captured in these tows, and during these surveys, siphonophores were observed on the trawls, as well as on other instrumentation, such as the CTD and video towbody, when they were brought on board. Other interannual changes in backscatter patterns were a decreasing trend in the ratio of water-column 38 kHz s_A from cells where all three frequencies were greater than the S_v threshold to all other s_A and, between 2001 and 2002, a drop in the ratios of 38 kHz s_A within scrutinized regions to s_A in the water column. Again the causes of these changes are unknown but may be indicative of biological changes in this area.

This classification method highlighted spatial distributions of backscatter patterns and changes in these patterns may be indicative of biological changes. For example, a composite echogram using the classification method for a transect conducted during daylight on 21 September 2003 is illustrated in Fig. 8. This transect was oriented north to south and different backscatter patterns are observed along the transect. The primary concentration of Atlantic herring is located at the base of the slope (near the 60 nmi mark). Backscatter represented by red (backscatter dominated by 120 kHz) is believed to be euphausiids (*Euphausia* sp.), and the small yellow (backscatter dominated by 38 and 120 kHz) aggregations (between 40 and 50 nmi marks) are believed to be either shrimp (*Pandalus* sp. or *Penaeus* sp.) or euphausiids. Backscatter patterns observed near the surface were especially interesting where 18 kHz backscatter dominated north of Georges Bank (between 0 and 50 nmi) then changed to backscatter dominated by all three frequencies (between 50 and 65 nmi) and then to backscatter dominated by 38 kHz (between 65 and 80 nmi) over Georges Bank. The organisms or mix of organisms causing these patterns can only be speculated on at this time, but this emphasizes the need for multiple types of sampling gear during acoustic surveys.

This paper presents a classification method and metrics to evaluate the performance of an objective method relative to prior methods. These metrics have the additional benefit of being able to monitor changes in the acoustic landscape, which may be indicative of changes in the ecosystem. As fisheries management moves toward ecosystem-based assessments (e.g., NOAA 2004), the need to measure and monitor multiple species and trophic levels will require objective and timely data processing. Multifrequency acoustics address several data needs for ecosystem-based management such as quantifying the spatial and temporal distributions of living marine resources and measuring multiple size and trophic levels. Objective methods to classify or remotely identify living marine resources and metrics to evaluate these methods, such as those presented here, are needed for producing timely abundance estimates and will lead to an improved understanding of the aquatic environment.

Acknowledgements

The authors thank the numerous scientists and volunteers who have participated on the survey cruises for their dedication to collecting high quality acoustic and biological data.

The authors also thank two anonymous reviewers for their insightful comments. Any use of trade names does not imply endorsement by NOAA. Support for this work was supported in part by the Office of Naval Research.

References

Anderson, V.C. 1950. Sound scattering from a fluid sphere. J. Acoust. Soc. Am. **22**: 426–431.

Cochrane, N.A., Sameoto, D., Herman, A.W., and Neilson, J. 1991. Multiple-frequency acoustic backscattering and zooplankton aggregations in the inner Scotian shelf basins. Can. J. Fish. Aquat. Sci. **48**: 340–355.

Diner, N. 2001. Correction on school geometry and density: approach based on acoustic image simulation. Aquat. Living Resour. **14**: 211–222.

Foote, K.G., Knudsen, H.P., Vestnes, G., MacLennan, D.N., and Simmonds, E.J. 1987. Calibration of acoustic instruments for fish density estimation: a practical guide. ICES Coop. Res. Rep. 44.

Goss, C., Rodhouse, P., Watkins, J.L., and Brierley, A.S. 1998. Attribution of acoustic echoes to squid in the South Atlantic. CCAMLR Science, **5**: 259–271.

Greenlaw, C.F., and Johnson, R.K. 1983. Multiple-frequency acoustical estimation. Biol. Oceanogr. **2**: 227–252.

Haslett, R.W.G. 1965. Acoustic backscattering cross sections of fish at three frequencies and their representation on a universal graph. Br. J. Appl. Phys. **16**: 1143–1150.

Higginbottom, I.R., Pauly, T.J., and Heatley, D.C. 2000. Virtual echograms for visualization and post-processing of multiple-frequency echosounder data. *In* Proceedings of the Fifth European Conference on Underwater Acoustics, ECUA 2000, 10–13 July 2000, Villeurbanne, France. Office for the Official Publications of the European Communities, Luxembourg. pp. 1497–1502.

Holliday, D.V. 1972. Resonance structure in echoes from schooled pelagic fish. J. Acoust. Soc. Am. **51**: 1322–1333.

Holliday, D.V. 1977. Extracting bio-physical information from the acoustic signature of marine organisms. *In* Oceanic sound scattering prediction. *Edited by* N.R. Anderson and B.J. Zahuranec. Plenum Press, New York. pp. 619–624.

Holliday, D.V., and Pieper, R.E. 1995. Bioacoustical oceanography at high frequencies. ICES J. Mar. Sci. **52**: 279–296.

Horne, J.K., and Jech, J.M. 1999. Multi-frequency estimates of fish abundance: constraints of rather high frequencies. ICES J. Mar. Sci. **56**: 184–199.

Kalish, J.H., Greenlaw, C.F., Pearcy, W.G., and Holliday, D.V. 1986. The biological and acoustical structure of sound scattering layers off Oregon. Deep-Sea Res. **33**: 631–653.

Kang, M., Furusawa, M., and Miyashita, K. 2002. Effective and accurate use of difference in mean volume backscattering strength to identify fish and plankton. ICES J. Mar. Sci. **59**: 794–804.

Kirkegaard, E., and Lassen, H. 1990. Mean volume backscattering strength at 38 kHz and 120 kHz and echogram classification. Rapp. P-V. Reun. Cons. Int. Explor. Mer, **189**: 73–81.

Kjærgaard, N., Bjorno, L., Kirkegaard, E., and Lassen, H. 1990. Broadband analysis of acoustical scattering by individual fish. Rapp. P-V. Reun. Cons. Int. Explor. Mer, **189**: 370–380.

Kloser, R.J., Ryan, T., Sakov, P., Williams, A., and Koslow, J.A. 2002. Species identification in deep water using multiple acoustic frequencies. Can. J. Fish. Aquat. Sci. **59**: 1065–1077.

Korneliussen, R.J., and Ona, E. 2002. An operational system for processing and visualizing multi-frequency acoustic data. ICES J. Mar. Sci. **59**: 293–313.

Korneliussen, R.J., and Ona, E. 2003. Synthetic echograms generated from the relative frequency response. ICES J. Mar. Sci. **60**: 636–640.

MacLennan, D.N., and Holliday, D.V. 1996. Fisheries and plankton acoustics: past, present, and future. ICES. J. Mar. Sci. **53**: 513–516.

Madureira, L.S.P., Everson, I., and Murphy, E.J. 1993. Interpretation of acoustic data at two frequencies to discriminate between Antarctic krill (*Euphausia superba* Dana) and other scatterers. J. Plankton Res. **15**: 787–802.

McNaught, D.C. 1969. Developments in acoustic plankton sampling. Proc. Conf. Gt. Lakes Res. **12**: 61–68.

Mitson, R.B., Simard, Y., and Goss, G. 1996. Use of two-frequency algorithm to determine size and abundance in three widely spaced locations. ICES J. Mar. Sci. **53**: 209–215.

NOAA. 2004. Priorities for the 21st century: NOAA Fisheries' Strategic Plan, updated for FY2005–FY2010. US Department of Commerce, National Oceanic and Atmospheric Administration, NMFS, Silver Spring, Maryland.

Reeder, D.B., Jech, J.M., and Stanton, T.K. 2004. Broadband acoustic backscatter and high-resolution morphology of fish: measurement and modeling. J. Acoust. Soc. Am. **116**: 747–761.

Reid, D.G., Fernandes, P.G., Bethke, E., Couperus, A., Goetze, E., Hakansson, N., Pederson, J., et al. 1998. On visual scrutiny of echograms for acoustic stock estimation. ICES CM 1998/B:1.

Sætersdal, G., Stromme, T., Bakken, B., and Piekutowski, L. 1982. Some observations on frequency dependent back scattering strength. *In* Symposium on fisheries acoustics. *Edited by* O. Nakken and S.C. Venema. FAO Fisheries Report No. 300. pp. 150–156.

Simard, Y., and Lavoie, D. 1999. The rich krill aggregation of the Saguenay – St. Lawrence Marine Park: hydroacoustic and geostatistical biomass estimates, structure, variability, and significance for whales. Can. J. Fish. Aquat. Sci. **56**: 1182–1197.

Simmonds, E.J., and Armstrong, F. 1990. A wideband echo sounder: measurements on cod, saithe and herring, and mackerel from 27 to 54 kHz. Rapp. P-V. Reun. Cons. Int. Explor. Mer, **189**: 381–387.

Simmonds, E.J., Armstrong, F., and Copland, P.J. 1996. Species identification using wideband backscatter with neural network and discriminant analysis. ICES J. Mar. Sci. **53**: 189–195.

Swartzman, G., Brodeur, R., Napp, J., Walsh, D., Hewitt, R., Demer, D., Hunt, G., and Logerwell, E. 1999. Relating spatial distributions of acoustically determined patches of fish and plankton: data viewing, image analysis, and spatial proximity. Can. J. Fish. Aquat. Sci. **56**(Suppl. 1): 188–198.

Towler, R.H., Jech, J.M., and Horne, J.K. 2003. Visualizing fish movement, behaviour, and acoustic backscatter. Aquat. Living Resour. **16**: 277–282.

Zakharia, M., and Sessarego, J.P. 1982. Sonar target classification using a coherent echo processing. *In* Proceedings of the IEEE International Conference on Acoustics, Speech and Signal Processing, Vol. 7, 3–5 May 1982, Paris, France. The Institute of Electrical and Electronics Engineers, Inc., Piscataway, N.J. pp. 331–334.

Zakharia, M.E., Magand, F., Hetroit, F., and Diner, N. 1996. Wideband sounder for fish species identification at sea. ICES J. Mar. Sci. **53**: 203–209.

Salinity controls phytoplankton response to nutrient enrichment in the Great Salt Lake, Utah, USA

Amy M. Marcarelli, Wayne A. Wurtsbaugh, and Olivia Griset

Abstract: To examine how salinity and nutrient supply interact to control phytoplankton community composition, nutrient limitation, and dinitrogen (N_2) fixation rates in the Great Salt Lake (Utah, USA), we conducted a series of bioassay experiments with plankton from both Gilbert Bay, where salinities are near 160 $g\cdot L^{-1}$, and Farmington Bay, where salinities range from 10 to 90 $g\cdot L^{-1}$. Six-day nutrient addition bioassay experiments showed that the extant phytoplankton communities in both bays were limited by nitrogen (N). However, in 28- to 30-day factorial bioassay experiments in which both salinities and nutrient supply were manipulated, phosphorus stimulated chlorophyll *a* as much as 500% when salinities were less than 70 $g\cdot L^{-1}$ and N_2-fixing cyanobacteria were present. At salinities greater than 70 $g\cdot L^{-1}$, or with additions of combined N, N_2 fixation ceased. When N_2-fixing cyanobacteria were absent, the plankton community was routinely N-limited regardless of salinity. The results of these experiments suggest that nutrient limitation of phytoplankton communities may change depending on salinity levels, because salinity controls whether N_2-fixing cyanobacteria will be present in the phytoplankton community. Therefore, both salinity and nutrient supply must be considered when making water quality decisions for hypersaline systems such as the Great Salt Lake.

Résumé : Afin d'examiner comment la salinité et l'apport des nutriments contrôlent la composition de la communauté phytoplanctonique, la limitation par les nutriments et la fixation de diazote (N_2) dans le Grand Lac Salé (Utah, É-U.), nous avons mené une série de bioessais avec du plancton provenant de la baie Gilbert où les salinités s'approchent de 160 $g\cdot L^{-1}$ et de la baie Farmington où les salinités varient de 10–90 $g\cdot L^{-1}$. Des bioessais d'addition de nutriments pendant 6 jours montrent que les communautés actuelles de phytoplancton dans les deux baies sont limitées par l'azote (N). Cependant, dans des bioessais factoriels de 28–30 jours, dans lesquels à la fois la salinité et l'apport de nutriments sont manipulés, le phosphore stimule la chlorophylle *a* par autant que 500 %, lorsque les salinités sont inférieures à 70 $g\cdot L^{-1}$ et qu'il y a des cyanobactéries fixatrices de N_2 présentes. Aux salinités supérieures à 70 $g\cdot L^{-1}$ ou après l'addition de N combiné, la fixation de N_2 cesse. Lorsque les cyanobactéries fixatrices de N_2 sont absentes, la communauté planctonique est généralement limitée par N, quelle que soit la salinité. Les résultats de ces expériences indiquent que la limitation des communautés phytoplanctoniques peut changer en fonction des niveaux de salinité, parce que la salinité contrôle la présence des bactéries fixatrices de N_2 dans la communauté phytoplanctonique. C'est pourquoi on doit tenir compte à la fois de la salinité et de l'apport de nutriments lorsque l'on prend des décisions sur la qualité de l'eau dans les systèmes hypersalés tels que le Grand Lac Salé.

[Traduit par la Rédaction]

Introduction

Nitrogen (N) is believed to control primary production in estuaries, coastal oceans (Paerl 1996), and most saline lakes (Javor 1989), whereas phytoplankton growth in fresh waters is thought to be more frequently limited by phosphorus (P). However, many bioassays and whole-lake experiments have shown that N is limiting in lakes and streams as frequently as P (Elser et al. 1990; Francoeur 2001). Schindler (1977) argued that N should never limit production in lakes because dinitrogen (N_2) fixing cyanobacteria should be able to make up N deficits so that P becomes the limiting nutrient. Consequently, the question of N versus P limitation can be restated to ask what factor(s) limit N_2 fixation in aquatic systems (Vitousek and Howarth 1991). Despite its importance, the factors that limit N_2 fixation in both fresh and saline waters are poorly understood (Vitousek et al. 2002). In some saline systems, iron or molybdenum supplies (Howarth and Cole 1985; Evans and Prepas 1997) or zooplankton grazing coupled with low cyanobacterial growth rates (Marino et al. 2002) may be important, but it is unclear how broadly applicable these control mechanisms are. Salinity and P concentrations

Received 5 December 2005. Accepted 21 July 2006. Published on the NRC Research Press Web site at http://cjfas.nrc.ca on 26 September 2006.
J19031

A.M. Marcarelli,[1,2] W.A. Wurtsbaugh, and O. Griset.[3] Department of Aquatic, Watershed and Earth Resources / Ecology Center, Utah State University, Logan, UT 84321-5210, USA.

[1] Corresponding author (e-mail: amy.marcarelli@gmail.com).

[2] Present address: Center for Ecological Research and Department of Biological Sciences, Idaho State University, Pocatello, ID 83209-8007, USA.

[3] Present address: College of Education and Human Development, University of Southern Maine, Gorham, ME 04038, USA.

Can. J. Fish. Aquat. Sci. **63**: 2236–2248 (2006)

doi:10.1139/F06-113

are important control mechanisms on cyanobacterial growth, toxin production, and N_2 fixation in the Baltic Sea and elsewhere (Lehtimäki et al. 1997). Interactions between these different factors may be important for controlling N_2 fixation and cyanobacterial abundance in hypersaline systems such as the Great Salt Lake (Utah, USA).

Previous bioassays have indicated that plankton in the main basin of the Great Salt Lake are N-limited (e.g., Stephens and Gillespie 1976; Wurtsbaugh 1988), but the factor(s) controlling N_2 fixation, and thus perpetuating N limitation, are not understood. In the Baltic Sea, Lehtimäki et al. (1997) found that the same factors (salinity, temperature, light flux, and phosphate concentration) favored both growth and N_2 fixation by one cyanobacterium species. Salinity controls on growth and N_2 fixation by cyanobacteria have been reported by others (Fernandes et al. 1993; Pinckney et al. 1995; but see Moisander et al. 2002), and some argue that increasing the sulfate (SO_4^{2-}) content of the water inhibits molybdenum (Mo) uptake and, consequently, N_2 fixation by cyanobacteria (Howarth and Cole 1985; Marino et al. 2002). However, Wurtsbaugh (1988) found that lowering the ratio of SO_4^{2-} to Mo did not stimulate planktonic growth or N_2 fixation in the Great Salt Lake. Evans and Prepas (1997) argue that high salinities (or alkalinities) inhibit iron uptake and thus restrict N_2 fixation. Recently, Mills et al. (2004) performed bioassay experiments indicating that low iron and P supplies simultaneously limit N_2 fixation in the ocean. Despite these advances, the factor(s) controlling plankton growth and N_2 fixation in hypersaline systems remain elusive.

The Great Salt Lake experiences variable salinity both spatially and temporally as a result of human-constructed causeways and seasonally fluctuating freshwater inputs. Variable salinities, coupled with heavy nutrient loading into one of the bays, provided an opportunity to study how salinity and nutrient supply interact to control phytoplankton nutrient limitation. We conducted laboratory experiments to determine whether N or P control phytoplankton growth and N_2 fixation at a variety of salinities found in the Great Salt Lake. The goal of these experiments was to determine whether nutrient limitation of phytoplankton production changes at different salinities and, therefore, which nutrients should be the focus of management to control eutrophication in the Great Salt Lake.

Materials and methods

Study area

The Great Salt Lake is a 5180 km^2 closed-basin lake in Utah, USA (Fig. 1), and during our study, the mean lake depth was near 5 m. Because of its shallow morphometry, the size of the lake can increase or decrease markedly with climatic fluctuations. The lake has been highly impacted by the construction of causeways that divide the system into three large bays. Gunnison Bay (2520 km^2), located in the northwest area of the lake (Fig. 1), has salt concentrations between 280 and 300 g·L^{-1}. Gilbert Bay (2400 km^2), in the central portion of the lake, has salinities typically between 120 and 180 g·L^{-1} and supports a thriving brine shrimp population. Farmington Bay (260 km^2) is very shallow and the mean depth was <1 m during our study. It is bordered on its eastern and southeastern shores by the greater metropolitan area of Salt Lake City. Farmington Bay receives a large portion of the fresh water flowing into Great Salt Lake via the Jordan River and sewage canals and therefore also receives a large portion of the nutrient loading to the lake. Wetlands at the southern end of the bay intercept and process an undetermined portion of the nutrients, but nutrient loading rates to the bay remain high. Phytoplankton chlorophyll *a* levels in the bay usually exceed 100 µg·L^{-1} and sometimes exceed 500 µg·L^{-1}. Secchi depth transparencies are normally near 0.2 m. Salinity in Farmington Bay is highly variable, ranging from 5 to 100 g·L^{-1} depending on annual climate variations and lake elevation. The phytoplankton community in the Great Salt Lake is highly variable, depending on ambient salinities. At salinities between 5 and 50 g·L^{-1}, the phytoplankton community is sometimes dominated by the N_2-fixing cyanobacteria *Nodularia spumigena*. At higher salinities, the phytoplankton community is a mix of diatom and green algal species, most notably *Dunaliella viridis* (Carter 1971; Rushforth and Felix 1982; Stephens 1990).

Fig. 1. Map of the Great Salt Lake (Utah, USA; see inset) showing the location of the major bays. This study was conducted in Farmington Bay (salinity 10–100 g·L^{-1}) and Gilbert Bay (salinity 150–170 g·L^{-1}). Automobile and railroad causeways separate Farmington Bay and Gunnison Bay, respectively, from Gilbert Bay. Breaches in the west ends of each causeway allow limited bidirectional exchanges of water between the bays. Hatched area indicates the greater Salt Lake City population area. WTP identifies the locations of wastewater treatment plants that discharge directly into Farmington Bay.

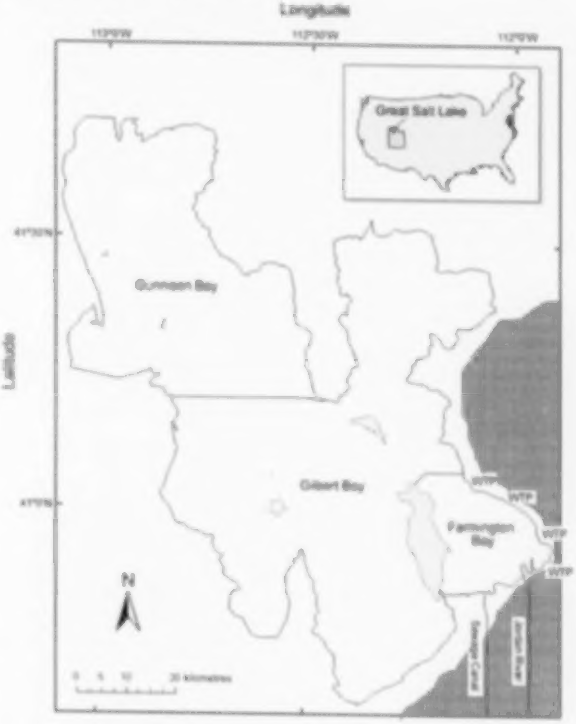

Simple bioassay design

A series of four simple bioassays was conducted to evaluate the extant nutrient status of the phytoplankton communities (Table 1). Water was collected either from the central region of Farmington Bay or from its northern shore in November 2003 when low water levels prevented boat access. Additionally, water was collected in Gilbert Bay on 29 August 2003 to compare nutrient limitation between the two bays of differing salinity. Water was collected with an 8 L horizontal Van Dorn bottle from 0.5 m depth and transported to the laboratory in 10 L polyethylene containers.

In the laboratory, macrozooplankton were removed by filtering through 153 μm netting, and twelve 800 mL aliquots of water were randomly distributed into 900 mL glass jars with plastic lids. Jars were randomly assigned to four treatments with three replicates each: control (C), + nitrogen (N), + phosphorus (P), and + nitrogen + phosphorus (NP). Concentrations added to the treatments were 100 $\mu mol \cdot L^{-1}$ N (as NH_4NO_3) and 6.5 $\mu mol \cdot L^{-1}$ P (as Na_2HPO_4). Jars were then placed randomly in a temperature-controlled incubation room at 20 °C, with light intensities of approximately 150 μmol $photons \cdot s^{-1} \cdot m^{-2}$ and an 18 h light – 6 h dark photoperiod. Experiments lasted 6 days. Jars were agitated twice daily and re-randomized once daily to ensure even irradiance. Each jar was sampled for N_2 fixation and chlorophyll *a* after 3 and 6 days to examine phytoplankton responses to enrichment. Phytoplankton community composition was sampled only after 6 days.

Factorial bioassay design

We conducted four factorial bioassays in which nutrient and salinity levels were manipulated simultaneously (Table 1). Water was collected as above from the same sites. Salinities were manipulated in the source water from a low of 10 $g \cdot L^{-1}$, where cyanobacteria thrive, to 130 $g \cdot L^{-1}$, where we hypothesized that cyanobacteria, and therefore N_2 fixation, would be absent (Table 1). To change salinities, an aliquot of source water was diluted with either deionized water or saline water (made with NaCl and $MgSO_4$ in a 7.8:1 ratio in deionized water) to provide the desired salinities. The same aliquot volume of source water was used in all the salinity treatments of each experiment to ensure that the same initial amount of phytoplankton biomass was present in each nutrient–salinity treatment. These volumes varied between experiments depending on the salinity of the source water, which ranged from 15 to 170 $g \cdot L^{-1}$ (Table 1). Because these salinities varied widely, the proportion of source water placed into each jar also varied widely to achieve the target salinities, i.e., much less 170 $g \cdot L^{-1}$ source water needed to be used than 50 $g \cdot L^{-1}$ source water, if our maximum target salinity was 110 $g \cdot L^{-1}$. In all experiments, the water was filtered in the laboratory through 153 μm netting to remove macrozooplankton, and the aliquots were placed in 900 mL glass jars. Jars were randomly assigned to salinity treatments, and the aliquots were diluted to 800 mL using deionized water or saline water to reach the desired end salinity. Salinity was measured after mixing with a refractometer. Additionally, 2.3 mL of supplementary inocula water from low-salinity sites in Great Salt Lake and surrounding wetlands and from a high-salinity site in Gilbert Bay was added to each jar to insure that a variety of phytoplankton with different salinity

Table 1. Initial conditions and experimental treatments for the simple and factorial bioassays.

Experiment	Type	Source	Date	Source salinity ($g \cdot L^{-1}$)	Source Chl *a* ($\mu g \cdot L^{-1}$)	Source water used (%)	Source N_2 fixation ($\mu g \cdot L^{-1} \cdot h^{-1}$)	Salinity treatments ($g \cdot L^{-1}$)	Nutrient treatments
1	Simple	FB	6 June 2003	53	52.2	100	0.1	na	C, N, P, N+P
2	Simple	FB, GB	29 August 2003	103, 154	85.2, 5.9	100	nm	na	C, N, P, N+P
3	Simple	FB	9 October 2003	104	114.5	100	0.0	na	C, N, P, N+P
4	Simple	FB	4 November 2003	86	166.5	100	0.0	na	C, N, P, N+P
A	Factorial	GB	10 October 2002	84	105	24	nm	30, 60, 130	C, N, P
B	Factorial	FB	3 July 2003	72	11.2	14	0.0	10, 30, 50, 70	C, N, P
C	Factorial	FB	9 October 2003	100	nm	10	0.0	10, 40, 70, 100	C, N, P
D	Factorial	GB	20 October 2004	170	11	17	0.0	30, 50, 70, 90, 110	C, N, P
I	Short-term factorial	FB	19 May 2005	15	200	50	2.0	20, 40, 50, 60, 70, 80, 90	C, P

Note: "Source" indicates whether the initial water used in the experiment was from Farmington Bay (FB) or Gilbert Bay (GB). Nutrient treatments: C, control; N, nitrogen enriched; P, phosphorus enriched; N+P, nitrogen and phosphorus enriched. Chl *a*, chlorophyll *a*; nm, not measured on initial day; na, not applicable.

tolerances were present at the start of the experiment. The jars within each salinity treatment were randomly assigned to three nutrient treatments: control (C), + nitrogen (N), and + phosphorus (P). Each salinity–nutrient combination had three replicates. Jars were enriched with nutrients, incubated, and agitated as described for the simple experiments. The four factorial experiments lasted 28–30 days and were sampled approximately every 7 days for N_2 fixation and chlorophyll *a*. Phytoplankton community composition samples were collected on the final day of the experiment.

A final short-term factorial bioassay experiment (experiment I) was conducted in May 2005, when a large bloom of *N. spumigena* was present in Farmington Bay. The goal of this experiment was to look at salinity tolerance of N_2 fixers present in the bay at that time. We chose to use a large number of salinity treatments for this experiment to allow a finer determination of the salinity at which N_2 fixation ceased (Table 1). Because of the larger number of salinity treatments, we reduced the nutrient treatments to only a control and P enrichment and used only two replicates per salinity–nutrient combination. Experiment I lasted 6 days and was sampled on days 1, 3, and 6 for chlorophyll *a* and N_2 fixation. This experiment was terminated after 6 days because visual observations indicated that the phytoplankton community had changed drastically by day 6 (color change from green to brown; senescence visually obvious).

Sample analysis

On sampling days, 50 mL aliquots of water were collected from each sample jar, placed in a 62 mL glass serum vial, and sealed with a septum for N_2-fixation analysis. N_2 fixation was measured using an acetylene reduction assay (Stewart et al. 1967; Flett et al. 1976). Once in the serum vial, assay samples and standard vials with deionized water were injected with 4 mL of acetylene, agitated for 1 min to evenly mix gas between the water and vapor stages, and incubated for 2 h in the incubation chamber in which the bioassay was conducted. The standard vials were also injected with known concentrations of ethylene so that a standard curve could be constructed. At the end of the incubation, vials were again agitated and gas samples were collected in cleaned, re-evacuated 3 mL Vacutainers®. Ethylene and acetylene in each sample were measured within 2 months using a SRI 8610 gas chromatograph (SRI Instruments, Torrance, Calif.) with a Poropak T column (Waters Associates, Milford, Mass.) and a flame ionization detector. Ethylene concentration was converted to amount of N_2 gas fixed using an assumed 4:1 molar ratio (Postgate 1998).

An index of phytoplankton biomass was estimated using chlorophyll *a* analysis. An aliquot was removed from the serum vial after termination of the acetylene reduction assay and filtered through a 25 mm Millipore AP 40 glass fiber filter with a nominal pore size of 1.0 µm. The filter was wrapped in foil and immediately frozen to prevent sample degradation. Within 30 days of sample collection, filters were extracted in 95% ethanol, and chlorophyll *a* concentration was measured fluorometrically using a nonacidification technique with a Turner 10-AU fluorometer (Turner Designs, Sunnyvale, Calif.; Welschmeyer 1994).

Phytoplankton were collected from one replicate of each treatment at the beginning and end of each experiment. Approximately 40 mL of sample was preserved with 3% Bouin's solution (80% formaldehyde, saturated with picric acid; 20% glacial acetic acid) or with 3% formalin. Phytoplankton cell density was determined by settling in Utermöhl chambers and counting on an inverted Olympus microscope at 1000× (Wetzel and Likens 2000). Phytoplankton were identified to the lowest taxonomic group possible (usually genus or species) using Felix and Rushforth (1979). Length and width measurements were made on 10 individuals of each taxa, and biovolume was calculated using equations from Hillebrand et al. (1999).

Data analysis

Results were analyzed both as simple treatment responses and as responses relative to controls. Percent of control responses were calculated using the following equation:

$$\text{(1)} \qquad \text{percent of control} = [(\text{treatment value} - \text{control value}) / \text{control value}] \times 100$$

All statistical analyses were conducted with SAS (version 8e; SAS Institute Inc. 2000). For the simple bioassays, treatment effects on chlorophyll *a* and N_2 fixation were analyzed statistically using one-way analysis of variance (ANOVA, PROC GLM, factor = nutrient). Results were analyzed for the final day of the experiment, with the exception of experiment 2, where very different responses were observed on day 3 and so both days 3 and 6 were analyzed. Significance was determined using Bonferroni-adjusted *p* values, where α (set at 0.05) was divided by the number of tests ($n = 6$ for simple bioassays; Zar 1999). Biovolume was not analyzed statistically because only one replicate was counted per treatment. Post-hoc Tukey's Studentized range tests were used to compare treatments. Factorial bioassays were analyzed using three-way, repeated-measures ANOVA (PROC MIXED, factors = treatment, salinity, repeated = date) for chlorophyll *a* and N_2 fixation. Five repeated-measures models with different covariance structures were fit to the data sets before selecting the model with the lowest Akaike's information criterion (AIC) value and least parameters. Degrees of freedom (df) were calculated in PROC MIXED using the Kenward–Roger method, which permits decimal df values. When necessary, transformations were applied to the data to meet the ANOVA assumptions that the residuals had a mean and standard deviation of zero and were normally distributed. A range of transformations was applied and the most appropriate for meeting the assumptions was selected, usually log or cube root. Significance was again determined using Bonferroni-adjusted *p* values ($n = 4$ for factorial bioassays; Zar 1999).

Results

Simple bioassays

Similar responses to nutrient additions were obtained in all four simple nutrient addition experiments. For simplicity, the results of experiment 2, where nutrient limitation was measured in both Farmington and Gilbert bays, will first be discussed and then related to results observed in all of the simple bioassays.

In experiment 2, initial chlorophyll *a* concentrations in Farmington Bay water were extremely high (>350 $\mu g \cdot L^{-1}$;

Fig. 2. Chlorophyll *a* concentrations in simple bioassay experiment 2 conducted with water from (*a*) Farmington Bay and (*b*) Gilbert Bay. Note different scales on *y* axes of (*a*) and (*b*). Error bars are ±1 standard error. One-way analysis of variance (see Table 2) indicated significant nutrient effects in Farmington Bay on day 3. In Gilbert Bay, a nutrient effect was significant by day 6. Asterisks (*) indicate treatments that were significantly different than controls as determined by a post-hoc Tukey's Studentized range test. Control, diamonds; nitrogen, squares; phosphorus, triangles; nitrogen + phosphorus, circles.

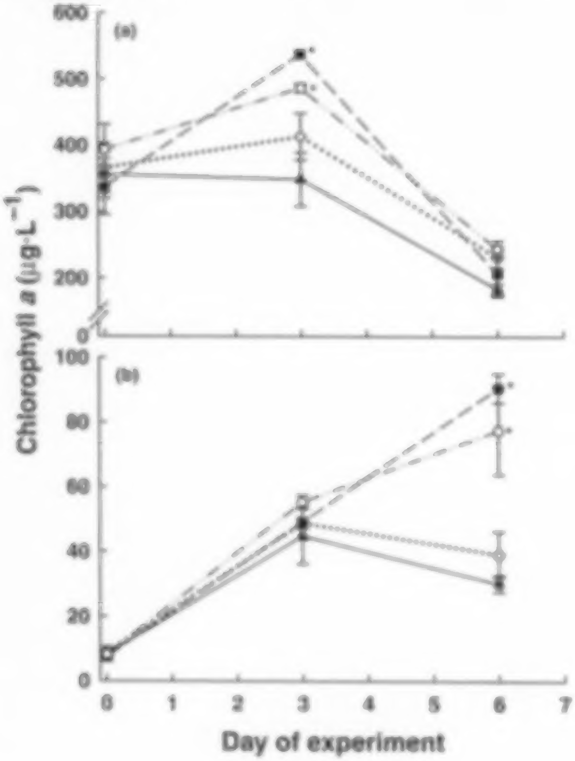

Fig. 2*a*). Nevertheless, chlorophyll *a* increased significantly within 3 days when N or NP was added to the cultures, indicating strong N limitation of the phytoplankton community (Fig. 2*a*; Table 2). However, by day 6 of the experiment, the response had subsided, which was unusual among all of the short-term bioassays (Table 2). In Gilbert Bay, initial chlorophyll *a* levels were much lower than in Farmington Bay, but a significant response to N and NP was also evident after 6 days (Fig. 2*b*; Table 2).

Table 2. One-way analysis of variance values (*F* ratios with degrees of freedom (df) and *p* values) testing the effects of nutrient additions (factor) in the simple bioassay experiments on chlorophyll *a* (µg·L^{-1}) and nitrogen fixation (µg·L^{-1}·h^{-1}).

		Chlorophyll *a*		Nitrogen fixation	
Experiment	Day	$F_{[df]}$	*p*	$F_{[df]}$	*p*
1	6	$175.0_{[3,8]}$	**<0.01**	$7.3_{[3,8]}$	**<0.01**[a]
2 Farmington	3	$9.3_{[3,8]}$	**<0.01**	$2.0_{[3,8]}$	0.19
	6	$1.9_{[3,8]}$	0.21	$0.8_{[3,6]}$	0.56
2 Gilbert	3	$0.7_{[3,8]}$	0.6	$2.3_{[3,8]}$	0.16
	6	$14.4_{[3,8]}$	**<0.01**	$1.2_{[3,8]}$	0.38
3	6	$119.1_{[3,8]}$	**<0.01**	ND	ND
4	6	$67.1_{[3,8]}$	**<0.01**	$1.0_{[3,8]}$	0.44

Note: Bold type indicates Bonferroni-adjusted significance, $p < 0.008$. ND indicates that *F* ratio and *p* value could not be determined because every value was zero for all treatments and replicates.

[a] Although this was significant, the nitrogen-fixation rates here were actually very low and near the detection limit of the measurement technique.

Fig. 3. Phytoplankton biovolume on day 6 in simple bioassay experiment 2 conducted with water from both Farmington Bay and Gilbert Bay. C, control; N, + nitrogen; P, + phosphorus; NP, + nitrogen + phosphorus. Diatoms, open bars; green algae, hatched bars; cyanobacteria, solid bars; chrysophytes, shaded bars.

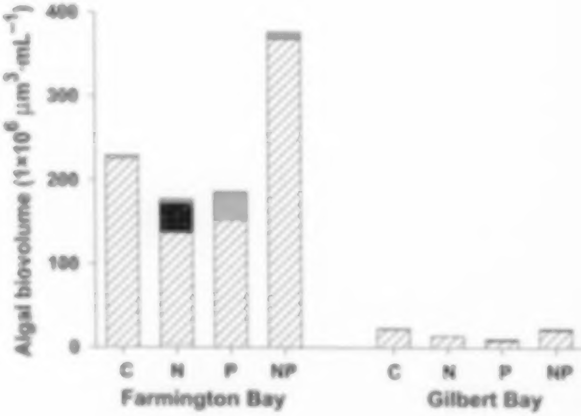

Responses of phytoplankton biovolume to nutrients were not as striking as the responses of chlorophyll *a* during experiment 2. In treatments utilizing Farmington Bay water, the greatest biovolume was observed in the NP treatments and was dominated by the chlorophyte *Carteria* sp., with additional biovolume contributed by *Dunaliella salina*, *D. viridis*, and *Oocystis* sp. (Fig. 3). The N treatment stimulated the cyanobacterium *Microcoleus* sp. In contrast, little difference in biovolume was observed between the treatments in Gilbert Bay, all of which were dominated by the small *D. viridis* (Fig. 3).

When the results from all of the simple bioassays are compared, it is clear that N and NP treatments routinely stimulated chlorophyll *a* (Fig. 4*a*). In every experiment except experiment 2, N limitation was strongly indicated by chlorophyll *a* responses on day 6 (Fig. 4*a*). Low, negative responses in chlorophyll *a* were usually observed in P treatments, although these differences were never significant. Generally, phytoplankton biovolume decreased relative to controls, except for small positive or negative responses in the NP treatments (Fig. 4*b*). N_2 fixation showed very small and usually insignificant responses (Table 2) to nutrient additions in the simple bioassay experiments, and rates were routinely near or below the level of detection of the acetylene reduction assay used (Fig. 4*c*). The lack of N_2-fixation

Fig. 4. Summary of responses of phytoplankton to nutrient additions in all experiments on day 6 in the simple bioassays. Responses are reported as percent responses above mean control levels for (*a*) chlorophyll *a*, (*b*) total phytoplankton biovolume, and (*c*) nitrogen fixation. Zero (0) indicates no difference from the response of control treatments. Missing bars indicate that no comparison was possible because of lack of either control or nutrient treatment. Treatments were + nitrogen (N, solid bars), + phosphorus (P, open bars), + nitrogen + phosphorus (NP, hatched bars). Experiment numbers (Table 1) shown are, from left to right, 1, 2 Farmington Bay, 2 Gilbert Bay, 3, and 4. An asterisk (*) indicates the treatment response was significantly different from the control value in (*a*) and (*c*). Significance was assessed using a one-way analysis of variance for nutrient treatment followed by a post-hoc Tukey's Studentized range test; test statistics are shown in Table 2. No replicates were analyzed for biovolume measurements shown in (*b*), so treatments could not be compared statistically.

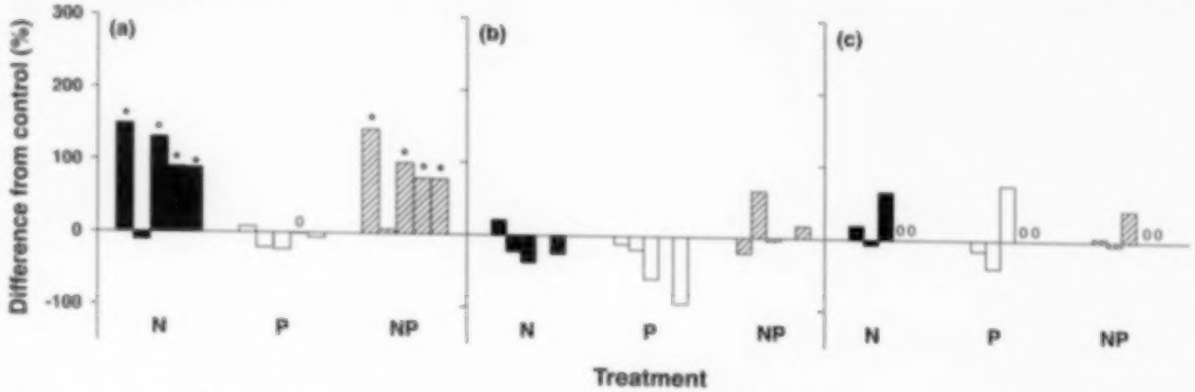

responses in these short-term assays was expected, given that few, if any, N_2-fixing taxa were present (e.g., Fig. 3).

Factorial bioassays

Very different results were obtained between the four long-term factorial bioassay experiments. Again for simplicity we will first discuss the results of a single experiment (experiment B), where we observed interesting responses to nutrient and salinity treatments, and then relate these to results from all the factorial bioassays.

In experiment B, there were short-term responses to N additions, but in the long-term, the plankton responded primarily to P additions (Fig. 5*a*; Appendix A). In the lowest salinity (10 g·L^{-1}) treatments, there were only small responses of chlorophyll *a* to the nutrient treatments (Fig. 5*a*). N stimulated chlorophyll *a* production after 9 days only in the 70 g·L^{-1} salinity treatment (Fig. 5*d*). However, after 30 days, P stimulated chlorophyll *a* above control treatments in the 30, 50, and 70 g·L^{-1} salinity treatments (Figs. 5*b*–5*d*). A three-way repeated-measures ANOVA indicated a significant three-way interaction between salinity, nutrient, and day of experiment for chlorophyll *a* (Table 3).

N_2-fixation rates in this experiment were initially near zero, but rates increased both in the controls and particularly in P treatments during the long incubation (Figs. 5*e*–5*h*). In the controls, N_2-fixation rates increased most in the 10 and 30 g·L^{-1} treatments (Figs. 5*e*, 5*f*), with limited increases at 50 and 70 g·L^{-1}. At 10 g·L^{-1} salinity, peak N_2-fixation rates in the P treatment were observed by day 15 (Fig. 5*e*), but at higher salinities, the peak was delayed to day 23 (30 and 50 g·L^{-1}; Figs. 5*e* and 5*g*) or day 30 (70 g·L^{-1}; Fig. 5*h*). The relatively high N_2-fixation rate on day 30 in the + P, 70 g·L^{-1} salinity treatment was due to a high rate in only one of the three replicates. A three-way repeated-measures ANOVA indicated a significant three-way interaction between salinity, nutrient, and day of experiment for N_2 fixation (Table 3). Cyanobacteria comprised 60%–80% of the phytoplankton biovolume in P treatments at all salinities on day 30 of the experiment (Fig. 6). *Nodularia spumigena*, a N_2-fixing taxon with heterocytes, was the dominant cyanobacteria. N additions suppressed N_2 fixation (Figs. 5*e*–5*h*) and cyanobacterial abundances (Fig. 6). When N_2-fixation rates are normalized to the biomass of cyanobacteria on day 30 of the experiment, P stimulated N_2 fixation of cyanobacteria 98% above control levels, whereas N suppressed N_2 fixation 100% below control levels.

Salinity exerted an important control on N_2 fixation in all of the factorial experiments. When maximum N_2-fixation rate measurements from the control and P treatments from all factorial experiments are combined, the results, although variable, indicate that maximum N_2-fixation rates were relatively independent of salinity between 10 and 70 g·L^{-1}. However, little or no N_2 fixation was observed at salinities greater than 70 g·L^{-1} (Fig. 7). In all four experiments, repeated-measures ANOVA indicated a significant three-way interaction between salinity, nutrient supply, and day that controlled both N_2 fixation and chlorophyll *a* (Table 3). However, examining the mean N_2-fixation rates from the experiments showed that the stimulatory response to P additions at low salinities observed in factorial experiment B was rare. Very small increases in N_2 fixation due to P addition were observed on day 28 in experiment A, days 14 and 21 in experiment C, and day 28 in experiment D (Appendix A). However, these increases only translated into a stimulation of chlorophyll *a* production by P in three salinity treatments in the first two experiments (experiment A, day 28, 30 g·L^{-1}; experiment B, days 23 and 30, 30 and 50 g·L^{-1}; Appendix A). These increases were all concurrent with a response of N_2 fixation to P. However, in a majority of the salinity treatments less than 70 g·L^{-1}, there was no stimulation of N_2 fixation by P, and N limitation of chlorophyll *a* was routinely observed. In

Fig. 5. (*a*–*d*) Chlorophyll *a* and (*e*–*h*) nitrogen-fixation responses of plankton from Farmington Bay grown in four salinities (*a* and *e*, 10 g·L^{-1}; *b* and *f*, 30 g·L^{-1}; *c* and *g*, 50 g·L^{-1}; *d* and *h*, 70 g·L^{-1}) to N or P additions during factorial experiment B. Note the delays in peak nitrogen-fixation rates with increasing salinities. Error bars are ±1 standard error. Control, diamonds; nitrogen, squares; phosphorus, triangles. A three-way repeated-measures analysis of variance indicated a significant three-way interaction between nutrient, salinity, and date; test statistics are shown in Table 3.

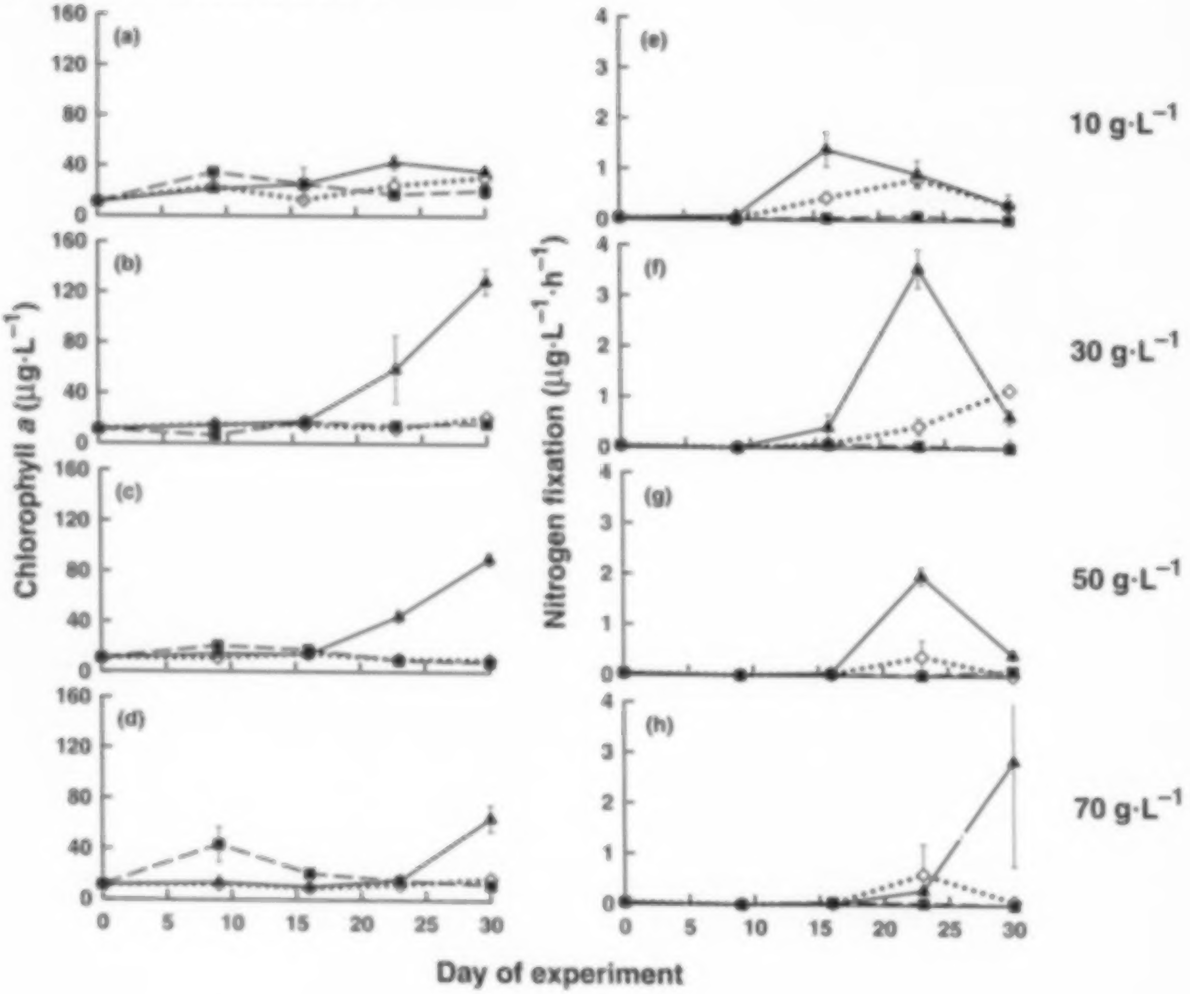

each of these instances, there were no cyanobacteria with heterocytes observed at the end of the experiment, indicating that N_2 fixation could not occur to facilitate the switch from N to P limitation because of the lack of N_2-fixing taxa. At salinities greater than 70 g·L^{-1}, strong limitation of chlorophyll *a* by N was uniformly noted, with no stimulation of chlorophyll *a* by P in any instance (Appendix A).

In the short-term factorial experiment I, salinity exerted a very clear effect on both chlorophyll *a* and N_2 fixation (Fig. 8). In this experiment, there was no significant difference in chlorophyll *a* and N_2-fixation rates between the control and P treatments, indicated by repeated-measures three-way ANOVA (Fig. 8). Chlorophyll *a* concentrations decreased in the salinity treatments greater than 50 g·L^{-1} through the duration of the experiment, while increasing in salinity treatments less than 50 g·L^{-1} (Fig. 8*a*). N_2 fixation ceased at salinities greater than 60 g·L^{-1} on all days of the study, but continued at high rates at 20 and 40 g·L^{-1} salinities (Fig. 8*b*).

Discussion

Nutrient effects on phytoplankton growth

Both the short-term bioassays and high salinity treatments in the factorial bioassays demonstrated that the extant phytoplankton populations in Farmington Bay and Gilbert Bay were typically N-limited. N limitation has been found in previous studies of Great Salt Lake phytoplankton. Stephens and Gillespie (1976) found that densities of *D. viridis* increased in response to N additions but not to P additions in laboratory cultures of Gilbert Bay water (salinity 135 g·L^{-1}). Porcella and Holman (1972) also found a positive response of *Dunaliella* sp. to N and not to P when salinity in Gilbert

Table 3. Statistics (*F* ratios with degrees of freedom (df) and *p* values) for the factorial experiments.

Factor	Chlorophyll *a* $F_{[df]}$	Chlorophyll *a* p	Nitrogen fixation $F_{[df]}$	Nitrogen fixation p
Experiment A				
Nut	$49.0_{[2,19.6]}$	**<0.01**	$7.3_{[2,18]}$	**<0.01**
S	$2.4_{[2,19.6]}$	0.12	$33.6_{[2,18]}$	**<0.01**
D	$22.2_{[3,22]}$	**<0.01**	$10.0_{[1,18]}$	**<0.01**
Nut × S	$8.8_{[4,19.6]}$	**<0.01**	$8.6_{[4,18]}$	**<0.01**
D × Nut	$17.9_{[6,27.2]}$	**<0.01**	$15.5_{[2,18]}$	**<0.01**
D × S	$13.3_{[6,27.2]}$	**<0.01**	$5.0_{[2,18]}$	0.02
D × Nut × S	$3.2_{[12,31.5]}$	**<0.01**	$19.9_{[4,18]}$	**<0.01**
Experiment B				
Nut	$69.2_{[2,25.3]}$	**<0.01**	$118.8_{[2,31]}$	**<0.01**
S	$4.2_{[2,25.3]}$	0.02	$19.7_{[4,37]}$	**<0.01**
D	$50.1_{[3,44]}$	**<0.01**	$120.8_{[4,14.6]}$	**<0.01**
Nut × S	$10.6_{[6,25.3]}$	**<0.01**	$5.3_{[6,31.2]}$	**<0.01**
D × Nut	$61.0_{[6,50.1]}$	**<0.01**	$13.5_{[6,49.7]}$	**<0.01**
D × S	$8.6_{[9,52.0]}$	**<0.01**	$7.0_{[9,52.2]}$	**<0.01**
D × Nut × S	$6.9_{[18,54.1]}$	**<0.01**	$6.6_{[17,52.2]}$	**<0.01**
Experiment C				
Nut	$119.8_{[2,24.7]}$	**<0.01**	$37.4_{[2,18.4]}$	**<0.01**
S	$10.0_{[3,24.7]}$	**<0.01**	$88.7_{[3,18.4]}$	**<0.01**
D	$138.1_{[4,51.9]}$	**<0.01**	$6.6_{[3,19.3]}$	**<0.01**
Nut × S	$4.8_{[6,24.6]}$	**<0.01**	$25.4_{[6,18.2]}$	**<0.01**
D × Nut	$33.0_{[8,61.7]}$	**<0.01**	$10.1_{[6,24.8]}$	**<0.01**
D × S	$5.9_{[12,66.2]}$	**<0.01**	$5.0_{[9,28.2]}$	**<0.01**
D × Nut × S	$4.3_{[24,69.2]}$	**<0.01**	$7.0_{[18,32.1]}$	**<0.01**
Experiment D				
Nut	$449.2_{[2,31.9]}$	**<0.01**	$1.5_{[2,32.2]}$	0.24
S	$38.6_{[4,31.8]}$	**<0.01**	$8.8_{[4,32]}$	**<0.01**
D	$107.4_{[3,35.6]}$	**<0.01**	$23.3_{[3,45.9]}$	**<0.01**
Nut × S	$30.2_{[8,31.8]}$	**<0.01**	$1.1_{[8,31.9]}$	0.36
D × Nut	$131.0_{[6,44.4]}$	**<0.01**	$2.8_{[6,52.1]}$	0.02
D × S	$105.6_{[12,52.0]}$	**<0.01**	$13.1_{[12,50]}$	**<0.01**
D × Nut × S	$27.5_{[24,56.5]}$	**<0.01**	$2.4_{[23,56.0]}$	**<0.01**

Note: Analyses were three-way repeated-measures analysis of variance (factors = nutrient (Nut), salinity (S), and date (D)). Bold type indicates Bonferroni-adjusted significance, $p < 0.0125$. The two response variables measured were chlorophyll *a* (μg·L^{-1}) and nitrogen fixation (μg·L^{-1}·h^{-1}).

Bay was near 160 g·L^{-1}. Wurtsbaugh (1988) tested Gilbert Bay water during high water years (1985–1986) when salinities were 50 g·L^{-1} and found that chlorophyll *a* concentrations responded significantly to N additions, but only marginally to P additions in 8-day bioassays. Moreover, Javor's review (1989) of the literature on saline lakes indicates that phytoplankton production in most saline lakes is N-limited.

The phytoplankton in our experiments always responded to N additions within 3–8 days by incrementing chlorophyll *a* levels, often as much as 150%–250% above controls. Phytoplankton biovolume did not, however, respond consistently to the nutrient additions in the simple or factorial bioassays. A linear regression between biovolume and chlorophyll *a* from factorial bioassay treatments where both were collected revealed a significant but weak relationship (r^2 = 0.16, $F_{[1,37]} = 6.5$, $p = 0.02$, chlorophyll *a* μg·L^{-1} = 3.1×10^{-6} × (biovolume μm^3·mL^{-1}) + 9.2). This response has been described in other similar experiments in lake and stream ecosystems (e.g., Greenwood and Rosemond 2005). This response could result in an increased capacity to capture sunlight and, in turn, increase photosynthesis in light-limited

Fig. 6. Phytoplankton biovolume on day 30 of factorial experiment B at salinities of 10, 30, 50, and 70 g·L^{-1}. Note higher biovolume of cyanobacteria in the control and P treatments, particularly at low salinities. C, control; N, + nitrogen; P, + phosphorus. Diatoms, open bars; green algae, hatched bars; cyanobacteria, solid bars; chrysophytes, shaded bars.

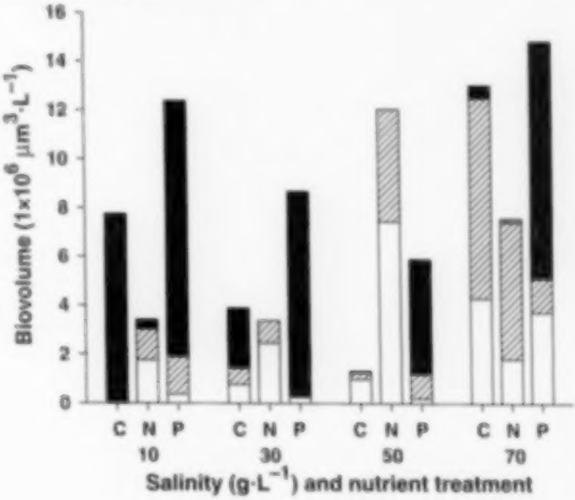

Fig. 7. Maximum nitrogen-fixation rates observed in relation to treatment salinities for all factorial experiments in the control (solid circles) and phosphorus (open circles) treatments. Maximum nitrogen-fixation rates showed no clear relationship with salinity from 10 to 70 g·L^{-1}, but declined to near zero at salinities greater than 70 g·L^{-1}. Maximum nitrogen-fixation rates occurred on different days in the different experiments. Note log scale on the y axis.

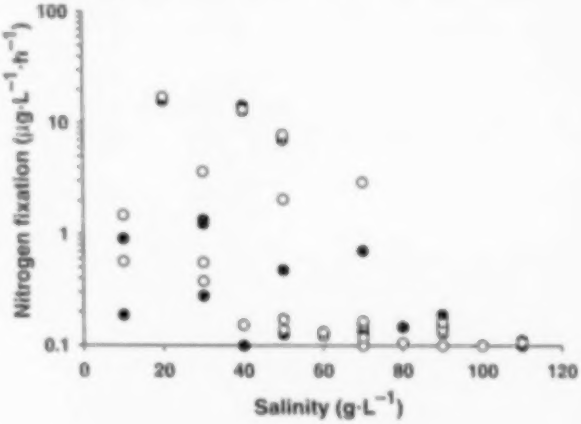

Fig. 8. (*a*) Chlorophyll *a* and (*b*) nitrogen-fixation results from short-term factorial experiment I on the three sampling dates of the experiment. Note (*i*) how nitrogen fixation peaks later at higher salinities and (*ii*) how nitrogen fixation ceases on all days at greater than 60 g·L^{-1} salinity. Error bars are ±1 standard error. A three-way repeated-measures analysis of variance showed significant interactions between date and salinity on chlorophyll *a* ($F_{[12,27.6]}$ = 92.8, $p < 0.01$) and on nitrogen fixation ($F_{[12,18.4]}$ = 18.4, $p < 0.01$). There was no significant individual or interaction effect of nutrient treatment for either response, so results from the control and phosphorus treatments were combined for this figure. Day 1, diamonds; day 3, squares; day 6, triangles.

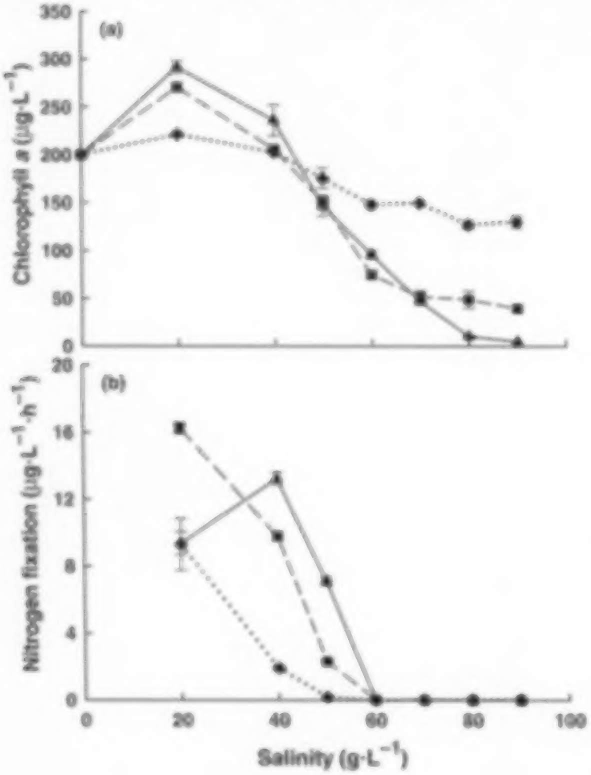

situations. However, increasing chlorophyll *a* per cell could also be a response to shading, either because our experimental light intensities were moderate or because of shading differences within each treatment. Chlorophyll *a* – biovolume ratios did not show a clear pattern related to treatment. However, without biovolume estimates from all sampling dates, it was difficult to uncover relationships using this ratio.

Fig. 9. Generalized relationship between phosphorus and salinity identifying domains where nitrogen fixation can or cannot occur in the Great Salt Lake, causing nutrient limitation of the phytoplankton community to vary between nitrogen and phosphorus limitation.

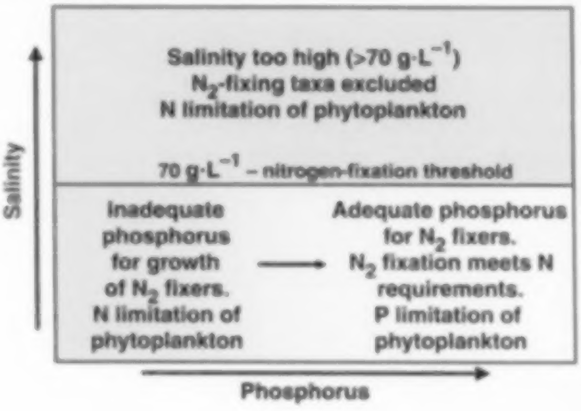
Salinity too high (>70 g·L⁻¹)
N₂-fixing taxa excluded
N limitation of phytoplankton
70 g·L⁻¹ – nitrogen-fixation threshold
Inadequate phosphorus for growth of N₂ fixers. N limitation of phytoplankton
Adequate phosphorus for N₂ fixers. N₂ fixation meets N requirements. P limitation of phytoplankton
Salinity
Phosphorus

In most of the short-term bioassay experiments that have been conducted with Great Salt Lake water, P additions actually decrease phytoplankton abundances. A decrease in chlorophyll *a* and biovolume occurred as a result of P addition in our short-term bioassays, and it was also reported in those of Stephens and Gillespie (1976) and Porcella and Holman (1972), but not in the assays of Wurtsbaugh (1988). This decrease could be due to competition between phytoplankton and heterotrophic bacteria for P, as the latter are superior competitors for this nutrient (Brussaard and Riegman 1998). The increased bacterial populations might then compete with phytoplankton populations for some other limiting nutrient, such as N. Although this mechanism has not been demonstrated in the Great Salt Lake, the potential that it may occur reminds us that the phytoplankton open-water community is a diverse, interacting assemblage of microbes and metazoans, and complex responses to experiments may be driven by these often ignored interactions.

Effects of salinity on N_2 fixation and N_2-fixing cyanobacteria

Salinity exerted an important control on N_2 fixation in the long-term experiments and sometimes interacted with P to control N_2 fixation. Our results generally showed that N_2 fixation could occur up to salinities of 50–70 g·L^{-1}. These salinities were higher than levels found by Lehtimäki et al. (1997) and Mazur-Marzec et al. (2005) that restricted growth, N_2 fixation, and hepatotoxin production of Baltic Sea *N. spumigena* (<30 g·L^{-1}). Pinckney et al. (1995) found that decreasing salinity from 90 to 45 g·L^{-1} significantly increased N_2-fixation rates in a microbial mat dominated by *Microcoleus chthonoplastes*, which lacked heterocytes, and rates were increased approximately 75% by P addition to cultures held in the dark. Herbst (1998) found that the N_2 fixation by a benthic periphyton community from Mono Lake was decreased by nearly 50% when salinities increased from 50 to 100 g·L^{-1}, and rates were reduced by 90% at 150 g·L^{-1} salinity. Dubinin et al. (1992) reported N_2 fixation by *M. chthonoplastes* in salinities up to 150 g·L^{-1}, but in those experiments, the organism was grown at 60 g·L^{-1} salinity and only exposed to the higher test salinities for 6 h. Camacho and de Wit (2003) also noted P stimulation of N_2 fixation in *M. chthonoplastes* communities at 80 g·L^{-1} salinity. However, they indicate that N_2 fixation was more likely carried out by heterotrophic bacteria in the biofilm because *M. chthonoplastes* does not contain nitrogenase. It is also possible that low-salinity and anoxic microzones in biofilms allow N_2 fixation at salinities higher than those possible in the homogenous water column. In our experiments, biofilms sometimes developed in the bottom of the incubation jars towards the end of the long-term experiments, but because we did not assay these communities, it is impossible to determine whether N_2 fixation was occurring in these mats. All of these results indicate that increasing salinity dramatically depresses N_2-fixation rates in a variety of environments and are consistent with the responses to salinity observed in our experiment.

Salinity likely limits the survival and distribution of cyanobacteria in hypersaline lakes. A monitoring study of a salinity gradient in Farmington Bay in 1971 (Carter 1971) indicated that *Nodularia* sp. was usually not abundant in areas where salinities were greater than 70 $g \cdot L^{-1}$ but was abundant at lower salinities. Stephens (1990) noted that *N. spumigena* appeared in Gilbert Bay of the Great Salt Lake when salinities decreased to 60 $g \cdot L^{-1}$ during the mid-1980s. It is possible, however, that *N. spumigena* was primarily found in Farmington Bay and had advected into Gilbert Bay. A mesocosm study in Mono Lake examined the community composition of benthic periphyton mats at five salinity levels between 50 and 150 $g \cdot L^{-1}$. The filamentous cyanobacteria *Oscillatoria* sp. only occurred in salinity treatments between 50 and 100 $g \cdot L^{-1}$, and no other cyanobacteria species were present at any salinity (Herbst and Blinn 1998).

Hypersaline conditions are stressful for all organisms because of the coupled effects of osmotic stress and ionic stress resulting from high concentrations of ions. Mackay et al. (1983) demonstrated that cyanobacteria that live in saline environments (both marine and hypersaline) have the ability to synthesize osmoregulatory compounds that permit growth in saline solutions. These compounds inhibit Na^+ influx into cells, in turn allowing cyanobacteria to tolerate saline conditions (Apte et al. 1987). More recent work has shown that N_2-fixing cyanobacteria are more susceptible to ionic stress than to osmotic stress, and *Anabaena* species will cease N_2 fixation and decrease growth by 50% within 5 days of exposure to salinity stress (Fernandes et al. 1993). This suggests that the salinity effects we see on N_2 fixation in Farmington Bay are likely a combination of salinity stress leading to (*i*) decreased N_2-fixation rates and (*ii*) decreased growth and (or) death of N_2-fixing cyanobacteria.

Salinity and nutrient interactions in Farmington Bay

The compiled results of all our factorial bioassay experiments suggest that given the salinities normally observed in Farmington Bay (<70 $g \cdot L^{-1}$), P can stimulate growth and N_2-fixation rates of cyanobacteria, indicating that the phytoplankton community there is P-limited (Fig. 9). In our experiments, this stimulation by P was certainly due to increased growth of cyanobacteria, but not always due to increased N_2-fixation rates per cyanobacterial cell. When N_2-fixation rates are normalized for cell biovolume, they range from 40% lower to 100% greater in P treatments than in the controls at salinities of <70 $g \cdot L^{-1}$. During droughts when lake elevations drop, salinities can rise above 70 $g \cdot L^{-1}$ in Farmington Bay, and in Gilbert Bay, salinities are almost always above 70 $g \cdot L^{-1}$. At salinities greater than 70 $g \cdot L^{-1}$, the phytoplankton community would remain N-limited, regardless of the P concentrations, because N_2-fixing taxa are excluded from the phytoplankton community (Fig. 9). This has clearly been illustrated in our experiments, where N limitation is always observed at salinities greater than or equal to 70 $g \cdot L^{-1}$, and cyanobacteria are usually absent from the phytoplankton community. If nutrients were to be controlled to reduce eutrophication in Farmington Bay, the expected salinity levels would thus need to be incorporated into the decision process. At low salinities (approximately <70 $g \cdot L^{-1}$), P may need to be controlled. At higher salinities, N control would be appropriate (Fig. 9).

It should also be noted from our results that P limitation of phytoplankton communities was not always observed at low salinities, because cyanobacteria were not always present in our low-salinity treatments. It is possible that this occurred because in some of the assays there may not have been sufficient N_2-fixing cyanobacteria available in the initial water or in the inocula added. Although we added plankton from a variety of salinities, it was not always possible to find waters of intermediate salinities that could contain salt-tolerant N_2-fixing species such as *N. spumegina*. It is also possible that appropriate organisms were present in the inocula, but that N_2 fixation and (or) cyanobacterial growth was limited by factors other than P, such as trace elements (Howarth and Cole 1985; Evans and Prepas 1997), grazing (Marino et al. 2002), temperature (McQueen and Lean 1987; Marcarelli and Wurtsbaugh 2006), and light (Lewis and Levine 1984).

Light limitation of N_2 fixation may be particularly important in Farmington Bay because light penetration is low as a result of eutrophic conditions. Therefore, photosynthesis by cyanobacteria may be light-limited, leading to a lack of energy to carry out the energetically expensive N_2-fixation reaction (Lewis and Levine 1984). Some cyanobacterial taxa are adapted to low-light conditions. However, *N. spumegina*, at least in the Baltic Sea, prefer greater irradiances (45–155 $\mu mol\ photons \cdot s^{-1} \cdot m^{-2}$) than other cyanobacteria taxa (Lehtimäki et al. 1997). In Farmington Bay, this light intensity only penetrated, on average, to 0.5 m in the water column during the summer of 2005, suggesting that growth and N_2 fixation of *N. spumegina* would have been light-limited in approximately 50% of the water column. However, on several occasions in 2005 we observed floating surface scums of *N. spumegina*, suggesting that this taxa may be able to outcompete other phytoplankton taxa for light, leading to a further growth advantage in Farmington Bay under low-salinity conditions.

Laboratory bioassays also have limitations, and field experiments are needed to unequivocally determine nutrient limitation in Farmington and Gilbert bays. Laboratory assays impart controlled conditions on the microbial communities, thus simplifying environmental variables and the interpretation of results. However, these assays also modify the environment so that experimental artifacts could occur. For example, we removed macrozooplankton (primarily brine shrimp) from the assays, but we did not remove microzooplankton. Consequently, grazing and nutrient recycling by zooplankton was not the same in the assays as in the lake, and this could alter the response to nutrients. Additionally, the jar experiments we used do not evaluate nutrient cycling between the benthic sediments and the water column, which can have important implications for the relative balance of N and P limitation in lakes (Levine and Schindler 1992). Consequently, to determine whether nutrient control is an appropriate management strategy for Farmington Bay, field experiments in limnocorrals or shore-based mesocosms should be used to study nutrient limitation under more natural conditions.

In conclusion, our laboratory experiments showed that under the high-salinity conditions typical in the Great Salt Lake, N limited phytoplankton growth, as has been suggested by previous researchers. However, when salinities were $<70\ g{\cdot}L^{-1}$, the N_2-fixing *N. spumegina* can join the phytoplankton community, leading to high rates of N_2 fixation and shifts of the phytoplankton community from N to P limitation. If nutrients were to be controlled to reduce eutrophication in Farmington Bay, the expected salinity levels would thus need to be incorporated into the decision process. This knowledge is particularly relevant as interest in improving water quality in the Great Salt Lake is currently growing, and potential management plans may examine scenarios such as breaching causeways to increase water, salt, and nutrient circulation. Interactions between these factors, including salinity and nutrient supply, will increase the difficulty associated with predicting the impacts of different management approaches. To that end, our experiments may help predict the interacting impacts of salinity and nutrient supply on eutrophic conditions in hypersaline systems, including the Great Salt Lake.

Acknowledgements

Invaluable field and lab assistance was provided by D. Gross, P. Brown, K. Goodman, M. Kanaga, and L. Quantz. Funding for the project was provided by the Utah Department of Water Quality, the Central Davis Sewer District, and the Community/University Research Initiative (CURI) program at Utah State University. This paper was greatly improved by the comments of two anonymous reviewers.

References

Apte, S.K., Reddy, B.R., and Thomas, J. 1987. Relationship between sodium influx and salt tolerance of nitrogen-fixing cyanobacteria. Appl. Environ. Microbiol. **53**(8): 1934–1939.

Brussaard, C.P.D., and Riegman, R. 1998. Influence of bacteria on phytoplankton cell mortality with phosphorus or nitrogen as the algal-growth-limiting nutrient. Aquat. Microb. Ecol. **14**(3): 271–280.

Camacho, A., and de Wit, R. 2003. Effect of nitrogen and phosphorus additions on a benthic microbial mat from a hypersaline lake. Aquat. Microb. Ecol. **32**(3): 261–273.

Carter, C.K. 1971. Some ecological considerations of the Farmington Bay estuary and adjacent Great Salt Lake Park. University of Utah, Salt Lake City, Utah.

Dubinin, A.V., Gerasimenko, L.M., and Zavarzin, G.A. 1992. Nitrogen-fixation by cyanobacterium *Microcoleus chthonoplastes* from hypersaline lagoons of Lake Sivash. Microbiology, **61**(5): 593–597.

Elser, J.J., Marzolf, E.R., and Goldman, C.R. 1990. Phosphorus and nitrogen limitation in the freshwaters of North America: a review and critique of experimental enrichments. Can. J. Fish. Aquat. Sci. **47**(7): 1468–1477.

Evans, J.C., and Prepas, E.E. 1997. Relative importance of iron and molybdenum in restricting phytoplankton biomass in high phosphorus saline lakes. Limnol. Oceanogr. **42**(3): 461–472.

Felix, E.A., and Rushforth, S.R. 1979. The algal flora of the Great Salt Lake, Utah, U.S.A. Nova Hedwigia, **31**: 163–195.

Fernandes, T.A., Iyer, V., and Apte, K. 1993. Differential responses of nitrogen-fixing cyanobacteria to salinity and osmotic stresses. Appl. Environ. Microbiol. **59**(3): 899–904.

Flett, R.J., Hamilton, R.D., and Campbell, N.E.R. 1976. Aquatic acetylene-reduction techniques: solutions to several problems. Can. J. Microbiol. **22**(1): 43–51.

Francoeur, S.N. 2001. Meta-analysis of lotic nutrient amendment experiments: detecting and quantifying subtle differences. J. North Am. Benthol. Soc. **20**(3): 358–368.

Greenwood, J.L., and Rosemond, A.D. 2005. Periphyton response to long-term nutrient enrichment in a shaded headwater stream. Can. J. Fish. Aquat. Sci. **62**(9): 2033–2045.

Herbst, D.B. 1998. Potential salinity limitations on nitrogen fixation in sediments from Mono Lake, California. Int. J. Salt Lake Res. **7**: 261–274.

Herbst, D.B., and Blinn, D.W. 1998. Experimental mesocosm studies of salinity effects on the benthic algal community of a saline lake. J. Phycol. **34**(5): 772–778.

Hillebrand, H., Durselen, C.D., Kirschtel, D., Pollingher, U., and Zohary, T. 1999. Biovolume calculation for pelagic and benthic microalgae. J. Phycol. **35**(2): 403–424.

Howarth, R.W., and Cole, J.J. 1985. Molybdenum availability, nitrogen limitation, and phytoplankton growth in natural waters. Science (Washington, D.C.), **229**(4714): 653–655.

Javor, B. 1989. Hypersaline environments. Springer-Verlag, Berlin, Germany.

Lehtimäki, J., Moisander, P., Sivonen, K., and Kononen, K. 1997. Growth, nitrogen fixation, and nodularin production by two Baltic Sea cyanobacteria. Appl. Environ. Microbiol. **63**(5): 1647–1656.

Levine, S.N., and Schindler, D.W. 1992. Modification of the N–P ratio in lakes by in situ processes. Limnol. Oceanogr. **37**(5): 917–935.

Lewis, W.M., Jr., and Levine, S.N. 1984. The light response of nitrogen fixation in Lake Valencia, Venezuela. Limnol. Oceanogr. **29**(4): 894–900.

Mackay, M.A., Norton, R.S., and Borowitzka, L.J. 1983. Marine blue-green algae have a unique osmoregulatory system. Mar. Biol. **73**: 301–307.

Marcarelli, A.M., and Wurtsbaugh, W.A. 2006. Temperature and nutrient supply interact to control nitrogen fixation in oligotrophic streams: an experimental examination. Limnol. Oceanogr. **51**(5): 2278–2289.

Marino, R., Chan, F., Howarth, R.W., Pace, M., and Likens, G.E. 2002. Ecological and biogeochemical interactions constrain planktonic nitrogen fixation in estuaries. Ecosystems, **5**(7): 719–725.

Mazur-Marzec, H., Zeglinska, L., and Plinski., M. 2005. The effect of salinity on the growth, toxin production, and morphology of *Nodularia spumigena* isolated from the Gulf of Gdansk, southern Baltic Sea. J. Appl. Phycol. **17**(2): 171–179.

McQueen, D.J., and Lean, D.R.S. 1987. Influence of water temperature and nitrogen to phosphorus ratios on the dominance of blue-green algae in Lake St. George, Ontario. Can. J. Fish. Aquat. Sci. **44**(3): 598–604.

Mills, M.M., Ridame, C., Davey, M., La Roche, J., and Geider, R.J. 2004. Iron and phosphorus co-limit nitrogen fixation in the eastern tropical North Atlantic. Nature (London), **429**(7039): 292–294.

Moisander, P.H., McClinton, E., and Paerl, H.W. 2002. Salinity effects on growth, photosynthetic parameters, and nitrogenase activity in estuarine planktonic cyanobacteria. Microb. Ecol. **43**(4): 432–442.

Paerl, H.W. 1996. A comparison of cyanobacterial bloom dynamics in freshwater, estuarine and marine environments. Phycologia, **35**(Suppl. 6): 25–35.

Pinckney, J., Paerl, H.W., and Bebout, B.M. 1995. Salinity control of benthic microbial mat community production in a Bahamian hypersaline lagoon. J. Exp. Mar. Biol. Ecol. **187**(2): 223–237.

Porcella, D.B., and Holman, J.A. 1972. Nutrients, algal growth, and culture of brine shrimp in the southern Great Salt Lake. *In* The Great Salt Lake and Utah's water resources. *Edited by* J.P. Riley. Utah Water Research Laboratory, Logan, Utah. pp. 142–155.

Postgate, J.R. 1998. The fundamentals of nitrogen fixation. 3rd ed. Cambridge University Press, Cambridge, UK.

Rushforth, S.R., and Felix, E.A. 1982. Biotic adjustments to changing salinities in the Great Salt Lake, Utah, USA. Microb. Ecol. **8**:157–161.

SAS Institute Inc. 2000. SAS [computer software]. Version 8e. SAS Institute Inc., Cary, North Carolina.

Schindler, D. 1977. Evolution of phosphorus limitation in lakes. Science (Washington, D.C.), **195**(4275): 260–262.

Stephens, D.W. 1990. Changes in lake levels, salinity and the biological community of Great Salt Lake (Utah, USA), 1847–1987. Hydrobiologia, **197**(1): 139–146.

Stephens, D.W., and Gillespie, D.M. 1976. Phytoplankton production in the Great Salt Lake, Utah, and a laboratory study of algal response to enrichment. Limnol. Oceanogr. **21**(1): 74–87.

Stewart, W.D.P., Fitzgerald, G.P., and Burris, H.R. 1967. *In situ* studies on N-fixation using the acetylene reduction technique. Proc. Nat. Acad. Sci. U.S.A. **58**(5): 2071–2078.

Vitousek, P.M., and Howarth, R.W. 1991. Nitrogen limitation on land and in the sea: how can it occur? Biogeochemistry, **13**: 87–115.

Vitousek, P.M., Cassman, K., Cleveland, C., Crews, T., Field, C.B., Grimm, N.B., Howarth, R.W., Marino, R., Martinelli, L., Rastetter, E.B., and Sprent, J.I. 2002. Towards an ecological understanding of biological nitrogen fixation. Biogeochemistry, **57**(1): 1–45.

Welschmeyer, N.A. 1994. Fluorometric analysis of chlorophyll *a* in the presence of chlorophyll *b* and phaeopigments. Limnol. Oceanogr. **39**(8): 1985–1992.

Wetzel, R.G., and Likens, G.E. 2000. Limnological analyses. 3rd ed. Springer, New York.

Wurtsbaugh, W.A. 1988. Iron, molybdenum and phosphorus limitation of N_2 fixation maintains nitrogen deficiency of plankton in the Great Salt Lake drainage (Utah, USA). Verh. Int. Ver. Limnol. **23**: 121–130.

Zar, J.H. 1999. Biostatistical Analysis. 4th ed. Prentice Hall, Upper Saddle River, New Jersey.

Appendix A

Table A1. Responses of chlorophyll *a* and nitrogen fixation to nutrient and salinity treatments on each sampling date in the four factorial bioassay experiments.

Day of experiment	Salinity ($g \cdot L^{-1}$)	Nitrogen fixation ($\mu g \cdot L^{-1} \cdot h^{-1}$)			Chlorophyll *a* ($\mu g \cdot L^{-1}$)		
		Control	+ Nitrogen	+ Phosphorus	Control	+ Nitrogen	+ Phosphorus
Experiment A							
6	30	nm	nm	nm	9.3 (0.9, 3)	7.1 (0.5, 3)	8.7 (0.8, 3)
	60	nm	nm	nm	7.0 (1.0, 3)	4.3 (0.0, 3)	3.2 (1.6, 3)
	130	nm	nm	nm	1.5 (0.3, 3)	1.2 (0.3, 3)	0.7 (0.0, 3)
14	30	0.0 (0.0, 3)	0.0 (0.0, 3)	0.0 (0.0, 3)	5.8 (1.1, 3)	19.4 (4.7, 3)	5.0 (1.7, 3)
	60	0.0 (0.0, 3)	0.0 (0.0, 3)	0.0 (0.0, 3)	6.5 (1.6, 3)	20.5 (2.5, 3)	7.8 (0.5, 3)
	130	0.0 (0.0, 3)	0.0 (0.0, 3)	0.0 (0.0, 3)	7.8 (0.7, 3)	33.4 (6.4, 3)	5.0 (0.1, 3)
21	30	nm	nm	nm	3.9 (0.1, 3)	12.1 (0.9, 3)	6.8 (1.2, 3)
	60	nm	nm	nm	4.2 (0.4, 3)	8.1 (0.9, 3)	4.5 (1.0, 3)
	130	nm	nm	nm	5.3 (0.5, 3)	23.9 (3.3, 3)	4.8 (0.1, 3)
28	30	0.0 (0.0, 3)	0.0 (0.0, 3)	0.1 (0.0, 3)	4.6 (0.4, 3)	11.2 (1.8, 3)	15.8 (3.5, 3)
	60	0.0 (0.0, 3)	0.0 (0.0, 3)	0.0 (0.0, 3)	6.7 (0.4, 3)	8.2 (1.5, 3)	6.1 (1.0, 3)
	130	0.0 (0.0, 3)	0.0 (0.1, 3)	0.0 (0.0, 3)	4.0 (0.4, 3)	13.9 (1.1, 3)	3.9 (0.1, 3)
Experiment B							
9	10	0.0 (0.0, 3)	0.0 (0.0, 3)	0.1 (0.0, 3)	23.2 (2.0, 3)	34.4 (3.7, 3)	21.1 (0.2, 3)
	30	0.0 (0.0, 2)	0.0 (0.0, 2)	0.0 (0.0, 2)	15.0 (0.9, 3)	6.3 (0.6, 3)	14.2 (0.1, 3)
	50	0.0 (0.0, 2)	0.0 (0.0, 2)	0.0 (0.0, 2)	11.3 (1.6, 3)	20.8 (0.3, 3)	14.5 (0.9, 3)
	70	0.0 (0.0, 3)	0.0 (0.0, 3)	0.0 (0.0, 3)	12.1 (0.0, 3)	43.3 (13.7, 3)	13.3 (0.2, 3)
16	10	0.4 (0.0, 3)	0.0 (0.0, 3)	1.4 (0.3, 3)	12.7 (1.3, 3)	25.1 (12.9, 3)	25.1 (4.4, 3)
	30	0.1 (0.0, 3)	0.1 (0.0, 3)	0.4 (0.3, 3)	14.8 (0.9, 3)	16.9 (1.6, 3)	17.7 (2.8, 3)
	50	0.0 (0.0, 3)	0.0 (0.0, 3)	0.1 (0.0, 3)	14.8 (0.2, 3)	17.9 (0.7, 3)	14.3 (0.4, 3)
	70	0.0 (0.0, 3)	0.0 (0.0, 3)	0.0 (0.0, 3)	9.3 (0.1, 3)	20.5 (0.9, 3)	10.0 (0.7, 3)
23	10	0.8 (0.1, 3)	0.1 (0.0, 3)	0.9 (0.3, 3)	24.2 (6.5, 3)	17.0 (3.1, 3)	42.4 (5.5, 3)
	30	0.4 (0.2, 3)	0.0 (0.0, 3)	3.5 (0.4, 3)	11.9 (1.7, 3)	14.3 (0.5, 3)	58.9 (26.5, 3)
	50	0.4 (0.3, 3)	0.0 (0.0, 3)	2.0 (0.2, 3)	10.4 (0.3, 3)	9.6 (0.4, 3)	44.4 (4.6, 3)
	70	0.6 (0.6, 3)	0.0 (0.0, 3)	0.3 (0.1, 3)	12.0 (0.6, 3)	15.0 (0.1, 3)	15.5 (0.7, 3)
30	10	0.3 (0.1, 3)	0.0 (0.0, 3)	0.3 (0.2, 3)	30.7 (2.2, 3)	20.2 (5.2, 3)	35.4 (2.8, 3)
	30	1.1 (0.0, 3)	0.0 (0.0, 3)	0.6 (0.1, 3)	21.1 (2.9, 3)	16.1 (1.1, 3)	129 (10.1, 3)

Table A1 *(concluded).*

Day of experiment	Salinity ($g \cdot L^{-1}$)	Nitrogen fixation ($\mu g \cdot L^{-1} \cdot h^{-1}$)			Chlorophyll *a* ($\mu g \cdot L^{-1}$)		
		Control	+ Nitrogen	+ Phosphorus	Control	+ Nitrogen	+ Phosphorus
	50	0.0 (0.0, 3)	0.1 (0.1, 3)	0.4 (0.1, 3)	10.1 (0.1, 3)	8.3 (1.1, 3)	90.0 (4.8, 3)
	70	0.1 (0.0, 3)	0.0 (0.0, 3)	2.8 (2.1, 3)	17.0 (1.5, 3)	12.1 (0.3, 3)	64.6 (10.3, 3)
Experiment C							
7	10	0.1 (0.0, 3)	0.0 (0.0, 3)	0.0 (0.0, 3)	39.4 (5.8, 3)	91.8 (6.3, 3)	29.9 (2.3, 2)
	40	0.0 (0.0, 3)	0.0 (0.0, 3)	0.0 (0.0, 3)	21.9 (10.8, 3)	62.5 (1.1, 3)	39.4 (3.3, 4)
	70	0.0 (0.0, 3)	0.0 (0.0, 3)	0.0 (0.0, 3)	28.2 (0.2, 3)	82.1 (1.7, 3)	30.7 (1.4, 3)
	100	0.0 (0.0, 3)	0.0 (0.0, 3)	0.0 (0.0, 3)	20.4 (0.9, 3)	70.7 (2.5, 3)	16.9 (1.9, 3)
14	10	0.1 (0.0, 3)	0.0 (0.0, 3)	0.2 (0.1, 3)	29.8 (7.1, 3)	38.4 (2.2, 3)	26.7 (11.8, 2)
	40	0.0 (0.0, 3)	0.0 (0.0, 3)	0.0 (0.0, 3)	11.8 (2.4, 3)	29.9 (5.5, 3)	20.5 (3.5, 4)
	70	0.0 (0.0, 3)	0.0 (0.0, 3)	0.0 (0.0, 3)	16.6 (0.8, 3)	64.8 (0.5, 3)	16.3 (1.0, 3)
	100	0.0 (0.0, 3)	0.0 (0.0, 3)	0.0 (0.0, 3)	18.1 (1.6, 3)	62.4 (3.5, 3)	15.3 (1.7, 3)
21	10	0.0 (0.0, 3)	0.0 (0.0, 3)	0.5 (0.3, 3)	15.5 (1.2, 3)	37.6 (3.3, 3)	16.6 (0.4, 2)
	40	0.0 (0.0, 3)	0.0 (0.0, 3)	0.0 (0.0, 2)	7.6 (1.8, 3)	15.7 (1.9, 3)	11.7 (0.2, 3)
	70	0.0 (0.0, 3)	0.0 (0.0, 3)	0.0 (0.0, 2)	8.1 (3.4, 3)	36.9 (4.8, 3)	7.2 (2.0, 3)
	100	0.0 (0.0, 3)	0.0 (0.0, 3)	0.0 (0.0, 3)	7.9 (0.6, 3)	35.2 (3.6, 3)	8.8 (0.4, 3)
28	10	0.0 (0.0, 3)	0.0 (0.0, 2)	0.0 (0.0, 3)	17.7 (1.6, 3)	42.2 (5.4, 3)	19.5 (5.5, 2)
	40	0.0 (0.0, 3)	0.0 (0.0, 2)	0.1 (0.1, 3)	7.7 (1.0, 3)	13.4 (1.6, 3)	11.3 (1.5, 4)
	70	0.0 (0.0, 2)	0.0 (0.0, 3)	0.0 (0.0, 3)	9.1 (0.8, 3)	15.7 (2.9, 3)	12.3 (0.8, 3)
	100	0.0 (0.0, 3)	0.0 (0.0, 3)	0.0 (0.0, 3)	7.4 (0.3, 3)	15.3 (4.6, 3)	6.0 (0.6, 3)
Experiment D							
8	30	0.0 (0.0, 3)	0.4 (0.4, 3)	0.0 (0.0, 3)	54.8 (4.8, 3)	59.0 (1.8, 3)	54.1 (2.7, 3)
	50	0.0 (0.0, 3)	0.0 (0.0, 3)	0.0 (0.0, 3)	50.3 (2.4, 3)	78.6 (2.8, 3)	46.9 (2.4, 3)
	70	0.0 (0.0, 3)	0.1 (0.1, 3)	0.0 (0.0, 3)	18.6 (0.2, 3)	20.3 (1.2, 3)	16.7 (0.1, 3)
	90	0.0 (0.0, 3)	0.0 (0.0, 3)	0.0 (0.0, 3)	6.3 (0.7, 3)	6.5 (1.6, 3)	5.0 (0.1, 3)
	110	0.0 (0.0, 3)	0.0 (0.0, 3)	0.0 (0.0, 3)	11.8 (0.4, 3)	13.7 (0.2, 3)	13.5 (0.7, 3)
16	30	0.1 (0.0, 3)	0.1 (0.0, 3)	0.1 (0.0, 3)	22.5 (1.2, 3)	22.9 (2.2, 3)	20.9 (0.9, 3)
	50	0.0 (0.0, 3)	0.0 (0.0, 3)	0.0 (0.0, 3)	27.4 (1.6, 3)	150 (4.6, 3)	30.2 (0.6, 3)
	70	0.0 (0.0, 3)	0.0 (0.0, 3)	0.0 (0.0, 3)	35.8 (1.8, 3)	152 (2.7, 3)	36.7 (1.2, 3)
	90	0.0 (0.0, 3)	0.0 (0.0, 3)	0.0 (0.0, 3)	25.2 (2.7, 3)	89.8 (6.4, 3)	21.2 (3.8, 3)
	110	0.0 (0.0, 3)	0.0 (0.0, 3)	0.0 (0.0, 3)	18.7 (1.9, 3)	50.2 (8.1, 3)	15.0 (1.5, 3)
24	30	0.0 (–, 1)	0.0 (0.0, 2)	0.0 (0.0, 2)	9.7 (2.0, 3)	11.0 (2.8, 3)	10.2 (0.6, 3)
	50	0.0 (0.0, 2)	0.0 (0.0, 2)	0.0 (0.0, 3)	17.4 (1.2, 3)	60.6 (1.4, 3)	19.1 (0.1, 3)
	70	0.1 (0.1, 2)	0.0 (0.0, 2)	0.0 (0.0, 3)	24.0 (2.5, 3)	127 (3.5, 3)	28.7 (0.7, 3)
	90	0.0 (0.0, 3)	0.0 (0.0, 2)	– (–, –)	21.9 (1.4, 3)	106 (14.0, 3)	14.7 (1.0, 3)
	110	0.7 (0.5, 2)	0.0 (0.0, 3)	0.0 (0.0, 2)	15.5 (2.8, 3)	97.6 (5.8, 3)	15.7 (0.6, 3)
28	30	0.2 (0.0, 3)	0.2 (0.0, 3)	0.3 (0.1, 3)	10.2 (1.0, 3)	12.6 (2.2, 3)	13.3 (0.6, 3)
	50	0.0 (0.0, 3)	0.0 (0.0, 3)	0.0 (0.0, 3)	17.2 (0.9, 3)	35.3 (1.7, 3)	13.9 (0.6, 3)
	70	0.0 (0.0, 3)	0.0 (0.0, 3)	0.0 (0.0, 3)	17.9 (2.7, 3)	93.5 (5.7, 3)	23.5 (1.9, 3)
	90	0.0 (0.0, 3)	0.0 (0.0, 3)	0.0 (0.0, 3)	16.0 (1.7, 3)	107 (15.3, 3)	12.0 (0.4, 3)
	110	0.0 (0.0, 3)	0.0 (0.0, 3)	0.0 (0.0, 3)	12.1 (2.8, 3)	80.0 (15.3, 3)	14.2 (1.4, 3)

Note: Mean values are shown, followed in parentheses by standard error (left) and *n* (right). "nm" indicates that a parameter was not measured on that experiment date; –, missing data or that standard error could not be calculated because of lack of replicates.

The fisheries management implications of maternal-age-dependent larval survival

Michael R. O'Farrell and Louis W. Botsford

Abstract: A common goal of conventional fisheries management is to maintain fishing mortality at a rate that ensures an adequate level of lifetime egg production (LEP) for population sustainability. However, larvae from young spawners can experience higher mortality rates than larvae of older spawners, reducing the effect of egg production by young females (hereafter, maternal age effects). This reduction leads to an error in LEP that can be accounted for by reducing the fishing mortality rate, but raises the question of the magnitude of these errors if they are present but not accounted for. Calculations using parameters from a typical long-lived fish demonstrated that maternal age effects resulted in large errors in estimates of lifetime reproduction when there was a large contrast in the larval mortality rate extending over the reproductive life span. Errors were small when maternal age effects reduced the reproductive potential of only the very youngest spawners, at ages when a small fraction of females are mature. A specific example using the empirically derived maternal age effect for black rockfish (*Sebastes melanops*) indicated that errors in traditional management would be small for this species.

Résumé : Un objectif généralement poursuivi par la gestion conventionnelle des pêches est le maintien de la mortalité due à la pêche à un taux qui permette un niveau de production d'oeufs pendant la vie entière (LEP) suffisant pour le maintien de la population. Cependant, les larves nées des jeunes reproducteurs peuvent encourir une mortalité supérieure à celle des larves issues des reproducteurs plus âgés, ce qui réduit l'effet de la production d'oeufs par les jeunes femelles (ci-après, les effets de l'âge maternel). Cette réduction entraine une erreur dans LEP qui peut être corrigée en réduisant le taux de mortalité due à la pêche; cependant si ces erreurs existent mais ne sont pas prises en considération, il reste la question de leur importance. Des calculs faits à partir des paramètres d'un poisson typique à forte longévité démontrent que les effets de l'âge maternel causent d'importantes erreurs dans les estimations de la reproduction au cours de la vie entière lorsqu'il y a de fortes différences dans la mortalité larvaire au cours de l'ensemble de la vie reproductive. Les erreurs sont faibles lorsque les effets de l'âge maternel réduisent le potentiel reproductif de seulement les tout jeunes reproducteurs, aux âges où seulement une petite fraction des femelles sont matures. Un exemple précis utilisant l'effet de l'âge maternel obtenu de façon empirique chez le sébaste noir (*Sebastes melanops*) indique que, chez cette espèce, les erreurs seraient faibles dans le cadre d'une gestion traditionnelle.

[Traduit par la Rédaction]

Introduction

In a recent paper, Berkeley et al. (2004*a*) demonstrated that the time for 50% mortality of unfed, experimentally reared black rockfish (*Sebastes melanops*) larvae was longer for progeny of older females relative to the youngest spawners. These results have led several investigators to suggest that the truncation of a population's age distribution may have more severe consequences for the sustainability of fish populations than previously understood, requiring management by marine reserves or size limits that reduce mortality on large fish (Berkeley et al. 2004*b*; Palumbi 2004; Birkeland and Dayton 2005). Fisheries biologists account for sustainability by estimating and attempting to maintain the ability of individuals in a population to replace themselves through reproduction (Sissenwine and Shepherd 1987; Myers and Mertz 1998). The metric generally used to set the target fishing mortality rate (F) is lifetime egg production (LEP), the number of eggs produced by a female over the course of her lifetime. Yet there is accumulating evidence that egg and larval survival rates are not always homogeneous, but rather may depend on maternal factors (e.g., Hislop 1988; Trippel 1997; Berkeley et al. 2004*a*). Ignorance of maternal effects on egg or larval survival could lead to lower levels of per-recruit reproduction than predicted when using the LEP metric to set target levels of F.

The most common goal of conventional fisheries management is to recommend a level of F that simultaneously pro-

Received 21 November 2005. Accepted 27 March 2006. Published on the NRC Research Press Web site at http://cjfas.nrc.ca on 27 September 2006.
J19013

M.R. O'Farrell[1,2] and L.W. Botsford. Department of Wildlife, Fish and Conservation Biology, University of California, 1 Shields Avenue, Davis, CA 95616, USA.

[1] Corresponding author (e-mail: michael.ofarrell@noaa.gov).

[2] Present address: National Oceanic and Atmospheric Administration (NOAA), National Marine Fisheries Service, Santa Cruz Laboratory, Southwest Fisheries Science Center, 110 Shaffer Road, Santa Cruz, CA 95060, USA.

Can. J. Fish. Aquat. Sci. 63: 2249–2258 (2006) doi:10.1139/F06-130

duces a near-maximum sustainable yield and allows the population to maintain a healthy level of spawning stock biomass (SSB). To attain this goal, the level of *F* that reduces the fraction of unfished LEP (FLEP, analogous to the spawning potential ratio (SPR)) to a specific level is chosen. Generally, levels of FLEP used to set target values of *F* have been estimated to range from 30% to 60%, depending on the resiliency of the stock (Clark 1991; Mace and Sissenwine 1993; Dorn 2002). These calculations account for a population's age structure and the age dependence of egg production, yet they typically assume that all eggs have an equal chance of producing future progeny. The results of Berkeley et al. (2004*a*) and others indicate that this assumption may not be true because of a dependence of heterogeneous egg and larval survival on maternal age. When such maternal age effects are known to exist, they can be accounted for in conventional fisheries management by lowering *F* so that the desired level of the fraction of unfished lifetime reproduction is attained.

Laboratory experiments suggest that Atlantic cod (*Gadus morhua*) experience heterogeneous survival of eggs and larvae as a result of maternal age and spawning experience (Marteinsdottir and Steinarsson 1998; Trippel 1998), and the management implications have been investigated (Murawski et al. 2001). The models, parameterized with typical cod estimates, demonstrated that ignorance of maternal effects could result in a recommended *F* that was too high to preserve the desired levels of reproduction per recruit. While this may be the case for cod, it is not clear how severe the fisheries implications of maternal age effects can be for other stocks. There remains a need to assess the general severity of this problem for fisheries management by describing the consequences of various possible forms of maternal-age-dependent survival from the egg stage.

Here we evaluate how well conventional methods of fisheries management represent the fishery-induced decline in a population's reproductive potential when maternal age effects are present. We consider various plausible forms of maternal-age-dependent larval mortality, in a model using life history parameters typical of a long-lived fish, to evaluate the magnitude of errors that could occur if managers were ignorant of the maternal age effect. We then provide a specific example using the life history traits, fishery characteristics, and maternal age effects for black rockfish from Oregon and California, USA.

Materials and methods

Maternal-age-dependent larval mortality

Berkeley et al. (2004*a*) demonstrated in the laboratory that larvae born of older females survived longer in unfed conditions than larvae born of younger females. The mechanism apparently responsible for this result is a greater volume of the oil globule, hence a greater source of endogenous energy, for progeny of older females. In the highly variable marine environment, the ability to wait for suitable prey to become available for exogenous feeding can have a large effect on larval survival (Blaxter and Hempel 1963; Kamler 1992). The results of Berkeley et al. (2004*a*) suggest that older females will produce larvae having greater average survival than the larvae of young females.

To describe the time to 50% mortality for unfed black rockfish larvae that were the progeny of mothers aged 5–17, Berkeley et al. (2004*a*) fit a nonlinear relationship to their data. Using this relationship, we calculated the instantaneous, maternal-age-dependent larval mortality rate (Z_a) that would result in this pattern of mortality (Berkeley et al. 2004*a*):

$$(1) \qquad d_{50} = -15.23 + 28.79(1 - e^{-0.23a})$$

where d_{50} is the number of days for 50% of larvae, produced by mothers of age *a*, to die. To obtain the equivalent value of Z_a that would lead to the relationship in eq. 1, we assumed exponential decline from an initial larval abundance $N(0)$ on the day of hatching to abundance $N(t)$ on day *t*:

$$(2) \qquad \frac{N(t)}{N(0)} = e^{-Z_a(d_{50})}$$

Setting $N(t)/N(0) = 0.50$ to represent 50% mortality, substituting eq. 1 into eq. 2, and solving for Z_a produces the black rockfish maternal age effect:

$$(3) \qquad Z_a = -\frac{\ln(0.5)}{13.56 - 28.79\,e^{-0.23a}}$$

This maternal age function results in declining larval mortality rate with increasing maternal age to an asymptotic minimum (Fig. 1*a*).

The specific form of eq. 3 depends on the choice of functions Berkeley et al. (2004*a*) used to fit to their data, but the data in Berkeley et al. (2004*a*) suggest that Z_a declines approximately exponentially from a high value to a low value. To explore other assumptions of how larval mortality rates vary with maternal age, we specified a family of exponentially declining larval mortality rate functions similar in form to eq. 3. As in eq. 3, larvae of young mothers experience mortality rates greater than the asymptotic rate, which we assumed to be the normal larval mortality rate (Z_n) of the population (i.e., the rate at which all larvae would die if maternal age dependence did not exist). Anticipated, similar larval mortality rate functions could vary in two fundamental ways: (*i*) variability in the rate at which the larval mortality rate approaches Z_n with increasing maternal age and (*ii*) variability in the multiple by which the larval mortality rate exceeds Z_n for larvae of young mothers. We characterized the decline in Z_a from its maximum, $Z_{\max}$, to Z_n as $e^{(-a/A)}$, where *A* is termed the age constant and represents the number of years for Z_a to decline by a factor of 1/*e*. We allowed *A* to vary in our analyses from 1 year (a rapid approach to Z_n) to 10 years (a slow approach to Z_n) (Fig. 1*b*). Contrast (*C*) is the multiple by which larval mortality rates are increased from Z_n for larvae of the youngest spawning females: $C = Z_{\max}/Z_n$. In the analyses that follow, we allowed *C* to vary from 3 to 15 and assume that $Z_{\max}$ is the larval mortality rate for the progeny of 5-year-old females. The larval mortality rate at each maternal age was then computed with the following expression:

$$(4) \qquad \frac{Z_a}{Z_n} = 1 + (C - 1)\,e^{-(a-5)/A}$$

Fig. 1. (*a*) The relationship between maternal age and instantaneous larval mortality rate (Z_a), calculated for black rockfish (*Sebastes melanops*). (*b*) The general relationship between maternal age and Z_a used for analyses in the hypothetical population, demonstrating three values of the age constant (A) and a contrast (C) level of 8. Z_n is the normal, asymptotic, larval mortality rate. Solid line, $A = 1$; circles, $A = 5$; squares, $A = 10$.

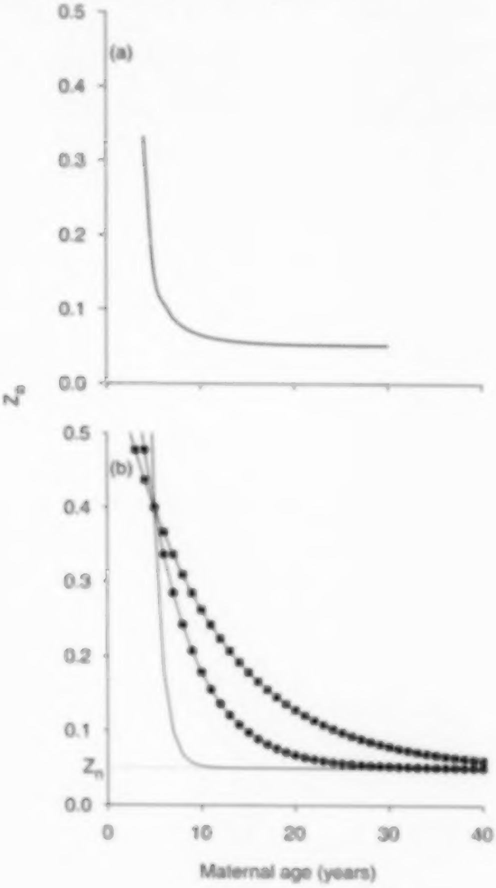

Distributions of reproduction at age

We evaluated how various forms of the maternal age effect changed the unfished reproductive contribution of a recruit at each age, relative to a recruit with homogeneous larval mortality rate, for a hypothetical population with life history traits typical of a long-lived fish species. Using the life history parameters in Table 1, we calculated egg production at each age (a)

$$\text{(5)}\qquad \text{eggs}(a) = l(a)\,p(a)\,m(a)$$

where $l(a)$ is survival to age a, $p(a)$ is the proportion mature at age a, and $m(a)$ is the number of eggs produced at age a. Here, in the unfished case, $l(a)$ was determined only by the natural mortality rate (M) of the population (i.e., $l(a) = e^{-M(a-a_0)}$). We assumed initially that maturity of females is knife-edged at age 5; $p(a)$ is 0 for maternal ages younger than 5 and 1 for ages 5 and older. Age-specific egg production was a function of length, represented by a von Bertalanffy growth model, with parameters given in Table 1. For each age, $m(a) = cL^b$, where L is the length of a fish at age a, and c and b are parameters.

To incorporate maternal age effects, we exposed egg production at each age to the maternal-age-dependent larval mortality rate Z_a for a larval duration of time (t) in days:

$$\text{(6)}\qquad \text{larvae}(a) = l(a)\,p(a)\,m(a)\,e^{-Z_a(t)}$$

We assumed $t = 10$ days, following conclusions regarding the maternal age mechanism of survival in starvation conditions (Berkeley et al. 2004*a*). We compared normalized distributions of egg and larval production at age for two levels of C (3 and 15) and three values of A (1, 5, 10) to evaluate how different forms of the maternal age effect change the relative, unfished contribution of reproduction at age.

In most fish populations, the proportion of reproductively mature fish is not a step function as assumed above, but rather an incremental function that increases until an age where all individuals are mature. To investigate how partial maturity and maternal age effects combine to affect the distribution of unfished reproductive output, we relaxed the knife-edged maturity assumption and specify $p(a)$ as a logistic function of age:

$$\text{(7)}\qquad p(a) = \frac{1}{1 + e^{-\kappa(a-\gamma)}}$$

The parameter κ determines the curvature of the logistic function, while γ determines the age at which 50% of the individuals are mature. We calculated normalized distributions of egg and larval production, as in eq. 5 and 6, using the logistic function for maturity (eq. 7). We assumed the curvature of the function to be constant at $\kappa = 1.0$, but examined cases where $\gamma = 5$, 7, and 9 years (Table 2). We compared normalized distributions of egg production at age and larval production at age, assuming three values of A (1, 5, 10) and a single value of C (13) for the maternal age effect.

Fishery effects

We evaluated the conditions under which maternal age effects could result in errors in fisheries assessment by calculating relative losses of lifetime spawning potential per recruit, in terms of eggs or larvae, from the hypothetical, long-lived fish population caused by a fishery. To represent conventional management with no knowledge of maternal age effects, we calculated LEP by integrating the egg production per recruit over all ages:

$$\text{(8)}\qquad \text{LEP} = \int_{a=0}^{a=\max} l(a)\,p(a)\,m(a)\,\mathrm{d}a$$

When no fishery exists, $l(a)$ is determined only by M. When a fishery exists, $l(a)$ is reduced by both M and F after the age at first capture (t_c).

$$\text{(9)}\qquad l(a) = \begin{cases} e^{-M(a-a_0)} & a < t_c \\ l(t_c)\,e^{-(M+F)(a-t_c)} & a \geq t_c \end{cases}$$

The degree of decline in LEP from the unfished state owing to a fishery was calculated as the ratio of fished LEP to unfished LEP (i.e., FLEP). FLEP as defined here is identical

Table 1. Life history and fishery parameter set for the model population.

Parameter	Value(s)	Definition
$a_{\max}$	40	Maximum age (years)
M	0.10	Natural mortality rate (year^{-1})
a_{mat}	5	Age at maturity (for knife-edged maturity case)
L_∞	45	von Bertalanffy asymptotic length (cm)
k	0.15	von Bertalanffy growth parameter
t_0	0	von Bertalanffy age at which individual length is 0
c	1	Coefficient of the allometric length–fecundity relationship
b	3	Exponent of the allometric length–fecundity relationship
t_c	5, 7, 9	Age of entry into the fishery (years)
F	0.05, 0.20, 0.50	Instantaneous fishing mortality rate (year^{-1})
Z_n	0.05	Instantaneous normal larval mortality rate (day^{-1})
C	3–15	Ratio of the larval mortality rate for 5-year-old females to Z_n
A	1–10	Age constant

Table 2. Logistic partial maturity schedules for three values of γ and $\kappa = 1.0$.

	Fraction mature		
Age	$\gamma = 5$	$\gamma = 7$	$\gamma = 9$
0	0.01	0.00	0.00
1	0.02	0.00	0.00
2	0.05	0.01	0.00
3	0.12	0.02	0.00
4	0.27	0.05	0.01
5	0.50	0.12	0.02
6	0.73	0.27	0.05
7	0.88	0.50	0.12
8	0.95	0.73	0.27
9	0.98	0.88	0.50
10	0.99	0.95	0.73
11	1.00	0.98	0.88
12	1.00	0.99	0.95
13	1.00	1.00	0.98
14	1.00	1.00	0.99
15	1.00	1.00	1.00
...	...	...	...
...	...	...	...
...	...	...	...
40	1.00	1.00	1.00

to SPR (Gabriel et al. 1989; Goodyear 1993), except that LEP is substituted for spawning stock biomass per recruit (SSBR). For species in which an egg production at age relationship is unavailable, weight at age for reproductive-aged fish is commonly used as a proxy for fecundity. We made the assumption that egg production is proportional to SSB, though this is not the case for all fish species (e.g., Love et al. 1990). By convention, we refer to FLEP as a percentage.

Lifetime larval production (LLP) was calculated by integrating the larval production of a recruit over all ages:

$$\text{(10)} \qquad \mathrm{LLP} = \int_{a=0}^{a=\max} l(a)\,p(a)\,m(a)\,e^{-Z_a(10)}\,da$$

Fractional LLP (FLLP) is the ratio of fished LLP to unfished LLP and is analogous to FLEP.

We evaluated the amount by which conventional fisheries management underestimates the normalized measure of reproductive potential when maternal age effects are present by calculating the percent difference between FLEP and FLLP (i.e., (FLEP – FLLP)/FLEP). This comparison was performed for three levels of F and t_c to represent nine separate fishery scenarios. Maturity was assumed to be logistic, with parameters $\kappa = 1.0$ and $\gamma = 7$. The role of maternal age effects in underestimating spawning potential was evaluated by examining the percent difference between FLEP and FLLP over a range of assumed A and C levels.

Black rockfish example

We examined the fisheries management implications of maternal age effects on larval mortality for a specific example with life history, fishery, and maternal age effect parameters (eq. 3) for black rockfish. Life history and fishery parameters were derived from the stock assessment and other literature and are detailed in Appendix A. We generated curves describing the dependence of LEP and LLP on F for two very different fisheries that target black rockfish. The California sport fishery begins removing black rockfish as sizes much smaller than the size at 50% maturity, while the California trawl fishery selects for larger, mature fish (Appendix A). Of the six fisheries modeled in the stock assessment, the California sport fishery was estimated to have the highest exploitation rate, while the California trawl fishery had the lowest exploitation rate on the black rockfish stock (Ralston and Dick 2003). Distributions of unfished egg and larval production at age were also computed to assess how maternal age effects affect the relative contribution of reproductive potential at each age.

Results

Distributions of reproduction at age

The effect of maternal-age-dependent larval mortality is to shift distributions of unfished larval production to older ages, relative to the distribution of unfished egg production (Fig. 2). The degree to which larval production shifts to older age classes depends both on *A* and *C*. Higher levels of *A* result in a greater dependence on older individuals for reproduction. The slow decline in Z_a over maternal age caused by a large *A* results in older females always producing larvae subjected to lower mortality rates than young females. For such cases, the larval mortality rate never reaches the asymptotic level, Z_∞. Higher levels of *C* increase the degree to which *A* shifts the distribution to the right. High values of *C* produce a greater dependence on older individuals for reproduction because larvae from young spawners are subjected to high levels of mortality.

Explicitly accounting for gradual, non-knife-edged maturity reduces the difference between the distributions of unfished egg and larval production at age (Fig. 3). Maternal age effects can be almost completely nullified when high larval mortality rates occur at ages in which only a small fraction of females are mature. This is most evident in Fig. 3*c*, where the distribution of egg production and larval production with $A = 1$ converge to be nearly identical. In this case, 50% of females are mature at 9 years of age (Table 2), while the maternal age effect with $A = 1$ reaches Z_∞ at approximately 10 years (Fig. 1). The result is the nullification of the maternal age effect by the partial maturity schedule. The maturity schedules considered here have very little effect on the distributions of larvae at age for maternal age effects with higher levels of *A*. The only changes to these distributions occur at the youngest of ages, from which very few larvae are produced.

Fishery effects

The efficacy of using FLEP to describe declines in lifetime reproductive potential when maternal age effects are present depends both on the form of the maternal age effect as well as the characteristics of the fishery (i.e., t_c and *F*; Fig. 4). Four general results can be observed in Fig. 4. First, the percent difference between FLEP and FLLP is relatively small for low levels of *C* for all *F* and t_c. Second, the percent difference between FLEP and FLLP can be small at low values of *A* over all levels of *F* and t_c. Third, percent differences are larger for higher levels of *F*, though absolute errors may be small because of low levels of FLEP at high *F*. Fourth, relative errors are nearly identical for different values of t_c. However, higher t_c results in higher levels of FLEP, and therefore the absolute difference between FLEP and FLLP are larger with increasing t_c.

These results can be understood by examining the integral that comprises the LEP and LLP calculations. LEP and LLP values are the result of integrating the product of two functions: (*i*) the survival function, which decreases with maternal age, and (*ii*) the egg or larval production function (in which the maturity schedule is embedded), which increases to an asymptotic level with maternal age. The product of these functions, integrated over age, reflects their degree of overlap. The effect of increased *F* and (or) decreased t_c is a shortening of the survival function (i.e., truncation of the age distribution). This results in decreasing the amount of overlap with the egg or larval production functions and a decrease in the integral of their product. The effect of increasing *C* and (or) increasing *A* is to decrease the larval production at young ages. This results in the larval production function shifting toward older ages, a lower amount of overlap with the survival function, and a decrease in the integral of their product. When both functions diverge to the point that there is no overlap, the integral is zero and no eggs or larvae are produced. The fishery parameters *F* and t_c were chosen in our analysis such that some overlap between the survival and egg production function always occurs, as FLEP is greater that zero in each panel (Fig. 4). However, the high *C* and high *A* forms of the maternal age effect can result in nonoverlapping functions at high *F*, an integral of zero, and thus percent difference values of 100%.

Fig. 2. Normalized distributions of the unfished egg and larval production as a function of maternal age, assuming that all females 5 years and older are mature. Larval distributions are calculated with three values of the age constant (*A*) and two values of contrast (*C*): (*a*) $C = 3$ and (*b*) $C = 15$. Solid line, eggs; circles, larvae $A = 1$; squares, larvae $A = 5$; diamonds, larvae $A = 10$.

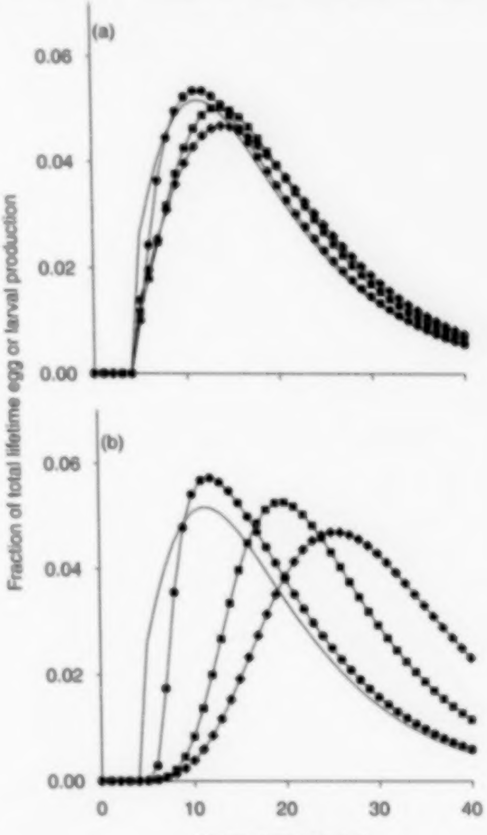

Black rockfish example

For the specific example of black rockfish, the parameterization of the maternal age effect produces a maximum larval mortality rate at age 4 ($Z_4 = 0.3322$) and a minimum larval mortality rate at the terminal age ($Z_{30} = 0.0512$) (Fig. 1). For comparison with the hypothetical population, *C* for black rockfish was 3.0649 (retaining the assumption from the hypothetical population that Z_{max} occurs for the progeny of 5-

Fig. 3. Normalized distributions of the unfished egg and larval production as a function of maternal age, assuming logistic maturity. Egg and larval distributions are calculated with three values of the age constant (A) at a contrast (C) of 13 and three values of the age of 50% maturity (γ): (*a*) $\gamma = 5$, (*b*) $\gamma = 7$, (*c*) $\gamma = 9$. Solid line, eggs; circles, larvae $A = 1$; squares, larvae $A = 5$; diamonds, larvae $A = 10$.

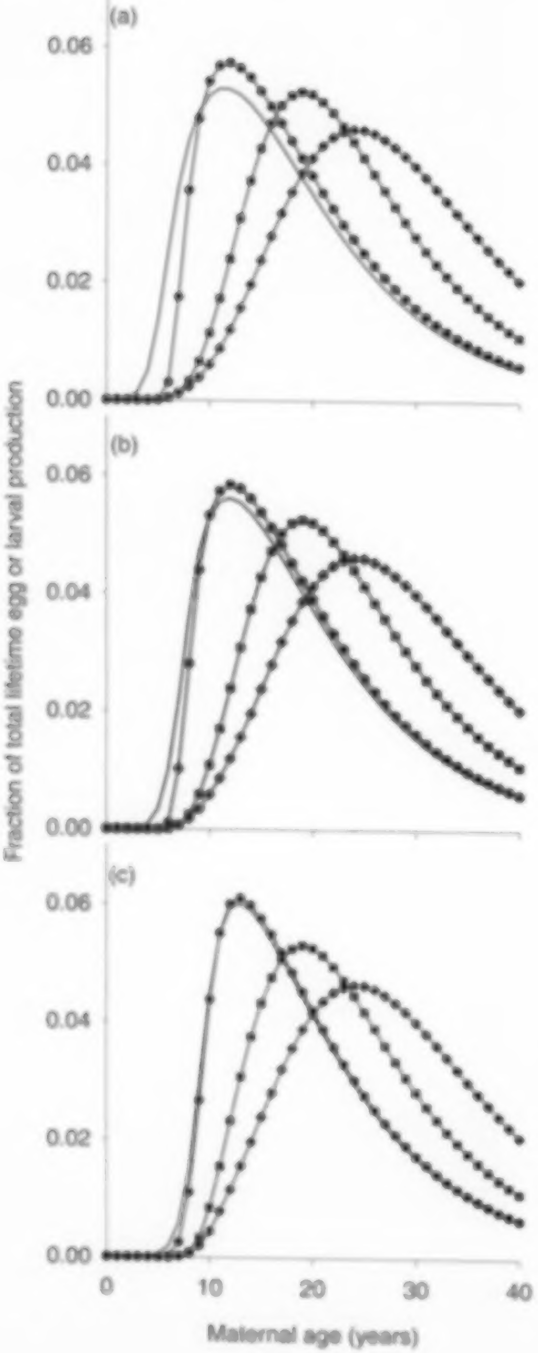

year-old females). A single value of A cannot be computed for the black rockfish larval mortality function, since it is not a simple, exponentially declining function as assumed for our hypothetical population. However, values for A fell in the range between 1.5 and 3.5, based on the predicted Z_y, Z_o, and C values from eq. 3. While the maturity ogive used in management is size-based, the conversion from size to age indicates that black rockfish first begin to mature at age 4, with 50% maturity occurring between ages 7 and 8, corresponding closely to the values reported in Love et al. (2002).

The maternal age effect has little influence on the decline in LEP and LLP curves for both the sport and trawl fisheries; the difference between LEP and LLP is small at all values of F (Fig. 5*a*). This result can be partially explained by the similarity between the distributions of unfished eggs and larvae at age (Fig. 5*b*). Here, the maternal age effect on larval survival discounts the reproductive output of young females relatively little, producing very similar distributions of egg and larval production. As a result, any fishery will impact the relative contribution of eggs and larvae at age in a similar manner.

Discussion

The fishery effects of maternal-age-dependent larval mortality depend critically on the form of the maternal age effect and the maturity schedule of females. The high mortality rates experienced by larvae produced from young mothers result in distributions of larval production at age shifting toward older ages relative to the distribution of egg production at age. The degree to which these distributions diverge depends on the contrast C, the age constant A, and the maturity schedule. In general, high C and high A result in more reproductive importance being placed on older individuals (i.e., the distribution of larvae is shifted far to the right relative to the distribution of eggs). Yet, when the change in larval mortality rates occurs for maternal ages that are only partially mature, this effect can be nullified. Truncation of the age distribution by a fishery greatly reduces FLLP relative to FLEP when the distribution of larval production is widely divergent from the distribution of egg production, with the result being that conventional management can misrepresent declines in reproductive potential. However, age truncation will have very similar effects on FLEP and FLLP when the unfished distributions of eggs and larvae at age are similar, such as when there is low C and low A. For populations such as these, errors in conventional management will be small.

For the specific example of black rockfish parameterized from the results of Berkeley et al. (2004*a*), addition of the maternal age effect had small fisheries implications. This appears to be due to the combination of (*i*) low C, (*ii*) a rapid decrease in larval mortality rate with increased maternal age (i.e., low A), and (*iii*) a maturity schedule that nullifies much of the increased larval mortality effects. The black rockfish form of the larval mortality function only penalizes egg production of the youngest spawners with high levels of larval mortality. At these young maternal ages, a relatively small proportion of females are actually mature, as the age of 50% maturity is approximately 7–8 years. The females producing larvae subjected to high larval mortality rates represent a very small proportion of the total reproductive potential of

Fig. 4. Percent difference between the fraction of unfished lifetime egg production (FLEP) and the fraction of unfished lifetime larval production (FLLP) plotted as a function of contrast (*C*) and the age constant (*A*). The percent difference between FLEP and FLLP is considered for three values of the fishing mortality rate *F* (0.05, 0.20, and 0.50) and three values of the age of entry into the fishery t_c (5, 7, 9). The FLEP at each combination of *F* and t_c appears in the upper right corner of each plot.

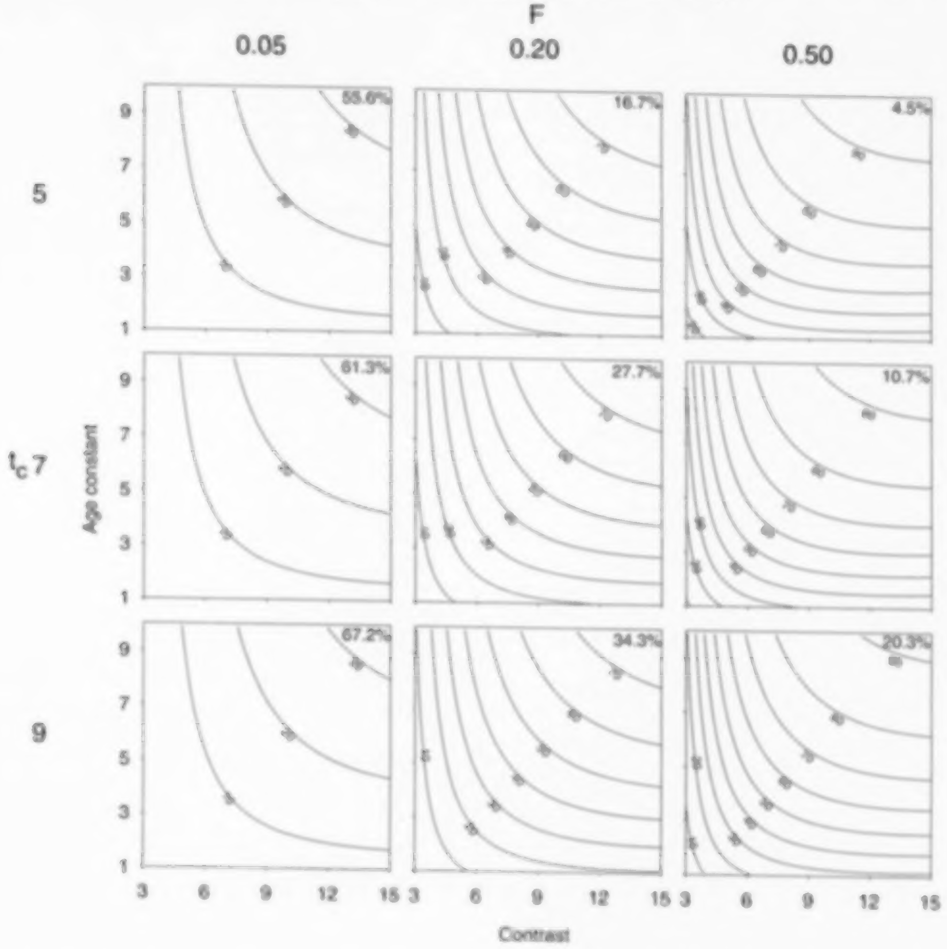

the population. As a result, assessment of reproductive potential is nearly identical regardless of whether maternal age effects are incorporated in the assessment.

The management implications of including maternal age effects have been investigated for the specific case of Atlantic cod (Murawski et al. 2001), which differ substantially from the black rockfish results presented here. Murawski et al. (2001) demonstrated that if the management goal is to preserve spawning intensity per recruit at 20% of the unfished level, the addition of maternal age effects requires a decrease in *F* from 0.43 (to preserve 20% of the unfished SSBR) to 0.28 (to preserve 20% of the unfished larvae per recruit). The difference in *F* is slightly smaller if LEP is used as the spawning metric instead of SSBR. In comparison, if we adopted the goal of keeping black rockfish at 20% of unfished LEP or LLP, the difference in *F* for the sport fishery is very small. Including maternal age effects would only require a decrease in *F* from 0.36 to 0.34 to maintain 20% of the unfished spawning intensity. The same comparison cannot be made for the trawl fishery, as it is nearly impossible to deplete LEP or LLP to 20% of the unfished level owing to the large lengths of first capture. The lack of sensitivity to the maternal age effect for black rockfish relative to Atlantic cod underscores how different life history characteristics and maternal age effects can result in very different implications for management.

The results presented in this paper pertain only to per-recruit egg and larval production quantities and how they differ when maternal age effects are considered. However, to fully assess how maternal age effects influence the sustainability of fished populations, knowledge of the slope of the stock–recruitment curve at the origin is necessary in conjunction with these per-recruit egg and larval production quantities. When the stock–recruitment curve is unknown or poorly known, the level of *F* corresponding to the maximum sustained yield (F_{MSY}) cannot be calculated with any degree

Fig. 5. (*a*) Decline in lifetime egg production (LEP) and lifetime larval production (LLP) as a function of fishing mortality rate (*F*) for black rockfish (*Sebastes melanops*) subjected to the selectivity patterns of the California sport and trawl fishery. (*b*) The distributions of unfished egg and larval production as a function of maternal age for black rockfish.

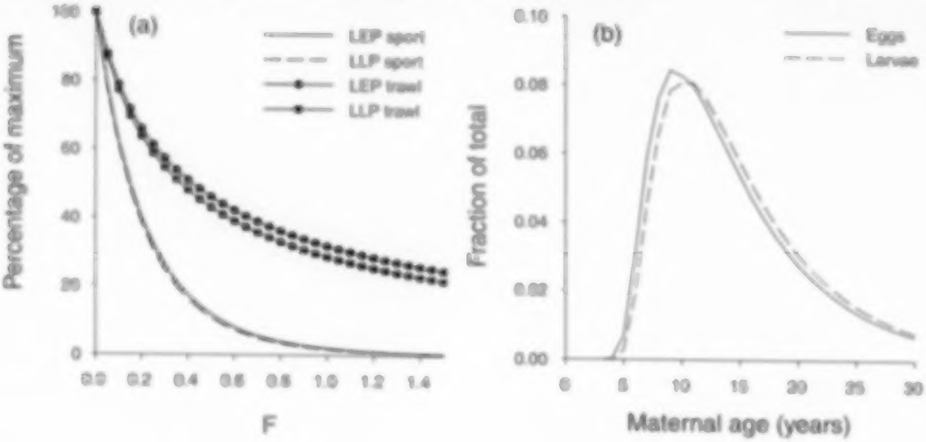

of certainty. In such cases, proxy levels of F_{MSY} are often calculated by setting F to a level that reduces LEP to a certain percentage of the unfished quantity (commonly 20%–60%). These commonly used levels of FLEP or SPR are employed to allow for a yield near the equilibrium, maximum level while ensuring persistence, given the uncertainty in the slope of the stock–recruitment relationship. However, these FLEP or SPR levels are based on analyses where SSB is generally used as the spawning metric (i.e., the independent variable in the stock–recruitment relationship). Results from two studies demonstrate that if viable larvae are instead used as the spawning metric in the stock–recruitment relationship, the level to which per-recruit reproduction can be reduced without causing collapse is increased. Murawski et al. (2001), using viable larvae as the spawning metric for the Georges Bank cod stock–recruitment relationship, found that the percentage of unfished viable larvae necessary for population persistence was lower than if SSB were used as the spawning metric. Similarly, another study (Spencer et al. 2007) found that resiliency of the stock–recruitment curve based on Gulf of Alaska Pacific ocean perch (*Sebastes alutus*) was increased if viable larvae were used as the spawning metric. The observed increase in resiliency with the addition of maternal age effects results from decreasing the measure of reproductive output (by computing viable larvae from SSB) while the number of estimated recruits remains constant. These stock–recruitment results are an important complement to the per-recruit results of this paper because they demonstrate that the previous SPR or FLEP values used to set proxy F_{MSY} levels will likely not apply if maternal age affects are included in assessment. Indeed, while fishing at a rate that reduces LEP to 20% of the unfished level will result in some lower percentage of unfished LLP, this may not necessarily lead to deterministic population collapse.

Our analysis treated only one measurable aspect of maternal age effects on early larvae. We assumed in both the hypothetical population and the black rockfish example that the maternal age effect only operates for the first 10 days of larval life, while the larval period for black rockfish and most other fishes is much longer. We restricted our analysis to this critical period of first exogenous feeding to approximate the experimental starvation conditions that produced the maternal age relationship (Berkeley et al. 2004*a*). The increased time to 50% mortality for the progeny of old females was attributed to increased oil globule volume for older females, promoting survival of unfed larvae. We therefore limited our analysis to this starvation tolerance mechanism. If we were to increase the larval duration for these analyses, the differences between FLEP and FLLP would increase. The larval survival term ($e^{-Z_a(t)}$) includes terms Z_a and t, the larval duration. As a result, an increase in larval duration would lower larval survival and increase the relative influence of maternal-age-dependent larval mortality. If the high mortality rates for larvae of young mothers continued into the active feeding stage, an increase in the assumed t would be warranted. Other maternal effects such as increased growth for progeny of older females (Berkeley et al. 2004*a*), if they continued into the active feeding stage, could result in better survival (Hare and Cowen 1997, and references therein) and increased importance of maternal age effects on persistence. However, if slow-growing larvae were the progeny of only very young females at ages where only a small proportion are mature, the effect of population dynamics would likely be small.

The importance of including maternal age effects in fisheries management does not appear to be universal for all species and possible maternal age functions. For maternal age effects where the contrast is low and higher mortality rates are restricted to larvae derived from females comprising a small fraction of the spawning biomass, the addition of maternal age effects does not result in conventional assessment methods grossly overestimating reproductive potential and persistence. Our results suggest that the black rockfish example falls into this category. Inclusion of maternal age effects in these cases does not require a large decrease in F to conserve adequate reproductive potential, as suggested by Berkeley et al. (2004*b*). Rather, low rates of exploitation may be required for long-lived species, regardless of whether maternal age effects are present. For many species, marine reserves may be beneficial for enhancing age structure and preserving adequate reproductive potential for populations dependent on old females for larval production (Halpern 2003). Whether specific marine reserve configurations can increase larval production to a greater degree than can be achieved by reducing F in conventional management, with less cost in terms of decreased catch, is an extant question.

Acknowledgements

Funding for this study was provided by NOAA Fisheries through the Partnership for Education in Marine Resource and Ecosystem Management (PEMREM). Alan Hastings and Chris Dewees critically read early versions of this manuscript. We also thank Paul Spencer and an anonymous reviewer for their insightful reviews.

References

Berkeley, S.A., Chapman, C., and Sogard, S.M. 2004*a*. Maternal age as a determinant of larval growth and survival in a marine fish, *Sebastes melanops*. Ecology, **85**: 1258–1264.

Berkeley, S.A., Hixon, M.A., Larson, R.J., and Love, M.S. 2004*b*. Fisheries sustainability via protection of age structure and spatial distribution of fish populations. Fisheries, **29**: 23–32.

Birkeland, C., and Dayton, P.K. 2005. The importance in fishery management of leaving the big ones. Trends Ecol. Evol. **20**: 356–358.

Blaxter, J.H.S., and Hempel, G. 1963. The influence of egg size on herring larvae. J. Cons. Int. Explor. Mer, **28**: 211–240.

Clark, W.G. 1991. Groundfish exploitation rates based on life history parameters. Can. J. Fish. Aquat. Sci. **48**: 734–750.

Dorn, M.W. 2002. Advice on west coast rockfish harvest rates from Bayesian meta-analysis of stock–recruitment relationships. N. Am. J. Fish. Manag. **22**: 280–300.

Gabriel, W.L., Sissenwine, M.P., and Overholtz, W.J. 1989. Analysis of spawning biomass per-recruit: an example for Georges Bank haddock. N. Am. J. Fish. Manag. **9**: 383–391.

Goodyear, C.P. 1993. Spawning stock biomass per-recruit in fisheries management: foundation and current use. *In* Risk evaluation and biological reference points for fisheries management. *Edited by* S.J. Smith, J.J. Hunt, and D. Rivard. Can. Spec. Publ. Fish. Aquat. Sci. No. 120. pp. 67–81.

Halpern, B.S. 2003. The impact of marine reserves: Do reserves work and does reserve size matter? Ecol. Appl. **13**(Suppl.): S117–S137.

Hare, J.A., and Cowen, R.K. 1997. Size, growth, development, and survival of the planktonic larvae of *Pomatomus saltatrix* (Pices: Pomatomidae). Ecology, **78**: 2415–3431.

Hislop, J.R.G. 1988. The influence of maternal length and age on the size and weight of the eggs and the relative fecundity of the haddock, *Melanogrammus aeglefinus*, in British waters. J. Fish Biol. **32**: 923–930.

Kamler, E. 1992. Early life history of fish: an energetics approach. Chapman and Hall, London.

Love, M.S., Morris, P., McCrae, M., and Collins, R. 1990. Life history aspects of 19 rockfish species (Scorpaenidae: *Sebastes*) from the Southern California Bight. NOAA Tech. Rep. NMFS 87.

Love, M.S., Yoklavich, M.M., and Thorsteinson, L. 2002. The rockfishes of the Northeast Pacific. University of California Press, Berkeley, Calif.

Mace, P.M., and Sissenwine, M.P. 1993. How much spawning per-recruit is enough? *In* Risk evaluation and biological reference points for fisheries management. *Edited by* S.J. Smith, J.J. Hunt, and D. Rivard. Can. Spec. Publ. Fish. Aquat. Sci. No. 120. pp. 110–118.

Marteinsdottir, G., and Steinarsson, A. 1998. Maternal influence on the size and viability of Icelandic cod *Gadus morhua* eggs and larvae. J. Fish Biol. **52**: 1241–1258.

Murawski, S.A., Rago, P.J., and Trippel, E.A. 2001. Impacts of demographic variation in spawning characteristics on reference points for fishery management. ICES J. Mar. Sci. **58**: 1002–1014.

Myers, R.A., and Mertz, G. 1998. The limits of exploitation: a precautionary approach. Ecol. Appl. **8**(Suppl.): S165–S169.

Palumbi, S.R. 2004. Why mothers matter. Nature (London), **430**: 621–622.

Ralston, S., and Dick, E.J. 2003. The status of black rockfish (*Sebastes melanops*) off Oregon and northern California in 2003. Pacific Fishery Management Council, Portland, Ore.

Sissenwine, M.P., and Shepherd, J.G. 1987. An alternative perspective on recruitment overfishing and biological reference points. Can. J. Fish. Aquat. Sci. **44**: 913–918.

Spencer, P., Hanselman, D. and Dorn, M. 2007. The effect of maternal age of spawning on estimation of F_{msy} for Alaskan Pacific ocean perch. *In* Biology, Assessment, and Management of North Pacific Rockfishes. Proceedings of the 2005 Wakefield Symposium, Anchorage, Alaska. *Edited by* J. Heifetz, J. DeCosimo, A.J. Gharrett, M.S. Love, T. O'Connell, and R. Stanley. Alaska Sea Grant College Program, University of Alaska Fairbanks. (In press.)

Trippel, E.A. 1997. Effects of adult age and size structure on reproductive output in marine fishes. *In* Early life history and recruitment in fish populations. *Edited by* R.C. Chambers and E.A. Trippel. Fish Fish. Ser. **21**. pp. 31–62.

Trippel, E.A. 1998. Egg size and viability and seasonal offspring production of young Atlantic cod. Trans. Am. Fish. Soc. **127**: 339–359.

Appendix A

Assessment of the fisheries management implications of maternal age effects for black rockfish (*Sebastes melanops*) required the use of external life history and fishery parameters. We obtained these parameters from the stock assessment and other literature. The definitions, values, and sources of the parameters used are listed in Table A1, and a description of the use of these parameters in the model follows.

A representation of variability in length at age was necessary to adequately incorporate the size-based maturity schedule and fishery selectivity patterns. Variation in length at age was produced by using the approximate coefficient of variation of length at age (CV_L) estimated by Ralston and Dick (2003). We assumed that length at age is normally distributed, with the mean value at each age determined by the von Bertalanffy parameters, and the standard deviation (SD) computed from the estimated value of CV_L (i.e., $\mathrm{SD} = \mathrm{CV}_L L_a$. Here, L_a is the fork length at age a predicted by the von Bertalanffy curve. We assume that the distributions of length at age extend to ±3 SD from the mean. Our results were not sensitive to the chosen value of CV_L. Simulations

Table A1. Life history parameters for black rockfish (*Sebastes melanops*).

Symbol	Definition	Value	Source
L_∞	von Bertalanffy asymptotic length (mm)	442.02	Bobko and Berkeley 2004
k	von Bertalanffy instantaneous growth parameter	0.33	Bobko and Berkeley 2004
t_0	von Bertalanffy parameter for age when length equals zero	0.75	Bobko and Berkeley 2004
CV_L	Coefficient of variation of length at age	0.08	Ralston and Dick 2003
Max age	Maximum age observed (years)	30	Bobko and Berkeley 2004
M	Instantaneous natural mortality rate (year^{-1})	0.14	Ralston and Dick 2003
c	Coefficient in the length–weight relationship	0.000 016 8	Ralston and Dick 2003
b	Exponent in the length–weight relationship	3.000	Ralston and Dick 2003

performed with values of CV_L from 0.04 to 0.12 resulted in negligible differences from the results presented here (M.R. O'Farrell, unpublished data).

Maturity was modeled as a logistic function of age. Bobko and Berkeley (2004) fit a logistic function to length and maturity data for black rockfish caught in Oregon. From Bobko and Berkeley (2004)

$$\text{(A1)}\quad P_L = \frac{e^{-26.731+0.068L}}{1+e^{-26.731+0.068L}}$$

where P_L is the percent mature at length L. Using this length-based maturity ogive and the estimated variability in length at age, we calculated the percent mature at each age (Fig. A1).

Egg production is not directly proportional to weight for black rockfish. To account for this, we first calculate weight at age as described in the Materials and methods. For each value of weight at age, we apply the following linear transformation to obtain the weight-specific egg production:

$$\text{(A2)}\quad \text{eggs per kilogram} = 289\,406 + 103\,076W$$

Here, W represents weight in kg (Ralston and Dick 2003).

Descriptions of the fishery selectivity patterns operating on black rockfish were needed to evaluate how lifetime egg production (LEP) and lifetime larval production (LLP) decline with an increase in the fishing mortality rate F. Size selectivity curves were estimated in Ralston and Dick (2003) for six fisheries that operate on black rockfish in California and Oregon. We used information on two of these six fisheries, which have the most diverse selectivity patterns.

The first fishery considered was the California sport fishery, which begins harvesting black rockfish at the smallest sizes of all six fisheries. Ralston and Dick (2003) estimated the California sport fishery selectivity to be dome-shaped (i.e., fish become fully recruited to the fishery at an intermediate size and vulnerability to the fishing gear declines at large sizes) (Fig. A1). Bobko and Berkeley (2004) estimated the length of 50% maturity for black rockfish to be 394 mm in fork length, and at this length, black rockfish have passed the fully recruited peak of the dome-shaped selectivity curve and have been already been exposed to the maximum F.

Fig. A1. Estimated maturity schedule (thick line) and fishery selectivity curves for black rockfish (*Sebastes melanops*). The sport (open circles) and trawl (solid squares) selectivity curves are estimated for the California fishery. Sources of these estimates are given in Table A1.

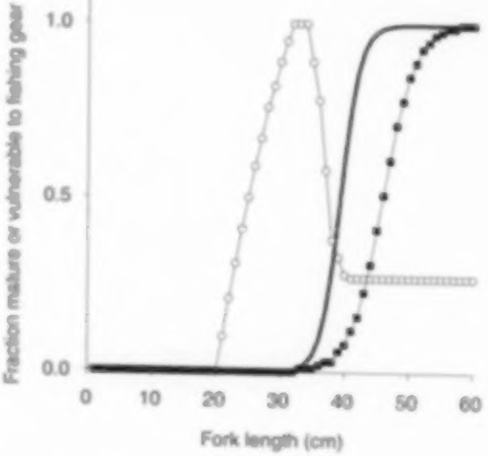

The second fishery considered was the California trawl fishery, which begins harvesting black rockfish at the largest sizes of all six fisheries. Ralston and Dick (2003) estimated the selectivity of the California trawl fishery as an asymptotic function of length (Fig. A1). This fishery represents the fishery least able to deplete reproductive potential, as most fish recruited to this fishery are mature. For example, at the length of 50% maturity, vulnerability to the fishing gear is only ~7%.

Appendix references

Bobko, S.J., and Berkeley, S.A. 2004. Maturity, ovarian cycle, fecundity, and age-specific parturition of black rockfish (*Sebastes melanops*). Fish. Bull. **102**: 418–429.

Ralston, S., and Dick, E.J. 2003. The status of black rockfish (*Sebastes melanops*) off Oregon and northern California in 2003. Pacific Fishery Management Council, Portland, Ore.

Consequences of inappropriate criteria for accepting age estimates from otoliths, with a case study for a long-lived tropical reef fish

Ross J. Marriott and Bruce D. Mapstone

Abstract: Fish ages estimated from increments in otoliths are uncertain because of various sources of error, including increment interpretation. Interpretation error is often addressed by reading each otolith multiple times and accepting age estimates only if readings satisfy certain consistency criteria. Choice of an inappropriate acceptance criterion may significantly bias the accepted age estimates and derived parameters such as mortality. The frequencies and magnitudes of discrepancies from replicate readings of otoliths increased with age for the red bass, *Lutjanus bohar*. The trend was best described by a constant probability of misinterpreting each increment, indicating an age acceptance criterion that allowed for increasing discrepancy between readings with age. Simulations of three error processes in reading otoliths, two processes of error accumulation within readings, and six acceptance criteria illustrated the biases in age-based metrics that arise from choosing inappropriate acceptance criteria. Biases were largest for static constant, rather than proportional, acceptance criteria, leading to elevated exclusion of older otoliths, overestimation of mortality, and underestimation of mean age. von Bertalanffy growth parameters were generally estimated with little bias. We recommend formal analysis of alternative models of ageing error to choose appropriate acceptance criteria and minimise biases in age-based demographic metrics.

Résumé : Les âges des poissons estimés à partir des zones de croissance des otolithes restent incertains à cause des diverses sources d'erreur, en particulier de l'interprétation des zones de croissance. On pallie souvent à cette erreur d'interprétation par des lectures multiples de chaque otolithe et par l'acceptation des estimations seulement si les lectures satisfont certains critères d'uniformité. Le choix d'un critère inadéquat d'uniformité peut générer des erreurs dans les estimations d'âge retenues et les paramètres dérivées, telles que la mortalité. La fréquence et l'importance des divergences dans les lectures multiples des otolithes augmentent en fonction de l'âge chez le vivaneau chien rouge, *Lutjanus bohar*. La tendance peut se décrire le mieux par une probabilité constante d'interprétation erronée de chaque zone; le critère d'acceptation de l'âge permet donc une divergence accrue entre les lectures en fonction de l'âge. Des simulations impliquant trois processus d'erreur dans la lecture des otolithes, deux processus d'accumulation d'erreurs dans ces lectures et six critères d'acceptation montrent les erreurs dans les métriques basées sur l'âge qui résultent du choix de critères d'acceptation inadéquats. Les erreurs sont plus grandes avec les critères d'acceptation statiques et constants qu'avec les critères proportionnels, ce qui mène à une exclusion accrue des otolithes de poissons plus âgés, à une surestimation de la mortalité et une sous-estimation de l'âge moyen. Les paramètres de croissance de von Bertalanffy's estiment généralement avec peu d'erreur. Nous recommandons de faire une analyse formelle de l'erreur des modèles de rechange pour la détermination de l'âge afin de choisir des critères d'acceptation appropriés et de minimiser les distorsions dans les métriques démographiques basées sur l'âge.

[Traduit par la Rédaction]

Introduction

Estimating age from counts of growth increments in fish otoliths usually involves judgement and some subjective interpretation (Brothers 1987; Campana 2001) and can result in errors that influence estimates of biological parameters (Barlow 1984) and age-based stock assessments (Powers 1983; Lai and Gunderson 1987; Eklund et al. 2000). Errors can arise because growth increments are not consistently periodic and so fail to reliably reflect the age of the fish or because of procedural errors in processing and interpreting otoliths and counting the increments. Systematic procedural errors will introduce biases in estimates, whereas random procedural errors are most likely to result in imprecision, either with or without bias. Procedures to ensure the accuracy (reviewed in Campana 2001; Panfili et al. 2002) and preci-

Received 8 December 2005. Accepted 22 May 2006. Published on the NRC Research Press Web site at http://cjfas.nrc.ca on 29 September 2006.
J19037

R.J. Marriott.[1,2] School of Marine Biology and Aquaculture, James Cook University, Townsville, Queensland, 4811, Australia.
B.D. Mapstone. Antarctic Climate and Ecosystems CRC, Private Bag 80, Hobart, Tasmania, 7001, Australia.

[1] Corresponding author (e-mail: rmarriott@fish.wa.gov.au).
[2] Present address: Western Australian Fisheries and Marine Research Laboratories, P.O. Box 20, North Beach, WA 6920, Australia.

Can. J. Fish. Aquat. Sci. 63: 2259–2274 (2006) doi:10.1139/F06-109

sion (Kimura and Lyons 1991; Campana et al. 1995; Morison et al. 1998) of fish ageing, therefore, are important for fisheries research and management.

Otoliths have been reported to be accurately readable chronometers for most temperate and tropical reef fish species so far examined (Secor et al. 1995). Various methods have been used to assess procedural errors in the interpretation of otolith increments once increments have been validated (Beamish and McFarlane 1983) as a sufficiently accurate measure of age (Francis et al. 1992). Repeated age estimation is used most often to ensure that a method of reading otoliths is applied consistently and to estimate characteristics of interpretation errors in readings of growth increments. In high volume "production ageing", a subset of otoliths may be read multiple times to estimate imprecision in age estimates that is then incorporated into assessment procedures or to account for systematic biases in estimates over time or among readers (Kimura and Lyons 1991; Morison et al. 1998). An alternative approach has involved independently repeatedly reading all specimens and accepting age estimates only when similarity between successive readings meets some specified criterion. The criterion used for acceptance is largely arbitrary and varies among studies. For example, Hesp et al. (2002) and Peres and Haimovici (2004) required repeat counts of annuli in otoliths to differ by no more than 2 and 0 annuli, respectively, for a final age to be accepted. Crabtree et al. (1995) required repeat counts to differ by no more than 10% for acceptance. Specimens for which "acceptable" agreement between successive readings is not achieved usually are excluded from subsequent age-based analyses.

Estimating age from the otoliths of long-lived fish can be particularly difficult and prone to error. For instance, Hesp et al. (2002) reported a higher rate of discrepancies between replicate readings of older otoliths than younger otoliths, while other studies (e.g., Lai and Gunderson 1987; Eklund et al. 2000) have observed that the variance of estimated ages increases with nominal fish age. Increasing discrepancies with age makes the choice of acceptance criterion for age estimates particularly important. If the rate or magnitude of discrepancies between repeated readings increases with nominal fish age and a static (age-independent) criterion for accepting age estimates is adopted (e.g., requiring that repeated readings match exactly or differ by no more than one or two), there will likely be a disproportionately high rate of rejection of age estimates from older otoliths. This is likely to result in underrepresentation of older age classes in estimated population age frequencies, potentially causing bias in derived fishery statistics such as mortality and growth parameters. Information about the relationship between ageing error and nominal age can be used to account for uncertainties in age estimation in age-structured stock assessment models (Fournier and Archibald 1982; Richards et al. 1992). This information could also potentially be used to decide which criterion is most appropriate for accepting estimates of age from individual otoliths in order to minimise risks of rejection-related biases in population samples and derived parameters.

In this paper, we present an approach to analytically evaluate the suitability of alternative criteria for accepting estimates of age from repeated readings of otoliths. We use otoliths from the long-lived tropical snapper *Lutjanus bohar* as a case study to illustrate how age-related patterns of discrepancy between replicate readings of otoliths can be used to identify which "age acceptance criterion" is most appropriate for filtering age estimates from otoliths. We then explore, through simulation, potential effects of adopting inappropriate age acceptance criteria on estimates of population age parameters, mortality, growth metrics, and von Bertalanffy growth parameters for a known population under different scenarios for the genesis of errors in reading otoliths. We investigate here the degree to which the choice of acceptance criterion, perhaps by convention, is likely to result in significant biases in some age-based parameters central to descriptions of population dynamics and stock assessments.

Materials and methods

Sample collection

Biological samples and associated field data were collected from the northern and central sections of the Great Barrier Reef (GBR:14°30′S, 145°20′E to 18°50′S, 147°40′) and the Seychelles Republic (3°50′S, 50°10′E to 10°10′S, 57°10′E) from 1995 to 2001 and 1999 to 2001, respectively. *Lutjanus bohar* were collected by line fishing from depths of 5–35 m on the Great Barrier Reef and 5–65 m in the Seychelles. *Lutjanus bohar* were collected from the GBR through two sampling programs: (*i*) research catch surveys of the CRC Reef Effects of Line Fishing Experiment (detailed sampling methods in Mapstone et al. 2004); and (*ii*) monthly samples from the landed catches of commercial reef line fishers. *Lutjanus bohar* were sampled approximately monthly from landed catches of the artisanal line fishing fleet in the Seychelles by the Seychelles Fishing Authority (Marriott 2005; Marriott and Mapstone 2006).

Sample processing and age estimation

Sagittal otoliths were dissected from frozen heads of *L. bohar* in the laboratory. Age estimates were then derived from the analysis of transverse sections of one otolith from each fish ($n = 1742$), sectioned using a standard procedure (Ferreira and Russ 1994). Otoliths were sectioned in random order to ensure that any effects of sampling date or geographic area of collection were not confounded with potential biases attributable to the order in which otoliths were sectioned and read. Otolith sections were then further processed to improve the definition of opaque zones before repeat age estimation using one of three "secondary preparation methods" (acid etching, hand polishing, or mechanical polishing) (Marriott and Mapstone 2006). Fish age, in years, was estimated by counting opaque increments along the ventral sulcus of otolith sections, from the nucleus to the proximal surface margin, when viewed with transmitted light under low (40×) to medium (100×) magnification.

All otoliths were read by the same reader (RJM) twice, with readings separated by at least 2 weeks. Age estimates from the first reading are hereafter deemed "nominal" ages. Increments were considered pseudoannuli and were excluded from counts if their position or optical density was inconsistent with other opaque increments that had been validated as annual (Marriott 2005; Marriott and Mapstone 2006). Where two or more opaque increments were overlapping in places or unusually closely spaced (Crabtree et al. 1995), they were interpreted as a single annulus. Otolith sections from up to five fish, if available, were randomly selected from each nominal age class, preparation method, and geographic area to test for any effects of secondary preparation method or geographic area on estimates of discrepancy characteristics.

Models of patterns in ageing error

We derived mathematical models for each of three credible, but not exhaustive, hypotheses about the genesis of discrepancies between repeated age estimates from the same otolith. The first hypothesis (H_1) was that discrepancies between readings arose principally because of difficulties in interpreting specific features common to all otoliths, such as the first increment (e.g., Marriott and Cappo 2000) or marginal increment (e.g., Smith and Deguara 2003), but that there was little likelihood of interpretation error for all other increments. Thus, the probability of not achieving exact agreement from replicate readings is independent of the number of increments counted and so constant over all otoliths and nominal ages. The second hypothesis (H_2) was that nominal fish age did not influence the clarity or interpretability of growth increments but that each increment had the same nontrivial likelihood of misinterpretation. Here, the probability of discrepancy between readings would increase with nominal age. The third hypothesis (H_3) was that growth increments become increasingly difficult to identify or interpret with increasing nominal age (and distance from the otolith nucleus), perhaps because of "bunching" of increments deposited by older fish (e.g., Stevenson and Secor 1999; Manickchand-Heileman and Phillip 2000; Andrews et al. 2001). Here, too, the probability of discrepancy would increase with nominal age but the probability of misinterpreting each annulus increases as more annuli are counted. The manifestations of the three hypotheses are shown (Fig. 1).

Under H_2, the probability (p) that a growth increment (annulus) is interpreted differently between readings will be the same for all annuli, as is the complement probability ($1 - p$) of each annulus being interpreted the same in both readings. Thus, the probability of getting different estimates of age in successive readings of the same otolith is derived from the binomial expansion:

$$J_t = 1 - (1 - p)^t \tag{1}$$

where t is the number of increments counted where interpretation errors are possible, p is constant probability that two interpretations of an increment will differ, and J_t is the probability that two readings of the same otolith of nominal age t', with t increments interpreted with error, will differ.

H_1 is essentially a special case of H_2 in which $t = 1$ for all otoliths if errors are likely at only the first or the marginal increment, or $t = 2$ for all otoliths if errors are likely at both and will take the form of

$$J = p' \tag{2}$$

where p' is a constant for all otoliths.

Fig. 1. Expected patterns in (*a*) the probability (J) of disagreement (PD) between successive readings of an otolith and (*b*) mean magnitude (m) of inter-read discrepancy (IRD) with increasing nominal fish age for three alternative hypotheses: H_1, J does not change with nominal fish age; H_2, J increases with nominal age because errors made at all annuli are equiprobable; H_3, J increases with nominal age at an increasing rate because increments become harder to distinguish at older ages.

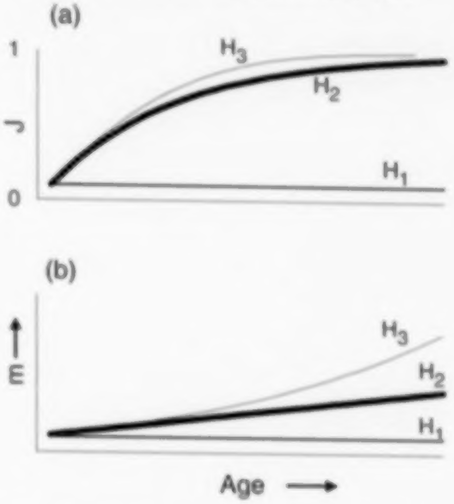

The plot of H_3 is similar to that of H_2 except that the rate of increase in probability of discrepancy is greater. Under H_3, the probability of different interpretation of each increment in successive readings can be expressed as

$$p_i = p(1 + b)^{i-1} \tag{3}$$

where p is the base rate of interpretation error for the first increment, b is the rate at which p changes with each additional increment interpreted, and p_i is the specific probability that two interpretations of increment i will differ. The probability of not estimating the same age in successive readings when errors arise according to H_3 is

$$J_t = 1 - \prod_{i=1}^{t}(1 - p_i) \tag{4}$$

where t, p, and J_t are as for eq. 1 and i and p_i are as for eq. 3. Probabilities of discrepancies in reading otoliths will be manifest as the proportion (or percentage) of otoliths that had not been assigned the same age in duplicate readings. We use the term "percentage disagreement" (PD) for the observed percentage of discrepant readings in a sample of otoliths.

The theoretical magnitude of discrepancy between successive readings of the same otolith also can be derived from each of the above models (Fig. 1*b*). Under H_2, the magnitude of discrepancy between readings is expected to increase linearly with nominal age. Because we are dealing only with data that are discrepant, however, the discrepancy data will have a minimum nonzero value for all fish, giving

$$m_t = tp + c \tag{5}$$

where p is the probability of different interpretation between readings common to all increments, as for eq. 1, t is the number of increments read where interpretation errors are likely, and so also the nominal age (t') of the otolith for H_2 and H_3, c is the expected minimum discrepancy between two readings of an otolith, and m_t is the expected magnitude of discrepancy between two readings of the otolith given increment count t. For H_1, $m = p + c$ when errors are likely only in one increment, or $m = 2p + c$ when errors are likely at both first and marginal increments. In practice, this would mean that the expected magnitude of discrepancies would be one or two, respectively. Under H_3, m is expected to increase roughly exponentially with the number of increments (age) read, again with a nonzero minimum, and can be described by

$$(6) \qquad m_t = \left[p \sum_{i=1}^{t} (1 + b)^{i-1} \right] + c$$

where t, m_t, c, and p are as for eq. 5 and b and i are as for eq. 3.

Because increment counts are integers, however, the observed magnitudes of discrepancies, termed the inter-read discrepancy (IRD) will be integral and is usually expressed as

$$(7) \qquad \mathrm{IRD} = \left| R_1 - R_2 \right|$$

where R_1 and R_2 are the first and second readings, respectively, of an otolith. Under H_1, IRD will typically be either 1 or 2 for all otoliths and c will be 1 in practice for all hypotheses. Under H_2 or H_3, IRD will typically follow a step function with increasing nominal age, with constant IRD for all ages within the range that the expected value of m_t falls between integers.

Each of the above models for H_1 to H_3 can be fitted to either observed PD (eqs. 1, 2, and 4) or IRD (eqs. 5 and 6) data. The best fit can be used to infer the most likely explanation of the frequency (Fig. 1*a*) and magnitude (Fig. 1*b*) of discrepancies and so the most appropriate age acceptance criterion. That is, if H_1 best described observations, a static constant acceptance criterion would be appropriate for fish of all ages, meaning that if repeated readings of an otolith differed by more than a fixed constant (e.g., 1 or 2), the otolith would be discarded as an unreliable indicator of age. If H_2 or H_3 were better approximations to the discrepancy data, however, then a constant or increasing rate criterion, respectively, would be more appropriate, with acceptable limits to discrepancies being proportions of nominal fish age.

Fitting models to discrepancies from ageing *L. bohar*

Percentage disagreement

The frequency data from the nominal age classes of *L. bohar* from different geographic areas and prepared with different secondary preparation methods were pooled into nominal age bins, each comprising three successive nominal age classes, before calculating rates of nonagreement. Binning age classes was necessary to provide larger sample sizes ($n \geq 3$; Table 1) for all categories and thus improve resolution in estimates of nonagreement. PD was then calculated for each of the nominal age bins from each geographic area and secondary preparation method. These data were then analysed using analysis of covariance (ANCOVA) to investigate the influence of geographic area and method on PD, while accounting for age bin (covariate). If plots of PD against nominal age bin indicated significant departures from linearity, a relevant linearizing transformation was applied before the ANCOVA. The ANCOVA was done principally to determine the validity of pooling data across these factors for a more powerful subsequent analysis.

Table 1. Number of observations analysed for the analysis of covariance of the observed percentage of discrepant readings (PD).

	GBR			Seychelles		
t' bin	AE	HP	MP	AE	HP	MP
1–3	7	9	5	5	10	5
4–6	15	14	15	3	15	13
7–9	12	16	15	5	16	13
10–12	15	15	15	5	15	14
13–15	5	10	15	11	14	9
16–18	3	7	7	7	14	9

Note: Factors: geographic area (Great Barrier Reef (GBR), Seychelles) and secondary preparation method (acid-etched (AE); hand-polished (HP); machine-polished (MP)). Covariate: nominal age (t') bin; t' bins that were judged to have too few observations to sufficiently represent the percentage of data that did not achieve agreement from replicate reads ($n < 3$ per cell) were excluded from the analysis and are not shown.

The models corresponding to each of the above hypotheses for the genesis of interpretation errors (Table 2) were then fitted to observed PD for nominal age classes using nonlinear regression. PD values calculated from less than five data were arbitrarily judged to be poor estimates and excluded from analysis. The fit of the models was compared using Akaike's information criterion for small sample sizes (AIC_c; Burnham and Anderson 1998) to infer which of the models best described these data. Models with an AIC_c value within two of that calculated for the best approximating model (lowest AIC_c) were considered to describe these data equivalently well (Burnham and Anderson 1998). The model that best described the data was then interpreted as evidence justifying the selection of an appropriate corresponding age acceptance protocol.

Magnitudes of discrepancies

Averages of observed IRD were calculated from discrepant readings only for each nominal age class or nominal age bin. IRD was calculated initially for the nominal age bins from different geographic areas and preparation methods and compared using ANCOVA, as was done for PD data, to test the validity of pooling data across these factors in subsequent analysis. The three models for trends in IRD with nominal age class corresponding to the three ageing error hypotheses (Table 3) were then fitted to these data. AIC_c values were again calculated from the fit of these models to determine which one best explained the data. This was done as a "reality check" of our evaluation of the trend of PD with age to account for the prospect of type II errors in the former analysis and verify consistency between our inferences of

Table 2. Candidate models used to investigate the likelihood of hypotheses about error generation processes leading to nonagreement between repeated readings of otoliths.

Hypothesis	Model	Functional form	Constraints
H_1	J uniform	$\mathrm{PD} = c$	None
H_2	p constant	$\mathrm{PD} = 100[1 - (1 - p)^t]$	$0 \le p \le 1$
H_3	p increasing	$\mathrm{PD} = 100[1 - \prod_{i=1}^{t}(1 - p(1 + b)^{i-1})]$	$0 \le p \le 1$; $b > 0$

Note: PD, the percentage of otoliths per nominal age (t') class or t' bin for which repeated readings were potentially discrepant. b, c, and p are model parameters, where b is the rate at which p changes, assuming H_3 ageing error propagation, c is the expected PD under H_1, and p is the probability that an increment is interpreted differently between readings, assuming H_2 or H_3 ageing error propagation.

Table 3. Candidate models used to describe the relationship between observed inter-read discrepancies (IRD) with nominal age (t').

Hypothesis	Model	Functional form	Constraints
H_1	J uniform	$\mathrm{IRD} = c$	None
H_2	p constant	$\mathrm{IRD} = p(t - 1) + c$	$0 \le p \le 1$
H_3	p increasing	$\mathrm{IRD} = \left[p\sum_{i=1}^{t}(1 + b)^{i-1}\right] + c$	$0 \le p \le 1$; $b > 0$

Note: Each model is that which predicts the expected magnitude of discrepancies at each age given the corresponding model of probability of discrepancy shown in Table 2. b, c, and p are model parameters, where b is the rate at which p changes, assuming H_3 ageing error propagation, c is the expected minimum discrepancy between two readings of an otolith, and p is the probability that an increment is interpreted differently between readings, assuming H_2 or H_3 ageing error propagation.

the most likely source(s) of error and the ultimate acceptance criterion based on the magnitude of IRDs.

Effects of adopting inappropriate age acceptance criteria

We used simulations to explore the consequences of adopting different age acceptance criteria when ageing errors arose according to each of the above hypotheses (H_1, H_2, H_3). The simulations involved the following steps. (*i*) Sample individuals from a model population with known parameters. (*ii*) "Read" the ages of the individuals multiple times with interpretation errors generated according to H_1, H_2, or H_3. (*iii*) Filter each of the resultant data sets according to six age acceptance criteria either commonly reported in the literature or corresponding to the above hypotheses. (*iv*) Calculate various age-based metrics from the accepted age data. (*v*) Compare the accepted sample metrics with the known true values of the sampled model population or those estimated from the samples had ages been determined without error. Full details of the modelling are available elsewhere (Supplemental data[3]) and only summary details for each step are provided here.

Generating and sampling the model population

We generated the hypothetical population data from an age-structured population model parameterised from field data for *L. bohar* (Marriott 2005; Table 4). Fork lengths (FL) of the model individuals were generated using the von Bertalanffy growth function (VBGF) with individual variation in length at age, again parameterised with field data for *L. bohar* (Table 4). The population comprised 109 744 individuals aged 1–56 years and was sampled randomly with replacement to generate samples of 1679 individuals (with age and FL data pairs), representing a sampling fraction of 0.0153 and providing a reasonable prospect of sampling at least one of the 100 individuals in the oldest age class and seven or more individuals (Kritzer et al. 2001) from around two-thirds of age classes (1–37 years). Three sets of 200 such samples were taken independently with one set (of 200 samples) destined to be "aged" with interpretation errors corresponding to H_1, H_2, or H_3.

Ageing the sample individuals

In most cases, neither counts of increments in otoliths nor discrepancies between multiple readings can provide direct estimates of interpretation errors because usually we do not know whether our interpretation of each increment is correct or the true age of the individual. Accordingly, the above hypotheses and associated models relate only to frequency and magnitudes of discrepancies, not the frequency or magnitudes of erroneous interpretations of increments or inaccuracies in single readings of an otolith. The latter properties, however, were those we wanted in order to generate data according to the error-generating processes described under H_1, H_2, or H_3.

We inferred an appropriate value for per-increment interpretation error (a) from the empirical discrepancy data that we had for *L. bohar* based on the premise that two main types of misinterpretation might occur in practice: an incre-

---

[3] Supplementary data for this article are available on the journal Web site (http://cjfas.nrc.ca) or may be purchased from the Depository of Unpublished Data, Document Delivery, CISTI, National Research Council Canada, Building M-55, 1200 Montreal Road, Ottawa, ON K1A 0R6, Canada. DUD 5080. For more information on obtaining material refer to http://cisti-icist.nrc-cnrc.gc.ca/irm/unpub_e.shtml.

Table 4. Input parameters used for simulations.

Parameter	Estimate	Source
y_{max}	56	Maximum age from *Lutjanus bohar* samples
Z_{μ}	0.081	Hoenig (1983) estimate from *L. bohar* data (Marriott 2005)
L_{∞}	650	*L. bohar* data (Marriott 2005)
K	0.15	*L. bohar* data (Marriott 2005)
y_0	0	*L. bohar* data (Marriott 2005)
$\sigma_{L\infty}$	31.81	*L. bohar* data (Marriott 2005)
p	0.1	This paper
σ_p	0.01	This paper
a	1	This paper
b	0.025	This paper

ment might not be counted when it should be or an increment might be counted twice (or, rarely, more). Each type of error can occur because of structural ambiguity in the otolith, such as the formation of apparent increments more or less frequently than expected (e.g., subannual "annuli"), because of poor preparation of otoliths for reading or because of mistakes by the observer when interpreting increments. Thus, in general, there are three possible outcomes from interpretation of each increment: an omission, a correct interpretation, or a multiple count of the same increment. If r_i is the difference between the correct interpretation and the realised interpretation, and so a measure of impact on the accuracy of estimated age, then these three outcomes correspond respectively to values of r_i of −1, 0, or +1 and theoretically have estimable probabilities of u, $1 - a$, or v, respectively, where $a = u + v$ is the probability of any interpretation error occurring. Given these probabilities of outcomes for interpreting each increment, the potential results from reading an entire otolith can be described by the terms of the trinomial expansion

$$(8) \qquad P(-1, 0, +1) = {}^{y}C_{l,k}(u)^{l}(v)^{k}(1-a)^{y-l-k}$$

where ${}^{y}C_{l,k} = \dfrac{y!}{l!k!(y-l-k)!}$, l is the number of $r_i = -1$, k is the number of $r_i = +1$, and $y - l - k$ is the number of $r_i = 0$. The probability density function of outcomes for a single reading R is thus

$$(9) \qquad \mathrm{Pl} = \sum_{l=0}^{y}\sum_{k=0}^{y-l} {}^{y}C_{l,k}(u)^{l}(v)^{k}(1-a)^{y-l-k}$$

Assuming the probability that an interpretation error will be made is independent among increments, it is possible that all increments will be interpreted without error, all increments will be interpreted erroneously, or some increments will be interpreted correctly and the remainder erroneously in a single reading of an otolith.

The discrepancy data we usually have available arise from two (or more) readings, each of which may involve errors arising as described above. "Acceptable" estimates of age are derived when any pair of readings satisfies a specified acceptance criterion. Two readings will match, giving discrepancies of zero, whenever the same outcome is reached from each reading, whether accurate or not. Thus, for two readings R_1 and R_2

$$(10) \qquad \mathrm{P(IRD = 0)} = \sum_{l=0}^{y}\sum_{k=0}^{y-l} [{}^{y}C_{l,k}(u)^{l}(v)^{k}(1-a)^{y-l-k}]^{2} + 2\sum \mathrm{CP}_{lk}$$

where CP_{lk} denotes the cross-product of each pair of different terms that produce the same count, and $\mathrm{P(IRD \neq 0)} = 1 - \mathrm{P(IRD = 0)}$.

From our observational data, $P(\mathrm{IRD} \neq 0)$ is estimated by J (eq. 1), and so by setting $J = 1 - \mathrm{P(IRD = 0)}$, we have a path to estimate the unknowns in eq. 10 for specific assumptions about the relationship between u and v. We can simplify eq. 10 if we use a parameter s that describes the likelihood that an interpretation error will be an error of inclusion (r_i = +1) rather than one of omission ($r_i = -1$) such that $v = as$ and so $u = a(1 - s)$, giving

$$(11) \qquad J = 1 - \left\{ \sum_{l=0}^{y}\sum_{k=0}^{y-l} [{}^{y}C_{l,k}(a(1-s))^{l}(as)^{k}(1-a)^{y-l-k}]^{2} + 2\sum \mathrm{CP}_{lk} \right\}$$

We can then solve eq. 11 for a under specific assumptions about the value of s. For example, if interpretation errors of omission and inclusion are equally likely, then $s = 0.5$. Equation 11 can be solved most easily for the special case of a single increment for which there are no terms in CP_{lk}, giving

$$(12) \qquad J = 2a - (2 - 2s + 2s^{2})a^{2}$$

We used the observed discrepancy data from readings of *L. bohar* otoliths to provide a value for the per-increment rate of discrepancy (p) of 0.1 (Tables 5, 6) and so estimate J from eq. 1 under H_2 when just one increment was read with error, giving a value for the per-increment probability of error (a) of 0.05203, from eq. 12 under the condition that $a \leq 1$. We estimated the standard error (SE) of a to be ~0.0054 by replacing p with $p \pm \mathrm{SE}_p$ (Tables 5, 6) in these calculations.

We applied an estimated rate of increase in interpretation error per increment (b') of 0.0265 to simulate interpretation errors according to H_3. Relating discrepancy rates, J, to interpretation error rates a, for H_3 is analytically less tractable than for H_1 and H_2. We derived the per-increment rate (b') of increase in the rate of interpretation error (a) approximately by calculating the instantaneous rate J_{H_3} at two increments, $i = 1$ and $i = 40$, from eq. 3 and using each of those rates to estimate corresponding rates of interpretation error at those ages. We then assumed that the increase in rate of interpretation error with increment count was of the same form as for increases in probability of discrepancies (eq. 3), giving

$$(13) \qquad a_i = a_1(1 + b')^{i-1}$$

and so estimated, by rearrangement of eq. 13, the rate of per-increment increase in interpretation error (b') from

Table 5. Model fits to variation in percentage of disagreements (PD) with nominal age class (t'; $n = 37$).

Model	Hypothesis	c	b	p	R^2	AIC$_c$	Δ
p constant	H_2	—	—	0.09 (0.007)	0.53	**86.06**	0.00
p increasing	H_3	—	0 (0)	0.10 (0.010)	0.46	90.79	4.73
J uniform	H_1	73.98 (3.09)	—	—	0.00	98.23	12.17

Note: The functional forms of each model and respective hypotheses are given in Table 2. Numbers in parentheses are standard errors of parameter estimates. AIC$_c$, Akaike's information criterion for small sample sizes; Δ, the difference in AIC$_c$ from that calculated for the best approximating model (in bold). PD values were excluded from the analysis if calculated from fewer than five data or if estimated for $t' > 43$ years.

Table 6. Model fits to mean inter-read discrepancy (IRD) with nominal age ($n = 33$).

Model	Hypothesis	c	b	p	R^2	AIC$_c$	Δ
p constant	H_2	0.959 (0.271)	—	0.107 (0.012)	0.73	**−4.15**	0.00
p increasing	H_3	1.273 (0.460)	0.025 (0.029)	0.064 (0.033)	0.75	−2.43	1.72
J uniform	H_1	3.171 (0.232)	—	—	0.00	12.76	16.31

Note: The functional forms of each model and respective hypotheses are given in Table 3. Data have been pooled across geographic areas and preparation methods (excluding sections that were acid-etched then machine-polished). Numbers in parentheses are standard errors of the estimates. AIC$_c$, Akaike's information criterion for small sample sizes; Δ, the difference in AIC$_c$ from that calculated for the best approximating model (in bold). IRD values were excluded from the analysis if calculated from fewer than five data or if estimated for $t' > 43$ years.

$$(14)\qquad b' = \left(\frac{a_t}{a_1}\right)^{\frac{1}{t-1}} - 1$$

We also simulated readings with values of a two and three times the base rate derived for *L. bohar* (0.05203) with correspondingly scaled standard errors. In addition, we simulated two scenarios for the accumulation of interpretation errors: one in which errors of omission or inclusion were equally likely ($s = 0.5$) and independent among increments within a reading and the other in which errors of only one type (omission or inclusion) occurred for each otolith ($s = \pm 1$), but the type was assigned randomly among otoliths, resulting in unidirectional error accumulation within readings. We used these two extreme scenarios to bracket the likely range of error accumulation scenarios manifest in real applications, which is likely to include various situations in which some otoliths are consistently difficult to interpret and so interpretations will not be completely independent among increments.

Three independent estimates of age were generated for each individual in each sample assigned to each of the three hypotheses described above (Tables 2, 3). In each case, the probability that each true increment on the otolith of an individual was interpreted incorrectly was calculated from a normal distribution of error rates $N(a, \sigma_a^2)$ and the error-generating hypothesis appropriate for that sample (H_1, H_2, H_3). Errors were either randomly assigned values of +1 or −1 and then accumulated within a reading, for the scenario of independent interpretation errors within readings, or accumulated first and then their sum randomly assigned a sign, for the scenario that errors accumulated unidirectionally within the reading. At the end of the reading, the (signed) sum of errors was added to the known true age to give the age estimated with error according to H_1, H_2, or H_3.

Applying age acceptance criteria

The readings for all otoliths were then filtered and an age estimate was either accepted or rejected according to each of six age acceptance criteria. An estimate of age was accepted if the selected criterion was satisfied for at least one of each of three pairs of readings as follows. If the criterion was satisfied for comparison of the first and second readings, then the first estimate was accepted as the final age. If this test failed, the first estimate was compared with the third age reading and accepted if the criterion was satisfied, and if that test failed, the second and third readings were compared, with the second accepted if the criterion was satisfied. If all three pairwise comparisons failed to satisfy the selected criterion, that otolith was excluded from subsequent calculations of age-based parameters. The six criteria applied were (*i*) exact agreement, two readings matched exactly; (*ii*) $H_1(1)$, two readings differed by no more than one; (*iii*) $H_1(2)$, two readings differed by no more than two; (*iv*) APE, percent error between two readings was ≤5%; (*v*) H_2, two readings differed by no more than $0.1t + 1$, rounded to an integer value; and (*vi*) H_3, two readings differed by no more than $0.1\sum_{i=1}^{t}(1 + 0.025)^{i-1} + 1$, rounded to an integer value. We included the APE statistic (Beamish and Fournier 1981) as an acceptance criterion following the recommendation of Morison et al. (1998) that 5% APE is an acceptable upper limit of imprecision for age estimate data. Note that the APE and H_2 criteria are analogous in that both represent allowable discrepancies that are constant proportions of nominal age and that another criterion sometimes used, the coefficient of variation (CV) (Chang 1982), has similar characteristics (Campana 2001; Kimura and Anderl 2005) and would be expected to perform qualitatively similarly to the APE and H_2 criteria.

We kept the same acceptance criteria for all data sets in the above simulations, irrespective of the rate of interpretation error used in reading the ages. To consider the impact of having a mismatch between the per-increment rate of discrepancy (p) used to derive acceptance criteria under H_2 and H_3, we also applied a discrepancy rate of $p = 0.267$ to the data sets generated with the highest rate of interpretation error ($a = 0.15609$) as these two values are congruent for eq. 12. The overall simulation experimental design is summarised in Fig. 2.

Calculated metrics from accepted age data

We used the data (FL and estimated age) for the "accepted" individuals to calculate the following 10 metrics for each sample under each acceptance criterion: mean age; longevity, estimated as the mean age of the oldest 10% of accepted individuals; maximum age; mean FL at estimated mean age; "oldest FL", being the mean FL of the oldest 10% of accepted individuals; K, the growth rate parameter estimated from the VBGF fitted to the accepted data; L_∞, the average asymptotic FL estimated from the VBGF fitted to the accepted data; $\hat{Z}$, the coefficient of total mortality estimated from the descending arm of the catch curve for the accepted data (Ricker 1975); $\hat{Z}$-ages, the number of ages included in the catch curve estimate of $\hat{Z}$; and $\hat{Z}_H$, Hoenig's (1983) estimate of natural mortality (in this case equivalent to total mortality), adjusted for the geometric mean regression as suggested by Ricker (in Hoenig 1983). Catch curves were fitted for accepted ages from $t' = 1$ to the last age class in the accepted sample before two consecutive frequencies of zero (Kritzer et al. 2001), there being no selectivity function applied when sampling from the parent population and so all age classes were "fully selected", resulting in no "ascending" limb of the catch curve.

Comparing estimated sample metrics with known values

We averaged the 200 estimates of the above metrics derived from the 200 samples selected for ageing with either H_1, H_2, or H_3 errors and calculated the percent difference between the mean estimates and the corresponding true population values (mean age, maximum age, FL at mean age, $\hat{Z}$, $\hat{Z}_H$) or true sample value (longevity, oldest FL, K, L_∞, $\hat{Z}$-ages). These mean deviations were plotted to explore patterns in bias arising from the various scenarios modelled.

Results

Trends in percentage of discrepant readings

A total of 412 discrepancies were recorded between repeated readings of 1742 *L. bohar* otoliths (23.7%). Inspection of plots of PD against nominal age bins (Table 1) indicated no obvious departure from linearity among groups, so a two-factor ANCOVA was done to compare the relationship among areas and preparation methods. Slopes of the relationship did not vary significantly with either geographic area ($F_{[1,24]} = 2.048$, $p = 0.165$) or preparation method ($F_{[2,24]} = 0.054$, $p = 0.948$) or their interaction ($F_{[2,24]} = 0.024$, $p = 0.977$). Accordingly, data were pooled across geographic areas and preparation methods, resulting in sufficient data to analyse trends in PD with nominal age rather than in bins of three year classes. The fits of empirical models to the relationship between PD and nominal age and parameter estimates are shown (Table 5).

Fig. 2. Basic experimental design for the simulations of ageing error and the influence of age acceptance criteria on estimation of age-based metrics. Two hundred samples, each of 1679 individuals, were sampled with replacement from a common parent population for application of each hypothesis about the genesis of ageing errors (H_1, H_2, H_3). Repeat age "observations" were then generated from each sample under the indicated rates of interpretation error (a) and type of error accumulation (s). The six acceptance criteria were then applied to each set of observations. Criteria: APE, readings within 5%; =, readings match exactly; ±1 or ±2, readings differ by no more than 1 or 2, respectively; ±% or ±%(t) (where t = age, indicating that the percent difference between readings varies with the number of increments read), readings differ by no more than a constant (%) or increasing (%(t)) percentage, respectively, of nominal age.

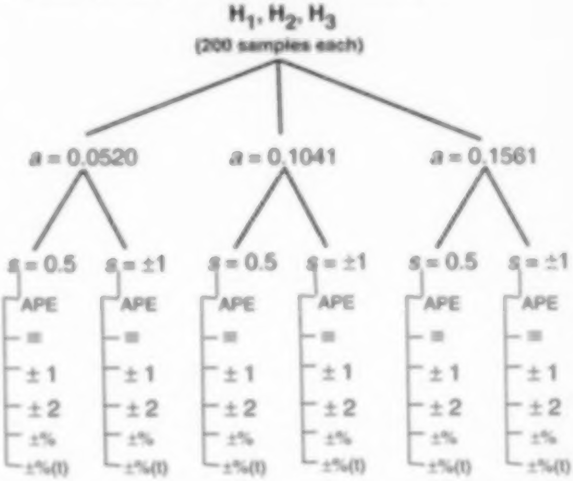

The "p constant" model (Table 2), representing H_2, fitted the observed data best ($R^2 = 0.53$; Fig. 3). The difference in AIC$_c$ between this model and next best (H_3, p increasing with age) was greater than 2, indicating that the H_2 model better described the data (Burnham and Anderson 1998). It is notable that the estimates of p did not differ significantly between these models (Table 5). The calculated AIC$_c$ for the "J uniform" model was more than 10 higher than that calculated for the best approximating model, which is sufficient evidence to reject that model (Burnham and Anderson 1998) and, by inference, H_1.

The estimate of $\hat{p}$ (the probability of successive interpretations of each annulus being discrepant) was not very high (0.09), but the cumulative effect of reading additional annuli resulted in a marked increase in J. The curve describing the expected cumulative rate of discrepancy (J) continued to increase with increasing numbers of annuli counted to 84.8% (PD) when 20 annuli were counted, and then to 97.9% or more after counting around 30 annuli (Fig. 3). It is also noteworthy that the spread of observed discrepancies about the expectation increased considerably when more than 20 annuli were counted (Fig. 3).

Trends in the magnitude of inter-read discrepancies

Because only those data from discrepant replicate readings (i.e., IRD > 0) were analysed, sample sizes were not

Fig. 3. Fit of the "*p* constant" model (H_2) to the observed percentage of samples for which first and second age readings disagreed (PD) per nominal age.

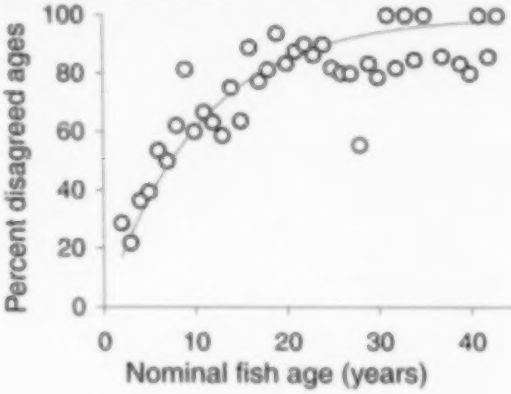

Fig. 4. Fit of the linear model (*p* constant, solid line) to observed mean inter-read discrepancy (IRD) with nominal fish age.

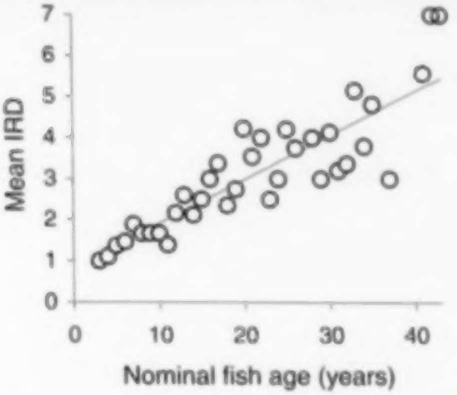

Fig. 5. Standard error of inter-read discrepancies (IRD) indicating the precision of calculated mean IRD for each nominal age class.

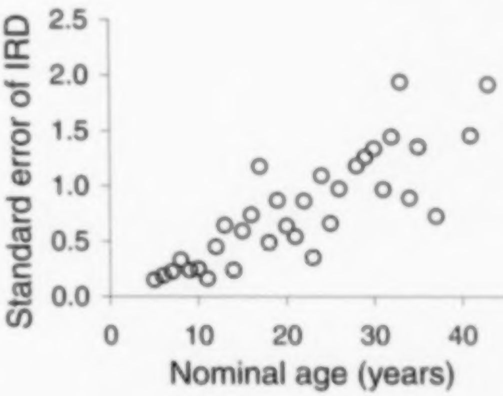

sufficient for a full model (main effects and interactions) two-factor ANCOVA for the factors of geographic area and preparation method. Accordingly, a main effects only analysis was done. An initial inspection of plotted mean IRD against age bins of 5 (i.e., 5–9, 10–14,…, 35–39 years) indicated no significant departures from linearity, so no transformations were required. There was no significant influence of geographic area ($F_{[1,14]}$ = 0.003, p = 0.96) or preparation method ($F_{[2,21]}$ = 2.60, p = 0.107) on the slope of mean IRD against bin, again indicating that data could be pooled across preparation methods and geographic areas, allowing fitting of models to mean IRD at single nominal age classes.

The *p* constant (H_2) model again provided the best approximation (Table 6), consistent with the results for trends in PD with nominal age. Although the difference in AIC_c between this and the *p* increasing model indicated that H_2 and H_3 might have explained the observations equally well ($\Delta \leq 2$; Burnham and Anderson 1998), the estimate for the rate at which *p* increased with nominal age (for H_3) was negligible and not significantly different from zero (b = 0.025 ± 0.029 SE).

The *p* constant model predicted a mean IRD of 0.96 increments for nominal age 1, which increased by 0.107 with each successive increase in nominal age (Fig. 4), providing further justification for establishing an acceptance criterion that was a constant proportion of nominal fish age. The observed trend in mean IRD was less precise for older age classes, however, because the standard error of IRD was shown to increase with nominal age (Fig. 5). This may be a result of the expected increase in variance with increasing nominal age, which has been observed in other ageing studies (Lai and Gunderson 1987; Eklund et al. 2000), and of having fewer fish of older nominal age in the sample.

Effects of age acceptance criterion on population parameter estimates

Base case: errors independent among increments, a = 0.0520

Percent biases introduced in estimates of nine of the metrics by applying each age acceptance criterion to each form of interpretation error (H_1, H_2, H_3) when interpretations were independent among increments and the mean per-increment error rate was 0.0520 are shown (Fig. 6). These conditions are referred to as the "base case" scenario. Two of the age metrics (mean age, longevity) and both length metrics (FL at mean age, FL of oldest 10%) were underestimated when ageing errors arose from H_2 or H_3 but were expected to match exactly or differ by no more than 1. Only biases introduced by requiring an exact match, however, exceeded 2 standard deviations (SD) of the estimator. Most biases were small and negative, except for those for data filtered by the APE criterion, which tended to be small and positive (Fig. 6). Biases in the age metrics (up to ~20%) were considerably greater than those in length metrics, which were mostly less than 1% (Fig. 6). Bias in growth parameter estimates was consistently very small (<0.6%) and never exceeded 2 SD of the estimator. *K* tended to be slightly overestimated and L_∞ underestimated except for data with interpretation errors generated according to H_1, for which the pattern was reversed (Fig. 6). Mortality metrics were those most affected by choice of acceptance criterion, with $\hat{Z}$ being consistently overestimated by up to 36.6%, and the number of ages from which it was calculated consistently and

Fig. 6. Percent bias (vertical axes) in estimates of nine age-based demographic metrics estimated from samples with different sources of ageing error (H_1, solid bars; H_2, shaded bars; H_3, open bars) after filtering duplicate age readings by six different age acceptance criteria: APE, readings within 5%; =, readings match exactly; ±1 or ±2, readings differ by no more than 1 or 2, respectively; ±% or ±%(*t*), readings differ by no more than a constant (%) or increasing (%(*t*)) percentage, respectively, of nominal age. Bias is expressed as the percent deviation between the estimator and the true population or sample value. Negative and positive values indicate underestimation and overestimation, respectively. Plotted results are for the base case conditions (interpretation error rate (*a*) = 0.0520, errors independent among increments within a reading). (*a*) Age metrics; (*b*) mortality metrics; (*c*) length metrics; (*d*) growth metrics.

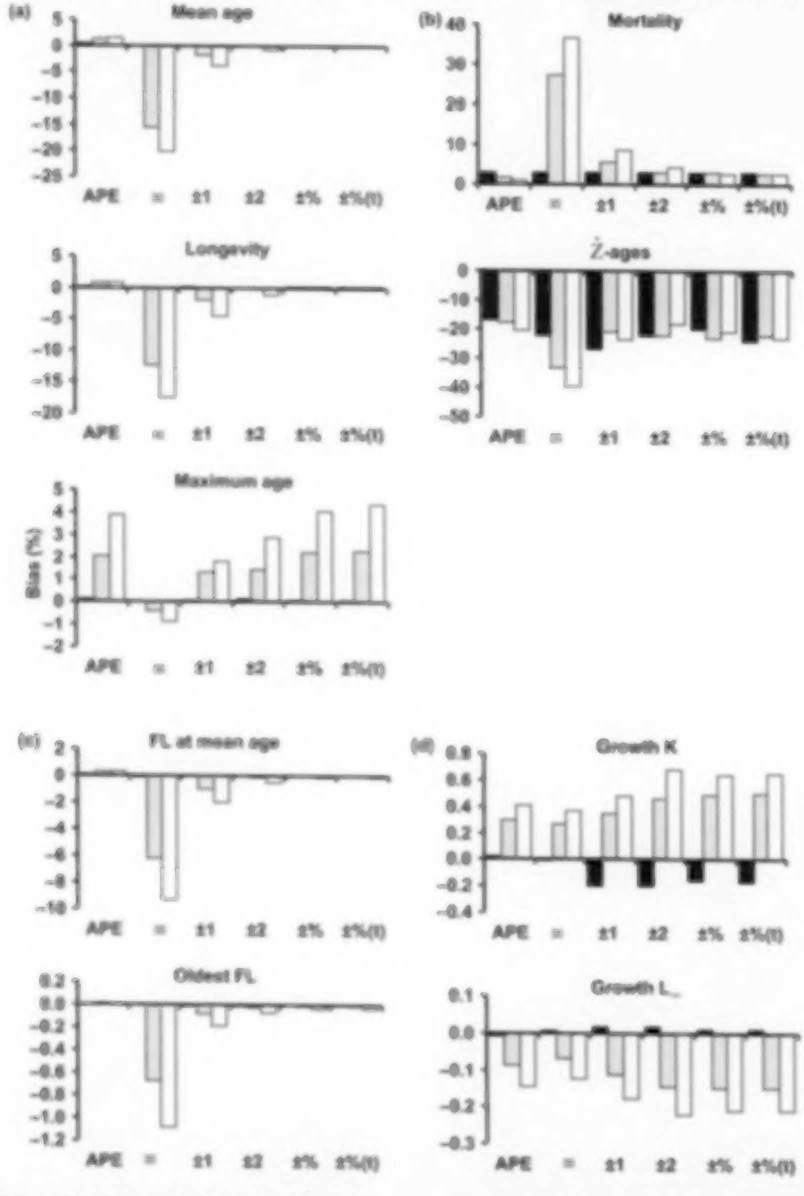

greatly (by ~20%–30%) underestimated (Fig. 6). All the results for $\hat{Z}$-ages (i.e., the number of age classes from which $\hat{Z}$ was calculated) exceeded 2 SD of the estimator but only estimates of $\hat{Z}$ from exactly matched readings of H_2 and H_3 data sets did so, despite overestimation by up to 9% in several other scenarios.

Maximum age was increasingly overestimated by increasingly liberal acceptance criteria for errors of types H_2 and H_3 (Fig. 6), though none of the biases exceeds 2 SD of the estimator. We deduce that maximum age is intrinsically prone to overestimation when ageing errors are random and unbiased because the oldest age estimates are likely to result in deviations from true fish ages that bracket (and therefore exceed) the true maximum age sampled. Accordingly, estimates of longevity sometimes are based on the average of some proportion of the oldest aged individuals (e.g., Begg et al. 2005). Bias in estimates of longevity or maximum age would be expected to bias estimates of mortality using Hoenig's (1983) method based on either metric. The percent bias in estimates of longevity under different defining criteria for longevity when increment interpretation errors were independent within readings is plotted (Fig. 7), as is the biases in Hoenig's estimate of mortality arising from each definition of longevity (Fig. 8). Analogous plots when interpretation errors accumulate unidirectionally within readings are provided (see Supplemental Figs. S1 and S2[3]).

Estimates of longevity clearly improved as smaller proportions of the oldest individuals were used to estimate the metric (Fig. 8). Most estimates were underestimates, though slight overestimation also occurred when liberal acceptance criteria were applied only to the very oldest individuals with data of types H_2 and H_3 (Fig. 8). Overall, the most generally reliable estimates of longevity were derived from the upper 0.5%–0.1% of age estimates. Bias varied with acceptance criterion only for H_2 and H_3 data and tended to be more extreme (underestimation) for the most conservative criteria (exact agreement or ±1). Biases were generally increased, both for under- and over-estimation of longevity, when errors accumulated unidirectionally within readings, with the changes being most extreme when the most stringent acceptance criteria were applied for errors generated under H_2 and H_3 (Supplemental Fig. S1[3]).

Bias in the Hoenig estimates changed considerably over the range of longevity estimates from overestimation when longevity was estimated from larger components of the population (upper 10%–5%) to underestimation when longevity was defined by increasingly smaller components of the population (Fig. 8). As with longevity estimates, acceptance criterion had no impact on bias in the Hoenig estimates for H_1 data but did influence biases for H_2 and H_3 data (Fig. 8). The more stringent acceptance criteria (especially exact agreement) precipitated the greatest overestimation bias, whereas the more liberal criteria tended to produce slightly greater underestimation bias (Fig. 8). In most cases, Hoenig estimates of mortality were generally relatively close to the correct value when based on longevity estimates from the oldest 5%–2.5% of the accepted ages (Fig. 8). As with longevity, accumulating errors consistently within readings increased both under- and over-estimation bias in the Hoenig estimators, and those increases were greater for the more stringent acceptance criteria applied when errors arose under H_2 and H_3 (Supplemental Fig. S2[3]).

Influence of error accumulation type

The biases arising when errors were independent among increments are plotted against biases arising when error accumulation was unidirectional within readings (Fig. 9). In all cases, the biases for different scenarios and similar metrics (age, length, mortality, or growth) are closely clustered around a linear fit, indicating that the type of error accumulation does not alter the pattern of biases among different scenarios. Moreover, the linear fits to the data differ little in slope among data sets from the three hypothesised sources of interpretation errors (Fig. 9). The slopes are generally less than 1 and mostly around 0.5–0.7, indicating that the type of accumulation of errors does impact on the magnitude of biases, with biases when interpretation errors are independently signed among increments around 50%–70% of those when errors are in the same direction for all increments within a reading. The slopes for the H_1 data tend to be greater and more variable than for other data sets, but the

Fig. 7. Comparison of biases in estimates of longevity for different definitions of "longevity" or "maximum age". Longevity was estimated from data above the percentiles of accepted ages indicated on the horizontal axis, and bias (vertical axis) is the percent deviation of the estimated from the known longevity (56 years). The three plots show fits for data generated with errors of each type modelled ((*a*) H_1; (*b*) H_2; (*c*) H_3) filtered by each of six acceptance criteria (APE, readings within 5% (- ◆ -); =, readings match exactly (- + -); ±1 (- ° -) or ±2 (— × —), readings differ by no more than 1 or 2, respectively; ±% (- ■ -) or ±%(*t*) (- ● -), readings within constant or increasing percentage of nominal age, respectively). Errors were independent among increments within a reading.

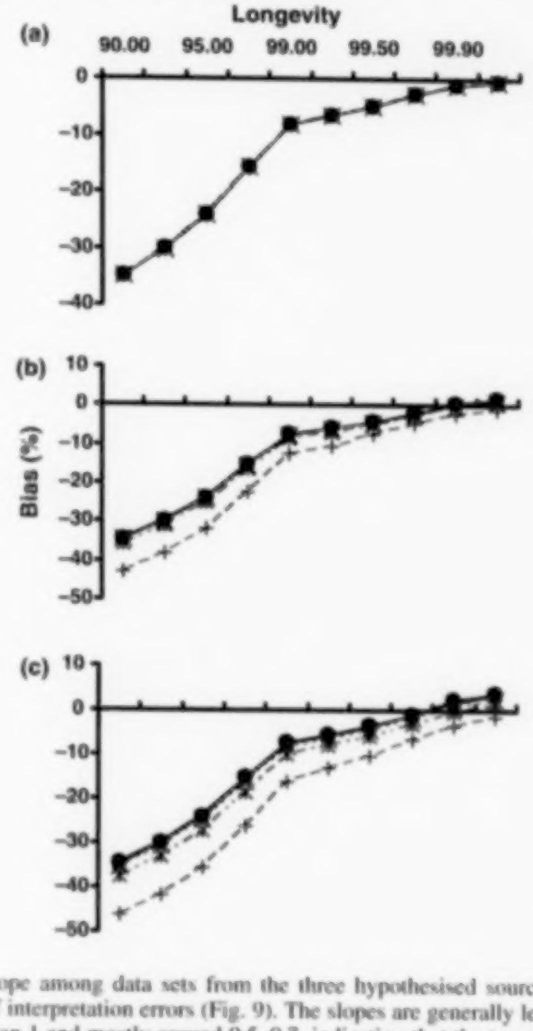

Fig. 8. Comparison of biases in estimates of mortality from Hoenig's (1983) method, after the adjustment of geometric regression suggested by Ricker (in Hoenig 1983), for different definitions of "longevity" or "maximum age". Longevity was estimated from data above the percentiles of accepted ages indicated on the horizontal axis, and bias (vertical axis) is the percent deviation of the estimated from the known rate of mortality (0.061). The three plots show fits for data generated with errors of each type modelled ((*a*) H_1; (*b*) H_2; (*c*) H_3) filtered by each of six acceptance criteria (APE, readings within 5% (- ◆ -); =, readings match exactly (- + -); ±1 (- * -) or ±2 (— × —), readings differ by no more than 1 or 2, respectively; ± % (- ■ -) or ±%(*t*) (- ● -), readings within constant or increasing percentage of nominal age respectively). Errors were independent among increments within a reading.

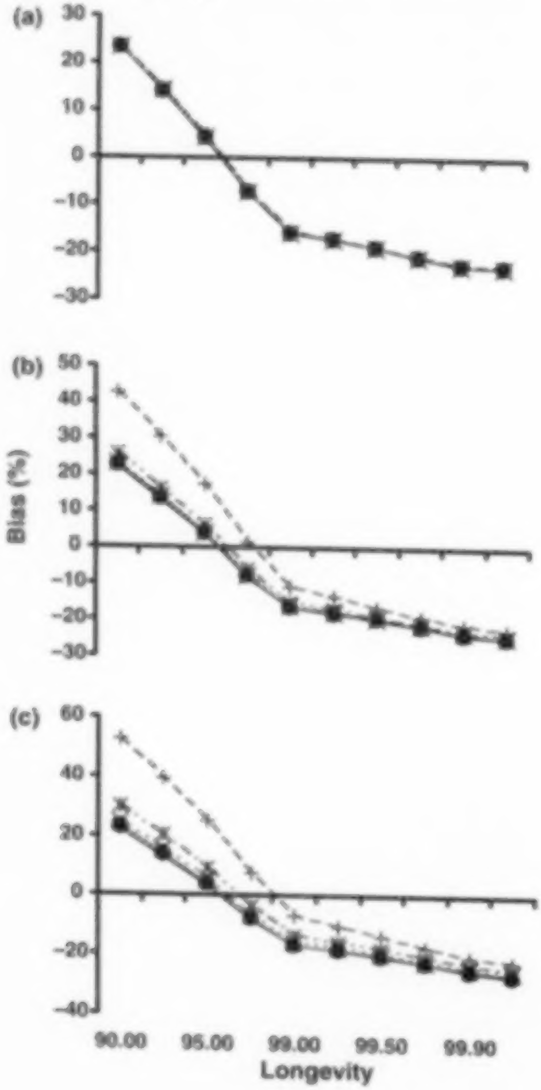

ranges of bias values for H_1 data are generally small and the slopes relatively poorly estimated. Errors that accumulated in the same direction within readings tended to increase the proportion of biases that exceed 2 SD of the relevant estimators, with the effects being most marked at the highest rate of interpretation error.

Effect of per-increment interpretation error rate

The relationships between biases arising from increased rates (to 0.1041 and 0.1561) of underlying interpretation errors (*a*) and the base case (a = 0.0520) are tabulated for the different error models in Table 7 (plots are provided in Supplemental Fig. S3[1]). Again, the relationships are tightly linear and, with the exception of the growth metrics, show remarkably little dependence on the source of errors in readings (H_1, H_2, H_3). Aside from the H_1 data, for which the slopes of the plots are again quite variable, the effect of increasing the interpretation error by 2- to 3-fold is to increase the magnitudes of biases by approximately 1.4- to 1.8-fold for age and length metrics, 1.3- to 1.4-fold for the mortality metrics, and around 2.5-fold (a = 0.1041) to 4.7-fold (a = 0.1561) for the growth metrics (Table 7). The magnitudes of biases also exceed 2 SD of the respective estimators more often as underlying rates of interpretation error increase.

The application of an acceptance criterion (based on p = 0.267) that corresponded to the highest rate of interpretation error (a = 0.1561) to data generated with this highest value of a had very little impact on the biases estimated from different scenarios. The plots of biases from the lower value of p against those with the higher value generally were tightly linear with slopes close to 1 (typically between 0.95 and 1.05).

There were marked patterns of bias among scenarios that were relatively consistent across all or most of the metrics we examined. First, with the exception of $\hat{Z}$-ages, biases from applying any of the acceptance criteria to H_1 data, with interpretation errors arising only in the first or marginal increments, were generally negligible and always the smallest for any metric. Second, again with the exception of results for $\hat{Z}$-ages, the H_3 data, for which rates of interpretation error increased with age, consistently caused the greatest biases under any acceptance criterion, with H_2 data (interpretation error constant for all increments) generally showing biases around 20%–30% smaller than for H_3 data for each acceptance criterion. Third, with the exception of the growth metrics, biases were generally greatest when an acceptance criterion of exactly matching readings was applied, with the criteria of requiring age estimates to be within 1 or 2 of each other usually the next most biased. Fourth, again with the exception of the growth metrics and $\hat{Z}$-ages, applying the acceptance criterion appropriate to H_2 or H_3 or the APE criterion generally produced trivial biases irrespective of the sources of interpretation error in the data, though this generalisation began to break down for the APE criterion at the highest rates of per-increment interpretation error. Finally, although biases in growth metrics generally were trivial, they displayed quite a different pattern among acceptance criteria than all the other metrics, with biases tending to be relatively constant (H_1 data) or increasing (H_2 and H_3 data) with the application of more liberal acceptance criteria.

Fig. 9. Comparison of biases in estimated metrics when increment interpretation errors accumulate consistently within a reading (horizontal axis) or independently within a reading (vertical axis) for data with errors arising according to H_1, H_2, or H_3. Linear fits to the data and R^2 values are shown, with subscripts on the left-hand side indicating the data set represented by each equation. Single linear regressions were fitted with all metrics combined in each category of (*a*) age (mean age, maximum age, longevity), (*b*) mortality ($\hat{Z}$, $\hat{Z}$-ages), (*c*) length (FL at mean age, mean FL of oldest 10%), and (*d*) growth (L_∞, K). Legend: H_1, ◇, – – –; H_2, □, —; H_3, △, - - -.

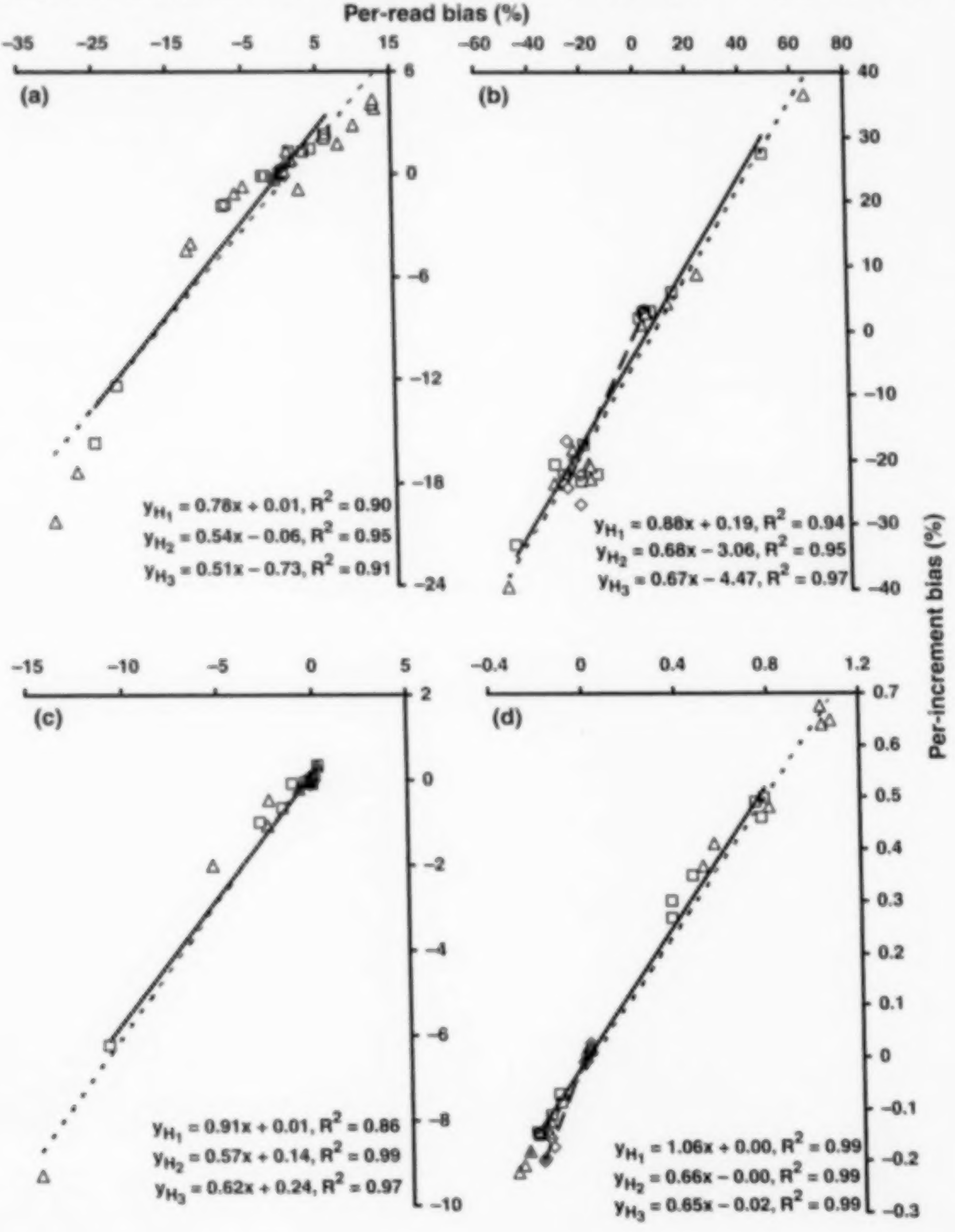

Table 7. Comparison of biases in estimated metrics under different rates of increment interpretation error when errors arose according to H_1, H_2, or H_3 and were independent among increments within a reading.

		Age		Mortality		Length		Growth	
Hypothesis	Error Rate	Slope	R^2	Slope	R^2	Slope	R^2	Slope	R^2
H_1	0.1041	3.02	0.92	0.91	0.95	2.95	0.86	1.84	0.98
H_1	0.1561	5.89	0.88	0.93	0.92	4.48	0.84	2.60	0.89
H_2	0.1041	1.43	0.96	1.31	0.97	1.62	0.85	2.65	0.96
H_2	0.1561	1.67	0.89	1.42	0.95	1.85	0.96	4.90	0.90
H_3	0.1041	1.43	0.95	1.28	0.98	1.36	0.99	2.43	0.96
H_3	0.1561	1.74	0.87	1.43	0.98	1.51	0.98	4.59	0.89

Note: Elevated interpretation error rates (a) of 0.1041 and 0.1561 were regressed against the "base case" (a = 0.0520), for which results are shown in Fig. 7, to estimate the relative impact of increased interpretation error on resultant bias in estimates. A regression slope of one would indicate no impact, whereas slopes greater than one indicate increased bias in estimates with increased per-increment error rates. Linear regressions were fitted with all metrics combined in each category of age (mean age, maximum age, longevity), mortality (Z, Z-ages), length (FL at mean age, mean FL of oldest 10%), and growth (L_∞, K). All intercepts were positive (0.9–3.0) but not significantly different from zero ($p > 0.05$) and so are not shown.

Discussion

Observation errors in age estimates

We have shown that discrepancies between repeated readings of *L. bohar* otoliths were consistent with a model for error generation in which all increments were interpreted with relatively constant probability of error. That rate of error was unaffected by a variety of methods used to prepare otoliths for reading or the geographic area from which the specimens came. Accordingly, the most appropriate criterion for filtering age estimates from multiple readings was a constant proportion of nominal fish age, rather than a constant absolute value. We reached this conclusion through a systematic analysis of the characteristics of discrepancies between paired readings of otoliths. The analyses are relatively simple and provide a straightforward means of determining empirically which criterion for acceptance of age estimates is likely to best suit the characteristics of reading errors associated with any ageing process. Although relationships between the rates and magnitudes of discrepancies and age are likely to be affected by the readability and structure of otoliths and the maximum age of the species being aged, our simulation results indicate some plausible general principles for the selection of age acceptance criterion. We suggest, however, that the approach we describe is a viable empirical approach to selecting age acceptance criteria and preferable to the automatic adoption of criteria from unrelated studies or by convention.

Other authors have simulated rates of ageing error with age to show that random ageing errors can bias estimates of mortality from the average age method (Powers 1983), catch-curve analysis (Barlow 1984), and optimum fishing mortality from yield per recruit analysis (Lai and Gunderson 1987). Eklund et al. (2000) demonstrated that between-reader biases increased with the nominal age and size of older Baltic herring (*Clupea harengus*), which had significant effects on estimates of mortality from cohort analysis. None of these studies, however, evaluated competing models for rates or magnitudes of ageing error with nominal age. We believe that the analytical approach adopted in this study provides three main benefits. First, it provides for the explicit testing of plausible hypotheses about the sources of ageing errors against easily quantified metrics on rates and magnitudes of discrepancies between readings that are routinely taken in ageing studies. Second, it provides a basis for discriminating among competing criteria for accepting or rejecting estimates of age based on the characteristics of the sample in hand. Third, it provides a mechanism for minimising the inevitable biases arising from a strategy of rejecting "unacceptable" age estimates and their effects on estimation of some important population parameters. It is important to note, however, that we explored only three credible models for the genesis of ageing discrepancy data and that other alternatives should not be ruled out in future work. For example, a reviewer of this paper noted unpublished evidence that interpretations errors in some species were more likely during the early years of life than later, meaning that interpretation errors might decrease, rather than increase, with the number of increments counted.

Simulations of effects on age-based parameters

We demonstrated through simulations parameterised from population data for *L. bohar* that the choice of age acceptance criterion could have substantial impacts on estimated population metrics, especially when overly conservative or strict acceptance criteria are applied to data for which interpretation errors were not similarly conservative. These biases were most apparent in the age and mortality metrics as a result of truncation of the age distribution or reductions in older age frequencies in "accepted" samples. Perhaps not surprisingly, greater rates of interpretation error increased the biases, in some cases several-fold.

We suggested above that the approach illustrated should be applied to each ageing study in which an age acceptance criterion is to be used to ensure that the applied criterion is appropriate. Our simulation results suggest, however, that if this empirical approach is not possible, the safest approach would be to apply a criterion of constant rate of error, with allowable discrepancies between readings increasing with nominal age (such as our H_2 type or APE), rather than a criterion of a static constant absolute allowable discrepancy for all ages (such as exact matches or differences of ±1 or ±2). The constant rate criteria generally produced the least biased estimates of most metrics irrespective of the underlying origin of interpretation errors and so would likely be most forgiving of being mismatched with the type of errors in an ageing data set.

The exception to the preceding generality was for the growth metrics, but in general, we also found that the VBGF parameters were estimated well and with fairly trivial biases in all but the most extreme error scenarios. This suggests that effects on the relative frequency of older age classes and (or) the maximum accepted age were not severe enough to result in a substantial extrapolation bias on L_∞, the most likely effect of rejection of older (and larger) fish from growth estimation. Extrapolation bias on L_∞ can arise when insufficient length-at-age data are sampled for older age classes in which asymptotic growth is inferred (but not demonstrated) to occur (Knight 1968; Francis 1988). The generally small biases in growth parameters might reflect the fact that even though higher proportions of older fish were excluded from analyses, those that were retained were safely within the inferred range of asymptotic growth for this species and thus not likely to have markedly influenced $\hat{L}_\infty$. Alternatively, if the readability of otoliths was demonstrated to change with the growth rate of individuals and this affected the probability of exact agreement, then the choice of age acceptance protocol might have an effect on the fit of the VBGF through the disproportionate rejection of data from faster- or slower-growing individuals.

Perhaps of greatest concern is the potential for significant biases in estimates of mortality if an inappropriately conservative acceptance criterion is applied. Bias in mortality estimates from catch curves reached over 100% if exactly matching readings were required under the highest rate of interpretation error we simulated and exceeded 20% for the widely used "static constant" criteria (±1 or ±2). Conversely, the marked overestimation of maximum age by the more liberal acceptance criteria, in the worst cases by ~37%, was accompanied by underestimation of mortality by the method of Hoenig (1983). Interestingly, the Hoenig method also tended to underestimate mortality even when longevity was reliably estimated, perhaps suggesting that the Hoenig estimates are intrinsically biased.

Longer-lived, slower-growing species are generally most vulnerable to overfishing (e.g., Adams 1980; Musick 1999). Sampling a sufficient number of individuals from the largest, oldest age classes of a population is often cited as difficult in the biological and fisheries literature (Knight 1968; Hoenig 1983). Biological data for the oldest age classes are particularly important for estimates of key demographic traits such as longevity and mortality rates. We demonstrated, using simulations, that the potential for increased rejection of samples from the oldest age classes due to application of unjustified, inappropriate, and potentially overly conservative age acceptance criteria (e.g., exact agreement) tends to accentuate this problem and leads to further bias in estimates of age-based population parameters. This, in turn, could lead to inappropriate management advice for the harvest of such populations, especially if natural mortality was significantly overestimated. We believe that these problems can be avoided using the approach demonstrated in this study.

In conclusion, we do not contend that the quantitative results we obtained for *L. bohar* will be general, again emphasizing the importance of analysis of each ageing process on its merits, but we do suggest that there are some general qualitative conclusions from this work. In particular, we consider that the adoption by convention of static constant age acceptance criteria should be abandoned. Such criteria are those most prone to bias in age estimation unless the underlying error-generating process matches the acceptance criterion (our H_1). If analytical choice of an appropriate acceptance criterion is not possible, adoption of a criterion of constant proportionality (e.g., APE, CV, or some form of our H_2) will be less likely to lead to biased age data than a static criterion under all the sources of interpretation error we considered and so will be more robust to mismatch between error-generation process and age acceptance criterion. We caution, however, that there may be interactions between the biases accompanying the acceptance criterion and the method of parameter estimation. For example, applying this generalisation is robust if estimating mortality from catch curves (Ricker 1975), but when mortality will be estimated by Hoenig's (1983) method, the constant rate criterion will produce poorer estimates of mortality than the use of a static constant criterion under some circumstances. Hence, as with all generalisations, caveat emptor.

Acknowledgements

We acknowledge financial support from the Australian Government's Cooperative Research Centres Programme through the Cooperative Research Centre for the Ecologically Sustainable Development of the Great Barrier Reef and the Antarctic Climate & Ecosystems Cooperative Research Centre. We thank the Effects of Line Fishing field team, commercial line fishers on the Great Barrier Reef, and Em. Prof. Howard Choat, Edwin Grandcourt, Jan Robinson, and the Seychelles Fishing Authority for assistance in the collection of samples. We also thank Gavin Begg, Andre Punt, Ashley Williams, and two anonymous reviewers for constructive comments on earlier drafts. This manuscript is a contribution from the CRC Reef Effects of Line Fishing Project.

References

Adams, P.B. 1980. Life history patterns in marine fishes and their consequences for fisheries management. Fish. Bull. **78**: 1–12.

Andrews, A.H., Burton, E.J., Coale, K.H., Cailliet, G.M., and Crabtree, R.E. 2001. Radiometric age validation of Atlantic tarpon, *Megalops atalanticus*. Fish. Bull. **99**: 389–398.

Barlow, J. 1984. Mortality estimation: biased results from unbiased ages. Can. J. Fish. Aquat. Sci. **41**: 1843–1847.

Beamish, R.J., and Fournier, D.A. 1981. A method for comparing the precision of a set of age determinations. Can. J. Fish. Aquat. Sci. **38**: 982–983.

Beamish, R.J., and McFarlane, G.A. 1983. The forgotten requirement for age validation in fisheries biology. Trans. Am. Fish. Soc. **112**: 735–743.

Begg, G.A., Mapstone, B.D., Williams, A.J., Adams, S., Davies, C.R., and Lou, D.C. 2005. Multivariate life-history indices of exploited coral reef fish populations used to measure the performance of no-take zones in a marine protected area. Can. J. Fish. Aquat. Sci. **62**: 679–692.

Brothers, E.B. 1987. Methodological approaches to the examination of otoliths in aging studies. *In* The age and growth of fish.

Edited by R.C. Summerfelt and G.E. Hall. The Iowa State University Press, Ames, Iowa. pp. 319–330.

Burnham, K.P., and Anderson, D.R. 1998. Model selection and inference: a practical information-theoretic approach. Springer-Verlag, New York.

Campana, S.E. 2001. Accuracy, precision and quality control in age determination, including a review of the use and abuse of age validation methods. J. Fish Biol. **59**: 197–242.

Campana, S.E., Annand, M.C., and McMillan, J.I. 1995. Graphical and statistical methods for determining the consistency of age determinations. Trans. Am. Fish. Soc. **124**: 131–138.

Chang, W.Y.B. 1982. A statistical method for evaluating the reproducibility of age determination. Can. J. Fish. Aquat. Sci. **39**: 1208–1210.

Crabtree, R.E., Cyr, E.C., and Dean, J.M. 1995. Age and growth of tarpon, *Megalops atlanticus*, from South Florida waters. Fish. Bull. **93**: 619–628.

Eklund, J., Parmanne, R., and Aneer, G. 2000. Between-reader variation in herring otolith ages and effects on estimated population parameters. Fish. Res. **46**: 147–154.

Ferreira, B.P., and Russ, G.R. 1994. Age validation and estimation of growth rate of coral trout, *Plectropomus leopardus* (Lacepede 1802), from Lizard Island, Northern Great Barrier Reef. Fish. Bull. **92**: 46–57.

Fournier, D., and Archibald, C. P. 1982. A general theory for analyzing catch at age data. Can. J. Fish. Aquat. Sci. **39**: 1195–1207.

Francis, R.I.C.C. 1988. Are growth parameters estimated from tagging and age–length data comparable? Can. J. Fish. Aquat. Sci. **45**: 936–942.

Francis, R.I.C.C., Paul, L.J., and Mulligan, K.P. 1992. Ageing of adult snapper (*Pagrus auratus*) from otolith annual increment counts: validation by tagging and oxytetracycline injection. Aust. J. Mar. Freshw. Res. **43**: 1069–89.

Hesp, S.A., Potter, I.C., and Hall, N.G. 2002. Age and size composition, growth rate, reproductive biology, and habitats of the West Australian dhufish (*Glaucosoma hebraicum*) and their relevance to the management of this species. Fish. Bull. **100**: 214–227.

Hoenig, J.M. 1983. Empirical use of longevity data to estimate mortality rates. Fish. Bull. **82**: 898–902.

Kimura, D.K., and Anderl, D.M. 2005. Quality control of age data at the Alaska Fisheries Science Centre. Mar. Freshw. Res. **56**: 783–789.

Kimura, D.K., and Lyons, J.L. 1991. Between-reader bias and variability in the age determination process. Fish. Bull. **89**: 53–90.

Knight, W. 1968. Asymptotic growth: an example of nonsense disguised as mathematics. J. Fish. Res. Board Can. **25**: 1303–1307.

Kritzer, J.P., Davies, C.R., and Mapstone, B.D. 2001. Characterising fish populations: effects of sample size and population structure on the precision of demographic parameter estimates. Can. J. Fish. Aquat. Sci. **58**: 1557–1568.

Lai, H.L., and Gunderson, D.R. 1987. Effects of ageing errors on estimates of growth, mortality and yield per recruit for walleye pollock (*Theragra chalcogramma*). Fish. Res. **5**: 287–302.

Manickchand-Heileman, S.C., and Phillip, D.A.T. 2000. Age and growth of the yellowedge grouper, *Epinephelus flavolimbatus*, and the yellowmouth grouper, *Mycteroperca interstitialis*, off Trinidad and Tobago. Fish. Bull. **98**: 290–298.

Mapstone, B.D., Davies, C.R., Little, L.R., Punt, A.E., Smith, A.D.M., Pantus, F., Lou, D.C., Williams, A.J., Jones, A., Ayling, A.M., Russ, G.R., and McDonald, A.D. 2004. The effects of line fishing on the Great Barrier Reef and evaluations of alternative potential management strategies. CRC Reef Tech. Rep. No. 52. CRC Reef Research Centre, Townsville, Australia.

Marriott, R.J. 2005. Population biology, dynamics and their implications for management of red bass: a large, long-lived reef fish. PhD. thesis, James Cook University, Townsville, Australia.

Marriott, R.J., and Cappo, M. 2000. Comparative precision and bias of five different ageing methods for the large tropical snapper *Lutjanus johnii*. Asian Fish. Sci. **13**: 149–160.

Marriott, R.J., and Mapstone, B.D. 2006. Geographic influences on the accuracy and precision of age estimates for the red bass, *Lutjanus bohar* (Forsskal 1775), a large tropical reef fish. Fish. Res. **80**: 322–328.

Morison, A.K., Robertson, S.G., and Smith, D.C. 1998. An integrated system from production fish ageing: image analysis and quality assurance. N. Am. J. Fish. Manag. **18**: 587–598.

Musick, J.A. 1999. Ecology and conservation of long-lived marine animals. *In* Life in the slow lane: ecology and conservation of long-lived marine animals. *Edited by* J.A. Musick. Am. Fish. Soc. Symp. **23**: 1–10.

Panfili, J., Pontual, H., Troadec, H., and Wright, P.J. 2002. Manual of fish sclerochronology. Ifremer–IRD Coedition, Brest, France.

Peres, M.B., and Haimovici, M. 2004. Age and growth of southwestern Atlantic wreckfish, *Polyprion americanus*. Fish. Res. **66**: 157–169.

Powers, J.E. 1983. Some statistical characteristics of ageing data and their ramifications in population analysis of oceanic pelagic fishes. *In* Proceedings of the International Workshop on Age Determination of Oceanic Pelagic Fishes: Tunas, Billfishes, and Sharks. *Edited by* E.D. Prince and L.M. Pulos. NOAA Tech. Rep. NMFS, **8**: 19–24.

Richards, L.J., Schnute, J.T., Kronlund, A.R., and Beamish, R.J. 1992. Statistical models for the analysis of ageing error. Can. J. Fish. Aquat. Sci. **49**: 1801–1815.

Ricker, W.E. 1975. Computation and interpretation of biological statistics of fish populations. Fish. Res. Board Can. Bull. No. 191.

Secor, D.H., Dean, J.M., and Campana, S.E. (*Editors*). 1995. Recent developments in fish otolith research. University of South Carolina Press, Columbia, South Carolina.

Smith, K.A., and Deguara, K. 2003. Formation and annual periodicity of opaque zones in sagittal otoliths of *Mugil cephalus* (Pisces: Mugilidae). Mar. Freshw. Res. **54**: 57–67.

Stevenson, J.T., and Secor, D.H. 1999. Age determination and growth of Hudson River Atlantic sturgeon, *Acipenser oxyrinchus*. Fish. Bull. **97**: 153–166.

Performance of time-varying catchability estimators in statistical catch-at-age analysis

Michael J. Wilberg and James R. Bence

Abstract: We used Monte Carlo simulations to evaluate how different methods of estimating fishery catchability within statistical catch-at-age analysis (SCA) performed when fishery catchability changed over time. Data-generating models included cases where catchability changed abruptly or gradually over time and where catchability was explicitly a function of population abundance, and we considered corresponding estimation models. In many cases, including fishery effort data in the estimation model and allowing catchability to follow a random walk provided the best (or nearly best) estimates of biomass in the last year as measured by the median of the absolute value of the relative error. Exceptions were cases where fishing mortality was low and catchability trended over time. The estimation model that ignored fishery effort data performed well in cases with a good survey, but performance degraded as survey precision decreased. The white noise estimation model performed poorly in situations where catchability trended over time. No estimation model was best for all underlying models of catchability, but the random walk estimation model performed well under most circumstances and should be used as a starting point for SCAs.

Résumé : Des simulations de Monte Carlo nous ont servi à évaluer comment fonctionnent les différentes méthodes d'estimation de la capturabilité de pêche dans des modèles statistiques de captures en fonction de l'âge (SCA), lorsque la capturabilité de pêche varie dans le temps. Les modèles de génération de données englobent des situations dans lesquelles la capturabilité change abruptement ou graduellement dans le temps et dans lesquelles la capturabilité est explicitement une fonction de l'abondance de la population et nous avons considéré les modèles d'estimation correspondants. Dans plusieurs cas, inclure les données d'effort de pêche dans le modèle d'estimation et laisser la capturabilité suivre un trajet aléatoire fournissent les meilleures (ou presque les meilleures) estimations de la biomasse de l'année précédente, d'après la mesure de la médiane de la valeur absolue de l'erreur relative. Les exceptions incluent les cas où la mortalité due à la pêche est basse et la capturabilité suit une tendance temporelle. Le modèle d'estimation qui ne tient pas compte des données d'effort de pêche fonctionne bien dans les cas qui comportent un bon inventaire, mais sa performance se dégrade à mesure que la précision des inventaires diminue. Le modèle d'estimation de bruit blanc fonctionne mal dans les situations où la capturabilté suit une tendance temporelle. Aucun des modèles d'estimation ne s'avère être le meilleur pour tous les modèles sous-jacents de capturabilité, mais le modèle d'estimation de trajet aléatoire fonctionne bien dans la plupart des circonstances et devrait servir de point de départ pour les SCA.

[Traduit par la Rédaction]

Introduction

Statistical catch-at-age analysis (SCA) is used to estimate abundance, recruitment, and fishing mortality for many exploited fish stocks throughout the US and the rest of the world (National Research Council (NRC) 1998; Quinn and Deriso 1999). In contrast to virtual population analysis and its variants, SCAs generally assume that fishing mortality rate at age can be modeled as a function of a year effect and an age effect (selectivity). This approach allows statistical estimation in which fishery catch-at-age data are assumed to be measured with error (Fournier and Archibald 1982; Megrey 1989). These models require catch-at-age data, as well as an index of abundance; other data sources can also be included in the model (Deriso et al. 1985). Under many conditions, SCA provides more accurate estimates of stock size and other important management quantities than other stock assessment techniques (NRC 1998; Punt et al. 2002; Radomski et al. 2005).

Many SCAs use fishery catch-per-unit-effort (CPUE) as an index of relative abundance and thus assume that fishery CPUE is proportional to abundance (Quinn and Deriso 1999). However, violations of this assumption can cause SCA models (and other stock assessment models) to produce

Received 8 September 2005. Accepted 18 May 2005. Published on the NRC Research Press Web site at http://cjfas.nrc.ca on 29 September 2006.
J18878

M.J. Wilberg[1,2] **and J.R. Bence.** Department of Fisheries and Wildlife, Michigan State University, 13 Natural Resources Building, East Lansing, MI 48824, USA.

[1] Corresponding author (e-mail: wilberg@cbl.umces.edu).
[2] Present address: Chesapeake Biological Laboratory, University of Maryland Center for Environmental Science, P.O. Box 38, Solomons, MD 20688, USA.

doi:10.1139/F06-111

biased estimates (NRC 1998). Time-varying catchability has been documented in a wide range of fisheries, spanning commercial and recreational fisheries and freshwater and marine systems. In some cases, catchability may change with abundance or the area inhabited by a stock (e.g., Peterman and Steer 1981; Winters and Wheeler 1985; Harley et al. 2001), environmental effects (Ziegler et al. 2003), or changes in fisherman behavior or gear (Hilborn and Walters 1992). Interactions between population size, stock area, and fisherman behavior can lead to hyperstable fishery CPUE, where CPUE remains high despite decreases in abundance (Hilborn and Walters 1992; Harley et al. 2001). Hyperstable CPUE in combination with a stock assessment model that does not account for this can lead to overestimated stock size and catch limits (NRC 1998).

Methods have been developed to account for time-varying fishery catchability (e.g., Fournier and Archibald 1982; Fournier 1983; Methot 1990), but there is little consensus about best practices in this area. Generally, fishery effort or CPUE data are ignored if an independent survey is available for a stock (NRC 1998). However, in many fisheries, survey data are not available and ignoring fishery effort data is not an option (NRC 1998). Likewise, ignoring fishery effort data may decrease the accuracy and precision of SCA estimates in some cases because fishery CPUE may be informative about changes in relative population size in comparison to survey data. Our objective was to determine how well different methods of estimating time-varying catchability performed within an SCA framework. Specifically, we tested four estimation models to determine how well they performed in scenarios where catchability changed over time.

Materials and methods

We used Monte Carlo simulations to compare how four different methods of estimating fishery catchability within an SCA model performed when models were confronted with different data-generating scenarios. Our data-generating models included five cases where catchability changed abruptly or gradually over time and where catchability was explicitly a function of population abundance. Our data-generating models also contained three levels of fishing mortality and three levels of survey measurement error. Although the general influence of fishing mortality level and survey measurement error on the performance of SCA methods is well understood (e.g., Bence et al. 1993), we included these factors to determine whether they act to change the relative performance of different approaches of modeling time-varying catchability. We generated 1000 data sets for each scenario (45 total scenarios). For data sets that included survey data, we fitted each data set with four different models that made different assumptions regarding fishery catchability: catchability was modeled as white noise, a random walk, or density-dependent or catchability was effectively estimated as a free parameter for each year. This last method ignores any information contained in fishery CPUE or effort because the fishing mortality rate for fully selected age classes is estimated as a parameter during the model fitting procedure (rather than calculated from estimated catchability and observed effort). This method can only be used if an independent index of abundance is available. For data sets that did not include survey data, we used the first three of these estimation methods. Each scenario used the same sets of random numbers.

All models contained 15 years of data and eight age classes, with the last age class representing all fish that age and older. Data-generating models were based on commercial fisheries for lake whitefish (*Coregonus clupeaformis*) in the upper Great Lakes. Symbols and equations defining the data-generating models and estimation models are presented in Tables 1, 2, and 3. Equations are referred to in the text as eq. T*x*.*y*, where *x* is the table number and *y* is the equation number within Table *x*. To avoid redundancy, equivalent quantities and parameters in estimation and data-generating models are not differentiated except when they both appear in the same equation, in which case, estimated quantities are denoted with a caret above the symbol.

Data-generating model

The data-generating model described the population dynamics and created data sets of total fishery catch, the age composition of the fishery catch, and in some scenarios, total survey CPUE and the age composition of the survey. For the population dynamics, we used an age-structured model that followed cohorts over time. Recruitment (abundance at age 1) was generated from a lognormal distribution with a log-scale standard deviation (SD) of 100%. The SD is approximately equal to the coefficient of variation on the arithmetic scale. Numbers-at-age in the first year were calculated assuming a stable age distribution with lognormal errors, where recruitment and mortality rates before the first year of the simulation were on average the same as in the first year (eq. T2.1). Cohorts were tracked over time by applying a simple exponential mortality model (eq. T2.2*a*); the last age class was treated as representing all fish age 8 and older (eq. T2.2*b*). Biomass each year was the sum of age-specific abundance multiplied by mean weight-at-age (eq. T2.3).

We used a separable model to generate fishing mortality rates. Total mortality rates were determined by the natural mortality rate and age-specific fishing mortality rates (eq. T2.4). Instantaneous natural mortality rate (M) was held constant across ages and years at 0.25. Instantaneous fishing mortality rate was a function of catchability, fishing effort, and age-specific selectivity (eq. T2.5). We used three levels of fishing mortality where F at fully selected ages was approximately $2M$ (high), M (medium), and $0.5M$ (low). We allowed fishing mortality to change over time by allowing effort to change (Fig. 1) and by incorporating several processes of time-varying catchability (see below). The pattern of increasing then decreasing effort provides contrast in fishing mortality rates, which is different than the pattern of catchability, and can be thought of as simulating periods of fishery development and subsequent regulation that reduces effort (although this is probably not the ideal evolution of management for a fishery). For a given level of fishing mortality, each of the models used the same effort series and each effort series had the same amount of contrast in absolute terms. The selectivity pattern for the fishery was dome-shaped to simulate a gill net fishery (Fig. 2).

We included five models for time-varying catchability, incorporating a range of possible ways that catchability could vary over time. The log of catchability was modeled as

Table 1. Symbols and descriptions of variables for data-generating and estimation models.

Symbol	Description	Value (if needed in the data-generating model)
$\bar{R}$	Average recruitment (numbers)	1 000 000
$N_{y,a}$	Abundance by age and year (numbers)	
B_y	Biomass (weight)	
$Z_{y,a}$	Total instantaneous mortality rate by age and year (year^{-1})	
$F_{y,a}$	Instantaneous fishing mortality rate by age and year (year^{-1})	
M	Instantaneous natural mortality rate (year^{-1})	0.25
$s_{a,f}$	Fishery age-specific selectivity	See Fig. 2
$s_{a,s}$	Survey age-specific selectivity	See Fig. 2
E_y	Fishery effort (effort)	See Fig. 1
$q_{y,f}$	Fishery catchability (effort^{-1})	
q_s	Survey catchability (effort^{-1})	0.0001
$\bar{q}_f$	Mean fishery catchability (effort^{-1})	0.05
$C_{y,a}$	Expected fishery catch-at-age (numbers)	
$I_{y,a}$	Expected survey catch-at-age (numbers)	
$\tilde{C}_y$	Observed total fishery catch (numbers)	
$\tilde{I}_y$	Observed total survey catch (numbers)	
$u_{y,a,f}$	Proportion of catch-at-age in fishery	
$u_{y,a,s}$	Proportion of catch-at-age in survey	
w_a	Mean weight-at-age (weight)	0.16, 0.45, 0.82, 1.2, 1.55, 1.86, 2.11, 2.3
γ_a	Deviations from mean recruitment	
δ_y	Deviations for white noise catchability	
ε_y	Deviations for first-order autoregressive catchability	
ω_y	Deviations for random walk catchability	
α	Parameter for density-dependent catchability (low, medium, high)	175; 90; 35
β	Parameter for density-dependent catchability (low, medium, high)	0.53; 0.49; 0.42
a, b	Parameters for linear increase in catchability	0.032, 0.00225
q_1, q_2	Parameters for abrupt change in catchability	0.0402, 0.0598
f_y	Fishing intensity by year (year^{-1})	
ρ	Correlation parameter for autoregressive catchability	0.9
σ_γ	Log-scale standard deviation (SD) for recruitment variation	1.0
σ_η	Fishery measurement error SD	0.1
σ_ν	Survey measurement error SD	0.25; 1.0
σ_δ	SD for white noise catchability deviations	0.2
σ_ε	SD for autoregressive catchability deviations	0.16
σ_ω	SD for random walk catchability deviations	0.165

Note: Units for most model quantities are arbitrary, but we denote the type of units in parentheses after the description. Unitless quantities have no parentheses. Units for effort and catchability are arbitrary, and therefore, units on quantities that describe catchability are not displayed.

white noise to simulate a fishery where catchability varied from year to year about a constant mean (eq. T2.6), perhaps resulting from environmental effects, but where year-to-year deviations were not correlated. We also included four treatments that had varying amounts of autocorrelation: first-order autoregressive (AR(1)), density-dependent, linear increase, and abrupt change. The AR(1) process was also on the log scale (eqs. T2.7*a*, T2.7*b*). The AR(1) process simulates a case where catchability varies about its mean in an autocorrelated way but is not related to population abundance. We set the correlation (ρ) of the AR(1) process to 0.9 and the SD (σ_ε) to 0.16. This level of autocorrelation and SD produced 15-year time series that on average had a sample SD of about 0.2. This sample SD is lower than the expected stationary SD because the time series is not long enough to display the full range of dynamics of an autocorrelated process with these parameters. Density-dependent catchability followed a power relationship where catchability declined with increasing abundance (eq. T2.8; Fig. 3; Paloheimo and Dickie 1964). Because each of the different levels of fishing mortality had different average levels of abundance, we used three sets of parameters (α and β) to define the density-dependent power function, one for each level of fishing mortality. In the linear increase scenario, catchability increased linearly over time (eq. T2.9), which could represent learning by fishers or increases in gear efficiency. In the abrupt change scenario, catchability was constant until year 8 of the time series and increased to a higher level, where it re-

Table 2. Data-generating and estimation model equations.

	Model equations	Application
Population model		
(T2.1)	$N_{1,a} = \bar{R}e^{-\sum_{i=1}^{a-1} Z_{1,a}+\gamma_a}; \gamma_a \sim N(0, \sigma_\gamma^2)$	Generation
(T2.2*a*)	$N_{y+1,a+1} = N_{y,a}e^{-Z_{y,a}}$	Both
(T2.2*b*)	$N_{y+1,8} = N_{y,7}e^{-Z_{y,7}} + N_{y,8}e^{-Z_{y,8}}$	Both
(T2.3)	$B_y = \sum_a N_{y,a}w_a$	Both
(T2.4)	$Z_{y,a} = M + F_{y,a}$	Both
(T2.5)	$F_{y,a} = q_y E_y s_a$	Both
Catchability model		
(T2.6)	White noise: $\log q_{y,f} = \log \bar{q}_f + \delta_y; \delta_y \sim N(0, \sigma_\delta^2)$	Both
(T2.7*a*)	First-order autoregressive: $\log q_{1,f} \sim N\left(\log \bar{q}_f, \frac{\sigma_\varepsilon^2}{1-\rho^2}\right)$	Generation
(T2.7*b*)	$\log q_{y+1,f} = \log \bar{q}_f + \rho(\log q_{y,f} - \log \bar{q}) + \varepsilon_y; \varepsilon_y \sim N(0, \sigma_\varepsilon^2)$	Generation
(T2.8)	Density-dependent: $q_{y,f} = \alpha N_y^{-\beta}$	Both
(T2.9)	Linear increase: $q_{y,f} = a + by$	Generation
(T2.10)	Abrupt change: $q_{y,f} = \begin{cases} q_1 \text{ if } y < 8 \\ q_2 \text{ if } y \geq 8 \end{cases}$	Generation
(T2.11)	$\log q_{y+1,f} = \log q_{y,f} + \omega_y; \omega_y \sim N(0, \sigma_\omega^2)$	Estimation
(T2.12)	Freely estimate f_y (ignore fishery effort): $F_{y,a} = f_y s_{a,f}$	Estimation
Observation model		
(T2.13)	$C_{y,a} = \frac{F_{y,a}}{Z_{y,a}}(1 - e^{-Z_{y,a}})N_{y,a}$	Both
(T2.14)	$\tilde{C}_y = e^{\tau_y}\sum_a C_{y,a}; \tau_y \sim N(0, \sigma_\tau^2)$	Both
(T2.15)	$I_{y,a} = q_s s_a N_{y,a}$	Both
(T2.16)	$\tilde{I}_y = e^{\upsilon_y}\sum_a I_{y,a}; \upsilon_y \sim N(0, \sigma_\upsilon^2)$	Both

mained for the rest of the time series (eq. T2.10). This scenario simulated the adoption of a more efficient technology by the fishery. All models were parameterized to have the same expected catchability (over the time series) and similar variances of log q_f (Fig. 4). We achieved this by simulating data sets and adjusting the catchability parameters until the mean and variance of catchability were the same as in the white noise case. We used a value of 0.2 for the SD as the standard for all other catchability models. This value is similar to estimates of the SD of catchability for commercial fisheries in New Zealand (Francis et al. 2003) but was less than median values of the SD of fishery CPUE estimated by Harley et al. (2001) for International Council for the Exploration of the Sea fisheries of 0.4–0.8, which should be an upper bound for catchability variation.

Fishery catch was calculated with the Baranov catch equation (eq. T2.13; Quinn and Deriso 1999). We multiplied total catch by a lognormal measurement error to calculate observed fishery catch (eq. T2.14); the measurement error SD for fishery catch was 10%. Observed age compositions were generated by drawing a sample from a multinomial distribution of size *n* (100 for the fishery) with proportions equal to the expected catch-at-age in the fishery. Survey CPUE-at-age was calculated as the product of survey catchability, abundance, and survey selectivity (eq. T2.15), and observed survey CPUE was the product of total survey CPUE and a lognormal measurement error (eq. T2.16). Our simulation model contained three levels of survey quality with differing levels of measurement error: good SD = 0.25, poor SD = 1.0, and no survey. Catchability of the survey was constant over time. Observed survey age compositions were generated by drawing a random sample from a multinomial distribution of size 75 with proportions equal to the expected CPUE-at-age in the survey. We chose a slightly smaller effective sample size for the survey to simulate a situation where ages are determined for fewer individuals in the survey than in the fishery catch.

Estimation model

The estimation models were largely the same as the simulation models except for how catchability was estimated and how numbers-at-age in the first year and recruitments were

Table 3. Objective function equations for statistical catch-at-age analysis simulation study.

(T3.1)	$L = \sum_i \ell_i$	Objective function
(T3.2)	$\ell_1 = \frac{1}{2\sigma_1^2}\sum_y (\log(\bar{C}_y) - \log(\hat{C}_y))^2$	Fishery catch
(T3.3)	$\ell_2 = \frac{1}{2\sigma_s^2}\sum_y (\log(\bar{I}_y) - \log(\hat{I}_y))^2$	Survey catch-per-unit-effort
(T3.4)	$\ell_3 = -n_f \sum_y \sum_a u_{y,a,f} \log(\hat{u}_{y,a,f})$	Proportion-at-age in the fishery catch
(T3.5)	$\ell_4 = -n_s \sum_y \sum_a u_{y,a,s} \log(\hat{u}_{y,a,s})$	Proportion-at-age in the survey catch
(T3.6)	$\ell_5 = \frac{1}{2\sigma_\delta^2}\sum_y (\hat{\delta}_y)^2$	White noise catchability
(T3.7)	$\ell_5 = \frac{1}{2\sigma_\omega^2}\sum_y (\hat{\omega}_y)^2$	Random walk catchability

Note: Equations T3.3 and T3.5 were only used in estimation models that considered survey data. Equations T3.6 and T3.7 were only used in estimation models that modeled fishery catchability as white noise or a random walk, respectively.

Fig. 1. Effort series used for low (dotted line), medium (broken line), and high (solid line) fishing mortality scenarios. The average fishing mortality rates for fully selected age classes were approximately 2*M* for the high scenario, *M* for the medium scenario, and 0.5*M* for the low scenario.

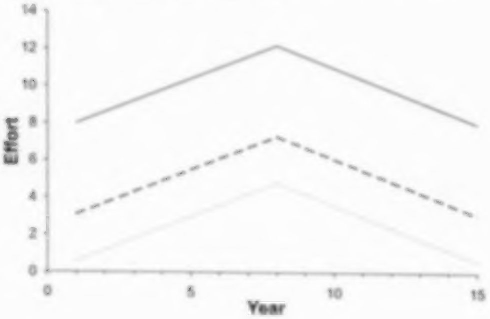

Fig. 2. Fishery (dotted line and open circles) and survey selectivity (solid line and solid circles) patterns used in the data-generating model.

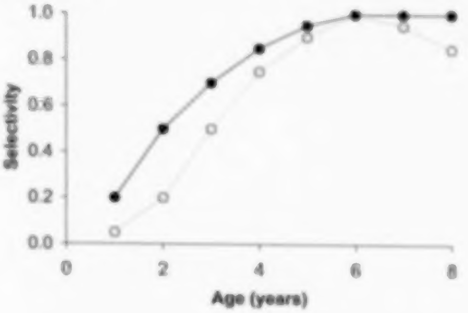

handled. Common parameters among models included $N_{1,1},\ldots,N_{15,1}$ (recruitment), $N_{1,2},\ldots,N_{1,8}$ (numbers-at-age in the first year), and $s_{1,f},\ldots,s_{7,f}$ (fishery selectivity); models with surveys also included $s_{1,s},\ldots,s_{7,s}$ (survey selectivity) and q_s (survey catchability). Numbers-at-age in the first year and recruitment for each year were estimated as parameters during the model fitting process. After the first year and age, abundance-at-age followed a standard exponential mortality model with the last age representing all fish that age and older (eqs. T2.2*a*, T2.2*b*).

The total mortality rate ($Z_{y,a}$) was the sum of M and $F_{y,a}$ (eq. T2.4); M was assumed known at 0.25 (the true value from the simulation models). Fishing mortality followed a separable model for all of our estimation models. Fishery and survey selectivities were estimated as individual parameters by setting selectivity at the oldest age class to one; selectivity for other ages were only constrained to be positive values, so fixing the selectivity of the oldest age class to one did not assume an asymptotic selectivity pattern. Estimation models contained four methods of estimating catchability: white noise, random walk, density-dependent, and no catchability (directly estimating fishing mortality) with survey data. The first estimation model allowed fishery catchability to vary with white noise about a constant mean (eq. T2.6). The second estimation model allowed fishery catchability to vary according to a random walk (eq. T2.11); in this estimation model, catchability in the first year is an estimated parameter. The third estimation model allowed catchability to be a density-dependent function (eq. T2.8). The density-dependent model did not contain any random deviations in order to match the assumptions from the density-dependent catchability data-generating model. In our fourth estimation model, we estimated the fishing mortality rate for fully selected age classes as a parameter and then applied the estimated fishery selectivity to calculate age-specific fishing mortality rates (eq. T2.17). This method does not use fishery effort as a data source. The estimation models also predicted proportions of fishery and survey catch-at-age.

Fig. 3. Density-dependent fishery catchability for low (short dash), medium (long dash), and high (solid line) fishing mortality scenarios in the data-generating model.

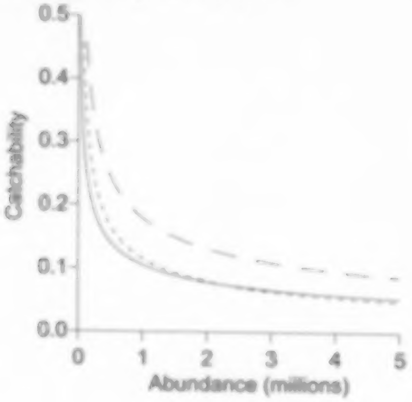

Model fitting and convergence

We fitted the models using a likelihood-based approach where we used a numerical search to find parameter values that minimized our objective function. The objective function was the sum of the likelihood components and each component was the negative of the log-likelihood for a single data source or a penalty related to time-varying catchability (eq. T3.1).

Our estimation models assumed lognormal distributions of errors for total catch for the fishery (eq. T3.2) and survey CPUE (eq. T3.3) and multinomial distributions for age compositions of the fishery (eq. T3.4) and the survey (eq. T3.5; Fournier and Archibald 1982). Effective sample sizes and SDs of the fishery and survey catch and age compositions were set to their true values from the data-generating models. The likelihood components for survey CPUE and age composition were only included in models that included survey data.

For estimation models that used fishery effort as a data source, fishery CPUE was not explicitly modeled. Instead, fishing mortality was an explicit function of effort, and catch was linked to abundance and fishery effort by estimating the catchability coefficient. We assumed lognormal deviations for catchability in the white noise (eq. T3.6) and random walk (eq. T3.7) estimation models. The SD for the white noise catchability was set to the true expected value, which was 0.2 for all data-generating models. For the random walk model, we set the SD to 0.165, the SD that on average created a time series with a sample SD of 0.2. This component in the objective function can be thought of as a penalty that produces a shrinkage estimator (in the Frequentist case) or as a Bayesian prior and penalizes large deviations from mean catchability (for the white noise model) or large year-to-year deviations (in the random walk model). Estimation models that contained density-dependent catchability or ignored effort data did not contain likelihood component ℓ_5.

We minimized the objective function iteratively using an efficient quasi-Newton implementation in AD Model Builder software (Otter Research Limited 2000) that takes advantage of automatic differentiation. We minimized the objective function in stages, where the initial stages were penalized if the model estimates deviated from the expected average fishing mortality rates under each scenario (early stages can be viewed as providing starting values for subsequent stages). This constraint was removed for the final stage of fitting and therefore did not penalize final model estimates. Iterative adjustment of the parameters terminated when the maximum gradient of parameters with respect to the objective function was less than 0.0001, or more than 1000 function evaluations had occurred. We denoted any terminated parameter estimates where the maximum gradient component was less than 0.0005 as converged, based on trial investigations after the completion of the simulations that used different parameter starting values.

Fig. 4. Examples of 15-year time series of catchability generated by a white noise process (solid line), an autocorrelated process (long dashed line), and a density-dependent process (short dashed line). Each of these time series has a sample standard deviation of about 0.2 on the log scale.

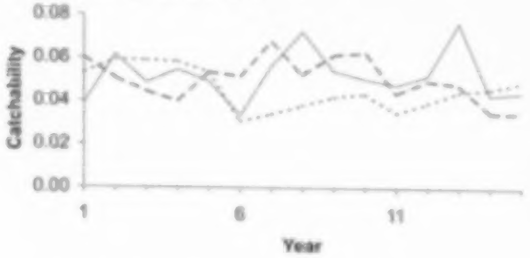

Evaluation of estimation model performance

In stock assessments, estimated quantities in the last year are often most important for forecasting and management. Therefore, we evaluated estimation model performance by calculating the relative error (RE) of estimated biomass in the last year:

$$\text{RE} = \frac{\text{estimated} - \text{true}}{\text{true}} \times 100 \qquad (1)$$

We report only results for stock size measured in biomass. Other common measures of stock size (e.g., measures of exploitable abundance) showed similar patterns and estimates of fully selected F or exploitation rate reflected similar but inverse patterns (i.e., if estimated biomass was higher than the true value, estimated F was usually lower than the true value and vice versa). We evaluated systematic over- or under-estimation using the median of the relative error (MRE). If MRE equals zero, half of the estimates are higher than the true value and half are lower than the true value. Throughout the rest of the paper, we use the term unbiased as meaning median unbiased (i.e., MREs near zero). We also compared estimation model performance using the median of the absolute values of relative error (MARE), which indicates the width of the distribution of REs if the median is zero. In situations where the REs are either all (or mostly) positive or negative, the MRE will equal the MARE. We compared relative performance of the estimation models by calculating the difference of their MAREs and report these differences as percentages because MAREs are reported as percentages. We used MRE and MARE instead of mean relative error and root mean squared error because mean values were heavily influenced by several cases with large relative errors (>100). We checked whether these outliers represented false convergence by restarting the estimation with different starting values. Convergence was verified and we obtained the same parameter estimates.

Results

All estimation models performed best in situations with high fishing mortality and low survey SD and worst in cases with low fishing mortality and no survey (Table 4, high, good). The performance of a given estimation model depended on the level of fishing mortality, survey quality, and data-generating model. In almost all cases, estimation models that made use of both survey CPUE and fishery effort outperformed models that used only fishery effort or survey CPUE. Performance of the estimation model that ignored fishery effort data was independent of the underlying catchability model that generated the data and was only a function of survey quality and fishing mortality. The estimation model that ignored effort data was relatively unbiased (MRE near zero) in all cases, but the MARE was often significantly higher than for estimation models assuming white noise and random walk catchability, and the relative performance of this method was highly dependent on survey quality. Small differences in performance among different catchability scenarios arose because differences in catchability dynamics created different patterns of fishing mortality and therefore slightly different population dynamics. For the other estimation models, the results can be separated into two categories: (*i*) all estimation models were relatively unbiased (scenarios without consistent trends in catchability; Table 4, WN, AR, DD) and (*ii*) some estimation models had substantial bias (linear increase and abrupt change; Table 4, LI, AC). Although the density-dependent estimation model was relatively unbiased in many cases, it performed relatively poorly overall because it failed to converge for 25%–85% (depending on the combination of underlying catchability model, survey SD, and level of fishing mortality) of the simulated data sets that did not contain density-dependent catchability; the other estimation models usually failed to converge less than 1% of the time. This lack of convergence likely occurred because the two parameters describing density-dependent catchability were confounded with one another (i.e., many combinations of α and β could produce equally good fits) for many data sets and thus the optimization procedure could not find a unique best solution. Because of the lack of convergence, results of the density-dependent model were omitted from the rest of the results section.

Scenarios without catchability trends

In cases where the data-generating models contained white noise catchability, first-order autoregressive catchability, or density-dependent catchability, all estimation models produced relatively unbiased estimates of biomass in the last year (i.e., MREs near zero; Table 4, WN, AR, DD), with the most biased estimation model in these scenarios having an MRE of only –8.7% (random walk estimation model fitting density-dependent generation model with low mortality and no survey). There were larger differences in precision among the estimators and this was reflected in MARE and the tightness of the distributions of relative errors (Table 4). For cases where the estimation model was the same as the data-generating model (white noise), the estimation model that matched the data-generating model performed best (i.e., had the lowest MARE and tighter distributions). In the case of the AR(1) data-generating model, the random walk model performed best in most cases. Differences in MARE among estimation models that modeled catchability as white noise or a random walk or ignored fishery effort were usually less than 5% for cases with good surveys (Fig. 5). However, MAREs of random walk and white noise estimation models were 10%–30% lower than estimation models that ignored fishery effort in cases with a poor survey. Differences in relative performance of estimation models were largely accounted for by differing performance of random walk and white noise catchability models because the performance of the estimation model that ignored fishery effort data was relatively constant for a given level of fishing mortality and survey quality.

Scenarios with catchability trends

The white noise and random walk estimation models were biased in cases where catchability increased linearly or increased abruptly, but the amount of bias depended on survey quality, fishing mortality rate, and data-generating model. The MREs of biomass in the last year for estimation models with white noise and random walk catchability were above zero in all cases, indicating a positive bias (Table 4, LI, AC). The positive bias seen in our simulations undoubtedly reflects the direction of change in catchability built into our simulations, where the estimation models did not fully account for the increase in fishery catchability. Neither the white noise nor the random walk estimation models performed well in cases with no survey, trending catchability, and low mortality. The amount of bias was highest in cases where fishery catchability changed abruptly and fishing mortality rates were low and decreased as the level of fishing mortality increased and as survey quality improved.

Although the random walk estimation model was biased, it usually had a lower MARE than the other estimation models, but performance relative to the other estimation models depended on the treatment. In cases with a good survey, the MARE of the estimation model that ignored fishery effort and the MARE of the random walk estimation model were within 5% of one another (Fig. 5). However, in cases with a poor survey, the random walk model usually had MAREs 8%–20% lower than the estimation model that ignored fishery effort. The estimation model that ignored fishery effort data only outperformed the random walk model in the scenario with an abrupt change in catchability and low or medium fishing mortality. The estimation model that ignored fishery effort and the random walk estimation model clearly outperformed the white noise estimation model in these cases and had MAREs 12%–50% lower than the white noise estimation model (Fig. 5).

Discussion

Often stock assessment scientists will not use or will substantially downweight (i.e., specify an arbitrarily large SD)

Table 4. Simulation results for statistical catch-at-age estimation model performance in cases where data-generating models included white noise catchability (WN), first-order autoregressive catchability (AR), density-dependent catchability (DD), linearly increasing catchability (LI), and an abrupt increase in catchability (AC).

			Estimation model					
			MRE (%)			MARE (%)		
q Model	Mortality	Survey	WN	RW	FF	WN	RW	FF
WN	Low	Good	–0.7	1.2	1.9	**19.3**	20.8	21.4
WN	Low	Poor	–0.2	–0.6	1.9	**21.4**	25.3	49.2
WN	Low	None	–0.4	–2.5		**23.7**	25.1	
WN	Medium	Good	0.2	1.4	2.7	**13.5**	14.7	16.6
WN	Medium	Poor	1.3	0.2	3.0	**15.9**	21.1	41.1
WN	Medium	None	1.3	–0.9		**17.9**	23.0	
WN	High	Good	1.1	0.7	3.2	**10.4**	12.4	14.9
WN	High	Poor	1.5	0.1	5.1	**12.7**	17.2	31.4
WN	High	None	1.8	0.8		**13.8**	19.1	
AR	Low	Good	–0.8	–0.2	0.4	26.2	**22.0**	23.0
AR	Low	Poor	0.0	–2.6	1.4	35.3	**33.2**	49.0
AR	Low	None	–0.2	–3.8		**39.6**	40.1	
AR	Medium	Good	0.1	0.5	3.5	20.6	**15.9**	17.2
AR	Medium	Poor	0.1	–4.9	2.1	29.5	**29.9**	41.1
AR	Medium	None	1.5	–4.3		32.9	**32.6**	
AR	High	Good	0.6	0.9	2.7	17.1	**13.2**	14.9
AR	High	Poor	0.6	–2.0	2.4	23.7	**19.6**	32.3
AR	High	None	1.0	–4.2		26.5	**23.7**	
DD	Low	Good	–2.2	1.6	1.7	23.1	**22.4**	23.2
DD	Low	Poor	–4.7	–2.3	4.3	32.4	**31.2**	51.1
DD	Low	None	–5.8	–8.7		36.8	**36.0**	
DD	Medium	Good	–3.0	1.3	2.8	17.0	**16.1**	17.9
DD	Medium	Poor	–3.2	–4.0	2.9	**24.6**	24.7	41.1
DD	Medium	None	–4.2	–7.1		**27.4**	27.7	
DD	High	Good	–0.3	1.1	3.2	13.0	**12.5**	15.0
DD	High	Poor	–0.1	–1.4	4.9	19.4	**17.9**	32.9
DD	High	None	–1.0	–3.4		21.5	**20.8**	
LI	Low	Good	35.4	5.1	2.3	35.4	**18.6**	23.0
LI	Low	Poor	78.4	41.2	4.1	78.4	**41.3**	49.3
LI	Low	None	75.6	62.0		75.6	**62.0**	
LI	Medium	Good	33.9	7.3	2.5	33.9	**14.4**	16.6
LI	Medium	Poor	67.5	30.1	3.7	67.5	**30.7**	38.5
LI	Medium	None	71.9	43.6		71.9	**43.6**	
LI	High	Good	30.8	7.2	3.1	30.8	**11.9**	14.3
LI	High	Poor	55.1	17.5	4.2	55.1	**19.0**	28.4
LI	High	None	61.2	21.8		61.2	**22.1**	
AC	Low	Good	52.5	16.6	2.1	52.5	25.4	**23.5**
AC	Low	Poor	110.3	65.9	6.0	110.3	65.9	**48.6**
AC	Low	None	149.7	127.0		149.7	**127.0**	
AC	Medium	Good	35.4	8.6	3.4	35.4	16.5	**16.4**
AC	Medium	Poor	69.3	27.9	2.5	69.3	**29.4**	38.6
AC	Medium	None	80.5	44.0		80.5	**44.0**	
AC	High	Good	27.5	3.6	2.6	27.5	**11.4**	14.4
AC	High	Poor	48.4	8.5	2.7	48.4	**14.6**	29.1
AC	High	None	53.7	10.7		53.7	**15.7**	

Note: Shown are median relative error (MRE) and median of the absolute values of relative error (MARE) for estimated biomass in the last year (year 15) from four statistical catch-at-age estimation models: white noise (WN), random walk (RW), density-dependent (power relationship; DD), and freely estimated F at maximum selectivity (*i.e.*, not fitted to fishery effort data; FF). Data-generating models included three levels of fishing mortality (high ($F = 2M$), medium ($F = M$), and low ($F = 0.5M$)), and three levels of survey precision (good (SD = 25%), poor (SD = 100%), and no survey). Bias is indicated by MREs different from zero, and lower MAREs indicate more accurate model predictions. Estimation models with the lowest MARE for each treatment are indicated in bold.

Fig. 5. Relative performance of (*a*) the estimation model that ignores fishery effort and (*b*) the white noise estimation model versus the random walk estimation model measured by the difference of the median of the absolute value of the relative errors (MARE). Points above zero indicate that the estimation model that ignored fishery effort data or the white noise estimation model had a larger MARE than the random walk estimation model and vice versa. Data-generating models are indicated by the symbol shape: white noise, ○; autoregressive, ■; density-dependent, ▲; linear increase, ◇; abrupt change, ●. Two letters identify each treatment: the first letter indicates the level of fishing mortality (L, low; M, medium; H, high) and the second letter indicates the level of survey quality (G, good; P, poor; N, none).

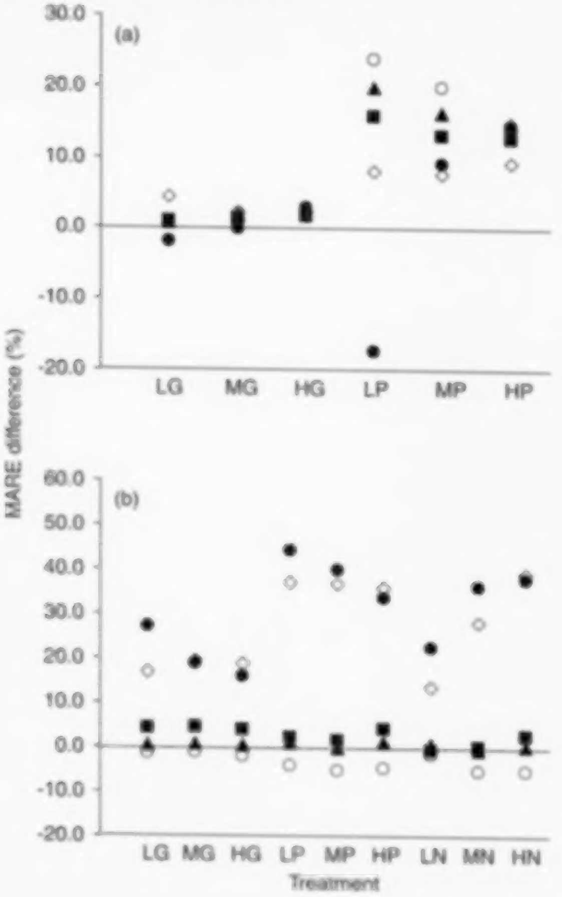

fishery effort or CPUE data in an SCA if a fishery-independent index of abundance is available for a given stock. Indeed, based on the results of their simulations, the NRC (1998) recommended that fishery-dependent indices of abundance should be ignored if an independent index of abundance is available, although many assessments will use both fishery-dependent and -independent data if they are available (Millar and Methot 2002; Francis et al. 2003). However, our results argue against automatically ruling out the use of fishery-dependent indices of abundance when a survey is present. In cases where the survey SD is large, we believe that use of fishery-dependent indices is justified if they are believed to contain information on stock size. Of course, fishery effort should be adjusted for known changes in fishing efficiency, and the estimation model should allow for flexible changes in catchability over time, as was the case for our random walk estimator. The reliability of fishery effort data may be suspect in some fisheries, and in these cases, it may make sense to ignore fishery effort. Using methods that do not allow for trends in catchability can lead to severely biased SCA estimates, and modeling fishery catchability as white noise (which is often done) may not provide the necessary flexibility for models to accurately depict system dynamics. Also, there may be a tendency to overstate the precision of survey data and understate the precision of fishery data in SCAs (Francis et al. 2003), which may degrade accuracy of SCA estimates.

Our recommendations are contrary to those of NRC (1998) because we evaluated a wider range of structural models for time-varying fishery catchability within SCAs, but our results yield similar insights for the cases they explored. In the NRC (1998) study, fishery catchability increased over time combined with density dependence; their survey had a SD of 30% (near the level of our "good" survey). Also, the NRC (1998) study mainly included SCA estimation models that contained white noise models for catchability or ignored fishery effort data (see Restrepo (1998) for details of models used in the NRC 1998 study). The exception was one estimation model where fishery catchability was modeled as a mixture of random walk and white noise processes. However, the SD of the white noise term was large relative to the SD of the random walk term (Ianelli and Fournier 1998), which likely caused the model to perform similarly to a white noise model. Similar to the results of NRC (1998), we also found that SCA models that ignored fishery effort data outperformed SCA models that modeled fishery catchability as white noise in cases with trending catchability.

Independent survey indices of abundance or relative abundance are extremely important for obtaining accurate SCA estimates, especially in situations with low fishing mortality. Our results agree with the NRC (1998) recommendation to use survey data if they are available. In our study, estimation models that utilized fishery effort data and survey data (even with a SD of 100%) outperformed models that used only fishery effort data, especially in cases where catchability trended over time and fishing mortality was not high.

It is important to standardize effort series to remove catchability trends to as large an extent as possible. Our experiments showed that SCA estimates were most biased when trends or abrupt changes in fishery catchability occurred and that all our estimation models performed reasonably well in cases where catchability did not trend over time. However, trending fishery catchability is probably a common phenomenon. Many mechanisms could lead to trends in fishery catchability, e.g., increasing power of the fishery, increasing aggregation of fish stocks and fishers, or trending recruitment dynamics and density-dependent catchability. Salthaug and Aanes (2003) presented a method to correct CPUE for the spatial distribution of fishing effort, which has been shown to affect catchability (Winters and Wheeler 1985; Rose and Kulka 1999). Also, improvements in vessels and other fisherman behaviors can be accounted for either by preprocessing (e.g., analyzing CPUE data to estimate mean CPUE by accounting for vessel characteristics and spatial and temporal patterns of fishing) fishery data or by integrating the standardization process into the stock assessment model (e.g., Maunder 2001; Maunder and Starr 2003; Maunder and Punt 2004).

Our results represent the relative performance of the estimation models rather than the absolute performance because, except for the catchability aspect, the structure and assumed values of some parameters of the estimation models were correct (i.e., the same as the data-generating model). Fishery selectivity may vary over time, which can cause biased estimates from SCA models if it is not accounted for (Radomski et al. 2005). Further, our data-generating models contained a survey with an asymptotic selectivity pattern, which allows SCA models to produce more accurate estimates than other survey selectivity patterns (Bence et al. 1993). Likewise, our models did not contain trends in survey catchability over time or correlation with changes in fishery catchability, which could cause models that used survey indices of abundance to generate less accurate estimates.

The results of our analysis are contingent on correctly specifying M. In reality, the data analyst will probably not know the true M, and M may vary among years and ages. Attempting to estimate M within stock assessment models is becoming more common (Fu and Quinn 2000); however, M is often confounded with catchability and other parameters in SCA models (Schnute and Richards 1995; Fu and Quinn 2000). In some cases, M may be estimable, but this procedure usually requires additional auxiliary data that we did not include in our analyses, such as estimates of population size or other parameters from a mark–recapture study (Quinn and Deriso 1999). For example, Fu and Quinn (2000) showed that M was estimable in a length-structured model, especially when survey catchability was specified at the correct value. For our simulations, M was generally not estimable (results not shown). It seems that often reliable auxiliary information on either M or catchability is essential for fitting an age-structured assessment.

The density-dependent estimator used in this study was not one that would probably be used in real assessments, and explicitly modeling density-dependent catchability seems to be rarely used in stock assessments. The formulation that has been suggested for including density-dependent catchability in SCAs includes white noise process error about the density-dependent relationship (Fournier 1983). We did not include the Fournier (1983) estimator in our simulation because we wanted a clear distinction between the white noise and density-dependent estimators. Because of problems with convergence of our density-dependent estimator in most cases without density dependence, we do not believe that the density-dependent estimation model is a viable omnibus estimator, although it may be worth considering when there are a priori grounds for suspecting density dependence.

The relative performance of the estimators we tested depends on the amount of variation in catchability used in our simulations (SD of 0.2). We used this amount of variability because it is similar to estimates of the SD of catchability for commercial fisheries in New Zealand (Francis et al. 2003), which to our knowledge is the only study that has attempted to characterize variability in catchability across many fisheries within a region. We also conducted a limited set of simulations (results not shown) where the SD for catchability was set to 0.4. Results of these simulations were similar to those for the 0.2 scenarios. However, the relative performance of the estimators would likely change with increasing variation in catchability above these levels. Some useful generalizations can be drawn from the similarity of the different estimators. The estimator that ignored effort data and the white noise and random walk estimators are all special cases of an AR(1) process. In the case of white noise and random walk estimators, the correlation coefficient is zero and unity, respectively; for the estimator that ignored fishery effort data, the SD is infinity. As the SD of catchability increases, the white noise and random walk estimators will perform more like the estimator that ignores effort data if the correct standard deviation is used in the estimation model. We attempted to implement an estimation model where catchability followed an AR(1) process and the correlation and SD parameters were estimated, but in most cases this model failed to converge (results not shown).

We believe that using a random walk to model fishery catchability in an SCA is currently the best available approach when both fishery-dependent and -independent indices of abundance are available. This approach allows the model to accommodate and adjust for trends in catchability over time, which can cause biased estimates of stock size and fishing mortality rates if they are unaccounted for. An alternative approach to simply using a random walk may be to use a composite estimator (i.e., fitting several alternative models and choosing the best model structure based on specific rules). Using a composite estimator may provide improved performance over simply using a random walk. However, increased performance from a composite estimator is likely to be small because the random walk model performed nearly as well as the as the best model in the cases we examined. A variety of alternative approaches exist for selecting among competing models or averaging over such competitors (Burnham and Anderson 2002; McAllister and Kirchner 2002; Spiegelhalter et al. 2002). The extent to which such methods can lead to improved stock assessments is an area warranting future research.

Acknowledgments

The authors thank two anonymous reviewers and Dan Hayes, Mike Jones, and Rob Tempelman for providing helpful comments, which improved this manuscript. This research was supported in part by the Michigan Sea Grant College Program, the Great Lakes Fish and Wildlife Restoration Act administered by the US Fish and Wildlife Service, the Great Lakes Fishery Commission, the International Association for Great Lakes Research, and Michigan State University. This is publication number 2006-01 of the Quantitative Fisheries Center, Michigan State University.

References

Bence, J.R., Gordoa, A., and Hightower, J.E. 1993. Influence of age-selective surveys on the reliability of stock synthesis assessments. Can. J. Fish. Aquat. Sci. **50**: 827–840.

Burnham, K.P., and Anderson, D.R. 2002. Model selection and multimodel inference: a practical information-theoretic approach. Springer-Verlag, New York.

Deriso, R.B., Quinn, T.J., II, and Neal, P.R. 1985. Catch–age analysis with auxiliary information. Can. J. Fish. Aquat. Sci. **42**: 815–824.

Fournier, D.A. 1983. An analysis of the Hecate Strait Pacific cod fishery using an age-structured model incorporating density dependent effects. Can. J. Fish. Aquat. Sci. **40**: 1233–1243.

Fournier, D., and Archibald, C.P. 1982. A general theory for analyzing catch at age data. Can. J. Fish. Aquat. Sci. **39**: 1195–1207.

Francis, R.I.C.C., Hurst, R.J., and Renwick J.A. 2003. Quantifying annual variation in catchability for commercial and research fishing. Fish. Bull. **101**: 293–304.

Fu, C., and Quinn, T.J., II. 2000. Estimability of natural mortality and other population parameters in a length-based model: *Pandalus borealis* in Kachemak Bay, Alaska. Can. J. Fish. Aquat. Sci. **57**: 2420–2432.

Harley, S.J., Myers, R.A., and Dunn, A. 2001. Is catch-per-unit-effort proportional to abundance? Can. J. Fish. Aquat. Sci. **58**: 1760–1772.

Hilborn, R., and Walters, C.J. 1992. Quantitative fisheries stock assessment. Chapman and Hall, New York.

Ianelli, J.N., and Fournier, D.A. 1998. Alternative age-structured analyses of the NRC simulated stock assessment data. *In* Analyses of simulated data sets in support of the NRC study on stock assessment methods. *Edited by* V.R. Restrepo. US Department of Commerce, Washington, D.C. NOAA Tech. Memo. NMFS-F/SPO-30. pp. 81–96.

Maunder, M.N. 2001. A general framework for integrating the standardization of catch per unit effort into stock assessment models. Can. J. Fish. Aquat. Sci. **58**: 795–803.

Maunder, M.N., and Punt, A.E. 2004. Standardizing catch and effort data: a review of recent approaches. Fish. Res. **70**: 141–159.

Maunder, M.N., and Starr, P.J. 2003. Fitting fisheries models to standardized CPUE abundance indices. Fish. Res. **63**: 43–50.

McAllister, M., and Kirchner, C. 2002. Accounting for structural uncertainty to facilitate precautionary fishery management: illustration with Namibian orange roughy. Bull. Mar. Sci. **70**: 499–540.

Megrey, B.A. 1989. Review and comparison of age-structured stock assessment models from theoretical and applied points of view. *In* Mathematical analysis of fish stock dynamics. *Edited by* E.F. Edwards and B.A. Megrey. Am. Fish. Soc. Symp. **6**: 8–48.

Methot, R.D. 1990. Synthesis model: an adaptable framework for analysis of diverse stock assessment data. *In* Proceedings of the Symposium on Application of Stock Assessment Techniques to Gadids. *Edited by* L. Low. International North Pacific Fisheries Commission Bulletin 50. pp. 259–277.

Millar, R.B., and Methot, R.D. 2002. Age-structured meta-analysis of U.S. West Coast rockfish (Scorpaenidae) populations and hierarchical modeling of trawl survey catchabilities. Can. J. Fish. Aquat. Sci. **59**: 383–392.

National Research Council (NRC). 1998. Improving fish stock assessments. National Academy Press, Washington, D.C.

Otter Research Limited. 2000. An introduction to AD Model Builder version 4 for use in nonlinear modeling and statistics. Otter Research Ltd., Sidney, B.C.

Paloheimo, J.E., and Dickie, L.M. 1964. Abundance and fishing success. Rapp. P-V Reun. Cons. Int. Explor. Mer, **155**: 152–163.

Peterman, R.M., and Steer, G.J. 1981. Relation between sport-fishing catchability coefficients and salmon abundance. Trans. Am. Fish. Soc. **110**: 585–593.

Punt, A.E., Smith, A.D.M., and Cui, G. 2002. Evaluation of management tools for Australia's south east fishery. 2. How well can management quantities be estimated? Mar. Freshw. Res. **53**: 631–644.

Quinn, T.J., II, and Deriso, R.B. 1999. Quantitative fish dynamics. Oxford University Press, New York.

Radomski, P.A., Bence, J.R., and Quinn, T.J., II. 2005. Comparison of virtual population analysis and statistical kill-at-age analysis for a recreational kill dominated fishery. Can. J. Fish. Aquat. Sci. **62**: 436–452.

Restrepo, V.R. 1998. Analyses of simulated data sets in support of the NRC study on stock assessment methods. US Department of Commerce, Washington, D.C. NOAA Tech. Memo. NMFS-F/SPO-30.

Rose, G.A., and Kulka, D.W. 1999. Hyperaggregation of fish and fisheries: how catch-per-unit-effort increased as the northern cod (*Gadus morhua*) declined. Can. J. Fish. Aquat. Sci. **56**(Suppl. 1): 118–127.

Salthaug, A., and Aanes, S. 2003. Catchability and the spatial distribution of fishing vessels. Can. J. Fish. Aquat. Sci. **60**: 259–268.

Schnute, J.T., and Richards, L.J. 1995. Influence of error on population estimates from catch-age models. Can. J. Fish. Aquat. Sci. **52**: 2063–2077.

Spiegelhalter, D.J., Best, N.G., Carlin, B.P., and van der Linde, A. 2002. Bayesian measures of model complexity and fit. J. R. Stat. Soc. Ser. B, **64**: 583–639.

Winters, G.H., and Wheeler, J.P. 1985. Interactions between stock area, stock abundance, and catchability coefficient. Can. J. Fish. Aquat. Sci. **42**: 989–998.

Ziegler, P.E., Frusher, S.D., and Johnson, C.R. 2003. Space–time variation in catchability of southern rock lobster *Jasus edwardsii* in Tasmania explained by environmental, physiological and density-dependent processes. Fish. Res. **61**: 107–123.

Diel vertical migration in the Lake Superior pelagic community. I. Changes in vertical migration of coregonids in response to varying predation risk

Thomas R. Hrabik, Olaf P. Jensen, Steven J.D. Martell, Carl J. Walters, and James F. Kitchell

Abstract: The distribution of fishes is influenced by a host of physico-chemical and biological variables, including temperature and oxygen, prey abundance, feeding or assimilation rates, and predation risk. We used hydroacoustics and midwater trawls to measure the vertical distribution of pelagic fishes during a series of research cruises on Lake Superior's western arm in 2001 and 2004. Our objective was to assess vertical structuring in the fish assemblage over varying light levels. We observed variability in vertical structuring of both ciscoes (*Coregonus* spp.) and their primary predator, the siscowet (*Salvelinus namaycush siscowet*). Our results indicate that deepwater predators and prey migrate extensively over a diel cycle. This migration pattern is most consistent with changes in the distribution of prey resources for siscowet and diel variability in predation risk controlled by changing light levels for ciscoes. The magnitude of vertical migration in ciscoes increased with higher abundance of siscowets, supporting predation risk as a driver of cisco distribution. This study describes the extent of vertical migration in each group of fish, provides a statistical description of the pattern, and discusses the implications for trophic interactions in the Lake Superior food web.

Résumé : La répartition des poissons est affectée par une quantité de variables physico-chimiques et biologiques, dont la température et l'oxygène, l'abondance des proies, les taux d'alimentation et d'assimilation et le risque de prédation. Nous avons utilisé des méthodes hydroacoustiques et des chaluts de mi-profondeur pour mesurer la répartition verticale des poissons pélagiques durant une série de croisières de recherche dans le bras occidental du lac Supérieur en 2001 et en 2004. Notre objectif était de déterminer la structuration verticale du peuplement de poissons en fonction de la variation des intensités lumineuses. Nous avons observé de la variabilité dans la structuration verticale tant chez les ciscos (*Coregonus* spp.) que chez leur prédateur principal, le touladi siscowet (*Salvelinus namaycush siscowet*). Nos résultats indiquent que les prédateurs et les proies d'eau profonde font d'importantes migrations sur un cycle journalier. Ce patron de migration s'accorde le mieux avec les changements dans la répartition des ressources des proies chez le siscowet et avec la variabilité journalière du risque de prédation contrôlée par les changements de l'intensité lumineuse chez les ciscos. L'étendue de la migration verticale des corégones augmente en fonction de l'abondance des siscowets, ce qui vient appuyer le risque de prédation comme facteur explicatif de la répartition des ciscos. Notre étude décrit l'étendue de la migration verticale chez chaque groupe de poissons et fournit une description statistique du patron de migration; les conséquences sur les interactions trophiques dans le réseau alimentaire du lac Supérieur font l'objet d'une discussion.

[Traduit par la Rédaction]

Introduction

The pelagic food web of Lake Superior is unique among the Laurentian Great Lakes in that it is dominated by native species that are well adapted to exist in cold, deep habitats found there. Among the native forage fish, coregonids (*Coregonus* spp.) represent the most abundant prey available to large piscivores. In addition, native lake trout (*Salvelinus namaycush*) are approaching historical levels of abundance (Bronte et al. 2003). Diel vertical migration (DVM) is evident in coregonids in many pelagic ecosystems (Brandt et al. 1991; Eshenroder and Burnham-Curtis 1999; Knudsen and Gjelland 2003). Furthermore, diel changes in the vertical distribution of coregonids have the potential to influence the

Received 8 November 2005. Accepted 28 June 2006. Published on the NRC Research Press Web site at http://cjfas.nrc.ca on 30 September 2006.
J18986

T.R. Hrabik.[1] Department of Biology, 207 Swenson Science Building, University of Minnesota, Duluth Campus, 1035 Kirby Drive, Duluth, MN 55812, USA.
O.P. Jensen and J.F. Kitchell. Center for Limnology, 680 N. Park Street, Madison, WI 53706, USA.
S.J.D. Martell and C.J. Walters. Fisheries Centre, The University of British Columbia, Vancouver, BC V6T 1Z4, Canada.

[1] Corresponding author (e-mail: thrabik@d.umn.edu).

Can. J. Fish. Aquat. Sci. 63: 2286–2295 (2006)   doi:10.1139/F06-124

extent to which prey are available to predators. Recent examinations of prey supply – predator demand discrepancies in Lake Superior suggest that predator demand is near the capacity of prey species to support them (Negus 1995; Mason et al. 2005). Increased migratory behavior by prey in response to higher predation risk and the resulting behavioral segregation may further decrease the availability of prey to predators.

The Lake Superior fish community has undergone substantial changes brought about by overfishing, habitat degradation, and the invasion of exotic species. Historically, the pelagic prey fish community in Lake Superior was dominated by a clade of coregonids (Dryer et al. 1965; Christie 1974). However, the community shifted from coregonids to one dominated by exotic rainbow smelt (*Osmerus mordax*) during the 1970s (Selgeby 1982; Bronte et al. 2003). Recently, however, native coregonids have increased in abundance and are the most abundant planktivore in many locations (Hansen 1994). This shift in prey species most likely resulted from increased predatory demand placed on prey species by recovering lake trout populations. Rainbow smelt, a primary prey item for the increasing lake trout, declined as a result of lake trout predation (Hansen 1994). The decline in adult rainbow smelt resulted in a reduction in the predation rate on age-0 coregonid larvae and reduced interaction intensity between rainbow smelt and coregonids (Hansen 1994; Cox and Kitchell 2004).

Although the vertical distribution of the pelagic coregonids in Lake Superior has been characterized using daytime bottom trawl surveys and bottom-set gill net surveys (Selgeby and Hoff 1996), there is no documentation of changes in the vertical distribution of ciscoes in Lake Superior over changes in light levels. Historically, trawl surveys most often were conducted during the day and did not account for day to night variability in the depth distribution of the various species. Currently, the three most abundant pelagic prey fish in the open water areas of Lake Superior are bloater (*Coregonus hoyi*), kiyi (*Coregonus kiyi*), and lake herring (i.e., cisco, *Coregonus artedi*). These ciscoes feed on opossum shrimp (*Mysis relicta*, hereafter referred to as *Mysis*), which exhibit a strong DVM (Beeton 1960; Bowers 1988). Characterization of the abundance and spatial distribution of cisco species based on surveys conducted during the daylight hours may show only a portion of their distribution and ecological niche if they exhibit DVM. Furthermore, there are reports of vertical migrations by bloater in Lake Michigan (Eshenroder and Burnham-Curtis 1999; TeWinkle and Fleischer 1999), although there may be physiological constraints on the magnitude of such migrations (Clemens and Stevens 2003). Eshenroder and Burnham-Curtis (1999) posit that DVM in deepwater ciscoes is an adaptation for feeding on *Mysis* and that ciscoes possess physiological adaptations allowing DVMs (also see TeWinkle and Fleischer 1999).

Native lake trout represent the dominant native predator in Lake Superior, with the deepwater subspecies the siscowet (*Salvelinus namaycush siscowet*) being several times more abundant than the shallow-water form (*Salvelinus namaycush namaycush*) (Bronte et al. 2003). Siscowet, which have flesh lipid content of up to 48% (Eschmeyer and Phillips 1965), are well adapted for extensive vertical movements in the Great Lakes and feeding on deepwater ciscoes (Eshenroder and Burnham-Curtis 1999). Siscowet are commonly caught in deep, bottom areas in depths >100 m (Thurston 1962; Selgeby and Hoff 1996), but have also been caught in surface waters at night, where they may feed on terrestrial insects and shallow-water organisms (Thurston 1962). Furthermore, Thurston (1962) indicated that siscowets do not experience problems with gas expansion in the swimbladder or bloating that is experienced by lean lake trout when pulled from depths >70 m. Combined, these reports suggest substantial variability in the vertical distribution of siscowets. The derived physiological adaptations that characterize this subspecies of lake trout (e.g., high lipid content and reduced swim bladders) suggest the possibility of extensive vertical migrations (Eshenroder and Burnham-Curtis 1999); however, DVM has not yet been documented for siscowets.

Analyses of stable isotope ratios of Lake Superior fishes indicate a linkage between siscowets and deepwater ciscoes. Siscowets are isotopically distinct from lean lake trout and feed to a large extent on deepwater ciscoes (Harvey and Kitchell 2000). Diet analyses support the contention that large siscowets rely on ciscoes much more so than do lean lake trout (Conner et al. 1993; Ray 2004). Isotopic signatures and diet studies suggest a pelagic food web with strong linkages among *Mysis*, deepwater ciscoes, and siscowets (Harvey and Kitchell 2000). Given that the open-water food web is largely dominated by native species that have adaptations that allow vertical migrations (Eshenroder and Burnham-Curtis 1999), the existence of vertical migration within the pelagic food web has the potential to influence predator–prey interactions. Documentation of the existence and extent of vertical movements and overlap between predator and prey populations are required before a full understanding of energy exchange is possible.

In this paper (part I of II), we examine the vertical distribution of fishes in the open-water area of Lake Superior's western arm during isothermal and thermally stratified periods and among years with varying abundance of predatory siscowets. We hypothesized that the distribution of ciscoes will be influenced by diel changes in light, where darkness represents a potential refuge from predation. In addition, we also hypothesized that the abundance of siscowet within the pelagia would also influence the extent to which cisco vertically migrate. We present and examine evidence of the vertical migration in ciscoes and siscowets based on in situ measurements with midwater trawl gear and scientific echosounders. In addition, vertical changes in the density of *Mysis*, which migrate to shallow-water areas at night, may result in shallow depth distribution of ciscoes at night. The results presented here are used in a companion analysis to explore whether predation avoidance or prey distributions or a combination therein drive the vertical distribution of predators and prey in the open-water area of Lake Superior (Jensen et al. 2006).

Materials and methods

Planktivore distribution

We conducted surveys in western Lake Superior on the research vessel *Blue Heron* on 17–21 May 2001, 21–23 Au-

Fig. 1. Location of sonar transects and sampling locations in western Lake Superior in 2001 and 2004.

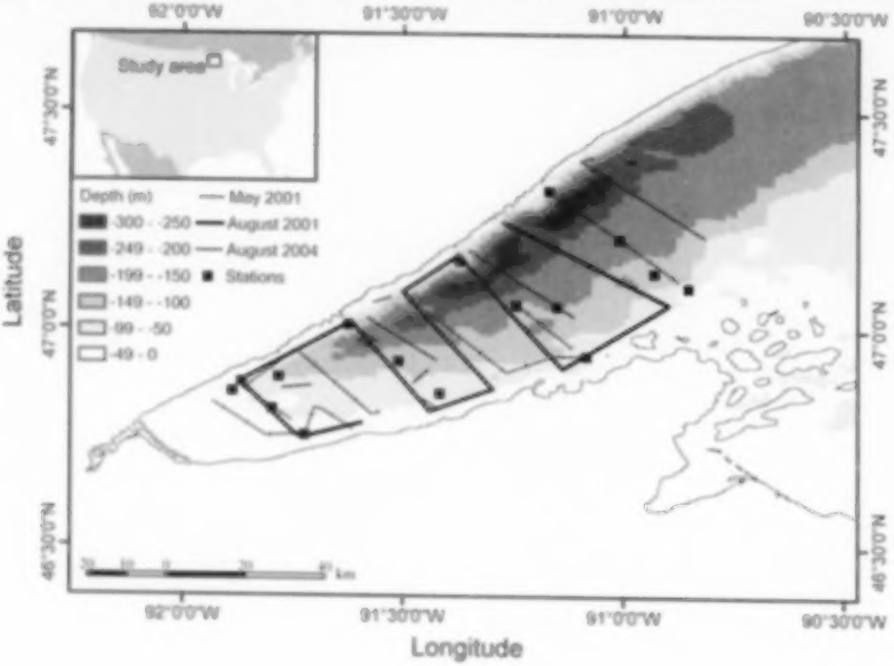

gust 2001, and 14–18 August 2004 (Fig. 1). During the sampling cruises, we estimated the depth distribution, size, and abundance of fish using a split-beam, 120 kHz Biosonics echosounder while performing transects spanning the western arm of Lake Superior during the day and at night on each outing. The software settings for the echosounder included a pulse duration of 0.4 ms and one pulse per second. Standard target calibration was performed shortly before each tow and after the sampling cruise, and target strength never varied significantly (<±1 dB) from the known target strength of the calibration sphere. Analysis procedures included eliminating any bottom anomalies using postprocessing software (Ecoview, SonarData Inc. V. 3.0) and estimation of fish density at each depth strata using echo integration and mean target strength after correcting for system configuration. The transducer was mounted on the Biosonics Inc. Biofin towbody and towed alongside the research vessel at a depth of 1 m from the surface at speeds of 4–5 knots (1 knot = 1.853 $km \cdot h^{-1}$) during day and night. In 2004, vertical distribution of fish during dawn, day, and dusk was estimated using stationary pinging, allowing target tracking and rates of movement of fish in the vertical plane to be estimated.

We used a threshold value of –65 dB during echo postprocessing for data used in the echo-squared integration analyses (Thorne 1983). Single target analysis using split-beam data (Ehrenberg 1983) used a threshold of –55 dB. Integrated values were identified for 5 m vertical intervals and horizontal intervals of 20 min. These criteria provided numerous samples for identification of mean backscatter for each depth and time interval.

We used split-beam analysis to determine the target strengths of fish identified within the acoustic beam. Mean backscatter of single fish targets was calculated for each 5 m vertical and 20 min time interval for each transect to convert echo-squared integration into measures of fish density. Target strength values at depth were converted to estimates of fish length using relationships developed using echoes from the dorsal aspect (Love 1977).

We estimated the volumetric density of predators using single target analyses and estimates of the volume of the acoustic beam. We assumed single targets > –32 dB in size represented predatory species; this target strength exceeded the maximum size of ciscoes captured in midwater trawls in the survey areas. We also assumed that a large proportion of predator targets would be single targets, that schooling behavior was uncommon in predatory species, and that prey fish aggregations would avoid a large predator. The number of predator targets was summed over 5 m vertical and 20 min time interval for each transect and divided by the beam volume sum to estimate predator density and depth distributions for a given time interval.

During day, dusk, and dawn periods in 2004, stationary pinging allowed single fish targets to be tracked in the vertical plane. The depth trajectory of prey fish (< –32 dB) tracked for a minimum of three pings in each time period was recorded, and slope was estimated using a linear regression (SAS REG Procedure, SAS Institute Inc., Cary, North Carolina) of target depth vs. time for each target. The mean slopes (i.e., rates of ascent or descent) for each time period (day, dusk, and dawn) were compared using analysis of variance (ANOVA, SAS GLM procedure) to determine if the

Fig. 2. Numerical proportion of species caught in nighttime midwater trawls in areas with bottom depths >150 m. The trawls were targeted to the primary scattering layer observed with hydroacoustics and maintained at a constant depth for approximately 1 h. Head rope depth of the trawls ranged between approximately 20 and 40 m and averaged 30 m. Hatched bars indicate coregonid species.

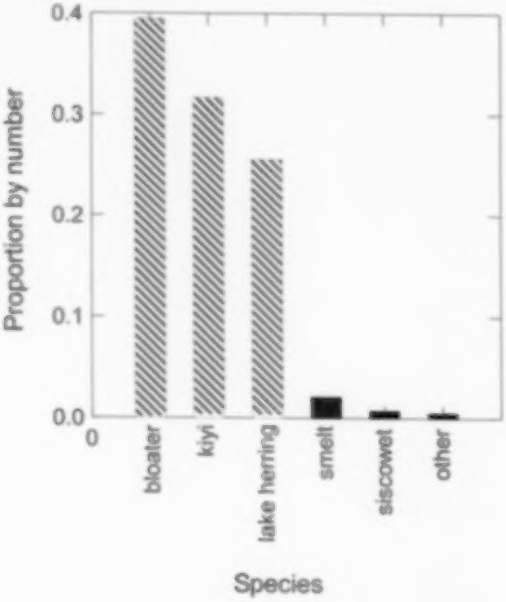

Fig. 3. Numerical proportion of various sizes of fish (10 mm bins) caught in nighttime midwater trawls. Coregonids, solid area; rainbow smelt (*Osmerus mordax*), shaded area; siscowet (*Salvelinus namaycush siscowet*), hatched area.

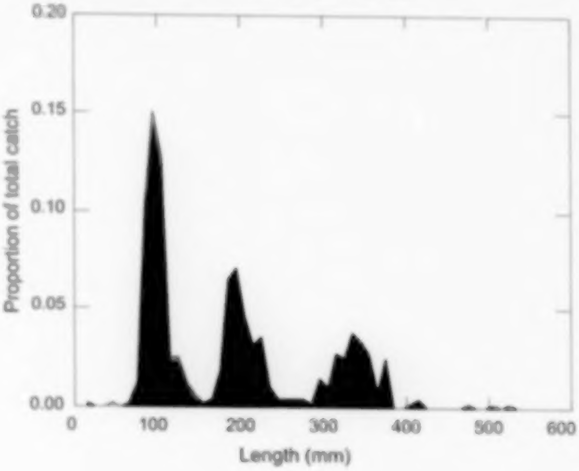

mean slope was substantially different (positive or negative) from zero (or no slope).

Biological and physical sampling

In 2004, we used a Gourock 20 m × 20 m box-type midwater trawl with 5 mm mesh cod end liner to sample fish species composition at various depths. We fished the trawl at discrete depths and aimed to sample scattering layers of fish. We monitored the trawl positions using Imagenex trawl mensuration system that contained a trawl sonar that measured the size of the trawl opening, depth of the trawl, and a temperature at the head rope. All fish captured in each trawl were identified, enumerated, and measured for total length and mass. No trawl information was available for 2001. However, information collected in 1997 and 2003 indicated that approximately 80% of open-water fish captured in midwater trawl surveys were deepwater coregonids (Mason et al. 2005; T.R. Hrabik, unpublished data), a finding that was similar to that observed in 2004. We therefore assume the species identified in 2004 were also representative of fish sampled by hydroacoustics in 2001.

We performed temperature casts near the beginning, midpoint, and end points of each sampling transect using Sea Bird model 19-01 conductivity, temperature, and depth profiler in 2001. In 2004, temperature profiles were recorded using a temperature sensor located within the Imagenex trawl mensuration system. Temperature profiles were recorded during the descent and ascent of each trawl. The average of each was used to estimate the temperature profile for transect segment during trawling (Fig. 1).

Statistical analysis of DVM trajectories

In addition to estimating regional and lake-wide abundance of different species, the hydroacoustic survey data can be used to describe diel changes in their depth distribution. To estimate DVM trajectories for coregonids and lake trout, targets of the appropriate target strength (< –32 dB for coregonids and > –32 for lake trout) were summarized by 5 m by 20 min depth–time bins for all targets observed in water depths >150 m. Data from all days and stations were combined based on the assumption that DVM trajectories did not vary over the short time scale (3 days) and limited spatial extent of the survey. However, densities of both coregonids and lake trout did vary among stations. Therefore, we standardized densities by dividing the number of targets in each depth–time bin by the total number of targets for that time interval. We also calculated the depth of the 0.01 lx isolume for May and August surface light intensity data for Duluth, Minnesota (NSRDB 2004), and the Beer–Lambert equation (Hutchinson 1957). We use 0.01 lx because it is below the threshold at which the reaction distance of many fish (including lake trout (Vogel and Beauchamp 1999) and coregonids (Link and Edsall 1996)) reaches a minimum.

Weighted, penalized regression splines were fit to the data where depth was the response variable, time the predictor, and the standardized targets were the weights (mgcv v1.0–9 for R v1.9.1). Penalized regression splines allow the flexibility of the curve to be optimized by "rewarding" model fit and "penalizing" model degrees of freedom (Wood and Augustin 2002) rather than setting the model degrees of freedom a priori. To make use of the cyclic nature of DVM without specifying cyclic functions (e.g., sine or cosine transformations), the data were wrapped, such that the last 3 h of the 24 h period were duplicated and added to the be-

Fig. 4. Box and whisker diagram showing the size of coregonids and siscowet (*Salvelinus namaycush siscowet*) in the open-water area of Lake Superior's western arm in 2004. Coregonids and siscowet represent approximately 97% of the total catch of fish in the open-water area.

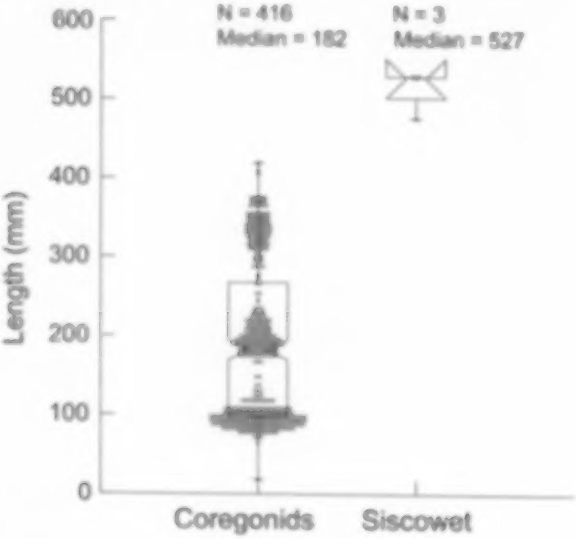

ginning of the 24 h period. Similarly, the first 3 h were duplicated and added to the end such that the curves were fit to data spanning the time interval –180 to 1620 min.

Although the spline curves show diel changes in mean depth for each species, clearly not all individuals are aggregated at the mean depth. Probability density fields for each species were created by overlaying a normal distribution with time-specific mean and standard deviation on each time interval. The assumption of normality was confirmed through histograms of the weighted residuals. In some time intervals where the curve approached the surface or the bottom, the tail of the distribution extended beyond the depth range. When more than 0.1% of the distribution in any time interval extended beyond the depth range, this missing portion was added proportionally to the existing depth bins such that the total probability in any time interval sums to one, and there is equal probability above and below the mean.

Results

Fish species composition and size

The numerical composition of fish species in Lake Superior's western arm was dominated by coregonines (97%; 75% represented by bloater and kiyi, 22% by lake herring), followed by rainbow smelt (2%), siscowet (0.7%), and other fish species (0.3%) (Fig. 2). All fish were captured between 12 and 60 m in depth at night. Trawls were performed in the same depth ranges during the day but captured no fish. The size of fish captured in trawls varied according to species. Coregonids ranged in size from 65 to 415mm total length (Fig. 3). Rainbow smelt sizes ranged from 45 to 145 mm total length (Fig. 3). Siscowets were the largest species captured and ranged from 475 to 535 mm total length (Fig. 3). There was no overlap in size between the predatory siscowet and prey fish species, which differed in median size by ~345 mm (Fig. 4).

Fig. 5. The mean difference between coregonid depths and bottom depth on three sampling dates. Predator density was substantially higher in May 2001 (*a*) than in August 2001 (*b*). Predator density in August 2004 (*c*) was substantially higher than in May 2001. Night, solid circles; day, open circles; dawn–dusk, shaded circles.

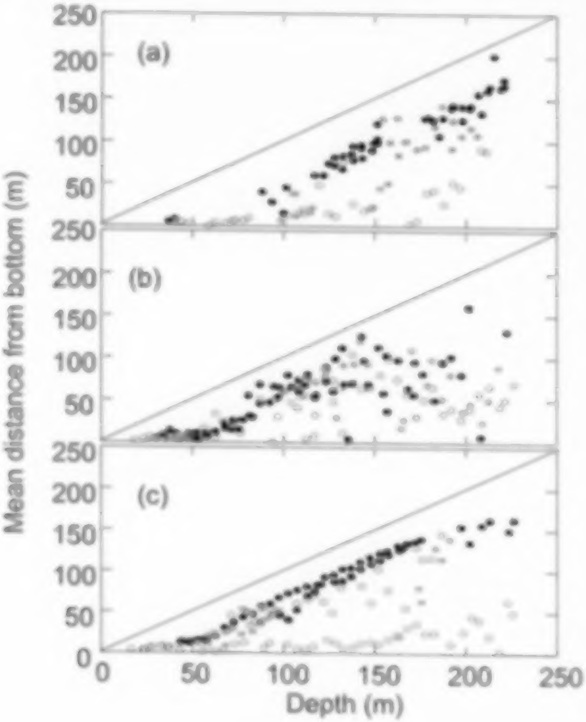

DVMs of fish in western Lake Superior

Data on ciscoes collected over varying light levels indicates that they perform a DVM in western Lake Superior. The difference between the mean depth of ciscoes estimated using hydroacoustics and bottom depth was greatest during night, intermediate at dawn–dusk, and much lower during the day (Fig. 5). The magnitude of difference between the mean depth of ciscoes and the bottom during the low light periods was greatest in areas where total depth exceeded 150 m and relatively small in areas shallower than 50 m (Fig. 5).

In August of 2004, single fish targets were tracked while stationary pinging and allowed directionality and rate of vertical movement during different periods of the daily cycle. The mean ± standard deviation (SD) vertical slope of 308 individually tracked fish at dawn was $-0.129 \pm 0.76\ \mathrm{m \cdot s^{-1}}$, which differed significantly from zero ($F = -5.98$, $p = 0.003$) (Fig. 6). At dusk, the mean ± SD vertical slope of 163 single fish targets was $0.011 \pm 0.068\ \mathrm{m \cdot s^{-1}}$, which differed significantly from zero ($F = 4.0$, $p = 0.049$) and from the dawn slope ($F = 5.5$, $p = 0.019$). The mean ± SD slope estimated for 91 targets identified during the day ($0.02 \pm 0.26\ \mathrm{m \cdot s^{-1}}$)

Fig. 6. Tracks of 50 randomly selected single targets tracked over a minimum of three sequential pings. Data for each light period was collected while the vessel was stationary. (*a*) Dawn, (*b*), day, (*c*) dusk.

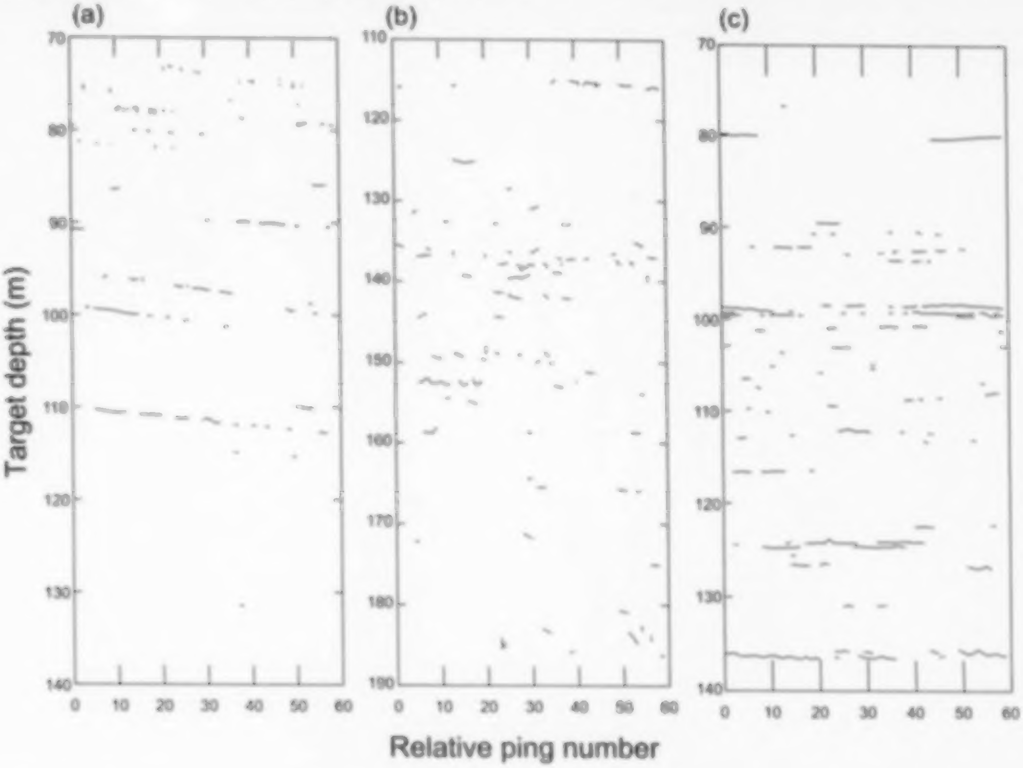

did not differ significantly from *zero* ($F = 0.51$, $p = 0.46$) (Fig. 6).

Analyses of vertical density estimates of both lake trout and ciscoes indicated synchronized vertical movements that corresponded to changing light conditions. In portions of the survey area >150 m in depth, the distribution of ciscoes and lake trout in May and August 2001 and in August 2004 was greatest during the day and most shallow at night (Fig. 7). Weighted, penalized regression spline fits of cisco density using time as a predictor explained 38% of variability in depth distributions in May 2001, 20.2% in August 2001, and 54.8% in 2004 (Table 1). A similar analysis of depth distribution of siscowet revealed model fits that explained 78.9% of the variability in depth distribution in May 2001, 25.2% in August 2001, and 77.5% in August 2004 (Table 1). In May and August 2001, however, the magnitude of vertical movement in ciscoes was much lower than that observed in August 2004. Results from the spline fits were consistent with the findings from analyses of tracked single targets. In 2004, the ascent at dusk occurred much more slowly than the descent at dawn (Fig. 7). The vertical movements of siscowet in August 2001 were lower in magnitude and much less predictable. In addition, the pattern of movement did not appear to be influenced by thermal stratification, and the fish appeared to remain below the thermocline when one was present. While the predatory lake trout also showed vertical movements, the magnitude of their movement appeared similar to that exhibited by ciscoes in May 2001 and August 2004 (Fig. 7). In 2004, however, the vertical movement was more pronounced in magnitude for both siscowet and ciscoes than that observed in 2001.

Temperature measurements taken in areas >150 m in depth show isothermal conditions in May 2001 and stratified conditions in August 2001 and 2004 (Fig. 8). Temperature in May 2001 was approximately 2.7 °C throughout the water column. In August 2001, the surface temperature averaged ~17.4 °C, with the average hypolimnion height of ~9 m. The surface temperature in August 2004 was ~12.4 °C, with an average hypolimnion height of ~9 m (Fig. 8). In areas >150 m, secchi depth readings during each sampling period averaged ~10 m and ranged from 7 to 13 m.

Variability in fish density

The extent of vertical migration by ciscoes was associated with changes in the density of large predators in deep areas of western Lake Superior. The density of predators and prey varied both among seasons in 2001 and between 2001 and 2004. The density of cisco was highest at 33 411 individuals·km^{-2} (±standard error (SE) = 375.43) in May 2001, followed by 26 993·km^{-2} (±1870.31) in August 2001, and lowest at 10 186·km^{-2} (±1063.53) in August 2004 (Fig. 9). The density of predators, however, showed a different pattern among dates. The density of predatory siscowet in open-water areas was highest in August of 2004 at approximately 62.66·km^{-2} (±3.01), followed by 33.14·km^{-2} (±3.10) in May of 2001 and 9.18·km^{-2} (±0.49) in August of 2001. The density of preda-

Fig. 7. Coregonid (*Coregonus* spp.; *a*, *c*, and *e*) and lake trout (*Salvelinus namaycush*; *b*, *d*, and *f*) densities at depth from May 2001 (*a* and *b*), August 2001 (*c* and *d*), and August 2004 (*e* and *f*) shown in proportions of total density for each time bin. Coregonid target weights are as follows: large dots, high (>0.33); medium dots, medium (0.1–0.33); small dots, low (<0.1). Lake trout target weights are as follows: large dots, high (>0.66); medium dots, medium (0.33–0.66); small dots, low (<0.33). Weighted, penalized regression splines (solid line) and the 0.01 lx isolume (broken line) are also shown.

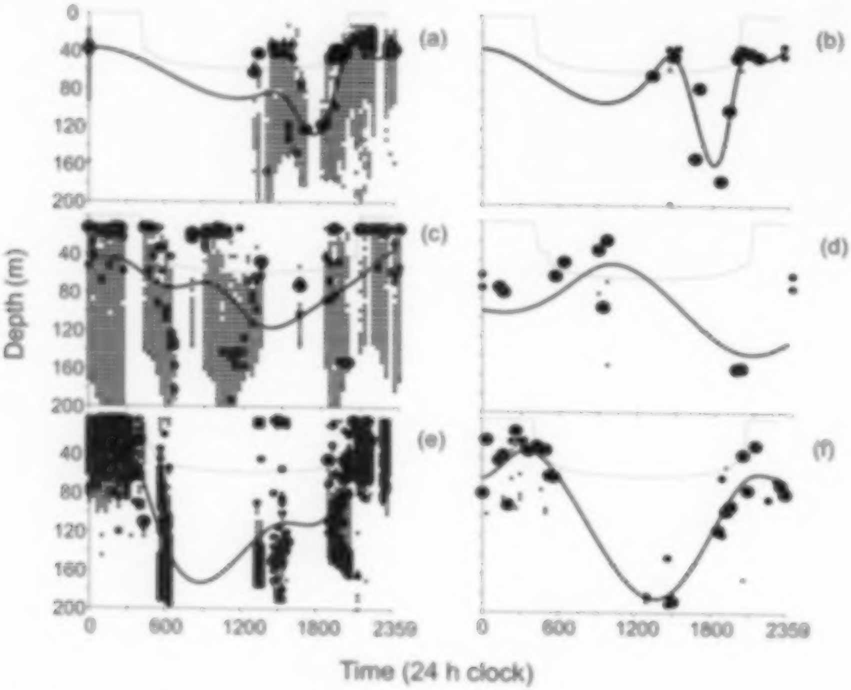

Table 1. Weighted, penalized regression spline fits predicting coregonids (*Coregonus* spp.) and siscowet (*Salvelinus namaycush siscowet*) depth based on time of day.

	Coregonids				Siscowet			
Sampling period	*N*	df	Dev. exp. (%)	*p*	*N*	df	Dev. exp. (%)	*p*
May 2001	995	8.7	38.9	<0.001	28	7.9	78.9	<0.001
August 2001	1788	8.7	20.2	<0.001	21	4.0	25.2	<0.001
August 2004	1180	8.8	54.8	<0.001	71	7.8	77.5	<0.001

Note: Model degrees of freedom (df) were chosen by generalized cross-validation (Wood and Augustin 2002) using mgcv v1.0-9 for R v1.9.1. *N*, the number of 5 m by 20 min intervals for which observations were available; Dev. exp., the percent of deviance explained.

tors corresponded to the magnitude of migration by ciscoes, such that the deepest migration and the fewest coregonids present above the depth of light penetration during the day occurred when predator density was highest (Fig. 7).

Discussion

The DVM pattern exhibited by ciscoes and siscowet in Lake Superior suggests a strong behavioral response to changing light levels that is consistent with predation avoidance and the distribution of their preferred prey, respectively. Our findings are consistent with other reports of DVM shown for bloaters in Lake Michigan (e.g., Brandt et al. 1991; Eshenroder and Burnham-Curtis 1999; TeWinkle and Fleischer 1999). Such movement patterns are often associated with thermoregulation and bioenergetic optimization, foraging maximization, or predation avoidance (Eggers 1978; Bevelhimer and Adams 1993; Scheuerell and Schindler 2003). The rates of vertical movement in ciscoes differ between dawn and dusk, suggesting that ciscoes may control their rate of ascent to compensate for decreasing hydrostatic pressure and positive buoyancy as they rise. Furthermore, the presence of a strong migration pattern has ramifications for interaction intensity between predators and prey and ongoing analyses of demand and supply in the Lake Superior food web.

Lake Superior is unique in that its food web is dominated by native fish species that are well adapted to the unique set of environmental conditions that include exceedingly cold temperatures and great depth. Lake Superior differs from

Fig. 8. Temperature profiles taken at deep (>130 m) locations in western Lake Superior during (*a*) spring 2001, (*b*) summer 2001, and (*c*) summer 2004. Different symbols indicate different sites deeper than 130 m.

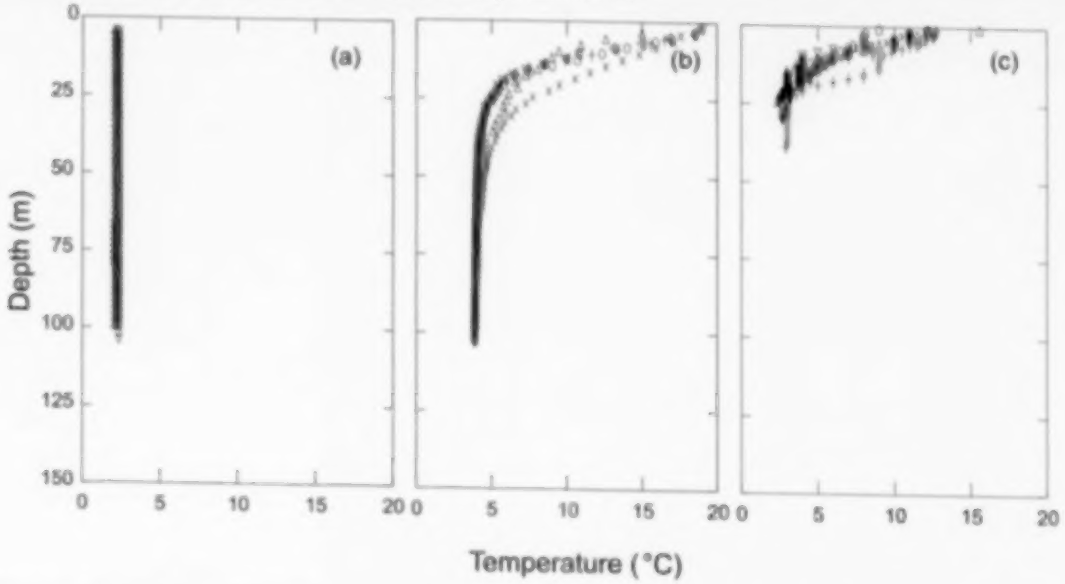

Fig. 9. The density of (*a*) coregonids and (*b*) predatory species estimated from hydroacoustic sampling in waters >150 m in total depth in Lake Superior's western arm on each sampling interval. Error bars indicate the standard error about the mean estimated using 1 km segments of transects as samples.

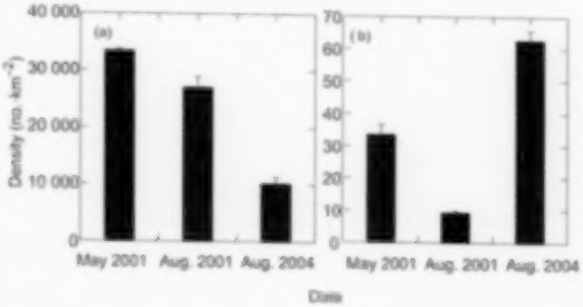

other Great Lakes in that the thermocline in open-water areas is often relatively shallow even in late summer. In addition, many of the open-water fish species remain below 30 m in depth even at night when at the shallowest point in their migration. This observation coupled with the consistent vertical migration in the isothermal period in May 2001 suggests that thermoregulation is not a major variable in the process.

The migration patterns of ciscoes observed in this study are consistent with those observed in other Great Lakes. Stationary acoustic tracking of single target data documented many individual fish rising during dusk and diving during the dawn periods. We detected no fish in shallow waters during daytime sampling. However, we often observed a large number of acoustic targets in water >150 m during the day. During dusk, repeated pings on single fish targets while stationary revealed rates of ascent that were lower than rates of descent, suggesting possible compensation for positive buoyancy while in the process of migration. These findings are consistent with reports of DVM in Great Lakes ciscoes by others (Brandt et al. 1991; Eshenroder and Burnham-Curtis 1999; TeWinkle and Fleischer 1999) and indicate that ciscoes are able to perform large vertical movements that may exceed 150 m in magnitude over the span of a few hours. The slower rate of ascent than descent at dusk may offer insight into how coregonids compensate for large decreases in hydrostatic pressure as they move vertically and contribute to the buoyancy compensation debate (Eshenroder and Burnham-Curtis 1999; Clemens and Stevens 2003).

The observed vertical movement by siscowets supports the contention that high fat content is associated with their ability to move readily over large depth ranges (Eshenroder and Burnham-Curtis 1999). In 2004, a year with the highest observed predator densities, the vertical movement by siscowets exceeded 150 m and was similar to that exhibited by ciscoes. The increase in the magnitude of migration in this year corresponds to the highest predator densities and lowest prey density and suggests that foraging opportunity may underlie the process. This finding supports previous reports of siscowet moving to upper portions of the water column at night (e.g., Thurston 1962) and that this species is well adapted to extensive and rapid vertical movements while foraging.

The depth distribution records for bloater and kiyi suggest that these species live in deep areas (>100 m) and rarely foray into shallow areas (Becker 1983; Selgeby and Hoff 1996). Our findings suggest that historical depth characterization based on information collected using daytime bottom trawls or gill nets set on the bottom may not reflect the true distributions of either bloater or kiyi in Lake Superior over a 24 h cycle. We routinely caught kiyi and bloater in midwater trawls deployed at depths near 30 m at night and very few fish below 50 m. These findings indicate these species may follow *Mysis* from deep areas and feed on abundant prey near 30 m during low light periods.

The existence of DVM patterns in the dominant prey fish species has implications for assumptions of prey availability for increasing siscowet and lean lake trout populations in Lake Superior. Predatory lake trout are now approaching historical abundance in Lake Superior (Hansen et al. 1995; Anonymous 1996). The rate of increase in abundance of siscowet is much higher relative to the lean lake trout (Kitchell et al. 2000; Bronte et al. 2003). Given an assumption of maximum prey size of ~50% of siscowet body length, ~78% of the coregonids collected would be vulnerable to predation by siscowets in our trawl samples. In 2004, the year in which the strongest migration pattern by both cisco and siscowet occurred, it was apparent that each moved extensively over a 24 h cycle. Our findings suggest that the magnitude of the migration pattern may be influenced by predator abundance and that the extreme depth range of the migration may be linked to higher densities of siscowet in the deep areas of western Lake Superior. However, given that a primary food item of ciscoes, the *Mysis*, undergoes a similar vertical migration pattern, testing of these hypotheses using a mathematical modeling approach is required to eliminate food supply as a likely mechanism (Jensen et al. 2006).

In summary, our findings document the existence of strong migratory behavior that has the potential to influence energy transfer between the planktivore and piscivore trophic levels and further complicate supply–demand analyses. Siscowets are capable of extensive vertical migrations. Given that the shallow-water lean lake trout is not, siscowet may indirectly influence prey resource availability for lean lake trout by inducing large migration patterns in the prey and possibly reducing prey density. As prey become more difficult to capture in the open water, siscowet may switch to alternative prey and place further competitive pressure on the shallow-water form (Harvey et al. 2003). Recent findings indicate that siscowets may foray into shallow water to feed on prey used by lean lake trout and that the dietary overlap between the two forms now exceeds 90% during the spring and early summer period (Ray 2004). These findings highlight the need to understand the mechanisms underlying the vertical migration patterns within the Lake Superior community and the consequences of this behavior for energy transfer through the food web to top predators exploited by fisheries.

Acknowledgements

We thank the crew of the R/V *Blue Heron* and the Large Lakes Observatory for their service during sampling cruises. We thank Don Schreiner and Steve Schram for providing support for portions of the field surveys. Funding for this research was provided by the Minnesota Department of Natural Resources, the Wisconsin Department of Natural Resources, the Minnesota Sea Grant College program, the Wisconsin Sea Grant, and the University of Minnesota, Duluth Campus.

References

Anonymous. 1996. Lake Superior lake trout restoration proclaimed a victory. Fisheries (Bethesda), **21**: 47–48.

Becker, G.C. 1983. Fishes of Wisconsin. The University of Wisconsin Press, Madison, Wis.

Beeton, A.M. 1960. The vertical migration of *Mysis relicta* in Lakes Huron and Michigan. J. Fish. Res. Board Can. **17**: 517–539.

Bevelhimer, M.S., and Adams, S.M. 1993. A bioenergetics analysis of diel vertical migration by kokanee salmon, *Oncorhynchus nerka*. Can. J. Fish. Aquat. Sci. **50**: 2336–2349.

Bowers, J.A. 1988. Diel vertical migration of the opossum shrimp *Mysis relicta* in Lake Superior — observations and sampling from the Johnson-Sea-Link II Submersible. Bull. Mar. Sci. **43**: 730–738.

Brandt, S.B., Mason, D.M., Patrick, E.V., Argyle, R.L., Wells, L., Unger, P.A., and Stewart, D.J. 1991. Acoustic measures of abundance and size of pelagic planktivores in Lake Michigan. Can. J. Fish. Aquat. Sci. **48**: 894–908.

Bronte, C.R., Ebener, M.P., Schreiner, D.R., Devault, D.S., Petzold, M.M., Jensen, D.A., Richards, C., and Lozano, S.J. 2003. Fish community change in Lake Superior, 1970–2000. Can. J. Fish. Aquat. Sci. **60**: 1552–1574.

Christie, W.J. 1974. Changes in the fish species composition of the Great Lakes. J. Fish. Res. Board Can. **31**: 827–854.

Clemens, B.J., and Stevens, E.D. 2003. Buoyancy range, gas bladder volume, and lipid content of adult bloater, *Coregonus hoyi* Gill, in the Laurentian Great Lakes. Environ. Biol. Fishes, **68**: 175–182.

Conner, D.J., Bronte, C.R., Selgeby, J.H., and Collins, H.L. 1993. Food of salmonine predators in Lake Superior, 1984–1987. Great Lakes Fish. Comm. Tech. Rep. 59.

Cox, S.P., and Kitchell, J.F. 2004. Lake Superior ecosystem, 1929–1998: simulating alternative hypotheses for recruitment failure of lake herring (*Coregonus artedi*). Bull. Mar. Sci. **74**: 671–683.

Dryer, W.R., Erkkila, L.F., and Tetzloff, C.L. 1965. Food of the lake trout in Lake Superior. Trans. Am. Fish. Soc. **94**: 169–176.

Eggers, D.M. 1978. Limnetic feeding-behavior of juvenile sockeye salmon in Lake Washington and predator avoidance. Limnol. Oceanogr. **23**: 1114–1125.

Eschmeyer, P.H., and Phillips, A.M. 1965. Fat content of the flesh of siscowets and lake trout from Lake Superior. Trans. Am. Fish. Soc. **94**: 62–74.

Eshenroder, R.L., and Burnham-Curtis, M.K. 1999. Species succession and sustainability of the Great Lakes fish community. *In* Great Lakes fisheries policy and management. *Edited by* W.W. Taylor and C.P. Ferreri. Michigan State University Press, East Lansing, Mich. pp. 145–184.

Ehrenberg, J.E. 1983. A review of in situ target strength estimation techniques. FAO Fish. Rep. 300: 85–90.

Hansen, M.J. (*Editor*). 1994. The state of Lake Superior in 1992. Great Lakes Fish. Comm. Spec. Publ. 94-1.

Hansen, M.J., Peck, J.W., Schorfhaar, R.G., Selgeby, J.H., Schreiner, D.R., Schram, S.T., Swanson, B.L., MacCallum, W.R., Burnham-Curtis, M.K., Curtis, G.L., Heinrich, J.W., and Young, R.J. 1995. Lake trout (*Salvelinus namaycush*) populations in Lake Superior and their restoration in 1959–1993. J. Gt. Lakes Res. **21**(Suppl. 1): 152–175.

Harvey, C.J., and Kitchell, J.F. 2000. A stable isotope study of the structure and spatial heterogeneity of the Lake Superior food web. Can. J. Fish. Aquat. Sci. **57**: 1395–1407.

Harvey, C.J., Schram, S.T., and Kitchell, J.F. 2003. Trophic relationships among lean and siscowet lake trout in Lake Superior. Trans. Am. Fish. Soc. **132**: 219–228.

Hutchinson, G.E. 1957. A treatise on limnology. Vol. I. Geology, physics, and chemistry. Wiley, New York.

Jensen, O.P., Hrabik, T.R., Martell, S.J.D., Walters, C.J., and Kitchell, J.F. 2006. Diel vertical migration in the Lake Superior pelagic community. II. Modeling trade-offs at an intermediate trophic level. Can. J. Fish. Aquat. Sci. **63**: 2296–2307.

Kitchell, J.F., Cox, S.P., Harvey, C.J., Johnson, T.B., Mason, D.M., Schoen, K.K., Aydin, K., Bronte, C., Ebener, M., Hansen, M., Hoff, M., Schram, S., Schreiner, D., and Walters, C.J. 2000. Sustainability of the Lake Superior fish community: interactions in a food web context. Ecosystems, **3**: 545–560.

Knudsen, F.R., and Gjelland, K.O. 2003. Hydroacoustic observations indicating swimbladder volume compensation during the diel vertical migration in coregonids. Fish. Res. **66**: 337–341.

Link, J., and Edsall, T.A. 1996. The effect of light on lake herring (*Coregonus artedi*) reactive volume. Hydrobiologia, **332**: 131–140.

Love, R.H. 1977. Target strength of an individual fish at any aspect. J. Acoust. Soc. Am. **62**: 1397–1403.

Mason, D.M., Johnson, T.B., Harvey, C.J., Kitchell, J.F., Schram, S.T., Bronte, C.R., Hoff, M.H., Lozano, S.J., Trebitz, A.S., Schreiner, D.R., Lamon, E.C., and Hrabik, T.R. 2005. Hydroacoustic estimates of abundance and spatial distribution of pelagic fishes in western Lake Superior. J. Gt. Lakes Res. **31**: 426–438.

Negus, M.T. 1995. Bioenergetics modeling as a salmonine management tool applied to Minnesota waters of Lake Superior. N. Am. J. Fish. Manag. **15**: 60–78.

NSRDB (National Solar Radiation Database). 2004. NSRDB hourly data files for Duluth (Weather Bureau Army Navy (WBAN) Identification Number 14913) [online]. Available from http://rredc.nrel.gov/solar/old_data/nsrdb/hourly/1990/14913_90.txt [accessed on 8 December 2004].

Ray, B.A. 2004. Spatial and temporal analysis of the Lake Superior fish community and predator diets. M.Sc. thesis, University of Minnesota, Duluth Campus, Minn.

Scheuerell, M.D., and Schindler, D.E. 2003. Diel vertical migration by juvenile sockeye salmon: empirical evidence for the antipredation window. Ecology, **84**: 1713–1720.

Selgeby, J.H. 1982. Decline of lake herring (*Coregonus artedi*) in Lake Superior: an analysis of the Wisconsin herring fishery 1936–78. Can. J. Fish. Aquat. Sci. **39**: 554–563.

Selgeby, J.H., and Hoff, M.H. 1996. Seaosonal bathymetric distributions of 16 fishes in Lake Superior, 1958–1975. Nat. Biol. Serv. Biol. Sci. Rep. 7.

TeWinkle, L.M., and Fleischer, G.W. 1999. Vertical migration and nighttime distribution of adult bloaters in Lake Michigan. Trans. Am. Fish. Soc. **128**: 459–474.

Thorne, R.E. 1983. Assessment of population abundance by hydroacoustics. Biol. Oceanogr. **2**: 253–262.

Thurston, C.E. 1962. Physical characteristics and chemical composition of two subspecies of lake trout. J. Fish. Res. Board Can. **19**: 39–43.

Vogel, J.L., and Beauchamp, D.A. 1999. Effects of light, prey size, and turbidity on reaction distances of lake trout (*Salvelinus namaycush*) to salmonid prey. Can. J. Fish. Aquat. Sci. **56**: 1293–1297.

Wood, S.N., and Augustin, N.H. 2002. GAMs with integrated model selection using penalized regression splines and applications to environmental modelling. Ecol. Model. **157**: 157–177.

Diel vertical migration in the Lake Superior pelagic community. II. Modeling trade-offs at an intermediate trophic level

Olaf P. Jensen, Thomas R. Hrabik, Steven J.D. Martell, Carl J. Walters, and James F. Kitchell

Abstract: Several hypotheses have been proposed to explain diel vertical migration (DVM); however, they have generally been applied to DVM behavior of a single trophic level. We evaluate the costs (predation risk) and benefits (foraging rate and growth rate potential) of different hypothetical and observed DVM trajectories for a three-level pelagic food chain in Lake Superior containing opossum shrimp (*Mysis relicta*), deepwater ciscoes (*Coregonus* spp.), and lake trout (*Salvelinus namaycush*). Lake trout appear to be maximizing foraging and growth rates by tracking vertically migrating ciscoes, while the DVM trajectories of ciscoes suggests a trade-off between predation risk and growth. For ciscoes, two alternative DVM trajectories both minimize the ratio of risk to growth: a shallow trajectory that follows low light levels down to 80 m during the day and a deep trajectory (below 150 m) that tracks highest *Mysis* densities. Observed cisco DVM trajectories appear to follow the shallow high risk – high growth trajectory in 2001, but switch to the deep, low risk – low growth trajectory in 2004 when lake trout density was higher and the density of ciscoes was lower.

Résumé : Plusieurs hypothèses cherchent à expliquer les migrations verticales journalières (DVM); elles ont, cependant, généralement été appliquées au comportement DVM d'un seul niveau trophique. Nous évaluons les coûts (risque de prédation) et les bénéfices (taux potentiels d'alimentation et de croissance) de différentes trajectoires DVM hypothétiques et réelles dans une chaine alimentaire pélagique à trois échelons au lac Supérieur comprenant la crevette opossum (*Mysis relicta*), des ciscos d'eau profonde (*Coregonus* spp.) et le touladi (*Salvelinus namaycush*). Le touladi semble maximiser ses taux d'alimentation et de croissance en poursuivant les ciscos en migration verticale, alors que les trajectoires DVM des ciscos semblent refléter un compromis entre le risque de prédation et la croissance. Chez les ciscos, deux trajectoires DVM de rechange permettent toutes deux de minimiser le rapport du risque de prédation sur la croissance, une trajectoire peu profonde qui suit les faibles intensités lumineuses pendant le jour jusqu'à une profondeur de 80 m et une trajectoire profonde (sous 150 m) qui suit les densités maximales de *Mysis*. Les trajectoires DVM observées chez les ciscos en 2001 semblent avoir suivi le type de trajectoire plus superficielle de risque élevé et de croissance rapide. En 2004 quand les densités de touladis étaient plus fortes et celles des ciscos réduites, les ciscos ont adopté plutôt la trajectoire de risque faible et de croissance lente.

[Traduit par la Rédaction]

Introduction

Understanding the mechanisms underlying diel vertical migration (DVM) continues to be one of the unresolved questions in limnology and behavioral ecology despite the many hypotheses that attempt to provide general explanations for this frequently observed phenomenon. Because this question sits at the intersection of several important ecological concepts (e.g., trophic interactions, bioenergetics, foraging theory), DVM has attracted a correspondingly diverse array of approaches. Implicit in many of these approaches are trade-offs between the costs and benefits of being at a given depth at a given time. We combine several of the most commonly advanced hypotheses regarding DVM in a modeling framework that elucidates these trade-offs and allows for comparisons between theoretically ideal DVM trajectories and those observed in the field. The model is applied to data on the diel vertical distribution of three trophic levels, opossum shrimp (*Mysis relicta*), deepwater ciscoes (*Coregonus* spp.), and lake trout (*Salvelinus namaycush*), in a Lake Superior pelagic food chain. The framework, however, is general and can be applied to any system for which depth–time distribution data exist.

Observations of similar DVM trajectories for fishes and their prey led to the development of foraging hypotheses (Narver 1970; Schoener 1971), which predict that DVM al-

---

Received 9 November 2005. Accepted 22 June 2006. Published on the NRC Research Press Web site at http://cjfas.nrc.ca on 30 September 2006.
J18987

O.P. Jensen[1] **and J.F. Kitchell.** Center for Limnology, 680 N. Park Street, Madison WI, 53706, USA.
T.R. Hrabik. University of Minnesota, Duluth Campus, 1110 Kirby Drive, Duluth, MN 55812, USA.
S.J.D. Martell and C.J. Walters. Fisheries Centre, The University of British Columbia, Vancouver, BC V6T 1Z4, Canada.

[1] Corresponding author (e-mail: ojensen@wisc.edu).

Can. J. Fish. Aquat. Sci. 63: 2296–2307 (2006) doi:10.1139/F06-125

lows fish to maximize consumption rates (or conversely to minimize foraging time required to obtain a given quantity of food). In the Laurentian Great Lakes, DVM in alewives (*Alosa pseudoharengus*; Janssen and Brandt 1980) and ciscoes (Eshenroder and Burnham-Curtis 1999, 2001) has been explained as a means of maximizing feeding rates on vertically migrating *Mysis*. Foraging hypotheses were extended by bioenergetic theories to include temperature-dependent metabolic costs as well as foraging benefits (Brett 1971). Bioenergetic hypotheses predict that DVM will allow fish to maximize growth rate, and they provide a rationale for migration trajectories that do not place fish in depths of highest prey density (Bevelheimer and Adams 1993). Foraging and bioenergetic hypotheses have been most successful at explaining DVM patterns for species at top trophic positions where predation risk is not a consideration.

Foraging and energetic approaches have failed to explain DVM at intermediate trophic levels for which predation is an important source of mortality (Levy 1990*a*, 1990*b*, 1991). Experimental evidence has shown that the addition of predators can induce changes in behavior and habitat use by fishes (Werner et al. 1983; He et al. 1993) and that the effects of such predator-induced changes depend on food availability (Biro et al. 2003*a*, 2003*b*). Eggers (1978) postulated predation risk as a driving factor in juvenile sockeye salmon (*Oncorhynchus nerka*) distributions in Lake Washington where zooplankton prey are comparatively abundant and observed that a variety of foraging strategies, including brief feeding near the surface and prolonged feeding at low light intensity, might all result in similar food intake and similar predation risk.

For a visual planktivore preyed upon by a visual piscivore, the ratio of predation risk (μ) to growth rate (*G*) (Werner and Gilliam 1984) is minimized at intermediate light intensity, assuming that the reaction distances of predator and prey are similar and respond in a similar manner to changes in light intensity (Clark and Levy 1988). In addition to predicting that sockeye salmon should use DVM to allow them to feed during crepuscular periods when foraging rates are high relative to predation risk (the "antipredation window"), the model used by Clark and Levy (1988) predicts that to achieve maximum fitness, sockeye should follow a DVM trajectory that would allow them to obtain a critical minimum size at the lowest possible risk.

For understanding DVM of fish at intermediate trophic levels, which are subject to the constraints of both growth and risk avoidance, the model of Clark and Levy (1988) was a substantial improvement over previous hypotheses, which focused on only one side of the equation. More recent laboratory feeding experiments, however, have shown that at least for some fish species, the relationship between reaction distance and light intensity differs substantially between planktivores and piscivores (De Robertis et al. 2003). Scheuerell and Schindler (2003) modified the Clark and Levy (1988) model for calculating μ/*G* by adding empirically derived reaction distance functions for both predators and prey and found that juvenile sockeye experience daily antipredation windows of seasonally varying duration and timing.

DVM has been documented at three trophic levels of the Lake Superior pelagic community. Vertical migration of *Mysis* has been observed in Lakes Superior (Bowers 1988), Michigan (Beeton 1960; Grossnickle and Morgan 1979; Janssen and Brandt 1980), and Huron (Beeton 1960). Recent work in Cayuga Lake, New York, and Lake Ontario has shown that *Mysis* vertical migration patterns are driven by diel changes in light intensity at depth (Gal et al. 1999), with the thermocline setting the upper limit of the nighttime migration (Gal et al. 2004). Hydroacoustic and trawl surveys show clear evidence of DVM among ciscoes in Lake Michigan (Eshenroder et al. 1998; TeWinkel and Fleischer 1999) and Lake Superior (Hrabik et al. 2006). Predation risk from piscivorous lake trout has been previously considered as a driver of DVM in sockeye (Stockwell and Johnson 1999; Hardiman et al. 2004), and DVM by lake trout has been observed in Lake Superior (Hrabik et al. 2006).

We consider DVM of ciscoes in light of three previously hypothesized goals of the behavior: (*i*) maximizing foraging or growth rate potential, (*ii*) minimizing predation risk, and (*iii*) minimizing the ratio of predation risk to growth rate potential. Predation risk is considered at both the individual and the population level. DVM patterns of lake trout are evaluated in terms of the first hypothesis, since adult lake trout are not subject to predation.

Materials and methods

Biomass fields

Depth- and time-specific costs and benefits of DVM for each trophic level were calculated for a hypothetical 0.0075 g *Mysis*, 125 g coregonid, and 675 g lake trout over a 200 m by 24 h depth–time field divided into 5 m by 20 min intervals. We consider only the pelagic fraction of each trophic level, since individuals near the bottom are difficult to distinguish using hydroacoustic methods. Biomass fields and DVM trajectories were derived from field observations of *Mysis*, ciscoes, and lake trout in Lake Superior.

Concurrent hydroacoustic and midwater trawl sampling of ciscoes and lake trout was conducted in May and August 2001 and August 2004 (Hrabik et al. 2006). Because the DVM pattern was clearest in 2004, the model is developed from data collected at that time; however, DVM trajectories of coregonids observed in 2001 are also considered. Probability density functions, which describe the depth distribution of ciscoes and lake trout by 20 min intervals, were developed by fitting cubic regression splines to the hydroacoustic data (Hrabik et al. 2006). To limit the effect of depth on DVM patterns, we used only those portions of the hydroacoustic survey track that occurred in depths of 150–250 m. Thermal profiles and secchi depths were measured during the course of the surveys and showed little interannual variation (Hrabik et al. 2006).

Mysis vertical migration patterns could not be evaluated using the hydroacoustic survey data because of low-level ship noise. We therefore used published data from vertical stage net tows and submersible collections in eastern Lake Superior on 26–27 July 1986 (Bowers 1988). This study collected data over three depth intervals: 0–50, 50–200, and 200–280 m. To evaluate vertical migration patterns over a 200 m depth range (the approximate average of our hydroacoustic survey), we proportionally compressed the two deeper strata to 50–150 and 150–200 m. In addition, field

Table 1. Biological and physical parameters used in the foraging and predation risk models.

Parameter	Value	Unit	Source
Biological			
Lake trout			
Weight (W_{T3})	675	g	Assumption
Swimming speed (v_{T3})	$11.7W_{T3}^{0.05}e^{(0.0405T)} = 20-24$	m·min^{-1}	Stewart et al. 1983
Areal density	0.000 063	individuals·m^{-2}	Hrabik et al. 2006
Coregonids			
Weight (W_{T2})	125	g	Assumption
Swimming speed (v_{T2})	$7.23W_{T2}^{0.25} = 24\ \text{cm}\cdot\text{s}^{-1} = 14.5$	m·min^{-1}	Rudstam et al. 1994
Areal density	0.01	individuals·m^{-2}	Hrabik et al. 2006
Mysis			
Length (L_{T1})	0.015	m	Johannsson 1995
Dry weight (W_{T1})	0.0075	g	Johannsson 1995
Swimming speed (v_{T1})	0.6	m·min^{-1}	Mason and Patrick 1993
Areal density	750	individuals·m^{-2}	Bowers 1988
Physical			
Extinction coefficient (k)	0.15	m^{-1}	Koenings and Edmundson 1991[a]
Turbidity (τ)	0.5	NTU	Koenings and Edmundson 1991[a]
Temperature (T)	6–10	°C	Measured
Light level at surface (I_0)	$0-5.7 \times 10^4$	lx	NSRDB 2004

[a] Based on relationships between average Secchi depth (10 m) and k and turbidity for clear lakes.

observations showed a high concentration of *Mysis* in the deep scattering layer just below the thermocline during thermally stratified periods (Beeton 1960; Bowers and Grossnickle 1978; Levy 1991). This high concentration of *Mysis* could not be adequately represented using the 0–50 m net data. We therefore assumed that 70% of the *Mysis* biomass recorded by Bowers (1988) in the 0–50 m interval at night was found in the 5 m interval at the top of the hypolimnion (15–20 m), with the remaining biomass for the 0–50 m interval spread equally among the other depth bins. The sensitivity of the model results to this assumption and to potential changes in *Mysis* density is evaluated.

Foraging model

Foraging rate potential (FRP) was calculated using the general encounter rate model of Gerritsen and Strickler (1977), as applied by Mason and Patrick (1993):

$$\text{(1)} \qquad \text{FRP} = \left(\frac{\pi R_{ij}^2}{3}\right)\left(\frac{3v_j^2 + v_i^2}{v_j}\right)d_i$$

where R_{ij} is the reaction distance of predator j (lake trout or ciscoes) preying on prey i (ciscoes or *Mysis*, respectively), v_j and v_i are predator and prey swimming speeds, respectively, and d_i is the depth- and time-specific prey density (depth and time subscripts are suppressed for clarity). Swimming speeds of *Mysis* and ciscoes were assumed to be constant, while swimming speed of lake trout is temperature-, and consequently depth-dependent, as defined in Table 1. FRP is a theoretical quantity based on encounter rates. It is useful for comparing foraging opportunities among different depths and times, but is not meant as an estimate of consumption.

Reaction distance

Reaction distance, or the distance at which fish show an attack response to prey, has been measured for coregonids and lake trout in laboratory feeding studies. It is important to distinguish between reaction distance and visual acuity. For piscivores, the latter may remain high at distances much greater than those that trigger a strike (Breck 1993). For ciscoes feeding on *Mysis*, we modified the parameters of the slope (β) equation of the reaction distance model developed by Wright and O'Brien (1984) for planktivorous white crappie (*Pomoxis annularis*) to fit reaction distances observed for lake herring (*Coregonus artedi*) feeding on *Limnocalanus macrurus* (2.46 mm) at light levels of 2–1500 lx (Link and Edsall 1996):

$$\text{(2)} \qquad R = 1.44\beta(l - 0.2)$$

where l is the length of *Mysis* (15 mm), and β is a function of turbidity (τ) and depth- and time-specific light intensity (I):

$$\text{(3)} \qquad \beta = 1.65[1.49 + 7.86\arctan(\log I)](1 - \tau/30 + 4.6)$$

Ciscoes are known to feed in the dark (TeWinkel and Fleischer 1999), indicating that there is a positive reaction distance even at 0 lx. Lacking laboratory studies of coregonids or similar planktivores feeding below 2 lx, this minimum reaction distance was adjusted until the daily growth rate predicted by the model was equal to the average daily growth increment predicted for a 125 g kiyi (*Coregonus kiyi*) from a von Bertalanffy growth model fit to data from Lake Michigan (Carlander 1969). The minimum reaction distance estimated using this method was 2 cm.

For lake trout feeding on ciscoes, we used the reaction distance function developed by Vogel and Beauchamp (1999):

$$(4a)\qquad R = 26.84 + 2.81\, I - 6.09 \ln(\tau) - 0.025 \ln(\tau) I$$

for light intensities less than the saturation intensity threshold (SIT, 17.83 lx) and

$$(4b)\qquad R = 77.79 + 0.046\, I - 6.09 \ln(\tau) - 0.025 \ln(\tau) I$$

for light intensities greater than SIT.

Light intensity at the surface, I_0, was based on the average irradiance (W·m^{-2}) recorded at Duluth, Minnesota, for August 1990 (NSRDB 2004), the most recent year for which data were available, and a conversion factor for visible light of 1 W·m^{-2} equals 120 lx (Lampert and Sommer 1997). All three hydroacoustic surveys were conducted under clear skies to light clouds and within 5 days of the new moon (i.e., low nighttime light). Light intensity at depth x was calculated using the Beer–Lambert equation (Hutchinson 1957):

$$(5)\qquad I_x = I_0 e^{-kx}$$

where k is the extinction coefficient (m^{-1}).

Bioenergetic model

A bioenergetic model based on the framework of Kitchell et al. (1977) was used to translate depth- and time-specific estimates of FRP into growth rate potential (GRP, sensu Brandt et al. 1992). Similar approaches to mapping GRP have been used by Tyler (1998) and Roy et al. (2004). All prey encounters predicted from the FRP model were assumed to have resulted in consumption up to a species- and temperature-specific maximum consumption rate ($C_{\max}$). The bioenergetic model used the same equations as those in Hanson et al. (1997), with parameters for ciscoes taken from the generalized coregonid model (Rudstam et al. 1994) and those for lake trout taken from Stewart et al. (1983). We refer interested readers to these two papers for details of the temperature dependency of $C_{\max}$, respiration, specific dynamic action, egestion, and excretion. The bioenergetic model used to calculate GRP was validated by comparison with Fish Bioenergetics v. 3.0 (Hanson et al. 1997).

Predation risk model

Predation risk is difficult to quantify precisely, since, as game-theory models have shown, different assumptions about the behavioral flexibility of predators and prey can lead to substantial differences in risk (Hugie and Dill 1994). To bracket this uncertainty, we consider two separate formulations of risk that represent extremes of behavioral flexibility: one based on observed predator and prey distributions and one based on the assumption that predator DVM trajectories will track (imperfectly) changes in the DVM trajectory of the prey population. The first formulation is relevant for assessing the implications of alternative DVM trajectories for an individual prey, since it holds predator and prey distributions constant. The assumption here is that predators are unlikely to change their distribution in response to an individual prey. The second formulation assumes that the observed overlap between lake trout and coregonid DVM trajectories represents the equilibrium outcome of a game between predators and prey (Iwasa 1982) (i.e., if prey change their DVM trajectory, predators will be able to adjust, so that the degree of overlap remains the same). Predator and prey densities in this case are defined as the average over a 24 h day of the predator and prey densities found along the mean prey DVM trajectory. In both cases, we can define the probability of dying due to predation in a given time and depth interval as the ratio of prey consumed (d_{cons}) to total prey (d_{total}) in that interval:

$$(6)\qquad \mu = d_{\text{cons}} / d_{\text{total}}$$

The number of consumed prey is defined by the depth- and time-specific FRP (up to $C_{\max}$) for an individual predator multiplied by the observed (the individual formulation) or average (the population formulation) predator density. Similarly, the total prey in the interval is either the observed or the average prey density. For the individual formulation, eq. 6 is not defined for intervals in which no prey were observed. Therefore, for these intervals, we follow Mason and Patrick (1993) and define μ based on the encounter rate with predators using eq. 1, with the substitution of predator density for prey density, d_r. Equation 1 gives an encounter rate (i.e., the expected number of predators encountered per unit of time). Predation risk, however, is defined as the probability of encountering any predator (again, we assume that all encounters result in consumption). If we assume that the encounter rate estimated using eq. 1 represents the mean of a Poisson distribution (appropriate for unbounded count data), this distribution can be used to calculate the probability of encountering one or more predators.

Balancing predation risk and growth rate potential

The trade-off hypothesis was evaluated by calculating the risk ratio (μ/G) based on DVM trajectories through the depth–time fields for μ and GRP according to the following formula:

$$(7)\qquad \frac{\mu}{G} = \frac{1 - \left[\prod_{t=1}^{72} (1 - \mu_t)\right]^{T_{\max}}}{\left(\sum_{t=1}^{72} \text{GRP}_t\right) T_{\max}}$$

where μ_t and GRP$_t$ are, respectively, the probability of dying due to predation and the GRP for the 20 min time interval t (there are 72 of these time intervals in a 24 h day), and $T_{\max}$ is the number of days over which μ/G is calculated. The risk ratio was calculated for 1-day and 100-day intervals to demonstrate how diel patterns in μ/G may vary depending on the time horizon.

We performed an individual parameter perturbation analysis (Bartell et al. 1986) on the parameters in Table 1, the minimum reaction distances of ciscoes and lake trout, and the vertical distribution of *Mysis*. Each parameter was increased and decreased by 20%, and the model was rerun with the new parameter value. Critical threshold densities of *Mysis* (i.e., the point at which qualitative changes occurred in the pattern of FRP, GRP, risk, and the risk ratio) were estimated.

Fig. 1. Volumetric densities (individuals·m^{-3}) of *Mysis relicta* (*a*), ciscoes (*Coregonus* spp.) (*b*), and lake trout (*Salvelinus namaycush*) (*c*) by depth and time of day. Broken lines in panels (*a*) and (*b*) show the diel vertical migration of ciscoes and lake trout, respectively, in 2004. Data for *Mysis* are from Bowers (1988). Data for ciscoes and lake trout are from Hrabik et al. (2006).

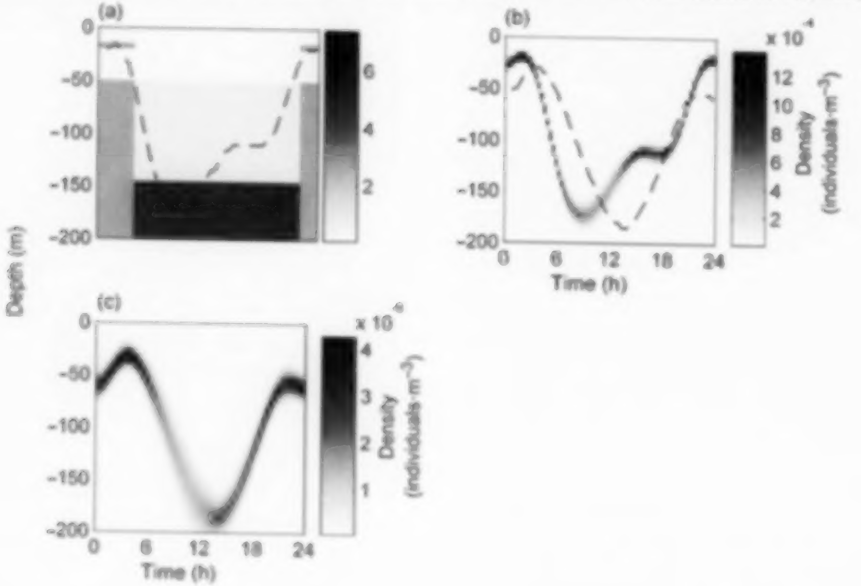

Fig. 2. Light level (log (lx)) by depth and time of day (*a*) based on surface light data recorded at Duluth, Minnesota, in August 1990 (NSRDB 2004) and reaction distance of ciscoes (*Coregonus* spp., broken line) and lake trout (*Salvelinus namaycush*, solid line) as a function of light level (*b*). The reaction distance function for ciscoes is based on experiments by Link and Edsall (1996). The function for lake trout is based on a study by Vogel and Beauchamp (1999).

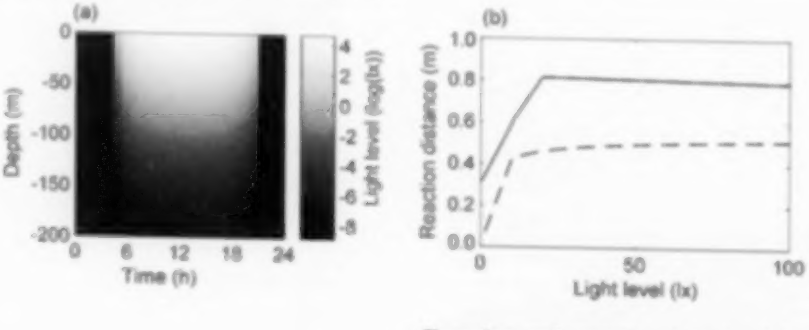

Results

Biomass fields

The biomass fields of all three trophic levels (Figs. 1*a*–1*c*) show distinct DVM behavior. The vertical net tow data from Bowers (1988) show that *Mysis* occur throughout the water column, with highest densities found at the thermocline–hypolimnion interface at night and in the deepest stratum during the day. Volumetric densities of *Mysis* from Bowers (1988) varied from 0.16 individuals·m^{-3} in the 0–50 m stratum during the day to 7.4 individuals·m^{-3} in the 150–200 m stratum during the day. Biomass fields of ciscoes and lake trout show fish density concentrated within only a few depth bins at any given time interval. Volumetric densities of ciscoes and lake trout ranged from 0 to 1.4×10^{-3} individuals·m^{-3} and 0 to 4.3×10^{-6} individuals·m^{-3}, respectively.

Foraging and growth rate potential

FRP for ciscoes and lake trout varied over time and depth because of the distribution of prey and because of differences in light intensity (Fig. 2*a*), which affects reaction distance (Fig. 2*b*), and temperature (Fig. 3), which affects lake trout swimming speed. The FRP field for ciscoes was dominated by light intensity and *Mysis* density (Fig. 4*a*). At night, FRP for ciscoes was greatest in the dense *Mysis* layer below the thermocline. During the day, highest FRP for ciscoes occurred at 50–80 m. Lowest FRP for ciscoes occurred in the unlit portions of the 0–50 m stratum, including the intervals just before sunrise and just after sunset. FRP in these areas was 0.06 *Mysis* consumed per 20 min time interval compared with a maximum FRP of 198 *Mysis* consumed at midday at 50 m. At this higher FRP, the maximum daily ration for a 125 g coregonid at 3 °C (1.25 g dry weight or 167

Fig. 3. Temperature (°C) profile from August 2004 taken in the western arm of Lake Superior.

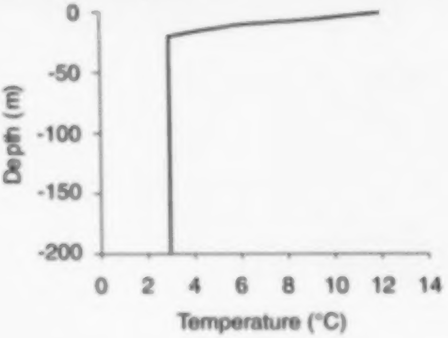

Mysis) could be consumed in less than 20 min. The daily FRP of a coregonid following the mean observed DVM trajectory for 2004 (white line in Fig. 4*a*) is ~60 *Mysis*.

FRP for lake trout (Fig. 4*b*) closely mirrors the distribution of ciscoes, since ciscoes generally remained in the dark. The maximum FRP for lake trout was approximately 0.15 ciscoes consumed in a 20 min time interval, compared with a maximum daily ration of 18.5 g (or equivalently one 125 g coregonid·week^{-1}) for a 675 g lake trout at 3 °C. The daily FRP of a lake trout following the mean observed DVM trajectory for 2004 (white line in Fig. 4*b*) is 0.64 ciscoes.

GRP for ciscoes (Fig. 4*c*) is strikingly different than FRP, with GRP patterns dominated by temperature. The region of highest GRP for ciscoes occurs in the warm, well-lit waters above the thermocline during the day. Regions of positive GRP for ciscoes occurred in daytime from the surface to depths of approximately 70–90 m, below which light intensity is extremely low. Positive daytime GRP resumed below 150 m because of increased *Mysis* density. At night, positive GRP for ciscoes occurred at depths >50 m and in the depth interval just below the thermocline (15–20 m). The region of highest FRP, from 50–80 m during the day, does not exhibit particularly high GRP because the high FRP in this region exceeds the maximum daily ration for a 125 g coregonid at 3 °C. Daily GRP of a coregonid following the mean observed DVM trajectory is 0.13 g.

GRP of lake trout (Fig. 4*d*) is dominated by the distribution of ciscoes, but a temperature effect is apparent as well above the thermocline. The peaks seen in the FRP field are flattened in the GRP field because many of the FRP peaks correspond to foraging rates greater than the maximum daily ration. Daily GRP of a lake trout following the mean observed DVM trajectory is 0.75 g.

Predation risk and the risk vs. growth trade-off

The individual risk field (Fig. 5*a*) for ciscoes closely matches the distribution of lake trout. Highest individual risk occurs in depth–time bins in which lake trout are most concentrated. By definition, there is zero individual risk in bins containing no lake trout. The lower individual risk in places where ciscoes and lake trout overlap reflects the reduction in individual risk associated with being one of many individuals in a large group. The population risk field (Fig. 5*b*), which assumes that lake trout would be able to track changes in the coregonid DVM trajectory, reflects differences in light intensity and temperature. Dark regions (i.e., at night or at depths below the depth of light penetration during the day) below the thermocline all show equal and low population risk. Highest population risk occurs in the surface layer during the day. Population risk in this region is ~28 times greater than that in dark regions below the thermocline.

The ratio of individual risk to GRP for ciscoes calculated over 1 day (Fig. 6*a*) reflects the distribution of lake trout as well as the location of depth–time bins in which GRP is negative. Population risk to GRP calculated over 1 day (Fig. 6*b*) is minimized at night in the high *Mysis* density layer below the thermocline. During the day, two alternative zones show approximately equal population risk to GRP: (*i*) a crescent of low light (approximately 0.2–1 lx) that extends from the surface at dawn, down to 80 m at noon, and back near the surface at dusk and (*ii*) the region from 150 to 200 m. Two regions of high population risk to GRP are evident: one in the shallowest depth bin during full daylight and one occurring in a semicircle above the low-light crescent. Risk becomes relatively more important when individual risk to GRP is calculated over a period of 100 days (Fig. 6*c*). When population risk/GRP is calculated over 100 days (Fig. 6*d*), there is a reversal in the high risk, high growth area near the surface during the day, which now becomes a minimum for the risk/GRP ratio.

Sensitivity analysis

Changes in swimming speed and prey density generally had a proportional effect on FRP (i.e., a 20% increase in either variable yielded a 20% increase in FRP), since encounter rate is a product of these variables and search area. The exception was the swimming speed of prey, which had very little effect. For example, a 20% change in swimming speed of ciscoes resulted in only a 10% change in FRP of lake trout. The swimming speed of *Mysis* had virtually no effect on FRP of ciscoes. The effect of swimming speed and prey density on GRP, risk, and the risk ratio was less pronounced than the effect on FRP, and in depths–times where FRP exceeded the maximum consumption rate, there was no effect. The assumed weight of prey had a proportional effect on consumption (by weight) of predators and a smaller effect on GRP, risk, and the risk ratio. An independent 20% perturbation in the length of *Mysis* (used in the reaction distance model for ciscoes) resulted in ~40% change in the maximum FRP of ciscoes, but no change in the FRP experienced by ciscoes along the mean DVM trajectory in 2004, since this trajectory was largely in the dark where reaction distance was set by the minimum reaction distance. The perturbation in *Mysis* length had a much smaller effect on GRP and the risk ratio, since the maximum FRP greatly exceeded the maximum consumption rate.

Perturbations to the light parameters (k, τ, I_0) resulted in vertical shifts in the daytime portions of the depth–time field for FRP. For example, a 20% decrease in k (the most sensitive of the light parameters) extended the region of maximum daytime FRP for ciscoes from 50–80 to 50–100 m because of increased light penetration. Maximum values of FRP for ciscoes (i.e., at 50 m at noon) increased by 28%. Smaller changes in FRP were observed at other depths and

Fig. 4. Foraging rate potential (FRP, individuals encountered·day^{-1}) of ciscoes (*Coregonus* spp.) (*a*) and lake trout (*Salvelinus namaycush*) (*b*) and growth rate potential (GRP, g·day^{-1}) of ciscoes (*c*) and lake trout (*d*) by depth and time of day. White lines represent the mean diel vertical migration trajectories of ciscoes (*a*, *c*) and lake trout (*b*, *d*) in 2004.

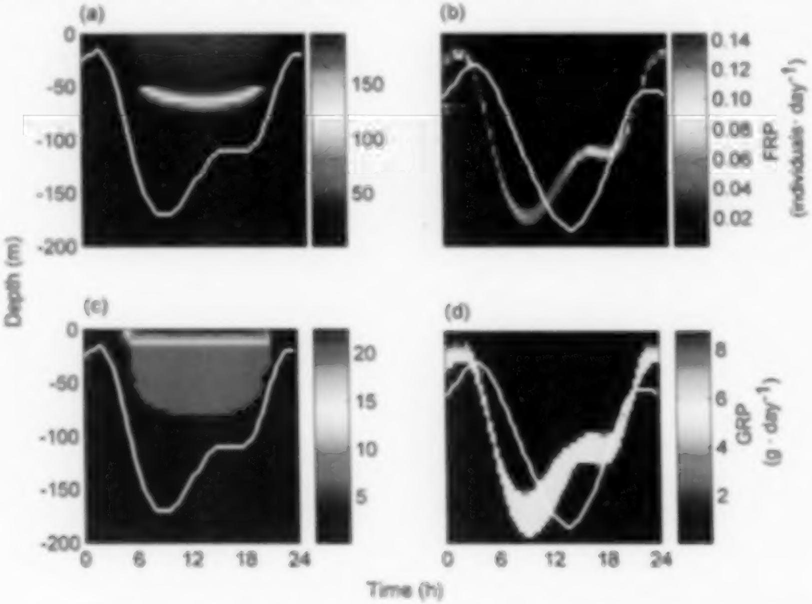

Fig. 5. Individual (*a*) and population (*b*) predation risk for ciscoes (*Coregonus* spp.) by depth and time. White lines represent the mean diel vertical migration trajectory of ciscoes in 2004.

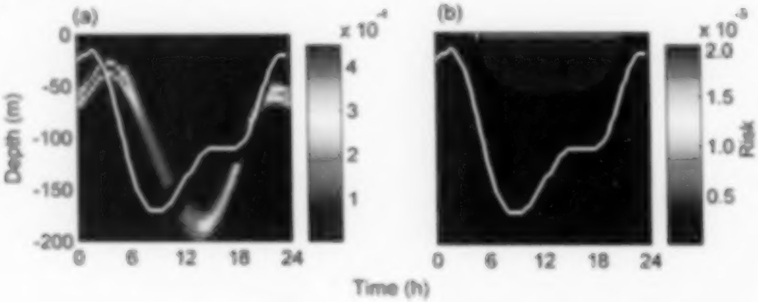

times. Changes in GRP, risk, and the risk ratio were less extreme. For example, the 20% decrease in *k* resulted in an 8% increase in μ for ciscoes at 50 m at noon.

Values of FRP for ciscoes and lake trout were sensitive to the minimum reaction distance. A 20% change in reaction distance resulted in a 40% change in FRP in the dark and lesser changes in the light.

The relatively high FRP and GRP for ciscoes just below the thermocline at night depended on the existence of a high-density *Mysis* layer. Such a layer has been frequently observed (Beeton 1960; Bowers and Grossnickle 1978; Levy 1991), but could not be quantitatively estimated from the available data on *Mysis* vertical distribution. If less than 62% of the *Mysis* observed by Bowers (1988) in the 0–50 m layer at night occurred in the depth bin just below the thermocline, higher FRP would be found below 50 m at night. During the day, the presence of highest FRP in the 50–80 m layer was based on modest densities of *Mysis* (0.94 individuals·m^{-3}) at these depths. These densities would need to be lower than 0.013 individuals·m^{-3} for higher FRP during the day to be found in deeper water.

Discussion

Do coregonids undergo vertical migration to increase foraging and growth or to reduce predation risk?

Previous consideration of coregonid vertical migration has focused on the potential foraging and growth benefits of migrating along with *Mysis*. Eshenroder and Burnham-Curtis (1999) suggested that vertical migration in deepwater ciscoes might have evolved in response to the vertical migration of *Mysis*. TeWinkel and Fleischer (1999) debated whether *Mysis* were driving the vertical migration, but noted that vertically migrating bloater (*Coregonus hoyi*) in Lake Michigan had a higher percentage of stomachs containing

Fig. 6. The ratio of predation risk to growth rate potential (GRP) for ciscoes (*Coregonus* spp.) by depth and time of day calculated over a time period of 1 day using individual (*a*) and population (*b*) risk formulas and calculated over 100 days using individual (*c*) and population (*d*) risk formulas. Depth–time bins in which GRP was less than 0.25 g·day^{-1} are unshaded. Lines represent the mean diel vertical migration trajectories of ciscoes in May and August 2001 (magenta and red, respectively) and August 2004 (black).

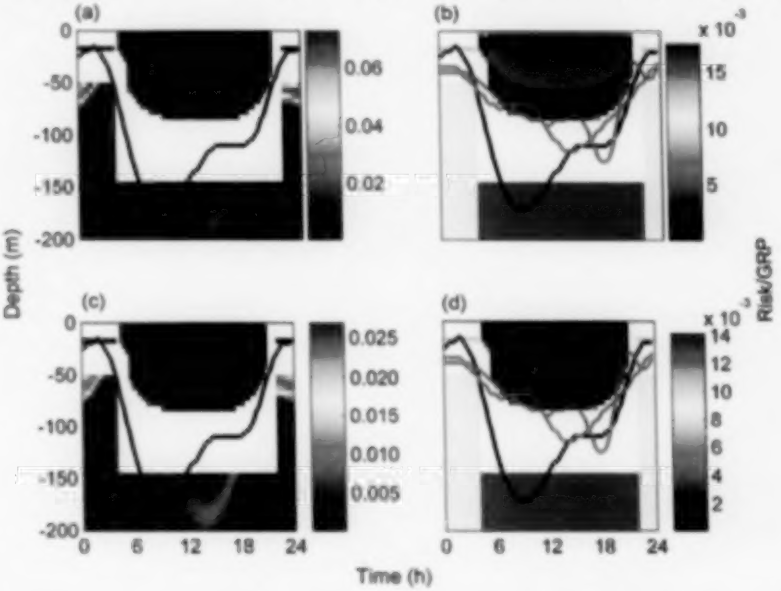

recently ingested prey than did bloater that remained on the bottom.

Our results offer little support for the hypothesis that a deep vertical migration confers a foraging or growth rate benefit for ciscoes. Higher foraging rates and GRP could be achieved through any number of alternative trajectories. At night, the maximum foraging rate and growth rate are found in the depth bin just below the thermocline, and DVM trajectories of ciscoes from all three time periods pass through or near this interval. During the day, however, substantially higher foraging rates and GRP can be found at depths with higher light levels, even though *Mysis* densities are dramatically lower at such depths. This is because even relatively low light levels increase the reaction distance of ciscoes, allowing them to search much larger volumes of water. Since all three observed DVM trajectories for ciscoes remain in low light and below the thermocline, they do not seem to be taking advantage of foraging opportunities available in higher light environments or more favorable temperatures for growth available near the surface. There are, of course, aspects of foraging behavior that are not captured by the model. For example, *Mysis* suspended in the water column may also be more visible to ciscoes from below if they are silhouetted against the surface. Other less understood aspects of visual predation such as polarization contrast (Sabbah and Shashar 2006) or near-ultraviolet light (Loew et al. 1993) may also be important.

Reducing predation risk is a more compelling explanation for the observed vertical migration of ciscoes, but is still incomplete. From the point of view of the individual, following the DVM trajectory chosen by the bulk of conspecifics results in lower individual risk; however, this observation begs the question: why does the group follow a particular DVM trajectory? The observed DVM trajectories of ciscoes kept them at low light levels, but not in complete darkness, throughout the day. A risk-minimizing population would stay entirely below the thermocline and below the depth of light penetration. This situation is approached by the deep DVM trajectory observed in 2004; however, all hypothetical DVM trajectories that avoid light and avoid the warmer epilimnion result in equally low risk.

The risk ratio based on population risk offers the best evidence for the benefit of a vertical migration. Two alternative minimum μ/G DVM trajectories are apparent. These trajectories overlap in the layer below the thermocline at night. During the day, the shallow trajectory follows a crescent that begins at the surface at dawn, moves progressively deeper during the day down to 80 m at noon, and ascends to near the surface at dusk. The deep trajectory descends from the layer below the thermocline into the 150–200 m stratum during the day. Both of these minimum μ/G trajectories are apparent in the risk ratio calculated over 1 and 100 days. The DVM trajectories observed in 2001 appear to follow the shallow (high risk, high growth) minimum μ/G trajectory. For 2004, when local lake trout densities were higher and coregonid densities were lower (Hrabik et al. 2006), the DVM trajectory is substantially deeper and appears to follow the deep (low risk, low growth) trajectory. This comparison assumes similar vertical distribution of light intensity and *Mysis* in 2001 and 2004.

Time-dependency of the risk ratio

Substantial differences in the μ/G patterns were apparent when these values were calculated over 100 days rather than 1 day. Werner and Gilliam (1984) proposed the ratio of risk to growth as a fitness-optimizing criterion for the timing of ontogenetic habitat shifts. Clark and Levy (1988) and Scheuerell and Schindler (2003) used the same criterion to understand trade-offs in juvenile sockeye vertical migration. Both growth and predation risk in Werner and Gilliam's (1984) example were instantaneous rates. In Scheuerell and Schindler's (2003) analysis and in the analysis presented here, growth and predation risk are modeled as discrete time functions, with the result that the value of μ/G depends on the time interval chosen, since survival probability is an exponential function of time, while over limited time periods, growth is approximately linear (Fig. 7; and see eq. 7 above). At very low or very high risk levels, the rate of increase in risk is low, and increases in growth dominate the equation. The opposite condition prevails at intermediate risk levels, where risk rises rapidly with time. Additionally, neither growth nor risk should be extrapolated indefinitely based on daily rates, as seasonal and ontogenetic changes in vital rates are likely. Figures *6b* and *6d* highlight a limitation of the risk ratio when extrapolated into the future. The shallow depth intervals in the daytime show relatively high μ/G when calculated for a single day, but low μ/G for the 100-day period. This result occurs because risk (the probability of predation mortality over the time period) reaches a maximum of one, while growth continues to accrue. Such time-dependency of μ/G must be considered when using discrete time calculations. The presence of size-dependent mortality bottlenecks (not considered here), such as winter periods when smaller individuals are likely to starve, will also influence the risk ratio (Schindler 1999).

Foraging and growth maximization by lake trout

In sharp contrast with ciscoes, lake trout appear to be following a DVM trajectory that offers substantial foraging and growth benefits. In Lake Superior, lake trout achieve high GRP not by seeking optimal temperatures, but by tracking the DVM trajectory of their coregonid prey. The fact that lake trout apparently do not follow a DVM trajectory that perfectly maximizes their GRP is not surprising considering that (*i*) ciscoes have likely evolved predator avoidance strategies and (*ii*) lake trout have limited sensory information regarding the location of their prey. Avoidance behavior by coregonids has been evaluated by Savitz and Bardygula (1989), who estimated that 60% of coregonid encounters with piscivores result in escape. This rate is undoubtedly sensitive to environmental conditions at the time of encounter, including the respective reaction distances of predator and prey (discussed below). Assuming a 40% capture efficiency, however, would lower the daily FRP of lake trout following the mean DVM trajectory from 0.64 to 0.26 ciscoes·day^{-1}, a value that is closer to the maximum consumption rate at 3 °C of one 125 g coregonid·week^{-1}. Previous applications of foraging models (e.g., Beauchamp et al. 1999) have also predicted that piscivores should encounter more than enough prey to satisfy observed growth and consumption. These results highlight the importance of understanding predator–prey interactions at fine temporal and spatial scales (Walters and Juanes 1993; Scheuerell 2004).

Changing trade-offs under changing conditions

The DVM patterns presented here represent a snapshot in space and time. Although all three components of this pelagic food chain have been shown to exhibit DVM in other times and places, the specific trajectories can differ substantially. For example, in 2001, ciscoes in the western arm of Lake Superior exhibited a much shallower and more variable DVM trajectory, with many individuals present in the 15–40 m depth range (Hrabik et al. 2006), well above the depth at which reaction distance of lake trout reaches a minimum. The model results suggest that ciscoes at this depth during the daytime experience high foraging rates, but also high risk. GRP is high above the thermocline and modest below it, because foraging rates that exceed the maximum daily ration are available at many depths. The risk ratio shows a crescent-shaped region of optimal conditions, discussed above, that occurs in deeper water.

Fig. 7. Predation risk (probability of dying due to predation during the given time period, broken black line), growth (solid black line), and risk/growth (solid gray line) as a function of time (days), assuming a daily predation risk of 0.001 and a daily growth rate of 0.01.

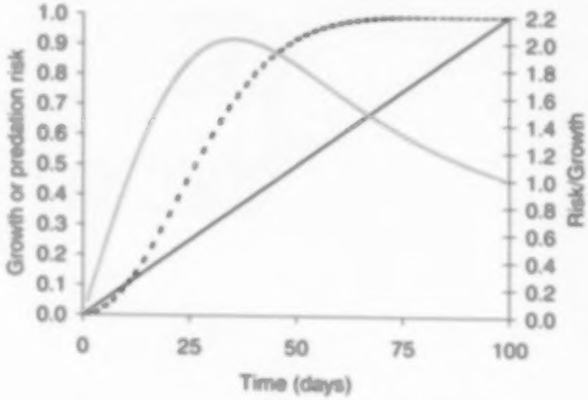

Why are ciscoes in 2001 using this high-risk, high-growth region rather than remaining in the relative safety of deeper water? The explanation may lie in the lower lake trout and higher coregonid densities in 2001 compared with 2004. The ratio of ciscoes to lake trout in the survey area in May and August 2001 was 1008 and 2940, respectively, while in August 2004 it was down to 163 (Hrabik et al. 2006). It appears that lower lake trout densities and higher densities of ciscoes in 2001 resulted in reduced predation risk per individual cisco, allowing ciscoes to take advantage of foraging and growth opportunities at shallower depths during the day. Density-dependent changes in risk-taking behavior (Walters and Juanes 1993) may also play a role if the lower coregonid densities in 2004 (70% and 62% lower compared with May and August 2001, respectively) resulted in less competition for food. The lack of data on *Mysis* densities for these two time periods unfortunately precludes a definitive test of this hypothesis.

The observed change in DVM behavior associated with a 7- to 18-fold decline in the coregonid to lake trout ratio suggests the possibility of a behavioral cascade (Romare and Hansson 2003). Predator-induced changes in DVM behavior have already been observed in the field for marine copepods (Frost and Bollens 1992) and *Daphnia* (Stirling et al. 1990). Cascading changes in DVM behavior could have potentially

Fig. 8. Relative reaction distance (i.e., the ratio of the reaction distance of ciscoes (*Coregonus* spp.) to that of lake trout (*Salvelinus namaycush*)) as a function of light level (lx) and turbidity (nephelometric turbidity units, NTU) (*a*) and over depth and time of day (*b*). Lines in panel (*b*) represent the diel vertical migration trajectory of ciscoes in May and August 2001 (magenta and red, respectively) and August 2004 (white).

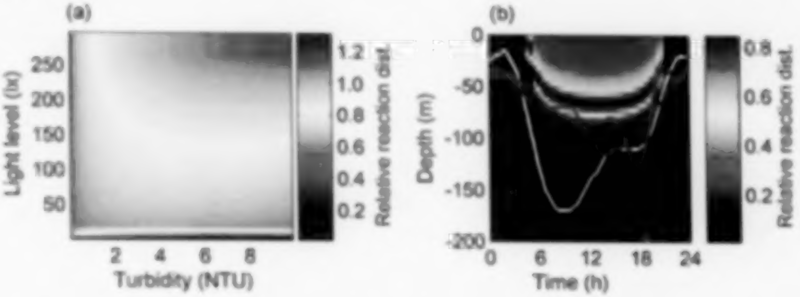

important practical and ecological consequences. For example, the two most common fishery-independent survey techniques, trawling and gill nets, target specific depths. If the vertical distribution of lake trout or coregonids changes with abundance, the catchability coefficient for these survey techniques will also change. Such changes have potentially dangerous implications for stock assessment, since they result in a violation of the assumption that catch per unit of effort is proportional to stock size. If ciscoes increasingly engage in risk avoidance behavior as the coregonid to lake trout ratio declines, then the predation rate will decline faster than simple "reaction vat" or Lotka–Volterra models suggest. This is one of the fundamental predictions of arena foraging theory (Walters and Juanes 1993). The potential for behavioral cascades in DVM behavior suggests that future studies of DVM should be broadened to include as many trophic levels as possible.

Large changes in turbidity are also likely to have an effect on the costs and benefits of different DVM trajectories. Increased turbidity results in greater light attenuation and therefore lower light intensity at depth, a result that would compress the region of highest FRP and highest risk into shallower depths. Experimental evidence, however, suggests that turbidity is likely to effect planktivores and piscivores differently. De Robertis et al. (2003) showed that feeding rates of piscivorous sablefish (*Anoplopoma fimbria*) were substantially reduced at turbidity levels that did not hamper feeding by planktivorous juvenile chum salmon (*Oncorhynchus keta*) and walleye pollock (*Theragra chalcogramma*). This result is consistent with the reaction distance models used here for lake trout and ciscoes. The relative reaction distance (i.e., the ratio of the reaction distance of ciscoes to that of lake trout) increases with turbidity, particularly at high light levels (Fig. 8*a*). The maximum relative reaction distance occurs at very low light intensity, but not in complete darkness when turbidity is low; however, at high turbidity, a second maximum appears at high light levels. Mapped across depth and time (Fig. 8*b*) at the low turbidities observed in the study area, the region of maximum relative reaction distance occurs in a crescent that is roughly coincident with the crescents seen in the illustration of risk/growth (Figs. 6*b*, 6*d*). At higher turbidities, such as those found on the south shore of the western arm of Lake Superior, the maximum relative reaction distance would occur at shallower depths during the day. This model prediction is consistent with observations that planktivorous rainbow smelt (*Osmerus mordax*) and larval lake herring are found nearer to the surface in high turbidity areas of the south shore of the western arm (Swenson 1978). Secchi disk casts conducted during the survey indicate low turbidity in the survey area and little difference in water clarity between 2001 and 2004 (Hrabik et al. 2006).

Model assumptions and sensitivity

The model assumptions of no predator avoidance ability and no silhouetting effect for prey viewed from below are discussed above. The limitations that the lack of *Mysis* data imposes on the interannual comparison are also stated. Two remaining assumptions deserve mention. First, fine-scale patchiness is not included in the model but is potentially important for calculations of μ. *Mysis* distributions were based on vertical net tows that integrate densities over wide depth intervals. The echo integration analysis (Hrabik et al. 2006) also precludes estimation of fine-scale patchiness of ciscoes. Patchiness of prey could increase foraging rates if patches were easier to locate than individual prey, but would otherwise make foraging rates more variable. Patchiness of predators would reduce μ, since risk is defined not by the number of encounters with predators, but by the probability of encountering any predators. If the patchiness of predators was known, its effect could be included in the model by adding an overdispersion parameter to the Poisson distribution used to calculate risk.

Reaction distances of lake trout and ciscoes are the most influential parameters in this model. Fortunately, feeding experiments have described the effect of a wide range of light intensities on reaction distance for both species. The experiments used to develop the reaction distance function for lake trout were conducted using a nested tank design in which prey were held in a small tank inside the larger experimental tank (Vogel and Beauchamp 1999). This design was used to eliminate all but visual stimuli. At short distances and in low light conditions, however, other sensory modes may increase the minimum reaction distance beyond what would be expected based on strictly visual experiments. Lake trout are known to be capable of feeding in near total darkness (Mazur and Beauchamp 2003), indicating that the minimum reaction distance is greater than zero and that nonvisual stimuli may be important at night or at depths below the limits of light penetration.

In conclusion, understanding the drivers of DVM requires a quantitative framework that allows foraging, growth, predation risk, and risk/growth trade-offs to be evaluated simultaneously for multiple trophic levels. Previous hypotheses concerning DVM in coregonids have focused on the putative foraging benefits of tracking vertically migrating *Mysis*. The model presented here indicates that predation risk is also an important factor and that a migration by ciscoes into deeper water during the day results in a more favorable trade-off between risk and growth and a greater relative reaction distance compared with lake trout. Lake trout feeding on ciscoes can generally achieve higher foraging and growth rates by tracking their vertically migrating prey. Such growth benefits suggest that the siscowet (*Salvelinus namaycush siscowet*) morphotype, with its high fat content and reduced swim bladder, may indeed be an evolutionary response to the vertical migration behavior exhibited by their coregonid prey, as suggested by Eshenroder and Burnham-Curtis (1999).

Acknowledgements

The helpful comments of Greg Sass on an earlier version of this manuscript are gratefully acknowledged. This work was funded by the University of Wisconsin Sea Grant Institute under grants from the National Sea Grant College Program, National Oceanic and Atmospheric Administration, US Department of Commerce, and from the State of Wisconsin (federal grant number NA16RG2257, project number R/LR-94). Additional funding was provided by a contract from the Minnesota Department of Natural Resources to T.R.H. and an Anna Grant Birge Memorial Fund award to O.P.J.

References

Bartell, S.M., Breck, J.E., Gardner, R.H., and Brenkert, A.L. 1986. Individual parameter perturbation and error analysis of fish bioenergetics models. Can. J. Fish. Aquat. Sci. **43**: 160–168.

Beauchamp, D.A., Baldwin, C.M., Vogel, J.L., and Gubala, C.P. 1999. Estimating diel, depth-specific foraging opportunities with a visual encounter rate model for pelagic piscivores. Can. J. Fish. Aquat. Sci. **56**: 128–139.

Beeton, A.M. 1960. The vertical migration of *Mysis relicta* in Lakes Huron and Michigan. J. Fish. Res. Board Can. **17**: 517–539.

Bevelheimer, M.S., and Adams, S.M. 1993. A bioenergetics analysis of diel vertical migration by kokanee salmon, *Oncorhynchus nerka*. Can. J. Fish. Aquat. Sci. **50**: 2236–2349.

Biro, P.A., Post, J.R., and Parkinson, E.A. 2003*a*. From individuals to populations: prey fish risk-taking mediates mortality in whole-system experiments. Ecology, **84**: 2419–2431.

Biro, P.A., Post, J.R., and Parkinson, E.A. 2003*b*. Density-dependent mortality is mediated by foraging activity for prey fish in whole-lake experiments. J. Anim. Ecol. **72**: 546–555.

Bowers, J.A. 1988. Diel vertical migration of the opossum shrimp *Mysis relicta* in Lake Superior — observations and sampling from the Johnson-Sea-Link II Submersible. Bull. Mar. Sci. **43**: 730–738.

Bowers, J.A., and Grossnickle, N.E. 1978. Herbivorous habits of *Mysis relicta* in Lake Michigan. Limnol. Oceanogr. **23**: 767–776.

Brandt, S.B., Mason, D.M., and Patrick, E.V. 1992. Spatially-explicit models of fish growth rate. Fisheries, **17**: 23–35.

Breck, J.E. 1993. Foraging theory and piscivorous fish — Are forage fish just big zooplankton? Trans. Am. Fish. Soc. **122**: 902–911.

Brett, J.R. 1971. Energetic response of salmon to temperature: a study of some thermal relations in the physiology and freshwater ecology of sockeye salmon. Fish. Bull. **70**: 99–113.

Carlander, K.D. 1969. Handbook of freshwater fishery biology. Vol. 1. The Iowa State University Press, Ames, Iowa.

Clark, C.W., and Levy, D.A. 1988. Diel vertical migrations by juvenile sockeye salmon and the antipredation window. Am. Nat. **131**: 271–290.

De Robertis, A., Ryer, C.H., Veloza, A., and Brodeur, R.D. 2003. Differential effects of turbidity on prey consumption of piscivorous and planktivorous fish. Can. J. Fish. Aquat. Sci. **60**: 1517–1526.

Eggers, D.M. 1978. Limnetic feeding behavior of juvenile sockeye salmon in Lake Washington and predator avoidance. Limnol. Oceanogr. **23**: 1114–1125.

Eshenroder, R.L., and Burnham-Curtis, M.K. 1999. Species succession and sustainability of the Great Lakes fish community. *In* Great Lakes fisheries policy and management. *Edited by* W.W. Taylor and C.P. Ferreri. Michigan State University Press, East Lansing, Mich. pp. 145–184.

Eshenroder, R.L., and Burnham-Curtis, M.K. 2001. Comment: Vertical migration of bloaters. Trans. Am. Fish. Soc. **130**: 166–167.

Eshenroder, R.L., Argyle, R.L., and TeWinkel, L.M. 1998. Evidence for buoyancy regulation as a speciation mechanism in Great Lakes ciscoes. Arch. Hydrobiol. **50**: 207–217.

Frost, B.W., and Bollens, S.M. 1992. Variability of diel vertical migration in the marine planktonic copepod *Pseudocalanus newmani* in relation to its predators. Can. J. Fish. Aquat. Sci. **49**: 1137–1141.

Gal, G., Loew, E.R., Rudstam, L.G., and Mohammadian, A.M. 1999. Light and diel vertical migration: spectral sensitivity and light avoidance by *Mysis relicta*. Can. J. Fish. Aquat. Sci. **56**: 311–322.

Gal, G., Rudstam, L.G., and Johannsson, O.E. 2004. Predicting *Mysis relicta* vertical distribution in lake Ontario. Arch. Hydrobiol. **159**: 1–23.

Gerritsen, J., and Strickler, J.R. 1977. Encounter probabilities and community structure in zooplankton — mathematical model. J. Fish. Res. Board Can. **34**: 73–82.

Grossnickle, N.E., and Morgan, M.D. 1979. Density estimates of *Mysis relicta* in Lake Michigan. J. Fish. Res. Board Can. **36**: 694–698.

Hanson, P.C., Johnson, T.B., Schindler, D.E., and Kitchell, J.F. 1997. Fish bioenergetics version 3.0. University of Wisconsin System Sea Grant Institute, Madison, Wis.

Hardiman, J.M., Johnson, B.M., and Martinez, P.J. 2004. Do predators influence the distribution of age-0 kokanee in a Colorado reservoir? Trans. Am. Fish. Soc. **133**: 1366–1378.

He, X., Wright, R., and Kitchell, J.F. 1993. Fish behavioral and community responses to manipulation. *In* The trophic cascade in lakes. *Edited by* S.R. Carpenter and J.F. Kitchell. Cambridge University Press, Cambridge, UK. pp. 69–84.

Hrabik, T.R., Jensen, O.P., Martell, S.J.D., Walters, C.J., and Kitchell, J.F. 2006. Diel vertical migration in the Lake Superior pelagic community. I. Changes in vertical migration of coregonids in response to varying predation risk. Can. J. Fish. Aquat. Sci. **63**: 2286–2295.

Hugie, D.M., and Dill, L.M. 1994. Fish and game: a game theoretic approach to habitat selection by predators and prey. J. Fish Biol. **45**: 151–169.

Hutchinson, G.E. 1957. A treatise on limnology. Vol. I. Geology, physics, and chemistry. Wiley, New York.

Iwasa, Y. 1982. Vertical migration of zooplankton: a game between predator and prey. Am. Nat. **120**: 171–180.

Janssen, J., and Brandt, S.B. 1980. Feeding ecology and vertical migration of adult alewives (*Alosa pseudoharengus*) in Lake Michigan. Can. J. Fish. Aquat. Sci. **37**: 177–184.

Johannsson, O.E. 1995. Response of *Mysis relicta* population dynamics and productivity to spatial and seasonal gradients in Lake Ontario. Can. J. Fish. Aquat. Sci. **52**: 1509–1522.

Kitchell, J.F., Stewart, D.J., and Weininger, D. 1977. Applications of a bioenergetics model to yellow perch (*Perca flavescens*) and walleye (*Stizostedion vitreum vitreum*). J. Fish. Res. Board Can. **34**: 1922–1935.

Koenings, J.P., and Edmundson, J.A. 1991. Secchi disk and photometer estimates of light regimes in Alaskan lakes: effects of yellow color and turbidity. Limnol. Oceanogr. **36**(1): 91–105.

Lampert, W., and Sommer, U. 1997. Limnoecology: the ecology of lakes and streams. Oxford University Press, Oxford, UK.

Levy, D.A. 1990*a*. Reciprocal diel vertical migration behavior in planktivores and zooplankton in British Columbia lakes. Can. J. Fish. Aquat. Sci. **47**: 1755–1764.

Levy, D.A. 1990*b*. Sensory mechanism and selective advantage for diel vertical migration in juvenile sockeye salmon, *Oncorhynchus nerka*. Can. J. Fish. Aquat. Sci. **47**: 1796–1802.

Levy, D.A. 1991. Acoustic analysis of diel vertical migration behavior of *Mysis relicta* and kokanee (*Oncorhynchus nerka*) within Okanagan Lake, British Columbia. Can. J. Fish. Aquat. Sci. **48**: 67–72.

Link, J., and Edsall, T.A. 1996. The effect of light on lake herring (*Coregonus artedi*) reactive volume. Hydrobiologia, **332**: 131–140.

Loew, E.R., McFarland, W.N., Mills, E.L., and Hunter, D. 1993. A chromatic action spectrum for planktonic predation by juvenile yellow perch, *Perca flavescens*. Can. J. Zool. **71**: 384–386.

Mason, D.M., and Patrick, E.V. 1993. A model for the space–time dependence of feeding for pelagic fish populations. Trans. Am. Fish. Soc. **122**: 884–901.

Mazur, M.M., and Beauchamp, D.A. 2003. A comparison of visual prey detection among species of piscivorous salmonids: effects of light and low turbidities. Environ. Biol. Fishes, **67**: 397–405.

Narver, D.W. 1970. Diel vertical movements of underyearling sockeye salmon and the limnetic zooplankton in Babine Lake, British Columbia. J. Fish. Res. Board Can. **27**: 281–316.

NSRDB (National Solar Radiation Database). 2004. NSRDB hourly data files for Duluth (Weather Bureau Army Navy (WBAN) Identification Number 14913) [online]. Available from http://rredc.nrel.gov/solar/old_data/nsrdb/hourly/1990/14913_90.txt [accessed on 8 December 2004].

Romare, P., and Hansson, L.A. 2003. A behavioral cascade: top-predator induced behavioral shifts in planktivorous fish and zooplankton. Limnol. Oceanogr. **48**: 1956–1964.

Roy, D., Haffner, G.D., and Brandt, S.B. 2004. Estimating fish production potentials using a temporally explicit model. Ecol. Model. **173**: 241–257.

Rudstam, L.G., Binkowski, F.P., and Miller, M.A. 1994. A bioenergetics model for analysis of food consumption patterns of bloater in Lake Michigan. Trans. Am. Fish. Soc. **123**: 344–357.

Sabbah, S., and Shashar, N. 2006. Polarization contrast of zooplankton: a model for polarization-based sighting distance. Vision Res. **46**: 444–456.

Savitz, J., and Bardygula, L. 1989. Analysis of the behavioral basis for changes in salmonid diets. Illinois–Indiana Sea Grant Report. IL-SG-R-89-3.

Scheuerell, M.D. 2004. Quantifying aggregation and association in three-dimensional landscapes. Ecology, **85**: 2332–2340.

Scheuerell, M.D., and Schindler, D.E. 2003. Diel vertical migration by juvenile sockeye salmon: empirical evidence for the antipredation window. Ecology, **84**: 1713–1720.

Schindler, D.E. 1999. Migration strategies of young fishes under temporal constraints: the effect of size-dependent overwinter mortality. Can. J. Fish. Aquat. Sci. **56**: 61–70.

Schoener, T.W. 1971. Theory of feeding strategies. Annu. Rev. Ecol. Syst. **2**: 369–404.

Stewart, D.J., Weininger, D., Rottiers, D.V., and Edsall, T.A. 1983. An energetics model for lake trout, *Salvelinus namaycush* — application to the Lake Michigan population. Can. J. Fish. Aquat. Sci. **40**: 681–698.

Stirling, D.G., McQueen, D.J., and Johannes, M.R.S. 1990. Vertical migration in *Daphnia galeata mendotae* (Brooks) — demographic responses to changes in planktivore abundance. Can. J. Fish. Aquat. Sci. **47**: 395–400.

Stockwell, J.D., and Johnson, B.M. 1999. Field evaluation of a bioenergetics-based foraging model for kokanee (*Oncorhynchus nerka*). Can. J. Fish. Aquat. Sci. **56**: 140–151.

Swenson, W.A. 1978. Influence of turbidity on fish abundance in western Lake Superior. Environmental Protection Agency, Washington, D.C. Rep. EPA-600/3-78-067.

TeWinkel, L.M., and Fleischer, G.W. 1999. Vertical migration and nighttime distribution of adult bloaters in Lake Michigan. Trans. Am. Fish. Soc. **128**: 459–474.

Tyler, J. 1998. A users guide for growth rate potential map maker version 2.0. Cooperative Institute for Limnology and Ecosystems Research, University of Michigan, Ann Arbor, Mich.

Vogel, J.L., and Beauchamp, D.A. 1999. Effects of light, prey size, and turbidity on reaction distances of lake trout (*Salvelinus namaycush*) to salmonid prey. Can. J. Fish. Aquat. Sci. **56**: 1293–1297.

Walters, C.J., and Juanes, F. 1993. Recruitment limitation as a consequence of natural selection for use of restricted feeding habitats and predation risk taking by juvenile fishes. Can. J. Fish. Aquat. Sci. **50**: 2058–2070.

Werner, E.E., and Gilliam, J.F. 1984. The ontogenetic niche and species interactions in size-structured populations. Annu. Rev. Ecol. Syst. **15**: 393–425.

Werner, E.E., Gilliam, J.F., Hall, D.J., and Mittelbach, G.G. 1983. An experimental test of the effects of predation risk on habitat use in fish. Ecology, **64**: 1540–1548.

Wright, D.I., and O'Brien, W.J. 1984. The development and field test of a tactical model of the planktivorous feeding white crappie (*Pomoxis annularis*). Ecol. Monogr. **54**: 65–98.

Could increased cyanobacterial biomass following forest harvesting cause a reduction in zooplankton body size structure?

Anas Ghadouani, Bernadette Pinel-Alloul, and Ellie E. Prepas

Abstract: Changes in phytoplankton and zooplankton communities were studied in 16 lake-years during a large-scale experimental before–after study as part of the Terrestrial Riparian Organisms Lakes and Streams (TROLS) project. After forest harvesting, phytoplankton biomass and especially cyanobacterial biomass increased in some of the experimental lakes, up to an order of magnitude. Although the response of phytoplankton was not directly related to the intensity of forest harvesting, this large-scale experiment provided a unique opportunity for studying the effects of an increasing gradient in cyanobacterial biomass on zooplankton communities. Cladoceran size structure and biomass were negatively correlated with cyanobacterial biomass, suggesting that large cladocerans and especially daphnids were inhibited by the increase in cyanobacterial biomass. The increase in cyanobacterial biomass seems to have caused a significant reduction in the size structure of zooplankton communities. As no correlation was found between cladocerans and cyanotoxins, our results point more towards feeding inhibition by filamentous and colonial cyanobacteria as a possible cause for the decline in the size structure and biomass of zooplankton communities. These results suggest that the increase in cyanobacterial biomass is likely to cause a shift in the size of zooplankton communities, which will lead to a profound change in functioning of lake systems.

Résumé : Nous avons étudié les changements dans les communautés de phytoplancton et de zooplancton dans 4 lacs durant 4 ans (16 lacs-années) lors d'une expérience à grande échelle dans le cadre du projet TROLS (« Terrestrial Riparian Organisms Lakes and Streams »). Après la coupe forestière, la biomasse phytoplanctonique et particulièrement celle des cyanobactéries a augmenté par un ordre de grandeur, dans certains des lacs expérimentaux. Bien que la réponse du phytoplancton ne soit pas directement reliée à l'intensité de la récolte forestière, cette expérience à grande échelle a fourni une occasion unique d'étudier les effets d'un gradient croissant de biomasse de cyanobactéries sur les communautés zooplanctoniques. La structure en taille et la biomasse des cladocères étaient négativement corrélés avec la biomasse des cyanobactéries, ce qui suggère que les cladocères de grande taille, et en particulier les daphniidés, sont inhibés par l'accroissement de la biomasse des cyanobactéries. L'augmentation de la biomasse des cyanobactéries semble avoir causé une réduction significative dans la structure de taille de la communauté de zooplancton. Dans l'absence de corrélation entre les cladocères et les cyanotoxines, nos résultats appuient la thèse d'une inhibition de l'alimentation par les cyanobactéries filamenteuses et coloniales comme cause possible du déclin de la structure en taille et de la biomasse des communautés de zooplancton. Ces résultats indiquent que l'augmentation de la biomasse des cyanobactéries cause vraisemblablement une réduction de la taille des communautés zooplanctoniques, ce qui peut mener à un profond changement dans le fonctionnement des systèmes lacustres.

[Traduit par la Rédaction]

Introduction

Understanding the interactions between zooplankton and phytoplankton is fundamental in aquatic ecology. Classical concepts in ecology such as biomanipulation, trophic cascades (Shapiro and Wright 1984; Carpenter et al. 1985), or bottom-up control (McQueen et al. 1986) are all based on efficient energy transfer through pelagic foodwebs. Some of these concepts have been used in attempts to control phytoplankton biomass in eutrophic systems with limited success

Received 3 November 2005. Accepted 20 June 2006. Published on the NRC Research Press Web site at http://cjfas.nrc.ca on 30 September 2006.
J18977

A. Ghadouani.[1] Aquatic Ecology and Ecosystem Studies, School of Environmental Systems Engineering, The University of Western Australia, 35 Stirling Highway, M015, Perth, Western Australia, 6009, Australia.
B. Pinel-Alloul. GRIL – Département de sciences biologiques, Université de Montréal, C.P. 6128, succ. Centre-ville, Montréal, QC H3C 3J7, Canada
E.E. Prepas. Faculty of Forestry and Forest Environment, Lakehead University, Thunder Bay, Ontario, P7B 5E1, Canada, and Department of Biological Sciences, University of Alberta, Edmonton, AB T6G 2E9, Canada.

[1] Corresponding author (e-mail: Anas.Ghadouani@uwa.edu.au).

Can. J. Fish. Aquat. Sci. 63: 2308–2317 (2006) doi:10.1139/F06-117

because of insufficient control of the primary producers by grazers (MacKay and Elser 1998). The inefficiency of zooplankton in controlling phytoplankton biomass in eutrophic lakes could be attributed to the dominance of phytoplankton communities by large inedible colonial and filamentous cyanobacterial species (MacKay and Elser 1998). Despite experimental evidence showing negative impact of some cyanobacterial species on large filter-feeding cladocerans such as *Daphnia* (Lampert 1982; Haney et al. 1994; Reinikainen et al. 1995), several studies support the idea that zooplankton may be able to control phytoplankton in eutrophic conditions (Boon et al. 1994; Brett and Goldman 1996; MacKay and Elser 1998). This dialectic has long been the center of a vigorous debate about the success of biomanipulation in eutrophic, cyanobacteria-dominated systems (Carpenter and Kitchell 1992; DeMelo et al. 1992).

Widely accepted empirical models predict that zooplankton are positively related to phytoplankton biomass in lakes (McCauley and Kalff 1981). In contrast, plankton succession models predict a decline in zooplankton biomass with the midsummer increase in the proportion of inedible phytoplankton (Sommer et al. 1986). This midsummer decline in total zooplankton biomass is usually attributed to loss of large cladocerans mainly due to fish predation (Sommer et al. 1986). Although the mechanism behind this phenomenon is not elucidated, it could be explained, at least partially, by a shift in phytoplankton community structure from small edible to large inedible phytoplankton, whereas it had been previously ascribed exclusively to predation (Threlkeld 1979; Benndorf et al. 2001). Many laboratory studies have shown that cladocerans (i.e., *Daphnia*) are negatively affected by cyanobacterial species (Lampert 1982; Haney et al. 1994; Reinikainen et al. 1999); however, there is no clear indication that cyanobacterial abundance can inhibit large zooplankton at the lake ecosystem level. Although it is generally believed that outbreaks of harmful algal blooms have been escalating in frequency and magnitude (Hallegraeff 1993), there have been only limited attempts to examine their impact at the whole-lake scale. This void makes it difficult to apply the information gained from laboratory studies or small-scale experiments to understand cyanobacteria–zooplankton interactions in natural systems.

The main objective of the present study is to test for the existence of negative effects of increased cyanobacterial biomass on zooplankton communities in eutrophic lakes at the whole-lake scale. Here, we examine cyanobacteria–zooplankton interactions over 4 years along a productivity gradient in four lakes that were subjected to a large-scale ecosystem manipulation whereby forest harvesting occurred in the lake watersheds (Prepas et al. 2001). Although there is consistent evidence that forest harvesting causes major changes to the hydrology and the cycling of nutrients and contaminants within the catchments (Likens et al. 1970; O'Driscoll et al. 2004), only a limited number of studies have investigated the effects of forest harvesting on various compartments of the aquatic foodwebs (Rask et al. 1998; Patoine et al. 2000). The first results from the Terrestrial Riparian Organisms Lakes and Streams (TROLS) programme showed no evidence that buffer-strip width had influenced lake response; however, there was indication that the interaction between forest harvesting and weather conditions (i.e., precipitation) resulted in an increase of 40% in total phosphorus after the manipulation (Prepas et al. 2001). Following the increase in nutrient export from the perturbed catchments, phytoplankton and especially the dominance of toxic cyanobacterial biomass have increased (Prepas et al. 2001). Based on results of previous studies on plankton succession in similar lakes (Ghadouani et al. 1998) and laboratory and field experiments (Ghadouani and Pinel-Alloul 2002; Ghadouani et al. 2003), we anticipated that increased cyanobacterial biomass and their secondary metabolites (e.g., microcystins) would result in (*i*) a shift in the size structure of zooplankton communities from large to small zooplankters, (*ii*) a decline in large cladoceran biomass, and (*iii*) little or no effect on the other zooplankton groups such as copepods. These changes would induce a shift in the zooplankton community structure from dominance by large cladocerans to smaller copepods and, consequently, a decline in the cladoceran–copepod ratio with increasing cyanobacterial biomass and microcystin concentrations. Major changes in zooplankton community size structure could significantly alter a wide range of lake processes such as primary production, energy transfer between trophic levels, and nutrient cycling, as well as heat budget and light penetration (Mazumder et al. 1990; Moore and Folt 1993; Steiner 2004).

Materials and methods

Study site and experimental design

The study lakes represent one subregion of the TROLS research project that evaluated the effects of forest harvesting and buffer strips on terrestrial and aquatic ecosystems (Prepas et al. 2001). The experimental lakes used in this study are all headwater and are located in the South Pelican Hills (SPH) in the southern portion of Alberta's boreal mixed-wood ecoregion. All four lakes used in the present study are relatively small and shallow, with surface areas ranging from 44 to 157 ha and mean depths ranging from 1.4 to 4.7 m (Table 1). Their drainage ratio, defined as the drainage basin area divided by the lake surface area, ranges from 6 to 22, resulting in important export of nutrients to the lakes. As a consequence, these lakes are quite productive and could be classified in the upper end of mesotrophic with average chlorophyll *a* (chl *a*) values of ~16 $\mu g \cdot L^{-1}$ (Prepas et al. 2001). More details about the limnological and physical features of the study lakes can be found in Prepas et al. (2001). Fish communities are typical of Alberta's boreal mixed-wood ecoregion lakes and are known to have low species richness (Tonn et al. 2004). Fathead minnow (*Pimephales promelas*), yellow perch (*Perca flavescens*), and brook stickleback (*Culaea inconstans*) are among the most common plantivorous fish species in these lakes (Beaudoin et al. 2001).

The experimental treatment consisted of harvesting the catchment up to a forested (buffer) strip around the lakes of 800, 200, 100, and 20 m in lakes SPH 800, SPH 200, SPH 100, and SPH 20, respectively. The study began in 1995 and lasted for 4 years. Forest harvesting took place in the experimental sites in the middle of the study period from October 1996 to February 1997, which resulted in a 4-year study that

Table 1. Selected lake and watershed characteristics for South Pelican Hill (SPH) lakes 20, 100, 200, and 800, where the numbers refer to the minimum width (in metres) of the forested buffer strip left after the experimental forest cut.

Lakes	Lake area (ha)	Maximum depth (m)	Average depth (m)	Drainage basin area (ha)	Drainage ratio	Percent total cut	Percent cut within 800 m
SPH 20	157	9.4	4.7	1053	6.7	28	33
SPH 100	56	2.6	1.4	840	15.0	10	30
SPH 200	44	9.1	3.7	964	21.9	22	21
SPH 800	65	3.9	2.3	650	10.0	6	0

Note: The drainage ratio is calculated from the drainage basin area divided by the lake surface area. The percentage of the cut area relative to the total drainage basin (percent total cut) and the percentage area cut within 800 m of each lake are presented as indication of the magnitude of the disturbance. Data in this table are from Prepas et al. (2001).

Fig. 1. Relationship between cyanobacteria biomass and chlorophyll biomass ($r = 0.95$, $P < 0.0001$) in the four experimental lakes from 1995 to 1998. Lakes: SPH 20, triangles; SPH 100, circles; SPH 200, squares; SPH 800, diamonds. Pretreatment (1995 and 1996) data are represented by open symbols; posttreatment (1997 and 1998) data are represented by solid symbols. A simple linear fit is displayed as a solid line; upper and lower 95% confidence intervals are indicated by broken lines.

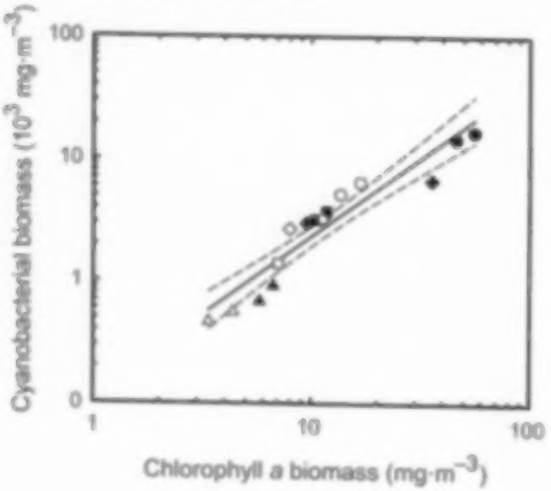

Fig. 2. (*a*) Cladoceran and (*b*) *Daphnia* spp. size structure represented in boxplots as a function of (*c*) cyanobacterial biomass gradient starting from low to high biomass in the four experimental lakes, SPH 20, SPH 100, SPH 200, and SPH 800, for four years (1995 to 1998). Each boxplot summarizes the size of cladoceran or *Daphnia* populations in one year and contains from 114 to 670 data points. Planktivorous fish density is shown in catch-per-unit-effort (CPUE). Numbers in parentheses are planktivorous fish densities for posttreatment years. Cyanobacterial biomass is shown as a seasonal average for each of the study years (1995 to 1998) in the four experimental lakes. Error bars are ± standard errors of the mean based on seasonal data.

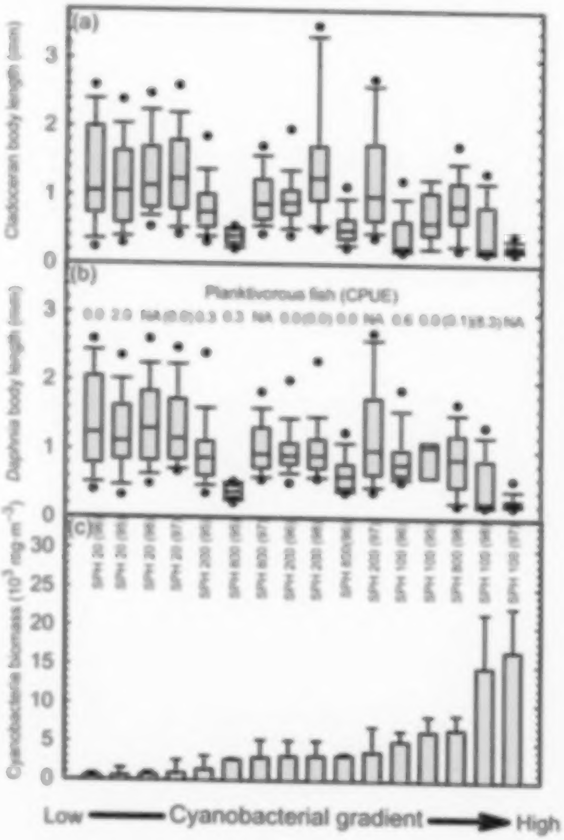

included 2-year pretreatment and 2-year posttreatment periods. The experimental forest harvesting resulted in clearing of 33%, 30%, and 21% within the 800 m around the lake in SPH 20, SPH 100, and SPH 200, respectively (Table 1). No harvesting occurred within 800 m of SPH 800, which is considered to be the control lake in this study. When the total catchment area for each lake is considered, only 28%, 10%, and 22% of the total catchment was cleared in SPH 20, SPH 100, and SPH 200, respectively, whereas about 6% of the catchment of the control lake, SPH 800, was cleared (Table 1). A series of logistic difficulties resulted in a deviation from the original experimental harvesting plan; however, the lake catchments were harvested with increased intensity, ranging from low or no perturbation in SPH 800 to high perturbation in SPH 20 (Table 1). Although not related to buffer-strip width, there is evidence that the combined effect of weather conditions and forest harvesting resulted in increased phosphorus export to the lakes and substantial increases in total

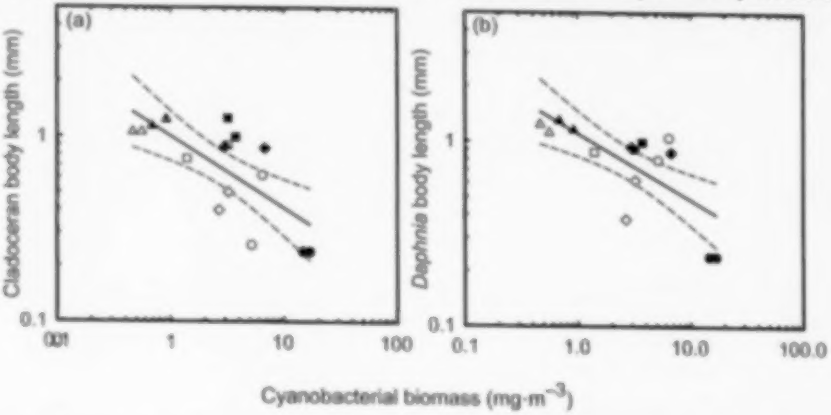

Fig. 3. Relationship between (*a*) cladoceran median body length ($r = -0.71$, $P < 0.01$), (*b*) *Daphnia* median body length ($r = -0.71$, $P < 0.01$), and cyanobacterial biomass. Lakes: SPH 20, triangles; SPH 100, circles; SPH 200, squares; SPH 800, diamonds. Pretreatment (1995 and 1996) data are represented by open symbols; posttreatment (1997 and 1998) data are represented by solid symbols. A simple linear fit is displayed as a solid line; upper and lower 95% confidence intervals are represented by broken lines.

phytoplankton and cyanobacterial biomass in some of the experimental lakes (Prepas et al. 2001).

Sampling and analyses

The lakes were sampled on a biweekly basis during the open-water season between May and September 1995 to 1998. On each sampling date, routine limnological measurements, including profiles of light penetration, water temperature, and dissolved oxygen, were taken at the deepest site of each lake. Integrated water samples of the euphotic zone, defined as the depth reached by 1% of incident light, were taken with a weighted Tygon tubing fitted with a one-way foot valve for chemical analyses. Chlorophyll *a* concentrations were estimated following a cold ethanol extraction method (Bergmann and Peters 1980). Lugol-preserved phytoplankton samples were analyzed and phytoplankton species were identified and counted with an inverted microscope according to the Utermöhl method (Lund et al. 1958). Microcystin-LR concentrations were estimated with a high-performance liquid chromatography method after extraction of lyophilized phytoplankton biomass (Zurawell et al. 1999). Microcystin-LR concentrations were then expressed in micrograms per gram of lyophilized seston dry mass. Seston collected with plankton net (53 µm mesh size) comprised both phytoplankton and zooplankton. The presence of zooplankton may cause microcystin measurement to be underestimated; however, on average, zooplankton represented only <5% of the total seston. It was therefore assumed that the presence of zooplankton in the samples would only have negligible effect on microcystin measurements.

Zooplankton samples were collected from the pelagic zone near the deepest point of each lake with a cantilevering net (53 µm mesh size) with a square opening (Filion et al. 1993). Vertical net hauls over the entire water column were performed at each sampling site. Zooplankton were preserved in 4% buffered formaldehyde solution after being narcotized in the field with carbonated water. In the laboratory, 5 mL subsamples, taken from the concentrated samples with a pipet outfitted with a wide opening, were analyzed with a stereomicroscope in a Ward cell (Ward 1955). Crustacean zooplankters were identified to species and their body lengths were measured. The body length of each individual was converted to dry mass by applying published length – dry mass relationships (Malley et al. 1989).

Statistical analyses

Correlation analysis was used to establish and measure the intensity of statistical associations between selected zooplankton and phytoplankton variables, especially in the context of increasing cyanobacterial biomass. To minimize the effect of temporal autocorrelation, data collected over a season have been averaged and only a single data point per lake-year is used in the statistical analyses (Hurlbert 1984). Each data point shown in the relationships is a seasonal average for a study year (1995 to 1998). All data used in statistical analyses were log-transformed and checked for normal distribution through the examination of the distribution of the residuals against the predicted values. A simple linear fit was used for the statistically significant correlations and displayed as a solid line with upper and lower 95% confidence intervals. All statistical analyses were performed with Systat 10.0 (Systat Software Inc. 2000).

Results

In the four experimental lakes, cyanobacterial biomass was strongly and positively correlated ($r = 0.95$, $P < 0.0001$) to chlorophyll biomass (Fig. 1). This relationship was mainly driven by SPH 100 and SPH 800, where cyanobacterial biomass increased by almost an order of magnitude after the watershed disturbance in 1997 and 1998 (Fig. 1). An examination of zooplankton communities along the productivity gradient revealed a trend by which cladocerans body length tended to decrease with increasing cyanobacterial biomass (Fig. 2). Lakes with relatively low cyanobacterial biomass tended to have large cladocerans (>1 mm), especially daphnids, whereas lakes with higher cyanobacterial biomass had only smaller cladocerans (<1 mm) (Fig. 2). At low cyanobacterial biomass, more than half of the cladocerans or daphnids were >1 mm in body length (Fig. 2). Lakes with moderate to high cyanobacterial biomass, with the exception of SPH 200, had only small cladocerans, where between 50% and up to 100% of the counted organisms were smaller than 1 mm in body length (Fig. 2). The same trend was observed when only daphnids were considered (Fig. 2). On the other hand, there was no indication that planktivorous predation increased along the same gradient (Fig. 2). Zooplankton size structure, as indicated by Cladoceran and *Daphnia* body length, were negatively correlated ($r = -0.71$, $P < 0.01$) to cyanobacterial biomass (Fig. 3). *Daphnia* and cladoceran biomass were also both negatively correlated ($r = -0.66$, $P < 0.01$, and $r = -0.56$, $P < 0.03$, respectively) to cyanobacterial biomass (Figs. 4*a*, 4*b*).

The strongest correlation between zooplankton and phytoplankton was found between the cladoceran–copepod ratio, used here as an indication of cladoceran dominance over copepods, and cyanobacterial biomass ($r = -0.79$, $P < 0.001$). This negative relationship suggests that the cladoceran dominance over copepods became weaker as lakes became more productive (Fig. 4*c*). In lakes where cyanobacterial biomass was the highest (i.e., SPH 100 in 1997 and 1998), copepods dominated over cladocerans and represented up to five times their biomass (Fig. 4*c*). However, there was no apparent correlation between copepod or total zooplankton biomass and chl *a* or cyanobacterial biomass (Fig. 5). None of the zooplankton variables showed any correlation with cyanotoxins, namely microcystin-LR (Fig. 6). It is important to note that although no correlations were found between cyanotoxins and zooplankton variables, cyanotoxin concentrations were an order of magnitude higher in the posttreatment period as shown by the distribution of the data points (Fig. 6).

Discussion

The interaction between the experimental forest harvesting and variations in annual precipitation resulted in important enhancement of productivity in some of the experimental lakes (Prepas et al. 2001). Although the response of the experimental systems was not proportional to the intensity of the perturbation, the experiment resulted in the creation of an ideal context for testing our main hypothesis with a gradient in cyanobacterial biomass ranging from low to extremely high. The highest cyanobacterial biomass was recorded in the posttreatment period of 1997 and 1998 in SPH 100. Our results showed that chl *a* concentration was strongly and positively correlated with cyanobacterial biomass, suggesting that along with the increase in lake productivity there was an increase in cyanobacterial biomass as well. Algal communities in SPH region lakes were mainly dominated by filamentous cyanobacterial species such as *Aphanizomenon* spp. and *Anabaena* spp., as well as colonial *Microcystis* spp. (Prepas et al. 2001). This species association is typical of eutrophic lakes in the Boreal plain (Zhang and Prepas 1996; Ghadouani et al. 1998; Zhang et al. 2001).

The main effect of increased cyanobacterial biomass following the experimental forest harvesting seems to be the decline in the size structure and the biomass of filter-feeding cladoceran populations and especially daphnids. This finding is consistent with previous studies in which large filter-feeding

Fig. 4. Relationship between (*a*) *Daphnia* biomass ($r = -0.66$, $P < 0.01$), (*b*) cladoceran biomass ($r = -0.56$, $P < 0.05$), and (*c*) Cladoceran–copepod ratio ($r = -0.79$, $P < 0.001$) and cyanobacterial biomass. Lakes: SPH 20, triangles; SPH 100, circles; SPH 200, squares; SPH 800, diamonds. Pretreatment (1995 and 1996) data are represented by open symbols; posttreatment (1997 and 1998) data are represented by solid symbols. A simple linear fit is displayed as a solid line; upper and lower 95% confidence intervals are represented by broken lines. The linear fit is only displayed for statistically significant correlations.

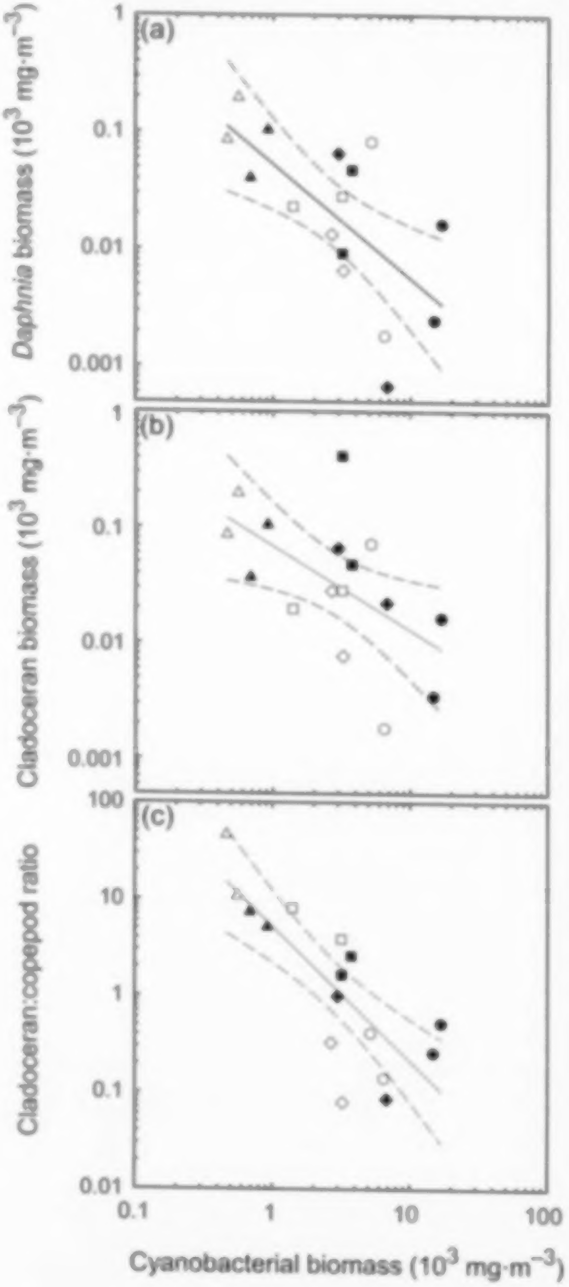

Fig. 5. Relationship between copepod biomass and (*a*) chlorophyll biomass ($r = 0.35$, $P = 0.19$) or (*b*) cyanobacteria biomass ($r = 0.13$, $P = 0.64$) and total zooplankton biomass and (*c*) chlorophyll biomass ($r = -0.28$, $P = 0.29$) or (*d*) cyanobacteria biomass ($r = -0.13$, $P = 0.62$). Lakes: SPH 20, triangles; SPH 100, circles; SPH 200, squares; SPH 800, diamonds. Pretreatment (1995 and 1996) data are represented by open symbols; posttreatment (1997 and 1998) data are represented by solid symbols. No fit was displayed, as none of the correlations was statistically significant.

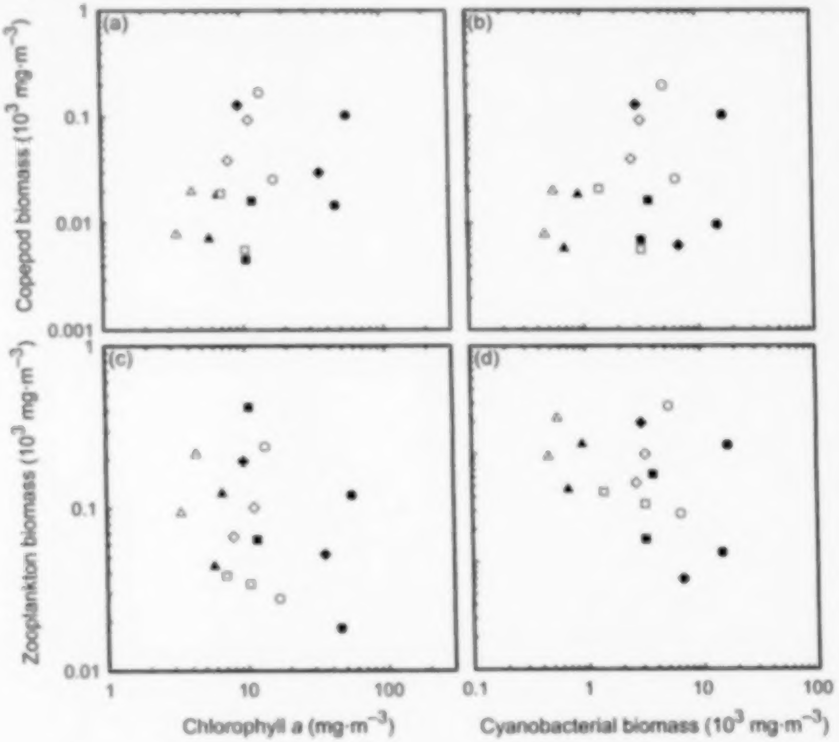

cladocerans were found to be inhibited by the presence of colonial and filamentous cyanobacterial species. It was suggested that smaller cladocerans may have a survival advantage because they can feed between cyanobacterial filaments, whereas larger cladocerans such as *Daphnia* may be severely inhibited (Webster and Peters 1978; DeMott et al. 2001). These patterns were also confirmed in large enclosure experiments where increased cyanobacterial biomass caused daphnids with body length >1 mm to decline significantly (Ghadouani et al. 2003). Early studies have shown that the presence of cyanobacterial filaments or colonies can cause daphnids to reject the total content of their food groove (Burns 1968) and to reduce their filtering rate (McMahon and Rigler 1963). This change in the feeding behavior is likely to cause higher mortality by starvation of large daphnids. More recently, it was demonstrated that the presence of even small numbers of cyanobacteria cells in the food mixture presented to daphnids caused a drastic increase in food rejection behavior (Ghadouani et al. 2004). A possible implication of these effects at the community level would be an overall reduction in size structure, especially of filter-feeding cladocerans such as daphnids, as shown in this study. It is important to note that although this hypothesis was proposed before, mainly based on findings from small-scale laboratory experiments, it has never been tested at the whole-lake scale before this study.

Following the increase in cyanobacterial biomass, zooplankton communities seem to have shifted from large cladocerans (>1 mm) to smaller zooplankters such as copepods. This is suggested by the strong negative correlation between cladoceran–copepod ratio and cyanobacterial biomass. These findings are consistent with those of established plankton models (i.e., PEG model), which predict a shift of zooplankton communities from a dominance by large species to a dominance by smaller species following eutrophication (Sommer et al. 1986). Copepods did not seem to have been affected by the change in lake productivity. This result was also predictable, as copepods have not been reported to be affected by the presence of cyanobacterial species. This resistance to cyanobacteria was attributed to their chemosensory feeding mechanism whereby they can choose between toxic and nontoxic food particles (Schaffner et al. 1994). It seems that cladocerans and especially large daphnids are the most affected by the increase in cyanobacterial biomass. These observations are in contrast with the size-efficiency hypothesis that predicts a competitive advantage for large zooplankton in food collection over smaller ones (Dodson 1974; Gliwicz and Lampert 1990). The dominance of large cladocerans is

Fig. 6. Relationship between (*a*) cladoceran biomass ($r = -0.31$, $P = 0.38$), (*b*) copepod biomass ($r = 0.37$, $P = 0.28$), (*c*) cladoceran–copepod ratio ($r = -0.57$, $P = 0.083$), and (*d*) total zooplankton biomass ($r = -0.09$, $P = 0.79$) and microcystin-LR concentrations (micrograms per gram of algal dry mass) in the four experimental lakes of SPH regions. Lakes: SPH 20, triangles; SPH 100, circles; SPH 200, squares; SPH 800, diamonds. Pretreatment (1996) data are represented by open symbols; posttreatment (1997 and 1998) data are represented by solid symbols. Microcystin-LR data were not available for 1995. No fit was displayed, as none of the correlations was statistically significant.

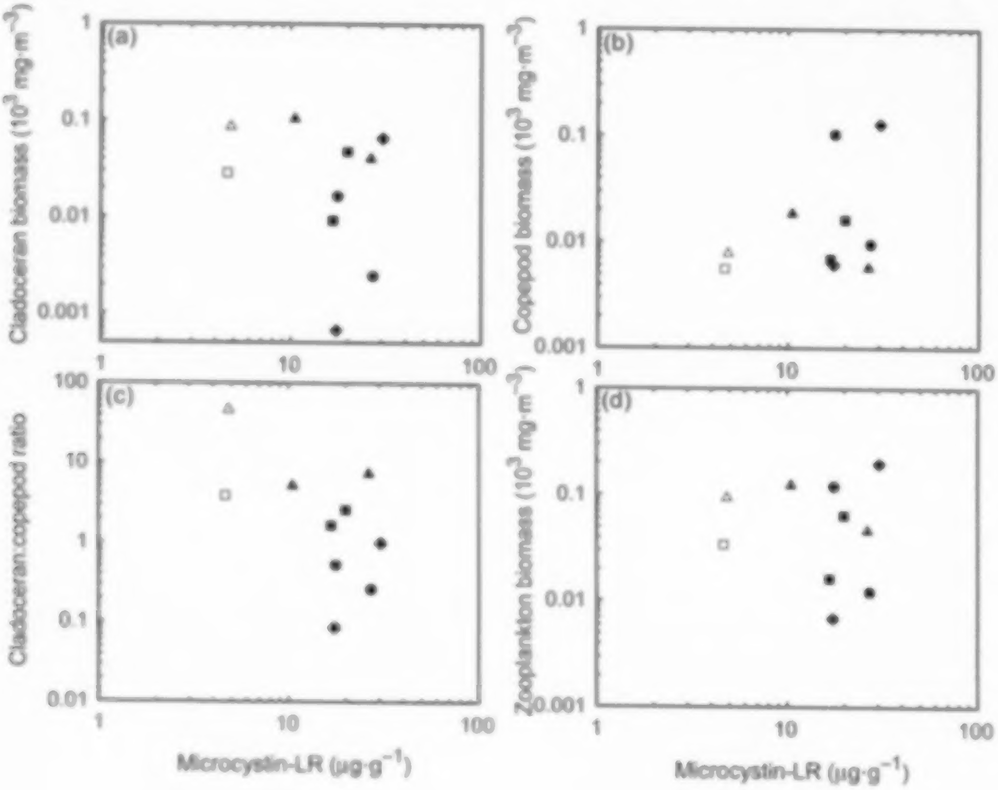

possible in conditions of low predation pressure and when phytoplankton are dominated by edible particles; however, it is not the case in cyanobacteria-dominated lakes, as shown by the clear negative relationship between the cladoceran–copepod ratio and cyanobacterial biomass. Several studies have previously reported midsummer declines of zooplankton biomass in eutrophic lakes as a result of a decline in large *Daphnia* concomitantly with the formation of cyanobacterial blooms (Threlkeld 1979; Ghadouani et al. 1998; Benndorf et al. 2001). However, these midsummer declines were attributed more to direct and indirect effects of predation than to changes in food quality or feeding inhibition by cyanobacteria (e.g., Benndorf et al. 2001). In the present study, the examination of variables associated with planktivory showed no likelihood of cladocerans being controlled by planktivorous fish as there was no relationship between the abundance of planktivorous fish and zooplankton variables (Prepas et al. 2001). Furthermore, there has been no report of increased predation following forest harvesting in similar studies (St-Onge and Magnan 2000). On the contrary, the authors of this study reported a decrease in small fish abundance in lakes with harvested watersheds (St-Onge and Magnan 2000).

There was no indication that cyanotoxins (i.e., microcystin-LR) had a notable effect on zooplankton communities. The lack of relationship may be indicative of the fact that the cyanotoxins are mainly endotoxins and therefore could only have an effect on the filter-feeding organism when ingested and fully digested. It is possible that some filter-feeding zooplankton could reduce or stop their feeding in presence of toxin-containing cyanobacterial cells and therefore may not ingest those cells. A detailed laboratory study on the feeding behavior of *Daphnia* in the presence toxin-containing *Microcystis* indicated that the animals were able to recover their normal feeding behavior only seconds after the replacement of toxic cells by nontoxic *Scenedesmus* cells (Ghadouani et al. 2004). Several studies have shown that the presence of dissolved microcystin can cause mortality in several zooplankton species; however, these experiments used concentrations orders of magnitude higher than the ones commonly reported in natural systems (Jungmann and Benndorf 1994). It is highly unlikely that natural blooms would release concentrations comparable to those used in the majority of ecotoxicological studies involving zooplankton species and where high mortalities were reported after 24–48 h exposures

(Christoffersen 1996; DeMott et al. 2001). It was clearly shown that only high concentrations of dissolved cyanotoxins could have a marked and permanent effect on the feeding behavior of cladocerans. Based on these observations and those of other studies (DeMott et al. 2001; Lürling 2003; Ghadouani et al. 2004), it seems that feeding inhibition produced by the presence of a high density of colonial and (or) filamentous cyanobacterial species could be more harmful than the cyanotoxins at the community level. In laboratory experiments, consistent indications of intoxication by direct exposure to purified microcystins were only observed when about 20% of known LC_{50} was added to the food of *Daphnia pulicaria* (Ghadouani et al. 2004). Mortality in daphnids was only observed when significantly higher concentrations of purified microcystin (typically $>30\ \mu g \cdot mL^{-1}$) than those normally found in natural systems were used in laboratory toxicity tests (DeMott et al. 1991; Jungmann 1992; Jungmann and Benndorf 1994). In natural conditions, cyanotoxins are contained in the cell and only released after senescence or destruction of the cyanobacterial cells, and hence, it is unlikely that animals could be exposed to high concentrations of cyanotoxins, high enough to cause mortality or even severe inhibition. The concentrations of microcystin in the present study, with an average of $\sim 15\ \mu g \cdot g^{-1}$, are rather low in comparison to concentrations reported in Alberta lakes and other lakes around the world (Kotak et al. 1995; Christoffersen 1996). Our experimental data suggest that *Daphnia* may be more severely affected by the presence of high concentrations of *Microcystis* colonies than by the presence of low concentrations of microcystin-LR (Ghadouani et al. 2004). However, it is still possible that sublethal concentrations of cyanotoxin could cause changes to the ecophysiology and the feeding behavior of filter-feeding zooplankters, especially in the short term (Ghadouani et al. 2004). The potential for bioaccumulation and biomagnification can still be possible when only sublethal concentrations of these toxins are released in the water. It was clearly shown that cyanotoxin concentrations can build up through terrestrial foodwebs, even causing serious health problems in some human populations (Cox et al. 2003). While some studies have reported cases of transfer to zooplankton (Kotak et al. 1996), snails (Zurawell et al. 1999), and even farmed shrimp (Kankaanpää et al. 2005), there is no evidence as to whether these invertebrates were actually accumulating toxins in their tissues. The toxins detected in invertebrates seem to come from phytoplankton cells accumulated in the digestive system of these animals. Furthermore, no case of biomagnification where toxins were detected in organisms at a higher trophic position such as planktivorous or piscivorous fish was reported (Kotak et al. 1996).

In summary, our results suggest that cladocerans are negatively affected by the occurrence of high biomass of cyanobacteria. To our knowledge, this is the first large-scale experiment providing a confirmation of patterns that were observed only in laboratory (McMahon and Rigler 1963; Burns 1968; Lampert 1982) or enclosure (Ghadouani et al. 2003) experiments. The main effect seems to be the reduction in the size structure and, consequently, the biomass of large filter-feeding cladocerans such as daphnids. Historically, fish predation has been considered to be the only control of zooplankton size structure, as planktivorous fish usually select for large cladocerans (Dodson 1974). Invertebrate predation has also been cited as a potential mechanism for the control of zooplankton size structure; however, this type of predation tends to select for small cladocerans and copepods, creating a contrasting picture from that of plantivorous fish predation (McNaught et al. 2004). Here we show that the increase of cyanobacterial biomass is likely to reduce the size structure of zooplankton communities most likely through the feeding-inhibition mechanism. A reduction in the size structure constitutes a fundamental change that is likely to have cascading effect on the functioning of the lakes. There are ecological fitness implications of the reduction of size structure whereby smaller females produce fewer and smaller eggs, which is likely to result in lower population growth (Moore and Folt 1993). Another likely consequence of reduction of size structure is the reduction of energy flow through foodwebs due to the reduction in grazing pressure by zooplankton on phytoplankton. It was also shown that the decline of zooplankton size structure may have far-reaching effects such as changes in the heat budget and light penetration in lakes (Mazumder et al. 1990). Furthermore, this study provides a potential explanation as to why management practice such as biomanipulation may not provide the desirable effects when large filter-feeding cladocerans are reduced or inhibited by the presence of high biomass of colonial and filamentous cyanobacteria (Shapiro and Wright 1984; Brett and Goldman 1996; MacKay and Elser 1998). Eutrophication constitutes a serious environmental problem that usually results in the occurrence of spectacular phytoplankton blooms, not only in lakes and reservoirs, but also in marine coastal systems (Sellner 1997). Eutrophication is not a new water quality problem; however, there is evidence that aquatic systems are experiencing severe algal blooms more frequently because of global warming and the consequential increase in lake water temperature (Hallegraeff 1993). Zooplankton communities constitute a fundamental link for energy transfer, nutrient cycling, and other ecosystem processes. It is crucial to better understand how these communities will respond to human-induced increases of cyanobacterial biomass in aquatic ecosystems.

Acknowledgments

Funding for this research was provided by the Natural Sciences and Engineering Research Council of Canada (NSERC) Collaborative Special Projects grant and University–Industry Cooperative Research and Development grant to EEP, Le Fonds Québécois de la Recherche sur la Nature et les Technologies (FQRNT), and the Québec Ministry of Education to BPA. Funding was also provided by Alberta–Pacific Forest Industries, Alberta Environment, Alberta Economic Development and Tourism, Manning Diversified Forest Products, Weyerhaeuser Canada, Syncrude Canada, Vanderwell, and Ainsworth. We are grateful to Emma Ivania Mangas for providing her expertise in zooplankton identification and analyses and Sharon Reedyk, M. Serediak, N. Scott, J. Burke, K. Gibson, S. Manchour, A. Smart, and C. Wichuk for their help in the field and with limnological analyses. We also thank S. Paquet for phytoplankton sample analyses. We are grateful to A. Cattaneo and H. Cyr for providing insightful comments on a previous version of this manuscript. This research was based at the Meanook Biological Research Sta-

tion of the University of Alberta and various TROLS field camps.

References

Beaudoin, C.P., Prepas, E.E., Tonn, W.M., Wassenaar, L.I., and Kotak, B.G. 2001. A stable carbon and nitrogen isotope study of lake food webs in Canada's Boreal Plain. Freshw. Biol. **46**(4): 465–477.

Benndorf, J., Kranich, J., Mehner, T., and Wagner, A. 2001. Temperature impact on the midsummer decline of *Daphnia galeata*: an analysis of long-term data from the biomanipulated Bautzen Reservoir (Germany). Freshw. Biol. **46**(2): 199–211.

Bergmann, M., and Peters, R.H. 1980. A simple reflectance method for the measurement of particulate pigment in lake water and its application to phosphorus–chlorophyll–seston relationships. Can. J. Fish. Aquat. Sci. **37**(1): 111–114.

Boon, P.I., Bunn, S.E., Green, J.D., and Shiel, R.J. 1994. Consumption of cyanobacteria by freshwater zooplankton: implications for the success of 'top-down' control of cyanobacterial blooms in Australia. Aust. J. Mar. Freshw. Res. **45**(5): 875–887.

Brett, M.T., and Goldman, C.R. 1996. A meta-analysis of the freshwater trophic cascade. Proc. Natl. Acad. Sci. U.S.A. **93**(15): 7723–7726.

Burns, C.W. 1968. Direct observations of mechanisms regulating feeding behavior of *Daphnia* in lakewater. Int. Rev. Ges. Hydrobiol. **53**(1): 83–100.

Carpenter, S.R., and Kitchell, J.F. 1992. Trophic cascade and biomanipulation: interface of research and management — a reply to the comment by DeMelo et al. Limnol. Oceanogr. **37**(1): 208–212.

Carpenter, S.R., Kitchell, J.F., and Hodgson, J.R. 1985. Cascading trophic interactions and lake productivity. Bioscience, **35**(10): 634–639.

Christoffersen, K. 1996. Ecological implications of cyanobacterial toxins in aquatic food webs. Phycologia, **35**(6): 42–50.

Cox, P.A., Banack, S.A., and Murch, S.J. 2003. Biomagnification of cyanobacterial neurotoxins and neurodegenerative disease among the Chamorro people of Guam. Proc. Natl. Acad. Sci. U.S.A. **100**(23): 13380–13383.

DeMelo, R., France, R., and McQueen, D.J. 1992. Biomanipulation: hit or myth? Limnol. Oceanogr. **37**(1): 192–207.

DeMott, W.R., Zhang, Q.X., and Carmichael, W.W. 1991. Effects of toxic cyanobacteria and purified toxins on the survival and feeding of a copepod and three species of *Daphnia*. Limnol. Oceanogr. **36**(7): 1346–1357.

DeMott, W.R., Gulati, R.D., and Van Donk, E. 2001. *Daphnia* food limitation in three hypereutrophic Dutch lakes: evidence for exclusion of large-bodied species by interfering filaments of cyanobacteria. Limnol. Oceanogr. **46**(8): 2054–2060.

Dodson, S.I. 1974. Zooplankton competition and predation: an experimental test of the size-efficiency hypothesis. Ecology, **55**(3): 605–613.

Filion, J.M., Chain, P., and Futter, M. 1993. Cantilevering vertical tow nets to reduce tow-line-induced zooplankton avoidance. J. Plankton Res. **15**(5): 581–587.

Ghadouani, A., and Pinel-Alloul, B. 2002. Phenotypic plasticity in *Daphnia pulicaria* as an adaptation to high biomass of colonial and filamentous cyanobacteria: experimental evidence. J. Plankton Res. **24**(10): 1047–1059.

Ghadouani, A., Pinel-Alloul, B., Zhang, Y., and Prepas, E.E. 1998. Relationships between zooplankton community structure and phytoplankton in two lime-treated eutrophic hardwater lakes. Freshw. Biol. **39**(4): 775–790.

Ghadouani, A., Pinel-Alloul, B., and Prepas, E.E. 2003. Effects of experimentally induced cyanobacterial blooms on crustacean zooplankton communities. Freshw. Biol. **48**(2): 363–381.

Ghadouani, A., Pinel-Alloul, B., Plath, K., Codd, G.A., and Lampert, W. 2004. Effects of *Microcystis aeruginosa* and purified microcystin-LR on the feeding behavior of *Daphnia pulicaria*. Limnol. Oceanogr. **49**(3): 666–679.

Gliwicz, Z.M., and Lampert, W. 1990. Food thresholds in *Daphnia* species in the absence and presence of blue-green filaments. Ecology, **71**(2): 691–702.

Hallegraeff, G.M. 1993. A review of harmful algal blooms and their apparent global increase. Phycologia, **32**: 79–99.

Haney, J.F., Forsyth, D.J., and James, M.R. 1994. Inhibition of zooplankton filtering rates by dissolved inhibitors produced by naturally occurring cyanobacteria. Arch. Hydrobiol. **132**(1): 1–13.

Hurlbert, S.H. 1984. Pseudoreplication and the design of ecological field experiments. Ecol. Monogr. **54**(2): 187–211.

Jungmann, D. 1992. Toxic compounds isolated from *Microcystis* PCC7806 that are more active against *Daphnia* than two microcystins. Limnol. Oceanogr. **37**(8): 1777–1783.

Jungmann, D., and Benndorf, J. 1994. Toxicity to *Daphnia* of a compound extracted from laboratory and natural *Microcystis* spp., and the role of microcystins. Freshw. Biol. **32**(1): 13–20.

Kankaanpää, H.T., Holliday, J., Schroder, H., Goddard, T.J., von Fister, R., and Carmichael, W.W. 2005. Cyanobacteria and prawn fanning in northern New South Wales, Australia — a case study on cyanobacteria diversity and hepatotoxin bioaccumulation. Toxicol. Appl. Pharmacol. **203**(3): 243–256.

Kotak, B.G., Lam, A.K.-Y., Prepas, E.E., Kenefick, S.L., and Hrudey, S.E. 1995. Variability of the hepatotoxin microcystin-LR in hypereutrophic drinking water lakes. J. Phycol. **31**(2): 248–263.

Kotak, B.G., Zurawell, R.W., Prepas, E.E., and Holmes, C.F.B. 1996. Microcystin-LR concentration in aquatic food web compartments from lakes of varying trophic status. Can. J. Fish. Aquat. Sci. **53**(9): 1974–1985.

Lampert, W. 1982. Further studies on the inhibitory effect of the toxic blue-green *Microcystis aeruginosa* on the filtering rate of zooplankton. Arch. Hydrobiol. **95**(1–4): 207–220.

Likens, G.E., Bormann, F.H., Johnson, N.M., Fisher, D.W., and Pierce, R.S. 1970. Effects of forest cutting and herbicide treatment on nutrient budgets in the Hubbard Brook watershed–ecosystem. Ecol. Monogr. **40**(1): 23–47.

Lund, J.W.G., Kipling, G., and LeCren, E.D. 1958. The inverted microscope method of estimating algal numbers and the statistical basis of estimations by counting. Hydrobiologia, **11**(2): 143–170.

Lürling, M. 2003. *Daphnia* growth on microcystin-producing and microcystin-free *Microcystis aeruginosa* in different mixtures with the green alga *Scenedesmus obliquus*. Limnol. Oceanogr. **48**(6): 2214–2220.

MacKay, N.A., and Elser, J.J. 1998. Factors potentially preventing trophic cascades: food quality, invertebrate predation, and their interaction. Limnol. Oceanogr. **43**(2): 339–347.

Malley, D.F., Lawrence, S.G., Mativer, M.A., and Findlay, M.W.J. 1989. Range of variations in estimates of dry weights for planktonic *Crustacea* and *Rotifera* from temperate North American lakes. Can. Tech. Rep. Fish. Aquat. Sci. No. 1666.

Mazumder, A., Taylor, W.D., McQueen, D.J., and Lean, D.R.S. 1990. Effects of fish and plankton on lake temperature and mixing depth. Science (Washington, D.C.), **247**(4940): 312–315.

McCauley, E., and Kalff, J. 1981. Empirical relationships between phytoplankton and zooplankton biomass in lakes. Can. J. Fish. Aquat. Sci. **38**(4): 458–463.

McMahon, J.W., and Rigler, F.H. 1963. Mechanisms regulating the feeding rate of *Daphnia magna* Straus. Can. J. Zool. **41**: 321–332.

McNaught, A.S., Kiesling, R.L., and Ghadouani, A. 2004. Changes to zooplankton community structure following colonization of a small lake by *Leptodora kindti*. Limnol. Oceanogr. **49**(4): 1239–1249.

McQueen, D.J., Post, J.R., and Mills, E.L. 1986. Trophic relationships in freshwater pelagic ecosystems. Can. J. Fish. Aquat. Sci. **43**(8): 1571–1581.

Moore, M., and Folt, C. 1993. Zooplankton body size and community structure — effects of thermal and toxicant stress. Trends Ecol. Evol. **8**(5): 178–183.

O'Driscoll, N.J., Lean, D.R.S., Loseto, L.L., Carignan, R., and Siciliano, S.D. 2004. Effect of dissolved organic carbon on the photoproduction of dissolved gaseous mercury in lakes: potential impacts of forestry. Environ. Sci. Technol. **38**(9): 2664–2672.

Patoine, A., Pinel-Alloul, B., Prepas, E.E., and Carignan, R. 2000. Do logging and forest fires influence zooplankton biomass in Canadian Boreal Shield lakes? Can. J. Fish. Aquat. Sci. **57**(Suppl. 2): 155–164.

Prepas, E.E., Pinel-Alloul, B., Planas, D., Méthot, G., Paquet, S., and Reedyk, S. 2001. Forest harvest impacts on water quality and aquatic biota on the Boreal Plain: introduction to the TROLS lake program. Can. J. Fish. Aquat. Sci. **58**(2): 421–436.

Rask, M., Nyberg, K., Markkanen, S.-L., and Ojala, A. 1998. Forestry in catchments: effects on water quality, phytoplankton, zoobenthos and fish in small lakes. Boreal Environ. Res. **3**(1): 75–86.

Reinikainen, M., Kiviranta, J., Ulvi, V., and Niku-Paavola, M.L. 1995. Acute toxic effects of a novel cyanobacterial toxin on the crustaceans *Artemia salina* and *Daphnia pulex*. Arch. Hydrobiol. **133**(1): 61–69.

Reinikainen, M., Hietala, J., and Walls, M. 1999. Reproductive allocation in *Daphnia* exposed to toxic cyanobacteria. J. Plankton Res. **21**(8): 1553–1564.

Schaffner, W.R., Hairston, N.G.J., and Howarth, R.W. 1994. Feeding rates and filament clipping in zooplankton consuming cyanobacteria. Verh. Int. Verein. Limnol. **25**(Part 4): 2375–2381.

Sellner, K.G. 1997. Physiology, ecology, and toxic properties of marine cyanobacteria blooms. Limnol. Oceanogr. **42**(5, Part 2): 1089–1104.

Shapiro, J., and Wright, D.I. 1984. Lake restoration by biomanipulation: Round Lake, Minnesota, the first two years. Freshw. Biol. **14**(4): 371–383.

Sommer, U., Gliwicz, Z.M., Lampert, W., and Duncan, A. 1986. The PEG-model of seasonal succession of planktonic events in fresh-waters. Arch. Hydrobiol. **106**: 433–471.

Steiner, C.F. 2004. *Daphnia* dominance and zooplankton community structure in fishless ponds. J. Plankton Res. **26**(7): 799–810.

St-Onge, I., and Magnan, P. 2000. Impact of logging and natural fires on fish communities of Laurentian Shield lakes. Can. J. Fish. Aquat. Sci. **57**(Suppl 2): 165–174.

Systat Software Inc. 2000. Systat 10.0 [computer software]. Systat Software Inc., Point Richmond, California.

Threlkeld, S.T. 1979. The midsummer dynamics of two *Daphnia* species in Wintergreen Lake, Michigan. Ecology, **60**(1): 165–179.

Tonn, W.M., Langlois, P.W., Prepas, E.E., Danylchuk, A.J., and Boss, S.M. 2004. Winterkill cascade: indirect effects of a natural disturbance on littoral macroinvertebrates in boreal lakes. Trans. Am. Fish. Soc. **23**(2): 237–250.

Ward, J. 1955. A description of new zooplankton counter. Q. J. Microsc. Sci. **96**: 371–373.

Webster, K.E., and Peters, R.H. 1978. Some size-dependent inhibitions of larger cladoceran filterers in filamentous suspensions. Limnol. Oceanogr. **23**(6): 1238–1245.

Zhang, Y., and Prepas, E.E. 1996. Regulation of the dominance of planktonic diatoms and cyanobacteria in four eutrophic hardwater lakes by nutrients, water column stability, and temperature. Can. J. Fish. Aquat. Sci. **53**(3): 621–633.

Zhang, Y., Ghadouani, A., Prepas, E.E., Pinel-Alloul, B., Reedyk, S., Chambers, P.A., Robarts, R.D., Methot, G., Raik, A., and Holst, M. 2001. Response of plankton communities to whole-lake $Ca(OH)_2$ and $CaCO_3$ additions in eutrophic hardwater lakes. Freshw. Biol. **46**(8): 1105–1119.

Zurawell, R.W., Kotak, B.G., and Prepas, E.E. 1999. Influence of lake trophic status on the occurrence of microcystin-LR in the tissue of pulmonate snails. Freshw. Biol. **42**(4): 707–718.

Disentangling local from macroenvironmental effects: quantifying the effect of human encroachments based on historical river catches of anadromous salmonids

Jan Henning L'Abée-Lund, Thrond O. Haugen, and Leif Asbjørn Vøllestad

Abstract: In this paper, we use dynamic factor and intervention analysis to identify and quantify the effect of human encroachments on anadromous salmonid catches in 22 Norwegian rivers over a 128-year period. In particular, we address effects of hydropower development, gravel removal, and stock enhancement (fish ladder construction and stocking). The methods allow for quantification of perturbation effects in the river environment on the annual catch, after removing long-term temporal trends at the appropriate spatial scale. The estimated effects of the encroachments differed among rivers, indicating that the mechanisms differ among rivers even for the same type of encroachment. In three rivers where hydropower development and stock enhancement had occurred, a significant increase of 0.8–9.8 tonnes (t) (34%–44%) was estimated, whereas a significant reduction of 11.2 t (38%) was estimated for the river where gravel removal had taken place. For rivers with additional biological information available, we find support for our estimated effects. In general, removal of gravel significantly reduced catch and there were positive effects of fish ladder constructions and variable effects of hydropower development and stocking (both positive and negative coefficients).

Résumé : Nous utilisons l'analyse factorielle dynamique et l'analyse d'intervention pour identifier et quantifier les effets des empiétements humains sur les captures de salmonidés anadromes dans 22 rivières de Norvège sur une période de 128 ans. En particulier, nous nous intéressons aux effets des développements hydroélectriques, des enlèvements de gravier et des améliorations de stock (constructions d'échelles à poissons et empoissonnements). Les méthodes permettent de quantifier les effets de perturbations dans l'environnement de la rivière sur la récolte annuelle, après avoir retiré les tendances temporelles à long terme à l'échelle spatiale appropriée. Les effets estimés des empiétements diffèrent d'une rivière à une autre, ce qui indique que les mécanismes varient en fonction des rivières pour un même type d'empiétement. Dans trois rivières (développement hydroélectrique, amélioration de stock), nous évaluons l'accroissement à 0,8–9,8 tonnes (t) (33–44 %), alors que dans la rivière d'où on a retiré du gravier, nous calculons une réduction significative de 11,2 t (38 %). Dans les rivières pour lesquelles il existe des informations biologiques additionnelles, nous obtenons des données qui appuient nos conclusions. En général, le retrait du gravier réduit la récolte de manière significative, la construction d'échelles à poissons a des effets positifs, alors que le développement hydroélectrique et l'empoissonnement ont des effets variables (coefficients positifs et négatifs).

[Traduit par la Rédaction]

Introduction

Most aquatic organisms spend their entire lives in either the marine or freshwater habitat, but individuals of species such as the anadromous salmonids may utilize both marine and freshwater habitats (Groot and Margolis 1991; Shearer 1992). Freshwater and marine habitats differ in many important features. For instance, in the northern hemisphere, productivity is higher in marine habitats compared with freshwater habitats (Gross et al. 1988). Seasonal changes (e.g., temperature) are more pronounced in freshwater temperate habitats, which also are spatially constrained compared with marine habitats. Anadromous salmonids reproduce in freshwater, and the juveniles stay in this habitat for up to several years before transforming into smolts and migrating to the marine environment (Groot and Margolis 1991; Shearer 1992; Elliott 1994). Because of the different characteristics of freshwater and marine habitats, the juveniles and adults are subjected to different selection pressures, and at least for Atlantic salmon (*Salmo salar*), it has been shown that growth and

Received 30 September 2005. Accepted 23 June 2006. Published on the NRC Research Press Web site at http://cjfas.nrc.ca on 3 October 2006.
J18911

J.H. L'Abée-Lund,[1,2] T.O. Haugen,[3] and L.A. Vøllestad. University of Oslo, Department of Biology, P.O. Box 1050, Blindern, N-0316 Oslo, Norway.

---

[1] Corresponding author (e-mail: lbl@nve.no).

[2] Present address: Norwegian Water Resources and Energy Directorate, P.O. Box 5091 Majorstuen, N-0301 Oslo, Norway.

[3] Present address: Norwegian Institute for Water Research, P.O.Box 173 Kjelsås, N-0411 Oslo, Norway.

Can. J. Fish. Aquat. Sci. 63: 2318–2329 (2006) doi:10.1139/F06-123

mortality are density-dependent in freshwater and density-independent at sea (Jonsson et al. 1998). Another important aspect of anadromous salmonids is their ability to home to their river of origin to spawn, increasing the potential for evolution of local adaptations (e.g., Ricker 1972; Hendry et al. 2004).

The effect on anadromous populations of human encroachments on the freshwater habitat may be difficult to detect and quantify, as it may be difficult to disentangle the local effects from the effects of macroclimatic and other large-scale effects (variation in growth and survival at sea). However, individuals from neighbouring populations intermingle at sea (Groot and Margolis 1991; Hansen and Jacobsen 2003), exposing them to more or less identical conditions during the postsmolt phase. Thus, the macroclimatic changes that may impact marine growth and survival act in the same way on populations utilising the same marine area (Beamish and Bouillon 1993; Friedland 1998; McKinnell and Karlström 1999). In contrast, changes in the freshwater habitat will affect individual populations differently. In a recent study, L'Abée-Lund et al. (2004) found coherence and similarity in the temporal variation in grilse proportion in Atlantic salmon from rivers draining into large fjord systems in Norway, indicating similarities in, for example, migration routes and environmental forcing at the regional scale. However, if population dynamics is mainly controlled by within-river factors, among-population abundance should be less correlated. Clearly, the relative role of marine and freshwater processes as agents affecting the population dynamics may change over time, and within-river perturbations will potentially result in such a change.

Throughout their range, anadromous salmonids are important commercial species, and recording of life history variables, number of spawners, or catch has been undertaken for more than 100 years in a number of populations (Groot and Margolis 1991; Shearer 1992). The existence of long-term data series makes anadromous salmonids valuable model organisms for understanding the underlying processes causing temporal and spatial variation in population size (Grenfell et al. 1998; Haydon et al. 2001). Such data series are valuable, as parameter estimates from models obtained from data-rich populations can be used for analysing variation in data-sparse populations (Prévost et al. 2003). Annual river catches from anglers may be considered an index of population size (Gee and Milner 1980; Crozier and Kennedy 2001; Thorley et al. 2005). It is also possible to remove any temporal trends in angling (changes is fishing regulations and fishing effort) using appropriate statistical techniques. However, this may not apply to very small populations (Peterman and Steer 1981; Beaumont et al. 1991).

In this paper, we present an analysis of Norwegian inter-river catch correlations and use dynamic factor and intervention analyses to test for possible effects of major human encroachments in a selected set of rivers. As the temporal trends were not the main focus of this study, we adjust the catch data for regional trends. In particular, we test the hypothesis that there is a relative decrease in annual catches in rivers where assumed negative human perturbations (hydropower development, depletion of gravel) have taken place and a relative increase in rivers where stock enhancement (stocking, fish ladder constructions) have occurred.

Fig. 1. Study rivers and their locations in Norway. The rivers of special interest for studying effects of human encroachments are marked with asterisks. River abbreviations are given in parentheses.

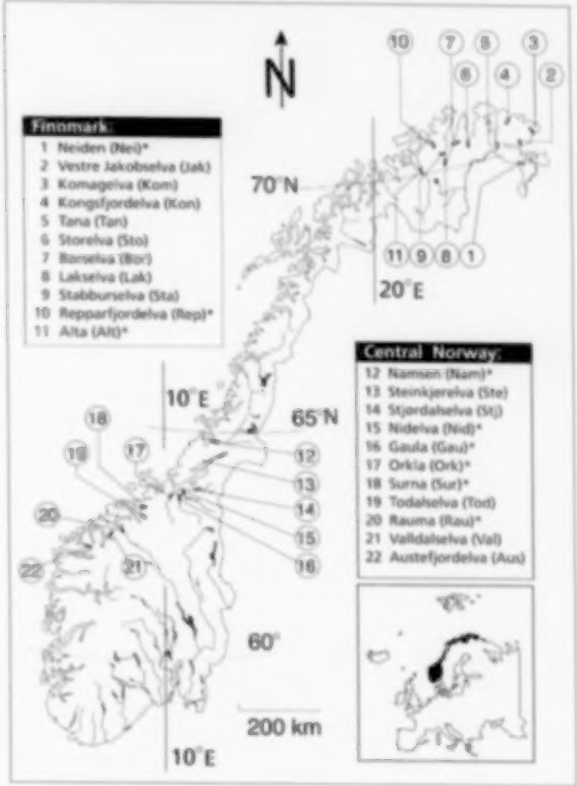

Materials and methods

Catch data

The present study is based on the Norwegian Official Statistics of nominal catch data (total weight) of Atlantic salmon, anadromous brown trout (*Salmo trutta*), and anadromous Arctic char (*Salvelinus alpinus*) from 22 rivers situated in two discrete regions in Norway (Fig. 1; Table 1). Data from nine of these rivers (Table 2) were used to test effects of human interventions using intervention analysis (IA). Data from the remaining 13 rivers were used in a dynamic factor analysis (DFA) to investigate the correlation structure among rivers to find the best covariation structure for the intervention analyses (see below).

The salmonid catch records have been collected by the Norwegian Official Statistics since 1876 (Hansen 1986). Since 1876, it has been an obligation for the local salmon management authorities to collect and report total catches in each river. Before 1968, the records comprised the total catches of Atlantic salmon, anadromous brown trout, and anadromous Arctic char; after 1968, the catches were divided between species. Originally, the catch was recorded in weight, but afterwards also including numbers. The legal fishing season is restricted to summer and early autumn, differing somewhat among rivers. For almost all rivers, the catches comprise

Table 1. Characteristics of 22 Norwegian rivers (from two regions: central Norway and Finnmark) where mean (± standard deviation (SD)) annual nominal catch (kg) of anadromous salmonids (1876–2003) and mean proportion (%; ±SD) of Atlantic salmon, *Salmo salar* (1983–2003), in the nominal catch of anadromous salmonids have been monitored.

River	Latitude (N)	Longitude (E)	River length (km)	Mean discharge ($m^3 \cdot s^{-1}$)	Mean annual catch (kg)	Proportion	*N*
Central Norway							
Austefjordelva	62°04′	6°19′	5.5	4.96	314±425	77.7±15.3	108
Valldalselva	62°18′	6°15′	17	15.08	686±652	61.8±19.0	122
Rauma	62°33′	7°41′	43	41.03	2517±1523	No data	125
Todalselva	62°49′	8°42′	8.5	14.63	230±199	45.1±25.0	101
Surna	62°58′	8°40′	58	55.15	3285±2632	73.4±9.5	125
Orkla	63°18′	9°50′	88	65.57	7678±5585	92.5±3.9	128
Gaula	63°21′	10°14′	112	95.43	14039±7466	89.1±5.8	128
Nidelva	63°16′	10°22′	6	85.12	1652±1207	75.9±11.8	128
Stjørdalselva	63°26′	10°54′	55	74.52	4231±3236	87.2±7.5	128
Steinkjerelva	64°02′	11°30′	6	64.25	802±858	73.8±26.4	116
Namsen	64°28′	11°35′	84	303.28	13889±7206	91.6±3.6	124
Finnmark							
Alta	69°58′	23°23′	46	90.77	7613±6439	86.5±5.0	110
Repparfjordelva	70°27′	24°20′	27	30.45	1908±1653	98.1±1.5	95
Stabburselva	70°11′	24°54′	15	21.33	1121±1142	88.3±4.6	120
Lakselva	70°04′	24°55′	70	25.56	2675±2039	88.7±3.7	126
Børselva	70°18′	25°32′	63	18.32	901±877	88.7±5.7	121
Storelva	70°22′	26°28′	31	14.41	481±456	92.6±4.3	79
Tana*	70°28′	28°20′	288	124.42	40151±29836	96.3±1.1	128
Kongsfjordelva	70°39′	29°15′	13	7.32	571±529	96.3±3.2	92
Komagelva	70°14′	30°32′	39	8.28	2479±2399	78.4±10.0	89
Vestre Jakobselva	70°06′	29°20′	3.5	12.54	458±487	96.5±2.9	110
Neiden*	69°42′	29°24′	79	5.95	2961±2727	95.1±3.5	118

Note: Latitude and longitude give geographical position of river mouth. River length (maximum distance that anadromous salmonids ascend in each river) and mean discharge (annual mean discharge) are river characteristics. *N*, number of years of observations.

*Catch in Finland is not included.

recreational rod catches only. In two rivers (Tana, Neiden), some commercial fishing with fixed and drifting nets is performed. Anadromous Arctic char occur in our study only in the Finnmark rivers. The annual incidence of anadromous brown trout and Arctic char in the nominal catches varied among rivers and among years within rivers, so it was not possible to estimate the catch for only Atlantic salmon for the whole study period. Thus, we analysed data for all salmonids combined.

The incidence of escaped farmed Atlantic salmon in the recreational river angling catch has been monitored annually since 1989 in several Norwegian rivers. Although considerable variation exists among rivers (0.3%–23.1%) in this period (1989–2000), the grand mean incidence of escaped salmon is low (<10%) and no significant time trend was observed (Fiske and Aas 2001). The effects of escaped farmed salmon in the analyses may be assumed to be random and negligible. None of the investigated rivers has been influenced by acidification.

In this study, all analyses have been performed on the nominal river catch of anadromous salmonids in the period 1876–2003. The analyses assume that the nominal catch reflects the fluctuations in catches and the development in the fisheries (Hansen 1986). Recent studies from Iceland and Great Britain demonstrate that catch statistics reflect the size of the spawning run (Gudjonsson et al. 1995; Crozier and Kennedy 2001; Thorley et al. 2005). Nominal catch statistics are used by the International Council for the Exploration of the Sea (ICES) to describe status and development of Atlantic salmon in Norway and other countries (ICES 2002).

The quality of the catch data has probably improved over time, introducing a possible bias. Despite this constraint, long-term data series are important for scientific hypothesis-making and management decisions. The Norwegian Official Statistics of nominal catch records of adult Atlantic salmon has undergone several improvements since their start in 1876. There was a change in reporting procedure in 1968 and 1992, but this only introduced more detail into the statistic and does not influence our set of data. Fishing method, effort, and recording of anglers' catch of anadromous salmonids in rivers changes over time. Our main assumption is that fishermen who report their catches are equally prone to report fish independently of fish size, i.e., the reported fish is a random sample of the fish that was captured in a specific river for a given year. There is no available data on the reporting behaviour of Norwegian salmon anglers that can be used to test this assumption. Further, we assume that any changes in reporting procedure or willingness will covary among rivers, at least within regions. Thus, a procedure

Table 2. Characteristics of the rivers studied.

River	Year of start of hydropower production	Watershed (km^2) (percent used for hydropower)	Runoff (million m^3) (percent stored)	Anadromous river length (km)	Natural production	Annual stocking	Stocking period
Neiden	1953	2960 (2)	946	67	450 juv	7–31 nn+n fry and juv	1965–1985
Repparfjordelva		1090	662	27+21	?	6–125 nn fry and juv	1931–1982
Gaula	1924	3659 (7)	3090 (5)	112	300–500 smolt	? nn+n fry and juv	1950s–1960s
						5 n smolt	1975–2000
Rauma	1948	1202 (11)	1356 (14)	43	?	0	
Alta	1987	7373 (80)	2333 (7)	46	?	0	
Surna	1968	1200 (50)	1883 (20)	40	80–140 smolt	35 n smolt	1968–2000
Namsen	1948	3283 (52)	9113 (13)	111+65	20–50 000 egg	0–400 nn+n fry	1881–1993
Orkla	1982	3053 (85)	2119 (7)	88	130–300 smolt	3–135 nn juv	1950–1979
						7–9 n smolt	1980–1988
Nidelva	1910	3110 (98)	2993 (41)	6	~25 smolt	6* nn juv	1950s–2000
						2–5 nn smolt	

Note: Estimated number (× 1000) of natural production and stocked Atlantic salmon (*Salmo salar*) of native (n) or non-native (nn) origin; juv, juvenile; ?, unknown; *, annual mean number. Increase in river length in Repparfjordelva and Namsen is due to construction of fish ladders.

adjusting for regional-scale temporal trends will remove such reported artefact effects.

Study sites

We focus mainly on nine Norwegian rivers from two different regions (central Norway and Finnmark) where different kinds of human encroachments (hydropower development, depletion of gravel, stock enhancement) have occurred during the 20th century (Fig. 1; Table 2). These rivers have in common that nominal catch records of anadromous salmonids exist for the period 1876–2003. Data from a set of rivers within the same regions were selected to represent the temporal variation at the regional scale. Three criteria were used in selecting these rivers. First, the catch records should contain data from almost the entire period. Rivers with missing values for more than 20 years at the start of the series are excluded. Single years without any data were treated as missing and not zero, as catch records before and after the year lacking data indicated that a zero catch was highly unrealistic. Second, the rivers should be clustered geographically with these nine rivers of specific interest. Third, because all nine rivers of interest contain a surplus of multi-sea-winter salmon, we excluded rivers dominated by grilse (one-sea-winter salmon). We expect that grilse behave differently from multi-sea-winter fish (Mills 1989), leading to differences in growth and survival (Hansen and Jacobsen 2003; Jonsson et al. 2003). In total, this resulted in a data set containing 11 rivers from central Norway and 11 rivers from Finnmark (Fig. 1; Table 1).

The effect of stock enhancement (fish release and fish ladder construction) has been tested in two rivers, Repparfjordelva and Neiden. Repparfjordelva is the least physically affected river in the present study. Initially, Atlantic salmon fry and juveniles were released in the natural Atlantic salmon reaches, but afterwards stocking took place in areas not normally accessible for anadromous salmonids. A fish ladder situated 27 km upstream from the estuary was constructed in 1956, increasing the passable river by another 21 km. In Neiden, Atlantic salmon fry and juveniles were released in the area with naturally reproducing Atlantic salmon. A fish ladder (situated 12 km from the estuary) was built in 1968 to improve the ascent of anadromous salmonids to 67 km of naturally occurring salmonid habitat. In both rivers, the number of juveniles released was small compared with the size of the natural production (Table 2; Fig. 2).

The effect of gravel removal has been tested in Gaula, which had been significantly altered during 1953–1985 by extraction of ~4 million m^3 of gravel. In some areas, this activity has lowered the river bottom by 2 m and, in other areas, left a clay bottom. Different age classes of young Atlantic salmon have been released since 1950s, mainly in the upper part of the river. However, the numbers released were small compared with the natural production (Table 2; Fig. 2).

Hydropower development may differ strongly among schemes. The effect on anadromous salmonids varies considerably between schemes, and we have investigated the effect of hydropower development in seven rivers (Table 2; Fig. 2). Rauma is least affected, whereas Nidelva is heavily affected both in water storage and by the fact that water from almost the entire watershed is lead through turbines. To reduce the

Fig. 2. Annual catches (tonnes (t)) of salmonids in the nine rivers of special interest. Periods with different kinds of encroachments are indicated: C, control period; H, hydropower; S, Atlantic salmon (*Salmo salar*) stocking; L, ladder; G, gravel removal. Numbers above horizontal line indicate intervention incidents.

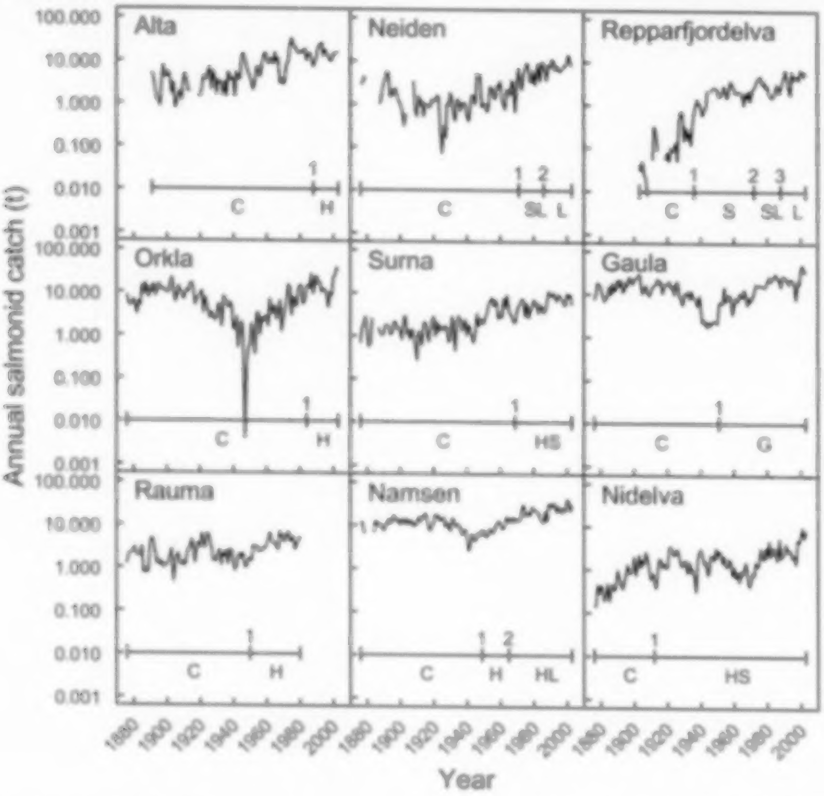

negative effect of hydropower, Atlantic salmon juveniles and smolts have been released in several rivers. The amount of this stocking varies considerably among rivers and between years in relation to the natural production (Table 2; Fig. 2). The numbers of released fish were low in Namsen and high in Nidelva and Orkla compared with the estimated natural production of similar age groups. In Namsen, nine fish ladders currently in operation have increased the passable river length for anadromous fish from 111 km to 176 km. Fish ladder construction started in the late 1950s, but they did not function satisfactorily until the late 1970s (A. Rikstad, County Environmental Administration, Statens Hus, N-7734 Steinkjer, Norway, personal communication). All stocking has been performed upstream of the natural anadromous reaches.

Two rivers used in this analysis (Rauma and Steinkjerelva) were infected by the parasitic monogenean *Gyrodactylus salaris* in the late 1970s. This led to a rapid and dramatic decline in the Atlantic salmon population (Johnsen and Jensen 1986). All catches from 1980 onwards were excluded from the data analyses for these rivers.

Statistical modelling

A number of studies have demonstrated that annual salmonid catch in a specific river is correlated with the catch in other rivers in the region (e.g., Friedland 1998; Peterman et al. 1998; McKinnell and Karlström 1999). Such a correlation is assumed to result from usage of similar ocean areas by populations in the same region. Hence, if one wants to explore effects of local environmental changes, general trends in the catches resulting from the common oceanic habitat use must be accounted for. However, as the spatial covariation scale is not predefined or fixed (Mueter et al. 2002), the spatial covariation structure in the time series data should be explored in order to find the most appropriate scale. Here we do so by employing dynamic factor analysis (DFA; Zuur et al. 2003) on standardized ln-transformed annual catches ($Y_{j,t}$):

$$(1)\qquad Y_{j,t} = (y_{j,t} - \bar{Y}_j)/s_{Y_j}$$

where $y_{j,t}$ is the ln-transformed total catch in river j for year t, $\bar{Y}_j$ is the population-specific overall mean for ln-transformed annual catches, and s_{Y_j} is the corresponding standard deviation. DFA is a multivariate time-series analysis technique used to estimate underlying common patterns in a set of time series. (*i*) We use this technique to assess the number of common temporal trends (M) in nontarget populations. (*ii*) By exploring the factor loading (z) pattern to the fitted trends, we can infer the most adequate spatial scale over which to estimate the regional covariate. The mathematical formulation used in DFA can be written as

$$(2)\qquad Y_{j,t} = z_{j,1}\alpha_{1,t} + z_{j,2}\alpha_{2,t} + \ldots + z_{j,M}\alpha_{M,t} + e_{j,t}$$

where $\alpha_{k,t}$ is the kth common trend, $z_{j,t}$ is the factor loading, and $e_{j,t}$ is noise. In matrix notation, this can be written as

$$(3)\qquad \mathbf{y}_t = \mathbf{Z}\boldsymbol{\alpha}_t + \mathbf{e}_t$$

where $\mathbf{y}_t$ is a $N \times 1$ vector containing the values of the N time series at time t, $\boldsymbol{\alpha}_t$ represents the values of the M common trends at time t, and $\mathbf{e}_t$ is a $N \times 1$ noise component, which is assumed to be normally distributed with mean 0 and covariance matrix $\mathbf{R}$. The $N \times M$ matrix $\mathbf{Z}$ contains the factor loadings and determines the exact form of the linear combinations of the common trends. The aim of DFA is to model all the time series using as low M as possible and still explain the data reasonably well. The optimal M is selected using a model selection metric called the consistent Akaike's information criterion (CAIC; Zuur et al. 2003). After finding the most supported M, we assign the individual rivers to the respective trend curves according to their factor loadings. Based on these trend curve assignments, we then estimate standardized annual mean catch values for each trend curve group ($X_{i,t}$) to be used as the regional covariates in intervention analyses (see below). All DFAs were performed using the R-based Brodgar software (http://www.brodgar. com/).

To estimate the effect of local human encroachments on within-river catch, we used IA (sensu Box and Tiao 1975). The general form of the intervention time series model can be written as

$$(4)\qquad Y_t = f(\boldsymbol{\beta}, \mathbf{x}, \xi, t) + e_t$$

where t is time, Y_t is the variable of interest at time t, e_t is a stochastic noise component, and $f(\boldsymbol{\beta}, \mathbf{x}, \xi, t)$ is the dynamic component of Y_t. The dynamic component includes an estimated set of parameters $\boldsymbol{\beta}$, a group of covariate series $\mathbf{x}$, and a set of intervention series ξ. Embedded in $\boldsymbol{\beta}$ are detrending parameters and parameters describing the magnitude of intervention effects. The covariate series $\mathbf{x}$ are additional time series that may be related to the time series of interest, in our case the mean regional catch (X_t). The intervention series, ξ, are used to signal the occurrence of an intervention in the dynamics of the time series of interest. In our case, all intervention events are a priori known (Fig. 2). Hence, the core model structure fitted the data in our study looks like this:

$$(5)\qquad Y_t = \omega_0\,\xi_t + x_t + \gamma_t + e_t$$

where γ_t is a detrending function (fitted as a polynomial function), x_t is the detrended X_t, ω_0 is the magnitude of a step intervention, and in the case of just one intervention incidence (I),

$$(6)\qquad \xi_t = \begin{cases} 0, & t < I \\ 1, & t \geq I \end{cases}$$

The noise term e_t was individually modelled for each river of interest based on the Ljung–Box chi-square white-noise test and augmented Dickey–Fuller stationarity test. For all models fitted, the temporal autocorrelation could be accounted for by fitting no higher than second-order ARMA models:

$$(7)\qquad \mu_t = \phi_1\mu_{t-1} + \phi_2\mu_{t-2} + \varepsilon_t - \theta_1\varepsilon_{t-1} - \theta_2\varepsilon_{t-2}$$

where ϕ_m and θ_m are the m-order autoregressive and moving average coefficients, respectively, ε_t is i.i.d. (i.e., independent and identically distributed), and μ_t is the expected value of Y_t. All the IA modelling was performed using PROC ARMA (with input variables) in SAS Version 9.1 (http://support.sas.com/documentation/onlinedoc/sas9doc.html). All models were fitted using the maximum likelihood method, and model selection was based on AIC.

Human perturbations in freshwater may affect catches of adult salmonids mainly via two processes — juvenile survival and the probability of capture of adults. Processes that affect juvenile survival will not be detected immediately after a perturbation (i.e., a delayed effect can be expected), whereas effects on the probability of capture will appear immediately and might decrease with time as the result of compensatory efforts. We fitted models including a delayed effect corresponding to the population-specific age of maturation (5–7 years; Alta, Namsen, Repparfjordelva (Dahl 1910; Jensen et al. 1999), Gaula (J.H. L'Abée-Lund, unpublished data), Orkla (Hvidsten et al. 2004), Surna (S.J. Saltveit, Natural History Museum, University of Oslo, P.O. Box 1172, Blindern, N-0318 Oslo, Norway, personal communication)). We found no evidence (comparing AIC values for pairs of similar models with and without delayed response) for delayed responses except for the case of Gaula. All the rest of the tests presented are therefore based on nondelayed intervention effects.

The data quality has probably improved over time and, hence, may potentially have caused a sampling bias in the data. We have dealt with this problem by including the regional mean catch of salmonids as a covariate in all models, assuming that the report rate is similar within regions. In addition to this action, we have performed resampling procedures (nonparametric bootstrapping; Manly 1997) where the direction and degree (variance) of sampling bias have been set to vary over time. We tested the effect of increasing and decreasing report rates over time, where the change ranged from 10% to 40% difference in report rate between first year and last year in the catch time series. Similarly, we also tested the effect of varying the sampling error over time (but with no net trend) between 10% and 40% of reported values. The resampled catch series were subjected to new intervention analyses under the originally favored model structure. Under each resampling regime (140 in total), 1000 resamples and intervention analyses were performed. Inferences on the robustness of the originally estimated intervention effects were made by comparing the original parameter estimates with the resulting variation in the bootstrapped intervention effect parameters (the median and 2.5 and 97.5 percentiles). The bootstrapping was conducted using the %BOOT macro developed for SAS (available from http://support.sas.com/ctx/samples/index.jsp?sid = 479).

Results

The DFA revealed that the temporal data of salmonid catches from all nontarget rivers could most effectively (i.e., lowest CAIC) be modelled by two general trends (embedded figure in Fig. 3). Although there was no distinct clustering into the two predefined central Norway and Finnmark regions

Table 3. Parameter estimates for the selected ARMA intervention models (based on Akaike's information criterion).

River	Intercept	Temporal autocorrelation structure				Detrending parameters	
		ar(1)	ar(2)	ma(1)	ma(2)	Linear	Quadratic
Gaula	−2.02±0.58 (0.0006)	0.85±0.07 (<0.0001)		0.32±0.12 (0.0087)		0.016±0.013 (0.2263)	0.0016±0.0004 (0.0003)
Repparfjordelva		−0.59±0.10 (<0.0001)		−0.44±0.11 (<0.0001)		0.024±0.005 (<0.0001)	−0.0004±0.0001 (0.0002)
Neiden	−0.62±0.16 (0.0002)	0.40±0.09 (<0.0001)				−0.003±0.004 (0.4394)	0.0004±0.0001 (0.0076)
Surna	0.95±0.23 (<0.0001)	0.27±0.09 (0.0041)				0.029±0.009 (0.0011)	−0.0002±0.0002 (0.4272)
Nidelva		0.52±0.08 (<0.0001)				0.022±0.008 (0.0078)	0.0011±0.0002 (<0.0001)
Namsen	−1.39±0.51 (0.076)	0.54±0.08 (<0.0001)				0.016±0.011 (0.1611)	0.0012±0.0003 (<0.0001)
Alta	−0.64±0.23 (0.0070)	1.53±0.13 (<0.0001)	−0.80±0.11 (<0.0001)	1.16±0.16 (<0.0001)	−0.58±0.13 (<0.0001)	0.011±0.004 (0.0044)	
Rauma		0.52±0.09 (<0.0001)					
Orkla		0.94±0.03 (<0.0001)		0.59±0.09 (< 0.0001)			

Note: Standard errors are provided and p values (t-based) appear in parentheses below each parameter estimate. ar and ma correspond to autocorrelation and they are indicated in Fig. 2.

[a] Note that this effect has been delayed by 6 years.

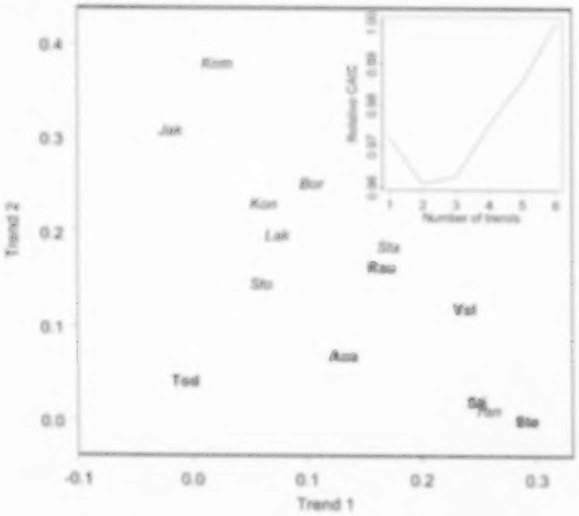

Fig. 3. Factor loadings for the salmonid catch data series obtained by the model containing two common trends. Based on the relative (to maximum) consistent Akaike's information criterion (relative CAIC), the model containing two common trends was the most supported one (inset figure). Rivers from central Norway are noted in bold, and Finnmark rivers are noted in italics. Factor loadings are unitless. River abbreviations: Tod, Todalselva; Aus, Austefjordelva; Rau, Rauma; Val, Valldalselva; Stj, Stjørdalselva; Ste, Steinkjerelva; Kom, Komagelva; Jak, Vestre Jakobselva; Bor, Børselva; Kon, Kongsfjordelva; Lak, Lakselva; Sta, Stabburselva; Sto, Storelva; Tan, Tana.

(Fig. 3), there was a general tendency for the Finnmark region rivers to cluster as a group with generally high loading to trend 2, whereas the central Norway rivers generally clustered with high loading to trend 1. Two rivers deviated from this pattern (Tana (Tan) and Todalselva (Tod)) and therefore were excluded when estimating regionwise standardized mean catches (X_t). These regionwise standardized mean catches were used as covariates in all the following intervention analyses.

The intervention analyses described 50%–91% of the variation in the individual time series (Table 3), and for all rivers except Repparfjordelva, regional mean catches had a significant positive effect on the individual river catches. The effects of the detrending using regional mean catch as covariate and of the interventions are illustrated (Fig. 4). The analyses further revealed that three of the four rivers (Alta, Orkla, Rauma, and Namsen) where effects from hydropower alone on annual salmonid catches could be estimated had positive effect coefficients. Although none of the hydropower effect coefficients was significant (p = 0.06–0.65), they were close to being so for the two rivers Namsen and Rauma (p values of 0.09 and 0.06, respectively). Only Alta showed signs of negative effect from hydropower development, but the estimated effect was far from significant (p = 0.66).

In the two rivers where hydropower development was combined with compensatory stocking (Surna and Nidelva), no significant effect was found. In Surna, there was a tendency that the combined effect was negative (p = 0.13). In Namsen, there was a significant positive effect of the combined hydropower development and construction of fish ladder actions (intervention 2), resulting in an increase of 9.8 t·year^{-1}. The increase corresponded to about 44% of the annual mean catch.

In both rivers where enhancement measures were undertaken (Neiden and Repparfjordelva), annual catches increased significantly after starting the stocking program (Table 3). The increase represented an estimated annual increase in catch of 0.8 t (39%) in Repparfjordelva and 1.6 t (34%) in

Cubic	Region	Intervention effects 1	2	3	R^2_{adj}
$1.25\times10^{-5} \pm 3.88\times10^{-6}$ (0.0017)	0.58±0.12 (<0.0001)	−1.49±0.36 (0.0001)[a]			0.80
	0.14±0.09 (0.1721)	0.39±0.10 (0.0001)	−0.04±0.23 (0.8580)	0.36±0.25 (0.1520)	0.91
	0.20±0.09 (0.0262)	0.55±0.18 (<0.0001)	−0.18±0.39 (0.8865)		0.69
$-3.36\times10^{-6} \pm 1.64\times10^{-6}$ (0.0428)	0.44±0.15 (0.0054)	−0.50±0.33 (0.1305)			0.71
$1.13\times10^{-5} \pm 2.22\times10^{-6}$ (<0.0001)	0.41±0.14 (0.0070)	−0.02±0.15 (0.8817)			0.71
$9.91\times10^{-6} \pm 2.68\times10^{-6}$ (0.0003)	0.56±0.13 (0.0001)	0.66±0.39 (0.0927)	0.84±0.38 (0.0296)		0.75
	0.56±0.12 (<0.0001)	−0.11±0.26 (0.6552)			0.75
	0.61±0.19 (0.0016)	0.51±0.26 (0.0552)			0.50
	0.43±0.16 (0.0086)	0.59±0.44 (0.1916)			0.65

and moving average, respectively. The intervention effect coding corresponds to their chronological appearance, and their nature is described in Table 2

Neiden. However, in both rivers, stocking was combined with construction of fish ladders. After terminating the stocking programs, annual catches remained unchanged.

Gravel removal in Gaula resulted in a significant decrease in annual salmonid catches (Table 3). The difference in catches before and after gravel removal corresponds to an annual reduction of 11.2 t or 38%.

The bootstrap tests demonstrated that the estimated intervention effects were generally robust to assumptions about temporal variation in sampling bias. We found a change in the degree of significance (α level = 0.05) in just 7.8% of the 140 bootstrap regimes performed. For instance, the weak positive effect of hydropower development on salmonid catches found for Rauma and Namsen became very significant when assuming that the report rate should increase to a 20% higher level than reported during the entire time series period. The same was the case for Nidelva, but here the intervention was both hydropower development and stocking of juvenile salmon. The negative tendency from hydropower development found in Alta became slightly significant (p = 0.046) when assuming that temporal variation in report error should be 20% higher than reported, but not for higher or lower levels of variation. In general, the intervention effects were most sensitive to high levels (i.e., >30%) in variation of the sampling error. For instance, although Gaula, Repparfjordelva, and Neiden had very robust intervention effect estimates towards temporal trends in sampling error and at lower levels of variation in sampling errors, the intervention effects changed markedly at variation levels above 30%. At such high levels of sampling variance, annual salmonid catches were estimated to drop markedly in Gaula (because of gravel removal), to not increase significantly in Repparfjordelva (after construction of fish ladder and enhancement stocking actions), and to decrease significantly in Neiden (after terminating the stocking actions).

Discussion

Here, we have used DFA and IA to identify and quantify the effects of various human encroachments on recreational catches of salmonid fishes in Norwegian rivers. In this way, we adjust for temporal trends that might occur at a regional scale, regional variation in reporting practice and fishing regulations, and temporal autocorrelation. We document strong negative effects of gravel removal, positive effects of fish ladder constructions, and variable effects of hydropower development and stocking (both positive and negative coefficients). The reported estimates of intervention effects were generally shown to be robust towards assumptions about temporal variation in sampling bias.

Marine environmental conditions are known to change over decades (Mann and Lazier 1991), and postsmolt survival has been documented to vary with these fluctuations (Friedland 1998; Mueter et al. 2002). Thus, it is reasonable to believe that variations in river catch records also reflect the effects of marine conditions. Other catch records of Atlantic salmon from the same area also show consistency for between-river comparisons (Friedland 1998; McKinnell and Karlström 1999), suggesting that the catches are influenced by the same marine conditions. The method presented here adjusts for temporal variation at the regional scale.

The DFA indicated that rivers in northern and central Norway exhibited different temporal trends in catch, indicating strong regional effects. Further, the analysis revealed synchrony in among-river catches within regions (with few exceptions). There is large variation in climatic condition along the Norwegian coast. The most striking variation occurs off the Lofoten area (69°N). The warm North Atlantic drift secures relatively high (although reduced in a northerly direction) and stable water temperature along the Norwegian coast. However, north of Lofoten the effect of the drift is considerably weakened and sea temperatures are more variable (see L'Abée-Lund et al. 1989; Orvik et al. 1995). Although the sea temperature is low in the Barents Sea, the density of zooplankton is still relatively high (Dalpadado et al. 2003) and gives rise to important marine fisheries. The feeding areas are situated near the mainland, and Rikardsen et al. (2004) show that Atlantic salmon after leaving their natal northern Norway rivers as smolt start feeding earlier than smolt from rivers in central Norway. The exact marine distribution of salmon from rivers in northern Norway is unknown, although available data indicate a northerly distribution compared with populations from southern Norway during the first year at sea (Hansen and Jacobsen 2003). Atlantic salmon in their second year at sea, however, may undertake a migration further south and intermingle with southern populations (Hansen and Jacobsen 2003). The Atlantic salmon during their first year at sea seem to follow the main surface currents northwards into the Norwegian Sea and then spread out over wide areas (Holm et al. 2000). However, the sampling effort has been very low in the Barents Sea and the Greenland Sea.

Our analyses are based on total river catches; thus, we are not able to detect possible within-river effects that do not affect the total river catches. This problem may arise in situations where the encroachment (e.g., power plant) has a negative local effect in one part of the river and positive effects in other parts. For instance, dramatic declines in the density of juveniles and catch of adult Atlantic salmon were registered in areas close to the hydropower plant in Alta, whereas increased catches have been reported for the lower parts of the river in the first decade of operation (Tor Fredrik Næsje, Norwegian Institute of Nature Research, Tungasletta 2, N-7485 Trondheim, Norway, personal communication).

Furthermore, other within-river changes occurring at the same time will be difficult to detect without detailed information and (or) study. For example, in Gaula and Orkla, substantial mining activities occurred from the late 1600s to the late 1980s and the termination of this activity improved water quality in the affected river sections (approximately 30 and 15 km, respectively). In Gaula, this water quality improvement may have masked an even larger negative effect of the encroachment than that observed. Unfortunately, data on water quality are only available for the later part of the time series (since the mid-1980s) and it was impossible to use water quality as a covariate in the analysis. In Orkla, we observed a nonsignificant positive trend after the hydropower development. This increase in catch was concurrent with reduced mining activity in the late 1970s, resulting in low contamination of heavy metals in the lower reaches of Orkla in the early 1980s and onwards (Jensen et al. 1998). As only the lower 15 km of the anadromous reach was affected, the improved water quality may have induced a small part of this positive effect on the salmonid catch.

The reliability of catch data is a subject for discussion. A critical assumption in our analyses is consistency in both fishing regulations and exploitation rate within and among rivers. Regulations of the river fisheries have remained consistent in Norway during most of the study period. The most pronounced change is a relatively recent reduction in the length of the fishing season, especially in rivers with small salmon populations (Fiske and Aas 2001). Our study rivers, however, have been little affected by this. In rivers where variation in exploitation rate has been estimated over time, no systematic trends are found. For instance, in two different Norwegian rivers, Aurland and Lærdal, it has been shown that anglers caught the same proportion of the spawning population 10 years after the hydropower plant came online as they did before this perturbation (Sættem 1995). For the rivers used in the present analyses, we do not have this kind of information.

Marine exploitation patterns have changed over time, with the most dramatic change being the start of offshore drift netting for Atlantic salmon in 1960. The Norwegian drift-net fishery was banned in 1989, significantly affecting the structure of the Norwegian spawning run (Jensen et al. 1999). After the cessation of the drift-net fishery, the mean size of grilse increased and the total catch of grilse increased in the four rivers where this has been studied in detail. No changes were observed for the catch of multi-sea-winter fish. It is thus evident that this fishery has affected grilse more strongly than larger fish. However, we have excluded time series from rivers dominated by grilse from our analyses, therefore the effect of this change in the marine fishery may be of minor importance. Other changes in marine exploitation have of course taken place during the 128 years covered by these time series. However, the effects have not been documented, and we have assumed that the changes are the same, at least on the regional scale used here. If so, the use of appropriate covariates in the statistical models has adjusted for these effects.

The observed effects of the encroachments differed both between encroachment types and among rivers with the same type of encroachment, indicating that the mechanisms differ among rivers. The largest observed effect was for Gaula, where ~4 million m^3 of gravel were removed from the river bed during 1953–1985. This extraction of gravel destroyed some of the best spawning areas for Atlantic salmon (Heggberget 1986), leaving the rearing habitat for juvenile fish consisting of substrate of small size and occasionally marine deposits such as clay. Densities of both invertebrates and juvenile salmon and brown trout in these areas are significantly lower than expected (JoVegard Arnekleiv, Freshwater and Inland Fisheries Laboratory, Norwegian University of Science and Technology, N-7491 Trondheim, Norway, personal communication). Also, more turbid water results from continuous flushing of the clay layer, which has been shown to negatively affect riverine ecosystems (Waters 1995). Thus, there is a clear relationship between production of invertebrates and juveniles and the catch of adult salmonids.

Enhancement measures such as stocking and building of fish ladders significantly increased annual catches. In Neiden and Repparfjordelva, stocking was combined with building fish ladders, thus the effect of each encroachment type could not be estimated. However, after terminating the stocking program, catches remained unchanged, indicating that the positive effect of the encroachment was mainly due to the building of fish ladders and the increase in the river area producing anadromous salmonids. The effect of building fish ladders was also positive Namsen. In Surna, hydropower development and stocking have taken place simultaneously, leading to a nonsignificant negative effect. However, it is impossible to

Fig. 4. Annual detrended catches (solid lines; standard deviation units with confidence bounds (dashed lines)) of salmonids in the nine rivers of special interest. The estimated effect sizes for the various interventions are displayed as thick solid lines.

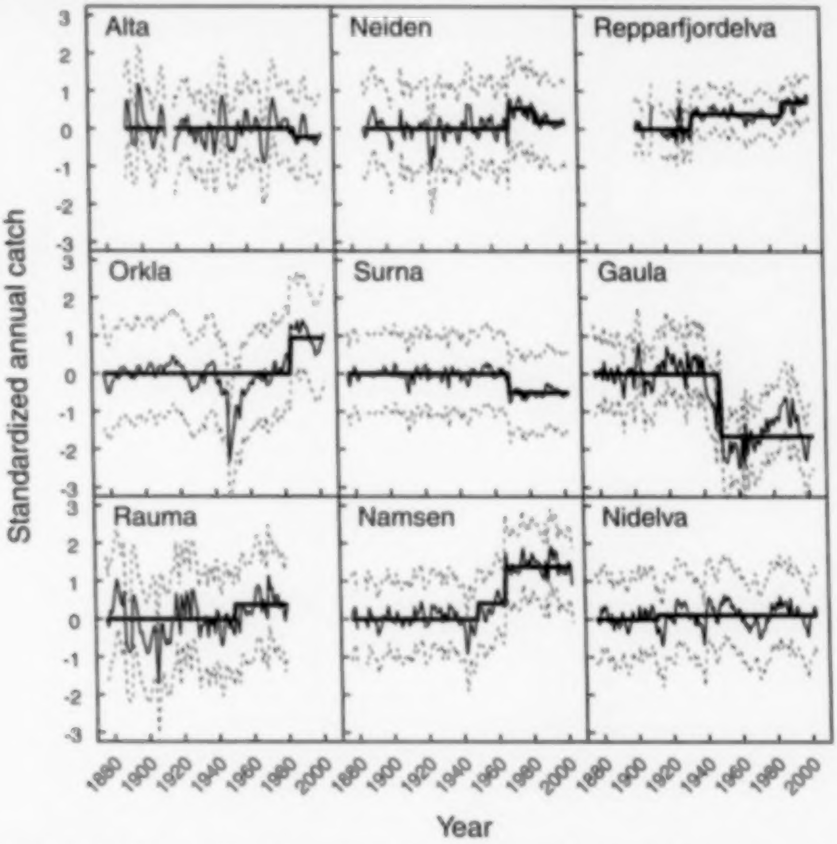

estimate the unique effects for the two encroachment types. Stocking was found to have a positive (nonsignificant) effect on annual catches when the fish was stocked as smolt and constituted a large proportion of the total smolt production, as in Surna. In total, there was no obvious positive or negative effect of fish stocking in these rivers. Also, this is the general conclusion from reviews on fish stocking, i.e., effect sizes vary strongly depending on the species, population, and environmental conditions (Einum and Fleming 2001). A number of authors suggest that the long-term effect in most cases will be negative because of the negative genetic and ecological interactions between hatchery-reared and native fish (Hindar et al. 1991; Einum and Fleming 2001; McGinnity et al. 2003).

In Orkla, estimated smolt production of Atlantic salmon has increased by a factor of up to 1.8 following hydropower development (Hvidsten 1993). This has been attributed to an increase in winter water discharge. In Alta, annual surveys since 1981 have revealed a decline in density of juvenile Atlantic salmon in the upper reaches concurrently with a decrease in the catch of adults (Forseth et al. 1996). In some rivers, stranding of juvenile salmonids has led to increased mortality (as shown for Nidelva; Hvidsten 1985). Hvidsten (1985) demonstrated that for anadromous brown trout, the stranding led to a significant reduction in productions, whereas the Atlantic salmon mortality was not affected. Furthermore, enhancement measures (stocking and fish ladders) significantly increased annual catches (Neiden and Repparfjordelva). For Repparfjordelva, it was especially interesting that the catch tended to increase after stocking was terminated.

For the regulated rivers, no significant effect of hydropower development on the annual catch of anadromous salmonids was observed. However, for Rauma and Namsen, we observed a positive and marginally significant effect. For Orkla, the effect was also positive, but nonsignificant. Only for Alta did we find a negative effect, but the estimate was nonsignificant. These results were contrary to our expectations of negative effects based on the scientific literature (e.g., Ward and Stanford 1979). Changes resulting from hydropower development may explain the deviation. For example, hydropower schemes have caused changes in the hydrological regime of the rivers by water being stored during periods of high discharge (mostly spring snowmelt) and released in periods with reduced runoff, as in winter when the power needs are greatest. However, water has not been diverted from the river systems. In Orkla, an increase in smolt production of Atlantic salmon following hydropower development has been attributed to an increase in winter water discharge (Hvidsten 1993). The increase in smolt production lends support to our analysis that the relative catch in Orkla has increased after hydropower development. A significant negative correlation between the size of the spring flood and the biomass and year-class strength of both Atlantic salmon and anadromous brown trout has been demonstrated for one undeveloped river (Jensen and Johnsen 1999). The water flow during spring, especially the intensity of spring flood, seems to determine to a large extend the recruitment of brown trout in Spanish and French rivers (Cattanéo et al. 2002; Lóbon-Cerviá and Rincón 2004). Thus, the reduced spring flood as a result of hydropower development may lead to increased recruitment in some rivers. To what extent increased recruitment is translated into increased smolt production will depend on how juvenile rearing habitat is influence by the encroachment. Given a surplus of spawners, it is often assumed that populations of salmonids in rivers are regulated by density-dependent processes. For Atlantic salmon, few stock–recruitment curves summarizing such density-dependent regulation have been published (but see Buck and Hay 1984; Chadwick 1985; Jonsson et al. 1998), and for the rivers studied here, no such information exists. Changes in hydrological regimes may also change the shape of the stock–recruitment relationships.

Acknowledgements

We thank R. Arvola, R. J. Bekvik, S. Brørs, M. Flood, B. Høgaas, I. Korsen, E. Lien, K. Moen, L. Nordseth, K. Ofstad, A. Rikstad, and L.M. Sættem for river information, K.B. Rian for providing the official catch records from Norwegian rivers, and R. Stubrud for technical assistance. We also thank J.E. Brittain, K. Friedland, E.M. Olsen, and K. Lekve for constructive comments on earlier versions of the paper. Finally, two anonymous reviewers are thanked for providing input that significantly improved the paper.

References

Beamish, R.J., and Bouillon, D.R. 1993. Pacific salmon production trends in relation to climate. Can. J. Fish. Aquat. Sci. **50**: 1002–1016.

Beaumont, W.C., Welton, J.S., and Ladle, M. 1991. Comparison of rod catch data with known numbers of Atlantic salmon (*Salmo salar* L.) recorded by a resistivity fish counter in a southern chalk stream. *In* Catch effort sampling strategies: their application in freshwater fisheries management. *Edited by* I.G. Cowx. Fishing News Books, Oxford, UK. pp. 49–60.

Box, G.E.P., and Tiao, G.C. 1975. Intervention analysis with applications to economic and environmental problems. J. Am. Stat. Assoc. **70**: 70–79.

Buck, R.J.G., and Hay, D.W. 1984. The relation between stock size and progeny of Atlantic salmon *Salmo salar* L. in a Scottish stream. J. Fish Biol. **24**: 1–11.

Cattanéo, F., Lamouroux, N., Breil, P., and Capra, H. 2002. The influence of hydrological and biotic processes on brown trout (*Salmo trutta*) population dynamics. Can. J. Fish. Aquat. Sci. **59**: 12–22.

Chadwick, E.M.P. 1985. Fundamental research problems in the management of Atlantic salmon, *Salmo salar*, in Atlantic Canada. J. Fish Biol. **27**(Suppl. A): 9–25.

Crozier, W.W., and Kennedy, G.J.A. 2001. Relationship between freshwater angling catch of Atlantic salmon and stock size in the River Bush, Northern Ireland. J. Fish Biol. **58**: 240–247.

Dahl, K. 1910. Alder og vekst hos laks og ørret belyst ved studiet av deres skjæl. Centraltrykkeriet, Kristiania. [In Norwegian.]

Dalpadado, P., Ingvaldsen, R., and Hassel, A. 2003. Zooplankton biomass variation in relation to climatic conditions in the Barents Sea. Polar Biol. **26**: 233–241.

Einum, S., and Fleming, I.A. 2001. Implications of stocking: ecological interactions between wild and released salmonids. Nordic J. Freshw. Res. **75**: 56–70.

Elliott, J.M. 1994. Quantitative ecology and the brown trout. Oxford University Press, Oxford, UK.

Fiske, P., and Aas, Ø. (*Editors*). 2001. Laksefiskeboka — Om sammenhenger mellom beskatning, fiske og verdiskaping ved elvefiske etter laks, sjøaure og sjørøye. NINA Temahefte, **20**. [In Norwegian.]

Forseth, T., Næsje, T.F., Jensen, A.J., Saksgård, L., and Hvidsten, N.A. 1996. The effects of new diversion valves in Alta hydropower station on the population of Atlantic salmon. NINA Oppdragsmelding, **392**: 1–28. [In Norwegian with English summary.]

Friedland, K.D. 1998. Ocean climate influences on critical Atlantic salmon (*Salmo salar*) life history. Can. J. Fish. Aquat. Sci. **55**(Suppl. 1): 119–130.

Gee, A.S., and Milner, N.J. 1980. Analysis of 70-year catch statistics for Atlantic salmon (*Salmo salar*) in the River Wye and implications for management of stocks. J. Appl. Ecol. **17**: 41–57.

Grenfell, B.T., Wilson, K., Finkenstädt, B.F., Coulson, T.N., Murray, S., Albon, S.D., Pemberton, J.M., Clutton-Brock, T.H., and Crawley, M.J. 1998. Noise and determinism in synchronized sheep dynamics. Nature (London), **394**: 674–677.

Groot, C., and Margolis, L. (*Editors*). 1991. Pacific salmon life histories. UBC Press, Vancouver, British Columbia.

Gross, M.R., Coleman, R.M., and McDowall, R.M. 1988. Aquatic productivity and the evolution of diadromous fish migration. Science (Washington, D.C.), **239**: 1291–1293.

Gudjonsson, S., Einarsson, S.M., Antonsson, T., and Gudbergsson, G. 1995. Relation of grilse to salmon ratio to environmental changes in several wild stocks of Atlantic salmon (*Salmo salar*) in Iceland. Can. J. Fish. Aquat. Sci. **52**: 1385–1398.

Hansen, L.P. 1986. The data on salmon catches available for analysis in Norway. *In* The status of the Atlantic salmon in Scotland. ITE Symposium No. 15, Banchory Research Station, Banchory, UK. *Edited by* D. Jenkins and W.M. Shearer. Institute of Terrestrial Ecology, Natural Environment Research Council, Banchory, UK. pp. 79–83.

Hansen, L.P., and Jacobsen, J.A. 2003. Origin and migration of wild and escaped farmed Atlantic salmon, *Salmo salar* L., in oceanic areas north of the Faroe Islands. ICES J. Mar. Sci. **60**: 110–119.

Haydon, D.T., Stenseth, N.C., Boyce, M.S., and Greenwood, P.E. 2001. Phase coupling and synchrony in the spatiotemporal dynamics of muskrat and mink populations across Canada. Proc. Natl. Acad. Sci. U.S.A. **98**: 13 149 – 13 154.

Heggberget, T.G. 1986. An aerial method of assessing spawning activity of Atlantic salmon, *Salmo salar* L., and brown trout, *Salmo trutta* L., in Norwegian streams. J. Fish Biol. **28**: 335–342.

Hendry, A.P., Castric, V., Kinnison, M.T., and Quinn, T.P. 2004. The evolution of philopatry and dispersal. Homing versus straying in salmonids. *In* Evolution illuminated. Salmon and their relatives. *Edited by* A.P. Hendry and S.C. Stearns. Oxford University Press, Oxford, UK. pp. 52–91.

Hindar, K., Ryman, N., and Utter, F. 1991. Genetic effects of cultured fish on natural fish populations. Can. J. Fish. Aquat. Sci. **48**: 945–957.

Holm, M., Holst, J.C., and Hansen, L.P. 2000. Spatial and temporal distribution of post-smolts of Altantic salmon (*Salmo salar* L.)

in the Norwegian Sea and adjacent areas. ICES J. Mar. Sci. **57**: 955–964.

Hvidsten, N.A. 1985. Mortality of pre-smolt Atlantic salmon, *Salmo salar* L., and brown trout, *Salmo trutta* L., caused by fluctuating water levels in the regulated River Nidelva, central Norway. J. Fish Biol. **27**: 711–718.

Hvidsten, N.A. 1993. High winter discharge after regulation increases production of Atlantic salmon (*Salmo salar*) smolts in the River Orkla, Norway. *In* Production of juvenile Atlantic salmon, *Salmo salar*, in natural waters. *Edited by* R.J. Gibson and R.E. Cutting. Can. Spec. Publ. Fish. Aquat. Sci. No. 118. pp. 175–177.

Hvidsten, N.A., Johnsen, B.O., Jensen, A.J., Fiske, P., Ugedal, O., Thorstad, E., Jensås, J.G., Bakke, Ø., and Forseth, T. 2004. Orkla – et nasjonalt referansevassdrag for studier av bestandsregulerende faktorer hos laks. NINA Fagrapport, **79**: 1–94. [In Norwegian with summary in English.]

International Council for the Exploration of the Sea. 2002. Report of the working group on North Atlantic salmon. ICES CM 2000/ACFM:14.

Jensen, A.J., and Johnsen, B.O. 1999. The functional relationship between peak spring floods and survival and growth of juvenile Atlantic salmon (*Salmo salar*) and brown trout (*Salmo trutta*). Funct. Ecol. **13**: 778–785.

Jensen, A.J., Grande, M., Korsen, I., and Hvidsten, N.A. 1998. Reduced heavy metal pollution in the Orkla River, Norway: effects on fish populations. Verh. Int. Verein. Limnol. **26**: 1235–1242.

Jensen, A.J., Zubchenko, A.V., Heggberget, T.G., Hvidsten, N.A., Johnsen, B.O., Kuzmin, O., Loenko, A.A., Lund, R.A., Martynov, V.G., Næsje, T.F., Sharov, A.F., and Økland, F. 1999. Cessation of the Norwegian drift net fishery: changes observed in Norwegian and Russian populations of Atlantic salmon. ICES J. Mar. Sci. **56**: 84–95.

Johnsen, B.O., and Jensen, A.J. 1986. Infestations of Atlantic salmon, *Salmo salar* L., by *Gyrodactylus salaris* in Norwegian rivers. J. Fish Biol. **29**: 233–241.

Jonsson, N., Jonsson, B., and Hansen, L.P. 1998. The relative role of density-dependent and density-independent survival of the life cycle of Atlantic salmon, *Salmo salar*. J. Anim. Ecol. **67**: 751–762.

Jonsson, N., Jonsson, B., and Hansen, L.P. 2003. The marine survival and growth of wild and hatchery-reared Atlantic salmon. J. Appl. Ecol. **40**: 900–911.

L'Abée-Lund, J.H., Jonsson, B., Jensen, A.J., Sættem, L.M., Heggberget, T.G., Johnsen, B.O., and Næsje, T.F. 1989. Latitudinal variation in life history characteristics of sea-run migrant brown trout, *Salmo trutta*. J. Anim. Ecol. **58**: 525–542.

L'Abée-Lund, J.H., Vøllestad, L.A., and Beldring, S. 2004. Spatial and temporal variation in grilse proportion of Atlantic salmon in Norwegian rivers. Trans. Am. Fish. Soc. **133**: 743–761.

Lobón-Cerviá, J., and Rincón, P. A. 2004. Environmental determinants of recruitment and their influence on the population dynamics of stream-living brown trout, *Salmo trutta*. Oikos, **105**: 641–646.

Manly, B.F.J. 1997. Randomization, bootstrap and Monte Carlo methods in biology. 2nd ed. Chapman and Hall, London, UK.

Mann, K.H., and Lazier, J.R.N. 1991. Dynamics of marine ecosystems. Biological–physical interactions in the ocean. Blackwell Scientific Publications, Oxford, UK.

McGinnity, P., Prodöhl, P., Ferguson, A., Hynes, R., Maoileidigh, N.O., Baker, N., Cotter, D., O'Hea, B., Cooke, D., Rogan, G., Taggart, J., and Cross, T. 2003. Fitness reduction and potential extinction of wild populations of Atlantic salmon, *Salmo salar*, as a result of interactions with escaped farmed salmon. Proc. R. Soc. Lond. B, **270**: 2443+2450.

McKinnell, S.M., and Karlström, Ö. 1999. Spatial and temporal covariation in the recruitment and abundance of Atlantic salmon populations in the Baltic Sea. ICES J. Mar. Sci. **56**: 433–443.

Mills, D. 1989. Ecology and management of Atlantic salmon. Chapman and Hall, London, UK.

Mueter, F.J., Ware, D.M., and Peterman, R.M. 2002. Spatial correlation patterns in coastal environmental variables and survival rates of salmon in the north-east Pacific Ocean. Fish. Oceanogr. **11**: 205–218.

Orvik, K.A., Lundberg, L., and Mork, M. 1995. Topological influence and the flow field off Lofoten-Vesterålen. *In* Ecology of fjords and coastal waters. *Edited by* H.R. Skjoldal, C. Hopkins, K.E. Erikstad, and H.P. Leinaas. Elsevier, Amsterdam. pp. 165–175.

Peterman, R.M., and Steer, G.J. 1981. Relation between sportfishing catchability coefficients and salmon abundance. Trans. Am. Fish. Soc. **110**: 585–593.

Peterman, R.M., Pyper, B.J., Lapointe, M.F., Adkinson, M.D., and Walters, C.J. 1998. Patterns of covariation in survival rates of British Columbian and Alaskan sockeye salmon (*Oncorhynchus nerka*) stocks. Can. J. Fish. Aquat. Sci. **55**: 2503–2517.

Prévost, E., Parent, E., Crozier, W., Davidson, I., Dumas, J., Gudbergsson, G., Hindar, K., McGinnity, P., MacLean, J., and Sættem, L.M. 2003. Setting biological reference points for Atlantic salmon stocks: transfer of information from data-rich to data-sparse situations by Bayesian hierarchical modelling. ICES J. Mar. Sci. **60**: 1177–1193.

Ricker, W.E. 1972. Hereditary and environmental factors affecting certain salmonid populations. *In* The stock concept in Pacific salmon. *Edited by* R.C. Simon and P.A. Larkin. MacMillan Lectures in Fisheries, University of British Columbia, Vancouver, B.C. pp. 19–160.

Rikardsen, A.H., Haugland, M., Bjørn, P.A., Finstad, B., Knudsen, R., Dempson, J.B., Holst, J.C., Hvidsten, N.A., and Holm, M. 2004. Geographical differences in marine feeding of Atlantic salmon post-smolts in Norwegian fjords. J. Fish Biol. **64**: 1655–1679.

Sættem, L.M. 1995. Gytebestander av laks og sjøaure — En sammenstilling av registreringer fra ti vassdrag i Sogn og Fjordane fra 1960–94. Direktoratet for naturforvaltning, utredning No. 7. [In Norwegian.]

Shearer, W.M. 1992. The Atlantic salmon — natural history, exploitation and future management. Fishing News Books, Oxford, UK.

Thorley, J.L., Eatherley, D.M.R., Stephen, A.B., Simpsons, I., MacLean, J.C., and Youngson, A.F. 2005. Congruence between automatic fish counter data and rod catches of Atlantic salmon (*Salmo salar*) in Scottish rivers. ICES J. Mar. Sci. **62**: 809–817.

Ward, J.V., and Stanford, J.A. (*Editors*). 1979. The ecology of regulated rivers. Plenum Press, New York.

Waters, T.F. 1995. Sediments in streams — sources, biological effects and control. Am. Fish. Soc. Monogr. **7**: 1–251.

Zuur, A.F., Tuck, I.D., and Bailey, N. 2003. Dynamic factor analysis to estimate common trends in fisheries time series. Can. J. Fish. Aquat. Sci. **60**: 542–552.

A model for evaluating fishing impacts on habitat and comparing fishing closure strategies

Jeffrey T. Fujioka

Abstract: In response to increasing concern with the effects of fishing on benthic habitat, I show a mathematical model using state transition equations to compute habitat reduction by unifying the processes of fishing impact and habitat recovery. The model assumes habitat is either in an unimpacted state or in an impacted state. The state transition equations describe that fishing decreases unimpacted habitat and the recovery process decreases impacted habitat. The equations are integrated under constant fishing effort for habitat trajectories over time, and the equilibrium habitat level is derived. A difference equation is also derived to model habitat trajectories under varying fishing effort. An exploration of the joint properties of the habitat reduction and catch equations provides guidance in choosing or designing habitat protection measures. Illustrations with the model demonstrate that when harvest levels are maintained, closing heavily fished areas rather than lightly fished areas can result in increased habitat reduction.

Résumé : En réponse aux préoccupations croissantes au sujet des effets de la pêche sur les habitats benthiques, mon modèle mathématique, qui utilise des équations de transition d'état, calcule la réduction d'habitat en unifiant les processus de l'impact des pêches et de la récupération des habitats. Le modèle assume que l'habitat est dans un état perturbé ou non perturbé. Les équations de transition d'état décrivent que la pêche réduit les habitats non perturbés et que les processus de récupération réduisent les habitats perturbés. Ces équations sont intégrées avec un effort de pêche constant dans des trajectoires de l'habitat dans le temps; un niveau d'habitat à l'équilibre est déterminé. Une équation de différence est aussi élaborée afin de modéliser les trajectoires de l'habitat sous un effort de pêche variable. Une exploration des propriétés communes de la réduction de l'habitat et des équations de capture fournit des critères pour choisir ou inventer des mesures de protection de l'habitat. Des exemples faits à partir du modèle montrent que lorsque les niveaux de récolte sont maintenus, la fermeture de zones fortement exploitées plutôt que de zones faiblement exploitées peut entrainer une augmentation de la réduction d'habitat.

[Traduit par la Rédaction]

Introduction

Increasing awareness of the utilization of various habitat features by marine fish has resulted in increased concerns about the effects of marine fisheries on habitat. The National Research Council (NRC 1994) considers this "perhaps the least understood of important environmental effects of fishing". Auster and Langdon (1999) present a conceptual model of the function of fishing effects on various habitat types. While simple mathematical equations have long been used to model the function of fishing effort on the reduction of fish numbers and have been the foundation for the population dynamics theory used to manage fisheries, the development of such equations for modeling fishing effects on habitat has only recently begun. A report by the NRC (2002) contains an equation that deals with the process of habitat removal by fishing.

The NRC equation does not specifically represent habitat recovery, but accounts for different recovery rates and habitat types indirectly by varying the impact rate. The impact rate for biogenic habitat or habitat not naturally disturbed would be higher than that for sand or habitat frequently disturbed by nature. This results in a ranking of effects of habitat type that seems reasonable with the findings of Auster and Langdon (1999) and Collie et al. (2000), who found that fauna in stable substrate and biogenic habitats are more adversely affected than fauna in less consolidated sediments and that recovery rate appeared to be most rapid in naturally disturbed habitat. Lindholm et al. (2001) classify habitat impact and suitability for juvenile fish by the complexity of habitat substrate and epifauna, but do not model the reduction process.

The Magnuson Stevens Fisheries Conservation and Management Act requires that adverse effects from fishing activities on essential fish habitat (EFH) be minimized to the extent practicable. The final regulations on EFH provide the guidance that US fishery management councils must act if "a fishing activity adversely affects EFH in a manner that is more than minimal and not temporary in nature" (National Oceanic and Atmospheric Administration – National Marine Fisheries Service (NOAA Fisheries) 2002). The North Pacific Fishery Management Council and the National Marine

Received 11 November 2005. Accepted 14 June 2006. Published on the NRC Research Press Web site at http://cjfas.nrc.ca on 3 October 2006.
J18996

J.T. Fujioka. National Marine Fisheries Service, Alaska Fisheries Science Center, Auke Bay Laboratory, 11305 Glacier Highway, Juneau, AK 99801, USA (e-mail: jeff.fujioka@noaa.gov).

doi:10.1139/F06-120

Fisheries Service's Alaska Regional Office asked scientists of the Alaska Fisheries Science Center to define criteria for determining whether a fishery has an effect "that is more than minimal and not temporary". Considering that the two terms are relevant to the rate of impact of fishing on habitat and the rate of habitat recovery, an approach is needed to unify the two aspects. The NRC equation does not explicitly account for habitat recovery and would be applicable for only a limited time period or for habitat that recovers very slowly or not at all.

During the development of the EFH-environmental impact statement (EIS) for the Alaska groundfish fishery (NOAA Fisheries 2005), the author proposed a mathematical model that combined the processes of fishing impact and habitat recovery in the calculation of habitat reduction. This model was used in the EIS to compare conditional impact levels of different fisheries over broad regions and habitat features.

Despite extensive review during the EIS process, a referee noted during the peer review for this paper that a term that appears in my original differential equations was incorrectly defined. Correctly defined, this term would equal 1, and the equations simplify to a system of state transition equations. Reduction levels are less than my original equations indicated, although the difference is slight at low recovery rates. At recovery rate $\rho = 0.01$, 0.10, and 0.20, the differences would be approximately 1%, 4%–7%, and 12%, respectively, depending on impact rate I. Here, I present the model developed as state transition equations, the model properties, and examples of how the model can be used to estimate or predict habitat reduction. While the examples are realistic, I deal only with the level of habitat reduction and do not evaluate all of the habitat issues involved. The linkage between habitat and fish productivity is a critical factor that is not evaluated by this model. Most of the model parameter values, such as habitat sensitivity and recovery rates, are unknown for the geographic area of application (Alaska), and the estimated habitat reductions are conditional.

Basic impact model

The basic model describes the state of habitat as either unaffected or affected. H is the amount of unaffected habitat, and h is the amount of affected habitat. H decreases in proportion to an impact rate I and increases in proportion to the recovery rate ρ on h. Let h that is not additionally impacted during an interval of time, Δt, be denoted by $e^{-I\Delta t}h$. That is, affected habitat is exposed to fishery impact at the same rate as unaffected habitat, but is already affected so that there is no increase in h. The amount of affected habitat that is not further impacted, $e^{-\Delta t}h$, recovers to the unaffected state at rate ρ. In the limit as $\Delta t \to 0$, $e^{-I\Delta t} = 1$ and the following state transition equations describe the rates of impact and recovery:

$$(1) \qquad \mathrm{d}H/\mathrm{d}t = -IH + \rho h$$

$$(2) \qquad \mathrm{d}h/\mathrm{d}t = +IH - \rho h$$

Letting $H = H_0$ and $h = 0$ at time $t = 0$, integrating the derivatives above for $t \geq 0$ (see Appendix A) results in

$$(3) \qquad H_t = H_0[Ie^{-(I+\rho)t} + \rho]/(I + \rho)$$

And because at $t = \infty$, $Ie^{-(I+\rho)t}$ will go to 0, H_t will reach an equilibrium level, H_{eq}, at

$$(4) \qquad H_{eq} = H_0\rho/(I + \rho)$$

Habitat reduction is expressed as $R_t = H_0 - H_t$. Relative concern for potential adverse effects may be defined as proportional reduction of habitat expressed by setting $H_0 = 1$:

$$(5) \qquad R_{eq} = 1 - H_{eq} = [1 - \rho/(I + \rho)] = I/(I + \rho)$$

Impact rate

The impact rate I can be expressed as $I = fq_H$, where f is the amount of fishing effort and q_H is the impact coefficient for unaffected habitat per unit effort. Consider a hypothetical bottom trawl fishery where effort is in random independent trawl sweeps and is measured in proportion to the area swept by the path of the trawl doors. If the amount of area swept by fishing effort is 20% more than the size of the area, then let $f = 1.2$. Some portions of the area will be swept more than once, while some may not be swept at all. If all habitat within the area swept is impacted by one pass of the gear, then $q_H = 1.0$ and $I = 1.2$. If half of the existing habitat is impacted, then $q_H = 0.5$ and $I = 0.6$. Each habitat type could have a different impact coefficient for each type of fishing activity. This coefficient is similar to a coefficient, q, used in equations to account for the catchability of fish.

The model was developed to provide a quantitative basis for relating fishing intensity and habitat impact and recovery. Data on fishing effort is typically available only for areas that are large in comparison with that impacted by an individual unit of gear, and thus intensity information is only available as the average for the area. Because habitat impact is not a linear function of fishing intensity, a bias can exist when using the average intensity to estimate the area's habitat reduction if fishing intensity is not uniformly distributed, which is seldom the case. The equilibrium (steady state) forms of the model (H_{eq} and R_{eq}) are asymptotically (in time) unbiased when applied to areas where fishing effort is randomly distributed or independently distributed each year. However, when applying the model in a nonequilibrium situation (e.g., to fit a time series) for an area of randomly (or contagiously) distributed fishing effort, a correction for bias would be required to compute the average value for the area. Such a correction, while cumbersome, can be easily determined numerically given information about the actual effort distribution. Rijnsdorp et al. (1998), Bergmann and van Santbrink (2000), and Pitcher et al. (2000) have dealt with this issue with a variety of approaches. Ellis and Pantus (2001) have derived a relationship for a family of distributions that scales up the impact of individual units of gear to the overall impact rate of a larger area.

If fishing effort within a unit area is thought to be concentrated consistently within a subarea or specific paths through the area, the area should be further subdivided and the model applied separately to each subarea or path. The results for habitat reduction from random fishing apply to the habitat that is within such an area or subarea. The results would also apply to clusters of areas where fishing effort is random and of similar intensity throughout. H_{eq} values would then be computed for each block or cluster of similar fishing intensity level for each habitat type.

Fig. 1. Equilibrium habitat reduction level R_{eq} as a function of impact rate I for different values of recovery rate ρ.

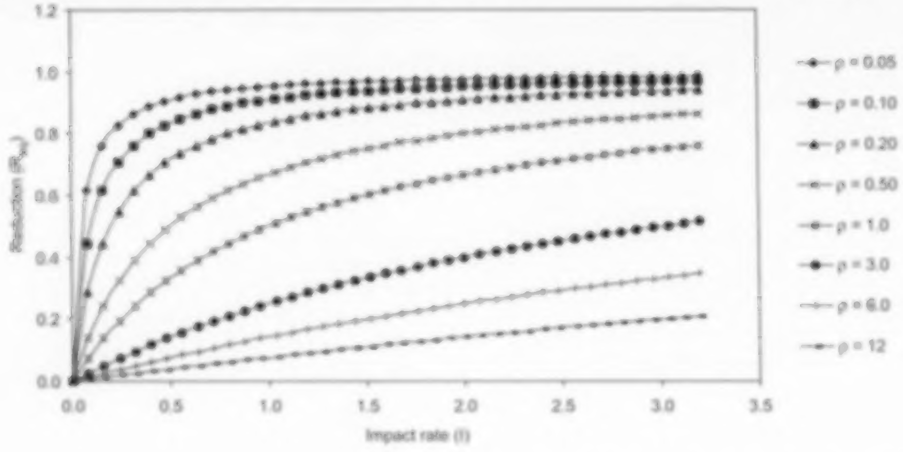

Recovery rate ρ

ρ reflects the rate of change of h back to H. In the absence of further impacts, h decreases exponentially until all habitat is in H, the unimpacted condition. The recovery time, T, can be thought of as the average amount of time that the impacted habitat stays in the impacted state, which equals $1/\rho$ (in the absence of further impacts). Each habitat type may have different recovery rates.

Modeling the instantaneous recovery process as a linear function of h serves as a simple approximation to what could be a very complex process. While the exponential recovery trajectories that result from the model are plausible, recovery of some habitat features may vary from the simple two-state model. If the recovery dynamics of a habitat was found to be more complex, a state transition model with additional states may provide reasonable means to represent the process.

Variable fishing rate

All the equations above apply to conditions of a constant level of effort. To model a variable fishing scenario, f_t, or a scenario starting at a habitat level other than the unfished level, H_0, the following difference equation can be used:

$$(6) \qquad H_{t+1} = H_t + (H_t - H'_{eq,t})[e^{-(I'+\rho)} - 1]$$

Note that $H'_{eq,t}$ is defined as at eq. 4, $I' = q_H f_t$.

Equation 6 can be used to model habitat reduction over time when the historical fishing effort is known. It can also be applied to track habitat change during a time series of alternating fishery openings and closures that may be proposed as a management approach.

The simplest conception of the model is to consider the quantity of habitat in either an unaffected or affected state. The definition of affected or unaffected is left to the user. The term R is referred to here as the reduction of unaffected habitat. While little is actually known about habitat function and its many possible links to fish productivity, the model could also be in terms of habitat function, and R could represent reduction of habitat function. R could also be a measure of habitat effect or impact on fish productivity. The value of R_{eq} is used to simplify comparisons of potential reduction, as the value of R_t depends on the duration of impact, which is often not known or is not at a constant rate.

Model properties

Equilibrium levels

As I increases, R_{eq} increases at a decreasing rate, and 100% reduction is approached asymptotically. At low ρ, R_{eq} will be higher, and 100% reduction will be approached at a lower I (Fig. 1). Both I and ρ are necessary to determine *Req*. Even a habitat that recovers in a year ($\rho = 1.0$) can be reduced by approximately 50% if the habitat is impacted once a year ($I = 1.0$). Likewise, it takes an extremely low impact rate to result in a minimal habitat effect if ρ is low.

Consideration of the relationship between ρ and f may help to evaluate proposed mitigation measures, such as closing an area to fishing. Whether a closure will result in more or less habitat reduction depends on the amount of status quo fishing effort, f_{SQ}, that is displaced, how much of the effort is reallocated, and to where the effort is reallocated. R_{eq} increases with increasing I at a decreasing rate throughout the function range, and R_{eq} approaches 100% asymptotically.

Catch in relation to reduction of habitat

A mitigation measure may involve closing areas to fishing without a commensurate reduction in catch quota. The measure will thus involve an increase in effort in the areas remaining open. Ideally, a net decrease of habitat reduction, R_{eq}, will occur while allowing the quota to be taken. However, to attain the quota, even more reduction in habitat could occur. Whether an intended mitigation will be effective depends on a variety of factors, such as distribution of target species, distribution of f_{SQ}, the f_{SQ} of the areas to be closed to fishing, effort redeployment under the mitigation measure, and the respective values of habitat recovery, sensitivity, q_H, and the fishing gear's fish catchability coefficient, q. The net effect of these factors, if known, could be estimated by incorporating the habitat model with a fishery catch model within a spatial modeling exercise. Although such an analysis is not presented here, the habitat model can

Fig. 2. Ratio of $dC/df : dR_{eq}/df$ in relation to fishing intensity f at selected recovery rates ρ. Ratios are in proportion to their maximum value for illustrative purposes.

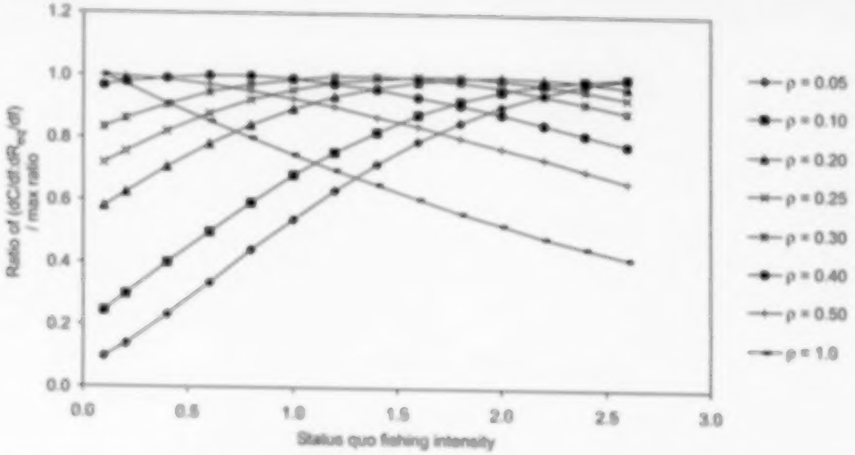

be combined with the catch equation to provide some general guidance in choosing areas to close or open relative to the areas' f_{SQ}. In particular, all else being equal, does an incremental increase in effort in one area result in more catch, C, relative to R_{eq} compared with increasing effort in another area of a different level of f_{SQ}?

For a given area, the level of f_{SQ} determines the corresponding exploitation rate and projected R_{eq}. If the distribution of unfished fish density and unfished habitat, H_0, is independent of and unrelated to the distribution of f_{SQ}, then comparing the ratio of the derivatives, dC/df and dR_{eq}/df, at respective values for areas' f_{SQ} will tell us whether C will increase faster than R_{eq} in one area than in the other. If the ratio is higher for one area compared with another, then the increase in C compared with the increase in R_{eq} will be greater if effort is increased in the former than if effort is increased in the latter. Taking the derivative with respect to f of the catch equation $C = N_0F/(F + M)[1 - e^{(-F-M)}]$ and eq. 3 results in

$$(7)\qquad dC/df = qM(1 - e^{-Z})/Z^2 + Fq\,e^{-Z}/Z$$

where $N_0 = 1.0$, $Z = F + M$, $F = fq$, and q is the effect of f on fish resulting in catch.

$$(8)\qquad dR_{eq}/df = H_{eq}q_H/(I + \rho) = H_{eq}R_{eq}/f$$
$$= H_{eq}(1 - H_{eq})/f$$

A plot of the ratio $dC/df : dR_{eq}/df$ at different levels of f_{SQ} and ρ (and at $q = 0.6$, $q_H = 0.15$) is shown (Fig. 2). For the higher values of ρ (0.40 to 1.00), the slope of the ratio vs. f_{SQ} is negative over the range of f_{SQ}. At the intermediate levels of ρ (0.20 to 0.30), the slope is positive at low levels of f_{SQ}, levels off, and becomes negative again at the high end of the range of f_{SQ}. For slower recovery rates ($\rho \leq 0.20$), the slope is positive for the full range of f_{SQ}.

The values of q and q_H influence the degree at which the ratio changes with ρ. A higher value of q results in a decrease of slope for a given ρ, while a higher value of q_H results in an increase of slope. Fishery and habitat interactions of most concern are where the habitat recovers slowly and the fishery is inefficient and the habitat is sensitive (i.e., a low q/q_H value). These conditions are more likely to result in a positive slope of the $dC/df : dR/df$ ratio. In this case, if two areas are equal in pristine fish density and habitat density, but are fished at different f_{SQ}, increasing effort in the heavier fished area would result in a bigger gain in catch relative to R_{eq} than if effort was increased in the lighter fished area. For the reverse case, reducing or closing effort in a lightly fished area would reduce catch less, relative to the decrease in R_{eq}, than closing a heavily fished area. By closing a more lightly fished area to attain the same decrease in habitat reduction as closing a heavily fished area, the decrease in catch would be less. It may be expected that f_{SQ} and pristine fish density are positively correlated. In that case, it would make even more sense to increase effort in the heavier fished area.

Time path to equilibrium

An obvious use of eq. 3 is prediction of the habitat over time, H_t, for given assumptions of f, q_H, and ρ. To explore some simple properties, eq. 3 with $H_0 = 1$ can be expressed as

$$(9)\qquad H_t = H_{eq} + R_{eq}e^{-(I+\rho)t}$$

or expressed in terms of habitat reduction

$$(10)\qquad R_t = 1 - H_t = R_{eq}[1 - e^{-(I+\rho)t}]$$

where H_t follows a simple exponential decrease from H_0 to H_{eq}, or equivalently, R_t approaches R_{eq} asymptotically. The amount of time it takes for R_t to reach some proportion, $P_{R_{eq}}$, of R_{eq}, is equal to

$$(11)\qquad t_{P_{R_{eq}}} = -\ln(1 - P_{R_{eq}})/(I + \rho)$$

where $0 \leq P_{R_{eq}} < 1$.

As I and ρ get larger, $t_{P_{R_{eq}}}$ decreases. The time in years that it takes to attain 95% of the equilibrium reduction for combinations of I and ρ is shown (Fig. 3). For habitat that takes 100 years to recover (e.g., long-lived corals), it takes

Fig. 3. Time (years) to reach 95% of equilibrium reduction R_{eq} at impact rate I and habitat recovery rate ρ.

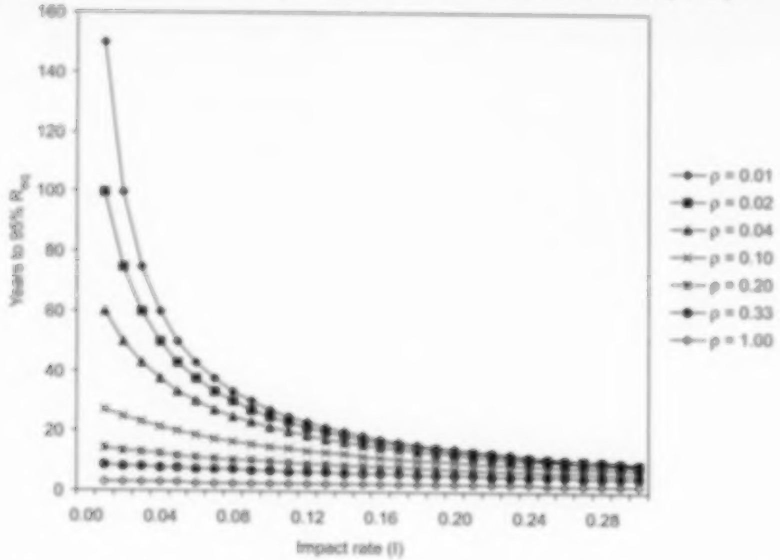

more than 150 years of fishing at $I = 1\% \cdot \text{year}^{-1}$ to approach the equilibrium level of reduction.

Application examples

Determining a threshold level of habitat reduction for groundfish stocks in the North Pacific Ocean is beyond the scope of the model and this paper, as well as current scientific knowledge. Little is known about relationships between habitat and productivity of fish stocks in the marine environment, and threshold values based on the measured interactions between habitat and fish production do not exist. The role of the model is to allow a quantitative estimate of the reduction of habitat, given assumptions of parameter values, so that the potential for adverse effects can be compared and concern focused where merited. The distribution of the habitat reduction in addition to the total or average reduction is an important factor that determines whether habitat reduction would have any effect on productivity. The appropriateness of any mitigative measure would depend on its practicability, plausibility of effect, and the level of precaution of decision makers.

In most of Alaska, information about habitat distribution is lacking, and therefore the actual amount and type of habitat in a fishing block is unknown. In such a case, the H_{eq} values for a block are considered conditional on the amount of each habitat type or habitat feature that actually exists or would have existed in the block if no fishing occurred. In much of Alaska, this data input will have to be estimated or hypothesized. One reason the Bering Sea shelf was chosen as an example area is that the bottom topography is relatively uniform over large areas relative to the available effort measurement units. There is little to suggest the habitat type varies greatly between area units or that fishing is clustered within measurement units. Thus, assumptions about equal habitat type and random fishing effort within blocks are not unreasonable.

Table 1. Equilibrium reduction (R_{eq}) levels as a function of plausible fishing intensity (f = area swept·25 km^{-2}) for the Bering Sea trawl fishery and two plausible sets of sensitivity parameters (q_H) and recovery rates (ρ) for biostructure habitat features.

	R_{eq} (%)	
f	Scenario 1	Scenario 2
0.00	0.0	0.0
0.10	2.0	17.4
0.25	4.8	34.4
0.50	9.1	51.2
1.00	16.7	67.7
2.00	28.6	80.8

Note: Scenario 1 combines low sensitivity (q_H = 0.10) and high ρ (0.50) to estimate low impact; scenario 2 combines higher sensitivity (q_H = 0.21) and lower ρ (0.10) to estimate a higher impact rate for a given fishing intensity.

Evaluating current effects on habitat

The habitat impact model is used to relate fishing intensity levels to habitat reduction from its unfished level. The corresponding R_{eq} values at different levels of fishing intensity are shown for two scenarios of habitat recovery rate and sensitivity to fishing operations (Table 1). The parameters chosen cover a plausible range for bioshelter habitat made up of organisms such as soft corals, tunicates, hydroids, and sponges that are present on the Bering Sea shelf area (Malecha et al. 2005). For scenario 1 habitat that recovers in 2 years (ρ = 0.5) and is only 10% impacted by one pass of the trawl, a fishing intensity of 1.00 results in a reduction of 16.7%. For scenario 2 habitat that takes 10 years (ρ = 0.10) to recover and is 21% impacted by a pass of the trawl, the

Table 2. Status quo Bering Sea bottom trawl fishery showing (*a*) frequency distribution of fishing intensity of and geometric mean of interval endpoints, (*b*) hypothetical biomass distribution (proportional to status quo effort) and catch distribution per intensity interval, and (*c*) habitat impact per intensity interval and mean impact per fished blocks under two scenarios of recovery rate (ρ) and sensitivity (q_H).

(*a*) Fishing intensity (f) distribution.

Interval	Frequency	Area (n.mi.^{2})[a]	Mean f
$0.01 \le f < 0.05$	1631	11 825	0.022
$0.05 \le f < 0.10$	1226	8 889	0.071
$0.10 \le f < 0.25$	1610	11 673	0.158
$0.25 \le f < 0.50$	1003	7 272	0.354
$0.50 \le f < 1.00$	822	5 960	0.707
$1.00 \le f < 2.00$	552	4 002	1.414
$2.00 \le f < 17.13$	277	2 008	2.850[b]
Total	7121		Total f = 2884

(*b*) Biomass and catch.

	Biomass		Catch[c]	
Interval	Per block (= 0.720f)	Per interval	Per block	Per interval
$0.01 \le f < 0.05$	0.016	26	0.000	0.3
$0.05 \le f < 0.10$	0.051	62	0.002	2.6
$0.10 \le f < 0.25$	0.114	183	0.010	16.6
$0.25 \le f < 0.50$	0.255	255	0.049	48.8
$0.50 \le f < 1.00$	0.509	418	0.176	144.7
$1.00 \le f < 2.00$	1.018	562	0.582	321.4
$2.00 \le f < 17.13$	2.052	568	1.681	465.6
Total		2076		1000

(*c*) Habitat reduction level (R_{eq}).

	$\rho = 0.5$, $q_H = 0.1$		$\rho = 0.1$, $q_H = 0.21$	
Interval	Per block	Per interval	Per block	Per interval
$0.01 \le f < 0.05$	0.004	7.26	0.045	73.153
$0.05 \le f < 0.10$	0.014	17.10	0.129	158.514
$0.10 \le f < 0.25$	0.031	49.35	0.249	401.327
$0.25 \le f < 0.50$	0.066	66.24	0.426	427.378
$0.50 \le f < 1.00$	0.124	101.85	0.598	491.205
$1.00 \le f < 2.00$	0.220	121.71	0.748	412.952
$2.00 \le f < 17.13$	0.363	100.57	0.857	237.344
	$\bar{R}_{eq} = 0.065$		$\bar{R}_{eq} = 0.309$	

[a] 1 nautical mile (n.mi.) = 1.852 km.

[b] Average interval intensity approximated as geometric mean of endpoints for intensity interval <2.0, median data value is used for last interval.

[c] Catch = $(1 - e^{-fq})$density; $q = 0.06$.

equilibrium reduction would be 67.7%, or reduced to H_{eq} = 32.3% (1 − 0.677) of its unfished level for fishing intensity of 1.00. Whether reductions of this degree could cause adverse effects to essential fish habitat depends on the amount and geographic extent of such reductions. Smaller amounts of isolated areas reduced to this extent may be less cause for concern.

For fisheries under federal management, Alaska has relatively good information on location and intensity of fishing effort owing to the Alaska Fisheries Science Center's North Pacific Groundfish Observer Program. For the bottom trawl fishery from 1998 to 2002, Rose and Jorgensen (2005) have estimated the amount of bottom area swept (distance towed × width of trawl gear, no correction for overlap) per area for each 5 km × 5 km cell in federally managed bottom trawl fisheries. These values can be considered units of effort for each block and are referred to as fishing intensity when expressed as a ratio of the bottom area swept to the area of each cell. This data will be used to illustrate applications of the model to estimate potential habitat reduction due to bottom trawl fishing in the Bering Sea and to estimate the effectiveness of closing areas to reduce impact on habitat.

The frequency distribution of Bering Sea bottom trawl fishing intensity calculated for the status quo (Table 2*a*) shows

Fig. 4. Geographic distribution of Bering Sea bottom trawl fishing intensity f (1998–2002) estimated for 5 km × 5 km blocks. At intensity level $f = 1$, area swept per block equals block area. Inset map shows study area's location in Alaska, USA.

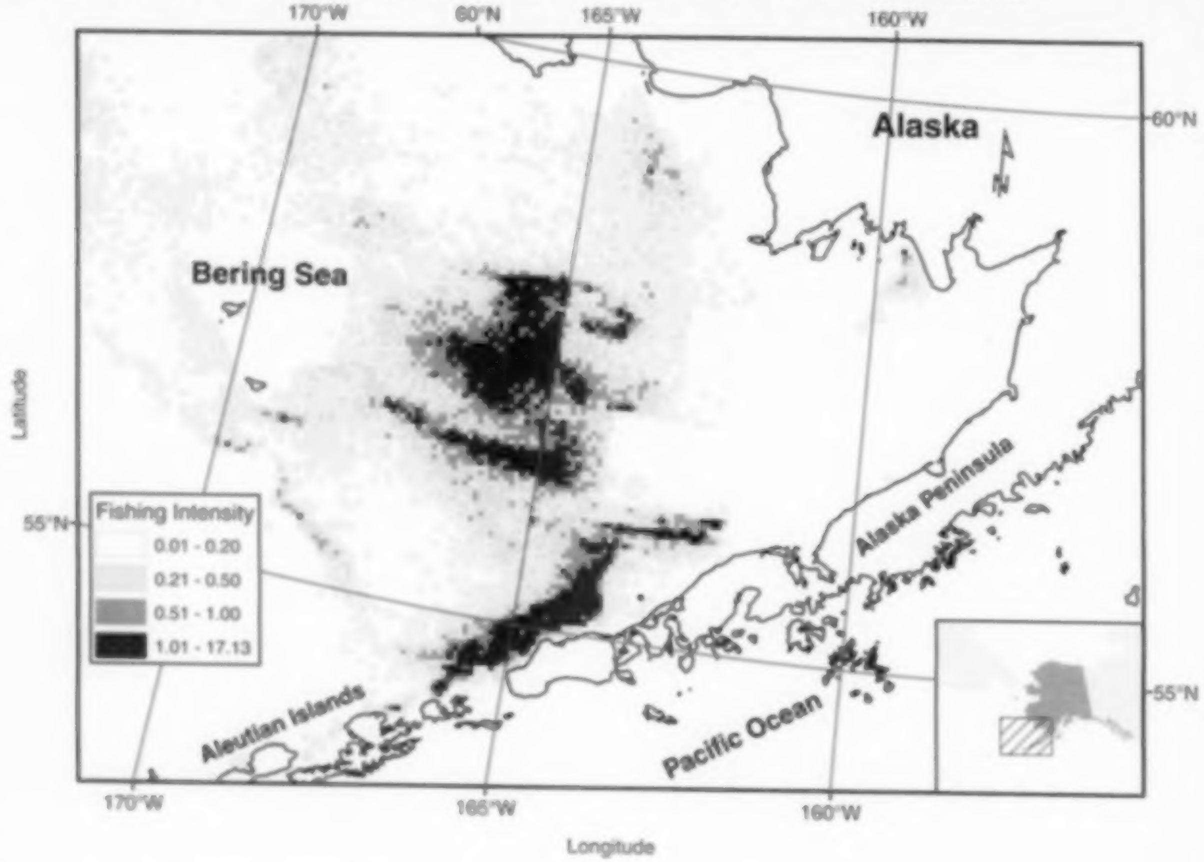

that 829 (552 + 277) 5 km × 5 km blocks are fished at an intensity of 1.00 or greater. The geographic distribution of these blocks is mainly in three large clusters (Fig. 4). Thus, if habitat is impacted and recovers as in scenarios 1 or 2 (Table 1), the model results indicate that the equilibrium level of habitat in these areas would be reduced by at least 16.7% or 67.7%, respectively, from their original unfished levels.

Comparing proposed closure measures

Area closures are a management option for minimizing adverse effects to habitat. An area closure would be expected to change the status quo distribution of fishing effort. For a prediction of the redeployed effort distribution, the habitat impact and recovery equations can be used to compare the habitat reduction levels under the closure strategy with reduction levels under current management. A complete evaluation should take into account the geographic distribution of the reduction and the distribution of the closed areas; however, this paper is limited to a simple look at the level of reductions.

R_{eq} averaged over all blocks under status quo, $\bar{R}_{eq}$, can be compared with the average under the closure measure, $\bar{R}'_{eq}$. The value for $\bar{R}_{eq}$ can be easily approximated by weighting the average R_{eq} for each fishing intensity level by the interval frequency, summing, and dividing by the total number of blocks (Table 2). The geometric mean of the interval endpoints is used as the fishing intensity in eq. 5 to estimate the interval's average reduction level. For example, the geometric mean of the intensity interval 1.00 to 2.00 is 1.414 (Table 2*a*). This results in an R_{eq} of 22.0% or 74.8% under parameter scenarios 1 and 2, respectively, (Table 2*c*). The weighted sum of the intervals divided by the number of fished blocks gives the $\bar{R}_{eq}$ over the fished area. $\bar{R}_{eq}$ is 6.5% or 30.9% under the status quo fishery for the two respective parameter scenarios. Dividing by the total number of blocks on the Bering Sea shelf gives the average over the entire shelf, fished and unfished.

This method approximates the more exact approach of calculating R_{eq} for each block. In the draft environmental impact statement (DEIS) for essential fish habitat in Alaska (EFH-DEIS, NOAA Fisheries 2005), R_{eq} was estimated for each block. Such a computation easily allows for specifying habitat quantities or values to individual blocks, which can be factored into the sum. However, because very little information exists on habitat value or even on the distribution of habitat, all blocks are treated the same in the EFH-DEIS, grouped only into general bottom types (C. Rose, Alaska Fisheries Science Center, 7600 Sand Point Way, Seattle, WA 98115, USA, personal communication). Here all blocks are treated the same as well. While $\bar{R}_{eq}$ compared with $\bar{R}'_{eq}$ alone is inadequate to fully evaluate habitat effects, it is used here as a simple criterion to compare closure alternatives.

Applying the procedures above to a proposed closure requires a prediction of fishing intensity distribution that would result from the proposed closure. The predictor may be simple or highly involved, depending on available information and the complexity of the assumptions made about behavior of fishermen.

Without information on current target species density, the target species density is assumed to be reflected by the status quo fishing intensity f_{SQ} in the fished blocks. Specifically, density is reflected by f_{SQ} in the function, density = af^b. At $b = 1$, density is proportional to fishing effort; at $b = 2$, density is proportional to the square of the effort; at $b = 0$, density is not related to effort. The scalar a is used to keep total biomass equal for different assumptions of b. Using the competitive form of the catch equation ($C = (1 - e^{-fq})$biomass) and $b = 1$, a value of a and the catchability coefficient q were chosen to achieve a status quo catch of 1 million metric tons (t) from a biomass of approximately 2 million t (Table 2*b*). An exploitation rate that may be higher than the actual fishery is used in this example to illustrate that a closure measure can be not only ineffective, but counterproductive.

As an example of a closure scenario, an approximation to the closure areas proposed under alternative 6 of the EFH-DEIS is used. This alternative was intended to prohibit bottom-tending gear within approximately 20% of waters shallower than 1000 m. The closures would be in addition to existing habitat protection measures. The Eastern Bering Sea shelf consists of three regions based on the three substrate types: sand, sand–mud, and mud. I do not distinguish habitat value among these substrate types in this example. Of the 7121 blocks fished under status quo (Table 2*a*), those that are centered within the proposed closed areas under alternative 6 are deleted from the frequency distribution of fishing intensities. This results in 5758 fished blocks (Table 3*a*).

Any increase in effort in the areas remaining open is assumed to be proportional to the original effort in those areas under status quo. The catch equation ($C = (1 - e^{-f'q})$biomass) is used, where $f' = \varepsilon f_{SQ}$, and ε is the fishing intensity expansion factor that results in a total catch level equal to the status quo catch (1 million t). This form of the catch equation accounts for the increased amount of effort required to achieve additional increments of catch. An ε of 1.308 is required to expand the fishing intensities to catch the status quo catch from the blocks remaining open (Tables 3*a*, 3*b*). After the fishing intensity distribution is predicted for the proposed closure, eq. 5 is applied to the frequency intervals using the expanded fishing intensities to compute R'_{eq} for the blocks remaining open (Table 3*c*).

Because of the nonlinear relationship of catch and habitat reduction to effort, an increase of effort results in a greater relative increase of R'_{eq} for blocks where status quo effort is low and there is a greater relative increase of R'_{eq} for habitat parameter scenario 1 than for scenario 2. This can be seen by comparing the reduction per block shown in Tables 2*c* and 3*c*. The increase is nearly proportional to the increase in effort ($\varepsilon = 1.308$) for the lightly fished blocks, but the increase is relatively much less than ε for the heavier fished blocks. The closing of blocks and increase of effort in the open blocks actually results in the average habitat reduction under the alternative, $\bar{R}'_{eq}$, being slightly greater (4.9%) than $\bar{R}_{eq}$ for the fast recovery scenario 1. $\bar{R}'_{eq}$ is only slightly less (5.5%) under the slow recovery scenario 2 (Table 3*c*).

Improvement of closure strategies

Properties of the model (Fig. 2) show that for the habitat of most concern (slow-growing, vulnerable), a strategy of closing lightly fished areas rather than heavily fished areas would be more likely to lower R_{eq} while maintaining status quo catch. If target species density is also positively correlated with f_{SQ}, the advantage of the strategy will be even greater. This section briefly examines whether these properties can be employed to improve on a closure strategy.

Note that for the EFH-DEIS alternative 6 closure, the proportion of blocks closed for each fishery intensity interval range from 18% to 23%, except for the highest interval, where 6% are closed. Closing areas of high effort where fish density may also be high will require greater effort to harvest the foregone catch than closing areas of low effort and presumably low density. Increased effort results in increased R_{eq} per fished block, and the relationship is nearly proportional when I is low as under scenario 1 compared with scenario 2. When reduction is already at a high level, additional effort results in a less than proportional additional reduction. Although alternative 6 happens to have closed a smaller proportion of the heavily fished areas than lightly fished areas, the improvement to the overall decrease from $\bar{R}_{eq}$ was minimal.

An attempt to apply the habitat model properties to improve on alternative 6 is shown (Table 4). Here the number of closed blocks in the two highest intensity intervals is reduced further, and the proportions of closed blocks in the lightly fished intervals are increased further. With this modification, only 10% (83), 4% (24), and 3% (8) of the blocks are closed in the three highest intensity intervals ($f = 0.5$–1.0, $f = 1.0$–2.0, and $f \geq 2.0$ intervals, respectively; Table 4*a*). For the lightly fished blocks, the proportion of blocks closed were increased considerably, but only a small fraction (1.95%) of the status quo catch came from these blocks ((0.3 + 2.6 + 16.6)/1000) (Table 2*b*). For the medium intensity interval, where 4.9% of the status quo catch is taken, the proportion of areas closed was also increased, from 16% (Table 3*a*) under alternative 6 to 20% (Table 4*a*). Under this closure distribution, the effort in the areas remaining open needs to be increased by 12.9% ($\varepsilon = 1.129$) to attain the status quo catch level (Table 4*a*) compared with an increase of 30.8% required under alternative 6 (Table 3*a*). The total effort required to catch the status quo catch is actually slightly less (3.4%) than that under status quo; this compares with the 11.4% increase required under alternative 6. The mean reduction $\bar{R}'_{eq}$ is reduced below status quo in both habitat parameter scenarios: 8.1% less for scenario 1 and 21.3% less for scenario 2 (Table 4*c*). While a greater proportion of blocks are closed, most of these are lightly fished and are

Table 3. Bering Sea bottom trawl fishery under alternative 6 showing (*a*) frequency distribution and estimated intensity required to catch status quo catch, (*b*) hypothetical biomass and catch distribution per intensity interval, and (*c*) habitat impact per intensity interval and mean impact per fished blocks under two scenarios of recovery rate (ρ) and sensitivity (q_H).

(*a*) Fishing intensity distribution.

Interval	No. of blocks closed	No. of blocks fished	% blocks closed	New f' ($\varepsilon = 1.308$)[a]
$0.01 \le f < 0.05$	378	1253	0.23	0.029
$0.05 \le f < 0.10$	280	946	0.23	0.092
$0.10 \le f < 0.25$	290	1320	0.18	0.207
$0.25 \le f < 0.50$	156	847	0.16	0.462
$0.50 \le f < 1.00$	131	691	0.16	0.925
$1.00 \le f < 2.00$	111	441	0.20	1.850
$2.00 \le f < 17.13$	17	260	0.06	3.728
Total	1363	5758		Total f' = 3213
				Compared with status quo: 11.4%

(*b*) Biomass and catch.

Interval	Biomass per block	Catch per block	Catch per interval
$0.01 \le f < 0.05$	0.016	0.000	0.35
$0.05 \le f < 0.10$	0.051	0.003	2.60
$0.10 \le f < 0.25$	0.114	0.013	17.53
$0.25 \le f < 0.50$	0.255	0.062	52.23
$0.50 \le f < 1.00$	0.509	0.217	149.81
$1.00 \le f < 2.00$	1.018	0.683	301.00
$2.00 \le f < 17.13$	2.052	1.833	476.48
Total			1000

(*c*) Habitat reduction.

Interval	$\rho = 0.5$, $q_H = 0.1$		$\rho = 0.1$, $q_H = 0.21$	
	Per block	Per interval	Per block	Per interval
$0.01 \le f < 0.05$	0.006	7.29	0.058	72.50
$0.05 \le f < 0.10$	0.018	17.18	0.163	153.85
$0.10 \le f < 0.25$	0.040	52.43	0.303	399.68
$0.25 \le f < 0.50$	0.085	71.70	0.493	417.29
$0.50 \le f < 1.00$	0.156	107.86	0.660	456.14
$1.00 \le f < 2.00$	0.270	119.09	0.795	350.71
$2.00 \le f < 17.13$	0.427	111.05	0.887	230.55
	$\bar{R}'_{eq} = 0.068$		$\bar{R}'_{eq} = 0.292$	
	Compared with status quo: 4.9%		−5.5%	

[a] ε is the fishing intensity expansion factor that results in a total catch level equal to the status quo catch (1 million t).

assumed (in this application) to have low target species density. As a result, there is a marked improvement over alternative 6 in terms of both $\bar{R}'_{eq}$ and effort.

Evaluation of rotating closures

Mitigation alternatives may contain forms of rotating closures. For example, an alternative may close an area for 10 years while allowing fishing in three other areas and then reopen the area for 30 years while rotating the closing of the other three areas. This results in the managed areas being closed for 10 years, then open for 30 years, with the cycle repeating every 40 years. Another alternative may close areas for a 15-year cycle of 5 years closed and 10 years open.

Equation 6 can be used to model a variable fishing scenario or a scenario starting at a habitat level other than the unfished level. Application to a time series of cyclical openings and closures shows the decrease in H_t during the opening and the recovery during the closures (Fig. 5). The decrease is greater at high I and low ρ, and recovery during the closed period is greater for higher ρ. Eventually, a stable repetition of H_t levels will result. Let R_{cyclic} equal the average reduction level, R_t, during a stable cycle. Depending on impact rate I (= fq_H) and recovery rate ρ, R_{cyclic} ranges from

Table 4. Bering Sea bottom trawl fishery under modification of alternative 6 showing (*a*) frequency distribution and estimated intensity required to catch status quo catch, (*b*) hypothetical biomass and catch distribution per intensity interval, and (*c*) habitat impact per intensity interval and mean impact per fished blocks under two scenarios of recovery rate (ρ) and sensitivity (q_H).

(*a*) Fishing intensity distribution.

Interval	No. of blocks closed	No. of blocks fished	% blocks closed	New f' ($\varepsilon = 1.129$)[a]
$0.01 \le f < 0.05$	1460	171	0.90	0.025
$0.05 \le f < 0.10$	985	241	0.80	0.080
$0.10 \le f < 0.25$	805	805	0.50	0.179
$0.25 \le f < 0.50$	200	803	0.20	0.399
$0.50 \le f < 1.00$	83	739	0.10	0.798
$1.00 \le f < 2.00$	24	528	0.04	1.597
$2.00 \le f < 17.13$	8	269	0.03	3.218
Total	3565	3556		Total $f' = 2786$
				Compared with status quo: –3.4%

(*b*) Biomass and catch.

Interval	Biomass per block	Catch per block	Catch per interval
$0.01 \le f < 0.05$	0.016	0.0002	0.04
$0.05 \le f < 0.10$	0.051	0.0024	0.57
$0.10 \le f < 0.25$	0.114	0.0116	9.31
$0.25 \le f < 0.50$	0.255	0.0542	43.53
$0.50 \le f < 1.00$	0.509	0.1937	143.18
$1.00 \le f < 2.00$	1.018	0.6275	331.32
$2.00 \le f < 17.13$	2.052	1.7542	471.87
Total			1000

(*c*) Habitat reduction.

Interval	$\rho = 0.5, q_H = 0.1$		$\rho = 0.1, q_H = 0.21$	
	Per block	Per interval	Per block	Per interval
$0.01 \le f < 0.05$	0.005	0.86	0.050	8.61
$0.05 \le f < 0.10$	0.016	3.79	0.144	34.60
$0.10 \le f < 0.25$	0.034	27.75	0.273	219.49
$0.25 \le f < 0.50$	0.074	59.37	0.456	366.17
$0.50 \le f < 1.00$	0.138	101.75	0.626	462.89
$1.00 \le f < 2.00$	0.242	127.80	0.770	406.70
$2.00 \le f < 17.13$	0.392	105.33	0.871	234.32
	$\bar{R}'_{eq} = 0.060$		$\bar{R}'_{eq} = 0.243$	
	Compared with status quo: –8.1%		–21.3%	

[a] ε is the fishing intensity expansion factor that results in a total catch level equal to the status quo catch (1 million t).

a proportion ($p_{open} < 1$) of R_{eq} to all of R_{eq}, where p_{open} is the proportion of years fished per cycle. Under the 40-year cycle of 10 years closed and 30 years open, $p_{open} = 0.75$. When I is low and ρ is high, $R_{cyclic} \approx p_{open}R_{eq}$. As I increases or ρ decreases, habitat is less able to fully recover during the closed period, and R_{cyclic} increases beyond $p_{open}R_{eq}$ and approaches R_{eq} (Fig. 6).

Thus, the best that the 10-year closed – 30-year open rotating closure for an area could achieve over a permanent closure would be a 25% decrease from R_{eq} for fast-recovering habitat within the area encompassed by the rotating closures. The best that the 5-year closed – 10-year open rotation could achieve would be a 33% decrease from R_{eq}. If recovery rate is slow, R_{cyclic} would be greater and would approach R_{eq} if the rotating open areas are fished the same as under status quo. If an adjacent closure displaces effort to open areas, the effort per open year would be greater than the original R_{eq} had been under the status quo. Depending on effort relocation, rotating closures could result in an increase rather than a decrease in habitat reduction for slow-recovering habitat.

Discussion

For some marine fisheries, there may be little or no conclusive information on whether the fishing causes adverse effects to fish habitat. The habitat in the ocean environment is difficult and expensive to observe. Many variables com-

Fig. 5. The habitat levels H_t under a rotating closure policy of fishing for 30 years and closed for 10 years. Results are shown for impact rates $I = 0.02$ and $I = 0.50$ and recovery rates $\rho = 0.10$ and $\rho = 0.02$. The higher I level causes faster reduction towards H_{eq} levels, while the higher ρ slows reduction during the fishing periods and allows faster recovery during the closed periods.

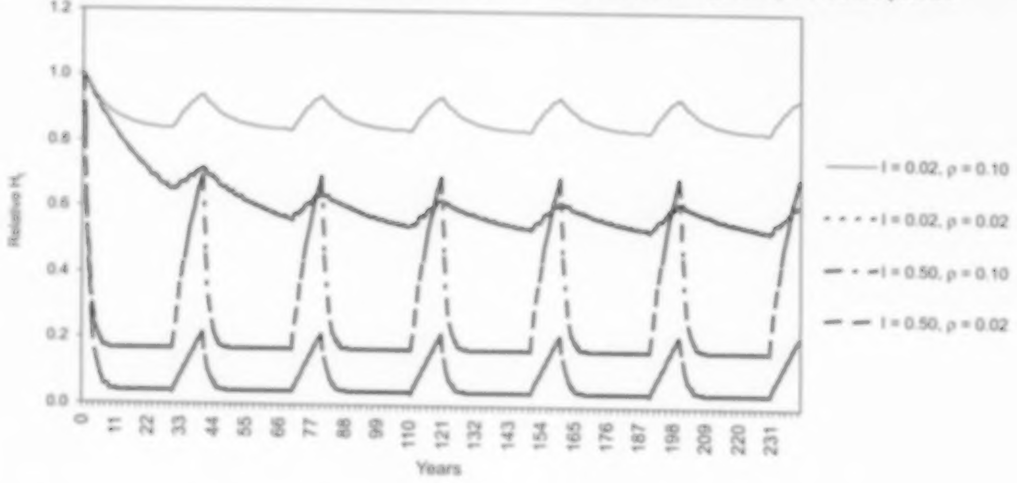

Fig. 6. Average habitat reduction R_{avg} for a rotating closure policy (30 years fishing, 10 years closed) at impact rate $I = 0.01$–0.50 and recovery rate $\rho = 0.02$–1.0, shown relative to the corresponding R_{eq}. For fast-recovering habitat ($\rho = 1.0$), the proportion of R_{avg} to R_{eq} will be at or barely above the proportion $P = 3/4$ of fishing days per cycle. R_{avg} will increase beyond P towards R_{eq} as recovery rates decrease or fishing intensity increases.

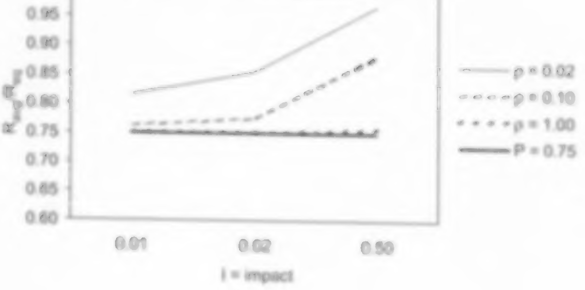

bine to determine fish stock productivity and distinguishing the role of habitat may be difficult, especially with the level of information available.

Estimates of H_{eq} and R_{eq} are applied in the EFH-DEIS to individual blocks to estimate the average percent reduction over broad habitat categories of the Bering Sea, Aleutian Islands, and the Gulf of Alaska. Using block-by-block estimates of fishing effort by various gears, the application was an example of how the model could be used to rank the potential effect of various fisheries on a variety of habitat features. A block-by-block calculation allows for specific habitat values, if they were known, for each block. This application provides a framework for accounting for the array of parameters and input information that determine habitat reduction over a region. Block-by-block estimates of target species density may also be attainable and easily incorporated. This information could improve the prediction of the effort redistribution and the resulting habitat and economic consequences that result from management proposals.

The comparison of their average or total habitat reduction is one facet of evaluating the effectiveness of management proposals. Examining the model properties indicates how the status quo fishing intensity of areas chosen to be closed or left open affects total or average habitat reduction as well as the effort required to catch the quota. Most of the applications in this paper treat habitat as simple additive quantities of equal value without regard to the frequency or geographical distribution of the habitat reductions. For example, is habitat equally valued when all of it is reduced to 50% or if half of it is pristine while the other half is reduced to near zero? Does it matter how the habitat reduction is distributed in relation to other areas and other geographic, topographic, and oceanographic features? The geographic distribution of bottom trawl intensity on the Bering Sea shelf can be used to show the potential level of reduction that may occur to biostructure for the corresponding intensity levels. Addressing the linkages of habitat to fish productivity and the actual effects on fish productivity are beyond the scope of this paper.

Conservative harvest management or optimal oceanographic conditions may overcome or mediate adverse effects to habitat. Not only can estimates of stock status be very uncertain, but the threshold levels chosen as reference criteria are usually generated by a management requirement and are seldom based on actual proof or well-accepted theory. Much of the information used to determine stock productivity may have been collected after habitat was already adversely affected, so estimates of stock threshold levels may be inherently biased.

If management decides to implement closures, what is a rational strategy under conditions of uncertainty? A practicable balance of the following objectives should be considered.

If little proof occurs for adverse fishing effects on habitat and stock productivity, economic impact on existing fisheries should be minimized by allowing large amounts of heavily fished areas to remain open while closing large amounts of lightly fished areas and only small amounts of heavily fished areas. The joint properties of the habitat and catch models suggest that such a strategy is compatible with minimizing habitat reduction and maintaining harvest.

There is seldom sufficient information to justify concluding that there are no effects of fishing; therefore, some amount of a representative sample of habitat should be closed. That is, closed and open areas should cover a cross-section of habitat factors, geography, and fishing intensity as much as practicable.

Because a better understanding of the ecosystem is needed to make informed decisions, closures should be designed to provide scientific information by creating contrasts of fishing intensity within a specific habitat–geographic type. In other words, do not close an entire cluster of intense fishing or close large, uninterrupted expanses of a lightly fished area, but place closure or open area boundaries to provide a comparison of the effect of fishing within a specific habitat. Areas open to fishing within expanses of proposed, or existing, closed areas may provide informative treatment contrasts.

The examples provided in this study utilize the equilibrium condition equations of the model because historical fishing effort is generally difficult to attain. If available, knowledge of the history of fishing effort could be applied in eq. 11 or eq. 6 to evaluate how close to the equilibrium reduction level a fishery habitat may currently be at. This may be important to note for a habitat that, while impacted at a very low rate, is extremely slow to recover. Current habitat levels may still be near pristine levels, H_0, but at equilibrium, the abundance could be quite a bit lower.

It should be remembered that habitat distribution and many of the model parameter values such as habitat sensitivity and recovery rates are unknown for the area of the example application, and the estimated habitat reductions are conditional. In such cases, the model can provide an additional function as a framework for sensitivity analysis to prioritize research on processes that contribute most to the uncertainty in estimating habitat reduction.

Acknowledgements

I thank the many people who acknowledged the relevance of my early model, especially Craig Rose, who first reviewed the model and applied it in his assessment of potential habitat effects of the federal groundfish fishery in the environmental impact statement for essential fish habitat in Alaska; Jon Heifetz, who provided encouragement and editorial suggestions to improve the manuscript; Jerome Pella, who provided many editorial suggestions that improved the manuscript; and Phil Rigby, who provided encouragement and time for me to work on the manuscript. I thank especially the anonymous referee who noted an erroneous term in my original equations.

References

Auster, P.J., and Langdon, R.W. 1999. The effects of fishing on fish habitat. *In* Fish habitat: essential fish habitat and rehabilitation. *Edited by* L.R. Benaka. American Fisheries Society, Bethesda, Md. pp. 150–187.

Bergmann, M.J., and van Santbrink, J.W. 2000. Mortality in megafaunal benthic populations caused by trawl fisheries on the Dutch continental shelf in the North Sea in 1994. ICES J. Mar. Sci. **57**: 1321–1331.

Collie, J.S., Hall, S.J., Kaiser, M.J., and Poiner, I.R. 2000. A quantitative analysis of fishing impacts on shelf-sea benthos. J. Anim. Ecol. **69**: 785–798.

Ellis, N., and Pantus, F. 2001. Management strategy modeling: tools to evaluate trawl management strategies with respect to impacts on benthic biota with the Great Barrier Reef Marine Park area. CSIRO Marine Research, Cleveland, Australia.

Lindholm, J.B., Auster, P.J., Ruth, M., and Kaufman, L. 2001. Modeling the effects of fishing and implications for the design of marine protected areas: juvenile fish responses to variations in seafloor habitat. Conserv. Biol. **15**: 42–437.

Malecha, P.W., Stone, R.P., and Heifetz, J. 2005. Living substrate in Alaska: distribution, abundance and species associations. *In* Benthic habitats and the effects of fishing. *Edited by* P.W. Barnes and J.P. Thomas. Am. Fish. Soc. Symp. 41, Bethesda, Md. pp. 289–299.

NOAA Fisheries. 2002. The final rule for implementing the essential fish habitat provisions of the Magnuson–Stevens Fishery Conservation Act. US Federal Register / Vol. 67, No. 12/ Thursday, 17 January 2002.

NOAA Fisheries. 2005. Final environmental impact statement for essential fish habitat identification and conservation in Alaska, April 2005 [online]. Available from http://www.fakr.noaa.gov/habitat/seis/efheis.htm [accessed 15 September 2006].

NRC. 1994. Improving the management of U.S. marine fisheries. National Academies Press, Washington, D.C.

NRC. 2002. Effects of trawling and dredging on seafloor habitat. National Academy Press, Washington, D.C.

Pitcher, C.R., Poiner, I.R., Hill, B.J., and Burridge, C.Y. 2000. Implications of the effects of trawling on sessile megazoobenthos on a tropical shelf in northeastern Australia. ICES J. Mar. Sci. **57**: 1359–1368.

Rijnsdorp, A.D., Buys, A.M., Storbeck, F., and Visser, E.G. 1998. Micro-scale distribution of beam trawl effort in the southern North Sea between 1993 and 1996 in relation to the trawling frequency of the sea bed and the impact on benthic organisms. ICES J. Mar. Sci. **55**: 403–419.

Rose, C.S., and Jorgensen, E.M. 2005. Spatial and temporal distributions of bottom trawling off Alaska: consideration of overlapping effort when evaluating the effects of fishing on habitat. *In* Benthic habitats and the effects of fishing. *Edited by* P.W. Barnes and J.P. Thomas. Am. Fish. Soc. Symp. 41, Bethesda, Md. pp. 679–690.

Appendix A. Integrating the differential equations

Assume habitat can be in two different conditions or states, let H = unimpacted habitat, h = impacted habitat, I = the rate habitat is impacted, and ρ = recovery rate of impacted habitat back to an unimpacted condition. The state transition equations for this process are

$$\text{(A1)}\quad \mathrm{d}H/\mathrm{d}t = -IH + \rho h$$

and

$$\text{(A2)}\quad \mathrm{d}h/\mathrm{d}t = +IH - \rho h$$

where there is no net loss of habitat (i.e., $H + h$ = constant amount). Combining the two equations and letting $H = H_0$ and $h = 0$ at time = 0, we get

$$\text{(A3)}\quad \mathrm{d}H/\mathrm{d}t = -IH + \rho(H_0 - H) = (-I - \rho)H + \rho H_0$$

Dividing each side of the equation by the right-hand value and multiplying each side by $\mathrm{d}t$ and $(-I - \rho)$ results in

$$\text{(A4)}\quad (-I - \rho)\, \mathrm{d}H/[(-I - \rho)H + \rho H_0] = (-I - \rho)\, \mathrm{d}t$$

Applying the integration rule $\int \mathrm{d}u/u = \ln(|u|) + C$ results in

$$\text{(A5)}\quad \ln[-[(-I - \rho)H + \rho H_0]] = \ln(IH + \rho H - \rho H_0)$$

$$= -(I + \rho)t + C$$

Exponentiating gives

$$\text{(A6)}\quad IH + \rho H - \rho H_0 = \mathrm{e}^{[-(I+\rho)t]}\mathrm{e}^{C}$$

at $t = 0$ and $H = H_0$, so $\mathrm{e}^{C} = IH_0$, thus

$$\text{(A7)}\quad IH + \rho H - \rho H_0 = \mathrm{e}^{[-(I+\rho)t]}IH_0$$

$$\text{(A8)}\quad H(I + \rho) = H_0[I\mathrm{e}^{[-(I+\rho)t]} + \rho]$$

and

$$\text{(A9)}\quad H = H_0[I\mathrm{e}^{[-(I+\rho)t]} + \rho]/(I + \rho)$$

so at time t

$$\text{(A10)}\quad H_t = H_0[I\mathrm{e}^{[-(I+\rho)t]} + \rho]/(I + \rho)$$

Changes in run timing and natural smolt production in a naturally spawning coho salmon (*Oncorhynchus kisutch*) population after 60 years of intensive hatchery supplementation

Michael J. Ford, Howard Fuss, Brant Boelts, Eric LaHood, Jeffrey Hard, and Jason Miller

Abstract: Supplementing natural fish populations with artificially propagated (hatchery) fish is a common practice. In evaluating supplementation, it is important to assess the relative fitness of both hatchery-produced and naturally produced fish when they spawn together in the wild and to evaluate how the absolute fitness of the natural population changes after many generations of supplementation. We evaluated the relative fitness of naturally produced and hatchery-produced coho salmon (*Oncorhynchus kisutch*) in Minter Creek, Washington, USA. We also evaluated long-term changes in natural smolt production in this stream after several decades of intensive hatchery supplementation. Total smolt production was estimated to be 14 660 and 19 415 in 2002 and 2003, respectively, compared with the average value of 28 425 from 1940 to 1955. We found no significant difference in relative fitness between hatchery and natural fish, probably because the natural population consists largely of fish produced from the hatchery a generation or two previously. There has been a long-term trend for adults to return to the stream earlier in the spawning season. We estimated standardized selection differentials on run timing, with results indicating stabilizing selection with an optimum run timing later than the mean contemporary run timing but earlier than the historical mean run timing.

Résumé : On ajoute couramment des poissons élevés artificiellement en pisciculture aux populations naturelles de poissons. En évaluant ces ajouts, il est important de mesurer la fitness relative tant des poissons de pisciculture que des poissons élevés en nature lorsqu'ils fraient ensemble dans le milieu et de déterminer comment la fitness absolue de la population naturelle change après plusieurs générations de ces ajouts. Nous évaluons la fitness relative de saumons coho (*Oncorhynchus kisutch*) élevés en pisciculture et en nature à Minter Creek, Washington, É.-U. Nous déterminons aussi les changements à long terme de la production naturelle de saumoneaux dans ce cours d'eau après plusieurs décennies d'ajouts importants de poissons de pisciculture. Nous estimons la production totale de saumoneaux à respectivement 14 660 et 19 415 en 2002 et 2003, alors que le nombre moyen était de 28 425 de 1940 à 1955. Nous ne trouvons aucune différence significative de fitness relative entre les poissons de pisciculture et les poissons sauvages, probablement parce que la population naturelle est composée en grande partie de poissons produits en pisciculture il y a une ou deux générations. Il y a chez les poissons une tendance à long terme à retourner au cours d'eau plus tôt dans la saison de fraie. Nous estimons les différentiels standardisés de sélection dans le calendrier de la montaison qui indiquent l'existence d'une sélection stabilisante; la montaison optimale se situe plus tard que la montaison actuelle, mais plus tôt que la période moyenne de montaison dans le passé.

[Traduit par la Rédaction]

Introduction

Releasing artificially propagated fish into the wild to enhance fisheries or boost natural population abundance is a common, but often controversial, fishery management strategy. The practice is particularly common for salmon and trout (especially *Oncorhynchus* spp. and *Salmo* spp.) and occurs nearly everywhere in the world where natural populations of these fish exist. In areas where native, natural salmon populations have declined, it is common for fish propagated and released from hatcheries (hatchery fish) to outnumber fish whose parents spawned naturally in a stream (natural fish). (Note that in this paper we follow the convention of the National Marine Fisheries Service (Hard et al.

Received 22 April 2006. Accepted 1 June 2006. Published on the NRC Research Press Web site at http://cjfas.nrc.ca on 3 October 2006.
J19286

M.J. Ford, E. LaHood, J. Hard, and J. Miller. National Marine Fisheries Service, Northwest Fisheries Science Center, Conservation Biology Division, 2725 Montlake Boulevard E, Seattle, WA 98112, USA.
H. Fuss[2] and B. Boelts. Washington Department of Fish and Wildlife, 600 Capital Way North, Olympia, WA 98501-1091, USA.

[1] Corresponding author (e-mail: mike.ford@noaa.gov).

[2] Howard Fuss died on 14 January 2004. This paper is dedicated to his memory.

doi:10.1139/F06-119

1992) and define a natural population as a group of fish that spawn in a stream under natural conditions. Natural fish (or naturally produced fish) are defined as the progeny of parents that spawned naturally, regardless of parental origin. In contrast, a wild population is defined as a natural population that has had essentially no genetic or demographic influence from artificially propagated, conspecific fish.) For example, the proportions of adult hatchery fish in natural Chinook salmon (*Oncorhynchus tschawytscha*) and steelhead (i.e., rainbow trout, *Oncorhynchus mykiss*) spawning populations in the Columbia River Basin are commonly >50% (McClure et al. 2003), and similar proportions are found elsewhere in the world (e.g., Dannewitz et al. 2003; NRC 2004).

Understanding the long-term effects of hatchery supplementation on natural population fitness and estimating the relative fitness of hatchery and natural fish when they spawn together in the wild have been identified as a two critical uncertainties in developing recovery actions for threatened salmon populations (e.g., ISAB 2005; Mobrand et al. 2005). Estimating relative fitness in any single generation is generally easier to accomplish than measuring long-term effects and is important for several reasons. First, the presence of large numbers of hatchery fish in natural spawning areas makes it difficult to accurately evaluate the viability of natural populations unless the relative fitness of the hatchery fish is known (McClure et al. 2003). Second, quantifying the relative fitness of hatchery fish is an important part of evaluating the risks and benefits that hatchery supplementation may provide to natural salmon populations (ISAB 2002). Supplementation is controversial in part because several studies have indicated that hatchery fish may have low fitness compared with natural fish when the hatchery fish spawn in the wild (reviewed by Berejikian and Ford 2004). A better understanding of hatchery fish relative fitness is therefore necessary for evaluating whether such supplementation programs are likely to provide a conservation benefit to natural populations.

Although important for evaluating and predicting the effects of hatcheries, estimates of hatchery fish relative fitness in any one generation are not sufficient for evaluating long-term changes in natural population fitness that may be caused by continuous hatchery supplementation. This is because a natural population may experience a loss of genetic fitness because of supplementation with hatchery fish, even if in any single generation the hatchery and natural fish have near equal average fitness in the wild (Ford 2002).

To evaluate the long-term genetic effects of hatchery supplementation on a natural population, it is therefore necessary to monitor how the natural population's fitness changes over time compared with, ideally, replicates of the population that were maintained in the same environment without supplementation. Such long-term experiments are obviously difficult to conduct with salmon, owing both to long generation times and the logistical difficulty of maintaining appropriate treatment and control populations. However, useful insights into the effects of long-term supplementation may be obtained by studying the characteristics of natural populations that have already experienced many generations of hatchery fish supplementation.

In this paper, we describe the initial results of a study to evaluate the effects of approximately 40 years of intensive supplementation of a naturally spawning population of coho salmon in Minter Creek, Washington (Fig. 1). We obtained estimates of the total smolt outmigration from the stream and compared these with estimates made from 1940 to 1955 at the start of the hatchery coho program (Salo and Bayliff 1958). Using genetic methods to estimate the number of offspring (fry, smolts, and adults) produced by individual parents, we also compared the ability of naturally spawning hatchery and natural fish to produce offspring at these life stages. Finally, we evaluated the effect of natural selection in the stream on adult run timing, a trait that has changed substantially in the Minter Creek Hatchery coho salmon population over the last 60 years.

Materials and methods

Study site

Our study site is on Minter Creek, a small stream draining into Henderson Bay in Puget Sound, Washington (Fig. 1). The creek drains a watershed of approximately 22 km^2. Coho salmon in Minter Creek have a life-history pattern typical for the stream's latitude (Sandercock 1991), with juveniles spending about a year in the stream prior to smoltification and migration to salt water. The fish then typically spend ~18 months in at sea, returning to fresh water as 3-year olds. There is a hatchery operated by the Washington Department of Fish and Wildlife (WDFW) located near the mouth of the creek. Coho salmon have been bred and released from the hatchery since 1938, when WDFW selected the stream as a study site representative of the hundreds of small Pacific Northwest streams inhabited by coho and chum (*Oncorhynchus keta*) salmon (Salo and Bayliff 1958). Production-scale coho salmon releases were initiated in 1960 (WDFW records, Olympia, Washington). The coho hatchery population was initially founded from wild Minter Creek salmon, but coho salmon from other nearby southern Puget Sound watersheds have been periodically imported and released as well, and Minter Creek Hatchery fish have also been widely released in other locations in southern Puget Sound. There have been no sustained attempts to keep the hatchery and natural populations isolated from each other, and in the years leading up to our study an unknown, but certainly high (probably >90%), fraction of the natural spawning population consisted of hatchery-produced fish. The natural population of coho salmon in Minter Creek is therefore clearly not a wild population, but rather is representative of many of the natural salmon populations in the Pacific Northwest that have experienced high levels of hatchery stocking for many decades.

Adult capture and sampling

An element of our study design was to capture and genetically analyze the entire population of coho salmon spawning naturally in Minter Creek. Adults were intercepted as they returned from the ocean to spawn by a weir located at the head end of tidewater (river kilometre (RK) 0.8). Fish were diverted into a multistep fish ladder that leads to a concrete holding tank. The hatchery crew operated a fish-sorting de-

Fig. 1. Map of study area in Washington, USA. Inset shows location in Pacific Northwest (BC, British Columbia; WA, Washington; OR, Oregon; ID, Idaho).

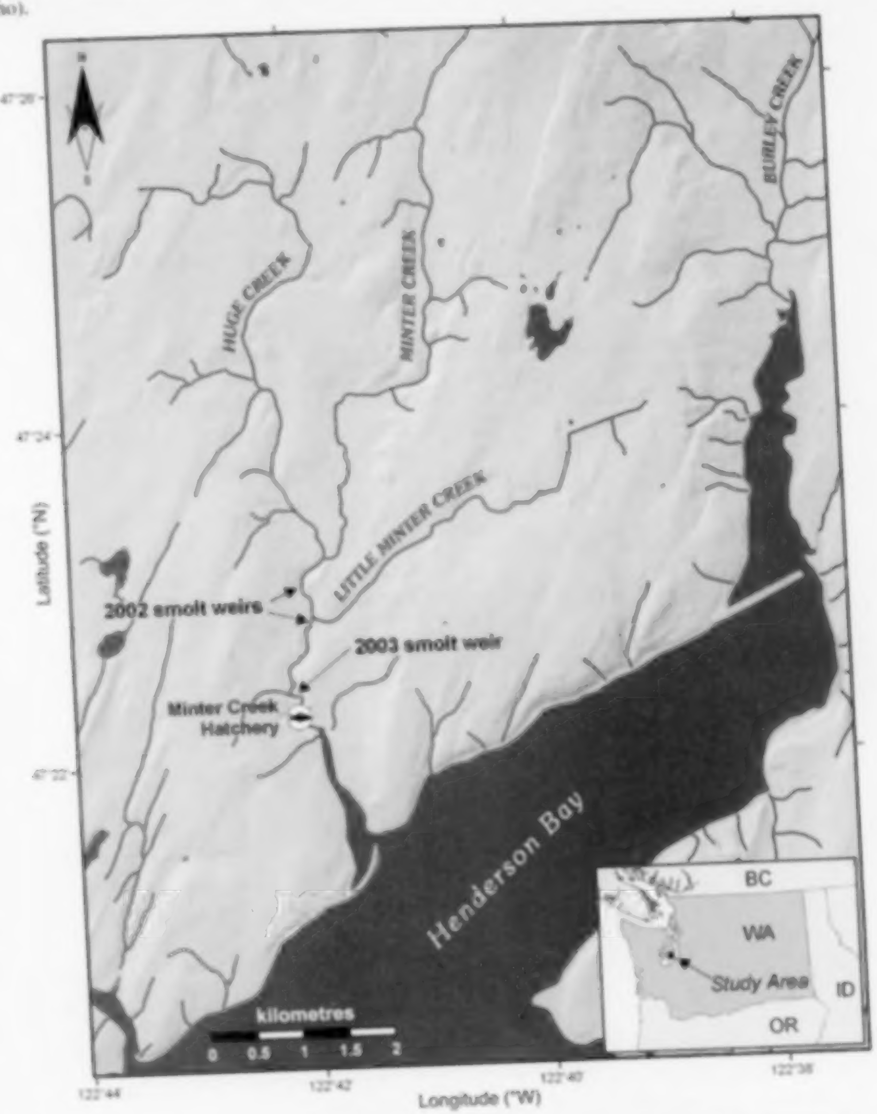
BURLEY CREEK
HUGE CREEK
MINTER CREEK
LITTLE MINTER CREEK
2002 smolt weirs
2003 smolt weir
Minter Creek Hatchery
Henderson Bay
kilometres
0
0.5
1
1.5
2
BC
WA
Study Area
ID
OR
47°26'
47°24'
47°22'
Latitude (°N)
122°44'
122°42'
122°40'
122°38'
Longitude (°W)

vice 2–5 days per week to enumerate each species entering the ladder. All coho salmon with an intact adipose fin were diverted into a 1.2 m diameter circular tank supplied with running fresh water. The hatchery routinely removes the adipose fin from >95% of the coho salmon they release. Adipose-intact coho salmon, therefore, were expected to be a mixture of natural origin fish and unmarked, hatchery-produced fish.

Up to 40 adult coho were held in the circular tank at once. One fish at a time was removed from the tank by dip net and placed in an anesthetic bath of tricaine methanesulfonate (MS-222). Once the fish was anesthetized, we recorded preliminary origin (adipose intact = potentially natural; missing = hatchery), sex, degree of maturity, jaw tag number, and body length measured from the post-orbital eye socket to the hypural plate. A small piece of caudal fin tissue was removed from each fish and stored for subsequent DNA analysis.

Fish were allowed to recover in fresh flowing water before release upstream. We attempted to pass upstream roughly equal numbers of hatchery-produced and naturally produced coho salmon. Hatchery fish were unambiguously identified by scale analysis performed by WDFW staff. Scales were collected from both nonclipped and clipped fish, and the origin (hatchery or natural) of the fish was determined by counting the number of circuli between the scale focus and the first annulus (origin determinations were performed by J. Sneva, WDFW, 600 Capitol Way North, Olympia, WA 98501-1091, USA). Fish of hatchery origin consistently have greater numbers of circuli present in this region than do natural fish because of faster growth in the hatchery environment (J. Sneva, personal communication). The updated numbers of hatchery and natural origin fish were determined the day following collection, and any adjustment in the number of hatchery origin fish needed were made in the subsequent sampling period by passing additional adipose-clipped fish upstream. In addition to the fish passed upstream, in 2000 we also spawned 63 females and 56 males in the hatchery (random, single pair matings) and planted their offspring into the creek gravel as eyed eggs as an internal control to test the pedigree reconstructions. A total of 139 240 eggs were collected, and 126 243 (90.7%) survived to be planted in the creek. In 2001, we crossed 102 females and 102 males in the hatchery, but sampled the progeny in the hatchery raceways rather than planting them in the stream.

Fry and smolt trapping

Fry were sampled using backpack electrofishing gear. On 9 and 18 May 2001, 1282 fry were sampled from 11 reaches throughout the watershed. On 13 and 19 June 2002, 1085 fry were sampled from similar locations as occurred in 2001. In 2002, an additional 500 fry resulting from the crosses we performed in the hatchery were also sampled. In 2001, all sampled fry were sacrificed in a lethal concentration of MS-222 and placed in 100% ethanol for storage; in 2002, small caudal fin clips were taken nonlethally and sampled fry were released back into the stream. Within the sampling reaches, fry distributions were patchy, presumably because of habitat preferences by the adult females for spawning sites, limited dispersal of fry after emergence from their nests, and preferences of the fry for certain habitats. To avoid chance overrepresentation of families, we sampled a large number of reaches throughout the stream and took care to avoid oversampling from any area within a reach. In particular, within a reach we electroshocked every area that was likely to contain fry (pools with good cover and a dark colored substrate) and only sampled a few fry from each area before moving on to the next. The subset of fry that were genotyped was selected such that number of fish genotyped from a reach was approximately proportional to that reach's representation in the total fry sample.

In spring of 2002 and 2003 (see Results for specific dates), a fence weir (or weirs) was installed to trap migrating smolts. In 2002, the primary weir was located at RK 2, and a secondary weir was installed at the mouth of Little Minter Creek (Fig. 1). In 2003, a single weir was installed just above the adult weir, at RK 0.8 (Fig. 1). The primary weirs consisted of 10 mm mesh fence panels configured in a V shape, with a 150 mm diameter polyvinyl chloride (PVC) pipe at the downstream apex (similar to that described by Blankenship and Hanratty 1990). The panels were installed over heavy ground cloth to prevent the substrate from washing out under the panels and were continually lined with sandbags and reinforced with wires connecting the panels to metal posts staked into the substrate upstream of the trap. Additional sandbags were used to anchor the panels to the shore and prevent water from washing around the sides of the traps during high-flow events. Fish migrating downstream were directed into the PVC pipe and deposited approximately 10 m downstream in a 1.3 m × 1.3 m × 1.3 m collection box. The Little Minter Creek weir consisted of a 0.05 m × 0.3 m × 4 m long board installed at the downstream end of a culvert to fit snugly against a metal lip. A 150 mm hole was cut in the board and a PVC pipe inserted to collect all water and fish. The pipe drained into a 1.5 m × 1.5 m × 0.5 m collection box. Each was designed to trap all downstream-migrating fish during the period it was installed, and the panels were inspected regularly for leaks or washouts. Each trap was checked during a several hour period beginning at dusk and again at ~0800, unless high flows and debris threatened operation of the trap. Fish were dipnetted from the trap box and anesthetized in MS-222. Each fish estimated to be over 70 mm in length was given a coded-wire tag (CWT). Length, weight, a tissue sample from the ventral fin, and a digital image were obtained for a random subset of the fish each day. In 2003, a subset of the smolts was also tagged with passive integrated transponder (PIT) tags (BioMark). Tags were injected into the abdominal cavity using a 12-gage syringe. Each PIT tag contained a unique alphanumeric code, which could be read by placing the fish in the vicinity of an appropriate electromagnetic tag reader.

Genetic analysis

DNA was extracted from the adult and juvenile samples using commercial kits following the manufacturer's (Qiagen) protocols. After DNA extraction and purification, genotypes at six (2000 cohort) or seven (2001 cohort) microsatellite loci were determined by polymerase chain reaction (PCR) amplification with dye-labeled primers followed by electrophoresis on an ABI 3100 automated sequencer–genotyper. Loci genotyped were as follows: Ocl-8 (Condrey and Bentzen 1998), Oki-10 (Smith et al. 1998) (2001 cohort only), Oki-23 (A. Spidle, Northwest Indian Fisheries Commission, 6730 Martin Way East, Olympia, WA 98516, USA, unpublished data; Genbank accession No. AF272822), Ots-3 (Banks et al. 1999), Ots-103 (Small et al. 1998), Ots-505 (Naish and Park 2002), and p53 (de Fromentel et al. 1992). PCR conditions and reagent concentrations were as follows (10 µL reaction volume): 0.2 $\mu mol \cdot L^{-1}$ for each primer (except Ots-505 and Ots-3, which were 0.4 $\mu mol \cdot L^{-1}$), 200 $mmol \cdot L^{-1}$ dNTPs, 500 $mmol \cdot L^{-1}$ KCl, 100 $mmol \cdot L^{-1}$ Tris–HCl (pH 9.0), 1% Triton X-100, 2 $mmol \cdot L^{-1}$ $MgCl_2$, and 5 Units (1 U = 16.67 nkat) *Taq* polymerase (Promega). Cycle conditions were as follows: 33 cycles with a 40 s denaturing step at 94 °C, 40 s anneal step at 60 °C (except for Ots-505, which was 54 °C and Ots-3 which was 47 °C), and a 40 s extension at 72 °C. A 40 min final incubation at 60° was used for all loci except Oki-23, p53, and Ots-103. Fragment sizes were estimated using ABI's Genescan software. The raw estimated allele sizes for the entire sample were plotted and generally clustered tightly at intervals corresponding to the repeat unit sizes for the loci scored. Bins of 1 to 1.5 base pairs every 2 to 4 base pairs apart were created from the plots, and the bins were used with ABI's Genotyper software to identify individual genotypes at each locus. Genotypic departures from random mating expectations and tests of population differentiation were conducted using permutation methods as implemented in the program GENEPOP

Table 1. Composition of the mating population.

	Total natural return			Natural fish passed upstream			Hatchery fish passed upstream			Unknown origin fish passed upstream		
Year	Total	Male	Female	Total	Male	Female	Total	Male	Female	Total	Male	Female
2000	541	283	268	486	250	236	360	192	168	51	33	18
2001	746	385	358	549	288	260	482	269	213	16	9	7

(Raymond and Rousset 1995). Each adult was also scored for a male-specific growth hormone pseudogene (Du et al. 1993) to help identify the sex of individuals that could not be morphologically sexed at the time of sampling. PCR conditions for the male-specific gene were the same as described above, except that primer concentrations were 0.1 μmol·L^{-1}.

Parentage assignments were made using the likelihood methods of Meagher and Thompson (1986) and Gerber et al. (2000) as implemented in the program FAMOZ (Gerber et al. 2003). Each individual in a sample of progeny was tested against all potential pairs of parents (discarding information on parent sex), and a log of odds (LOD) score was calculated for each potential parent pair – offspring triplet as the log of the ratio of the probability of a parent pair – offspring relationship compared with the probability they were drawn randomly from the population. The most likely pair of parents was compared with the second most likely, and the difference in LOD scores (ΔLOD) was calculated. The simulation function of the FAMOZ program was used to generate expected distributions of ΔLOD scores for correct and incorrect assignments.

Simulations and actual parental assignments were conducted assuming a genotyping error rate of 1.5% per locus and an analysis error rate of 0.01% per locus (i.e., the rate at which errors were produced in the simulations was 1.5% per locus, but the error rate assumed in the analysis of the simulated and real data was 0.01% per locus). The 1.5% error rate is approximately equal to what we have observed in our laboratory, and the 0.01% analysis error rate was used because it produced a higher fraction of correct assignments in the simulations than did an error rate of either 1.5% or 0%. In general, the highest fraction of correct assignments were obtained by assuming a non-zero but very small error rate, similar to what has been reported previously (Gerber et al. 2000; Sancristobal and Chevalet 1997). Individuals with missing genotypes at more than one locus (2000 cohort) or two loci (2001 cohort) were not included in the analysis. The difference in the allowable level of missing data between the cohorts is because the 2000 cohort was scored for six loci, while the 2001 cohort was scored for seven loci.

After preliminary assignments were made, the assignments were compared with the genetic and phenotypic sex data that had been collected earlier (see above). In a small fraction of cases, a preliminary assignment involved parents who were either two apparent males or two apparent females. In some cases, the parents involved were of ambiguous sex (e.g., the genetic and phenotypic sex calls disagreed with each other). In other cases, preliminary assignments clearly involved two parents of the same sex, and these were discarded from further analysis. Assignments were made for each cohort separately. The parents from the known crosses conducted in the hatchery were included in the analysis of the unknown parents as a control to test for accuracy of assignment but were not included in any post-assignment analyses.

Selection and fitness analysis

All statistical analyses were conducted using the general linear model (GLM) or analysis of variance (ANOVA) functions in the SYSTAT Version 11 (Systat Software Inc., Richmond, California) computer package. Comparisons of trait means by group (origin, sex, year) were done using ANOVA, after determining by visual inspection that the traits were approximately normally distributed. The statistical significance ($p < 0.05$) of mean progeny number differences among groups was made using the following GLM: progeny = constant + origin + sex + (origin × sex) + (origin × year) + (sex × year). Standardized selection differentials (Lande and Arnold 1983) and the effects of origin, sex, and year were estimated on run timing using the following GLM: progeny = constant + run time + (run time)^2 + (sex × run time) + (year × run time) + (origin ×run time) + [sex × (run time)^2] + [year × (run time)^2] + [origin × (run time)^2]. The significance of coefficients was determined using both standard parametric methods and by bootstrapping (1000 replicates). Unless the two methods differed, only the results from the parametric estimates are reported.

Results

Adult spawning run

The natural returns to Minter Creek in 2000 and 2001 are summarized in Table 1. In both 2000 and 2001, adult coho salmon started to return to Minter Creek in early September, and the last fish returned in late December. The mean return time (scored as number of days after 1 September) differed significantly by sex, origin, and year (Table 2). Both natural and hatchery fish returned on average over a month earlier than they did historically (Salo and Bayliff 1958), and records of return time kept at the Minter Creek Hatchery indicate a steady trend toward earlier return time from 1938 to 2001 (Fig. 2). Hatchery and wild fish did not differ significantly from each other in either length or weight, but males were significantly shorter than females and there were significant year and origin × year effects for both length and weight (Table 2).

Smolt sampling

A total of 2190 smolts were counted in 2002, and 9099 were counted in 2003. In 2002 and 2003, 95% and 99%, respectively, of the counted smolts were coded-wire tagged. In 2002 (2000 cohort), the main smolt trap was installed on 29 March and removed on 23 May. The Little Minter Creek smolt trap was installed on 11 April and removed on 22

Table 2. Trait information by origin, year, and sex (mean (sample size, standard deviation)).

	Trait			
	Male		Female	
Year	Hatchery	Natural	Hatchery	Natural
Run time (days after 1 September)[a]				
2000	49.6 (184, 24.4)	49.8 (234, 20.8)	47.8 (159, 20.7)	56.9 (230, 19.2)
2001	47.6 (316, 18.2)	47.1 (368, 17.6)	49.6 (246, 18.0)	50.2 (339, 16.3)
Length (cm)[b]				
2000	44.0 (184, 7.4)	44.8 (234, 5.2)	46.5 (159, 4.5)	47.1 (230, 3.7)
2001	47.2 (316, 6.6)	45.5 (368, 6.2)	48.2 (246, 5.1)	47.0 (339, 5.2)
Weight (g)[c]				
2000	2150.6 (126,1096.3)	2152.0 (160, 858.4)	2225.3 (108, 654.7)	2302.9 (172, 671.3)
2001	2454.3 (312, 1195.6)	2262.8 (359, 1081.7)	2414.2 (242, 847.0)	2291.3 (329, 902.7)

[a] Analysis of variance significance (*p* values) for run timing are as follows: origin, 0.007; sex, 0.003; year, 0.005; origin × sex, 0.004; origin × year, 0.008; sex × year, 0.943; origin × sex × year, 0.023.

[b] Analysis of variance significance (*p* values) for weight are as follows: origin, 0.239; sex, 0.284; year, 0.003; origin × sex, 0.496; origin × year, 0.049; sex × year, 0.235; origin × sex × year, 0.969.

[c] Analysis of variance significance (*p* values) for length are as follows: origin, 0.109; sex, 0.000; year, 0.000; origin × sex, 0.758; origin × year, 0.000; sex × year, 0.021; origin × sex × year, 0.533.

Fig. 2. Change in mean return time to Minter Creek Hatchery from 1938 to 2001 ($r^2 = 0.62$).

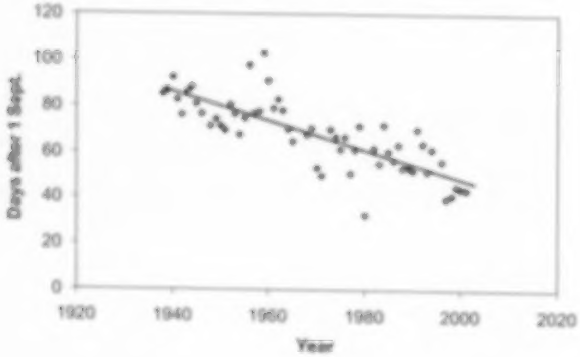

Fig. 3. Distribution of smolt outmigration days: 2002 (shaded line) and 2003 (solid line).

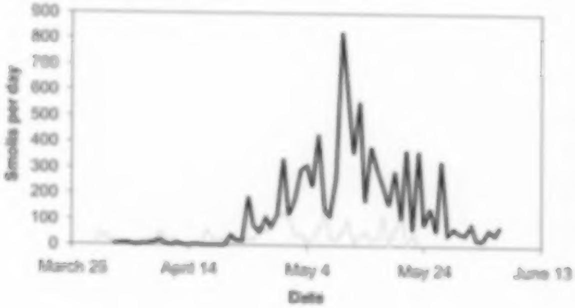

May. The main trap was destroyed by high flows on 14 April and reinstalled on 16 April. In 2003 (2001 cohort), the smolt trap was installed on 1 April and removed on 6 June. The panels on the trap were opened because of high water from 0800 on 13 April to 0900 on 14 April. In 2003, smolt migration clearly peaked in mid-May, while in 2002 there was no clear peak smolt migration time (Fig. 3).

Adult offspring sampling

As expected, the vast majority (97%–98%) of the coho salmon that returned to Minter Creek in 2003 and 2004 were 3 years old. A surprising result, considering the high proportion of smolts tagged, was the low proportion of CWT detections in the adults. In 2003, 943 natural origin coho returned to Minter Creek, of which 65 had a CWT. In 2004, 1837 fish returned, of which 289 had a CWT.

Genetic data

Of the loci analyzed, Ots-103 was the most variable with 60 observed alleles and an expected heterozygosity of 96%. Ots-3 was the least variable with 17 alleles and an expected heterozygosity of 72%. With the exception of Ots-103, observed heterozygosities were similar to those expected under random mating assumptions (average $F_{IS} = 0.0087$). Ots-103 generally had lower than expected heterozygosity across the entire sample and within sampling groups created on the basis of sampling year, life stage, and origin (average $F_{IS} = 0.095$). The excess of homozygotes at Ots-103 probably indicates the existence of either a null allele or an inability to observe very large alleles reliably. The Ots-103 locus was retained for use in parentage assignments, however, because of its very high level of variation and because the parentage assignments made with the locus included are accurate based on known hatchery crosses (see below).

Parentage assignment

Assuming a closed population, the simulations performed using FAMOZ indicated that ΔLOD thresholds of 2.28 and 3.21 would produce a correct closed population assignment rate of 95% for the 2000 and 2001 cohorts, respectively. At the other extreme, if none of the true parents are sampled, the percentage of individuals expected to exceed these thresholds when created from a random population with the same allele frequencies as the parental population is 13.6% and

Table 3. Summary of progeny assignments.

	Offspring analyzed (proportion assigned to a single parent pair)				
	Fry			Adults	
Cohort	Stream	Hatchery	Smolts	CWT	No CWT
2000	517 (0.51)	—	783 (0.44)	64 (0.34)	835 (0.23)
2001	700 (0.57)	370 (0.67)	677 (0.56)	249 (0.57)	1283 (0.28)

Note: The 2000 cohort refers to potential parents sampled in 2000, fry offspring sampled in 2001, smolt offspring sampled in 2002, and adult offspring sampled in 2003. The 2001 cohort refers to potential parents sampled in 2001, fry in 2002, smolts in 2003, and adults in 2004. CWT, coded-wire tag.

Table 4. Smolt counts and estimated total smolt abundance.

Year	Smolts counted	Smolts coded-wire tagged	Proportion tagged	Estimated proportion tag loss or nondetection	Proportion assigned adults with tags	Expanded proportion for tag loss	Expanded for proportion tagged	Expanded proportion for relative survival	Expanded smolts
2002	2190	2072	0.95	0.15[a]	0.10	0.12	0.13	0.15	14 660
2003	9099	8996	0.99	0.27[a]	0.29	0.39	0.39	0.47	19 415
2003	9099	8996	0.99	0.04[b]	0.29	0.30	0.30	0.36	25 298

[a] From genetic recaptures; in the 2000 cohort, 3/20 recaptures did not have a coded-wire tag (CWT); in the 2001cohort, 4/15 recaptures did not have a CWT.

[b] From passive integrated transponder (PIT) tag recaptures; in the 2001 cohort, 2/47 did not have a CWT.

7.57% for the 2000 and 2001 cohorts, respectively. Based on the ΔLOD thresholds, expected assignment rates were 51% for the 2000 cohort, 64% for the 2001 stream cohort, and 72% for the 2001 hatchery crosses. Actual assignment rates (after discarding a small number of same sex assignments) varied from 67% for the 2001 hatchery crosses to 23% for CWT-absent adults returning in 2003 (Table 3). In examining the assignment rates, a clear pattern emerged: the fry, smolt, and the tag-present adults all generally assigned at close to the expected rates, but the CWT-absent adults assigned at approximately half the rate expected (Table 3). Both the low tag proportions in the 2003 and 2004 spawning runs and the much lower than expected assignment rate for adult progeny compared with juvenile progeny imply that the 2003 and 2004 spawning runs contained many individuals that did not originate from Minter Creek, a finding that will be explored further in a subsequent report.

Estimated total smolt abundance

Even though many of the untagged natural origin adults may be strays, a large number of these fish nonetheless assign with high confidence to Minter Creek parents (Table 3). This result implies either a high rate of tag loss or nondetection or it could indicate that a large number of smolts left Minter Creek without being captured and tagged. We estimated the rate of tag loss or nondetection using the PIT tag recoveries and genetic recaptures (fish genetically sampled as both smolts and adults). We then estimated the total smolt runs in 2002 and 2003 by expanding the observed counts for (*i*) the proportion of captured smolts that were tagged, (*ii*) the estimated rates of tag loss or nondetection, (*iii*) the estimated proportion that were never captured, and (*iv*) the estimated survival of captured and tagged smolts compared with noncaptured smolts. The latter was assumed to be 0.84, based on the results of a study that estimated this parameter for Minter Creek coho salmon in the early 1980s (Blankenship and Hanratty 1990). The expanded smolt count estimates indicate <50% of the smolts were captured (Table 4).

Mating patterns and relative fitness by life stage

The minimum number of mates that a fish had was estimated from the progeny assignments. A mating between two individuals was counted if any progeny at any life stage were assigned to that pair of individuals. In neither year did the pattern of matings between hatchery and natural fish differ from what would be expected if the fish were mating randomly (data not shown).

For each sampled parent, we counted the mean number of mates (as described above) as well as the number of progeny in our sample at each life stage. Overall, mean progeny numbers were similar between sexes and between origins, although females had, on average, more mates than males (Table 5), a necessary outcome of the male-biased sex ratio. Depending on the life stage, sex, and year, relative fitness for hatchery compared with natural fish ranged from 0.61 to 1.27, although no values were significantly different from 1 (Table 5). The distributions of mate and offspring number at each life stage were roughly exponentially distributed (Fig. 4).

Araki and Blouin (2005) have demonstrated that estimates of relative fitness among groups can be biased because of errors in parentage assignment, and they describe two types of errors. A type A error occurs when a true parent is in the sample but a true offspring in the sample fails to assign to it (either assigning to no parent or to an incorrect parent), and a type B error occurs when a true parent is absent from the sample and its offspring assigns incorrectly to a parent that is in the sample. We estimated the type A and B error rates by conducting assignments using all of the potential 2001 cohort parents, including the 204 fish spawned in the hatchery, but only the 370 hatchery fry sampled from the known hatchery crosses. Of the 370 fry, 248 were assigned cor-

Table 5. Means of minimum inferred mate and progeny numbers by year, sex, and origin (mean, sample size, standard deviation).

	Progeny life stage					
	Male			Female		
Year	Hatchery (*H*)	Natural (*N*)	*H*/*N*	Hatchery (*H*)	Natural (*N*)	*H*/*N*
Mates						
2000	0.73 (184, 1.046)	0.75 (234, 1.222)	0.97	0.81 (159, 1.058)	0.84 (230, 1.228)	0.96
2001	0.74 (249, 1.118)	0.76 (273, 1.108)	0.97	0.82 (192, 1.324)	1.02 (243, 1.501)	0.80
Total	0.73 (433, 1.087)	0.75 (507, 1.161)	0.97	0.81 (351, 1.209)	0.93 (473, 1.376)	0.87
Fry						
2000	0.59 (184, 1.617)	0.46 (234, 1.27)	1.28	0.58 (159, 1.722)	0.54 (230, 1.293)	1.07
2001	0.74 (249, 2.067)	0.59 (273, 1.64)	1.27	0.97 (192, 2.768)	0.81 (243, 2.250)	1.20
Total	0.67 (433, 1.889)	0.53 (507, 1.48)	1.26	0.79 (351, 2.358)	0.68 (473, 1.851)	1.16
Smolts						
2000	0.63 (184, 1.732)	0.62 (234, 1.469)	1.02	0.67 (159, 1.541)	0.74 (230, 1.162)	0.91
2001	0.76 (249, 1.909)	0.62 (273, 1.704)	1.23	0.60 (192, 1.734)	0.99 (243, 2.599)	0.61
Total	0.70 (433, 1.835)	0.62 (507, 1.599)	1.13	0.63 (351, 1.647)	0.87 (473, 2.372)	0.72
Adults						
2000	0.40 (184, 0.831)	0.47 (234, 1.356)	0.85	0.42 (159, 0.896)	0.54 (230, 1.162)	0.78
2001	0.91 (249, 1.826)	0.87 (273, 1.622)	1.05	0.90 (192, 1.963)	1.28 (243, 2.430)	0.70
Total	0.69 (433, 1.506)	0.68 (507, 1.517)	1.01	0.68 (351, 1.588)	0.92 (473, 1.954)	0.74

Note: Tests of significance for differences in mate or progeny number between fish of different origin or sex were tested with the following general linear model: progeny (or mates) = constant + origin + sex + (origin × sex) + (origin × year) + (sex × year). The only significant term was mates, sex ($p = 0.03$), reflecting the biased sex ratio. *H*/*N* is the relative fitness of hatchery fish (hatchery mean divided by natural mean).

rectly, 116 were not assigned at all, and 6 were assigned incorrectly, resulting in a type A error rate of 33%. To estimate the type B error rate, we conducted assignments using the same 370 hatchery fry, but including only naturally spawning fish as potential parents (i.e., no true parents were included in the sample). Of these 371 fry, 31 had ΔLOD values greater than the assignment threshold of 3.21. Of these 31, 5 had incompatibilities at greater than two loci and an additional 6 involved incompatible sexes, resulting in a type B error rate of 5.4%. Using the error rates estimated above, the estimates of relative fitness reported in Table 5 changed by <1% when they were corrected using Araki and Blouin's (2005) method (data not shown).

Selection on run timing

We estimated standardized linear and quadratic selection differentials on run timing using the standardized number of mates, fry, smolts, or adults as alternative measures of fitness (Fig. 5; Table 6). Overall, the linear terms were positive and quadratic terms were negative, indicating stabilizing selection with an optimum greater than the mean. Linear selection differentials differed significantly by sex and year (Table 6).

Discussion

Smolt production

Minter Creek is a useful research site in part because of the long time series of smolt production data from the stream (Table 7). In addition to the smolt abundance data collected by Salo and Bayliff (1958) from 1940 to 1955, natural smolt counts were also made in the mid-1980s as part of a study to estimate mortality associated with capturing and tagging smolts (Blankenship and Hanratty 1990; L. Blankenship, Washington Department of Fish and Wildlife, 600 Capitol Way North, Olympia, WA 98501-1091, USA, personal communication). There has been a significant (~50%) decline in total smolt production from the stream between the period from 1940 to 1955 compared with the period from 1982 to 2003 (Table 7). The difference does not appear to be related to spawning abundance, which did not differ significantly between the two periods (Table 7). Two plausible alternatives for the decline are genetic changes in the population due to long-term selection in the hatchery and changes in the freshwater habitat in the Minter Creek watershed that have occurred over the last 60 years. We are in the process of conducting a study to evaluate habitat changes in the Minter Creek watershed using historical photographs and recent stream surveys. At this time, the relative contributions of hatchery and habitat effects cannot be determined, but it seems probable that selective changes in the hatchery have contributed to reduced smolt production in Minter Creek.

Run timing

Run timing distributions for Minter Creek coho salmon have been measured nearly annually since 1938 (Salo and Bayliff 1958; J. Tipping, WDFW 600 Capitol Way North, Olympia, WA 98501-1091, USA, unpublished data), and over that time period there has been a large shift in the distribution toward earlier run timing. The cause of this shift is not known, but a plausible hypothesis is that it is due at least in part to past breeding practices at the Minter Creek Hatchery. In particular, salmon hatcheries often have a target for the number of fish that they will spawn, and fish are spawned in roughly the order in which they arrive at the hatchery until the target is met. Fish arriving after that time

Fig. 4. Distribution of inferred minimum numbers of mates and progeny, combined across years, origin, and sex.

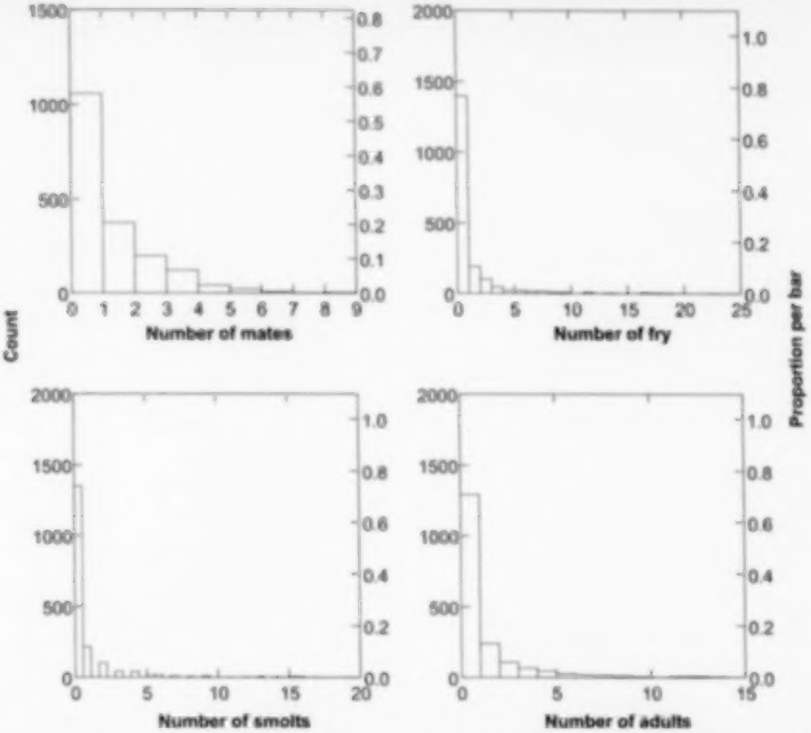

are either killed or are returned to the river. To the degree that run timing is heritable, the practice of preferentially spawning earlier-returning fish is expected to result in a shift in the population's run timing distribution toward earlier return times (Flagg et al. 1995; Quinn et al. 2002). If the natural population in the stream receives a high level of immigration from the hatchery population, theory suggests the run timing of the natural population will also shift toward earlier times (Ford 2002). In this study, we found that natural coho salmon returning to Minter Creek had a time of return similar to that of the hatchery fish. This result supports the conclusion that the characteristics of the natural population in Minter Creek have been largely replaced by those of the hatchery population over the last 60 years. It is therefore useful to examine selection gradients on run timing in light of the observed trend toward earlier run timing after initiation of the hatchery.

We found highly significant selection on run timing for naturally spawning coho salmon in Minter Creek. Overall, there was a clear pattern of stabilizing selection, with fish that returned at either end of the run timing distribution obtaining relatively few mates and producing fewer offspring compared with fish that returned in the middle of the distribution. There was a significant component of directional selection, however, with later-returning fish obtaining more mates and producing more offspring than earlier-returning fish. From the data at hand, it is not clear what is driving this selection. Assuming that the historical run timing is the optimum run timing for natural spawning in Minter Creek, it would be reasonable to expect to observe directional selection for later run timing in the current Minter Creek population. Although we did observe selection for later run timing in both years of the study, the optimum run timing was nonetheless much earlier than the mean run timing observed historically. It is possible that environmental conditions in Minter Creek have changed over the last 60 years so as to favor earlier run timing than was the case historically. Alternatively, stream conditions in 2000 and 2001 may have by chance not reflected the historical average even if there has been no long-term change. We suspect, however, that a more likely explanation is simply that it is disadvantageous to arrive at the stream when few other potential mates are present. In particular, fish arriving early are more likely to die before successfully spawning, and fish arriving late may simply have few other fish with whom to mate, even if environmental conditions might favor later spawning. Nonetheless, since the optimum spawning time in 2000 and 2001 was later than the mean, we predict that in the absence of continual immigration from early-returning hatchery fish, the mean run timing in the natural Minter Creek population will start to return toward what it was historically. The finding of natural selection for later run timing also suggests that the natural population productivity would increase if hatchery fish were prevented from spawning in the natural population, a conclusion also made by Salo and Bayliff (1958, p. 65) nearly 50 years ago.

Relative fitness of hatchery and natural fish

We found no significant difference in the average number of offspring produced by hatchery versus naturally produced

Fig. 5. Plots of standardized selection differentials on time of return to the weir using the inferred minimum numbers of mates, fry, smolts, and adults as alternative measures of fitness. Data are combined across cohorts, origin, and sex. Standardized (and nonstandardized in parentheses) time of return values are shown on the *x* axis. Each point represents a fitness estimate for an individual fish that was sampled at the weir in 2000 or 2001.

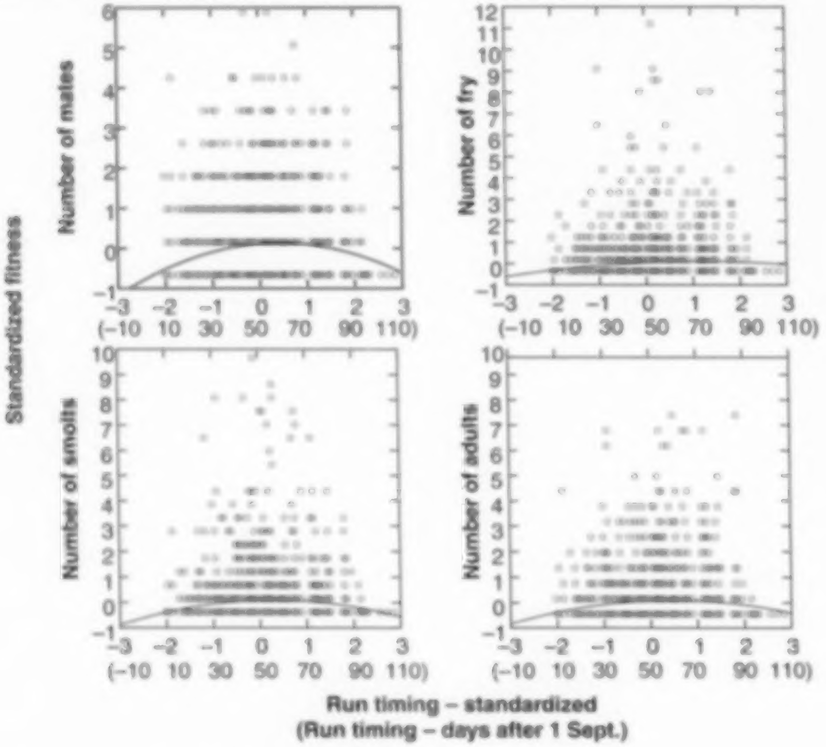

Table 6. Standardized linear and quadratic selection differentials on run timing.

	Estimate based on fitness at different life stages			
Effect[a]	Mates	Fry	Smolts	Adults
Run time	0.100***	0.092***	0.060*	0.076**
(Run time)^2	−0.108***	−0.040	−0.081***	−0.061**
Sex × run time; effect of male	−0.071**	−0.040	0.005	−0.030
Year × run time; effect of 2000	−0.022	−0.015	−0.019	−0.017
Origin × run time; effect of hatchery	0.052*	0.022	0.039	0.041
Sex × (run time)^2; effect of male	−0.007	−0.008	0.003	−0.007
Year × (run time)^2; effect of 2000	−0.009	−0.023	−0.028	−0.054**
Origin × (run time)^2; effect of hatchery	−0.017	0.006	−0.005	−0.011

Note: *, $p < 0.05$; **, $p < 0.01$; ***, $p < 0.001$.

[a] Effects are defined as parameters in the following model: fitness = constant + run time + (run time)^2 + (sex × run time) + (year × run time) + (origin × run time) + [sex × (run time)^2] + [year × (run time)^2] + [origin × (run time)^2].

fish for either males or females. This result is in contrast with most previous studies, which have found that hatchery-produced salmon are less successful than naturally produced salmon when fish of both origins spawn in the same stream (reviewed by Reisenbichler and Rubin 1999). For example, using behavioral observations, Fleming and Gross (1994) found that hatchery coho had a relative fitness of 0.61–0.81 over spawning through emergence portion of the lifecycle. Studies of hatchery steelhead have estimated that hatchery fish relative fitness ranges from 0.02 to 0.35 (Kostow et al. 2003; Leider et al. 1990; Reisenbichler and McIntyre 1977) and studies of Atlantic salmon (*Salmo salar*) have also documented low hatchery fish fitness (Fleming et al. 1996). One published study that did not find low hatchery fish relative fitness involved brown trout (*Salmo trutta*) (Dannewitz et al. 2003). This latter study, like the situation in Minter Creek,

Table 7. Historical and contemporary smolt production from Minter Creek.

Year	Females	Smolts
1940	967	35 452
1942	1393	32 085
1944	786	31 893
1945	906	23 117
1946	500	30 408
1948	500	41 848
1950	98	17 839
1951	114	27 781
1953	411	22 545
1954	753	31 363
1955	491	18 340
1982	450	10 123
1983	515	25 082
1984	800	12 426
1985	615	13 471
2002	422	14 660
2003	450	19 415

Note: Data from 1982 to 1984 were collected as part of a tagging mortality study on Minter Creek (Blankenship and Hanratty 1990) and were provided by L. Blankenship (Washington Department of Fish and Wildlife, 600 Capitol Way North, Olympia, WA 98501-1091, USA). Data prior to 1982 are from Salo and Bayliff (1958). Mean smolt numbers from 1940 to 1955 = 28 425 (standard deviation (SD) = 7379), mean from 1982 to 2003 = 15 863 (SD = 5469); $p = 0.001$ (t test). Mean number of spawning females did not differ significantly (745 for 1940–1955 vs. 542 for 1982–2003; $p = 0.12$).

involved a natural population that had been subject to high levels of hatchery stocking for many decades.

In the case of Minter Creek coho salmon, a likely explanation for the similar fitness of hatchery and natural origin fish stems from the history of the natural coho salmon population in Minter Creek. The hatchery population has been propagated since the late 1930s and was initially founded from coho salmon spawning in Minter Creek (Salo and Bayliff 1958). Since inception of the hatchery stock, there have been no consistent efforts to keep the hatchery stock from spawning naturally in the creek. The proportions of hatchery and natural origin fish spawning in the creek were unknown for several decades prior to the start of our study, but based on recent data it is likely that hatchery origin fish outnumbered natural origin fish by a large margin. For example, the mean annual return of hatchery-produced coho salmon to the Minter Creek Hatchery from 1990 to 2003 was 17 319 (WDFW hatchery records, WDFW, 600 Capitol Way North, Olympia, WA 98501-1091, USA). In this study, we deliberately limited the number of hatchery fish passed above the hatchery weir so that there would be roughly equal numbers of hatchery and natural origin fish. Had we passed fish above the weir in proportion to their abundance at the weir, hatchery fish would have outnumbered natural origin fish by a ratio of ~30:1. The actual ratio in the years leading up to our study would not have been so extreme because of a tendency to take fish into the hatchery early in run when hatchery fish proportions are highest and pass fish to spawn naturally later in the run when hatchery proportions are lowest. Even so, hatchery fish probably outnumbered natural fish on the spawning grounds by a considerable margin. Under those conditions, it is unlikely that any significant degree of differentiation between the natural and hatchery stocks could be maintained unless the hatchery fish had very low relative fitness from the very beginning of the hatchery program.

The high proportion of hatchery fish on the Minter Creek spawning grounds for many years is a likely explanation for the lack of significant fitness between hatchery and natural fish, but this result was not necessarily predictable prior to initiation of our study. In particular, in situations where a long-domesticated hatchery stock is introduced into a stream with an existing natural population, the hatchery fish may have sufficiently low relative fitness to limit introgression into the natural population. For example, Leider et al. (1990) found that the relative fitness of hatchery steelhead in the Kalama River was very low compared with natural steelhead, despite high proportions (>80%) of hatchery steelhead on the spawning grounds for many years. In the case of the Kalama steelhead, the hatchery stock was not native to the Kalama watershed and may also have experienced significant domestication selection prior to be introduced there. These factors appear to have limited genetic introgression into the native Kalama steelhead population despite high proportions of the hatchery stock on the spawning grounds. In contrast, the Minter Creek hatchery stock was originally founded from wild Minter Creek coho salmon, so the difference in relative fitness between hatchery and natural fish in Minter Creek may never have been large enough to prevent substantial interbreeding between hatchery and natural fish. Since the start of large-scale hatchery releases around 1960, the population has also presumably consisted predominantly of hatchery fish. Our finding of nearly identical allele frequencies between the hatchery and natural origin groups and the early run timing distribution of the naturally produced fish supports the hypothesis that the characteristics of the original natural coho salmon population in Minter Creek have been largely replaced by those of the hatchery population. Our results do indicate the hatchery rearing environment in Minter Creek did not lead to substantial, environmentally induced differences in fitness between hatchery and naturally produced fish, as has been observed in other studies (e.g., Fleming et al. 1997).

Assuming that the changes in run timing and smolt production are due to genetic effects of hatchery production, our results provide a worst case (or perhaps near worst case) bench mark for evaluating the long-term effects of supplementation. In particular, more conservation-oriented supplementation programs generally aim to limit fitness loss by keeping the proportion of hatchery fish in the population within some set limits (reviewed by Mobrand et al. 2005). To the degree that such limits are successfully implemented, theory suggests that fitness loss would occur more slowly than may have occurred in the more extreme case of Minter Creek coho salmon (Lynch and O'Hely 2001; Ford 2002). Starting in 2003, the proportion of hatchery coho salmon allowed to pass above the Minter Creek weir was reduced to ~15% (the lowest level that is logistically practical), allowing an opportunity to test the hypothesis that the natural population will increase in fitness in the absence of high rates of hatchery gene flow.

Acknowledgements

We particularly acknowledge the Minter Creek hatchery crew, especially Denis Popochock, Eric Kinney, and John Lovrak, whose kind assistance, patience, and unfailing good humor were essential to the success of this project. We also thank John Sneva for scale reading. Robin Waples, Kevin Williamson, Ewann Berntson, Barry Berejikian, and three anonymous reviewers provided useful comments on an earlier version of this paper. This project was funded in part by a grant from the Hatchery Scientific Review Group.

References

Araki, H., and Blouin, M.S. 2005. Unbiased estimation of relative reproductive success of different groups: evaluation and correction of bias caused by parentage assignment errors. Mol. Ecol. **14**: 4097–4109.

Banks, M.A., Blouin, M.S., Baldwin, B.A., Rashbrook, V.K., Fitzgerald, H.A., Blankenship, S.M., and Hedgecock, D. 1999. Isolation and inheritance of novel microsatellites in chinook salmon. J. Hered. **90**: 281–288.

Berejikian, B., and Ford, M.J. 2004. Review of relative fitness of hatchery and natural salmon. NOAA Tech. Memo. NMFS-NWFSC-61.

Blankenship, H.L., and Hanratty, P.R. 1990. Effects of survival of trapping and coded wire tagging coho salmon smolts. Am. Fish. Soc. Symp. **7**: 259–261.

Condrey, M.J., and Bentzen, P. 1998. Characterization of coastal cutthroat trout (*Oncorhynchus clarki clarki*) microsatellites and their conservation in other salmonids. Mol. Ecol. **7**: 787–789.

Dannewitz, J., Petersson, E., Prestegaard, T., and Järvi, T. 2003. Effects of sea-ranching and family background on fitness traits in brown trout *Salmo trutta* reared under near-natural conditions. J. Appl. Ecol. **40**: 241–250.

de Fromentel, C., Pakdel, F., Chapus, A., Baney, C., May, P., and Soussi, T. 1992. Rainbow-trout p53 – cDNA cloning and biochemical characterization. Gene, **112**: 241–245.

Du, S., Devlin, R., and Hew, C. 1993. Genomic structure of growth hormone genes in Chinook salmon (*Oncorhynchus tshawytscha*): presence of two function genes, GH-I and GH-II, and a male-specific pseudogene, GH-PSI. DNA Cell Biol. **12**: 739–751.

Flagg, T.A., Waknitz, F.W., Maynard, D.J., Milner, G.B., and Mahnken, C.V.W. 1995. The effect of hatcheries on native coho salmon populations in the lower Columbia River. Am. Fish. Soc. Symp. **15**: 366–375.

Fleming, I.A., and Gross, M.R. 1994. Breeding competition in a Pacific Salmon (coho: *Oncorhynchus kisutch*): measures of natural and sexual selection. Evolution, **48**: 637–657.

Fleming, I.A., Jonsson, B., Gross, M.R., and Lamberg, A. 1996. An experimental study of the reproductive behavior and success of farmed and wild Atlantic salmon. J. Appl. Ecol. **33**: 893–905.

Fleming, I.A., Lamberg, A., and Jonsson, B. 1997. Effects of early experience on the reproductive performance of Atlantic salmon. Behav. Ecol. **8**: 470–480.

Ford, M.J. 2002. Selection in captivity during supportive breeding may reduce fitness in the wild. Conserv. Biol. **16**: 815–825.

Gerber, S., Mariette, S., Streiff, R., Bodenes, C., and Kremer, A. 2000. Comparison of microsatellites and amplified fragment length polymorphism markers for parentage analysis. Mol. Ecol. **9**: 1037–1048.

Gerber, S., Chabrier, P., and Kremer, A. 2003. FAMOZ: a software for parentage analysis using dominant, codominant and uniparentally inherited markers. Mol. Ecol. Notes, **3**: 479–481.

Hard, J.J., Jones, R.P., Jr., Waples, R.S. 1992. Pacific salmon and artificial propagation under the Endangered Species Act. NOAA Tech. Memo. NMFS-NWFSC-2.

Independent Scientific Review Panel and Independent Science Advisory Board (ISAB). 2002. Hatchery surpluses in the Pacific Northwest. Fisheries, **27**: 16–27.

Independent Scientific Review Panel and Independent Science Advisory Board (ISAB). 2005. Monitoring and evaluation of supplementation projects. Report to the Northwest Power and Conservation Council, October 14, 2005. Available from http://www.nwcouncil.org/library/isrp/isrpisab2005-15.pdf [accessed April 2006; updated 14 October 2005].

Kostow, K., Marshall, A., and Phelps, S. 2003. Naturally spawning hatchery steelhead contribute to smolt production but experience low reproductive success. Trans. Am. Fish. Soc. **132**: 780–790.

Lande, R., and Arnold, S.J. 1983. The measurement of selection on correlated characters. Evolution, **37**: 1210–1226.

Leider, S.A., Hulett, P.L., Loch, J.J., and Chilcote, M.W. 1990. Electrophoretic comparison of the reproductive success of naturally spawning transplanted and wild steelhead trout through the returning adult stage. Aquaculture, **88**: 239–252.

Lynch, M., and O'Hely, H. 2001. Captive breeding and the genetic fitness of natural populations. Conserv. Genet. **2**: 363–378.

McClure, M.M., Holmes, E.E., Sanderson, B.L., and Jordan, C.E. 2003. A large-scale, multispecies status assessment: anadromous salmonids in the Columbia River Basin. Ecol. Appl. **13**: 964–989.

Meagher, T.R., and Thompson, E. 1986. The relationship between single parent and parent pair genetic likelihoods in genealogy reconstruction. Theor. Popul. Biol. **29**: 87–106.

Mobrand, L.E., Barr, J., Blankenship, L., Campton, D.E., Evelyn, T.T.P., Flagg, T.A., Mahnken, C.V.W., Seeb, L.W., Seidel, P.R., and Smoker, W.W. 2005. Hatchery reform in Washington State: principles amd emerging issues. Fisheries, **30**: 11–33.

Naish, K.A., and Park, L.K. 2002. Linkage relationships for 35 new microsatellite loci in chinook salmon *Oncorhynchus tshawytscha*. Anim. Genet. **33**: 316–318.

National Research Council (NRC). 2004. Atlantifc salmon in Maine. National Academies Press, Washington, D.C.

Quinn, T.P., Peterson, J.A., Gallucci, V.F., Hershberger, W.K., and Brannon, E.L. 2002. Artificial selection and environmental change: countervailing factors affecting the timing of spawning by coho and chinook salmon. Trans. Am. Fish. Soc. **131**: 591–598.

Raymond, M., and Rousset, F. 1995. GENEPOP. Version 1.2. Population genetics software for exact tests and ecumenicism. J. Hered. **86**: 248–249.

Reisenbichler, R.R., and McIntyre, J.D. 1977. Genetic differences in growth and survival of juvenile hatchery and wild steelhead trout, *Salmo gairdneri*. J. Fish. Res. Board Can. **34**: 123–128.

Reisenbichler, R.R., and Rubin, S.P. 1999. Genetic changes from artificial propagation of Pacific salmon affect the productivity and viability of supplemented populations. ICES J. Mar. Sci. **56**: 459–466.

Salo, E.O., and Bayliff, W.H. 1958. Artificial and natural production of silver salmon (*Oncorhynchus kisutch*) at Minter Creek, Washington. Washington Department of Fisheries, Olympia, Wash. Res. Bull. Rep. 4.

Sancristobal, M., and Chevalet, C. 1997. Error tolerant parent identification from a finite set of individuals. Genet. Res. **70**: 53–62.

Sandercock, F.K. 1991. Life history of coho salmon (*Oncorhynchus kisutch*). *In* Pacific salmon life histories. *Edited by* C. Groot and L. Margolis. University of British Columbia Press, Vancouver, B.C. pp. 395–446.

Small, M.P., Beacham, T.D., Withler, R.E., and Nelson, R.J. 1998. Discriminating coho salmon (*Oncorhynchus kisutch*) populations within the Fraser River, British Columbia, using microsatellite DNA markers. Mol. Ecol. 7: 141–155.

Smith, C.T., Koop, B.F., and Nelson, R.J. 1998. Isolation and characterization of coho salmon (*Oncorhynchus kisutch*) microsatellites and their use in other salmonids. Mol. Ecol. 7: 1614–1616.

Impaired detection of chemical alarm cues by juvenile wild Atlantic salmon (*Salmo salar*) in a weakly acidic environment

Antoine Olivier Henri Claude Leduc, Ellie Roh, Mark Charles Harvey, and Grant Edwin Brown

Abstract: Many prey fishes rely on damage-released chemical alarm cues to detect and avoid predators. The ability to use these cues has been shown to confer considerable survival benefits to individuals. While several laboratory studies and a single field study have demonstrated that an ambient pH of 6.0 impairs fishes in their ability to detect these alarm cues, no study had yet compared the response to alarm cue exposures across populations residing in multiple streams of a different acidity level. In our study, we conducted live behavioural observations in five nursery streams, ranging in pH from 5.71 to 7.49 on two age classes (young of the year and parr) of wild juvenile Atlantic salmon (*Salmo salar*). We aimed to assess if the detection of these chemical alarm cues was constantly dependant on the ambient pH or if variations in the detection occurred among populations of the different streams regardless of the ambient acidity level. Our results demonstrated that salmon present in any acidic stream did not respond to alarm cues, while those in neutral streams exhibited typical alarm responses.

Résumé : Plusieurs poissons proies utilisent les signaux d'alerte chimiques libérés par les blessures pour détecter et éviter les prédateurs. Il a été démontré que la capacité d'utiliser ces signaux procure aux individus des bénéfices significatifs de survie. Bien que plusieurs études de laboratoire et une seule étude de terrain aient prouvé qu'un pH ambiant de 6,0 compromet la capacité des poissons à percevoir ces signaux d'alerte, aucune recherche n'a encore comparé les réactions à la présence des signaux d'alerte dans une gamme de populations habitant des cours d'eau avec des niveaux différents d'acidité. Dans notre travail, nous avons mené des observations comportementales en nature dans cinq cours d'eau d'élevage dont les pH variaient de 5,71 à 7,49 chez deux classes d'âge (jeunes de l'année et tacons) de jeunes saumons atlantiques (*Salmo salar*) sauvages. Nous tentons de déterminer si la perception de ces signaux chimiques d'alerte dépend à tout coup du pH ambiant ou s'il existe des variations entre les populations des différents cours d'eau indépendantes des niveaux ambiants d'acidité. Nos résultats démontrent que tous les saumons qui habitent les cours d'eau acides ne réagissent pas aux signaux d'alerte, alors que ceux des cours d'eau neutres montrent des réactions typiques d'alerte.

[Traduit par la Rédaction]

Introduction

Acidification of freshwater ecosystems has considerable impacts on aquatic communities worldwide (Schindler 1988; Guerold et al. 2000). While in the past two decades anthropogenic acidic deposition has decreased by 30%–40% in many industrialized countries (Stoddard et al. 1999), weakly acidic water bodies (pH ~5.5–6.0) are still widespread (Mallory et al. 1998; Jeffries et al. 2000; Doka et al. 2003). In fishes, acidification is known to induce behavioural changes such as increased area avoidance (Johnson and Webster 1977; Åtland 1998), inhibition of migration (Ikuta et al. 2001), inhibition of spawning (Kitamura and Ikuta 2001), reduced feeding (Lacroix et al. 1985), and impairment of chemosensory risk assessment (Brown et al. 2002; Leduc et al. 2004*a*, 2004*b*). Several of these behavioural changes may represent sublethal effects of anthropogenic acidification. Despite its frequent occurrence, most studies investigating the effect of acidification on fish behaviour have concentrated on intermediate to severe acidification (pH value between 4.0 and 5.5; Lacroix et al. 1985; Gunn and Noakes 1986; Peterson et al. 1989), while the effects of weak acidification (pH of 6.0) has received much less attention (but see Ikuta et al. 2001). An acidification level of pH 6.0 corresponds to a threshold under which damage to aquatic biota will represent a major environmental problem (Holt et al. 2003).

A wide variety of aquatic vertebrates rely on chemosensory information to assess and avoid local predation risks (Smith 1992, 1999). Such risk assessment is mediated

Received 18 January 2006. Accepted 16 June 2006. Published on the NRC Research Press Web site at http://cjfas.nrc.ca on 3 October 2006.
J19115

A.O.H.C. Leduc,[1] E. Roh, M.C. Harvey, and G.E. Brown. Department of Biology, Concordia University, 7141 Sherbrooke St. West, Montréal, QC H4B 1R6, Canada.

[1] Corresponding author (e-mail: aleduc@alcor.concordia.ca).

doi:10.1139/F06-128

through the release and detection of chemical cues in the water column (Chivers and Smith 1998; Wisenden 2000). One extensively studied group of such chemicals is the damage-released alarm cues (reviewed in Chivers and Smith 1998; Brown 2003). These cues are present in the epidermis of taxonomically diverse prey fishes and typically enter the water column following mechanical damage to the skin, as would likely occur during a predation event (Brown and Smith 1997; Chivers et al. 1996). Alarm cues have been studied in several species of salmonids, including brook trout (*Salvelinus fontinalis*; Mirza and Chivers 2000, 2001*a*), brown trout (*Salmo trutta*; Mirza and Chivers 2001*a*), rainbow trout (*Oncorhynchus mykiss*; Mirza and Chivers 2001*a*; Leduc et al. 2004*a*), and Chinook salmon (*Oncorhynchus tshawytscha*; Berejikian et al. 1999). Their detection by nearby conspecifics and some sympatric, heterospecific prey-guild members may elicit a suite of short-term, antipredator, behavioural responses, including decreased activity level, increased use of shelter, and increased area avoidance (Smith 1992, 1999). Prey individuals responding to alarm cues have been shown to gain increased survival during staged encounters with live predators (Mirza and Chivers 2000, 2001*b*, 2003).

The ability to detect and respond to these critically important chemosensory cues may be impaired under acidic conditions. For example, Brown et al. (2002) demonstrated in a laboratory experiment that a weak level of acidification (pH of 6.0) renders two ostariophysan species, fathead minnow (*Pimephales promelas*) and finescale dace (*Phoxinus neogaeus*), unable to detect and respond to conspecific alarm cues. A similar loss of function of chemical alarm cues has been demonstrated for juvenile pumpkinseed (*Lepomis gibbosus*; Leduc et al. 2003) and rainbow trout (Leduc et al. 2004*a*). In all cases, the loss of response does not appear to be due to physiological damage to cue receptors, but rather to changes of the alarm cue molecule itself (Brown et al. 2002; Leduc et al. 2004*b*).

Laboratory conditions, however, lack the ecological relevance of the challenges prey individuals face in their natural habitat, and elements of controversy exist regarding the function of chemical alarm cues under natural conditions (see Magurran et al. 1996; Smith 1997). While several recent studies have shown that various prey fishes do rely on chemical alarm cues to assess risk under natural conditions (Brown et al. 1997; Wisenden et al. 2004), only a single field investigation has examined the potential effects of stream water acidification on the use of these cues. Leduc et al. (2004*a*) have shown that in a stream of mean pH 6.88, conspecific alarm cue injections elicited a major increase in antipredator response in brook trout compared with a control stimulus. However, in a stream of mean pH 6.11, no change in response was observed following injections of the chemical alarm cues. Population and strain-dependant variations in acid tolerance exist in many fish species, including salmonids (Robinson et al. 1976; Rosseland et al. 2001). While some strains may be adequately suited to live in more acidic conditions, others may suffer increased physiological stress leading to suboptimal behaviour (Åtland 1998). Thus, studying a single population at each acidity level cannot exclude the possibility that differences in alarm response may be the result of population differences in overall physiological condition and (or) olfactory sensitivity rather than from a direct loss in chemical alarm function. Thus, the general ecological relevance of the effects of weak acidification on chemosensory assessment of damage-released alarm cues remains difficult to assess.

In this study, we assess if the alarm response to conspecific chemical cues of juvenile wild Atlantic salmon (*Salmo salar*) is correlated with the ambient pH in nursery streams not directly disturbed by human activities (with the potential exception of acid precipitation). We test in young of the year (YOY; 0+) and parr (1+) for the presence of an alarm response following the exposure to chemical alarm cues in streams of different pH. If a loss of function of chemical alarm cues is linked to alterations of the alarm cue itself rather than population differences in acid tolerance, we predict that prey fish present in any of the acidic streams should show a reduced alarm response compared with fish present in neutral streams. Likewise, we would expect no difference in overall response intensity among populations present in streams of a similar acidity level.

We chose juvenile Atlantic salmon to investigate these questions owing to its territorial and site fidelity behaviour (Grant et al. 1998; Steingrimsson and Grant 2003), allowing for visual observations to be conducted with ease in its habitat. We compared four typical behavioural changes associated with antipredation response (see below) for two year classes (YOY and parr) in six sites of five different streams ranging in acidity from pH 5.74 to 7.33.

Material and methods

Test sites

This experiment was conducted in Northcumberland County, New Brunswick, Canada, in five different streams (Catamaran Brook, Little Southwest Miramichi River, Otter Brook, Devil's Brook, and Correy Creek) between 14–29 of June and 7–23 of August 2003. In these streams, a site of ~50 m in length (Fig. 1) was chosen for its physical characteristics (canopy cover, distance from the riverbank, and substrate type; Table 1). Because Corey Creek is a tributary of Devil's Brook, we chose to subdivide Devil's Brook into two test sites: one above and one below the mouth of Correy Creek. These two sites on Devil's Brook (named Devil's Brook "High", Devil's Brook "Low", respectively) had two distinct mean pH values (one-way analysis of variance, $p < 0.05$) but were otherwise similar it their physical characteristics (Table 2).

After each trial, the pH and water temperature were recorded (using a portable Accumet® EW-59333-20 pH meter), as well as the surface current speed (using a Flo-Mate velocity meter; Marsh McBirney Inc.), the depth (using a 1 m ruler), the cloud cover, and the canopy cover. The cloud cover was estimated by the same observer throughout the entire experiment by assessing the percentage of sky that was covered by clouds. The canopy cover was determined by estimating the proportion of sky that was blocked by branches and trees directly above the point of stimulus injection in a 2 m radius. Overall, test sites were grouped in two distinct categories, neutral or acidic, as a function of their mean pH (Table 1). Catamaran Brook, Little Southwest Miramichi River, and Otter Brook were considered neutral (pH range of

Fig. 1. The location of the study sites in New Brunswick, Canada. The inset map in the top right corner shows the location of the study sites within New Brunswick. The numbers 1–6 correspond to the study sites (each ~50 m in length) located on Catamaran Brook, Otter Brook, Little Southwest Miramichi River, Devil's Brook "High", Devil's Brook "Low", and Correy Creek, respectively.

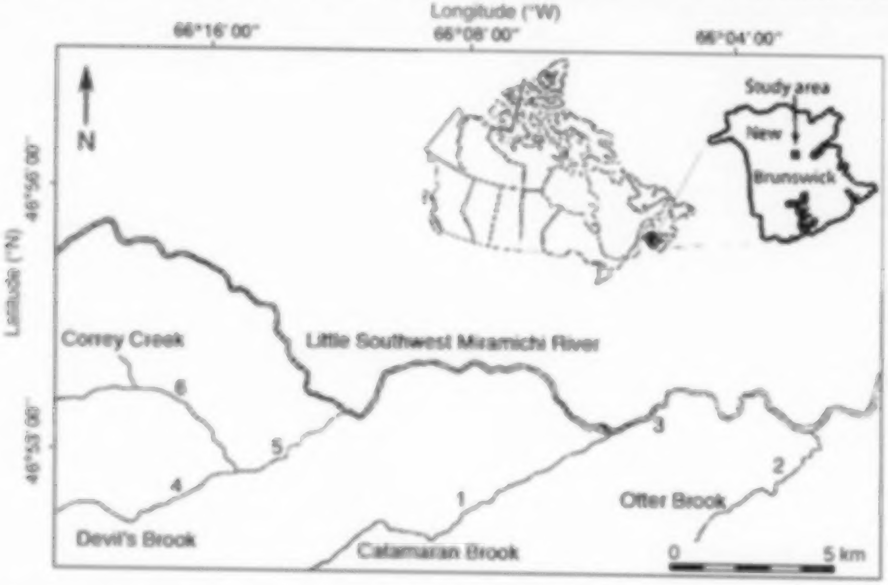

Table 1. Mean (± standard deviation) values for the physical and chemical variables of the studied streams.

Stream	pH	Water temperature (°C)	Current velocity ($cm \cdot s^{-1}$)	Canopy cover (%)	Cloud cover (%)	Depth (cm)
Catamaran Brook	7.25±0.17	17.0±0.5	52.3±18.9	63.0±20.0	43.2±12.7	37.0±11.8
Little Southwest Miramichi	7.16±0.07	16.7±0.6	69.9±18.2	12.5±3.4	19.6±21.4	51.7±11.3
Otter Brook	7.08±0.12	16.3±0.6	19.6±5.3	88.6±10.2	28.1±11.7	28.3±10.24
Correy Creek	6.03±0.06	17.7±1.2	40.3±11.1	74.3±18.2	33.8±17.9	34.0±6.8
Devil Brook "High"	5.85±0.12	15.8±1.0	35.3±19.7	57.9±17.6	56.1±12.3	28.4±7.8
Devil Brook "Low"	5.95±0.11	18.4±0.8	37.4±15.5	66.1±12.4	17.3±9.5	41.5±16.4

Table 2. Mean value (± standard deviation) of the physical and chemical variables between the neutral and acid sites for June and August.

Variable	Neutral	Acidic	*F*	df	*P*
June					
pH	7.11±0.19	5.88±0.10	149.83	6, 9	0.001
Water temperature (°C)	16.8±0.62	16.9±1.74	0.104	6, 9	0.748
Canopy cover (%)	49±30	57±23	7.673	6, 9	0.070
Cloud cover (%)	26±19	34±27	0.403	6, 9	0.528
Velocity ($cm \cdot s^{-1}$)	54±18	45±16	0.867	6, 9	0.355
Depth (cm)	42±10	36±16	0.097	6, 9	0.756
August					
pH	7.16±0.04	6.04±0.06	767.76	6, 9	0.002
Water temp (°C)	16.4±0.77	17.3±0.84	2.975	6, 9	0.089
Canopy cover (%)	47±28	56±21	0.969	6, 9	0.328
Cloud cover (%)	33±16	36±20	0.337	6, 9	0.564
Velocity ($cm \cdot s^{-1}$)	50±22	41±14	1.963	6, 9	0.166
Depth (cm)	38±16	32±8	1.706	6, 9	0.196

Note: One-way analysis of variance (ANOVA) was used to assess differences among groups of neutral and acidic streams for the surveyed variables.

6.96–7.33), while Devil's Brook "High", Devil's Brook "Low", and Corey Creek were considered acidic (pH range of 5.74–6.09). With the exception of the pH, no significant difference between the measured characteristics of the two groups of test sites was found (Table 2). Also, there was no significant difference in mean pH in each respective group of streams (neutral or acidic) between June and August (Table 2).

Stimulus collection

Skin from Atlantic salmon was collected as a source of the alarm cue substance on 13 June and 5 August 2003 from Little Southwest Miramichi River. Less than an hour after their capture, these Atlantic salmon were killed with a single blow on the head (in accordance to Concordia Animal Care Committee Protocol AC-2002-BROW), and skin fillets from both sides of their body were removed and immediately placed into an ice-chilled container filled with stream water of pH 7.04 and 7.08 (June and August, respectively). In June, we collected 327.74 cm^2 and 332.21 cm^2 of skin (parr and YOY, respectively), while in August we collected 348.21 cm^2 and 319.80 cm^2 of skin (parr and YOY, respectively). Fillets were homogenized and diluted with stream water, producing alarm cue solutions ranging from 0.150 to 0.158 $cm^2 \cdot mL^{-1}$.

This procedure has been shown to elicit a consistent antipredator response in cyprinids (Brown et al. 2002), in centrarchids (Leduc et al. 2003), and in salmonids (Brown and Smith 1997, 1998; Mirza and Chivers 2002). The resulting solution was frozen in 25 mL aliquots at −20 °C until needed. As a control, stream water was also frozen in 25 mL aliquots.

Experimental protocol

Field observations were conducted between 15–29 of June and 7–29 of August 2003 using the method of Leduc et al. (2004*a*) (modified from Steingrímsson and Grant 2003). Observation trials were conducted on focal test fish (found while snorkeling on the test sites) from ~1.5 m upstream from the test fish, at an angle of 45° relative to water current. This positioning was used to minimize visual obstruction of the focal fish and to reduce interference from drifting particulate matter. To ensure that the fish was behaving normally (i.e., it had resumed feeding and moving), it was left to acclimate to the observer's presence for a minimum of 2 min before any observations were recorded. Trials were 20 min in length and divided in 10 min pre-stimulus injection and 10 min post-stimulus injection periods. After the first 10 min elapsed (pre-stimulus), the observer injected the stimulus (either stream water or alarm cue solution for the control or experimental treatments, respectively) using a 60 mL syringe at a constant rate of 6 $mL \cdot s^{-1}$. The stimulus was injected approximately 1–1.5 m upstream of the test fish. The experimental treatment order and the year-class subjects were completely randomized, while the overall order of the test sites surveyed was partially randomized. All trials were conducted and videotaped by the same observer using an underwater Sea View® camera. As the camera was located between 1 and 1.5 m from the focal test fish, small-scale behavioural response could easily be monitored. In total, 144 trials were conducted (six replicates per treatment in six sites with two year classes). Each trial was conducted on a single fish that was used only once. To ensure that our injected stimulus reached our test fish, dye injection tests (commercial 2% milk) were conducted. These tests were done after the completion of 16 randomly assigned experimental trials in which the same experimental protocol was used. For all dye injection trials, the injected dye reached the test fish, suggesting that our injected stimuli were also reaching our test fish. Smith (1999) reported that a single exposure to alarm cue was sufficient to elicit an alarm response.

Behavioural measures

To assess the intensity of an alarm response from exposure to a stimulus as well as to increase our power of detection, five behavioural modalities were quantified: the number of feeding attempts, the number of aggressive interactions, the total time spent in motion (in seconds), the total time spent motionless on the substrate (in seconds), and the total time spent absent (in seconds). These behavioural responses were quantified by viewing videotapes on a 14-inch (35 cm) Toshiba™ flat screen monitor. All trials were viewed twice by the same observer. We chose these above-mentioned behavioural measures, as they allow us to gauge the alarm response intensity in several fish species (Leduc et al. 2004*a*; Mirza and Chivers 2002; Wisenden et al. 2004) and may confer survival benefits to individuals during predator encounters (Mirza and Chivers 2003). A feeding attempt was defined as a movement of at least half a body length toward a drifting particle or a particle on the substrate and where a biting attempt occurred. An aggressive interaction was defined as a movement of at least a body length toward another fish with or without a biting attempt. Time in motion was measured when an individual was changing its location by at least a body length. The time on substrate was measured when an individual was laying on the substrate without changing its location. Finally, the time absent was defined as the time when a fish was no longer observable on its stimulus injection location (either away or hiding). For the later parameter, if the test fish was seen more than 3 m away from its testing location, it was considered absent. This cutoff distance was used, since the observed displacements of territory-holding juvenile Atlantic salmon are generally under this distance (Steingrímsson and Grant 2003). In numerous cases, it was not possible to differentiate between hiding and fleeing; therefore, these two responses were indiscriminately grouped together. Because we cannot assess if certain response variables convey a stronger indication of fright, we interpreted the appearance of any of these behavioural patterns as an alarm response.

Statistical analysis

Our results were obtained by subtracting the pre-stimulus values from the post-stimulus values, thus giving the difference between the measured behavioural parameters (see above). We tested for any overall effect of pH with a nested multivariate analysis of variance (MANOVA) using treatment (stream water versus alarm cue) and pH (neutral versus acidic) as independent variables. We nested the variable stream in their respective pH level (neutral or acidic). Using subsequent analysis of variance (ANOVA), the effects of pH and stimuli were further investigated. The behavioural response of individuals was directly compared between control and experimental stimuli under neutral and acidic conditions for each year class (parr and YOY).

Results

For both parr and YOY, a significant effect of treatment that depended on the pH of the sites was found (MANOVA: treatment: $F_{[5,36]} = 8.73$, $P < 0.01$; pH: $F_{[5,36]} = 8.57$, $P < 0.01$; interaction: $F_{[5,36]} = 3.53$, $P < 0.01$). For each acidity level (acid or neutral streams), no effect of stream was found on the behavioural response of salmon (i.e., no significant difference in response among the acidic streams and likewise no significant difference in response among the neutral streams; $F_{[1,70]} = 0.57$; $P > 0.05$). Under neutral conditions, juvenile Atlantic salmon significantly decreased the time spent in motion ($t_{13} = 3.56$, $P = 0.0035$; Fig. 2*a*) and the number of feeding attempts ($t_{13} = 3.26$, $P = 0.0061$; Fig. 2*b*), while the time spent on the substrate and the time spent absent (or hiding) from the stimulus injection location increased ($t_{13} = 3.26$, $P = 0.012$ (Fig. 2*c*) and $t_{13} = 3.26$, $P = 0.0061$ (Fig. 2*d*), respectively) when exposed to conspecific alarm cue compared with stream water. However, no significant difference in the number of aggressive interactions between both treatments was found ($F_{[1,26]} = 4.22$; $P > 0.05$). Since the occurrence of such behaviour was rare (mean ± standard deviation = 0.08 ± 0.015 interactions per minute), we did not analyze it any further. Under weakly acidic conditions, however, there was no significant effect of treatment on the behavioural parameters tested (time spent in motion ($F_{[1,70]} = 1.59$; $P > 0.05$; Fig. 2*a*); number of feeding attempts ($F_{[1,70]} = 2.45$; $P > 0.05$; Fig. 2*b*); time spent on the substrate ($F_{[1,70]} = 0.09$; $P > 0.05$; Fig. 2*c*); time spent away from the stimulus injection area ($F_{[1,70]} = 0.45$; $P > 0.05$; Fig. 2*d*)). As control for potential temporal effects associated with our experimental design, the baseline (prestimulus) scores between stream water and alarm cue stimuli treatments for the neutral and acidic sites were compared using multiples one-way ANOVAs. No significant difference was found in any baseline activity scores between the two groups of sites nor among treatments (multiple one-way ANOVA, $P > 0.05$).

Subsequent one-way ANOVA revealed a significant difference in response intensity in the alarm cue treatment between parr and YOY in the neutral sites in two of the five behavioural measurements, but no significant difference in any of the behavioural measurements in the weakly acidic streams. Parr spent significantly more time on the substrate than YOY did ($F_{[1,19]} = 8.727$, $P < 0.05$; Fig. 2*c*), but significantly less time absent (or hiding) from the stimulus injection area than YOY did ($F_{[1,19]} = 7.34$, $P < 0.05$; Fig. 2*d*).

Discussion

These data demonstrate that juvenile Atlantic salmon found in the studied acidic streams were impaired in their ability to detect and respond to damage-released alarm cues. The response of individuals to alarm cue injections did not differ from stream water injections in any of the acidic sites. Also, the individuals' development stages had no effect on the response intensity in acidic condition, whereas in neutral condition, differences occurred. Overall, the findings of this experiment are consistent with the results obtained by Leduc et al. (2004*a*) and support the prediction that even weak levels of acidity directly affect chemosensory risk assessment.

Fig. 2. Mean (± standard deviation) differences (post-stimulus – pre-stimulus) in (*a*) time in seconds spent in motion, (*b*) number of feeding attempts, (*c*) time in seconds spent on the substrate, and (*d*) time spent in seconds away or hiding for juvenile Atlantic salmon (*Salmo salar*) exposed to either alarm cues (shaded bars) or stream water (open bars) under neutral (pH ~7.0) or acidic (pH ~6.0) conditions for young of the year (YOY; left column) and parr (right column).

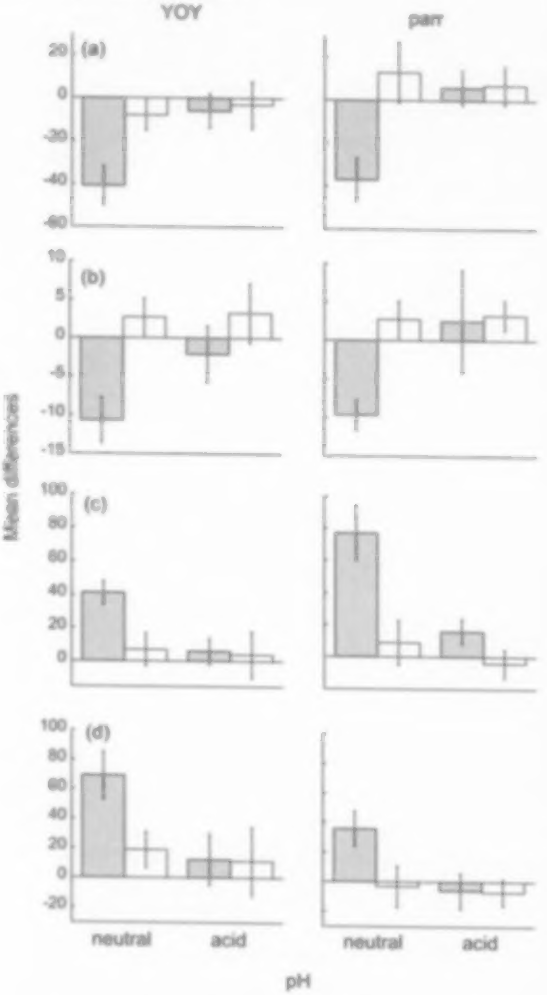

The loss of alarm function in acidic conditions may be due to the two following mechanisms. First, physiological stress and (or) olfactory damage may account for the apparent lack of response. We did not find, however, any significant difference in mean baseline activity level between individuals of the acidic streams and individuals of the neutral streams. Peterson et al. (1989) found that the threshold of pH avoidance for Atlantic salmon is ~4.5, while the most acidic condition we found was a pH of 5.71. Hence, the lack of difference in baseline behaviour and the relatively weak acidity level suggest that individuals present in both groups of streams were well suited to live in their habitat and did not experience much stress linked to acidity. Alternatively, damage to olfactory receptors may account for the lack of response. Leduc et al. (2004*b*) have shown that YOY rainbow trout could be conditioned to learn a novel odour when paired with damage-released chemical alarm cues. This learned response, however, did not occur when the odour was paired with acidified alarm cues (at pH ~6.0). In contrast, acidifying the odour had no effect on the retention of this novel learning as long as the paired alarm cue was not acidified. This result suggests that under weakly acidic conditions, the olfactory function of salmonids is not impaired and thus cannot explain the lack of alarm response. In the second proposed mechanism, the alarm cue may be completely degraded or the concentration of active alarm cues may be reduced below a detectable level because of ambient pH (Leduc et al. 2003). Several authors have shown that concentration of alarm cues below some population-specific threshold fails to elicit an overt antipredator response (Brown et al. 2001*a*; Mirza and Chivers 2003; Roh et al. 2004). We do not know the concentration of active alarm cue presented to our test fish; therefore, we cannot exclude the effect of covert response (i.e., a nonobservable response elicited by a concentration level of alarm cues that would be under the minimal concentration threshold to elicit an observable response; Brown et al. 2001*b*; Mirza and Chivers 2003). Leduc et al. (2004*b*) have shown that no acquired recognition of a novel odour paired with an alarm cue occurred under weakly acidic conditions, while recognition did occur under neutral conditions. These results suggest that a complete degradation of the alarm cues occurs under acidified conditions.

It is now well established that wild Atlantic salmon populations have steadily been declining over the last three decades (Parrish et al. 1998). The explanation of this decline includes a synergetic interaction of many deleterious effects, including invasion of farmed salmon, overfishing, habitat destruction, pollution (including acidification), and changing oceanic conditions (Parrish et al. 1998; Fleming et al. 2000). While many salmonid species are suited to live in a weakly acidic condition (Scott and Crossman 1973; Rosseland et al. 2001), there may be an indirect cost linked to increased predation success of predators. It was hypothesized that predation pressure is reduced in acidic conditions with predatory fish absent or reduced because of ambient pH (Bendell and McNicol 1987). We found in both our acidic and neutral streams several fish species that are known predators to juvenile Atlantic salmon, such as brook trout, slimy sculpin (*Cottus cognatus*), and 2+ Atlantic salmon parr (Henderson and Letcher 2003). Moreover, predation pressure on juvenile Atlantic salmon in their nursery streams may come from birds (Wood 1987) and mammals (Heggenes and Borgstrom 1988). Hence, the range of potential predators may not be directly affected by ambient acidity. As such, the observed alarm cue impairment could likely have major fitness costs linked to increased predation success of juvenile salmon's predators.

Fishes present in the acidified environment should face a considerable disadvantage compared with fishes living in neutral conditions, owing to their impaired ability to detect damage-released alarm cues. Responding to alarm cues of both conspecifics and heterospecifics has been shown to increase the survival of prey individuals in encounters with live predators (Mirza and Chivers 2000; Chivers et al. 2002). Likewise, the identity of a novel predator is learned faster from the detection of damage-released alarm cues than from visual cues (Brown et al. 1997). This difference in recognition time should be especially valid in a structurally complex environment, as is often found in many nursery streams used by Atlantic salmon. Hence, sublethal effects associated with acidity may exist for juvenile salmon, as for prey fishes in general. Aside from prey fishes, several taxa of aquatic vertebrates and invertebrates including amphibians, arthropods, and flatworms have been shown to respond to chemical alarm cues to mediate predation risk (Bouwma and Hazlett 2001; Kiesecker et al. 1996; Wisenden and Millard 2001). As such, anthropogenic acidification of natural water bodies may also influence a wide variety of aquatic organisms in their ability to use chemical alarm cues to assess predation risk.

As aquatic waterways may suffer from depleted buffering capacities in many areas affected by acid precipitations (Stoddard et al. 1999; Clair et al. 2004), deleterious effects on juvenile salmonid populations may arise. Therefore, even slight increases in acid precipitation may affect the ability of prey individuals to assess local predation risk via chemosensory cues, in spite of populations' tolerance to acidity. It is of interest to mention that other anthropogenic pollutants affect chemosensory risk assessment in fishes (McPherson et al. 2004; Scholz et al. 2000; Scott et al. 2003). As such, measures to effectively avoid deleterious direct and indirect effects linked to anthropogenic pollution in natural waterways should aim at looking at an integrated approach (Parrish et al. 1998). Changes in the chemistry of aquatic ecosystems may hinder juvenile salmonids from using an ecologically important source of information on local predation risk. Should it be the case, this may contribute to hinder wild Atlantic salmon stocks in recovering from a depleted state.

Acknowledgements

The authors thank Rick A. Cunjak for providing helpful suggestions and field support, James W. Grant and Emma Despland for helpful comments on the statistical method, and two anonymous reviewers to for comments on the manuscript. Concordia University and the Natural Sciences and Engineering Research Council of Canada (NSERC) provided the financial support to G. Brown and an NSERC post-graduate studies (PGS) D2 Scholarship to A. Leduc. All work reported herein was conducted in accordance with Concordia University Animal Care Committee protocol No. AC-2002-BROW. This paper is Contribution No. 87 to the Catamaran Brook Habitat Research Project.

References

Åtland, A. 1998. Behavioural responses of brown trout, *Salmo trutta*, juveniles in concentration gradients of pH and Al — a laboratory study. Environ. Biol. Fishes, **53**: 331–334.

Bendell, B.E., and McNicol, D.K. 1987. Cyprinid assemblages and the physical and chemical characteristics of small northern Ontario lakes. Environ. Biol. Fishes, **19**: 229–234.

Berejikian, B.A., Smith, R.J.F., Tezak, P.E., Schroder, P.E., and Knudsen, C.M. 1999. Chemical alarm signals and complex hatchery rearing habitats affect antipredator behavior and survival of chinook salmon (*Oncorhynchus tshawytscha*) juveniles. Can. J. Fish. Aquat. Sci. **56**: 830–838.

Bouwma, P., and Hazlett, B.A. 2001. Integration of multiple predator cues by the crayfish *Orconectes propinquus*. Anim. Behav. **61**: 771–776.

Brown, G.E. 2003. Learning about danger: chemical alarm cues and local risk assessment in prey fishes. Fish Fish. **4**: 227–234.

Brown, G.E., and Smith, R.F.J. 1997. Conspecific skin extract elicits antipredator responses in juvenile rainbow trout (*Oncorhynchus mykiss*). Can J. Zool. **75**: 1916–1922.

Brown, G.E., and Smith, R.F.J. 1998. Acquired predator recognition in juvenile rainbow trout (*Oncorhynchus mykiss*): conditioning hatchery-reared fish to recognize chemical cues of a predator. Can. J. Fish. Aquat. Sci. **55**: 611–617.

Brown, G.E., Chivers, D.P., and Smith, R.J.F. 1997. Differential learning rates of chemical versus visual cues of a northern pike by fathead minnows in a natural habitat. Environ. Biol. Fishes, **49**: 89–96.

Brown, G.E., Adrian, J.C., Jr., Patton, T., and Chivers, D.P. 2001*a*. Fathead minnows learn to recognize predator odour when exposed to concentrations of artificial alarm pheromone below their behavioural-response threshold. Can. J. Zool. **79**: 2239–2245.

Brown, G.E., Adrian, J.C., Jr., and Shih, M.L. 2001*b*. Behavioural responses of fathead minnows to hypoxanthine-3-*N*-oxide at varying concentrations. J. Fish Biol. **58**: 1465–1470.

Brown, G.E., Adrian, J.C., Jr., Lewis, M.G., and Tower, J.M. 2002. The effects of reduced pH on chemical alarm signaling in ostariophysan fishes. Can. J. Fish. Aquat. Sci. **59**: 1331–1338.

Chivers, D.P., and Smith, R.J.F. 1998. Chemical alarm signaling in aquatic predator–prey systems: a review and prospectus. Ecoscience, **5**: 315–321.

Chivers, D.P., Brown, G.E., and Smith, R.J.F. 1996. Evolution of alarm signals: attracting predators benefits alarm signal senders. Am. Nat. **148**: 649–659.

Chivers, D.P., Mirza, R.S., and Johnston, J.G. 2002. Learned recognition of heterospecific alarm cues enhances survival during encounters with predators. Behaviour, **139**: 929–938.

Clair, T.A., Dennis, I.F., Amiro, P.G., and Cosby, B.J. 2004. Past and future chemistry changes in acidified Nova Scotian Atlantic salmon (*Salmo salar*) rivers: a dynamic modeling approach. Can. J. Fish. Aquat. Sci. **61**: 1965–1975.

Doka, S.E., McNicol, D.K., Mallory, M.L., Woog, I., Minns, C.K., and Yan, N.D. 2003. Assessing potential for recovery of biotic richness and indicator species due to changes in acidic deposition and lake pH in five areas of southeastern Canada. Environ. Monit. Assess. **88**: 53–101.

Fleming, I.A., Hindar, K., Mjolnerod, I.B., Jonsson, B., Balstad, T., and Lamberg, A. 2000. Lifetime success and interactions of farm salmon invading a native population. Proc. R. Soc. Lond. B Biol. Sci. **267**: 1517–1523.

Grant, J.W.A., Steingrimsson, S.Ó., Keeley, E.R., and Cunjak, R.A. 1998. Implications of territory size for the measurement and prediction of salmonid abundance in streams. Can. J. Fish. Aquat. Sci. **55**: 181–190.

Guerold, F., Boudot, J.-P., Jacquemin, G., Vien, D., Merlet, D., and Rouiller, J. 2000. Macroinvertebrate community loss as a result of headwater stream acidification in the Vosges Mountains (N-E France). Biodivers. Conserv. **9**: 767–783.

Gunn, J.M., and Noakes, D.L.G. 1986. Avoidance of low pH and elevated Al concentration by brook charr (*Salvelinus fontinalis*) alevins in laboratory tests. Water Air Soil Pollut. **30**: 497–503.

Heggenes, J., and Borgstrøm, R. 1988. Effect of mink, *Mustela vison* Schreber, predation on cohorts of juvenile Atlantic salmon, *Salmo salar* L., and brown trout, *S. trutta* L., in three small streams J. Fish Biol. **33**: 885–886.

Henderson, N.J., and Letcher, B.H. 2003. Predation on stocked Atlantic salmon (*Salmo salar*) fry. Can. J. Fish. Aquat. Sci. **60**: 32–42.

Holt, C.A., Yan, N.D., and Somers, K.M. 2003. pH 6 as threshold use in critical load modeling for zooplankton community change with acidification in lakes of south-central Ontario: accounting for morphometry and geography. Can. J. Fish. Aquat. Sci. **60**: 151–158.

Ikuta, K., Munakata, A., Aida, K., Amano, M., and Kitamura, S. 2001. Effects of low pH on upstream migratory behavior in land-locked sockeye salmon *Oncorhynchus nerka*. Water Air Soil Pollut. **130**: 99–106.

Jeffries, D.S., Lam, D.C.L., Wong, I., and Moran, M.D. 2000. Assessment of changes in lake pH in southeastern Canada arising from present levels and expected reductions in acidic deposition. Can. J. Fish. Aquat. Sci. **57**: 40–49.

Johnson, D.W., and Webster, D.A. 1977. Avoidance of low pH in selection of spawning sites by brook trout (*Salvelinus fontinalis*). J. Fish. Res. Board Can. **34**: 2215–2218.

Kiesecker, J.M., Chivers, D.P., and Blaustein, A.R. 1996. The use of chemical cues in predator recognition by western toad (*Bufo boreas*) tadpoles. Anim. Behav. **52**: 1237–1245.

Kitamura, S., and Ikuta, K. 2001. Effects of acidification on salmonid spawning behavior. Water Air Soil Pollut. **130**: 875–880.

Lacroix, G.L., Gordon, D.J., and Johnston, D.J. 1985. Effects of low environmental pH on the survival, growth, and ionic composition of postemergent Atlantic salmon (*Salmo salar*). Can. J. Fish. Aquat. Sci. **42**: 768–775.

Leduc, A.O.H.C., Noseworthy, M.K., Adrian, J.C., Jr., and Brown, G.E. 2003. Detection of conspecific and heterospecific alarm signals by juvenile pumpkinseed under weak acidic conditions. J. Fish Biol. **63**: 1331–1336.

Leduc, A.O.H.C., Kelly, J.M., and Brown, G.E. 2004*a*. Detection of conspecific alarm cues by juvenile salmonids under neutral and weakly acidic conditions: laboratory and field tests. Oecologia, **139**: 318–324.

Leduc, A.O.H.C., Ferrari, M.C.O., Kelly, J.M., and Brown, G.E. 2004*b*. Learning to recognize novel predators under weakly acidic conditions: the effects of reduced pH on acquired predator recognition by juvenile rainbow trout. Chemoecology, **14**: 107–112.

Magurran, A.E., Irving, P.W., and Henderson, P.A. 1996. Is there a fish alarm pheromone? A wild study and critique. Proc. R. Soc. Lond. B Biol. Sci. **263**: 1551–1556.

Mallory, M.L., McNicol. D.K., Cluis, D.A., and Laberge, C. 1998. Chemical trends and status of small lakes near Sudbury, Ontario, 1983–1995: evidence of continued chemical recovery. Can. J. Fish. Aquat. Sci. **55**: 63–75.

McPherson, T.D., Mirza, R.S., and Pyle, G.G. 2004. Responses of wild fishes to alarm chemicals in pristine and metal-contaminated lakes. Can. J. Zool. **82**: 694–700.

Mirza, R.S., and Chivers, D.P. 2000. Predator-recognition training enhances survival of brook trout: evidence from laboratory and field-enclosure studies. Can. J. Zool. **78**: 2198–2208.

Mirza, R.S., and Chivers, D.P. 2001*a*. Are chemical alarm cues conserved within salmonid fishes? J. Chem. Ecol. **27**: 1641–1655.

Mirza, R.S., and Chivers, D.P. 2001*b*. Do chemical alarm signals enhance survival of aquatic vertebrates? An analysis of the current research paradigm. *In* Chemical signals in vertebrates. Vol. 9. *Edited by* A. Marchlewska-Koj, J.J. Lepri, and D. Müller-Schwarze. Kluwer, New York. pp. 19–26.

Mirza, R.S., and Chivers, D.P. 2002. Brook char (*Salvelinus fontinalis*) can differentiate chemical alarm cues produced by different age/size classes of conspecifics. J. Chem. Ecol. **28**: 555–564.

Mirza, R.S., and Chivers, D.P. 2003. Response of juvenile rainbow trout to varying concentrations of chemical alarm cue: response thresholds and survival during encounters with predators. Can. J. Zool. **81**: 88–95.

Parrish, D.L., Behnke, R.J., Gephard, S.R., McCormick, S.D., and Reeves, G.H. 1998. Why aren't there more Atlantic salmon (*Salmo salar*)? Can. J. Fish. Aquat. Sci. **55**(Suppl. 1): 281–287.

Peterson, R.H., Coombs, K., Power, J., and Paim, U. 1989. Response of several fish species to pH gradients. Can. J. Zool. **67**: 1566–1572.

Robinson, G.D., Dunson, W.A., Wright, J.E., and Mamolito, G.E. 1976. Differences in low pH tolerance among strains of brook trout (*Salvelinus fontinalis*). J. Fish Biol. **8**: 5–17.

Roh, E., Mirza, R.S., and Brown, G.E. 2004. Quality or quantity? The role of donor condition in the production of chemical alarm cues in juvenile convict cichlids. Behaviour, **41**: 1235–1248.

Rosseland, B.O., Kroglund, F., Staurnes, M., Hindar, K., and Kvellestad, A. 2001. Tolerance to acid water among strains and life stages of Atlantic salmon (*Salmo salar* L.). Water Air Soil Pollut. **130**: 899–904.

Schindler, D.W. 1988. Effects of acid rain on freshwater ecosystems. Science (Washington, D.C.), **239**: 149–157.

Scholz, N.L., Truelove, N.K., French, B.L., Berejikian, B.A., Quinn, T.P., Casillas, E., and Collier, T.K. 2000. Diazinon disrupts antipredator and homing behaviors in chinook salmon (*Oncorhynchus tshawytscha*). Can. J. Fish. Aquat. Sci. **57**: 1911–1918.

Scott, W.B., and Crossman, E.J. 1973. Freshwater fishes of Canada. Fish. Res. Board Can. Bull. No. 184.

Scott, G.R., Sloman, K.A., Rouleau, C., and Wood, C.M. 2003. Cadmium disrupts behavioural and physiological response to alarm substance in juvenile rainbow trout (*Oncorhynchus mykiss*). J. Exp. Biol. **206**: 1779–1790.

Smith, R.J.F. 1992. Alarm signal in fishes. Rev. Fish Biol. Fish. **2**: 33–63.

Smith, R.J.F. 1997. Does one result trump all others? A response to Magurran, Irving and Henderson. Proc. R. Soc. Lond. B Biol. Sci. **264**: 445–450.

Smith, R.J.F. 1999. What good is smelly stuff in the skin? Cross function and cross taxa effects in fish "alarm substances". *In* Advances in chemical signals in vertebrates. *Edited by* R.E. Johnston, D. Müller-Schwarze, and P.W. Sorensen. Kluwer, New York. pp. 475–487.

Steingrimsson, S.Ó., and Grant, J.W.A. 2003. Patterns and correlates of movement and site fidelity in individually tagged young-off-the-year Atlantic salmon (*Salmo salar*). Can. J. Fish. Aquat. Sci. **60**: 193–202.

Stoddard, J.L., Jeffries, D.S., Lukewille, A., Clair, T.A., Dillon, P.J., Driscoll, C.T., Forsius, M., Johannessen, M., Kahl, J.S., Kellogg, J.H., Kemp, A., Mannio, J., Monteith, D., Murdoch, P.S., Partick, S., Rebsdorf, A., Skjelkvale, B.L., Stainton, M.P., Traaen, T., van Dam, H., Webster, K.E., Wieting, J., and Wilander, A. 1999. Regional trends in aquatic recovery from acidification in North America and Europe. Nature (London), **401**: 575–578.

Wisenden, B.D. 2000. Olfactory assessment of predation risk in aquatic environment. Phil. Trans. R. Soc. Lond. B Biol. Sci., **355**: 1205–1208.

Wisenden, B.D., and Millard, M.C. 2001. Aquatic flatworms use chemical cues from injured conspecifics to assess predation risk and to associate risk with novel cues. Anim. Behav. **62**: 761–766.

Wisenden, B.D., Vollbrecht, K.A., and Brown, J.L. 2004. Is there a fish alarm cue? Affirming evidence from a wild study. Anim. Behav. **67**: 59–67.

Wood, C.C. 1987. Predation of juvenile Pacific salmon by the common merganser (*Mergus merganser*) on eastern Vancouver Island. II. Predation of stream-resident juvenile salmon by merganser broods. Can. J. Fish. Aquat. Sci. **44**: 950–959.

Altered growth and related physiological responses in juvenile Chinook salmon (*Oncorhynchus tshawytscha*) from dietary exposure to polycyclic aromatic hydrocarbons (PAHs)

J.P. Meador, F.C. Sommers, G.M. Ylitalo, and C.A. Sloan

Abstract: A dietary feeding study with polycyclic aromatic hydrocarbons (PAHs) was conducted with juvenile Chinook salmon (*Oncorhynchus tshawytscha*) to mimic exposure from urban estuaries during their transition from freshwater to seawater. A significant reduction in mean fish dry weight was observed only for the highest doses; however, analysis of variance (ANOVA) using standard deviations and examination of the cumulative frequency plots revealed high variability among all treatments. The skewed fish weight distribution revealed a large number of small fish in several treatments compared with control fish. Analyses of whole-body lipids and several parameters in blood plasma related to growth and metabolism indicated alterations for most treatments. These results and trends in growth, plasma chemistry, and lipids as a consequence of PAH exposure were similar to those in fish exhibiting starvation, which we have termed "toxicant-induced starvation". Based on these results, we conclude that PAHs are toxic to salmonids at this life stage and the reduction in biomass and lipid stores observed here would have the potential to cause increased mortality for individuals during their first winter.

Résumé : Nous avons mené une étude d'alimentation diététique avec des hydrocarbures aromatiques polycycliques (PAHs) chez de jeunes saumons chinook (*Oncorhynchus tshawytscha*) afin de mimer leur exposition aux estuaires urbains durant leur transition de l'eau douce vers la mer. Une réduction significative de la masse sèche des poissons s'observe seulement avec les doses les plus élevées; cependant, une analyse de variance (ANOVA), qui utilise les écarts types et qui examine les graphiques de fréquences cumulées, montre qu'il existe une forte variabilité dans tous les traitements expérimentaux. La distribution asymétrique des masses des poissons montre qu'il y a un grand nombre de petits poissons dans plusieurs groupes expérimentaux par comparaison aux groupes témoins. Les analyses des lipides du corps entier et de plusieurs variables du plasma sanguin reliées à la croissance et au métabolisme indiquent qu'il y a des modifications dans la plupart des groupes expérimentaux. Ces résultats et les tendances dans la croissance, la chimie du plasma et les lipides qui se développent à la suite de l'exposition aux PAH font penser aux conditions de poissons qui manquent de nourriture; nous qualifions cet état de « disette provoquée par les produits toxiques ». Sur la foi de ces résultats, nous concluons que les PAHs sont toxiques pour les salmonidés à cette étape de leur vie et que la réduction de biomasse et de réserves lipidiques observée peut potentiellement causer une augmentation de la mortalité individuelle durant leur premier hiver.

[Traduit par la Rédaction]

Introduction

Several studies and reviews have shown that polycyclic aromatic hydrocarbons (PAHs) are ubiquitous in aquatic systems, especially estuaries, and can often occur at high concentrations in sediment, water, and tissue (Meador et al. 1995; Eisler 2000; van Metre et al. 2000). These contaminants come from multiple sources, such as stormwater runoff, atmospheric transport, petroleum operations (including drilling, refining, transport, combustion, spills, and natural seeps),

Received 26 April 2006. Accepted 14 June 2006. Published on the NRC Research Press Web site at http://cjfas.nrc.ca on 3 October 2006.
J19293

J.P. Meador[1] and F.C. Sommers. Ecotoxicology and Environmental Fish Health Program, Environmental Conservation Division, Northwest Fisheries Science Center, National Marine Fisheries Service, NOAA, 2725 Montlake Boulevard East, Seattle, WA 98112, USA.
G.M. Ylitalo and C.A. Sloan. Environmental Assessment Program, Environmental Conservation Division, Northwest Fisheries Science Center, National Marine Fisheries Service, NOAA, 2725 Montlake Boulevard East, Seattle, WA 98112, USA.

[1] Corresponding author (e-mail: james.meador@noaa.gov).

Can. J. Fish. Aquat. Sci. 63: 2364–2376 (2006) doi:10.1139/F06-127

municipal and industrial wastewater, and combustion of most organic material.

During smoltification, juvenile salmonids, especially wild fish, lose significant amount of lipids, usually falling to 1%–3% of wet weight (Brett 1995; Beckman et al. 2000; Meador et al. 2002). While in the estuary and nearshore environment, juvenile Chinook salmon are voracious consumers of invertebrates and small fish (Weatherley and Gill 1995), leading to a rapid increase in growth and accumulated lipid stores that will be beneficial for their first winter (Burrows 1969; Healey 1980; Biro et al. 2004). This stage in the life cycle of juvenile Chinook salmon is one of the most critical for determining its survival and reproductive success (Spromberg and Meador 2005) and even slight impedance in growth or lipid storage may have severe consequences for survival.

Even though PAHs are ubiquitous and abundant in the environment, very few studies have examined organismal-level responses to these compounds. Only a handful of studies have considered growth impairment or energetics as a response in fish and a few of these reported severe effects at low exposure concentrations (Carls et al. 1996; Rice et al. 2000). This study was designed to examine growth and a selected number of associated metabolic parameters in juvenile Chinook salmon (*Oncorhynchus tshawytscha*) exposed to dietary PAHs. Our main focus was the juvenile stage that enters the estuary for several weeks to acclimate to seawater, increase in size, and accumulate lipid stores before migrating to open water. We selected fish growth, whole-body lipids, and several associated parameters in blood plasma as metrics for assessing toxic effects. The goal was to gauge the magnitude of effect on organismal properties such as body weight and whole-body lipid content that directly affect the survival of juvenile salmonids, in addition to several related blood chemistry parameters that may be useful as early indicators of adverse effects.

Materials and methods

Fish husbandry, experimental design, environmental parameters, and execution of these experiments followed the procedures described in Meador et al. (2005). The following is an abbreviated discussion of our methods.

Husbandry

Chinook salmon were cultured in our lab from eggs obtained from a local hatchery. Before the toxicity experiment, Chinook salmon fry were fed ad libitum with commercial food. Once large enough to consume pellets, juvenile Chinook salmon were fed at a rate of 1.5%–2.0% body weight (bw)·day^{-1} with fish pellets from Rangen Inc. (Buhl, Idaho). When juvenile fish weighed approximately 3 g, they were switched to a specially prepared fish pellet (Rangen Inc.) that contained a total lipid content of 11% dry weight that was formulated to mimic the lipid content of prey for wild fish. Water quality parameters (pH, dissolved oxygen, alkalinity, and hardness) were measured at least once every week and adjusted if outside the accepted range (Meador et al. 2005). Fish were raised in freshwater and introduced to saltwater during the new moon in June. The rate of change from freshwater to saltwater was approximately 5‰·day^{-1} until full-strength seawater was attained.

Experimental design

Individual fish were weighed and selected from a size window of 10.0 to 16.0 g wet weight (ww) (2.2–3.5 g dry weight (dw)), which was the range determined to provide the best achievable variance given the available pool of fish. Approximately 40% of the available fish fit the size selection criteria. Each tank contained 50 fish and the order of filling the tanks, as well as the assignment of treatment to each tank, was done randomly as determined with a random number generator.

Juvenile Chinook salmon were fed a mixture of PAHs intended to mimic those found in the stomach contents of field-collected fish both in magnitude and proportionality. Pellets were dosed using a stock solution of PAHs in dichloromethane ($MeCl_2$) (50 mg·mL^{-1}) that consisted of 21 PAHs (Table 1) at percentages similar to those found for stomach contents from field-collected fish (Varanasi et al. 1993) (Fig. 1). All fish food for a given treatment was made in one 3500 g batch. Fish pellets were placed in a stainless steel bowl, a calculated amount of stock solution was added to 4 L of $MeCl_2$, and the entire amount was added to the bowl covering all the pellets. The mixture was stirred occasionally and allowed to air dry. Once dried, the pellets were placed into plastic tubs with a tight-fitting lid and kept in a freezer at –20 °C until needed to feed fish.

An appropriate amount of food was weighed and supplied in two feedings (morning and afternoon). Fish in each experimental tank were fed 1.9% bw·day^{-1} based on their average day 0 wet weight, and that amount was increased each week by a quantity determined with a growth equation that assumed a conversion efficiency of 20%. In a separate tank, 50 fish were weighed frequently to determine their rate of growth, which allowed us to keep the amount that was to be fed to all tanks at 1.9% bw·day^{-1}. In treatments where growth was inhibited (or enhanced), those fish actually received a higher (or lower) percentage of food to body weight because the amount fed to each tank was incremented according the expected growth rate for control fish. Observations for each tank found that there was no aversion to pellets by fish in any treatment, and the entire allocation of pellets was consumed within a few seconds. Feeding was conducted 5 days per week; therefore, fish were fed 39 times over the 53-day dosing period starting on 27 July 2004 (day 0). The control fish were fed with pellets that were treated identically to those containing PAHs, including $MeCl_2$ soaking. The length of time for dosing was patterned after several studies showing estuarine residence time for juvenile salmonids ranging up to 60 days before migration to open water (Healey 1991; Thorpe 1994). The PAHs provided to fish are considered the administered dose. The administered dose is the amount given to an organism, whereas the acquired dose is the amount found within the tissues. Although food was delivered to the water in each tank, all pellets were consumed and therefore considered as the administered or ingested dose.

This study consisted of one control and five treatments, each with four replicate tanks. The Fiberglas tanks were round with a diameter of 1.3 m and contained 500 L of sea-

Table 1. Measured doses of each polycyclic aromatic hydrocarbon (PAH) in the experimental diet.

		Dose (µg·g fish^{-1}·day^{-1})				
	Control	0.7	2.3	6.1	18	22.1
Naphthalene (NPH)	0.0016	0.018	0.049	0.12	0.28	0.34
2-Methylnaphthalene	0.0036	0.038	0.106	0.28	0.70	0.85
Dimethylnaphthalene	0.0094	0.057	0.161	0.40	1.11	1.34
Total naphthalenes	**0.0146**	**0.112**	**0.315**	**0.80**	**2.10**	**2.53**
Dibenzothiophene (DBT)	0.0019	0.036	0.113	0.28	0.85	1.02
Acenaphthene (ACE)	0.0004	0.021	0.066	0.18	0.49	0.60
Fluorene (FLU)	0.0004	0.087	0.283	0.79	2.27	2.83
1,8-Dimethyl(9H)fluorene	0.0004	0.002	0.007	0.02	0.05	0.07
Total fluorenes	**0.0009**	**0.089**	**0.290**	**0.81**	**2.32**	**2.90**
Phenanthrene (PHN)	0.0032	0.102	0.321	0.87	2.64	3.21
9-Ethylphenanthrene	0.0004	0.006	0.019	0.05	0.15	0.18
9-Ethyl-10-methylphenanthrene	0.0004	0.003	0.010	0.03	0.08	0.10
1-Methyl-7-isopropylphenanthrene	0.0004	0.002	0.007	0.02	0.06	0.07
Total phenanthrenes	**0.0045**	**0.11**	**0.36**	**0.96**	**2.93**	**3.55**
Anthracene (ANT)	nd	0.023	0.072	0.19	0.59	0.72
Fluoranthene (FLA)	0.0002	0.117	0.378	1.02	3.02	3.78
Pyrene (PYR)	0.0002	0.094	0.321	0.83	2.46	3.02
Methyl pyrene	0.0004	nd	nd	nd	0.003	0.003
Total pyrenes	**0.0006**	**0.094**	**0.321**	**0.83**	**2.46**	**3.03**
Benz[a]anthracene (BAA)	0.0004	0.032	0.111	0.28	0.91	1.15
Chrysene (CHR)	0.0005	0.057	0.185	0.49	1.53	1.89
Benz[a]pyrene (BaP)	0.0004	0.015	0.053	0.13	0.40	0.49
Benzo(k)fluoranthene (BKF)	0.0005	0.009	0.032	0.09	0.25	0.28
Benzo(g,h,i)perylene (BZP)	0.0004	0.002	0.007	0.02	0.06	0.07
Dibenzanthracene (DBA)	0.0003	0.003	0.009	0.02	0.07	0.09

Note: Each value is expressed in micrograms of PAH per gram of wet fish per day. Values in bold are totals for groups of PAHs. The top line is the summed dose for each treatment. nd is not detected.

water. The tanks were inside a building and arranged in a grid pattern. The flow-through seawater system provided 4 L·min^{-1} of sand-filtered and ultraviolet (UV) sterilized water to each tank. Fish were maintained at 10–11 °C for the entire experiment. At the end of the dosing period (17 September 2004), the fish were not fed for 3 days before samples were taken for bile, blood chemistry, and tissue concentrations on day 56. Fish were fed uncontaminated food once on day 56 (after sampling) to prevent starvation conditions, but not again before weighing. All fish were weighed individually on day 58 on a Sartorius 4000 balance to 0.1 g accuracy. Fish length was not analyzed in this study because we consider fish weight to be a more important variable for assessing growth impacts resulting from toxicant exposure. This is supported by a few studies noting that fish weight was more affected than fish length for salmonids exposed to toxicants (Moles and Rice 1983; Heintz et al. 2000).

Samples

Chemical analyses were conducted with composite samples or a combination of individual fish and composites. For all bile, whole-body lipid, and plasma chemistry analyses, each value was determined on a composite of three fish. Whole-body lipids for each treatment were determined for three individual fish from one of the blood chemistry composites in addition to the two composites (three fish each) used for PAH determination for a total of five values. Tissue moisture content was determined for two of the PAH chemistry composites, and each was analyzed in duplicate with two separate aliquots from each composite. In all cases, each composite sample was composed of three fish from a given tank. Three of the four replicate tanks per treatment were chosen at random to make up the three separate composites.

Blood chemistry

Blood plasma samples were analyzed using an automated blood chemistry analyzer (Idexx VetTest 8008 Chemistry Analyzer; IDEXX Laboratories, Inc., Westbrook, Maine). Eleven blood chemistry parameters were measured simultaneously for each plasma sample. A quality control procedure (Idexx Vetrol control lot number J00951101) was run before samples to verify both the VetTest optics groups and the integrity of the test slides.

Blood was taken from stunned juvenile Chinook salmon by transection of the caudal peduncle and direct transfer of blood to heparinized 1.3 mL sample vials (heparin grade 1-A, 25 000 units). When approximately 1 mL was collected from three fish (one composite replicate), samples were immediately centrifuged at 18 800 rpm for 150 s in a Statspin veterinary centrifuge (Iris Sample Processing, Norwood, Mass.). Plasma was transferred via pipette to a sample cup, which allowed for aliquots to be taken up with the VetTest auto pipette and injected into the machine. The minimum amount of sample required was 40 µL, which was used for initiation and the first parameter tested. Each additional parameter

Fig. 1. Percent occurrence of each polycyclic aromatic hydrocarbon (PAH) in stomach contents of field-collected Chinook salmon (*Oncorhynchus tshawytscha* (open bar)), and dosed fish pellets used in this experiment (shaded bar). Mean and standard error percentages (error bars shown) are for PAHs in stomachs of juvenile Chinook salmon collected from the Duwamish and Hylebos waterways near Seattle, Washington. Data are from Varanasi et al. (1993). Each value is the mean of 12 composite samples, each with 10 fish. Fish food PAHs are mean measured percentages for this study (no error bars). C1, C2, C3, and C4 designate the total number of carbons in the alkylated homologs. ACY, acenaphthylene; BBF, benzo[b]fluoranthene; INP, indenopyrene. See Table 1 for all other abbreviations. Bars for total NPH, FLU, DBT, PHN, PYR, and CHR show summed percentages for parent plus alkyl homologs. ANT was not measured in stomach contents.

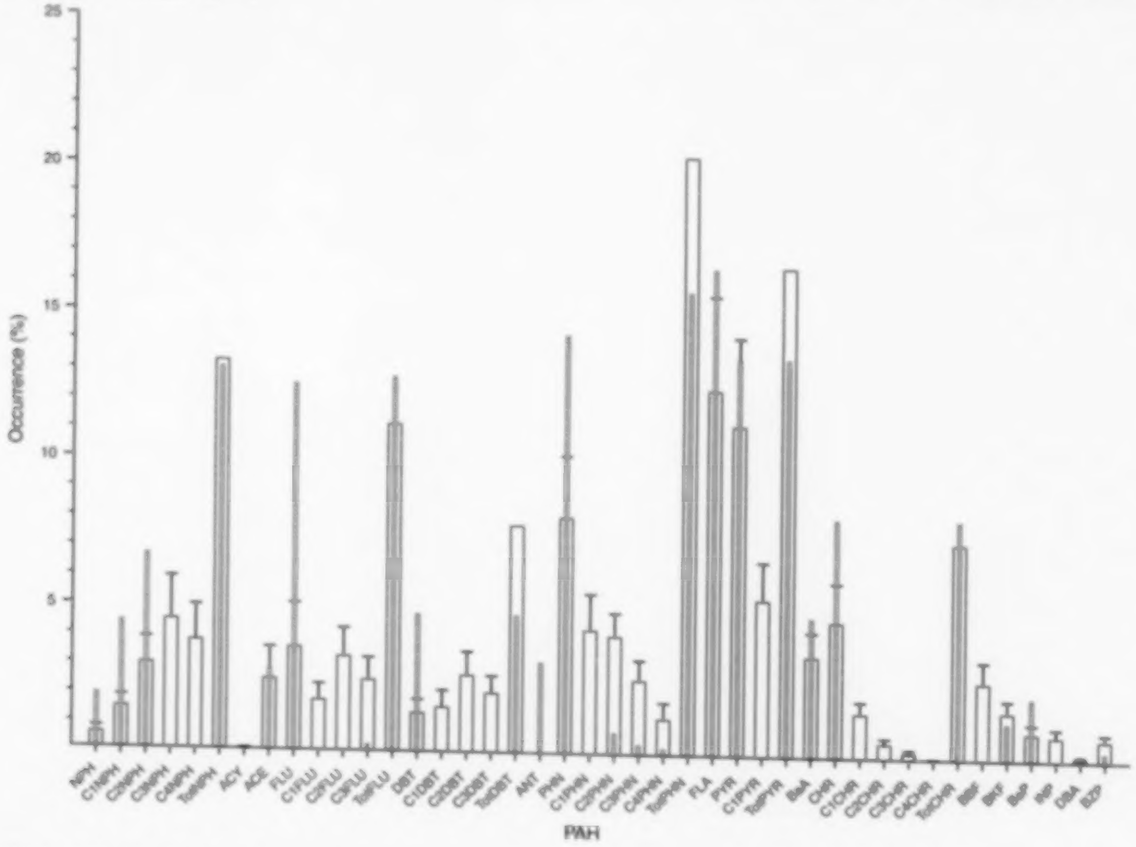

required 10 µL. The time lag between sampling plasma and analysis was less than 20 min. Blood plasma was analyzed for albumin (ALB), alanine aminotransferase (ALT), amylase (AMYL), calcium (CA), cholesterol (CHOL), creatinine (CREA), glucose (GLU), lipase (LIPA), inorganic phosphate (PHOS), total protein (TP), and triacylglycerols (TAG).

Lipid analysis for whole bodies

Whole-body fish were homogenized and analyzed for triacylglycerols (TAGs), cholesterol (CHOL), free fatty acids (FFA), sterol esters – wax esters (SE–WE), and polar lipids (PL). Total lipid concentrations (reported as percent total lipid) were calculated by summing the concentrations of the five lipid classes for each sample. Lipids were determined by a thin-layer chromatography – flame ionization detection (TLC–FID) method (Ylitalo et al. 2005) using an Iatroscan Mark 6 (Iatron Laboratories, Tokyo, Japan). In this method, fish whole bodies were mixed with sodium sulfate and magnesium sulfate and extracted with dichloromethane using an accelerated solvent extractor (Sloan et al. 2005). Various classes of lipids were separated based on polarity, with the nonpolar compounds eluting before the more polar lipids (e.g., phospholipids). Duplicate TLC–FID analyses were performed for each sample extract and the mean value was reported.

Whole-body PAHs and metabolites in fish bile

Composite bile samples of Chinook salmon were analyzed by high performance liquid chromatography (HPLC) for PAH metabolites as described in Krahn et al. (1986). Biliary fluorescent aromatic compounds (FACs) are determined by fluorescence at excitation/emission (ex/em) wavelength pairs. For this study we analyzed for biliary metabolites fluorescing at PHN (ex/em 260/380 nm) and BaP (ex/em 380/430 nm) wavelengths. Whole-body concentrations of PAHs were determined according to the methods of Sloan et al. (2005) using a gas chromatograph – mass spectrometer (GC–MS). Fish were not sampled for 3 days after the last dose to allow for gut purging. At the time of sampling, the stomach and alimentary canal were removed; however, it was difficult to assure total removal of these organs.

Because fish were not fed for 3 days before sampling for tissue concentrations, a large percentage of the PAHs were likely metabolized after the dosing period. From these data and the estimated half lives for selected PAHs found in the literature for salmonids (Niimi 1987; Niimi and Dookhran 1989), we calculated an expected whole-body tissue concentration for total PAHs (excluding metabolites) using eq. 1:

$$(1) \qquad [\text{tissue}_{t=0}] = [\text{tissue}_{t=\text{end}}]/e^{-k_2 T}$$

where $[\text{tissue}_{t=0}]$ and $[\text{tissue}_{t=\text{end}}]$ are the beginning and ending tissue concentrations, respectively, for the time period T and k_2 (elimination rate constant) = half live in days/0.693.

Analysis of treatment effects

Fish weights, wet to dry weight ratios, whole-body lipids, and blood chemistry were analyzed by analysis of variance (ANOVA). To test for effects on fish growth, an ANOVA was used to examine treatment differences based on mean fish weights for replicate tanks. To avoid pseudoreplication (Hurlbert 1984), the tank, not individual fish, was treated as the experimental unit. Therefore, replicate tanks in each treatment were not pooled and individual fish were not part of the statistical analysis. The hypothesis of equal variance among tank means (homoscedasticity) was tested with Levene's test. Simple linear regression was also conducted for several parameters as a function of dose.

The ANOVA is generally used to test for differences in treatment means. Performing only this test misses important information that characterizes the growth response in these treatments. Testing for differences in variance heterogeneity can be informative and useful as evidence for adverse effects (Green and Montagna 1996). To test for treatment differences caused by variability in fish weight resulting from PAH exposure, a second ANOVA was performed using tank standard deviation (SD) of fish weights. For this ANOVA, the SD was computed among fish within a tank. The hypothesis we tested was that treatment had no effect on the variability of weight among fish. As with testing for mean fish weight, tanks are the experimental units and each tank yielded a single observation, in this case, the SD of fish weight. This procedure is not an alternative to Levene's test, which examines equality of variances across experimental units, in this case replicate tank means.

All comparisons were considered significantly different from the control at the $\alpha = 0.05$ level. Additionally, a number of p values in the range of $0.05 < p \leq 0.15$ were noted because these low values indicate a substantial response. The α value to determine the level of significance is not a bright line separating significance from nonsignificance. For example, a p value of 0.1 indicates that there is only a 10% chance that the observed treatment effect or one more extreme (i.e., a larger difference between treatment means) would be obtained if there were indeed no treatment effect (a true null hypothesis). This low probably indicates that it is likely that the null hypothesis is not true. Based on this, we believe that these low p values ($p \leq 0.15$) provide a reasonable level of certainty for concluding that there are real treatment effects for many of these parameters.

Control versus treatment differences were determined with Fisher's protected least significant difference (PLSD) post-hoc test. Standard deviations were reported to show the range in the data, and the standard error of the mean (SEM, a statistic of the mean) was reported when comparisons of means were intended. Statistical analyses were conducted with SYSTAT (Systat Software Inc. 2004), JMP (SAS Institute Inc. 2004), and Statview (SAS Institute Inc. 1998).

Results

Chemistry

The measured concentrations in fish pellets were very close to nominal values. The mean (SD) for the ratio of observed to expected concentrations was 1.0 (0.08) for all five treatments. The percentage contribution of each compound in the experimental diet is shown along with the percentages found in stomach concentrations of field-collected fish (Fig. 1). For many PAHs, our measured percentages for pellets were very close to the percentages of PAHs in the stomach contents observed in field-collected fish. Because we could not obtain many of the alkylated homologs, we increased the amounts for some parent and alkyl compounds so that totals (e.g., TotNPH, TotFLU, TotPHN) were similar to the field values. The dose for each PAH is shown by treatment (Table 1), as are the total PAH concentration for fish pellets and total administered dose (as μg and $\text{nmol}\cdot\text{g fish}^{-1}\cdot\text{day}^{-1}$; Table 2). A few compounds were detected in control food, which resulted in an overall dose to fish of $0.026\ \mu\text{g}\cdot\text{g fish}^{-1}\cdot\text{day}^{-1}$.

Overall, whole-body tissue concentrations were very low (Table 2). Based on eq. 2 and an average half-life of 2 days for PAHs in salmonids, the concentrations of total PAHs measured in the whole body on day 56 would have been approximately three times higher if the sampling had been done immediately after the dosing period ended. This would lead to adjusted whole-body concentrations ranging from 0.06 to $2.3\ \mu\text{g}\cdot\text{g}^{-1}$ ww (0.4 to $12.4\ \text{nmol}\cdot\text{g}^{-1}$ ww) total PAHs (Table 2). The results for biliary FACs (Table 2) indicated a highly positive correlation with dose (PHN $r^2 = 0.98$ and BaP $r^2 = 0.97$). The proportional increases in biliary FACs over treatment indicate that fish in all treatments were consuming the dosed food, which was supported by behavioral observations.

Fish weights

Mean fish weight for each tank on day 0 (start of dosing) varied from 12.8 to 13.1 g ww (2.8 to 2.9 g dw) with an average SD of 1.5 g ww (0.31 g dw) (Table 3). The ANOVA using all individual fish weights on day 0 indicated that there were no differences among any of the tanks ($p = 0.99$). The post-hoc test (Fisher's PLSD) found no differences in mean weights between any of the tanks, when examined as pairwise comparisons for all tanks ($n = 276$; mean (SD) p value = 0.66 (0.21)). When replicate tanks were grouped by treatment, an ANOVA showed no difference between treatments ($p = 0.47$) for the day 0 mean weights (Table 3). The distribution is shown for day 0 fish by treatment ($n = 200$;

Table 2. Polycyclic aromatic hydrocarbons (PAHs) in food and fish tissue.

Treatment	Mortality (%)	Fish dose (µg [nmol]·g^{-1}·day^{-1})	Pellet concentration (µg [nmol]·g^{-1})	Whole-body concentration µg·g^{-1} (obs)	Whole-body concentration µg·g^{-1} (adj)	Whole-body concentration nmol·g^{-1} (adj)	Biliary FACs (µg·mg protein^{-1}) PHN	Biliary FACs (µg·mg protein^{-1}) BAP
Control	0	0.026 [0.15]	1 [7]	0.023	0.065	0.41	2.5 (0.3)	0.20 (0.03)
1	1.5	0.7 [3.9]	38 [210]	na	na	na	3.5 (0.1)	0.11 (0.02)
2	2.5	2.3 [12.3]	122 [650]	0.025	0.073	0.47	6.3 (0.6)	0.23 (0.03)
3	2.0	6.1 [32.7]	324 [1730]	0.13 (0.10)	0.38 (0.28)	2.1 (1.5)	11.7 (1.2)	0.25 (0.02)
4	0	18.0 [95.2]	951 [5040]	0.81 (0.46)	2.3 (1.3)	12.4 (7.0)	35.8 (5.5)	0.72 (0.11)
5	0	22.1 [117.1]	1171 [6200]	0.67 (0.25)	1.9 (0.73)	9.9 (3.5)	36.8 (8.2)	0.85 (0.14)

Note: Dose is expressed in µg [nmol] total PAH·g wet fish^{-1}·day^{-1} that was ingested. Pellet concentration is the observed dry weight concentration of total PAHs for fish pellets. Observed (obs) whole-body PAH concentrations shown for day 56 along with the metabolism adjusted (adj) concentrations (µg·g^{-1} and nmol·g^{-1}). Whole-body concentration is the mean and standard error of the mean (SEM) concentration (wet weight) of total PAHs measured in one or two composites (n = 3 fish·composite^{-1}). Biliary FACs (fluorescent aromatic compounds) are the mean (SEM) phenanthrene (PHN) and benzo[a]pyrene (BaP) equivalents in bile (µg·mg protein^{-1}). na, not analyzed.

Fig. 2), which are expressed as dry weights using the wet to dry weight ratio for our control fish (Table 3).

The ANOVA for mean fish wet weight (by tanks) at the end of the experiment (day 58) was highly significant, with a p value of <0.0001. Based on Levene's test (p = 0.16), the null hypothesis of equal variances was accepted. A Fisher's PLSD post-hoc test determined that only the 22.1 µg·g fish^{-1}·day^{-1} treatment was significantly lower than the control (p = 0.0009); however, the mean weight for the 18.0 µg·g fish^{-1}·day^{-1} treatment was substantially reduced (p = 0.17) (Table 3). When dry weights were considered, an ANOVA determined that the two highest treatments (4 and 5) exhibited significantly lower weights (p < 0.0001 and p = 0.01, respectively) (Table 3) when compared with the control.

An analysis of the moisture content of fish from each treatment revealed an increasing trend with treatment concentration on day 58. An ANOVA determined that fish from the two highest doses exhibited substantially elevated ratios of wet weight to dry weight compared with the control fish (p = 0.16 and p = 0.04 for the 18.0 and 22.1 µg·g fish^{-1}·day^{-1} treatments, respectively). Because of the extensive randomization during the experiment setup, there was no reason to suspect differences in ratios of wet weight to dry weight among treatments on day 0. This ratio was determined instead of moisture content because it is a useful multiplier for interconverting between wet and dry weight concentrations.

Although only the two highest doses produced significant reductions in overall fish weight, considerable variability among experimental units (tanks) occurred in all PAH treatments. The ANOVA using tank SD as an indicator of variability in fish weights was significantly different (overall ANOVA p = 0.0098). The result of Levene's test for this ANOVA was not significant (p = 0.9), indicating equal variances. Pairwise comparison of treatments with Fisher's PLSD determined that all control versus treatment comparisons were significantly different (Table 3) because the variability among replicate tanks was higher for each treatment compared with the control. An ANOVA using tank SD was conducted for day 0 fish weights and was not significant (p = 0.75).

Another indication of the increased variability for the day 58 fish is evident in Fig. 2. The cumulative distributions show that all treatments contained fish that were smaller than those in the control tanks when the lower percentiles were considered but were as large or larger in the higher percentile groups. Statistical tests were run for several percentile groups (Table 4), and the results show generally lower weights for those percentiles below the median and higher weights in the upper percentiles. In general, fish in the upper percentiles (e.g., 75th and 95th) of most treatments (except 22.1 µg·g fish^{-1}·day^{-1}) were larger than control fish. Treatment 3 (6.1 µg·g fish^{-1}·day^{-1}) stands out with a significant increase in fish weight for the 95th percentile fish. Also shown is the treatment variance (Table 3), which was determined using the data for all individual fish from a treatment (n ~ 200).

Whole-body lipids

Whole-body lipid content in our control fish was very similar to values observed in wild (and some hatchery) juve-

Table 3. Summary statistics for fish weights.

		Day 0	Day 58				
Treatment	Dose	Mean tank wet weight	Mean tank wet weight	Mean tank dry weight	Mean tank SD (dry weight)	Treat Var	Wet:dry
Control		13.1 (0.10)	27.6 (0.36)	6.18 (0.08)	0.91 (0.06)	0.85	4.47 (0.05)
1	0.7	13.1 (0.07)	28.2 (0.07)	6.15 (0.02)	**1.09** (0.04)	1.1	4.59 (0.04)
2	2.3	12.8 (0.07)	26.9 (0.55)	5.95 (0.12)	**1.19** (0.09)	1.41	4.53 (0.15)
3	6.1	12.9 (0.19)	28.3 (0.64)	6.20 (0.14)	**1.10** (0.07)	1.25	4.47 (0.09)
4	18.0	13.0 (0.17)	26.3 (0.77)	**5.63** (0.17)	**1.28** (0.05)	1.56	4.67 (0.04)
5	22.1	13.0 (0.17)	**22.3** (1.0)	**4.66** (0.21)	**1.09** (0.04)	1.16	**4.80** (0.17)

Note: Dose is expressed in µg total polycyclic aromatic hydrocarbons (PAHs)·gram wet fish^{-1}·day^{-1}. Table shows the mean fish weight for day 0 (wet weight) and day 58 (dry and wet weight) in addition to the mean tank standard deviation (SD) on day 58 (dry weight only) for each treatment (n = 4 experimental units per treatment). Treat Var shows the variance for all individual fish weights in a treatment (all tanks combined, n ~ 200 fish). Analysis of variance was conducted for each, except Treat Var. Wet:dry is the ratio of fish wet weight to dry weight. All bold values were significantly different from the control at α = 0.05. Most values are presented as mean with standard error of the mean (SEM) in parentheses.

Fig. 2. Cumulative frequency distribution of fish weights by treatment. Plots are shown for day 0 and day 58 (end of experiment). All fish from a treatment were combined for each line (n ~ 200). All treatments are shown for day 0, which occur on the left side of the figure. Day 0 wet weights were converted to dry weights by a constant factor of 0.22.

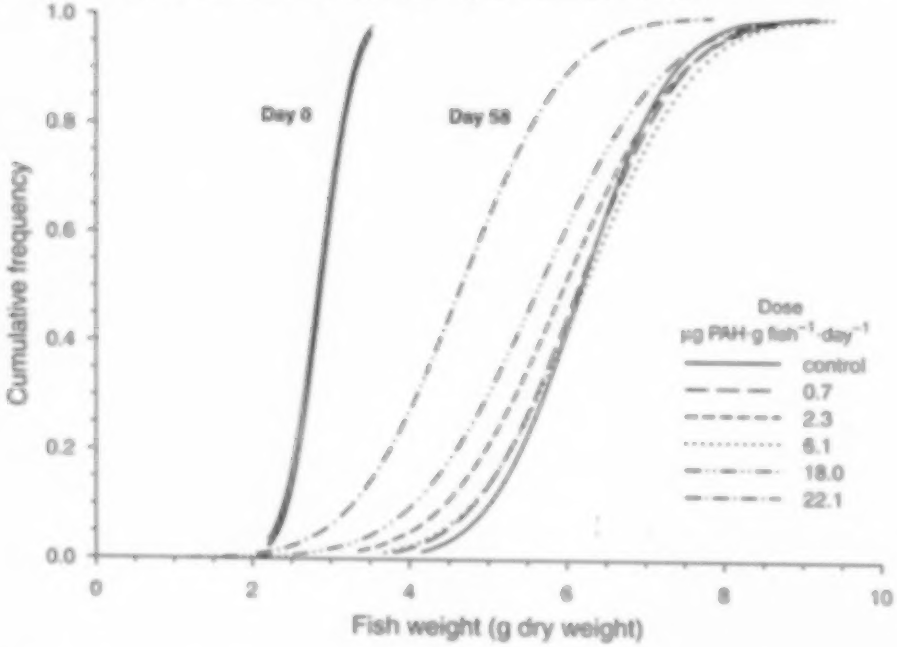

nile Chinook salmon at this life stage (11.2% dry weight = 2.5% wet weight) (Meador et al. 2002). Whole-body lipids generally follow the same pattern as that seen for fish weights. Based on ANOVA, the two highest doses exhibit significant reductions in whole-body lipids and triacylglycerols (Table 5). Other noteworthy values are for CHOL and SE–WE for the 6.1 µg·g fish^{-1}·day^{-1} dose and the general downward trend for TAGs in all PAH treatments (Table 5). No trend was observed for whole-body CHOL. Also, the large increase in free fatty acids and elevated cholesterol for the 6.1 µg·g fish^{-1}·day^{-1} treatment are responsible for the boost in total lipid (TotLip). Significant regression equations were observed for total lipid and TAG in whole body, which were best fit by linear equations. TAG = 49.86 – 1.59Dose, r^2 = 0.73, p = 0.018. TotLip = 11.0 – 0.242Dose, r^2 = 0.49, p = 0.07. Without the 6.1 µg·g fish^{-1}·day^{-1} dose, TotLip = 10.19 – 0.229Dose, r^2 = 0.89, p = 0.01.

Plasma chemistry

Plasma lipids exhibited similar results to those observed for whole-body lipids (Table 6). A declining trend was observed over all treatments for both CHOL and TAGs in plasma, and linear regression equations were the best fit for each. The regression equations are TAG = 107.1 – 2.37Dose, r^2 = 0.72, p = 0.02, and CHOL = 119.4 – 2.24Dose, r^2 = 0.96, p = 0.0004. Several noteworthy patterns were seen in the other blood chemistry parameters analyzed, many significantly different from the control. A declining trend was

Table 4. Fish weights by percentile.

Dose	5th	10th	25th	50th	75th	95th
Control	4.72 (0.17)	5.00 (0.23)	5.55 (0.11)	6.16 (0.08)	6.76 (0.10)	7.71 (0.12)
0.7	4.53 (0.11)	4.78 (0.13)	5.35 (0.03)	6.10 (0.04)	6.93 (0.06)	7.82 (0.03)
2.3	4.34 (0.19)	*4.52* (0.22)	**4.98** (0.24)	5.84 (0.22)	6.85 (0.10)	7.87 (0.10)
6.1	4.51 (0.12)	4.91 (0.09)	5.51 (0.15)	6.06 (0.18)	6.90 (0.18)	**8.18** (0.22)
18.0	**3.71** (0.38)	**4.18** (0.23)	**4.90** (0.11)	**5.56** (0.14)	*6.37* (0.21)	7.84 (0.20)
22.1	**3.17** (0.12)	**3.35** (0.14)	**3.96** (0.19)	**4.66** (0.24)	**5.30** (0.27)	**6.41** (0.23)

Note: Dose is expressed in µg total polycyclic aromatic hydrocarbons (PAHs)·g wet fish^{-1}·day^{-1}. Values are presented as mean fish dry weight (grams) with standard error of the mean (SEM) in parentheses for all four replicate tanks per treatment. All bold values were significantly different from the control at $\alpha = 0.05$. Italicized values indicate $0.05 < p \leq 0.15$. Each Levene's test was not significant.

Table 5. Whole-body lipids.

Dose	Total lipid (%)	TAG	FFA	CHOL	PL	SE–WE
Control	11.2 (1.2)	58.6 (17.1)	31.7 (14.7)	15.9 (2.2)	5.2 (0.9)	0.35 (0.25)
0.7	9.8 (1.5)	49.9 (17.3)	27.0 (13.0)	16.9 (2.5)	3.8 (0.6)	0.40 (0.26)
2.3	8.7 (2.2)	32.9 (13.4)	28.8 (12.9)	20.0 (4.1)	4.9 (1.1)	0.35 (0.15)
6.1	12.9 (2.0)	43.4 (8.9)	53.8 (12.0)	**25.4** (4.7)	5.6 (1.3)	**1.1** (0.38)
18.0	**6.8** (1.5)	**20.5** (9.2)	25.4 (11.3)	16.4 (2.1)	5.2 (0.7)	0.43 (0.26)
22.1	**4.9** (1.3)	**16.5** (11.3)	14.0 (7.3)	14.7 (1.4)	3.4 (0.9)	0.46 (0.19)

Note: Dose is expressed in µg total polycyclic aromatic hydrocarbons (PAHs)·g wet fish^{-1}·day^{-1}. Values are presented as mean with SEM in parentheses for all five samples per treatment (six for control). TAG, triacylglycerols; FFA, free fatty acids; CHOL, cholesterol; PL, polar lipids; SE–WE, sterol esters and wax esters. Total lipids are expressed as percent of dry weight; all others are expressed in mg·g dry weight^{-1}. Bold values are significantly different from the control at $\alpha = 0.05$. Each Levene's test for these variables was not significant.

Table 6. Plasma chemistry.

	Treatment					
Blood chemistry	Control	0.72	2.3	6.1	18.0	22.1
Albumin (g·dL^{-1})	0.38 (0.07)	*0.20* (0.06)	**0.12** (0.06)	*0.16* (0.09)	**0.12** (0.07)	*0.13* (0.10)
ALT (U·L^{-1})	25.3 (6.3)	26.7 (3.3)	30.3 (6.9)	30.3 (12)	21.7 (6.9)	16.3 (1.3)
Amylase (U·L^{-1})	599 (14)	561 (19)	*526* (48)	614 (42)	568 (17)	**507** (27)
Calcium (mg·dL^{-1})	12.1 (0.2)	11.6 (0.5)	11.6 (0.4)	12.1 (0.07)	11.7 (0.17)	*11.3* (0.5)
Cholesterol (mg·dL^{-1})	125 (11)	118 (10)	110 (2)	*104* (3)	**79** (7)	**72** (14)
Creatinine (mg·dL^{-1})	0.15 (0.02)	0.17 (0.04)	0.22 (0.03)	0.20 (0.03)	0.20 (0.05)	**0.29** (0.03)
Glucose (mg·dL^{-1})	79 (2.9)	77 (3.2)	79 (5.4)	79 (2.1)	**64** (1.1)	**65** (4.0)
Lipase (U·L^{-1})	74 (12.5)	*44.7* (11.5)	**32.3** (5.3)	**30.7** (8.8)	**30.7** (21.1)	**11.0** (11.0)
PHOS (mg·dL^{-1})	13.1 (0.3)	13.0 (0.5)	12.9 (0.5)	13.2 (0.14)	12.4 (0.4)	*11.8* (0.5)
Total protein (g·dL^{-1})	3.1 (0.11)	2.7 (0.08)	2.7 (0.14)	2.7 (0.13)	2.6 (0.3)	2.5 (0.5)
Triacylglycerols (mg·dL^{-1})	122 (13)	105 (14)	**81** (10)	95 (10)	**72** (8)	**52** (30)

Note: Mean and standard error of the mean (SEM) in parentheses for various parameters measured in blood plasma. Treatments are expressed in µg polycyclic aromatic hydrocarbon (PAH)·g wet fish^{-1}·day^{-1}. Composite samples ($n = 3$) are from different replicate tanks and each contained plasma from three fish. Bold values are statistically different from the control at $\alpha = 0.05$. Italicized values show those parameters that exhibited a p value between 0.05 and 0.15. ALT, alanine transaminase; PHOS, inorganic phosphate; U·L^{-1}, units per liter; dL, deciliter. None of the Levene's tests for these variables was significant.

generally observed for albumin, amylase, and lipase over PAH treatments; however, other blood parameters were relatively constant across treatments, declining only at the highest doses (ALT, phosphorus, and glucose) (Table 6). Only creatinine exhibited an increasing trend with dose (Table 6). Because the post-hoc power ranged from 0.2 to 0.5 for these ANOVAs, there was a higher probably of type II error, meaning that there was an increased likelihood of false negatives (i.e., accepting the null hypothesis of no treatment effect when in fact there is an effect). With additional statistical power, these parameters would have likely exhibited much lower p values. Even with low power, several parameters exhibited low p values (0.05–0.15) that were considered noteworthy because of the trend observed for other doses (Table 6). Significant regression equations were observed for albumin and lipase, which were best fit with an inverse first-order polynomial:

$$\text{albumin} = 0.144 + (0.0047/\text{Dose}),\ r^2 = 0.89,\ p = 0.003$$

$$\text{lipase} = 29.44 + (0.898/\text{Dose}),\ r^2 = 0.69,\ p = 0.025$$

Discussion

PAH concentrations

The PAH concentrations tested here were environmentally realistic because of the similar proportions and magnitude of individual compounds observed in stomach contents for juvenile Chinook salmon in contaminated estuaries. This is based on the data in Varanasi et al. (1993) showing a median stomach contents concentration of 23.8 µg total PAH·g^{-1} ww (range 3–365 µg·g^{-1} ww) for 12 composite samples (each with 10 fish) from two contaminated estuaries around Puget Sound, Washington. When based on this median concentration, the dose for field-collected fish would translate to approximately 3.8 µg total PAH·g fish^{-1}·day^{-1}, which is comparable to our middle dose. This dose was determined with the data from Varanasi et al. (1993) for mean fish weight (7 g) and PAHs in stomach contents, in addition to published growth rates of 3%–5%·day^{-1} (Healey 1980; Weatherley and Gill 1995) for this life stage. The growth rates reported by these authors for Chinook salmon and the reported food conversion efficiency for ingested prey of ~25% (Weatherley and Gill 1995) would imply an average consumption rate of 16% body weight·day^{-1} (based on wet weights), or more, for many salmonids (Weatherley and Gill 1995). In our study, the food conversion efficiency was 23% for the control fish.

The doses calculated above are based on dietary exposure only. Concentrations of PAHs in water also need to be considered when calculating the dose. For many species that have high ventilation rates, such as salmonids, a substantial dose can be obtained with relatively low water concentrations. Water concentrations of PAHs in the low parts-per-billion range, which are not unusual in urban environments and oil spills (Eisler 2000), can lead high doses of PAHs in fish (micrograms of total PAH per gram fish per day) (J.P. Meador, unpublished data). Therefore, it is necessary to consider both dietary and ventilatory sources for determination of dose to salmonids and other species of fish.

The PAH profile for the dosed food was very similar to that observed for PAHs in stomach contents from field-collected fish when most compounds and major classes were considered. Many of the compounds found in stomach contents were not represented in the dosed food. The missing compounds included many of the alkylated PAHs, which comprised from 12% to 88% (mean (SEM) = 48.5% (7.5%)) of the total PAH concentration in stomach contents from juvenile Chinook salmon residing in two different urban estuaries (Varanasi et al. 1993). Because the alkylated PAHs are generally more persistent and toxic than their parent compound (Irwin et al. 1997; Jonsson et al. 2004), our doses (mean alkylated component of 16%) likely underestimated the effects that would be observed in the fish from urban estuaries exposed to dietary PAHs with a higher percentage of alkylated homologs.

The expected concentrations for total whole-body PAHs indicate that more than 99% of the assimilated PAHs were metabolized. Based on the PAH values presented here and the high elimination rates determined by Niimi and Dookhran (1989), these adjusted values are likely close to the maximum that would be observed for this exposure. This implies that the observed adverse responses occurred at very low tissue concentrations. As seen in the results section, whole-body tissue concentrations at low exposure concentrations provide very little information regarding toxic exposure to PAHs. A better approach may be to assess PAH toxicity in fish based on throughput (micrograms of PAH per gram fish per day) or biliary FACs, which shows promise as a metric for PAH exposure in salmonids.

Fish growth

Although the ANOVA and post-hoc tests for mean dry weight determined significant reductions only for the two highest doses, evidence of altered growth on day 58 was observed in most treatments with the distribution plots, ANOVA with SDs, and ANOVA of dry weight by percentile. The observation that fish dry weight was a more accurate indicator of reduced growth and adverse effects is an important observation for the higher doses in this study. In general, the moisture content increased with increasing dose, which was likely due to altered lipid metabolism (Navarro and Gutierrez 1995). At the highest doses (18 and 22.1 µg·g fish^{-1}·day^{-1}), the reduction in mean weight compared with that of control fish was magnified when dry weight was considered. This observation is noteworthy because the higher moisture content indicates that these fish would exhibit a lower energy content per gram wet weight, which is important physiological information that would not be readily apparent if wet weights were considered.

We consider the significant ANOVA using standard deviations and the post-hoc tests showing significant differences for each treatment compared with the control an important result. Although no significant differences in mean fish weights were observed for the low doses, the observed variability and general trend of small fish below the median and larger fish above the median is noteworthy. If exposure had continued for a longer period of time, it is likely that fish from these treatments would have further diverged from the control fish, leading to significant differences in growth. As noted by Green and Montagna (1996), heterogeneity of variance can be an indicator of impact. A very similar experiment in our lab with a different toxicant was also analyzed by ANOVA with SDs, and no significant differences were observed (J.P. Meador, unpublished data), indicating that PAHs are potent inhibitors of metabolic pathways relating to organismal growth.

Comparison to other studies

Only a few studies have examined the toxicity of PAHs to fish from dietary sources and the results are mixed. Wu et al. (2003) examined several responses to dietary exposure of one PAH, benzo[a]pyrene, and concluded that their high dose of 12 µg·g fish^{-1}·day^{-1} did not affect growth or metabolic processes related to growth for the grouper *Epinephelus areolatus*. Another feeding study exposed polychaetes to creosote-contaminated sediment and then fed these worms to juvenile English sole (*Parophrys vetulus*; ~1 g ww) (Rice et al. 2000). In one experiment from that study, fish exposed to a dose of 0.12 µg total PAH·g fish^{-1}·day^{-1} exhibited a significant reduction in growth rate that was 10-fold lower than the observed rate for control fish (Rice et al. 2000; C. Rice, NOAA Fisheries, 2725 Montlake Blvd. East, Seattle, WA 98112, USA, personal communication, 2006). Another dietary study by Carls et al. (1996) examined the responses in pink salmon (*O. gorbuscha*) exposed to oil-contaminated food. These authors reported growth inhibition at their lowest dose of 0.14 μg PAHs·g fish^{-1}·day^{-1}, which is based on the published data and data from M. Carls (NOAA Fisheries, Auke Bay Laboratory, 11305 Glacier Highway, Juneau, AK 99801, USA, personal communication, 2006).

In another study on Chinook salmon, Palm et al. (2003) fed PAH-dosed pellets to juvenile fish for 28 days and reported no effects on growth. The doses in that study (approximately 0.33, 1.3, and 5 μg·g fish^{-1}·day^{-1}) were similar to our low and midrange doses. The methods in Palm et al. (2003) differed substantially from those in our experiment in that no alkylated PAHs were included, a limited subset of fish were weighed, the exposure period was substantially shorter, and no attempt was made to start the experiment with statistically indistinguishable experimental units with low variance.

A field study (Willette 1996) found a significant decrease in growth for pink salmon that were released in moderately oiled areas compared with those released in a lightly oiled area. This reduction in growth was associated with an increase in cytochrome P4501A, which is used as an indicator of PAH exposure. This study ruled out prey density, prey abundance, and feeding rate as possible causes of reduced growth. Willette (1996) concluded that the reduction in growth was likely the cause of the observed reduction in survival to adulthood for these fish.

Plasma chemistry

Several of the blood chemistry parameters for our control fish were in the same range as those reported for migrating juvenile Chinook salmon by Wagner and Congleton (2004). These included lipase, total protein, TAGs, calcium, and total phosphorus. For example, the mean lipase values for our control fish (74 U·L^{-1}) were very similar to the values observed in migrating juvenile Chinook salmon (64–93 U·L^{-1}) (Wagner and Congleton 2004). A few parameters (glucose, cholesterol, and ALT) were lower in our control fish compared with the observed values in that study. Downward trends for cholesterol, TAGs, and lipase are all indicative of impairment to the pathways involved with lipid storage and utilization. Because several of these parameters are interrelated, many are expected to be altered. For example, albumin functions as a transport protein for free fatty acids in the blood stream (Tocher 2003) and will exhibit decline during starvation (Mommsen 1998; Wagner and Congleton 2004).

Very few studies have examined the effects of PAHs on fish by measuring parameters in blood plasma. A review by Folmar (1993) reported only two studies that had examined plasma chemistry as a result of PAH exposure and both had studied English sole. This review also lists control values for several serum and plasma parameters; however, very few values for salmonids are reported. As seen in the review by Folmar (1993), the responses of blood chemistry parameters to toxicant exposure are quite varied. This is no doubt a result of differences among researchers using a variety of tests, life stages, and exposure times. Additionally, the variability in mechanism of action among the different toxicants will elicit increases in some parameters and declines in others. The results presented here are from one time point, which does not capture the potential dynamics of increases and decreases in blood chemistry parameters. Relative responses of the metabolic system to short-term exposure are expected to produce the pattern in blood chemistry parameters seen in our study, whereas longer-term exposure that results in tissue damage would likely produce increases in several blood parameters, especially enzymes.

Physiological condition and implications for the population

The high values for mean fish weight, fish weight by percentile, and total lipid for the 6.1 μg·g fish^{-1}·day^{-1} dose imply hormesis, which is defined as low dose stimulation (Calabrese and Baldwin 2003). Based on these parameters, it appears that fish in this treatment were in better health than the control fish. Examination of other parameters, such as lipid classes and plasma chemistry, indicate that fish from this treatment were strongly affected by PAHs and were not resistant to the toxic effects. The metrics that indicated no toxic effects were likely enhanced by physiological parameters (e.g., mobilized TAGs) or a shift in energy allocation that allowed a boost in growth that would likely not persist over time.

For the PAH-dosed fish, several of the lipid and blood chemistry parameters were depressed and exhibited similar patterns to those observed in fish undergoing starvation. For example, a number of studies report a reduction in lipids, glucose, lipase, and albumin in plasma, in addition to whole-body lipids, in salmonids that have been subjected to fasting (Navarro and Gutierrez 1995; Mommsen 1998; Krogdahl et al. 1999). In this experiment, many of these starvation-like alterations in physiology occurred even though these fish consumed all food supplied to them.

The proximal cause(s) of the starvation-like physiological parameters from PAH exposure in these juvenile Chinook salmon is not known. The physiological and biochemical factors that control and regulate growth and metabolism are diverse and only partially understood (Mommsen 1998). The enzyme lipase may be a key component for this "toxicant-induced" starvation syndrome. Several forms of lipase are known (Mommsen 1998; Tocher 2003) and these are regulated by transcription or phosphorylation. The enzyme responsible for triacylglycerol mobilization is hormone-sensitive lipase (HSL) (Tocher 2003). Under conditions of starvation, the activity of most forms of lipase is severely reduced (70%–90%) (Mommsen 1998).

Although the actual toxic mechanism(s) is not known, it is likely that these toxicants are acting on one or more components creating a cascade of interrelated abnormal physiological responses leading to toxicant-induced starvation. One hypothesis is that some or all of the PAHs absorbed from the diet are affecting lipase via the aryl hydrocarbon receptor (AhR). One study has shown that 2,3,7,8-tetrachlorodibenzo-*p*-dioxin (TCDD) and some PCB congeners reduce lipase activity as a result of interaction with the AhR and may be responsible for TCDD-induced "wasting syndrome" (Olsen et al. 1998). PAHs are also well-known agonists of the AhR (Varanasi et al. 1989) and may affect lipase activity via the

AhR. Barron et al. (2004) have published fish potency factors (FPF) for PAHs based on their function as AhR agonists, which are based on toxic equivalent factors (TEFs) indexed to TCDD potency.

The reduction in fish size and altered physiological parameters have important ramifications for survival of juvenile salmonids (Burrows 1969; West and Larkin 1987; Beamish and Mahnken 2001) and other species of fish (Cowan et al. 2000). A critical period in the salmonid life cycle occurs during their first winter in lakes, streams, or the marine environment. For many salmonid species, prey availability is greatly reduced during the winter months (Cooney et al. 2001) and fish often need to survive on lipid reserves. Additionally, predation is an important factor for first-year survival, which has been shown to be a function of size. According to Beamish and Mahnken (2001), juvenile salmon that do not attain a critical size during their first summer do not survive the winter.

Reduced lipid stores, which often occur in salmonids during winter months (Gardiner and Geddes 1980; Biro et al. 2004), can directly affect survival. For example, Burrows (1969) found that juvenile fall-run Chinook salmon with a lipid content of 4.1% (wet weight) exhibited a return rate to the hatchery that was approximately half of that for fish with a lipid content of 7.9%. As shown by Biro et al. (2004), the critical lipid level for *O. mykiss* is approximately 1% wet weight (≈5% dry weight), which was determined in lab and field studies. Below this critical level, mortality was very high. This value is supported by Finstad et al. (2004), who determined a critical body energy level of approximately 4400–4800 joules·g^{-1} for winter survival of Atlantic salmon, which translates to a TAG value of approximately 23 mg·g^{-1} dw. Some of the whole-body lipid and TAG values measured in our fish were at or below these critical levels determined by Biro et al. (2004) and Finstad et al. (2004).

The combination of reduced size and lipid content are critical for first year fish. For example, MacFarlane and Norton (2002) demonstrated a large increase in growth rate and a concomitant decline in TAGs when juvenile Chinook salmon exited the estuary to the open ocean. These high growth rates are likely beneficial to juvenile fish by decreasing predation and increasing their success for taking prey; however, they depend on ample prey for lipid accumulation before the winter months of low productivity. If juvenile fish exit the estuary with reduced lipid reserves, they will likely be unable to increase their growth rate and will be more susceptible to predation and less able to catch prey.

Based on the data from Biro et al. (2004) and Finstad et al. (2004), the rate of mortality for fish from our two highest treatments (18.0 and 22.1 μg·g fish^{-1}·day^{-1}) would likely approach 100%. Additionally, Biro et al. (2004) demonstrated that even small differences in fish size and lipid content led to increased mortality over winter months. Because of the reduction in size and lipid content observed for many of the fish in our experiment, especially from the lower percentiles, an increased probability for mortality would be expected for their first winter over that predicted for control fish. An increase in mortality for juvenile fish exposed to relatively low levels of PAHs would be an important stress for those populations that already experience myriad habitat alterations.

Acknowledgements

We gratefully acknowledge the following people for assistance with this study: Tiffany Linbo and O. Paul Olson for help with sample collection and Karl Shearer and Lyndal Johnson for their thorough and thoughtful review of this manuscript. We extend a special thanks to Stuart Hurlbert, Michael Paine, and Susan Picquelle for statistical advice and for recommending the ANOVA with standard deviations procedure.

References

Barron, M.G., Heintz, R., and Rice, S.D. 2004. Relative potency of PAHs and heterocycles as aryl hydrocarbon receptor agonists in fish. Mar. Environ. Res. **58**: 95–100.

Beamish, R.J., and Mahnken, C. 2001. A critical size and period hypothesis to explain natural regulation of salmon abundance and the linkage to climate and climate change. Prog. Oceanogr. **49**: 423–437.

Beckman, B.R., Larsen, D.A., Sharpe, C., Lee-Pawlak, B., Schreck, C.B., and Dickhoff, W.W. 2000. Physiological status of naturally reared juvenile spring chinook salmon in the Yakima River: seasonal dynamics and changes associated with smolting. Trans. Am. Fish. Soc. **129**: 727–753.

Biro, P.A., Morton, A.E., Post, J.R., and Parkinson, E.A. 2004. Over-winter lipid depletion and mortality of age-0 rainbow trout (*Oncorhynchus mykiss*). Can. J Fish. Aquat. Sci. **61**: 1513–1519.

Brett, J.R. 1995. Energetics. *In* Physiological ecology of Pacific salmon. *Edited by* C. Groot, L. Margolis, and W.C. Clarke. UBC Press, Vancouver, B.C. pp. 3–68.

Burrows, R.E. 1969. The influence of fingerling quality on adult salmon survivals. Trans. Am. Fish. Soc. **98**: 777–784.

Calabrese, E.J., and Baldwin L.A. 2003. Hormesis: the dose-response revolution. Annu. Rev. Pharmacol. Toxicol. **43**: 175–97

Carls, M.G., Holland, L., Larsen, M., Lum, J.L., Mortensen, D.G., Wang, S.Y., and Wertheimer, A.C. 1996. Growth, feeding, and survival of pink salmon fry exposed to food contaminated with crude oil. Am. Fish. Soc. Symp. **18**: 608–618.

Cooney, R.T., Allen, J.R., Bishop, M.A., Eslinger, D.L., Kline, T., Norcross, B.L., McCroy, C.P., Milton, J., Olsen, J., Patrick, V., Paul, A.J., Salmon, D., Scheel, D., Thomas, G.L., Vaughan S.L., and Willette, T.M. 2001. Ecosystem controls of juvenile pink salmon (*Oncorhynchus gorbuscha*) and Pacific herring (*Clupea pallasi*) populations in Prince William Sound, Alaska. Fish. Oceanogr. **10**(Suppl. 1): 1–13.

Cowan, J.H., Rose, K.A., and DeVries, D.R. 2000. Is density-dependent growth in young-of-the-year fishes a question of critical weight? Rev. Fish Biol. Fish. **10**: 61–89.

Eisler, R. 2000. Polycyclic aromatic hydrocarbons. *In* Handbook of chemical risk assessment: health hazards to humans, plants, and animals. Vol 2. Organics. Lewis Publishers Inc., Boca Raton, Fla. pp. 1343–1411.

Finstad, A.G., Ugedal, O., Forseth, T., and Næsje, T.F. 2004. Energy-related juvenile winter mortality in a northern population of Atlantic salmon (*Salmo salar*). Can. J. Fish. Aquat. Sci. **61**: 2358–2368.

Folmar, L.C. 1993. Effects of chemical contaminants on blood chemistry of teleost fish: a bibliography and synopsis of selected effects. Environ. Toxicol. Chem. **12**: 337–375.

Gardiner, W.R., and Geddes, P. 1980. The influence of body composition on the survival of juvenile salmon. Hydrobiologia, **69**: 67–72.

Green, R.H., and Montagna, P. 1996. Implications for monitoring: study designs and interpretation of results. Can. J. Fish. Aquat. Sci. **53**: 2629–2636.

Healey, M.C. 1980. Utilization of the Nanaimo River estuary by juvenile chinook salmon, *Oncorhynchus tshawytscha*. Fish. Bull **77**: 653–668.

Healey, M.C. 1991. Life history of chinook salmon (*Oncorhynchus tshawytscha*). *In* Pacific salmon life histories. *Edited by* C. Groot and L. Margolis. UBC Press, Vancouver, B.C. pp. 313–393.

Heintz, R.A., Rice, S.D., Wertheimer, A.C., Bradshaw, R.F., Thrower, F.P., Joyce, J.E., and Short, J.W. 2000. Delayed effects on growth and marine survival of pink salmon, *Oncorhynchus gorbuscha*, after exposure to crude oil during embryonic development. Mar. Ecol. Prog. Ser. **208**: 205–216.

Hurlbert, S.H. 1984. Pseudoreplication and the design of ecological field experiments. Ecol. Monogr. **54**: 187–211.

Irwin, R.J., Van Mouwerik, M., Stevens, L., Seese, M.D., and Basham, W. 1997. Entry on alkyl PAHs (alkyl homologs of PAHs). Environmental contaminants encyclopedia. National Park Service, Water Resources Division, Fort Collins, Colorado. *Available from* http://www.nature.nps.gov/hazardssafety/toxic/index.cfm.

Jonsson, G., Bechmann, R.K., Bamber, S.D., and Baussant, T. 2004. Bioconcentration, biotransformation, and elimination of polycyclic aromatic hydrocarbons in sheepshead minnows (*Cyprinodon variegatus*) exposed to contaminated seawater. Environ. Toxicol. Chem. **23**: 1538–1548.

Krahn, M.M., Moore L.K., and MacLeod, W.D., Jr. 1986. Standard analytical procedures of the NOAA National Analytical Facility, 1986: metabolites of aromatic compounds in fish bile. US Department of Commerce Tech. Memo. No. NMFS F/NWC-102.

Krogdahl, A., Nordrum, S., Sorensen, M., Brudseth, L., and Rosjo, C. 1999. Effects of diet composition on apparent nutrient absorption along the intestinal tract and of subsequent fasting on mucosal disaccharidase activities and plasma nutrient concentration in Atlantic salmon, *Salmo salar* L. Aquac. Nutr. **5**: 121–133.

MacFarlane, R.B., and Norton, E.C. 2002. Physiological ecology of juvenile chinook salmon (*Oncorhynchus tshawytscha*) at the southern end of their distribution, the San Francisco Estuary and Gulf of the Farallones, California. Fish. Bull. **100**: 244–257.

Meador, J.P., Stein, J.E., Reichert, W.L., and Varanasi, U. 1995. A review of bioaccumulation of polycyclic aromatic hydrocarbons by marine organisms. Rev. Environ. Contam. Toxicol. **143**: 79–165.

Meador, J.P., Collier, T.K., and Stein, J.E. 2002. Use of tissue and sediment based threshold concentrations of polychlorinated biphenyls (PCBs) to protect juvenile salmonids listed under the U.S. Endangered Species Act. Aquat. Conserv. Mar. Freshw. Ecosyst. **12**: 493–516.

Meador, J.P., Sommers, F.C., Wolotira, R.J., and Kubin, L. 2005. Conducting dose-response feeding studies with salmonids: growth as an endpoint. *In* Techniques in aquatic toxicology. Vol. 2. *Edited by* G.K. Ostrander. CRC Press, Boca Raton, Fla. pp. 93–115.

Moles, A., and Rice, S.D. 1983. Effects of crude oil and naphthalene on growth, caloric content, and fat content of pink salmon in seawater. Trans. Am. Fish. Soc. **112**: 205–211.

Mommsen, T.P. 1998. Growth and metabolism. *In* The physiology of fishes. *Edited by* D.H. Evans. CRC Press, Boca Raton, Fla. pp. 65–97.

Navarro, I., and Gutierrez, J. 1995. Fasting and starvation. *In* Biochemistry and molecular biology of fishes. *Edited by* P.W. Hochachka and T.P. Mommsen. Elsevier, Amsterdam, the Netherlands. pp. 393–434.

Niimi, A.J. 1987. Biological half-lives of chemicals in fishes. Rev. Environ. Contam. Toxicol. **99**: 1–46.

Niimi, A.J., and Dookhran, G.P. 1989. Dietary absorption efficiencies and elimination rates of polycyclic aromatic hydrocarbons (PAHs) in rainbow trout (*Salmo gairdneri*). Environ. Toxicol. Chem. **8**: 719–722.

Olsen, H., Enan, E., and Matsumura, F. 1998. 2,3,7,8-Tetrachlorodibenzo-*p*-dioxin mechanism of action to reduce lipoprotein lipase activity in the 3T3-L1 preadipocyte cell line. J. Biochem. Mol. Toxicol. **12**: 29–39.

Palm, R.C., Powell, D.B., Skillman, A., and Godtfredsen K. 2003. Immunocompetence of juvenile chinook salmon against *Listonella anguillarium* following dietary exposure to polycyclic aromatic hydrocarbons. Environ. Toxicol. Chem. **22**: 2986–2994.

Rice, C.A., Myers, M.S., Willis, M.L., French, B.L., and Casillas, E. 2000. From sediment bioassay to fish biomarker — connecting the dots using simple trophic relationships. Mar. Environ. Res. **50**: 527–533.

SAS Institute Inc. 1998. Statview statistical software. SAS Institute Inc., Cary, N.C.

SAS Institute Inc. 2004. JMP software. SAS Institute Inc., Cary, N.C.

Sloan, C.A., Brown, D.W., Pearce, R.W., Boyer, R.H., Bolton, J.L., Burrows, D.G., Herman, D.P., and Krahn, M.M. 2005. Determining aromatic hydrocarbons and chlorinated hydrocarbons in sediments and tissues using accelerated solvent extraction and gas chromatography/mass spectrometry. *In* Techniques in aquatic toxicology. Vol. 2. *Edited by* G.K. Ostrander. CRC Press, Boca Raton, Fla. pp. 631–651.

Spromberg, J.A., and Meador, J.P. 2005. Population-level effects on chinook salmon from chronic toxicity test measurement endpoints. Integr. Environ. Assess. Manag. **1**: 9–21.

Systat Software Inc. 2004. SYSTAT 11. Systat Software Inc., Richmond, Calif.

Thorpe, J.E. 1994. Salmonid fishes and the estuarine environment. Estuaries, **17**: 76–93.

Tocher, D.R. 2003. Metabolism and functions of lipids and fatty acids in teleost fish. Rev. Fish. Sci. **11**: 107–184.

van Metre, P.C., Mahler, B.J., and Furlong, E.T. 2000. Urban sprawl leaves its PAH signature. Environ Sci. Technol. **34**: 4064–4070.

Varanasi, U., Stein, J.E., Nishimoto, M. 1989. Biotransformation and disposition of polycyclic aromatic hydrocarbons (PAH) in fish. *In* Metabolism of polycyclic aromatic hydrocarbons in the aquatic environment. *Edited by* U. Varanasi. CRC Press, Boca Raton, Fla. pp. 94–149.

Varanasi, U., Casillas, E., Arkoosh, M.R., Hom, T., Misitano, D.A., Brown, D.W., Chan, S-L., Collier, T.K., McCain, B.B., and Stein, J.E. 1993. Contaminant exposure and associated biological effects in juvenile chinook salmon (*Oncorhynchus tshawytscha*) from urban and nonurban estuaries of Puget Sound. NOAA Technical Memorandum NMFS NWFSC-8.

Wagner, T., and Congleton, J.L. 2004. Blood chemistry correlates of nutritional condition, tissue damage, and stress in migrating chinook salmon (*Oncorhynchus tshawytscha*). Can. J. Fish. Aquat. Sci. **61**: 1066–1074.

Weatherley, A.H., and Gill, H.S. 1995. Growth. *In* Physiological ecology of pacific salmon. *Edited by* C. Groot, L. Margolis, and W.C. Clarke. UBC Press, Vancouver. pp. 103–158.

West, C.J., and Larkin, P.A. 1987. Evidence for size-selective mortality of juvenile sockeye salmon (*Oncorhynchus nerka*) in Babine Lake, British Columbia. Can. J. Fish. Aquat. Sci. **44**: 721–722.

Willette, M. 1996. Impacts of the *Exxon Valdez* oil spill on the migration, growth, and survival of juvenile pink salmon in Prince William Sound. Am. Fish. Soc. Symp. **18**: 533–550.

Wu, R.S.S., Carmel, P.A., Au, D.W.T., Zheng, G.J., Yuen, B.B.H., and Lam, P.K.S. 2003. Evaluation of biomarkers of exposure and effect in juvenile areolated grouper (*Epinephelus areolatus*) on food borne exposure to benzo[a]pyrene. Environ. Toxicol. Chem. **22**: 1568–1573.

Ylitalo, G.M., Yanagida, G.K., Hufnagle, L., Jr., and Krahn, M.M. 2005. Determination of lipid classes and lipid content in tissues of aquatic organisms using a thin layer chromatography/flame ionization detection (TLC/FID) microlipid method. *In* Techniques in aquatic toxicology. Vol. 2. *Edited by* G.K. Ostrander. CRC Press, Boca Raton, Fla. pp. 227–237.

A spatial model to estimate gear efficiency and animal density from depletion experiments

Paul J. Rago, James R. Weinberg, and Christopher Weidman

Abstract: Depletion experiments are conducted to estimate efficiency of sampling gear and density of organisms. Traditional models for analyzing these experiments make restrictive assumptions that are often violated. We present a new spatial model, suitable for sessile benthic invertebrates, that does not depend on these restrictive assumptions. The new model (*i*) allows flexibility during the experiment in choosing the spatial location of successive samples, (*ii*) does not require organisms or successive samples to be randomized over the entire area of the experiment, and (*iii*) permits target organisms to be lost or added during the experiment. The model treats total catch per sample as a sum of catches from smaller cells with different, but known, sampling histories. A negative binomial model is used to describe the distribution of catches from tows made during the depletion experiment. Maximum likelihood methods are used to estimate parameters, derive confidence regions for parameters, and evaluate goodness of fit between data and the model. Data from an experiment involving Atlantic surfclams (*Spisula solidissima*) are used to demonstrate the model.

Résumé : Des expériences d'épuisement nous permettent d'estimer l'efficacité des engins d'échantillonnage et la densité des organismes. Les modèles couramment utilisés pour analyser ces expériences font des présuppositions restrictives qui sont souvent violées. Nous présentons une nouvelle modélisation spatiale applicable aux invertébrés benthiques sessiles qui ne dépend pas de ces présuppositions restrictives. Le nouveau modèle (*i*) permet une flexibilité durant l'expérience pour choisir le site des échantillonnages successifs, (*ii*) ne requiert pas que les organismes ni les échantillons successifs soient répartis au hasard sur toute la surface expérimentale et (*iii*) permet que des organismes ciblés soient perdus ou ajoutés au cours de l'expérience. Le modèles traite la capture totale par échantillon comme la somme des captures de cellules plus petites avec des histoires d'échantillonnage différentes, mais connues. Un modèle binomial négatif sert à décrire la distribution des captures provenant des traits de récolte durant l'expérience d'épuisement. Des méthodes de vraisemblance maximale permettent d'estimer les paramètres, de déterminer les intervalles de confiance de ces paramètres et d'évaluer l'ajustement entre les données et le modèle. Des données provenant d'une expérience avec les mactres de l'Atlantique (*Spisula solidissima*) nous servent à faire la démonstration du modèle.

[Traduit par la Rédaction]

Introduction

A central problem in fisheries science is estimation of the catchability coefficient, a scalar that converts measures of relative abundance to absolute estimates of abundance. One can estimate the catchability coefficient of sampling gear by carrying out a depletion experiment, in which samples are taken without replacement from a closed population and catch per unit of sampling effort is monitored. Depletion experiments (e.g., Lasta and Iribarne 1997) are needed when it is not feasible to sample organisms directly with box cores, grab samples, or in situ sampling by divers. Direct sampling with divers may be too risky or impractical. Even when direct sampling is feasible, it may not be possible to sample a sufficient number of organisms or to cover a large enough area of the bottom (e.g., Caddy 1968; Smolowitz and Nulk 1982). Additionally, direct sampling methods can have certain biases related to the scale of observation or selectivity of the gear for limited size ranges.

The first depletion models for closed populations were developed by Leslie and Davis (1939) and DeLury (1947). Those early models included the following primary assumptions: (*i*) all extant individuals have the same probability of being caught in a sample, (*ii*) the expected catch in a sample is proportional to sampling effort, (*iii*) the catch depends on the cumulative catch of preceding samples, and (*iv*) all removals are known. In sampling a population of sessile organisms with a dredge, these assumptions are violated in subtle but important ways. A dredge sample can be viewed as the summation of a set of quadrats linked by the tow path. Because of an inability to accurately control the tow path of a dredge in deep water, one cannot assume that the probability of sampling a particular quadrat is random. The length of the tow and the number of previous tows through each

Received 24 May 2005. Accepted 25 February 2006. Published on the NRC Research Press Web site at http://cjfas.nrc.ca on 6 October 2006.
J18706

P.J. Rago[1] and J.R. Weinberg. National Marine Fisheries Service, Northeast Fisheries Science Center, 166 Water Street, Woods Hole, MA 02543, USA.
C. Weidman. Waquoit Bay National Estuarine Research Reserve, P.O. Box 3092, Waquoit, MA 02536, USA.

[1] Corresponding author (e-mail: paul.rago@noaa.gov).

doi:10.1139/F06-121

quadrat determine the number of animals caught in a particular tow. In a traditional experiment, one expects the number of animals per tow to decline monotonically with the number of tows. For sessile animals being sampled with a dredge, the catch in later tows may increase depending on the location of the tow. Another source of variation arises when availability of organisms changes during an experiment (e.g., Kendall and Bjorkland 2001; Peterson et al. 2004). Thus the variation in catches can exceed that expected under a standard depletion model that assumes a multinomial distribution for catches from a closed, nonspatially distributed population (Gould and Pollock 1997). The excess variation (i.e., overdispersion, sensu McCullagh and Nelder 1989) is not all due to the spatial distribution of animals, but also arises from the sampling process itself. This is related to the problem of heterogeneous capture probabilities described in Pollock et al. (1984) and Hilborn and Walters (1992).

Several models have been developed to address cases in which one or more of the traditional depletion model assumptions are violated (Carle and Strub 1978; Chien and Condrey 1985; Wang and Loneragan 1996). Mohn and Elner (1987) demonstrated that when the population is not uniformly distributed, the Leslie–Davis model underestimates abundance and overestimates gear efficiency. Miller and Mohn's (1993) analysis of sources of bias in depletion experiments demonstrates the need to consider spatial heterogeneity of organisms. Joll and Penn (1990) explicitly addressed the spatial aspect of sampling in their analyses of scallop (*Amusium balloti*) and western king prawn (*Penaeus latisulcatus*) populations.

Beginning with Taylor (1953) and continuing to Power and Moser (1999), various investigators have characterized the empirical distributions of catches of aquatic animals using a negative binomial distribution –$\mathrm{NB}(\mu,k)$. We also employed this distribution in our model. The applicability of the NB model can be demonstrated theoretically as the summation of a Poisson random process with randomly varying capture probabilities (see Johnson et al. (1993) and references therein), as well as empirically (Houser and Dunn 1967; Welch and Ishida 1993; White and Bennetts 1996). The NB model explicitly accounts for the extra variation in observed catches and reduces to the Poisson distribution as the dispersion parameter K becomes large.

Two additional properties of the NB distribution make it appropriate for the analysis of catches in a depletion experiment. First, the catch in a tow is the sum of catches from individual patches, each with the number of organisms distributed as NB random variables. The sum of individual random variables drawn from a NB distribution with parameters μ and k_i is also distributed as a NB random variable with parameters μ and Σk_i (Johnson et al. 1993). Second, the dispersion parameter K is invariant with respect to changes in density, which would occur as a result of removals (Pielou 1977, p. 128).

Overdispersion of count data has been demonstrated in many applications of the Leslie–Davis and DeLury removal models (e.g., Paloheimo 1963; Otis et al. 1978; Schnute 1983). Both parametric (e.g., Wang and Loneragan 1996) and semiparametric (e.g., Gould and Pollock 1997) methods for dealing with overdispersion have been applied to depletion experiments. Following the rationale of Lawless (1987), who emphasized the utility of relating the overdispersion to the underlying processes, we chose the NB model as a parametric approach to describe overdispersion. Our application of the NB model uses the cumulative spatial pattern of animal removals to define the probabilities of capture and expected catch per tow. This approach is tailored to sessile organisms sampled by a device the position of which is difficult to control. The likelihood function for the NB in our model explicitly conditions the parameters in each successive probability density function of the likelihood function on the cumulative spatial pattern of removals.

Our new model has been used to estimate dredge efficiency in National Marine Fisheries Service (NMFS) research surveys of the Atlantic surfclam, *Spisula solidissima* (Northeast Fisheries Science Center (NEFSC) 2003), ocean quahog, *Arctica islandica* (NEFSC 2004), and sea scallop, *Placopecten magellanicus* (NEFSC 2001). In the model, animals are distributed across the sea floor in a matrix of square cells. The catch in a single sample (i.e., tow) represents the sum of catches from all cells (under the constraint that cell width ≥ the width of the sampling device) that were contacted. The total catch depends not only on the number of cells sampled, but also on the sampling history of each cell in the tow path. A NB model is used to describe the distribution of catches, and maximum likelihood methods are used to estimate parameters, derive confidence regions, and evaluate goodness of fit. Parameters that are estimated include initial (presampling) density of animals, efficiency of sampling gear, indirect effects of sampling gear on catches (such as the burial of clams by a clam dredge), and the clumping parameter of the NB model. To demonstrate the model, we applied it to data from a field experiment on clams.

Existing theory

The expected catch $E(C)$ in a sample from a closed population can be expressed as the product of population abundance (N), sampling effort (f), and efficiency (e) of the sampling device. If we assume that f is equal to the area swept by the gear (a) divided by the total area (A) of the closed population, then expected catch can be expressed as

$$E(C) = e(a/A)N \tag{1}$$

where e is the probability of capture given encounter with the fishing gear, and a/A is the probability of encounter. If the animals are randomly (i.e., Poisson) distributed within the potential sampling area before each sample is taken, then the probability of encounter will be proportional to the area sampled by the gear, a, divided by the total area of the experiment, A. Likewise, if the animals are randomly distributed as groups, with varying numbers of individuals, then the probability of encountering a group will still be proportional to a/A but the expected variance of C will be higher (Sampson 1988).

The Leslie and Davis (1939), DeLury (1947), and Ricker (1975) models for depletion experiment data begin with the premise that the catch is equal to the probability of capture × population size in a fixed area at the start of the interval. Average density following a removal is equal to initial population size minus the catch, all divided by the total area. Every time sampling takes place, all individuals are assumed to have the same probability of being captured. The Leslie–Davis model is obtained by recursively applying eq. 1, which gives the population size after each catch. Writing the terms $e(a/A)$ in eq. 1 as q and recursively applying eq. 1 results in the Leslie–Davis equation:

$$(2) \qquad E(C_i) = q(N_0 - T_{i-1})$$

where $T_{i-1} = \sum_{j=1}^{i-1} C_j$ for tow number i. Thus the expected catch in the ith sample $E(C_i)$ is proportional to the initial population size minus the cumulative catch from previous samples (T_{i-1}). Although eq. 2 can be written as a linear regression, a least squares method is not appropriate in this case because the variance of C_i changes with each observation (Seber 1973; Schnute 1983). Gould and Pollock (1997) showed that maximum likelihood estimation (MLE) was the most appropriate method for estimating the parameters of the Leslie–Davis model.

Need for spatial approach

Existing theory models catches from a closed population without considering the organism's spatial distribution or the location where the sample was taken. For sessile animals, a removal experiment may be more properly viewed as sampling from a collection of cells in a grid, each of which may be subject to sequential sampling. The expected value of catch in any single sample depends on which cells were sampled and the number of times that each was sampled previously.

The following example demonstrates how failure to consider the spatial pattern and temporal sequence of catches in a depletion experiment can dramatically bias the estimates of true underlying population size and gear efficiency. Consider an experiment with sessile organisms in which the experimental area is wider than the width of the sampling device (Fig. 1). Assume that the experimental area is three paths wide, true population size is 300 individuals, gear efficiency is 0.5, a total of nine tows are taken, and each of the paths is sampled three times. We consider three hypothetical scenarios in which the paths are swept in different orders. In scenario 1, the first three tows are taken in the same path, the second three tows occur in the next path, and the last three tows occur in the remaining path. Naïve application of maximum likelihood methods to the scenario 1 data results in a very low and biased estimate of efficiency (0.06) along with an incorrect high estimated population size (~595). In scenario 2, each of the first three tows occurs in a different path, with no overlap between them. The same occurs for the next three tows (numbers 4–6) and again for the last three tows (numbers 7–9). MLE-based estimates for scenario 2 were also biased, with an efficiency estimate of 0.18 and population estimate of 312. One could recover the true parameters from either scenario 1 or scenario 2 by appropriately summing the tows related to the first, second, and third passes within a path. To show this, we derive scenario 3 from scenario 2 by summing tows 1 to 3, 4 to 6, and 7 to 9. Estimates of efficiency and population size for scenario 3 were equal to their true values, 0.5 and 300, respectively. The idealized experiments described above would be much more complicated if tows had partial overlap with each other, as they would in a field experiment.

Fig. 1. Three hypothetical depletion experiments demonstrating that parameter estimates will be biased unless spatial information on sample location is incorporated.

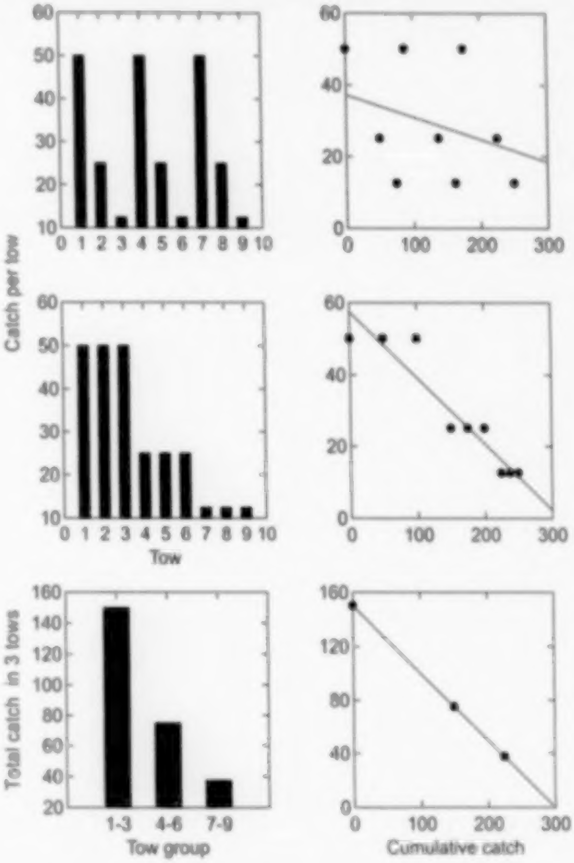

Extending the model to allow partially overlapping paths

Failure to consider the spatial pattern of samples biases parameter estimates. Partial overlap of tows, due to inability to control the exact tow path, results in observed catches that are a function of the numbers removed on previous tows *and* the locations of previous removals. A starting place for modeling this complex situation is to model catch data from depletion experiments in terms of average density in the experimental area, rather than total population size N. Population size, a parameter in the Leslie–Davis model, is less useful as an abundance index in this case because the size of the experimental area A is arbitrary, depending on the set of realized tow paths. Average density, however, is a useful measure of abundance because it does not rely on the particular set of tow paths.

Reparameterization of the Leslie–Davis model in terms of average density rather than population number can be shown for a restricted case in which the area swept by a single tow

a and the experimental area A are constant. The average density is $D = N/A$, so that $A = N/D$. Substituting for A in eq. 1 gives $C = eaD$. The average density in the cell after removal of C animals is $(N - C)/A = N/A - C/A = D - (eaD/A) = D(1 - (ea/A))$. Recursive computation of catch, population size, density, and cumulative catch is summarized for three time steps (Table 1). The elemental equation derived in Table 1 demonstrates that the expected catch in a cell that has been swept j times is

$$(3) \qquad E(C_j) = eaD_0(1 - e(a/A))^{j-1}$$

Equation 3 expresses catch per sample as a function of animal density, but further development of the model is needed to handle the case in which the probability of capture for animals inside the tow path is e and the probability for animals outside the tow path is zero. To address this issue, we treat a tow path as a string of individual cells, each of which is characterized with the same nonzero sampling probability. Cells that are not sampled by that tow are not included, in contrast with an analysis that considered all animals in the entire experimental area as equally vulnerable.

To implement this concept, it is necessary to define a "hits" matrix that represents the path of a tow as a discrete string of adjacent cells and retains a record of the number of previous contacts of these cells by the sampling device. The expected value of catch from an individual cell along a tow path can be predicted using eq. 3. The expected catch for the entire tow can now be represented as the sum of the expected catches from all cells. In effect, each cell within in a tow can be viewed as an individual depletion experiment. Because the catch in the ith tow is the sum of catches from individual cells, it is the sum of catches from cells hit 1 to i times. Thus the expected catch for a tow depends not only on the path of the sampling device, but also on the sampling history of each cell (Fig. 2). Equation 3 can be modified to account for hits of cells:

$$(4) \qquad E(C_i) = ea_iD_0\sum_{j=1}^{i} f_{i,j}(1 - e\gamma)^{j-1}$$

where C_i is the number caught in tow i ($i = 1,\ldots,I$), e is the efficiency, i.e., Prob(capture|encounter), a_i is the area swept by tow i, D_0 is the initial density (number/area), and $f_{i,j}$ is the fraction of tow i that was hit i times, where $\sum_{j=1}^{i} f_{i,j} = 1$. The parameter γ is analogous to the a/A term in eq. 3 and is defined as the ratio of the width of the sampling device w_{dredge} to the width of the cell Δx:

$$(5) \qquad \gamma = w_{dredge}/\Delta x$$

When applying the model, the choice of cell width is an important practical decision related to the accuracy and precision of gear location and gear size. The parameter γ would be 1.0 in an ideal situation with perfect information on the location of the sampling device, a tow width equal to cell width, and a tow path restricted to one and only one cell per unit time. In practice, these conditions are violated to varying degrees. This can be dealt with in a model by selecting a cell width that is commensurate with the imprecision of data on location of the sampling device. For instance, if the location $\{x,y\}$ of the sampling device is known to within some

Table 1. Expected values of density, number (or abundance), catch, and cumulative catch in a hypothetical depletion experiment in one cell, with complete mixing within the cell after each tow.

Dredge pass (i)	Density (D_i)	Number (N_i)	Catch (i – 1 to i) = C_i	Cumulative catch (T_i)
0	$D_0 = N_0/A$	N_0	—	—
1	$D_1 = N_1/A$ $= (N_0/A)(1 - e(a/A))$	$N_1 = N_0 - C_1$ $= N_0 - e(a/A)N_0$ $= N_0(1 - e(a/A))$	$C_1 = eaD_0$ $= e(a/A)N_0$	$T_1 = 0$
2	$D_2 = N_2/A$ $= (N_0/A)(1 - e(a/A))^2$ $= D_0(1 - e(a/A))^2$	$N_2 = N_1 - C_2$ $= N_0(1 - e(a/A)) - e(a/A)N_0(1 - e(a/A))$ $= N_0(1 - e(a/A))(1 - e(a/A))$ $= N_0(1 - e(a/A))^2$	$C_2 = e(a/A)N_1$ $= e(a/A)N_0(1 - e(a/A))$	$T_2 = C_1$ $= e(a/A)N_0$
3	$D_3 = N_3/A$ $= (N_0/A)(1 - e(a/A))^3$ $= D_0(1 - e(a/A))^3$	$N_3 = N_2 - C_3$ $= N_0(1 - e(a/A))^2 - e(a/A)N_0(1 - e(a/A))^2$ $= N_0(1 - e(a/A))^2(1 - e(a/A))$ $= N_0(1 - e(a/A))^3$	$C_3 = e(a/A)N_2$ $= e(a/A)N_0(1 - e(a/A))^2$	$T_3 = C_2 + C_1$ $= e(a/A)N_0 + e(a/A)N_0(1 - e(a/A))$ $= e(a/A)N_0\ (1 + 1 - e(a/A))$ $= e(a/A)N_0(2 - e(a/A))$

Note: The overall area is denoted as A and the area swept by an individual tow is denoted as a. Efficiency, e, is the probability of capture given encounter.

Fig. 2. Diagram of depletion experiment with multiple passes over a spatially distributed population. Grids in the left column represent example tow paths; histograms in the right column represent the number of cells that are "hit" one or more times in each tow.

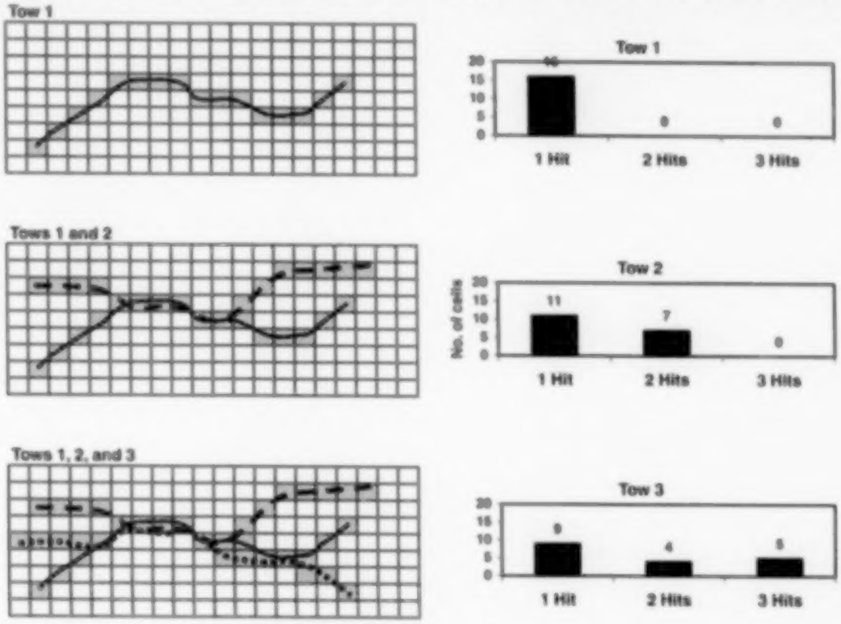

error level δ, then the size of the individual cell within a tow path can have an area proportional to the width of the sampling device ± δ.

Adding "indirect" effects to the model

"Indirect" effects in depletion experiments occur when the sampling process alters the catchability and availability of some individuals to the sampling gear during the experiment. For example, indirect effects may occur if the zone of influence of a clam dredge, used in a depletion experiment, is greater than the width of the dredge or if the availability of clams changes because of the dredge's effects on the bottom. Clams could be blown out of the area or buried, without being caught by the dredge (Meyer et al. 1981; Murawski and Serchuk 1989*a*).

With these types of indirect effects, the population available for capture on subsequent passes will be less than that expected based on eq. 4. Alternatively, if buried clams become more exposed to the dredge with each tow, then the reverse would be true. To deal with this general problem, we allow the parameter γ to take on additional meaning. We now use it to represent not only the size of the sampling device relative to cell size, but also the device's indirect effects on the probability of capture:

$$\gamma = (w_{\mathrm{dredge}}/\Delta x) + \varepsilon \tag{6}$$

where w_{dredge} is the width of dredge, Δx is the width of cell, and ε is a factor related to indirect effects. When there are no indirect effects, γ equals its nominal value (i.e., the ratio of dredge width to cell width). γ will be greater than the nominal value if animals become less available to the sampling gear with repeated passes over the same cell, or if they are lost before they can be counted in the catch. Conversely, γ will be less than its nominal value if animals become more available, or new animals become vulnerable to the sampling gear, with repeated passes. If indirect effects exist, it is necessary to estimate γ in a mathematical model, preferably utilizing external empirical information.

Parameter estimation from the NB distribution

Standard approaches for estimating NB parameters do not apply here because in most depletion experiments tows vary in length. Bissell (1972) showed how to apply the NB model to counts based on varying element sizes, and we applied his results to depletion experiments by writing the tow area as a function of the area swept in tow *i*, *e*, γ, and the pattern of overlap with other tows. We define this as the "effective" area, $a_i^{\bullet}$, of each tow:

$$a_i^{\bullet} = e a_i \sum_{j=1}^{i} f_{i,j} (1 - e\gamma)^{j-1} \tag{7}$$

Effective area represents the area sampled after adjusting it downward for cells in the tow path that were sampled a variable number of times during previous tows, which reduces the number of animals available for capture. Our formulation of the NB model is similar to that developed by Power and Moser (1999), who parameterized a model for trawl catches in terms of the volume of water filtered by the *i*th tow. Our definition of $a_i^{\bullet}$ differs in that it depends on both the area swept by the current tow and all previous tows. In effect, this definition normalizes the area swept in any given tow with respect to the locations and areas swept by all previous tows.

The NB distribution for catch can be expressed as a function of D_0, K, and a_i^*:

$$(8) \quad \Pr(C = C_i | D_0, K, a_i^*) = \left(\frac{K}{D_0 a_i^* + K}\right)^K \left(\frac{D_0 a_i^*}{D_0 a_i^* + K}\right)^{C_i} \times \prod_{j=1}^{C_i}\left(\frac{K + j - 1}{j}\right)$$

The log-likelihood function for the parameters K, D_0, e, and γ given C_i and a_i is

$$(9) \quad \mathrm{LL}(K, D_0, e, \gamma | C_i, a_i) = K\sum_{i=1}^{I}(\log(K) - \log(D_0 a_i^* + K)) + \sum_{i=1}^{I} C_i(\log(D_0 a_i^*) - \log(D_0 a_i^* + K)) + \sum_{i=1}^{I}\sum_{j=1}^{C_i}\log(K + j - 1) - \sum_{i=1}^{I} C_i!$$

Note that in this formulation, the likelihood function for successive probability density functions of catch are linked by the a_i^* (eq. 7). This dependency between successive terms in our formulation of the likelihood function for the NB distribution is analogous to the multinomial distribution (used in a standard Leslie–Davis model) obtained from a sequence of linked binomial distributions (Gould et al. 1997, p. 900).

Profile likelihood confidence intervals

Profile likelihood methods (Venzon and Moolgavkar 1988; Hirst 1994) can be used to estimate approximate confidence intervals for single parameters and confidence regions for two parameters. If $\boldsymbol{\theta}^* = \{D_0, e, K, \gamma\}$ represents the vector of parameters that maximizes the negative $\mathrm{LL}(D_0, e, K, \gamma | C_i, a_i)$, then the profile likelihood for any parameter θ_k may be obtained by finding the roots of

$$(10) \quad \mathrm{Sup}[\mathrm{LL}(\theta_k, \boldsymbol{\theta}^*_{-k})] = \mathrm{LL}(\boldsymbol{\theta}^*_{-k}) + \frac{\chi^2_{1,\alpha}}{2}$$

where $\boldsymbol{\theta}^*_{-k}$ denotes the parameter vector with all parameters except θ_k equal to their maximum likelihood estimates, Sup is the supremum function (Mood et al. 1974), and χ^2 is the chi square value for a selected α with 1 df.

Confidence intervals for catch are calculated in the new model by solving for $C_{\min}$ and $C_{\max}$ in the following equation:

$$(11) \quad 1 - \alpha = \mathrm{Prob}(C_{\min} < C(a_i^*) < C_{\max}) = \sum_{C_{\min}}^{C_{\max}} \mathrm{NB}(C_i | a_i, \boldsymbol{\theta}^*)$$

In the new model, the G test, following White and Bennetts (1996), measures goodness of fit of observed catches to predicted catches.

Application to an Atlantic surfclam depletion experiment

The Atlantic surfclam has been harvested commercially along the east coast of the USA for over 40 years, and it is the basis of a multimillion-dollar fishery (Murawski and Serchuk 1989*b*; Weinberg 1999; Weinberg et al. 2002*a*). The National Marine Fisheries Service has carried out fishery-independent surveys of this species with the NOAA R/V *Delaware II* (48 m in length) using a 1.52 m wide, hydraulic clam dredge. The dredge has a submersible pump and weighs 3.2 tonnes. Estimates of dredge efficiency from experiments have been used to convert survey estimates of catch per tow to estimates of total abundance (NEFSC 1998, 2003, 2004). We analyze one depletion experiment here to illustrate the new model and to compare it with the Leslie and Davis (1939) and Gould and Pollock (1997) models. This experiment was conducted off Atlantic City, New Jersey, USA (39°17.64′N latitude, 73°51.55′W longitude) between 5 June 1997 and 11 June 1997 in 34 m of water. The bottom was sand and gravel, the typical substratum for surfclams. Sixty-two tows were made over the same approximate location in an attempt to deplete the area of surfclams. The number of surfclams captured by the dredge in each tow was recorded.

The tow path of the dredge was assumed to match the ship's position, which was measured at 1-s intervals with a differential global positioning system (GPS). Each tow in this experiment was made with a 2:1 scope (tow line length to bottom depth) at 1.5 knots for 2 min, not counting the time that it took to set out and recover the dredge. The average distance between measurements of ship position was 1.25 m. An inclinometer, mounted on the dredge, electronically recorded the dredge angle and allowed us to estimate when the dredge was in contact with the bottom and sampling (Weinberg et al. 2002*b*).

To apply the model to an actual experiment, it is necessary to estimate the fractional overlap values $f_{i,j}$ for each tow (eq. 4). The procedure for converting a set of tow-specific coordinates into a set of proportions involves constructing a grid of cells for the experimental area, overlaying the tow tracks over the grid, and computing the number of times that each cell had been previously sampled through the ith tow. The fraction of the swept area for tow i that is hit j times is computed as the ratio of the number of cells hit j times divided by the total number of cells within tow i. By definition, $j \le i$. These concepts are illustrated in Fig. 2 for a simplified example. The data matrix used for estimation of parameters in eq. 8 consists of the total catch per tow C_i and the estimated fraction of the tow i hit j times (i.e., $f_{i,j}$).

Programs to preprocess position data, obtain maximum likelihood estimates, and evaluate goodness of fit were written in FORTRAN. International Mathematics and Statistics Library (IMSL) routines were used for optimization (eq. 9) and root finding (eq. 10). Optimization used Nelder and Mead's (1965) Simplex method, as described in Press et al. (1992). Confidence intervals (eq. 11) were found by evaluating the cumulative distribution function for values of a_i and $f_{i,j}$. After convergence, the model was restarted nine times, with different sets of initial parameter values, to determine if parameter estimates were stable.

Fig. 3. The area of each tow in the surfclam (*Spisula solidissima*) experiment is decomposed into the fraction that, at the conclusion of the tow, has been sampled j ($j = 1, 2, \ldots, 6$) times. Each column represents a tow. Elements within columns sum to one.

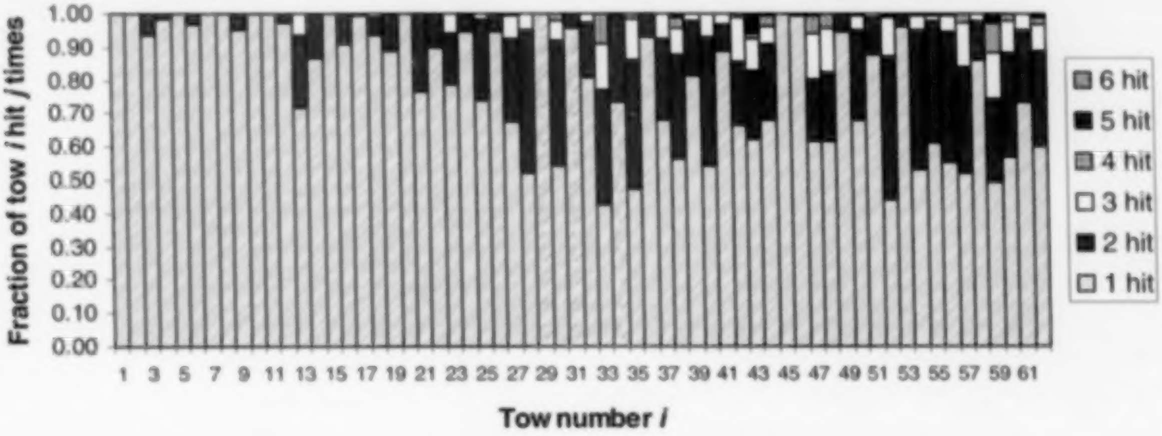

Table 2. Results (point estimates and 95% confidence intervals) from depletion models fit to data from a surfclam (*Spisula solidissima*) experiment.

Model	Dredge efficiency	Clam density (number·m^{-2})
Leslie–Davis (linear regression)	0.552 (0.372–0.731)	0.990 (0.872–1.109)
Gould and Pollock (MLE)	0.535 (0.497–0.573)	1.012 (0.969–1.066)
New model (3.0 × 3.0 m cell size)	0.645 (0.461–0.816)	0.775 (0.646–1.001)
New model (1.5 × 1.5 m cell size)	0.673 (0.557–0.674)	0.700 (0.646–0.818)

Note: The Leslie–Davis interval is a standard confidence interval from a linear regression in which errors are assumed to be normally distributed. Other intervals are from profile likelihoods for the multinomial model (MLE (maximum likelihood estimation); Gould and Pollock 1997) and the new, negative binomial model presented in this paper.

This depletion experiment sampled a rectangular area approximately 500 m × 175 m (NEFSC 1998). We used a 3.05 × 3.05 m cell size because of uncertainty in the exact position of the dredge in the sampling grid and because successive ship position measurements were, on average, 1.22 m apart.

Following eqs. 4 to 5, we computed the hit frequency matrix (Fig. 3). For the first 12 tows, carried out at the beginning of the experiment, 90%–100% of their areas were sampled for the first time. As the experiment progressed, tows tended to have a greater fraction of their total area sampled previously. The tows in this experiment were dispersed over a relatively large area, so even the final tows were still sampling new ground for approximately 50%–60% of their paths. For the entire experiment, the maximum number of times that any cell was contacted was six. The observed catch ranged from about 50 to 400 individuals per tow, and catch per tow declined over the course of the experiment (Fig. 4).

Fig. 4. Number of surfclams (*Spisula solidissima*), by tow, captured and counted during the depletion experiment.

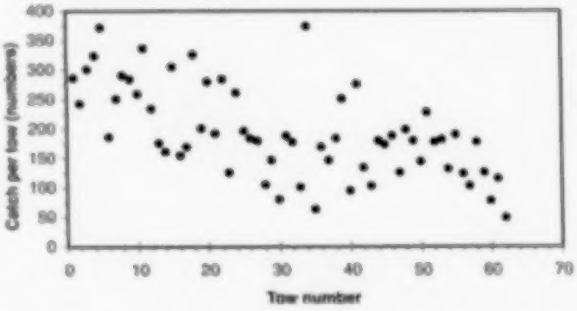

Parameter estimates were 0.645 for dredge efficiency and 0.775 clams·m^{-2} for density (Table 2). The 95% confidence interval for efficiency ranged from 0.46 to 0.82, whereas the interval for density ranged from 0.65 to 1.00 surfclams·m^{-2} (Table 2). The elliptical joint 95% confidence region for efficiency and density, based on profile likelihood, demonstrated the negative correlation between these parameters (Fig. 5*a*), expected in depletion studies. For this experiment, the confidence regions for γ and efficiency (Fig. 5*b*) and γ and density (Fig. 5*c*) were relatively small. Estimates of γ and density were positively correlated, whereas the joint confidence region for γ and efficiency suggested that estimates of these parameters were nearly independent. Other applications of our model suggest that this may not be true in all cases.

There was a positive relationship between observed catch per tow and effective area sampled (eq. 7) per tow (Fig. 6). This relationship occurred because catch per tow was affected not only by the density of clams at the start of the experiment and tow length, but also by catch history and spatial aspects of sampling. Residuals for observed and predicted catches (Fig. 7) and comparison of observed and pre-

Fig. 5. Profile likelihood confidence regions for (*a*) surfclam (*Spisula solidissima*) density (number·m^{-2}) and capture efficiency, (*b*) gamma and capture efficiency, and (*c*) gamma and surfclam density (number·m^{-2}) in the surfclam experiment. Outermost ellipse is a 95% joint confidence interval.

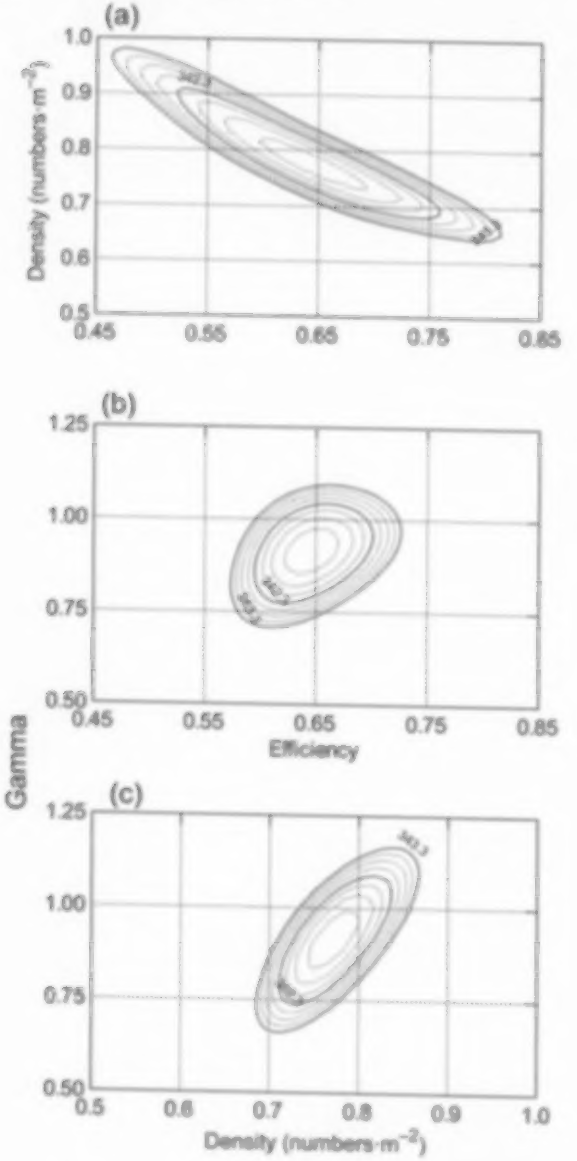

Fig. 6. Observed (●) and predicted (lines) surfclam (*Spisula solidissima*) catch per tow as a function of effective area sampled. Predicted values are from a parametric percentile method, computed with eq. 10. They represent the median and 95% confidence interval.

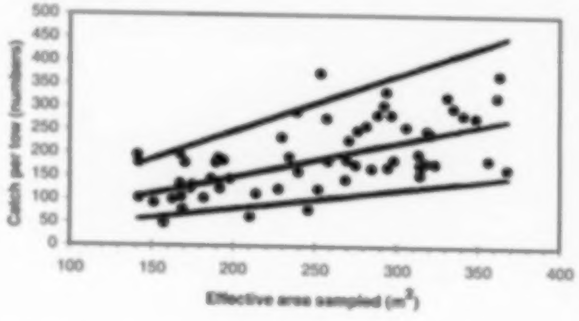

Fig. 7. Plot of residuals (observed (Obs.) – predicted (pred.) surfclam (*Spisula solidissima*) catch) vs. tow number.

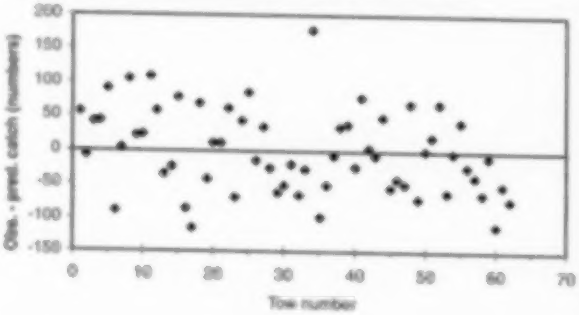

Fig. 8. Observed (open bars) and predicted (solid bars) frequency distributions for surfclam (*Spisula solidissima*) catch per tow. Predicted catch is based on the negative binomial model.

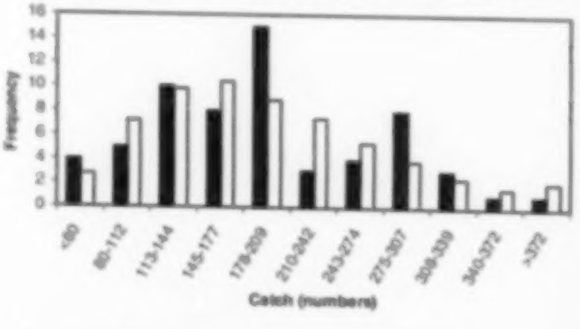

dicted frequency distributions for catch per tow (Fig. 8) suggested good model fit. Based on a *G* test, there was not a significant difference between these frequency distributions ($G = 13.51$, df = 10, $p = 0.197$; Fig. 8).

γ was estimated to be 0.918, which is greater than the nominal (*i.e.*, expected) value based only on the ratio of dredge width to cell width (0.5). This suggested that indirect losses of clams took place during this experiment. Because γ is a dimensionless ratio, it is difficult to grasp the meaning of a change in γ from 0.5 to 0.918. To clarify this, we did a sensitivity analysis to measure the impact on the predicted catch of changing γ (following eq. 4). In the sensitivity analysis, γ was varied between 0.4 and 1.2, while density, efficiency, and the dispersion parameter *K* were held at their optimal values. Lowering γ from 0.918 to 0.4 caused the predicted average catch per tow to increase by +10%. Raising γ from 0.918 to 1.2 decreased the predicted average catch per tow by –6%. Reducing γ below its optimal solution of 0.918 simulated reducing the number of clams lost due to indirect factors and raised the predicted catch in the dredge. Conversely, raising γ above 0.918 simulated even greater loss of clams due to indirect effects and lowered the predicted catch in the dredge.

We pointed out that γ may be difficult to determine. Because of this, we examined the sensitivity of efficiency and density to the assumed value of γ. Fixed γ values between 0.5 and 1.0 were used to the new model, assuming a 3.05 m × 3.05 m cell size, while the solutions for the other parameters were not constrained. Estimates of dredge efficiency were negatively correlated with γ, whereas density was positively correlated with γ. As γ increased from 0.5 to 1.0, dredge efficiency estimates decreased from about 0.9 to about 0.6, whereas density increased from about 0.5 to 0.8 surfclams·m^{-2} (Fig. 9).

Given the quality of spatial information for this experiment, a cell size of 3.05 m × 3.05 m was judged appropriate. In one model run, we explored the sensitivity of parameter estimates to cell size using a smaller cell size of 1.52 m × 1.52 m. Point estimates for density and efficiency did not change substantially from those in the run with 3.05 m × 3.05 m cells, but reducing the cell size caused the confidence intervals to be smaller (Table 2). Thus, using a cell size that is too small does not appear to cause much bias in parameter estimates, but it causes underestimation of variances of the parameters.

Comparison of results with other depletion models

Point estimates for capture efficiency ranged from 0.54 in the Gould and Pollock model to 0.67 in the present model, with a 1.52 m × 1.52 m cell size (Table 2). Point estimates from the Leslie–Davis model and the Gould and Pollock model were similar to each other, as were the estimates from the two runs of the spatial model using different cell sizes. For dredge efficiency, the narrowest confidence interval (0.08) was associated with the Gould and Pollock model. The spatial model with a 1.52 m × 1.52 m cell size produced a slightly wider interval (0.12). The widest confidence interval (0.36) was associated with the Leslie–Davis model and the present model, in which we used a 3.05 m × 3.05 m cell size.

Discussion

Traditional models for analyzing depletion experiments do not take into account important factors such as the history of catches from individual cells, the inability of sessile organisms to redistribute themselves between tows, indirect effects of sampling gear on availability and probability of capture of organisms, and differences in sampling intensity between locations. The model presented here considers these factors. The new model is appropriate to use when accurate information is available on the location of each sample and the overlap between samples, when organisms do not redistribute themselves quickly, when indirect effects occur, and (or) when it is necessary to sample with large dredges, the positions of which are hard to control. In situations when information about the location of each sample is not available, the model reduces to a simpler model comparable to model 2 of Schnute (1983).

Fig. 9. Gamma was varied from 0.5 to 1.0 to determine its effect on two other parameters in the new model, clam (*Spisula solidissima*) density (○) and capture efficiency (▲).

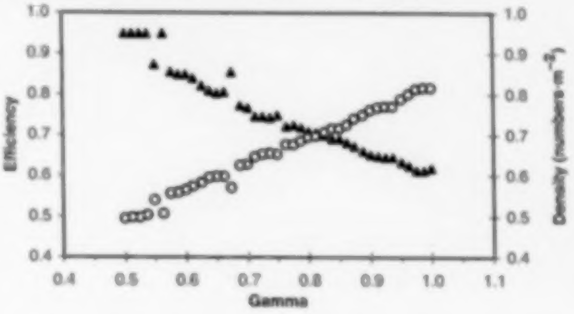

Implementing the new spatial model and collecting the necessary data require technologies such as GPS and geographical information system (GIS). GPS is used in the field to position the ship and record instantaneous location during each tow, and GIS is used in data analysis to visualize tow paths and compute degree of overlap among tows. Improvements in our ability to locate the dredge in two-dimensional space will let us reduce cell size and increase the precision of the overlap ("hits") indices. The effect of imprecise location information is an important topic for future research.

The new model allows for analyses of depletion experiments that vary in total area and in which tows vary in length. To our knowledge, this is the first model for analysis of depletion experiments that utilizes the NB distribution, an appropriate statistical model for overdispersed catches of organisms in nature (Power and Moser 1999). Gould and Pollock (1997) addressed overdispersed catches using quasi-likelihood methods in their analysis of the lobster (*Homarus americanus*) data of Paloheimo (1963). Wang and Loneragan (1996) proposed a more complicated compound distribution wherein the catchability parameter was distributed as a beta random variable. Either approach would be sufficient to address the effects of overdispersion.

Under the usual assumptions of the Leslie–Davis model, the joint distribution of the realized set of catches reduces to a multinomial distribution. The multinomial distribution can be used because (*i*) the mean and variance of a single tow can be expressed as a function of the probability of capture and the total population at the time of the sample, and (*ii*) the realization of catch in all previous tows alters the probability density function (pdf) of each catch in the series.

Although the multinomial distribution is a convenient closed-form expression of the joint distribution, other approaches could be used to model the salient features of a depletion experiment. Any model that is used must describe the capture process and link the distributions between successive tows. Explicit linkage of the pdfs is evident in earlier literature in which the multinomial distribution for removal experiments was called a "chain binomial" (Pielou 1977). As another illustration, Wang and Loneragan (1996) characterized the joint pdf as a beta-binomial distribution.

In our formulation of the depletion experiment, we chose to explicitly model the capture process with a NB model allowing a transition from random to overdispersed catches. The magnitude of overdispersion is indexed by K: when K is large the model converges to a Poisson distribution, which can be approximated by a binomial distribution (Mood et al. 1974). Our model also preserves the explicit dependency in the likelihood function such that each catch is dependent on previous tows. However, this dependency is not based on order as in the standard depletion model. Instead, it depends on the degree of spatial overlap of the current catch with all previous catches, as represented by their respective tow paths. The dependency of terms in the joint density function for catches in a depletion experiment for sessile organisms is handled through the computed measures of spatial overlap $f_{i,j}$ and the spatially explicit cell- or patch-based formulation in which each tow path hits a linked set of cells. The resulting joint distribution of catches may have a closed-form distribution, but we have not investigated this.

Differences in parameter estimates between the new model and traditional depletion models are caused by at least two factors. First, there is no explicit treatment of degree of tow overlap in the Leslie–Davis model; therefore, one might incorrectly interpret a high catch resulting from sampling new ground late in a depletion experiment as a low dredge efficiency. Second, indirect effects are not included in the Leslie–Davis model, so it might overestimate dredge efficiency by incorrectly attributing a low catch per tow to efficiency rather than to indirect effects of the gear in cases when it lowers the catchability of animals. These two factors bias the efficiency estimate in opposing directions and could even cancel each other out. Because the new model can realistically incorporate information on tows paths and indirect effects, it might yield more accurate estimates of the parameters and their variances. Thus far, the new model has been applied, for stock assessment, to data from numerous depletion experiments involving clams and scallops from the US Atlantic coast (NEFSC 2001, 2003, 2004).

When applied to the surfclam data, the Gould and Pollock model produced the smallest confidence intervals for both dredge efficiency and clam density. However, low variance may have resulted from model misspecification because the model did not consider the spatial distribution of clams. Wang and Loneragan (1996) showed that uncertainties in estimates of N and q were underestimated by standard approaches, which did not address overdispersion of organisms. They attempted to incorporate the spatial pattern of organisms by treating the catchability parameter q in their model as a random number from a beta distribution. Earlier, Crittenden (1983) attempted to model the capture process by explicitly incorporating an aggregation factor into the Leslie–Davis model. Variations in catchability have also been modeled as explicit functions of environmental parameters (Yamakawa et al. 1994), competing species (Polovina 1986), and independent signs of animal activity (Routledge 1989). We have modeled catchability as an explicit function of the spatial pattern of overlap among tows.

Gamma, cell size, and the catchability parameter

In practice, direct and indirect information about the behavior of the dredge, the animals, and their interactions could be used in a Bayesian approach to specify a likely range of values for γ. For the experiment considered here, empirical studies (Meyer et al. 1981; Murawski and Serchuk 1989*a*) indicated that the influence of the dredge on clams could extend half a dredge width beyond its nominal value. A lower bound would be one dredge width. Using a γ value greater than the ratio of the dredge width to cell width would imply that the expected population size within a cell that is available to the dredge on subsequent passes has been reduced beyond that explained by observed catches.

The γ parameter is also related to the selection of the appropriate cell size for applying the spatial model. At the extreme, as the cell size in the model increases, approaching the size of the area of the entire multiple-tow experiment, the new spatial model converges to the nonspatial Leslie–Davis model. Choice of cell size must be scaled to the degree of uncertainty about the position of the sampling gear and the tenability of the assumption of equal catchability of animals between samples, at the level of the cell. In the surfclam experiment, it was possible to run the spatial model with a cell size equal to or less than one dredge width. In that case, variances of parameters would be underestimated because the true position of the dredge is not known with such accuracy. This explains why the confidence intervals were much smaller when the new model was run with a 1.52 m × 1.52 m cell size, compared with the more appropriate 3.05 m × 3.05 m cell size. The cell size of 3.05 m × 3.05 m was more appropriate given the distance between successive ship positions, the dredge width, and uncertainty about dredge location. Using a cell size greater than the width of the dredge reflected the positional uncertainty of the dredge appropriately, but using a larger cell made the assumption about equal catchability of animals within cells between tows less tenable. Thus, there is a trade-off between cell size and satisfying the equal-catchability assumption. This assumption is more likely to be satisfied if a sensor could be used to track the location of the dredge directly (e.g., Takeda et al. 1995), making it appropriate to choose a smaller cell size for modeling.

Through the γ parameter, we presented one formulation of the capture process in which indirect losses of individuals may occur. Schnute (1983) considered other hypotheses, which could be included in our model by modifying eq. 4. Schnute considered the situation in which catchability declined with successive samples. For example, the efficiency of the first pass over an area can differ from that in subsequent samples, leading to a model with two efficiency parameters (Schnute 1983, model 2, p. 2155). A similar concept has been incorporated in models for electroshocking of fish in streams (Riley and Fausch 1992). In wildlife studies, the M_h and M_t models of Otis et al. (1978) allow for changes in catchability among animals and among recapture periods, respectively. Kendall and Bjorkland (2001) addressed the problem of temporary emigration of sea turtles (*Eretmochelys imbricata*) from the study area by allowing the probability of detection in a time period to vary. Their model was able to obtain unbiased estimates of survival and breeding probabilities.

Our model does not explicitly model variations in initial density over the area of the depletion experiment. Such variations might arise from habitat discontinuities (e.g., discrete beds of scallops; Caddy 1975). Nevertheless, the *K* parameter in the NB model provides some indirect information on the spatial heterogeneity (Pielou 1977; White and Bennetts 1996). The biases inherent in a nonspatial treatment of depletion experiments for sessile animals were demonstrated herein. Because the new model considers the spatial pattern of the animals and the tows, it should reduce the potential for these biases. Although many models can be used to describe overdispersion, the NB model has proved useful in many fisheries applications. A formal validation of the new model via extensive simulation experiments will be the subject of a future paper. Preliminary simulations have shown that the model can effectively recover the underlying parameters. In our application of the model to other species (NEFSC 2000*b*, 2001, 2004), we have found that the γ parameter is not always identifiable. The ability to estimate all four model parameters is related to the overlap pattern of tows within a depletion experiment. Tows that overlap extensively will be more informative about the joint effects of the efficiency and γ parameters.

This paper presents a realistic and flexible model for analyzing depletion experiments to estimate catch efficiency and density of organisms in an area. When combined with population abundance indices from standardized surveys, gear efficiency estimates can play an important role in direct stock size estimation (Vølstad et al. 2000; NEFSC 2003, 2004). Because gear efficiency may vary with habitat (NEFSC 2000*a*, 2000*b*), surveys that include multiple habitats may require multiple depletion experiments. From a statistical perspective, the benefit of measuring catch efficiency in several habitats may surpass the value of increasing the number of samples (tows) in a survey (Vølstad et al. 2000). Our conclusions are consistent with those of Schnute (1983), who advanced the notion that parametric descriptions of changing catchability were important aspects of depletion experiments in fisheries.

Acknowledgments

We are very grateful to the captain, crew, and scientists of the R/V *Delaware II* and staff of the Ecosystems Survey Branch for assisting with data collection and to L. D. Jacobson, S. A. Murawski, F. Serchuk, J. Hoenig, and anonymous reviewers for improving earlier versions of the manuscript. We also note the important role of W. Wakefield for his contributions on gear mensuration and underwater photography.

References

Bissell, A.F. 1972. A negative binomial model with varying element sizes. Biometrika, **59**: 435–441.

Caddy, J.F. 1968. Underwater observations on scallop (*Placopecten magellanicus*) behaviour and drag efficiency. J. Fish. Res. Board Can. **25**: 2123–2141.

Caddy, J.F. 1975. Spatial model for an exploited shellfish population, and its application to the Georges Bank scallop fishery. J. Fish. Res. Board Can. **32**: 1305–1328.

Carle, F.L., and Strub, M.K. 1978. A new method of estimating population size from removal data. Biometrics, **34**: 621–630.

Chien Y.H., and Condrey, R.E. 1985. A modification of the DeLury method for use when natural mortality is not negligible. Fish. Res. **3**: 23–28.

Crittenden, R.N. 1983. An evaluation of the Leslie–Davis method and of a weighted method for estimating the size of a closed population. Fish. Res. **2**: 149–158.

DeLury, D.B. 1947. On the estimation of biological populations. Biometrics, **3**: 145–167.

Gould, W.R., and Pollock, K.H. 1997. Catch-effort maximum likelihood estimation of important population parameters. Can. J. Fish. Aquat. Sci. **54**: 890–897.

Gould, W.R., Stefanski, L.A., and Pollock, K.H. 1997. Effects of measurement error on catch-effort estimation. Can. J. Fish. Aquat. Sci. **54**: 898–906.

Hilborn, R., and Walters, C.J. 1992. Quantitative fisheries stock assessment: choice, dynamics and uncertainty. Chapman and Hall, London.

Hirst, D. 1994. An improved removal method for estimating animal abundance. Biometrics, **50**: 501–505.

Houser, A., and Dunn, J.E. 1967. Estimating the size of threadfin shad population in Bull Shoals Reservoir from midwater trawl catches. Trans. Am. Fish. Soc. **96**: 176–184.

Johnson, N.L., Kotz, S., and Kemp, A.W. 1993. Univariate discrete distributions. 2nd ed. Wiley Inc., New York.

Joll, L.M., and Penn, J.W. 1990. The application of high resolution navigation systems to Leslie–DeLury depletion experiments for the measurement of trawl efficiency under open-sea conditions. Fish. Res. **9**: 41–55.

Kendall, W.L., and Bjorkland, R. 2001. Using open robust design models to estimate temporary emigration from capture–recapture data. Biometrics, **57**: 1113–1122.

Lasta, M.L., and Iribarne, O.O. 1997. Southwestern Atlantic scallop (*Zygochlamys patagonica*) fishery: assessment of gear efficiency through a depletion experiment. J. Shellfish Res. **16**: 59–62.

Lawless, J.F. 1987. Negative binomial and mixed Poisson regression. Can. J. Stat. **15**: 209–225.

Leslie, P.H., and Davis, D.H.S. 1939. An attempt to determine the absolute number of rats in a given area. J. Anim. Ecol. **8**: 94–113.

McCullagh, P., and Nelder, J.A. 1989. Generalized linear models. 2nd ed. Chapman & Hall Inc., New York.

Meyer, T.L., Cooper, R.A., and Pecci, K.J. 1981. The performance and environmental effects of a hydraulic clam dredge. Mar. Fish. Rev. **43**(9): 14–22.

Miller, R.J., and Mohn, R.K. 1993. Critique of the Leslie method for estimating sizes of crab and lobster populations. N. Am. J. Fish. Manag. **13**: 676–685.

Mohn, R.K., and Elner, R.W. 1987. A simulation of the Cape Breton snow crab, *Chionoecetes opilio*, fishery for testing the robustness of the Leslie method. Can. J. Fish. Aquat. Sci. **44**: 2002–2008.

Mood, A.M., Graybill, F.A., and Boes, D.C. 1974. Introduction to the theory of statistics. 3rd ed. McGraw-Hill, New York.

Murawski, S.A., and Serchuk, F.M. 1989*a*. Environmental effects of offshore dredge fisheries for bivalves. *In* International Council for the Exploration of the Sea, 1989 Statutory Meeting, The Hague, Netherlands. ICES CM 1989/K:27.

Murawski, S.A., and Serchuk, F.M. 1989*b*. Mechanized shellfish harvesting and its management: the offshore clam fishery of the eastern United States. *In* Marine invertebrate fisheries: their assessment and management. *Edited by* J.F. Caddy. Wiley Inc., New York. pp. 479–506.

Northeast Fisheries Science Center. 1998. 26th Northeast Regional Stock Assessment Workshop (26th SAW). B. Surfclams. Northeast Fisheries Science Center (NEFSC), Woods Hole, Massachusetts. NEFSC Ref. Doc. No. 98-03. pp. 51–169.

Northeast Fisheries Science Center. 2000*a*. 30th Northeast Regional Stock Assessment Workshop (30th SAW). E. Surfclams.

Northeast Fisheries Science Center (NEFSC), Woods Hole, Massachusetts. NEFSC Ref. Doc. No. 00-03. pp. 311–477.

Northeast Fisheries Science Center. 2000*b*. 31st Northeast Regional Stock Assessment Workshop (31st SAW). C. Ocean quahog. Northeast Fisheries Science Center (NEFSC), Woods Hole, Massachusetts. NEFSC Ref. Doc. No. 00-15. pp. 172–304.

Northeast Fisheries Science Center. 2001. 32nd Northeast Regional Stock Assessment Workshop (32nd SAW). B. Sea scallops. Northeast Fisheries Science Center (NEFSC), Woods Hole, Massachusetts. NEFSC Ref. Doc. No. 01-05. pp. 58–190.

Northeast Fisheries Science Center. 2003. 37th Northeast Regional Stock Assessment Workshop (37th SAW). C. Atlantic surfclam. Northeast Fisheries Science Center (NEFSC), Woods Hole, Massachusetts. NEFSC Ref. Doc. No. 03-16. pp. 284–433.

Northeast Fisheries Science Center. 2004. 38th Northeast Regional Stock Assessment Workshop (38th SAW). A. Ocean quahogs. Northeast Fisheries Science Center (NEFSC), Woods Hole, Massachusetts. NEFSC Ref. Doc. No. 04-03. pp. 8–173.

Nelder, J.A., and Mead, R. 1965. A simplex method for function minimization. Comput. J. **7**: 308–313.

Otis, D.L., Burnham, K.P., White, G.C., and Anderson, D.R. 1978. Statistical inference from capture data on closed animal populations. Wildl. Monogr. **62**.

Paloheimo, J. 1963. Estimation of catchabilities and population sizes of lobsters. J. Fish. Res. Board Can. **20**: 59–88.

Peterson, J.T., Thurow, R.F., and Guzevich, J.W. 2004. An evaluation of multipass electrofishing for estimating the abundance of stream-dwelling salmonids. Trans. Am. Fish. Soc. **133**: 462–475.

Pielou, E.C. 1977. Mathematical ecology. Wiley Inc., New York.

Pollock, K.H., Hines, J.E., and Nichols, J.D. 1984. The use of auxiliary variables in capture–recapture and removal experiments. Biometrics, **40**: 329–340.

Polovina, J. 1986. A variable catchability version of the Leslie model with application to an intensive fishing experiment on a multispecies stock. U.S. Fish. Bull. **84**: 423–428.

Power, J.H., and Moser, E.B. 1999. Linear model analysis of net catch data using the negative binomial distribution. Can. J. Fish. Aquat. Sci. **56**: 191–200.

Press, W.H., Teukolsky, S.A., Vettering, W.T., and Flannery, B.P. 1992. Numerical recipes in FORTRAN, the art of scientific computing. Cambridge University Press, Cambridge.

Ricker, W.E. 1975. Computation and interpretation of biological statistics of fish populations. Fish. Res. Board Can. No. 191.

Riley, S.C., and Fausch, K.D. 1992. Underestimation of trout population size by maximum-likelihood removal estimates in small streams. N. Am. J. Fish. Manag. **12**: 768–776.

Routledge, R.D. 1989. The removal method for estimating natural populations: incorporating auxiliary information. Biometrics, **45**: 111–121.

Sampson, D.B. 1988. Fish capture as a stochastic process. J. Cons. Int. Explor. Mer, **45**: 39–60.

Schnute, J. 1983. A new approach to estimating populations by the removal method. Can. J. Fish. Aquat. Sci. **40**: 2153–2169.

Seber, G.A.F. 1973. The estimation of animal abundance. Haefner Press, New York.

Smolowitz, R.J., and Nulk, V.E. 1982. The design of an electrohydraulic dredge for clam surveys. Mar. Fish. Rev. **44**(4): 1–18.

Takeda, S., Kakihara, T., Sakamoto, M., Zjan, Z., and Satoh, K. 1995. A study on the determination of underwater position of towed bodies. J. Tokyo Univ. Fish. **82**: 11–21.

Taylor, C.C. 1953. Nature of variability in trawl catches. Fish. Bull. **54**:145–166.

Venzon, D.J., and Moolgavkar, S.H. 1988. A method for computing profile-likelihood based confidence intervals. Appl. Stat. **37**: 87–94.

Vølstad, J.H., Sharov, A., Davis, G., and Davis, B. 2000. A method for estimating dredge catching efficiency for blue crabs, *Callinectes sapidus*, in Chesapeake Bay. Fish. Bull. **98**: 410–420.

Wang, Y-G., and Loneragan, N.R. 1996. An extravariation model for improving confidence intervals of population size estimates from removal data. Can. J. Fish. Aquat. Sci. **53**: 2533–2539.

Weinberg, J.R. 1999. Age-structure, recruitment, and adult mortality in populations of the Atlantic surfclam, *Spisula solidissima*, from 1978 to 1997. Mar. Biol. **134**: 113–125.

Weinberg, J.R., Dahlgren, T.G., and Halanych, K.M. 2002*a*. Influence of rising sea temperature on commercial bivalve species of the U.S. Atlantic coast. Am. Fish. Soc. Symp. **32**: 131–140.

Weinberg, J.R., Rago, P., Wakefield,W., and Keith, C. 2002*b*. Estimation of tow distance and spatial heterogeneity using data from inclinometer sensors: an example using a clam survey dredge. Fish. Res. **55**: 49–61.

Welch, D.W., and Ishida, Y. 1993. On the statistical distribution of salmon in the sea: application of the negative binomial distribution, and the influence of sampling effort. Can. J. Fish. Aquat. Sci. **50**: 1029–1038.

White, G.C., and Bennetts, R.E. 1996. Analysis of frequency count data using the negative binomial distribution. Ecology, **77**: 2549–2557.

Yamakawa, T., Matsumiya, Y., Nishimura, M., and Ohnishi, S. 1994. Expanded DeLury's method with variable catchability and its application to catch-effort data from spiny lobster gillnet fishery. Fish. Sci. **60**: 59–63.

ERRATUM / ERRATUM

Erratum: Basin-scale availability of salmonid spawning gravel as influenced by channel type and hydraulic roughness in mountain catchments

John M. Buffington, David R. Montgomery, and Harvey M. Greenberg

Ref.: Can. J. Fish. Aquat. Sci. **61**: 2085–2096 (2004).

Plane-bed and pool–riffle channels were incorrectly identified in the caption for Fig. 2. The second sentence of the caption should have read "... PB, plane-bed (circles); PR, pool–riffle (open triangles)...". In addition, the exponents reported in Fig. 2 for PR, wfPR, SP, and CA channels should have read 0.50, 0.59, 0.63, and 0.71, respectively. The corrected figure is shown.

Fig. 2. Bank-full Shields stress (τ^*_{bf}) as a function of total bank-full shear stress (τ) and channel type in Pacific Northwest rivers (morphologic definitions of Montgomery and Buffington 1997, 1998; Buffington et al. 2003). PB, plane-bed (circles); PR, pool–riffle (open triangles); wfPR, wood-forced pool–riffle (squares); SP, step–pool (diamonds); CA, cascade (solid triangles). PB, PR, and wfPR data are from Buffington and Montgomery (1999*a*, 2001); SP and CA data are from Montgomery and Buffington (1997).

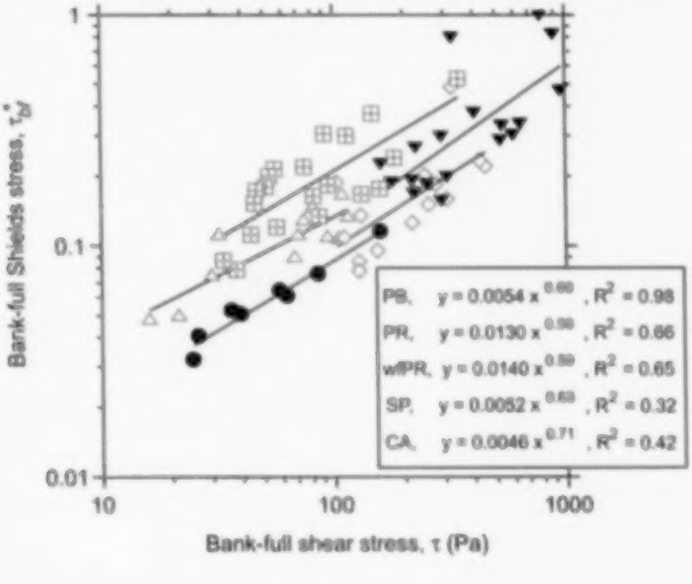

Received 19 September 2006. Accepted 20 September 2006. Published on the NRC Research Press Web site at http://cjfas.nrc.ca on 6 October 2006.
J17862E

J.M. Buffington.[1] USDA Forest Service, Rocky Mountain Research Station, 322 E. Front Street, Boise, ID 83702, USA.
D.R. Montgomery and H.M. Greenberg. Department of Earth and Space Sciences, University of Washington, Seattle, WA 98195-1310, USA.

[1] Corresponding author (e-mail: jbuffington@fs.fed.us).

doi:10.1139/F06-143

30th Congress of the International Association of Theoretical and Applied Limnology

30ième Congrès de l'Association internationale de limnologie théorique et appliquée

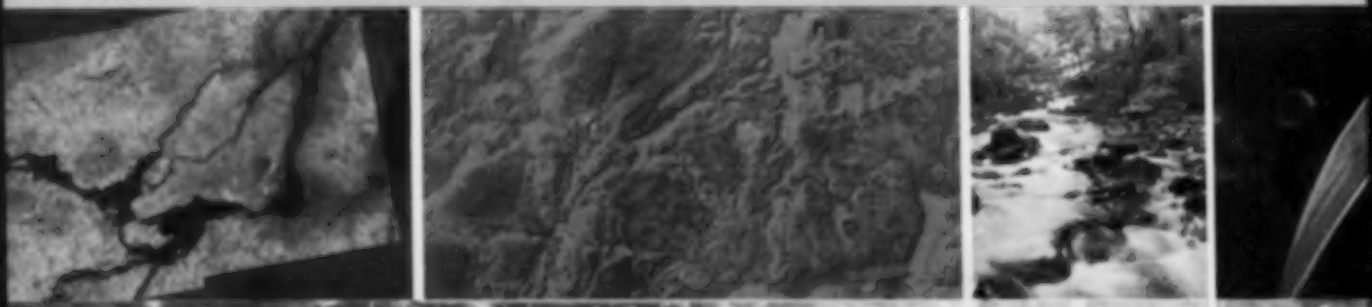

Montréal, Canada

12 - 18

août | August

2007

Montréal sera l'hôte du 30è Congrès de l'Association internationale de limnologie théorique et appliquée du 12 au 18 août 2007.

Ce congrès sera l'un des plus importants rassemblements de limnologistes venant des quatre coins du monde. Il fournira une opportunité unique d'interagir et de partager des données provenant de différents champs d'étude, régions et cultures. Ce congrès scientifique reliera la recherche de pointe aux problèmes majeurs auxquels font face les eaux douces dans le monde entier.

SIL 2007 vous fournira également l'opportunité de découvrir Montréal, une ville entourée du majestueux Fleuve St-Laurent de toutes parts. Reconnue mondialement pour sa joie de vivre, sa vie culturelle et sa gastronomie, Montréal est une ville propre, stimulante, abordable et sécuritaire.

Visitez-nous au **www.sil2007.org** !

Montreal will host the 30th Congress of the International Association of Theoretical and Applied Limnology from the 12th to 18th of August 2007

This promises to be one of the largest gatherings of freshwater scientists from around the globe. It will provide a unique opportunity to share ideas and data from diverse studies, regions and cultures. This scientific congress will link cutting-edge research with the important applied problems the world's freshwaters currently face.

SIL 2007 will be an opportunity for you to discover Montréal, an island city surrounded by the majestic freshwaters of the St-Lawrence River. Renowned for its cultural life and gastronomy, Montréal is also stimulating, safe and affordable.

Visit us at **www.sil2007.org** !

Montréal

Ross J. Marriott and Bruce D. Mapstone 2259–2274 Consequences of inappropriate criteria for accepting age estimates from otoliths, with a case study for a long-lived tropical reef fish

Michael J. Wilberg and James R. Bence 2275–2285 Performance of time-varying catchability estimators in statistical catch-at-age analysis

Thomas R. Hrabik, Olaf P. Jensen, Steven J.D. Martell, Carl J. Walters, and James F. Kitchell 2286–2295 Diel vertical migration in the Lake Superior pelagic community. I. Changes in vertical migration of coregonids in response to varying predation risk

Olaf P. Jensen, Thomas R. Hrabik, Steven J.D. Martell, Carl J. Walters, and James F. Kitchell 2296–2307 Diel vertical migration in the Lake Superior pelagic community. II. Modeling trade-offs at an intermediate trophic level

Anas Ghadouani, Bernadette Pinel-Alloul, and Ellie E. Prepas 2308–2317 Could increased cyanobacterial biomass following forest harvesting cause a reduction in zooplankton body size structure?

Jan Henning L'Abée-Lund, Thrond O. Haugen, and Leif Asbjørn Vøllestad 2318–2329 Disentangling local from macroenvironmental effects: quantifying the effect of human encroachments based on historical river catches of anadromous salmonids

Jeffrey T. Fujioka 2330–2342 A model for evaluating fishing impacts on habitat and comparing fishing closure strategies

Michael J. Ford, Howard Fuss, Brant Boelts, Eric LaHood, Jeffrey Hard, and Jason Miller 2343–2355 Changes in run timing and natural smolt production in a naturally spawning coho salmon (*Oncorhynchus kisutch*) population after 60 years of intensive hatchery supplementation

Antoine Olivier Henri Claude Leduc, Ellie Roh, Mark Charles Harvey, and Grant Edwin Brown 2356–2363 Impaired detection of chemical alarm cues by juvenile wild Atlantic salmon (*Salmo salar*) in a weakly acidic environment

J.P. Meador, F.C. Sommers, G.M. Ylitalo, and C.A. Sloan 2364–2376 Altered growth and related physiological responses in juvenile Chinook salmon (*Oncorhynchus tshawytscha*) from dietary exposure to polycyclic aromatic hydrocarbons (PAHs)

Paul J. Rago, James R. Weinberg, and Christopher Weidman 2377–2388 A spatial model to estimate gear efficiency and animal density from depletion experiments

ERRATUM ERRATUM

John M. Buffington, David R. Montgomery, and Harvey M. Greenberg 2389 Erratum: Basin-scale availability of salmonid spawning gravel as influenced by channel type and hydraulic roughness in mountain catchments

National Research Council Canada
Ottawa, Canada
K1A 0R6

Conseil national de recherches Canada
Ottawa, Canada
K1A 0R6

Postage paid at Ottawa
Publications mail
Registration No. 40062591

Port payé à Ottawa
Poste-publication
Enregistrement n° 40062591

USPS periodical postage paid at Plattsburgh, NY 12901, USA

Canadian Journal of Fisheries and Aquatic Sciences

Journal canadien des sciences halieutiques et aquatiques

Volume 63, Number 10, October 2006

Volume 63, numéro 10, octobre 2006

RAPID COMMUNICATION / COMMUNICATION RAPIDE

Ray Hilborn, John Annala, and Daniel S. Holland	2149–2153	The cost of overfishing and management strategies for new fisheries on slow-growing fish: orange roughy (*Hoplostethus atlanticus*) in New Zealand

ARTICLES / ARTICLES

John R. Sibert, Molly E. Lutcavage, Anders Nielsen, Richard W. Brill, and Steven G. Wilson	2154–2166	Interannual variation in large-scale movement of Atlantic bluefin tuna (*Thunnus thynnus*) determined from pop-up satellite archival tags
Brent A. Murry, John M. Farrell, Mark A. Teece, and Peter M. Smyntek	2167–2172	Effect of lipid extraction on the interpretation of fish community trophic relationships determined by stable carbon and nitrogen isotopes
R. John H. Hoxmeier, David H. Wahl, Ronald C. Brooks, and Roy C. Heidinger	2173–2182	Growth and survival of age-0 walleye (*Sander vitreus*): interactions among walleye size, prey availability, predation, and abiotic factors
Dina M. Leech and Sönke Johnsen	2183–2190	Ultraviolet vision and foraging in juvenile bluegill (*Lepomis macrochirus*)
H. Baumann, H.-H. Hinrichsen, C. Möllmann, F.W. Köster, A.M. Malzahn, and A. Temming	2191–2201	Recruitment variability in Baltic Sea sprat (*Sprattus sprattus*) is tightly coupled to temperature and transport patterns affecting the larval and early juvenile stages
Torsten Schulze, Ulrich Baade, Hendrik Dörner, Reiner Eckmann, Susanne S. Haertel-Borer, Franz Hölker, and Thomas Mehner	2202–2212	Response of the residential piscivorous fish community to introduction of a new predator type in a mesotrophic lake
Michael J. Paterson, Paul J. Blanchfield, Cheryl Podemski, Holger H. Hintelmann, Cynthia C. Gilmour, Reed Harris, Nives Ogrinc, John W.M. Rudd, and Ken A. Sandilands	2213–2224	Bioaccumulation of newly deposited mercury by fish and invertebrates: an enclosure study using stable mercury isotopes
J. Michael Jech and William L. Michaels	2225–2235	A multifrequency method to classify and evaluate fisheries acoustics data
Amy M. Marcarelli, Wayne A. Wurtsbaugh, and Olivia Griset	2236–2248	Salinity controls phytoplankton response to nutrient enrichment in the Great Salt Lake, Utah, USA
Michael R. O'Farrell and Louis W. Botsford	2249–2258	The fisheries management implications of maternal-age-dependent larval survival

Continued on inside back cover / Suite au verso

Canada

Printed in Canada by / Imprimé au Canada par
NRC Reprographic Services / Service de reprographie CNRC
Page production by / Mise en page par
NRC Research Press / Presses scientifiques du CNRC

0706-652X(200610)63:10;1-U